THE EVOLUTION OF THE PROTEROZOIC GNEISSES AND OTHER METAMORPHITES BETWEEN SPRINGBOK AND VIOOLSDRIF, SOUTH AFRICA

BY

GERHARD VAN ASWEGEN

PROMOTOR:

PROFESSOR A.E. SCHOCH

SUBMITTED IN FULFILMENT OF THE REQUIREMENTS FOR THE DEGREE OF

PHILOSOPHIAE DOCTOR

IN THE FACULTY OF SCIENCE (DEPARTMENT OF GEOLOGY)

UNIVERSITY OF THE ORANGE FREE STATE, BLOEMFONTEIN

JANUARY 1988

ABSTRACT

This study covers aspects of the stratigraphy, structure and metamorphism of part of the Proterozoic Namaqua Metamorphic Complex in northern Namaqualand, between Vioolsdrif in the north and the area around Springbok in the south. The investigation formed part of the Namaqua Geotraverse, National Geodynamics Project (Blignault et al., 1983). The study area is subdivided into four thrust bounded tectonic domains. The Richtersveld Domain in the north is seperated from the centrally situated Steinkopf Domain by the Transition Zone. The Copper District occurs in the south while the Geselskapbank Domain represents a small easterly extension of the study area. The latter domain was not part of the original geotraverse, but a brief study of the metamorphites provided important insights into the tectonic development of the region. The stratigraphy of this domain is not discussed. The major Steinkopf fault juxtaposes the Nama Group (+/- 600 Ma) and the Proterozoic rocks and forms a natural western boundary for the study area.

The Namaqua Metamorphic Complex is the product of two orogenies, the Orange River orogeny (1730 - 2000 Ma) and the Namaqua orogeny (1000 - 1300 Ma). The stratigraphy of the supracrustal rocks are possibly related to the Orange River orogeny, while most of the observable metamorphic and structural features are the products of the Namaqua orogeny.

The supracrustal rocks of the Namaqua Metamorphic Complex are considered to belong to a single Group, the Bushmanland Group, subdivided into the Haib, Eenriet and Khurisberg Subgroups. The Haib Subgroup in the study area consists of a lower felsic unit (Tsams Formation), which straddles the boundary between the Richtersveld Domain and the Transition Zone, and the more mafic Nous Formation, the latter being confined to the Richtersveld Domain. The Eenriet Subgroup comprises three spatially seperated metasedimentary units, namely the Groothoek Formation (mainly mica schists, confined to the Transition Zone), the Kabina Formation (metaquartzite and schistose metapelite; which builds the Eenriet Mountain Range) and the Besondermeid Formation (penetratively retrogressed metapelites and minor dark metaquartzite which occurs as a xenolitic enclave in the Steinkopf Domain). The Khurisberg Subgroup comprises the supracrustal rocks of the Copper District, i.e. white metaquartzite, high grade metapelites and minor metabasites.

The supracrustal rocks are engulfed in granitic batholiths and cut by smaller intrusive bodies. The most voluminous units are the Vioolsdrif, Gladkop, Little Namaqualand and Spektakel Suites. The Nariams metadolerite dykes, Koperberg Suite, Blesberg (pegmatite) Suite and the Gannakouriep (dolerite) Suite complete the list of significant intrusive units.

The Vioolsdrif Suite (granodiorite to leucogranite) is mainly confined to the Richtersveld Domain and, together with the Haib Subgroup, forms the Orange River Igneous Belt, the igneous products of the Orange River orogeny.

The Gladkop Suite constitutes the main lithological entity of the Steinkopf Domain. Three major units are distinguished, namely the Steinkopf Gneiss (granodioritic to granitic), the Brandewynsbank Gneiss (granitic) and the Noenoemaasberg Gneiss (leucogranitic). Together they form a grey gneiss complex similar to basement

complexes elsehwere. The gneisses exhibit well-developed banding shown to be of secondary origin through processes of mechanical flattening of primary heterogeneities coupled with metamorphic and/or metatectic differentiation. By distinguishing primary from secondary features, it is shown that the precursors to the three gneiss units were homogeneous in terms of composition, texture and structure. The gneisses do not exhibit primary banding. Intrusive relations are established on grounds of the recognition of xenoliths and observation of contamination and assimilation at the contacts. It is shown that the Steinkopf Gneiss is intrusive into metasediments of the Khurisberg and Eenriet Subgroups (i.e. it is not a basement for these supracrustal rocks), that the Brandewynsbank Gneiss is intrusive into the Steinkopf Gneiss and that the Noenoemaasberg Gneiss is intrusive into both the older units. Both the Gladkop and Vioolsdrif Suites are intrusive into the Eenriet Subgroup and are in turn intruded by the Little Namaqualand Suite. Isotopic characteristics confirm the suggested time equivalence while chemical, stratigraphic, structural and metamorphic evidence point to a spatial separation of the two suites during early Proterozoic times.

The Konkyp Gneiss of the Transition Zone is correlated with the Little Namaqualand Suite augen gneisses of the Copper District on grounds of similar structural, textural and stratigraphic relations. A slightly more silicic and iron rich compositions of the Konkyp Gneiss relative to other augen gneisses in the Geotraverse is interpreted to reflect inhomogeneities of the source area. The augen of the Little Namaqualand Suite are best interpreted as primary phenocrysts which are large due to growth during very slow cooling.

The Spektakel Suite includes the Concordia, Rietberg and Kweekfontein Granite of the Copper District and the Eyams Granite and Middelplaat dykes (normatively potassium-rich nepheline syenite for most part) of the Steinkopf Domain. The Eyams and Kweekfontein Granites are very similar in terms of their migmatitic characters and modes of emplacement.

The structural development spans 1000 million years and the older structures are largely obliterated by the main deformational phases of the Namaqua tectogenesis. Pre-Namaqua deformation in the Gladkop Suite is inferred and correlated with pre-Namaqua northeasterly directed thrusting in the Richtersveld Domain. The most important deformation phase involved early Namaqua, deep seated thrusting which imparted a regionally penetrative foliation to the augen gneisses and because of which lithological units were subhorizontally displaced over distances as much as 100 km from the northeast to the southwest. This was followed by a second phase of thrusting (commonly referred to as the Skelmfontein phase) which produced zonally developed refoliation in the augen gneisses and in the gneisses of the Gladkop Suite and which produced the foliation in the Concordia and Rietberg Granites. The direction of tectonic transport during Skelmfontein thrusting was essentially the same as for the early thrusting. The Kweekfontein and Eyams Granites are in part syn-tectonic with the Skelmfontein thrusting. The present distribution of lithological units in the Geotraverse is mainly the result of the two thrust phases. Late structures include the open folds, the Ratelpoort shearing (easterly trend), the Dabbiknik shearing (northwesterly trend) and the development of steep structures.

The Richtersveld Domain comprises a core zone charcterized by

greenschist facies mineral assemblages, the products of thermal overprinting during the Namaqua orogeny, superimposed on the kinematic fabrics of the Orange River orogeny. Outside the core zone the metamorphic grade increases to lower amphibolite facies. The Transition Zone is characterized by middle amphibolite facies mineral assemblages with prominent retrogression, involving the growth of andalusite at the expense of sillimanite, during late thrusting. In the Konkyp area higher grade prograde features are spatially associated with the Konkyp Gneiss. Mineral assemblages and compositions indicate peak metamorphic conditions of 650° C and less than 4 kb pressure for the Eenriet region. Penetrative reworking during Skelmfontein deformation tranformed dolerite dykes, which transect early Namaqua fabrics, to amphibolites in the Steinkopf Domain. Geothermometry indicates temperatures of around 700° C for the central and southern parts of the Steinkopf Domain during the late Namaqua metamorphism. The Copper District is a granulite terrane. Peak metamorphic around 800° and 5 kb pressure during Skelmfontein deformation is indicated. Metamorphic recrystallization of minerals in bodies of Koperberg Suite leucodiorite suggest elevated temperatures during emplacement of these rocks. Temperatures around 500° C indicated by biotite-garnet compositions of metapelites penetratively deformed in steep structures may reflect retrogression at a much later stage. The Geselskapbank Domain contains exotic stratigraphic units (including early Namaqua granulites) tectonically emplaced during late thrusting. These granulites formed at a temperature of about 750° C. Retrogression similar to that experienced by the rocks of the Transition Zone produced andalusite + chlorite in cordierite-sillimanite-garnet rocks. Geothermometry and geobarometry yield about 500° C and less than 3 kb respectively, consistent with the observed retrograde mineralogy.

The grey gneissses of the Gladkop Suite display maximum migmatization correlated with the Orange River orogeny at the northern extremities of Gladkop Suite outcrops, in the Transition Zone. Most significant migmatization developed during early Namaqua metamorphism and is located adjacent to the Copper District in the south and spatially associated with the Konkyp Gneiss in the north.

A tectonic model that fits the data includes high grade metamorphism and migmatization of the Gladkop Suite during the Orange River orogeny, culminating in the thrusting of the Steinkopf Domain over the Richtersveld Domain in a northeasterly direction. During the Namaqua orogeny the sense of thrusting reversed and first caused the overriding of thrust sheets, rendered hot and ductile due to high volumes of the Little Namaqualand Suite magmas, over the Richtersveld Domain. Later the Richtersveld Domain was undercut by foot wall propagation of thrust faults. The Richtersveld Domain then started to override the Steinkopf Domain along the Groothoek thrust, transporting a superjacent augen gneiss sheet. Late Namaqua thrusting caused rejuvenation of the Groothoek thrust and new movement along the Skelmfontein thrust. The distribution of thrust sheets with high volumes of still hot augen gneisses and recently added Spektakel Suite magmas caused high grade metamorphism at the leading edge of the Skelmfontein thrust sheet and retrograde metamorphism at the trailing end.

CONTENTS

APPENDICES

LIST OF FIGURES

LIST OF TABLES

1. INTRODUCTION

1.1 GENERAL

This thesis reports the results of the author's involvement in the contribution of the University of the Orange Free State (UOFS) to the International Geodynamics Project which focussed attention on the Namaqua Geotraverse. The locality and outline of the Geotraverse as well as the author's share of the regional mapping (henceforth referred to as the 'mapped area'), is illustrated by the printed map 'The Namaqualand Geotraverse' (Annexure 1). Subsequent to the completion of the Geodynamics project, mapping to the east of the geotraverse added significantly to a better understanding of the Proterozoic geology of the region (Strydom, 1985; Strydom and Visser 1986). The area covered by this study excludes most of the northern and eastern parts of the geotraverse, but includes part of the Geselskapbank area (Figures 1.1 and 1.2).

Henceforth the meaning of the terms Richtersveld Domain, Transition Zone, Steinkopf Domain, Copper District and Geselskapbank Domain will be as shown in Figure 1.3. The Richtersveld Domain is as defined by Blignault et al. (1983). The term 'Transition Zone' for the Groothoek Thrust Zone and environs was first used by Theart (1980). Van der Merwe (1986) used it more or less synonymously with Groothoek Thrust Zone. The Transition Zone is here considered to be the area between the Richtersveld Domain and the Steinkopf Domain proper. Thus the southern boundary is taken further south than was done by the Van der Merwe (1986). The mapped area (present study) includes the Steinkopf Domain and the Konkyp area of the Transition Zone.

In the chapters to follow, the lithology and stratigraphy of the mapped area is described and brought into context with lithological successions in the neighbouring regions. This is followed by a synthesis of the structural evolution of the rocks in the study area in order to provide the framework within which the metamorphic development can be discussed. Finally, an interpretation of the tectonic evolution of the Proterozoic rocks in Northern Namaqualand is given.

The investigation commenced in July 1975 and was continued until the end of 1977 in a full-time capacity, while the rest of the work was completed on a part-time basis. At first, the field work involved mapping of the area between the Copper District in the south and the Konkyp Mountain in the northwest, on aerial photographs (scale 1:30000). The mapping was later transferred to topographic maps (scale 1:50000) and eventually incorporated in the Geotraverse map (Annexure 1).

Routine petrographical analyses were carried out on specimens of the different lithological types. Chemical analyses of selected samples were supplied by the Geological Survey of South Africa (GSSA) in Pretoria as well as by the University of the Orange Free State. Microprobe analyses were carried out by the author at the University of Cape Town's Department of Geochemistry, at the research laboratory of the GSSA in Pretoria and in the laboratory of the Geochemistry Division, Department of Geology, UOFS.

1.2 HISTORICAL BACKGROUND

Wyley (1857), Dunn (1872) and Rogers (1915) were early visitors to the Steinkopf area who recorded their impressions. The report on the corundum bearing schist near the town of Steinkopf by Rogers (op. cit.) is important, because the deposit has been exhausted. Gevers (in Gevers et al., 1937) described the schist, quartzite and gneiss of the Eenriet area and pointed out the apparent similarity with metasediments which occur further to the south in the Copper District. He also considered the fine-grained gneiss structurally underlying the Eenriet metasediments to be the marginal aplitic phase of the "....great Namaqualand batholith...". His "batholith" included the Little Namaqualand Suite, the Spektakel Suite and probably also the Gladkop Suite. Mathias (1941, p. 176) described a gneiss sample from near Brandewynsbank in the Steinkopf Domain.

The southernmost part of the Steinkopf area was mapped by staff of the O'okiep Copper Company (OCC) and descriptions of these parts are embodied in unpublished company reports. Descriptions of two specific localities were, however, published (O'okiep Copper Company, 1975).

1.3 GENERAL GEOLOGY OF THE STEINKOPF DOMAIN

Except for those parts immediately to the north of the Copper District, where mapping was done by the OCC, the Steinkopf area had, for most part, never been mapped before. The mapped area is largely underlain by the grey gneisses of the Gladkop Suite (Chapter 4) which tend to form a flat monotonous landscape. In the southern and western regions, gneiss domes are the dominant landforms. In the north, prominent hills, known as the Eenriet Mountains, consist of metaquartzites of the Eenriet Formation (Chapter 2). The Konkyp hill, in the extreme northeast, represents most of the Little Namaqualand Suite present in the mapped area.

TABLE 1.1 THE STRATIGRAPHIC SUCCESSION OF THE MAJOR PRECAMBRIAN UNITS IN THE STUDY AREA

GROUP OR SUITE	DOMINANT ROCK TYPE and/or LOCAL NAME	AGE (Ma)
Nama Group	Not investigated	<= 600
Gannakouriep Suite	Dolerite dykes	+/-800
Late Pegmatites	Pegmatites	<=1000
Koperberg Suite	Diorite, anorthosite, hypersthenite, norite	<=1100
Spektakel Suite	Eyams Granite Rietberg Granite	<=1100
Little Namaqualand Suite	Konkyp Gneiss	<=1200(?)
Gladkop Suite	Noenoemaasberg Gneiss Brandewynsbank Gneiss Steinkopf Gneiss	>1800
Kinderlê Gneiss	Stratigraphic status unclear	
Okiep Group	Eenriet Subgroup Khurisberg Subgroup	> 1800

The Palaeozoic sediments of the Nama Group unconformably overlie the

Proterozoic rocks. The abovementioned sediments are tectonically undisturbed, except for some warping along the major Steinkopf fault. This north-trending fault has placed the Nama rocks in juxtaposition to the Proterozoic rocks, forming a natural western boundary for the study area. The Nama Group was not studied.

The stratigraphical succession of the mapped area (excluding Tertiary and Recent cover rocks), is presented in Table 1-1 above.

1.4 NOMENCLATURE

Term definitions are, as far as possible, in line with popular usage in South Africa. A number of terms are, however, used differently by different authors and it is necessary to explain some of the preferences adopted in this study.

The terms schist and gneiss are largely used as suggested by Winkler (1979, p. 341). A schist is characterized mainly by its schistose texture. In marginal cases, a 20 percent upper limit on the feldspar content is used to distinguish it from a gneiss. In the definition of a gneiss a significant feldspar content is considered to be essential. Most of the gneisses in this study are granitic in composition. Rocks with little or no feldspar and a gneissic texture are simply called foliated XYZ-rocks, where the XYZ represents the dominant or most characteristic constituent phases. Additional adjectives are used, if necessary, to describe the fabric more fully. A mineral name as prefix to a rock name (e.g. biotite gneiss) does not imply that that mineral is the only or most abundant constituent of the rock. It indicates, rather, that the particular mineral distinguishes that rock from other rocks (e.g. muscovite gneiss).

To describe different types of foliation the scheme put forward by Powell (1979) is adhered to. The gneisses of the study area generally exhibit an anastomosing foliation, defined by cleavage traces which follow the outlines of lense shaped felsic microlithons. Such a texture can also be descibed as 'domainal' since it consists of domains which are internally homogeneous (generally granoblastic), separated from each other by thin schistose zones. The adjectives 'embayed', 'decussate', 'helicitic', 'mimetic' and other similar terms to describe metamorphic grain shapes and interrelationships are used as defined by Spry (1969).

The term 'granoblastic' was taken by Winkler (1979) to describe the textures of rocks from the 'regional hypersthene zone' exclusively. His Figure 16-1 (after Moore, 1970), provides a useful classification system for granular metamorphic rocks and is applied here to rocks of all metamorphic grades. Furthermore, the term granoblastic is not restricted to rocks without foliation. The main characteristics are that most grains meet at triple junctions (indicating metamorphic crystallization) and that the majority of mineral grains are not strongly anisotropic. Since granoblastic literally means a combination of granular and blastic, it is unnecessary to include the term 'grained' (as in fine-grained) in the description; fine-granoblastic or coarse-granoblastic is sufficient.

Winkler's metamorphic classification system, introduced in 1974 with the third edition of his book 'The Petrogenesis of Metamorphic Rocks', according to which the old facies concept is replaced by a

simplified system, using terms such as 'very low-grade', 'high-grade' etc. and his suggestions pertaining to the nomenclature of metamorphites containing typomorphic orthopyroxene (granolite versus granulite), are widely used in South Africa. It has not, however, been widely accepted in the English literature on metamorphism. For this reason, the old classification system and accompanying terminology, as recently again advanced by Turner (1981), is followed here. Accordingly, metamorphites in the study area are classified in terms of the greenschist, lower amphibolite, upper amphibolite and granulite facies.

An important distinction between the greenschist facies and the amphibolite facies is the composition of the calcic amphibole in rocks with appropriate composition - actinolite for the greenschist facies and hornblende for the amphibolite facies. Accordingly, the term 'amphibolite' to describe a metamorphite, should be restricted to rocks in which hornblende is the dominant mafic phase (Winkler, 1979, p. 342).

Unless otherwise stated, mineral name abbreviations are used in accordance with the suggestions of Kretz (1983).

2 THE EENRIET SUBGROUP

2.1 THE BESONDERMEID FORMATION

Quartzites of the Besondermeid Formation build the prominent hill, called Spitskop, next to the main road a few kilometres south of Steinkopf. The formation constitutes a refolded synformal enclave of metasedimentary rocks within the Gladkop Suite (see Chapter 9 for the structural interpretation).

2.1.1 LITHOSTRATIGRAPHY

The details of the lithostratigraphic succession are unclear owing to poor outcrop. The formation consists for the most part of a major unit of altered biotite-sillimanite-garnet schist with lesser bands of calc-silicate rock and metaquartzite. There is no indication of the stratigraphic facing direction and no such facing is implied by the sequence in which the lithologic types is discussed. The progression described below is roughly in the sequence as encountered along a traverse from east to west accross the inlier.

Metaquartzite and calc-silicate rock

A banded sequence of metaquartzite and calc-silicate rock structurally underlies the major aluminous schist horizon (locality 1, Figure 2.1). The quartzite and calc-silicate rock occur as thin resistant bands (< .5 m) in host rock that seems to be dominated by feldspathic metaquartzite.

Mineralogically the calc-silicate rock consist of garnet, quartz and plagioclase, with or without the following minor constituents: hornblende, epidote, diopside, sphene and opaque minerals. The calc-silicate rocks do not exhibit prominent internal banding and the texture varies from fine-granoblastic to coarse-granoblastic.

At least two different types of metaquartzite are found in the "basal" banded sequence, namely fine-granoblastic white metaquartzite and medium-granoblastic to coarse-granoblastic purple-brown metaquartzite. Another rock type in the banded sequence can be described as a pink-weathering, schistose metaquartzite. It is fine-granoblastic with minor coarse quartz bands (veins?) of a few millimetres thick. It contains approximately 20 percent biotite (altered to white mica and opaque minerals) and 5 percent epidote.

The altered aluminous schist.

The banded sequence is structurally overlain by thick aluminous schist (> 100 metres) that forms the bulk of the Besondermeid Formation. The schist is a soft, massive, greenish rock consisting almost entirely of very fine-grained compact sericite (identified by X-ray diffractometry), with lesser amounts of quartz, garnet, remnants of biotite and, in some cases, plagioclase. Porphyroblasts of muscovite are also observed at certain places.

The process of retrograde metamorphism which caused the sericitization, is discussed in Chapter 10. The southern end of the Besondermeid enclave represents an area that to some extent escaped this process. Here, in an excavation next to the main road (locality 2, Figure 2.1), biotite-sillimanite-garnet schist is

exposed (Figure 2.2). No primary muscovite is present in the rock. To what extent this biotite-rich schist represents the unretrogressed precursor to the sericite schist in the rest of the Besondermeid Formation, is uncertain. The large number of pseudomorphs after sillimanite in the sericite-schist indicates, however, that the rock must formerly have been more sillimanite-rich than the biotite schist.

Another variety of the altered rock exhibits dark coloured boudinaged forms (altered to chlorite and white mica) rather than the common garnet relicts. These features are reminiscent of the cordierite nodules in the cordierite schist in the Transition Zone, discussed in Chapter 10.

The "upper" metaquartzite and calc-silicate rocks

In the northern part of the Besondermeid enclave, the structural top of the Besondermeid Formation is marked by relatively thin, dark-coloured metaquartzite. The quartzite has a coarse texture and glassy appearance. In the southern portion of the enclave, white metaquartzite is also present at the same structural horizon.

Associated with the dark metaquartzite are thin bands of calc-silicate rock. They differ from those at the structural base of the sequence in that they do not contain garnet. The rock is fine-granoblastic (<= 1 millimetre) to very fine-granoblastic (< 0.2 millimetre). The different bands vary somewhat in mineralogical composition. Quartz is the most prominent phase in all varieties, while only a few samples were found that do not contain significant amounts of plagioclase (broken down to sericite). Additional phases are biotite (broken down to white mica and chlorite) and epidote, with one occurrence of accessory diopside.

2.1.2 CORRELATIVES IN THE GLADKOP SUITE

The Gladkop Suite (Chapter 4) contains many large and small xenolithic remnants of metasedimentary rocks. On grounds of structural interpretation, geographical proximity and lithological character a number of occurrences are considered to be direct correlatives of the Besondermeid Formaton.

Metaquartzite and iron formation

In the inner arc of the macro-fold (locality 3, Figure 2.1) about 200 metres west of the main road, a band of metaquartzite, approximately 90 metres in length, is found within the Gladkop Suite grey gneiss. It follows the northeasterly strike of the regional foliation in the country rock and is less than 2 metres wide. The quartzite is fine-granoblastic (<=1 millimetre) and dark-coloured due to the presence of approximately 10 percent biotite, the latter partially broken down to opaque minerals and other alteration products.

Further to the south (locality 4, Figure 2.1), a minor band of iron formation is present within leuco-gneiss next to the regional contact between the gneiss and the metasediments. The rock is fine-grained, consisting of approximately 50 percent opaque minerals together with about equal amounts of quartz and saussuritized plagioclase. Small garnets are also present and, in thin section, small zircon crystals can be seen. The rock is black in colour and heavy, exhibiting banding of the order of 2 to 20

millimetres. The opaque phase is non-magnetic.

Corundum schist

In the early part of the century corundum was recovered economically from the corundum bearing schist 7 kilometres east-northeast of Steinkopf (locality 5, Figure 2.1). The schist band is approximately 50 metres wide, strikes northerly and has a vertical dip, parallel to the regional foliation in the adjacent gneiss. The corundum was evidently concentrated in the eluvium owing to the weathering of the schist. Apparently the schist itself was subeconomic but the rich surficial concentrations were entirely depleted. The early workers knew where to look for corundum and they left a trail of small pits and trenches, exposing corundum bearing schist to the north and south of the main occurrence and as near as 1 kilometre to the Besondermeid enclave (see Figure 2.1)

The corundum occurs as euhedral porphyroblasts (up to 10 centimetres long) in the schist, which consists of about equal volumes of biotite and K-feldspar. Minor amounts of completely saussuritized plagioclase and accessory opaque minerals and chlorite are also present. The corundum is replaced by white mica for a large part.

Pelitic granulite

About 100 metres to the south of the southernmost outcrop of corundum bearing schist, a small but mineralogically important occurrence of hypersthene bearing metapelite is found (locality 6, Figure 2.1). It constitutes a band with a width of 0.5 m, enveloped in the Gladkop gneiss. It can be followed for about 20 metres along the northern foot of a domal gneiss outcrop. The rock consists of hypersthene, gedrite, biotite, garnet, quartz and plagioclase. The proximity to the Besondermeid enclave suggests correlation with the Besondermeid schists, the high grade mineral assemblage having been protected from retrogression by the shielding effect of the gneiss.

2.2 THE KABINA FORMATION

2.2.1 LITHOSTRATIGRAPHY

White metaquartzite of the Kabina Formation builds the Eenriet Mountain Range to the northeast of Steinkopf. The metaquartzite structurally overlies a banded sequence consisting of aluminous schist and minor bands or lenses of magnetite-quartz rock, amphibolite, cordierite-garnet rock and ultramafic metabasite.

The stratigraphic sequence was severely disrupted by deformation and the emplacement of granites, both early and late in the tectonic history. The sequence structurally underlying the metaquartzite weathers negatively and is poorly exposed. The lithological sequence varies from traverse to traverse, owing to the discontinuous nature of individual units. The lithology is discussed below in terms of a generalized structural sequence. The sequence is synthetized from observations along different traverses. A detailed stratigraphic analysis was not attempted and the description given below should be regarded as a first approximation.

Biotite-sillimanite-muscovite schist

A few metres of biotite-sillimanite/muscovite schist structurally overlies the white metaquartzite at locality 1, Figure 2.3. Because of the presence of a late kinematic granite in this structural position, it is impossible to observe the remaining supracrustal sequence above the metaquartzite. The schist is fine-grained and consists of quartz, plagioclase, biotite, sillimanite (partially broken down to muscovite) and a minor amount of K-feldspar. At locality 1, Figure 2.3, the schist displays a prominent kink structure.

The main white metaquartzite

White metaquartzite, with the coarse texture and glassy appearance which is so typical of white metaquartzites elsewhere in the Namaqua Metamorphic Complex, has a thickness of more than 100 metres in the southeast (locality 2, Figure 2.3). It does, however, become much thinner (2 - 3 metres) in the northwest (i.e. northeast of locality 1, Figure 2.3). The metaquartzite is thickly bedded and appears massive from a distance.

Banded metaquartzite

In the region of locality 3 (Figure 2.3) a metre thick, thinly bedded metaquartzite band is present immediately below the main metaquartzite.

Iron formation

A metre thick purplish-brown metaquartzite band was found immediately below the main metaquartzite at locality 3 (Figure 2.3). A minor lense of banded iron formaton (bif) is present in the same structural position at locality 4 (Figure 2.3). More purple-brown metaquartzite forms a band, approximately 40 metres long and oriented parallel to the regional foliation, within the Kinderle Gneiss. This band occurs 50 metres south of a metapelite band at locality 5 (Figure 2.3).

Quartz-sillimanite schist

Fine-grained to medium-grained quartz-sillimanite schist is commonly found immediately below the metaquartzite. Similar schist is however also found throughout the banded sequence, associated with minor metaquartzite bands or with cordierite-garnet rock.

Biotite-sillimanite schist

Schist similar to the schist above the main metaquartzite appears to have formed a major component of the banded sequence prior to replacement by the migmatitic Eyams Granite (Chapter 7.4). The composition of the relicts and restites in the migmatite varies according to the local precursor composition. Thus can the high frequency of biotite-sillimanite schist relicts in the migmatite, where it occurs in the banded sequence, be interpreted to indicate the former presence of the schist. It appears, in fact, as if the migmatite formed preferentially at the expense of the biotite-sillimanite schist.

Minor metaquartzite bands

Minor bands of metaquartzite (< 2 metres thick) are common in the banded sequence. They are generally white to blue-grey, but a prominent greenish band is found at locality 3 (Figure 2.3).

Quartz-feldspar gneiss

Fine-grained, dark coloured quartz-feldspar-biotite-sillimanite gneiss is part of the banded sequence at some places (e.g. localities 1 and 3, Figure 2.3). It is easily confused with a deformed, alumina-contaminated variation of Wyepoort Granite (Chapter 7.5), which is also emplaced into the banded sequence. The fine-grained gneiss is also frequently found as relicts in the Eyams Granite where the latter is emplaced into the banded sequence, indicating a former wide distribution.

Amphibolite

Thin (< 1 metre), discontinuous amphibolite bands are present at different structural levels and in different lithological associations. They are common hornblende-plagioclase rocks, medium-grained and penetratively foliated. No relict features indicating the origin of the amphibolites were recognized. The small size and apparent lack of stratigraphic association with any particular unit, suggests an intrusive origin.

Ultramafic rock

A small, but petrologically interesting body of ultramafic rock is found at locality 6, Figure 2.3. The rest of the banded sequence at this locality does not form outcrops and it is uncertain whether the ultramafic rock is in situ. It is fairly clear, however, that the body is part of the banded sequence on grounds of its position relative to the surrounding outcrops. The rock is coarse-grained with a metamorphic mineralogy and texture (orthopyroxene and clino-amphibole)

Garnetiferous metapelite

Volumetrically insignificant, but petrologically important garnet-bearing rock is part of the banded sequence at localities 7 and 8. It occurs within the Kinderlê Gneiss at locality 5 (Figure 2.3). The outcrop at locality 6 (Figure 2.3) is only 30 metres across, lying in the hinge zone of a mesoscopic and isoclinally folded synformal enclave within the surrounding Gladkop gneiss. The structural sequence within the synform is (from top to bottom):

garnet-anthophyllite rock
metaquartzite (< 1 metre)
quartz-sillimanite schist
amphibolite

At locality 8 (Figure 2.3) a similar sequence structurally underlies a prominent bluish-grey metaquartzite band, the latter also part of the banded sequence.

At locality 5 (Figure 2.3) the garnet-rich rock is found in two small xenolithic lenses, each approximately 8 X 2 metres in size. They are approximately 100 metres apart and are oriented with their longest dimensions parallel to the regional foliation. Each xenolithic lense consists of garnet-biotite rock together with minor quartz-sillimanite schist.

2.2.2 CORRELATION

On grounds of broad lithological similarity and geographical proximity, the metasedimentary sequence building the Eenriet Mountains is correlated with a thicker metasedimentary sequence to the west, together constituting the Kabina Formation of the Eenriet Subgroup, as is shown on the printed map (Annexure 1). No evaluation of the stratigraphically important correlation between the Kabina Formation and the formations of the Khurisberg Subgroup of the Copper District can be made before detailed stratigraphic studies in both areas are done.

3. THE KHURISBERG SUBGROUP

3.1 INTRODUCTION

The Khurisberg Subgroup is described in SACS (Joubert et al., 1980) as consisting of two major metaquartzite units (the Ratelpoort and Springbok metaquartzites) interbanded with a number of aluminous schist units. Martens (1979) described the structural succession of the metasediments in the immediate vicinity of Khurisberg.

Strydom (1985) gives a more complete description and stratigraphic subdivision of the metasediments to the east and inter alia gives a new definition to the 'Khurisberg Subgroup'. The supracrustal rocks in the eastern nose area of the Ratelpoort Synform is classified by him as (i) undifferentiated metaquartzite and schist of the Khurisberg Subgroup and (ii) fine-grained biotite gneiss and amphibolite tentatively correlated with the Haib Subgroup. The author is, however, not convinced of the significant presence of fine-grained biotite gneiss in the area that can not be directly correlated with the Gladkop Suite. A traverse across the westerly extension of the mafic unit in question, as found on the eastern side of Skelmfontein se Poort, is summarized below. At this position, the Khurisberg Subgroup is split into two parts by the intrusion of major granite sills (Leeupoort augen gneiss and Kweekfontein aplogranite). The traverse described below covers only that part of the sequence structurally below the granite sheets and it represents approximately one third of the Khurisberg sequence in this area.

Width	Rock type	Comment
	Kweekfontein Granite	Struct. top of traverse
5m	Brandewynsbank Gneiss	With xenolithic lenses of amphibolite
10m	Amhibolite and hbe-gneiss	Minor biotite gneiss bands
6m	Steinkopf Gneiss	
2m	Kweekfontein Granite	
2m	Metapelite ('granitized')	An elongate lense of ultramafic rock occurs at this structural level 1400m to the east
1m	Metaquartzite	
1m	Metapelite ('granitized')	
2m	Biotite gneiss	Origin unknown
4m	Steinkopf Gneiss	
50m	Amphibolite, hbe-gneiss, minor calc-silicate rock	A banded unit, also exposed in Ratelpoort
10m	Steinkopf Gneiss	
4m	Hbe gneiss	Texture similar to Brandewynsbank Gneiss
2m	Steinkopf Gneiss	
1m	Noenoemaasberg Gneiss	
15m	Steinkopf Gneiss	
1m	Hornblende gneiss	
2m	Brandewynsbank Gneiss	
.5m	Amphibolite	
	'Steinkopf Domain'	

The sequence consists for a large part of Gladkop Suite gneiss and

mafic rocks. The intimate interbanding of the supracrustal rocks with the Gladkop Suite gneisses reflect the extreme shear strain imposed on the rocks in this area during Skelmfontein shearing (thrusting). A banded sequence of metapelite and varieties of mafic granulite occurs at the structural position of the last thin amphibolite band of the above traverse, less than 1 km to the east, as well as to the west, e.g. west of Ratelpoort. A similar banded sequence of metapelitic rock and granulite occurs structurally above the sill of Kweekfontein Granite which marks the upper limit of the traverse described above, to the west of Skelmfontein se Poort. Structural duplication is not unlikely. The entire supracrustal succession, as encountered along a generalised traverse from within the Steinkopf Domain across the 'Ratelpoort lineament' into the Ratelpoort Synform, plus the 'Springbok quartzite' and it's associated metasediments, is here taken to belong to the Khurisberg Subgroup and no stratigraphic subdivision of the Subgroup is attempted. Although this simplistic approach is bound to be proven incorrect by future stratigraphic analysis, our present knowledge is not adequate for any detailed stratigraphic subdivision of these rocks.

The broad structural succession found along a traverse, from within the area of the best development of Gladkop gneisses, southwards to the main metaquartzite in the northern limb of the Ratelpoort synform, is then as follows:

Banded metapelitic unit: aluminous schist/gneiss interbanded with several varieties of two-pyroxene granulite.

Mafic unit: Amphibolite, mafic gneiss, calc-silicate rock, biotite gneiss.

Banded metapelitic unit: similar to the unit at the base.

Main metasedimentary unit: especially well developed in the eastern nose area of the Ratelpoort Synform, it consists of biotite-sillimanite-garnet schist/gneiss and prominent metaquartzite.

The metapelites and mafic rocks weather more readily than the surrounding gneisses and good outcrops are scarce. No attempt was made to document the full nature of the supracrustal sequence during the course of the regional mapping. In the following paragraphs only brief descriptions of typical outcrops are given.

3.2. LITHOLOGICAL ASPECTS OF THE NORTHERN LIMB, RATELPOORT SYNFORM

3.2.1 THE GARNET-CORDIERITE-SILLIMANITE ROCKS

Immediately east of the Bulletrap settlement some of the best outcrops of aluminous schist/gneiss are found. The total thickness of the metapelitic unit in the area under discussion is at least 200 metres and the weathering and denudation of these rocks produced a valley rimmed by more resistant granitoid gneisses. The few small isolated outcrops found in the valley are not topographically prominent, but they are conspicuous due to their dark colour.

The outcrops in the immediate vicinity of Bulletrap consist for most part of dark red-brown weathering garnet-cordierite-sillimanite rock. The sillimanite is in the form of light-coloured needles set in a dark matrix of quartz, K-feldspar, cordierite and garnet. The texture varies from medium-granoblastic to coarse-granoblastic; the regional foliation, also penetratively developed in these rocks, is defined by the preferred orientation of sillimanite, flattened garnet and cordierite, and minor biotite.

Thin bands (< 20 centimetres) of fine-granoblastic, leucocratic, plagioclase-quartz rock with minor small garnets, may represent primary compositional layering in the metapelite. At the northern margin of the metapelite unit (locality 1, Figure 3.1), thin (<50 centimetres), discontinuous bands of fine-granoblastic, two-pyroxene granulite are found. Minor mafic granulite bands are common in the metapelite unit and more details are given below.

Stromatic leucosomes of two ages constitute about 30 percent of the metapelite and enhance the secondary banding. Closer to the contact with the adjacent Rietberg Granite (e.g. locality 2, Figure 3.1), the younger (pegmatitic) leucosomes are more abundant and here they are particularly rich in garnet. The garnet is present in the paleosome and in both ages of neosomes, but is more prominent in the younger neosome.

The presence of a high proportion of quartzo-feldspathic leocosomes in the metapelite renders the rock more resistant to weathering and at locality 3, (Figure 3.1) the metapelite horizon even builds positive topography. Here the rock consists of about 40 percent discrete neosome and the 'paleosome' is also impregnated with quartz and feldspar on millimetre scale.

At locality 4, (Figure 3.1), minor bands, a few centimetres thick, with a schistose texture due to a high biotite and low feldspar content, are found in the metapelite. This is one of the few examples of true schist in this stratigraphic unit which is locally known as the 'Ratelpoort schist'. For most part the metapelite contains too much feldspar and too little mica to be called schist. The high feldspar content can, for most part, be attributed to 'granitization', either in the form of stromatic leucosomes, or in the form of pervasive impregnation (millimetre scale) as mentioned above. In many other instances, however, the rock contains very little feldspar and little or no biotite, consisting chiefly of cordierite, garnet, sillimanite and quartz. It has a domainal foliation, i.e. a 'gneissose' texture.

In the east the supracrustal units, together with the gneisses, are more severely sheared. The cordierite-garnet-sillimanite rock here represents a 'matrix' in which other lithological types are present in the form of thin bands or lenses.

3.2.2 MAFIC ROCKS

Amphibolite and mafic granulite

Apart from the prominent amphibolite and hornblende gneiss in the mafic unit, minor amphibolite bands are also associated with two-pyroxene granulite within the banded metapelitic horizons on either side of the mafic unit. The maximum thickness of the bands and lenses is 1 metre and some bands are less than 4 centimetres thick. Textural variation is greater than could be expected considering the relatively small compositional variation. The

following types are found interbanded with each other or as individual bands or lenses: (i) very fine-granoblastic (< 1 millimetre) massive hypersthene-diopside-plagioclase rock, (ii) fine-granoblastic, thinly banded hypersthene-diopside-plagioclase-quartz rock with banding defined by narrow (<= 1 millimetre) quartz bands, isoclinally folded on meso and micro-scale, (iii) fine-granoblastic to medium- granoblastic, foliated, hypersthene-diopside-hornblende- plagioclase rock, with or without minor quartz and/or biotite, (iv) very coarse-granoblastic (> 5 millimetres) hypersthene-diopside-plagioclase rock, with or without hornblende and (v) common amphibolite (i.e. foliated hornblende-plagioclase rock with minor quartz and/or biotite). It is not possible to attribute these mafic metamorphites to a particular stratigraphic horizon in the lower metapelite unit and they appear to be randomly distributed along the entire outcrop area.

Ultramafic metamorphite

At locality 5, (Figure 3.1) east of Skelmfontein se Poort, a lense (boudin?) of ultramafic rock is interbanded with grey gneiss of the Gladkop Suite. Lying within orthogneiss, the stratigraphic status is not directly discernible, but its projected structural position is just above the mafic unit. At maximum, the lense is 10 metres wide, but thins out over a short distance. It has a strike continuation of at least 200 metres. At the widest part the rock consists solely of oriented pyroxene and amphibole, defining a penetrative foliation. Further westwards the body consists of less mafic two-pyroxene granulite, similar to the mafic granulites within the 'lower' metapelites described above.

About 5 metres structurally above the ultramafic/mafic band a thin calc-silicate band, consisting mainly of plagioclase with some diopside and quartz, can be followed for about 200 metres.

3.3 SOME OUTCROPS WITHIN THE RATELPOORT SYNFORM

3.3.1 Noubestaan

At Noubestaan, in the eastern part of the Ratelpoort Synform (locality 6, Figure 3.1) a map scale xenolith of metasediments lies in contact with granites and metagranites of the Gladkop, Little Namaqualand and Spektakel Suites. The structural sequence consists of the following units:

Banded iron formation:	banded fine-granoblastic quartz-garnet and quartz-limonite rock.
Metapsammite:	bands of metaquartzite (5 to 20 centimetres thick), consisting of at least 80 per cent quartz plus lesser quantities of plagioclase, garnet, biotite and opaque grains and with a fine-granoblatic to medium-granoblastic texture, alternating with sillimanite-bearing schist.
Metapelite:	foliated rock consisting chiefly of garnet, sillimanite, cordierite, quartz and feldspar.

The rocks are largely altered. Feldspar and sillimanite are replaced by white mica. Biotite is also replaced by white mica with

the resulting excess Fe (and Mg?) contained in an opaque phase concentrated along the relict cleavage planes. Cordierite is completely pinitized and garnet is replaced by a compact aggregate of chlorite.

The schist that is found in contact with the Steinkopf Gneiss (as described in Chapter 4.4.3) consists virtually only of the two phases sillimanite and garnet. Small subgrains of garnet testify to the advanced state of strain in the schist. The sillimanite is similarly fragmented into small subhedral subgrains. These phases do not, however, show signs of compositional alteration and the deformation which caused the strained state appears to be unrelated to the retrogressive metamorphism that caused the alteration of the rocks described above. The penetrative foliation in the garnet-sillimanite schist is parallel to the regional foliation and is correlated with the Skelmfontein fabric (see Chapter 9.4.2).

3.3.2 Klipvloer

At locality 7 (Figure 3.1), a structural sequence comparable to the generalized Bushmanland sequence, is found: pink gneiss, overlain by aluminous metapelite, followed by white metaquartzite. The pink gneiss in this case is Noenoemaasberg Gneiss (see Chapter 4.4.1). In general, the aluminous gneiss/schist in this region differs from similar units in the Ratelpoort area therein that the common migmatitic neosomes are largely absent.

In the metapelite, sillimanite is ubiquitous in the form of thick (up to 2 millimetres) needles, commonly randomly oriented. At locality 8 (Figure 3.1), sillimanite is concentrated in radial clusters which postdate the regional foliation (Figure 3.2). They are, however, flattened in zones of Skelmfontein shearing (see Chapter 9).

4 THE GLADKOP SUITE

4.1 INTRODUCTION

A thorough understanding of the grey and pink gneiss of the Gladkop Suite is desirable in the light of the following:

(i) "Grey gneiss complexes" of the Precambrian have received much attention as they yield clues for an understanding of the oldest crust (e.g. Bogdanova, 1979).

(ii) Lithologically the grey gneiss of the Steinkopf area resemble "basement gneiss" of mobile belts such as the Limpopo Belt (Van Biljon and Legg, 1983) and the Grenville orogenetic belts (e.g. Wynne-Edwards, 1969). However no basement for the metasedimentary rocks of Namaqualand has yet been unequivocally identified. The Achab Gneiss in Bushmanland, lithologically similar to the Gladkop Gneisses, is considered to be the basement for the Aggeneys type metasediments by some research workers (e.g. Moore, 1977, Watkeys, 1986).

(iii) The origin of the pink gneiss of Namaqualand and Bushmanland has long been in dispute. In Bushmanland the pink gneiss may be:
   (a) part of the supracrustal sequence,
   (b) part of the basement for the supracrustal rocks, or,
   (c) intrusive into both the supracrustal sequence and the basement.

(iv) In terms of outcrop area in the Namaqualand Geotraverse, the Gladkop Suite constitutes a major lithological unit forming a tectonic unit on its own.

In the following paragraphs the lithological varieties and the field relations are described. Emphasis is placed on those features that have a bearing on the evolution of the rocks. Finally, chemical comparisons are made and an interpretation is advanced for the origin of the rocks.

4.2 DISTRIBUTION

The distribution of the Gladkop Suite in the Geotraverse is shown in Figure 4.1. The Gladkop Suite constitutes virtually the entire lithology of the Steinkopf Domain. The three members of the Gladkop Suite, namely the Steinkopf, Brandewynsbank and Noenoemaasberg Gneiss, are areally intimately associated, even on outcrop scale.

4.3 FIELD CRITERIA REGARDING THE ORIGIN OF GRANITOID GNEISSES

When dealing with a gneiss complex such as the Gladkop Suite, certain criteria can be used in the field to facilitate the recognition, classification and interpretation of individual entities. These logical field criteria can be helpful in establishing the origin of the gneiss.

The first objective of the investigation is to distinguish between primary and secondary features and then to concentrate on those

primary aspects which have a bearing on the origin of the rocks. Secondary features in the Steinkopf Domain include the following:

(i) Complete metamorphic recrystallization and textural reconstitution. In this regard the constraints imposed by essentially isochemical metamorphism on outcrop scale is a prerequisite for the establishment of the nature of the pre-metamorphic parent rock. As far as granitoid gneiss is concerned, it is generally possible in the field to distinguish between subdomains of significant chemical alteration and those of lesser reconstitution, on grounds of textural and compositional appearance. Compositional variation, whether primary or secondary, is normally accompanied by textural variation.

(ii) Metamorphic or anatectic differentiation. The Gladkop gneisses exhibit various chorismatic structures and at some places the paleosome is not recognisable on outcrop scale. For most part, however, the neosomes form a subordinate proportion of the gneiss and it is possible to study the rock from the viewpoint of metamorphism and deformation of a pre-existing rock.

(iii) Deformation. Apart from the general structural complexities that arise from the deformation processes, it is important to be aware of the secondary characteristics of the gneiss attributed to penetrative deformation on regional scale. In these terms, the development of banded gneiss through the deformation of igneous rocks, as, for example, described by Myers (1978), must be taken into account by all investigators of mobile belts.

Basically, granitoid gneiss may form as a result of the metamorphism of arkose, wacke, felsic to intermediate volcanites or granitoids. Each different mode of origin could impart distinguishable and even unique properties to the final gneissic product. Some of the important properties are summarized in Table 4.1

TABLE 4.1

SOME THEORETICAL PROPERTIES OF GRANITOID GNEISSES OF DIFFERENT PRIMARY ORIGINS

	Precursor		
Characteristic	Granitoid	Volcanic	Sedimentary
Well-developed primary banding		X	XX
Poorly developed primary banding		XX	XX
No primary banding	XX	X	
Compositionally heterogeneous		X	XX
Compositionally homogeneous	XX	XX	
Texturally homogeneous	XX	X	
Very small primary grain size		XX	

Combinations of certain characteristics of a gneiss unit could be used to indicate the origin. More unequivocal evidence for the

origin of a gneiss is, however, found at its contact with other rock units. Some important features of the contact relationships between metamorphites of different origin can be considered in terms of a theoretical example.

In the case of a contact between a granite gneiss and a metapelite of which the stratigraphic facing direction is not known, the following possible pre-metamorphic conditions could be visualized for the association (the contact is taken to be "primary" i.e. there is no evidence that the contact represents a fault plane):

(i) an arkosic sediment overlying a pelite
(ii) a pelite overlying an arkosic sediment
(iii) a felsic volcanite overlying a pelite
(iv) a pelite overlying a felsic volcanite
(v) a pelite overlying a granitic floor
(vi) an intrusion of granite into a pelite

Some of the characteristics of such contacts are summarized in Table 4.2, from which it is clear that contamination and assimilation effects could distinguish meta-intrusions from the rest. Insight into these phenomena was obtained by observation of the contacts of the late-tectonic Spektakel Suite (Marais and Joubert, 1980b) in the study area. The Eyams Granite (Chapter 7.4) is generally compositionally altered at the contacts, at some places to such an extent that its composition approaches that of the country rock. In the Rietberg Granite the effects are less dramatic, but an increase in garnet content at the contacts with metapelites is well known. Such occurrences of garnet near the contacts with aluminous rocks are also generally found in the granitoids of the Little Namaqualand Suite in the Copper District. Assimilation of pelitic or intermediate to mafic xenoliths is generally incomplete, resulting in mafic restites concentrated at the contacts between the granite and the xenolith. Where assimilation is more complete, all that remains of the xenoliths are melanocratic schlieren (Mehnert, 1968).

The interaction between igneous and country rock affects a particular distribution of chemical components in the rocks near to the contact. After solidification of the magma, deformation can only change the shape and spatial positions of such phenomena, but the relative positions of the chemical components with respect to the contact remain fixed and are reflected by the distribution of metamorphic phases.

In the case of the Gladkop Suite, the gneiss has been penetratively sheared on millimetre scale. All original and most secondary planar structures have been drawn into parallelism. Original intrusive relations such as cross-cutting contacts, are all but obliterated and xenoliths have the appearance of concordant bands.

TABLE 4.2

PREDICTED CHARACTERISTICS OF A CONTACT BETWEEN A GRANITOID GNEISS AND A METAPELITE FOR DIFFERENT MODES OF ORIGIN

Characteristic	Origin (see text) i	ii	iii	iv	v	vi
The contact is gradational on grain scale	A	A	-	-	-	-
The contact is interbanded gradational	A	A	A	A	-	E
The contact is sharp	A	A	A	A	A	A
Inclusions of metapelite are present in the gneiss	B?	-	D?	-	-	A
Inclusions of gneiss are present in the metapelite	-	C	-	C?	-	F?
The gneiss is contaminated by the metapelite	-	-	-	-	-	A
The metapelite is partially assimilated by the gneiss; restite rims	-	-	-	-	-	A

Explanation:
- A Common geological process
- B Mud-pebble conglomerate
- C Boulder of floor in sediment
- D Agglomerate
- E Lit-par-lit intrusion
- F An apophysis seen in two dimensions

4.4 FIELD ASPECTS OF THE GLADKOP SUITE

In this section the field aspects of the Gladkop gneiss are described in terms of the principles set out above and in terms of the individual peculiarities of the different types.

4.4.1 NOENOEMAASBERG GNEISS

General

The Noenoemaasberg Gneiss is typically a fine-grained leucogranitic gneiss that weathers reddish brown. Fresh surfaces are light grey to white, and the pink appearance is only a characteristic of weathered surfaces. This rock type is compositionally homogeneous and no primary banding is visible. Typical Noenoemaasberg Gneiss forms the hill named Rooiberg northwest of Leeupoort and also T'Gybiekop in the central part of the Steinkopf domain.

The rock is commonly fine-grained (more or less 1 millimetre) with a penetrative anastomosing foliation (Powell, 1979). There is, however, a range of textural types reflecting primary as well as secondary crystallization phenomena. Basically three different textural types can be distinguished, the T'Gybiekop-type, the Rooiberg-type and the N2 type.

The prevalent leucogneiss: T'Gybiekop-type

The typical leucogneiss of the Steinkopf domain is fine-grained

(more or less 1 millimetre) and contains less than four volume percent biotite. It is texturally and compositionally homogeneous on meso and macro-scale. The homogeneity of the leucogneiss is reflected by the domal style of weathering so typical of the gneissic granites of Namaqualand. The distribution of mineral grains define small elongate leucocratic domains which impart a penetrative fine gneissic texture. The term domain, as used here, pertains to a particular gneissic texture in which the foliation is usually "anastomosing" (the descriptive terminology of foliated rock textures is treated by Powell (1979)). On a regional scale the term domain is also used to separate areas of different tectonic character. The shape of the individual leuco-domains vary according to the amount of total strain and in areas of relatively low strain they measure about 12 X 6 X 3 millimetres. Each little domain consists of an aggregate of equidimensional quartz and feldspar grains. The domainal texture is best seen on a weathered surface that is perpendicular to the regional stretching lineation. Where the biotite content is low the rock exhibits a granular texture on unweathered surfaces and apparently has no planar fabric. On weathered surfaces, however, a well-developed planar fabric, often band-like, is invariably discernible.

Texturally the T'Gybiekop-type leucogneiss is similar to the prevalent Brandewynsbank Gneiss, with a subtle difference in total biotite content. This creates mapping problems, but, wherever exposed, the contact between the two units is invariable found to be sharp.

The intrusive relations between the T'Gybiekop-type leucogneiss and the Brandewynsbank Gneiss is best illustrated at the eastern slope of Gladkop Hill. From a distance a raft (more or less 100 X 50 metres) of the grey gneiss is seen to be enclosed by leucogneiss (Figure 4.2). Smaller inclusions of Brandewynsbank or Steinkopf Gneiss is fairly common in the leucogneiss, usually in the form of thin bands.

The marginal zone of the T'Gybiekop-type leucogneiss, where in contact with older rock, is in many instances more leucocratic by virtue of a decrease in the amount of biotite, and has a sugary texture. At some places such phenomena are due to later remobilization (see below), but generally these marginal aspects are considered to be primary. At two localities, one east of Sabies and the other close to Steinkopf, such a primary marginal phase appears to traverse a pre-existing foliation in the Brandewynsbank Gneiss, but on those particular outcrops the recognition of structural features in the leucogneiss is difficult because the weathering of the rock has not emphasized the structure as usual. Apart from these possible examples, the T'Gybiekop-type gneiss is nowhere found to cut across older structures and exhibits the same structural imprints as the grey gneiss.

The homogeneous domainal texture reflects an important primary textural feature. In areas of least strain, relict feldspar phenocrysts are still recognised. At Awahaigaskop all transitions from a "small augen gneiss", with discrete K-feldspar phenocrysts in a more or less deformed state, through the prevalent T'Gybiekop-type, to a banded Rooiberg-type are found. Northeast of Noenoemaasberg the textural development of the leucogneiss is also admirably illustrated. On weathered surfaces an augen texture is displayed, with individual augen up to 200 millimetres across, enveloped in relatively little matrix. The overall impression is of a coarse-grained rock. However, when examined from nearby the augen

proves to be composite and the rock is clearly fine-grained (more or less 1 millimetre), reflecting recrystallization of both augen and matrix to an equidimensional granoblastic texture. The relative distribution of most components are not disturbed, with the result that a coarse palimpsest texture is still discernible under favourable circumstances (Figure 4.3 and Figure 4.4). A few metres from this locality, again on a weathered surface, the augen are seen to be progressively flattened and banding is developed (see below). The present texture of both the bands and the ghost augen is once again fine-grained and granoblastic, identical to the previously described example.

It is concluded that, in general, the gneissic texture of the T'Gybiekop-type leucogneiss is the result of deformation and recrystallization of a pre-existing medium-grained to coarse-grained leucogranite.

The banded leucogneiss: Rooiberg-type

The prevalent T'Gybiekop-type and the banded Rooiberg-type leucogneiss together constitute more than 95 percent of the Noenoemaasberg Gneiss. It was, however, impossible to separate the two types on mapping scale as illustrated below.

The banding is most conspicuous on weathered surfaces (Figure 4.5) because of differential weathering. Important characteristics of the banding are:

(i) The distribution of plagioclase defines the banding. The composition of the white-coloured bands is plagioclase and quartz in more or less equal parts, while the intervening bands consist of K-feldspar, quartz and minor amounts of plagioclase and biotite.

(ii) The transition from homogeneous T'Gybiekop-type gneiss to the well-banded Rooiberg-type is gradational over distances of up to 5 metres. Contacts which appear sharp at first sight usually prove to be gradational over a few centimetres. The banding is everywhere concordant to the regional planar shear fabric in the surrounding gneiss. This planar fabric is in most cases the oldest penetrative fabric, which explains why it is sometimes intensely folded. The change from non-banded rock to banded rock involves an intensification of the shear fabric of the gneiss, including an overall reduction in the size and shape of textural domains, and is especially noticeable where pre-kinematic feldspar megacrysts are progessively flattened until unrecognisable in the banded zones. Some thin non-continuous plagioclase bands are recognisable as deformed plagioclase grains.

(iii) The width of bands generally vary from 1 to 5 millimetres, but it can be as much as 10 millimetres. Alternating bands are more or less of the same width, which is relatively constant in any given zone.

(iv) The stratigraphical succession is significantly simple; if the different types of bands were numbered, the succession would everywhere be 1,2,1,2,1,2...

(v) The banding is very regular, but it is generally not possible to follow a single band for more than a metre.

(vi) The banding occurs in zones varying in thickness from a few centimetres to tens of metres. The most regular banding is restricted to relatively narrow zones.

(vii) The banding is especially well-developed in the immediate vicinity of schlieric xenolithic streaks of grey gneiss.

(viii) The alternative bands are texturally similar, i.e. they consist of equidimensional fine-grained (+- 1 millimetre) granoblastic feldspar and quartz. The internal texture is non-domainal.

(ix) The absence of boudin structures throughout, suggests that the viscosities of the two types of bands were the same during deformation subsequent to their development.

The above-mentioned features (i), (iii), (viii) and (ix) are in combination atypical of primary sedimentary or volcanic banding, while (ii), (vi) and (vii) are consistent with the conclusion that the banding was formed by a type of metamorphic differentiation during deformation.

Features (viii) and (ix) may be related to the principle of "equilibrium banding". According to this principle, strain induced secondary banding continues to develop in the form of alternating micaceous and non-micaceous bands, until the viscosities of the two types approach equality (Robin, 1979). Although the components involved here do not include a significant amount of mica, the fact that the alternative bands ended at similar viscosities during the development of the secondary banding suggests that viscosities may have controlled the process.

While a kinematic, metamorphic origin is evidently responsible for the banding, the regularly spaced or "homogeneous" banding remains to be explained (see (iii) above). In this regard one may recall one of the conclusions of Cobbold (1977) concerning the development of banding as a result of deformation; he suggested that "... the presence of heterogeneities is essential for the appearance of bands ...". Considering the initiation of the banding on millimetre to centimetre scale (as at Awahaigaskop), and the size and distribution of pre-kinematic feldspars and quartz, the scale of the banding is of the same order as the scale of the primary heterogeneities in the leucogneiss. The regular distribution of these primary heterogeneities should be reflected in the subsequent secondary banding.

The character of the contacts between the finely banded leucogneiss and the older country rock should reflect the primary intrusive origin of the leucogneiss. Thin band-like xenoliths of Steinkopf Gneiss within the Rooiberg-type leucogneiss are shown in Figure 4.6. An apophysis of the leuco-gneiss into the grey gneiss is also still recognisable despite high strain and metamorphism.

N2 Leucogneiss: Remobilised Noenoemaasberg Gneiss

The oldest set of neosomes that are superimposed on the oldest tectonic fabric in the Steinkopf Domain, is labelled N2. Anatexis and migmatization is discussed in Chapter 14. In this section a brief description is given of the N2 development in the Noenoemaasberg Gneiss because it complicates the textural character of the unit. In extreme cases the "new rock" (neosome) forms

leucosome veins having sharp contacts with the "old rock" (paleosome). For most part, however, the transition from paleosome to neosome is both gradational and incomplete and the progressive development can be studied in many places.

Where fully developed, the N2 leucogneiss is compositionally similar to the parent rock. The texture is medium-grained (+- 2 millimetre) and the dimensional orientation of constituent minerals imparts a continuous planar fabric (see Chapter 1.4 for reference to the textural terminology) to the rock; the texture is distinctly non-domainal. The development of N2 neosomes at the contact between leucogneiss and grey gneiss obscures the primary contact relations in many instances. Furthermore, it is difficult at some places to distinguish between the primary granular contact phase and the N2 phase, especially on fresh surfaces where the strain fabric is not distinct.

In the south of the Steinkopf domain the N2 leucogneiss is distinguished from satellite bands of relatively fine-grained Rietberg Granite by the dark colour of the quartz grains against a background of nearly white feldspars in the latter granite. It is also readily distinguishable from bands of Kweekfontein Granite (Marais and Joubert, 1980b), which usually has an inequidimensional texture and little or no kinematic fabric.

The age relation between the N2 type leucogneiss and the above-mentioned members of the Spektakel Suite is demonstrated in the area of the eastern nose of the Ratelpoort synform. There, near Waterval (Martens, 1979), xenoliths of leucogneiss, including the N2 variety, are found in a granite that represents an intermediate phase between the Kweekfontein and the Rietberg Granite. The relationships between the latter two granites are discussed by Martens (1979).

A coarser-grained leucogneiss

In addition to the types already described, more variations of the Noenoemaasberg Gneiss may exist. In the area to the east of the town of Steinkopf, xenoliths of fine-grained leucogneiss, with or without the fine banding, are found in a medium-grained leucogneiss. The latter leucogneiss is reminiscent of the T'Gybiekop-type except for (i) a slightly coarser grain size, and (ii) clearcut contacts and intrusive relations with the finer-grained types. No evidence has been found to indicate that the coarser-grained gneiss transects an older tectonic fabric in the finer-grained gneiss. It is not clear whether the coarser variety should be regarded as a late Gladkop-type phase or an early Klein Namaqualand-type gneiss.

4.4.2 BRANDEWYNSBANK GNEISS

General

The granitic Brandewynsbank Gneiss is generally distinguished from the Noenoemaasberg Gneiss by the grey colour, on both fresh and weathered surfaces. The grey tinge is due to a small grain size, the presence of biotite and the colour of the feldspars, which is not pink as in the case of some leucogneisses of Namaqualand and Bushmanland. The type locality is at the Brandewynsbank farm homestead about 15 km south of the town of Steinkopf, next to the national road. Excellent exposures of the rock type are very common in the Steinkopf domain and unweathered material is readily

available, as at the quarry a few hundred metres south-east of the roadside petrol-station at Steinkopf.

Composition and homogeneity

The chemistry of the Brandewynsbank Gneiss is discussed below (see 4.5). Mineralogically the prevalent Brandewynsbank Gneiss consists of approximately equal amounts of quartz, K-feldspar and oligoclase plus about five percent of biotite. A more mafic variety with as much as 12 percent biotite and with the textural appearance of Brandewynsbank Gneiss, forms a small proportion of the mapped unit. Generally, however, the mafic type is more highly strained and was grouped with the Steinkopf Gneiss. The contacts between the different compositional types are sharp.

The prevalent Brandewynsbank Gneiss is compositionally homogeneous on all scales and, as in the case of the Noenoemaasberg Gneiss, smooth domal outcrops result. The small variation in chemical composition illustrates the homogeneous nature of these rocks (see Chapter 4.5). At some places hornblende blastesis or diatexis have caused a change in mineral composition, as described in Chapter 11.

Contact Relations

Minor bands of calc-silicate rock and other less prevalent lithological types are widely distributed in the Brandewynsbank Gneiss. Although very noticeable in an otherwise homogeneous gneiss, these minor bands do not constitute a significant proportion of the gneiss. Because the junctions are parallel to the regional tectonic fabric it is generally difficult to ascertain the primary contact relations. In some places, however, the included rocks occur in the form of discrete bodies that are best explained as deformed xenoliths (e.g. Figure 4.7). The oldest recognisable tectonic fabric traverses the contacts between the bodies under discussion and the gneiss. The gneissic fabric generally does not warp around the bodies and when this is coupled with the fact that there are no extensions along the foliation strike, the possibility that these structures represent boudinaged remains of once continuous primary bands is precluded.

The contact relations between Brandewynsbank Gneiss and Noenoemaasberg Gneiss is described in Chapter 4.4.1. Xenoliths of the more mafic variety of Brandewynsbank Gneiss, as described above, are found in the domal outcrops of prevalent Brandewynsbank Gneiss east of Steinkopf. In areas of higher strain, analogous situations exist, but in such cases the xenoliths are elongated bands of Steinkopf Gneiss.

Contamination of the Brandewynsbank Gneiss near the contacts with xenoliths of country rock, is a fairly common phenomenon in the Steinkopf domain. In the Konkyp area, for example, the composition of the Brandewynsbank Gneiss changes, close to the contact with calc-silicate xenoliths, from that of the normal granitic type towards that of a calc-silicate rock. The contaminated rock contains hornblende in place of biotite and is enriched in plagioclase relative to K-feldspar. The transition is completely gradational over one metre, although the contact of the contaminated gneiss with the xenolith is abrupt. Contamination effects such as these are considered further evidence for the primary intrusive nature of the Brandewynsbank Gneiss.

Texture

As with the Noenoemaasberg Gneiss, the textural variation in the Brandewynsbank Gneiss reflects aspects of its evolution. The Brandewynsbank Gneiss is commonly fine-grained, with individual grains rarely exceeding 1 millimetre in diameter. Biotite distribution follows an anastomosing pattern resulting in a distinct domainal texture as in the case of the T'Gybiekop-type leucogneiss. However, at some places it contains small discrete K-feldspar megacrysts. In the Sabies area the frequency and size of the megacrysts are greater and the rock grades into an augen-gneiss, in which K-feldspar augen up to 10 millimetres in diameter are set in a fine-grained biotite-rich matrix.

The phenomenon of feldspar augen in granitoid gneisses in Namaqualand and Bushmanland is very common and the term "porphyroblast" is often used to describe them without due consideration of the strict meaning of this term. The conclusions reached with regard to the feldspar augen in the Brandewynsbank Gneiss could have implications for the entire region.

Some notable features that may have a bearing on the origin of the megacrysts may be listed:

(i) The megacrystic gneiss is generally more mafic than the average Brandewynsbank Gneiss, in the sense that the matrix contains more biotite.

(ii) The oldest recognizable tectonic foliation of the gneiss warps around the megacrysts. Microscopic studies of a large number of specimens revealed no crystals with helicitic inclusions of any older fabric.

(iii) Where seen in cross sections normal to the mineral lineation, the megacrysts have rounded forms (Figure 4.8). Sections containing the lineation exhibit elongated forms; in many places the elongation reflects the addition of quartz and feldspar in the pressure shadows of the rounded feldspars.

(iv) The size variation of the megacrysts is from very small, barely exceeding the matrix grain size, to as much as 10 millimetres and a continuous variation of sizes can be found in small bodies of rock.

(v) Flecky hornblende-rich neosomes, formed at the expense of biotite and with the production of new K-feldspar, is superimposed on the megacrystic texture. This is also the case for all generations of stromatitic neosomes, which are generally enriched in K-feldspar.

K-feldspar porphyroblastesis is a general result of the "granitisation" of rocks near the contacts with intruding granites (e.g. Mehnert, 1968). In principle such porphyroblastesis would require

(i) a chemical potential gradient,
(ii) a diffusion transport medium (fluid), and
(iii) permeability with regard to metasomatic fluids.

In most occurrences where these conditions could have been met in the Namaqualand geotraverse, such as xenoliths and xenolithic rafts

enveloped by the potassium-rich granitoids of the Vioolsfdrif, Gladkop, Little-Namaqualand and Spektakel suites, K-feldspar porphyroblastesis on any significant scale is not found.

In the case of the granitoid gneiss of the Gladkop Suite metasomatic porphyroblastesis is unlikely because:

(i) a chemical gradient could hardly have existed; the composition of the non-megacrystic gneiss is already granitic and, furthermore, no extensive outcrops of potassium-rich Little Namaqualand or Spektakel granites exist in the Steinkopf domain;

(ii) the rocks are metagranites in terms of their suggested intrusive origin, implying that they are relatively "dry" rocks as far as the common crustal fluids are concerned;

(iii) the gneisses are poorly endowed with micas, generally less than 10 percent by volume, so that permeability would have been low.

From the structural features listed above, it is evident that the megacrysts can be classified as pre-kinematic. Apart from the obvious strain effects one should note that in general the phenomenon of a tectonic fabric that warps around a megacryst implies deformation subsequent to the formation of the megacryst, and not the pushing apart of the fabric by the dynamic growth of the mineral (Ferguson et al., 1980). Furthermore, the rounding of a relatively strongly anisotropic mineral such as feldspar, is readily explained in terms of abrasion during flow, either magmatic or tectonic (e.g. Higgens, 1971). In this regard, the fact that more biotite-rich varieties of the Brandewynsbank Gneiss contain a greater proportion of megacrysts, could be significant. In general, if a given amount of shear strain has to be absorbed by a given volume of rock consisting of a mixture of feldspar crystals and mica, the mica would serve as lubricant. A higher proportion of the total strain will be taken up by movement along schistosity planes than through the deformation of individual feldspar crystals. In the absence of mica more strain will have to be absorbed by the deformation of the feldspar crystals. It is suggested that the feldspar megacrysts in the Brandewynsbank Gneiss were protected from mechanical destruction during deformation owing to a preponderance of biotite.

Where the geochemical mobility of the constituent elements of K-feldspar in the Brandewynsbank, Steinkopf and Noenoemaasberg gneiss was high during metamorphism, the development of neosomes took place rather than K-feldspar porphyroblastesis (Chapter 11). The Brandewynsbank Gneiss is therefore a metagranite that, at least in part, contained K-feldspar megacrysts prior to deformation. Such megacrysts are most readily explained as representing relict primary phenocrysts.

In general, the realization that a domainal texture in a granitic gneiss is probably of primary origin, assisted greatly in the subsequent classification of the gneiss in the geotraverse.

4.4.3 STEINKOPF GNEISS

General

When dealing with "grey gneiss" it is important not to generalize;

each gneiss unit should be considered in terms of its primary distinguishing features. This is especially true in the case of the grey gneiss of the Steinkopf Domain where secondary structural or metamorphic effects are so dominant that they were erroneously used to distinguish between different types of gneiss during the mapping phase of the investigation. The Steinkopf Gneiss (e.g. Figure 4.11) is distinguished from the Brandewynsbank Gneiss mainly on textural and structural grounds while the existence of transitional types indicate a common origin.

In terms of paleosome lithology, the Steinkopf Gneiss is, for most part, a fine-grained grey biotite gneiss with a granitic to granodioritic composition. The biotite content is of the order of 10 volume percent. Hornblende partially or completely replaces biotite in certain areas; this is for most part interpreted as a metamorphic effect. The foliation varies from penetrative and continuous on millimetre scale to fine-domainal, similar to the Brandewynsbank Gneiss but with smaller individual domains.

Leucocratic grey gneiss (4 to 6 percent biotite) that displays fine-spaced banding was also included in the Steinkopf Gneiss during mapping. It is compositionally the same as the common Brandewynsbank Gneiss and grades into that rock type in areas of lower strain. Mesocratic gneiss with a dioritic composition forms an important minor component of the Steinkopf Gneiss and was mapped out separately. It consists of plagioclase and hornblende with lesser quantities of quartz, K-feldspar and biotite.

The type locality of the Steinkopf Gneiss is a strip from Korrogas (a layby 10 km south of Steinkopf along the national road) towards Perdewater in the west, a distance of 4 km. At Perdewater the mesocratic gneiss occurs as a band with a maximum true thickness of 20 metres near the base of the easterly-dipping grey gneiss unit.

Homogeneity

Mesoscopically the Steinkopf Gneiss is compositionally heterogeneous owing to the presence of leucocratic bands. Macroscopically, however, the consistent nature of the heterogeneity becomes monotonous and, when viewed from a distance, the gneiss has an unvarying grey appearance. Since the banding observed on the mesoscopic scale is of secondary origin (see below) it is necessary to distinguish between "palaeosome" and new rock formed by combinations of metamorphism, migmatization and deformation, in order to evaluate the nature of the precursor.

Ignoring the secondary effects, it is found that the description given above for the palaeosome lithology is applicable to the Steinkopf Gneiss over the entire Geotraverse. The replacement of biotite by hornblende is restricted to small zones of pronounced flecky hornblende blastesis (see Chapter 11), so that, in general, the Steinkopf Gneiss has a simple biotite-granite to granodiorite mineralogy, which does not vary significantly.

The compositional homogeneity is reflected in the chemistry (Chapter 4.5), with relatively small variation in the vicinity of the granite-granodiorite boundary on chemical classification diagrams.

Minor bands of calc-silicate rock, metapelite and amphibolite are widely distributed in the Steinkopf Gneiss, as in the

Brandewynsbank Gneiss, representing features that have an important bearing on the origin of the gneiss. It should be noted, however, that they constitute less than one percent of the gneiss.

Contact relations

The contacts between individual rock types within the Steinkopf Gneiss and between the Steinkopf Gneiss and other metamorphic units, are sharp. The junctions are everywhere parallel to the regional penetrative planar fabric.

Within the eastern nose area of the Ratelpoort Synform, a kilometre-sized northwest-trending outcrop of metasediments of the Khurisberg Subgroup (Joubert et al., 1980), is enveloped by grey gneiss of the Gladkop Suite (Figure 4.9). The gneiss immediately to the southwest of the metasediments fits the description of the average Steinkopf Gneiss given above; the presence of ptygmatically folded leucosome veins are typical, although not exclusive to the Steinkopf Gneiss. Near the contact with the garnetiferous metapelite, small garnets in the gneiss are conspicuous, and at the contact the gneiss is particularly rich in garnet. Also present at the contact is one discrete xenolith and many small schlieric remnants of metasediments in the gneiss .

Similar garnet enrichment of Steinkopf Gneiss is found at the contact with a minor band of metapelitic granulite east of Dabbiknik (locality 6, Figure 2.1). The grey gneiss close to the contact of the nearby metapelites of the Besondermeid Formation contains sillimanite aggregates. At Korrogas a thin band of metasediment (aluminous schist and metaquartzite) can be followed for a considerable distance along strike in the Steinkopf Gneiss. Small xenolithic lenses and schlieren of the metasediment within the grey gneiss, in contact zones, demonstrate the primary relations between the rock types.

A few minor mafic bands are also present at Korrogas. The one extremity of a small mafic lense is frayed in a manner that is strongly suggestive of partial assimilation by the grey gneiss (Figure 4.10).

Secondary Banding

The most conspicuous general characteristic of the Steinkopf Gneiss is the well-developed secondary banding (Figure 4.11). The banding is generally migmatitic in character, but the Rooiberg-type, pure deformational types and combinations are also found.

Banding, characterized by the concentration of plagioclase, as in the case of the Rooiberg variety of Noenoemaasberg Gneiss, is developed on a restricted scale in the grey gneiss. The characteristics listed under Chapter 4.4.1 are applicable, except for the amount of biotite involved. The biotite is concentrated in the plagioclase-poor bands while the plagioclase-rich zones contain only a minor amount of the mica. Biotite is not concentrated at the contacts with the alternating bands, but are evenly distributed, emphasizing the difference between the Rooiberg-type banding and migmatitic banding. The modal compositions of the different bands for a typical case is given in Table 4.3.

TABLE 4.3

MODAL COMPOSITION OF PLAGIOCLASE-RICH AND PLAGIOCLASE POOR BANDS IN AN EXAMPLE OF STEINKOPF GNEISS (FROM THE KORROGAS AREA) WITH ROOIBERG-TYPE BANDING.

Mineral	Plagioclase-rich band	Plagioclase-poor band
K-feldspar	-	50 %
Plagioclase	60 %	21 %
Quartz	36 %	19 %
Biotite	4 %	8 %
Opaque minerals	0.3 %	2 %

The most common type of banding in the Steinkopf Gneiss exhibits thin leucosome bands (leucogranitic in composition) alternating with melanosomes and palaeosomes - i.e. the rock can be described as a stromatitic migmatite (Mehnert, 1968). Two main stages of concordant neosome development are distinguished, namely N1s and N2s (see Chapter 11). N1s is characteristically fine-grained with a similar grain size as the palaeosome and is concordant with the oldest recognizable planar strain fabric. N2s is medium-grained and concordant to the regional foliation, but discordant with respect to the oldest fabric in some places.

The migmatitic banding is distinguished from the Rooiberg-type banding because

(i) the leucosomes, with minor biotite, are rich in K-feldspar,
(ii) a melanosome (restite rim) is present, and
(iii) plagioclase and biotite are associated in the melanosome and palaeosome.

The frequency of occurrence of the concordant leucosomes varies in the exposed rock from 0 to 90 percent, but is commonly less than 15 percent. The modal composition of a leucosome from a typical N2s is given in Table 4.4 for comparison with the Rooiberg type bands (Table 4.3).

TABLE 4.4

MODAL COMPOSITION OF A STROMATIC NEOSOME (N1s) IN STEINKOPF GNEISS AT KORROGAS

Mineral	%
K-feldspar	41
Quartz	36
Plagioclase	23
Biotite	<1

4.4.4 DEVELOPMENT OF BANDED GREY GNEISS IN THE STEINKOPF DOMAIN

Ductile shears of different ages and magnitudes are the most important structural elements in the Steinkopf domain and many of the general characteristics of the gneiss can be attributed to shearing. An indication of the high measure of strain involved is given by the presence of a small structure near Sabies which is interpreted as a sheath fold (Figure 4.12) (see, for example, Cobbold and Quinquis (1980) for a description of the nature and significance of sheath folds). It is present in a zone in which the development of the oldest recognisable strain fabric of the Brandewynsbank Gneiss is so well developed that the rock has been reduced to a fine-grained, finely banded grey gneiss with a few relict porphyroclasts. The flattening of the megacrysts into millimetre-wide bands also shows that high strain values are applicable. The deformation was extreme and produced a banding by flattening of primary heterogeneities.
Ductile shearing apparently took place in a number of stages during the early subhorizontal deformation but, in general, a distinction is made between an earlier regional phase and the later Skelmfontein phase of subhorizontal shearing. Both these main phases of shearing are zonally developed and areas of higher and lower strain can be identified. Generally, the result of the Skelmfontein shearing is an intensification of the earlier strain effects and discordant shearing is not commonly observed. Relatively late subvertical shears, such as the Ratelpoort and Dabbiknik shear zones, are also ductile. It is difficult at some places to distinguish between the effects of the early and late events, because all planar structures have been drawn into parallelism in the subvertical shear zones. In general, however the textural and structural characteristics of the gneiss were determined by the main subhorizontal shearing and relatively minor transformations evidently took place during the subvertical deformation.

The general effect of the early shearing on the grey gneiss was the reduction in grain size (down to a limit imposed by concomitant high-grade metamorphic recrystallization) and the destruction of the domainal texture, in the advanced stages. In this way a rock with the typical texture of Steinkopf Gneiss could have been produced by the deformation of Brandewynsbank Gneiss. The effect of shearing was, however, different in different rock types on account of viscosity differences controlled by compositional variations. This explains why gneiss with the typical Brandewynsbank texture, but of more basic composition than usual, is found only in subdomains of relatively low total strain, while rock of similar composition in subdomains of high strain have typical Steinkopf Gneiss texture. Transitional types are common and presented mapping problems at a time when the distinction between Brandewynsbank Gneiss and Steinkopf Gneiss was based only on textural grounds.

The banding caused by the physical flattening of rock entities is enhanced by metamorphic or metatectic differentiation. The role of deformation in the development of the Rooiberg-type banding is discussed above. The migmatitic banding is also directly related to deformation. The Nls-type neosomes are only found where the early strain fabric is well developed. This is illustrated at Korrogas where megacrystic Brandewysbank Gneiss grades into a finely banded rock. The geometry of the fabric and the neosomes indicate a mechanism of shearing with simultaneous (or subsequent) metatectic differentiation (Figures 4.13 and 4.14).

N2s neosomes are concordant with the regional foliation for most part. In subdomains not deformed by later deformation the lack of internal fabric indicates a passive mode of emplacement, consistent with metatectic differentiation along existing planes. The N1s neosomes probably caused the distribution of components that controlled the attitude of the N2s bands. The general effect of Skelmfontein-type deformation was a flattening parallel to the existing foliation; ptygmatic folding at some places shows that not all N2s veins were formed concordantly.

Neosomes that have developed along closely spaced minor shears within the large shear zones have imparted a new banding to the gneisses and it is not uncommon to find one or two phases of new banding developed in a single outcrop, superimposed on the regional foliation/banding.

One notable difference between the average Brandewynsbank Gneiss and the Steinkopf Gneiss is the relative abundance of neosome bands. It is common to find the two types of gneiss interbanded on outcrop scale in such a way that metamorphic and kinematic conditions during the formation of the neosomes would have been the same for both, yet the neosome bands are generally scarce in the Brandewynsbank-type and abundant in the Steinkopf-type. Because both are metagranitoids, the main source of water for the initial metatexis could only have been the biotite. Because the biotite content of average Steinkopf Gneiss is double that of the Brandewynsbank Gneiss, it is to be expected that neosomes should be more prevalent in the former. The primary viscosity difference between the two gneisses, likewise the result of the relative abundance of mica, evidently allowed more shearing to take place within the Steinkopf Gneiss, and could have enhanced the mobility of metamorphic fluids. Considering the additional factors of strain heating and strain softening (e.g. Brun and Cobbold, 1980), it seems possible that relatively small primary compositional differences could, under favourable conditions, lead to prominent textural-structural differences in high-grade dynamic metamorphites.

In the area to the north and east of Bulletrap, pretectonic metasediments, granitoid gneiss of the Gladkop Suite and satellite bands of Rietberg Granite, occur in a structurally composite zone. This zone was sequentially subjected to at least three penetrative deformation events, namely the early subhorizontal deformation, the Skelmfontein refoliation and the Ratelpoort shearing. The apophyses of Rietberg Granite were emplaced more or less synkinematically with the Skelmfontein shearing and prior to the Ratelpoort shearing. The final result is a zone of intimately interbanded rocks of diverse though mostly intrusive origins. Technically the zone could be described as a melange, but the general appearance is that of a simple "banded sequence".

4.4.5 THE RELATIONSHIP BETWEEN THE LAMMERHOEK GNEISS AND THE STEINKOPF GNEISS

From the preceding paragraphs it should be clear that the Steinkopf Gneiss is considered to be essentially a metagranitoid. It is also, however, a highly deformed and metamorphosed rock in which secondary banding is strongly developed.

Geologists of the O'okiep Copper Company distinguished a fine-grained grey gneiss (the Lammerhoek-type) in the Copper

District and further to the south. Although this gneiss has broadly the same appearance as the Steinkopf Gneiss, it can, allegedly, nowhere be shown to resemble an orthogneiss. Its intimate association with metasediments and consistent fine non-domainal banded structure, even where in contact with relatively coarse-grained Brandewynsbank Gneiss (D. Gadd-Claxton, pers. comm., 1980) indicate a supracrustal origin; in terms of its composition it would probably represent metamorphosed felsic to intermediate volcanites. The possibility that such a "supracrustal" grey gneiss may form part of the Steinkopf Gneiss unit cannot be discounted. The author is, however, not convinced that such a supracrustally derived grey gneiss forms any significant part of the grey gneiss outcrops in the Copper District. During the occasion of one excursion, led by F.G.J. Schreuder and accompanied by S.W. van der Merwe, to the southern part of the Copper District, extensive outcrops of grey gneiss (allegedly Lammerhoek gneiss) were inspected on the farms Eendoorn and Platjes Fontein. On the latter property, small ellipsoidal mafic xenoliths were discovered in the grey gneiss, here with an anastomosing foliation. In local zones of low strain, the xenoliths are 3 to 5 centimetres long and 1 to 3 centimetres wide. These xenoliths remind strongly of similar mafic bodies which are characteristic of a significant part of the Vioolsdrif Suite granitoids.

All of the outcrops visited during this study can, on grounds of compositional and textural similarity, be directly correlated with either the Brandewynsbank Gneiss or the Steinkopf Gneiss. As a stratigraphic unit then, the Steinkopf Gneiss represents a granitic to granodioritic orthogneiss that contains minor xenolithic bands of metasediments and possibly a lesser component of metavolcanites.

4.5 CHEMISTRY

4.5.1 GENERAL

It is the intention in this section to briefly state the chemical character of the Gladkop Suite and to report on the fair amount of chemical data available.

4.5.2 SAMPLING

The different lithological units of the Gladkop Suite were sampled on a routine basis. The samples were broken down by tungsten-jaw core splitter, to yield pieces with an average diameter of 2 centimetres which were washed, dried and dispatched to the Geological Survey in Pretoria for further treatment. A number of samples were prepared and analysed by W.A. van der Westhuizen of the Department of Geochemistry, UOFS. A third set of samples of Gladkop Gneiss was collected on four special excursions (twice attended by E. Barton) for the purpose of geochronological investigation. Isotope analyses were carried out on these samples by E. Barton at the BPI (University of the Witwatersrand), and major and trace element analyses were done on the same samples by D. Reid (Department of Geochemistry, UCT) (see Reid and Barton, 1983). It was consistently attempted to collect specimens of unweathered palaeosome material, especially in the case of those samples collected for geochronology. This probably caused a measure of sampling bias because, as pointed out above, the more biotite-rich grey gneiss are generally more affected by migmatisation leaving less "clean" palaeosome to sample. Furthermore, the mica-rich types weather more readily than the

others. Nevertheless, the analyses listed in Appendix 3.2 are considered to be fairly representative of the spectrum of chemical variation in the grey gneiss, as care was taken to specifically include a number of mesocratic specimens.

4.5.3 NOENOEMAASBERG GNEISS

Major element analyses of 13 samples of Noenoemaasberg Gneiss are given in Appendix 3.2. The averange SiO_2 weight percentage is 75.66; the range is from 71 percent to 78 percent and the total composition is directly comparable to that of "aplogranites". The compositional overlap with the Brandewynsbank Gneiss (see Figure 4.15) is consistent with the genetic association observed in the field.

4.5.4 GREY GNEISSES

The Brandewynsbank Gneiss and the Steinkopf Gneiss are treated together in the light of the intimate genetic relationship and compositional overlap. (Note that the field terms used in Appendix 3.2 describe the rocks in terms of texture. It can be shown, however, that "mafic Brandewynsbank" grades into Steinkopf Gneiss in areas of higher strain and that "leuco-Steinkopf" grades into average Brandewynsbank Gneiss in areas of lower strain). In general, the Brandewynsbank Gneiss contains between 70 and 75 weight percent SiO_2, and the Steinkopf Gneiss between 64 and 70 percent, while the mesocratic unit within the Steinkopf Gneiss contains less than 64 weight percent. The bulk of the grey gneiss scatters around the diagrammatic granite-granodiorite boundary and it tails off towards tonalite and diorite (Figure 4.15).

4.5.5 COMPARISON WITH THE VIOOLSDRIF SUITE

The Vioolsdrif Suite is of similar age as the Gladkop Suite in terms of field relations, because both intrude the Bushmanland Group and are intruded by members of the Klein Namaqualand Suite (see Blignault et al., 1983). These relationships are also reflected by the isotopic ages (Barton, 1983). The composition of the two intrusive suites are compared on three standard composition-variation diagrams (Figures 4.15, 4.16 and 4.17). When the best fit trend lines in Figures 4.15 and 4.16 are compared, they can be described as parallel, the difference between the two suites pertaining mainly to the alkali content. More specifically, the Gladkop Suite appears depleted in potassium, compared to the Vioolsdrif Suite. In Figure 4.17 the deviation from the Vioolsdrif Suite calc-alkaline trend towards a tholeitic affinity for the Gladkop Suite, is shown.

In Figure 4.15 six samples of Vioolsdrif gneiss (penetratively foliated Vioolsdrif granitoids) from the Groothoek thrust zone, is shown for comparison (van der Merwe, 1986). Two of these correspond to the Gladkop Suite, two compare well with the Vioolsdrif granitoids and the last two deviate completely from all others. Inspection of the last two analyses show alkali enrichment in the one case and Fe-enrichment in the other.

Figure 4.18 is an adapted form of the QAP diagram for igneous rock classification (Streckeisen, 1976). Norm calculations were performed in the way explained in Appendix 2. The compositions of the different samples and of the averages of the different units in the Vioolsdrif Suite (Reid, 1977) were expressed in terms of the following phases: quartz, sphene, hornblende, magnetite, biotite,

anorthite, albite and K-feldspar. The biotite compositions of the Gladkop Suite grey gneisses (as in Appendix 6) and the average composition of igneous hornblende from Vioolsdrif Suite granodiorite (Reid, 1977) were employed. The resultant norms were then used to calculate QAP values according to the method of Le Maitre (1976). The 'Vioolsdrif trend' appears to form an upper boundary for the alkali-feldspar content of the grey gneisses.

4.5.6 SUMMARY AND DISCUSSION

The Gladkop Suite underlies virtually the whole of the Steinkopf domain and is also found west of the escarpment (Theart, 1980). Remnants of the Gladkop Suite are present in the Copper District, but the possible continuation of these rocks further south in Namaqualand or east into Bushmanland is not known.

In some places the Noenoemaasberg Gneiss has a remarkable banding attributable to the combined effects of deformation and metamorphic differentiation. For the most part it is a homogeneous leucogranitic gneiss that intruded the Steinkopf and Brandewynsbank gneisses prior to or contemporaneous with gneissification.

The Brandewynsbank Gneiss is a homogeneous orthogneiss intrusive into the Steinkopf Gneiss and metasedimentary country rock.

The Steinkopf Gneiss is characterised by secondary banding, but in terms of palaeosome lithology has all the characteristics of an orthogneiss. The intrusive relations with metapelites of the Khurisberg Subgroup and the Besondermeid Formation is of paramount importance, indicating that the grey gneisses of the Steinkopf domain was not the basement onto which these sediments were deposited. On the contrary, it is consistent with the interpretation that those sediments and the metavolcanites of the Haib Subgroup are all part of a pre-Vioolsdrif volcano-sedimentary pile - the Bushmanland Group.

Correlation of the Gladkop Suite with the Vioolsdrif Suite is strongly suggested by similar isotopic ages (Barton, 1983) and the fact that both intrude metasediments of the Eenriet Subgroup. There are, however, important differences:

(i) The Gladkop Suite is highly deformed and metamorphosed while the Vioolsdrif Suite, sensu stricto, is only marginally affected by the Namaqua Orogeny.

(ii) The Vioolsdrif Suite was emplaced into a calc-alkaline volcanic pile for most part; the Gladkop Suite was emplaced mainly into pelites, psammites and chemical sediments (today calc-silicate rocks).

(iii) Compositionally the Gladkop Suite differs from the Vioolsdrif Suite in two respects, namely that it deviates from the calc-alkaline Vioolsdrif Suite trend towards a tholeiitic affinity and that it is depleted in potassium relative to the Vioolsdrif Suite.

The Vioolsdrif-type isotopic age of the Gladkop Suite has been retained despite penetrative reworking during the Namaqua Orogeny. This suggests that the rocks were subjected to high-grade metamorphism shortly after emplacement, that caused relative dehydration prohibiting large-scale isotopic resetting during later

deformation and metamorphism. Such an interpretation is supported by the history of migmatite development in the gneisses of the Gladkop Suite (Chapter II).

Isoclinal folding of volcanites prior to the emplacement of the Vioolsdrif Granitoids (Blignault et al., 1983) suggests an early Proterozoic orogeny that affected the Vioolsdrif/Haib igneous complex. The fact that the Vioolsdrif Suite for the most part escaped high-grade metamorphism during such an early orogeny could be explained in terms of a wide spatial separation between the Vioolsdrif Suite and the Gladkop Suite prior to the Namaqua Orogeny. A wide geographic separation is suggested by the different environments of emplacement mentioned under (ii) above. The two intrusive suites were brought into juxtaposition by significant movement along the Groothoek Thrust Zone.

Although the lower potassium content of the Gladkop Suite relative to the Vioolsdrif Suite could be explained by potasium depletion during penetrative metamorphism and migmatisation, a loss in potassium alone could not explain an anti-clockwise rotation of the Gladkop Suite trend line relative to the Vioolsdrif Suite trend line in Figure 4.16. Considering, however, the difference in potassium content and the more tholeitic affinity as primary features and in addition applying modern plate tectonic theory, an interesting interpretation arises, namely that the Gladkop Suite represents a magmatic domain positioned towards an oceanic environment, compared to the high-K calc-alkaline Vioolsdrif Suite which would represent a continental or near-continental magmatic arc environment (see Green, 1980, for chemical characteristics of igneous rocks from different positions relative to ocean, subduction zone and continent). Such an interpretation would be consistent with the features mentioned under (ii) above.

5 THE KINDERLê GNEISS

5.1 GENERAL DESCRIPTION

The most important stratigraphic unit in the Steinkopf Domain after the Gladkop Suite is the Kinderlê Gneiss. It underlies a significant area south of the Eenriet Mountain Range and in the central part of the Steinkopf Domain (Annexure 1). Despite this relatively wide distribution, unambiguous field evidence regarding the origin of the unit is lacking. It is, by definition, not the same as the 'Kinderlê Metamorphic Complex' of van der Merwe (1986) which consists for a large part of sillimanite bearing granite and migmatite of Spektakel age (see Chapter 7 for a description of the Spektakel Suite).

The gneiss unit is characterized by 'pink nodular gneiss', i.e. a quartzo-feldspathic rock with sillimanite bearing nodules (centimetre scale, Figure 5.1). In the majority of cases, the nodules are quartz-rich, but all variations are found between those consisting of as much as 95 percent quartz and those that consist of sillimanite alone. The volumetric ratio of nodules: nodules plus matrix is not constant; parts of the gneiss are devoid of nodules. Generally, a lower limit of about 0.05 percent was observed.

Due to mechanical differences, the nodules, which are triaxial ellipsoids in shape, tend to be more oblate or prolate when they are sillimanite-rich than when they are quartz-rich. Near hinge zones of folds, oblate sillimanite nodules often define the only apparent axial planar fabric. In many places where the matrix contains sufficient biotite; it is notable that flattened sillimanite rich nodules define a new fabric at an angle to the prevalent foliation/banding of the gneiss while the biotite remains orientated parallel to the older fabric.

The nodules are distributed in zones from a few centimetres to 100 metres in width, generally parallel to major lithological stratification. The Kinderlê Gneiss contains numerous minor, discontinuous bands of biotite-sillimanite schist, at some places associated with metaquartzite. A few such occurrences are large enough to be shown on the 1:250 000 printed map (Annexure 1). The gneiss surrounding the aluminous metasedimentary bands is enriched in sillimanite nodules.

The matrix is generally fine-granoblastic and the rock is often banded; the texture varies between that of the T'Gybiekop-type and the Rooiberg-type of the Noenoemaasberg Gneiss. Although relict augen texture (as in Figure 4.3) was not observed, those parts of the rock which are devoid of nodules, are indistinguishable from the ordinary varieties of the Noenoemaasberg Gneiss. The chemical compositions of two matrix samples, listed in Appendix 3.5, are also indistinguishable from that of the Noenoemaasberg Gneiss (or from most aplogranites). In a few places, notably in the inner arc of the Spitskop enclave, the matrix contains more biotite and the rock resembles the surrounding Steinkopf Gneiss (apart from the presence of sillimanite-rich nodules).

5.2 DISCUSSION

Descriptions of similar sillimanite bearing quartzo-feldspathic

gneisses are given by Lipson (1978), Moore (1977) and Paizes (1975). Sillimanite-rich nodules are not confined to quartzo-feldspathic rocks. Colliston (1983) and Strydom (1985) reported sillimanite-rich nodules in feldspathic metaquartzite and biotite bearing metaconglomerate respectively. In the Aggeneys-Gamsberg area, sillimanite nodules occur in quartz-muscovite schist (e.g. Lipson, 1978; Rozendaal, 1975), biotite-sillimanite schist and pink gneiss (Van Aswegen, 1983b). In the western part of the Ratelpoort Synform, sillimanite nodules consisting of radial patterns of sillimanite occur in cordierite-rich metapelite of the Khurisberg subgroup (Figure 3.2).

In an extensive review of literature and based on his own contributions, Losert (1968) described the general characteristics of sillimanite bearing nodules in metamorphic rocks. He ascribed the formation of the nodules to de-alkalinization of selected small domains - the sites of the nodules. Moore (1977) elaborated this hypothesis in order to explain the origin of nodular gneiss in the Namiesberg area.

Some characteristics of quartzo-feldspathic rocks with sillimanite bearing nodules are of importance. Where the main field track from Aribes to Blesberg crosses the southern limit of Groothoek schist (see Annexure 1), a leucogranite dyke transects a junction between mica schist and Konkyp Gneiss. The dyke contains quartz-sillimanite-muscovite nodules where it has intruded the schist, but where it crosses the gneiss it contains no sillimanite. This phenomenon is illustrated in Figure 5.2. The 'Kinderlê Metamorphic Complex' of van der Merwe (1986) underlies most of the area between the locality described above and the Eenriet Mountain Range. This complex consists of a mixture of Kinderlê Gneiss (as defined in this study), and Eyams Granite, the latter with its associated migmatite and pegmatite. The Eyams Granite in this region contains numerous zones with nodules. The granite is deformed for most part and has a medium-grained to coarse-grained gneissic texture. The sillimanite nodules are generally flattened (oblate ellipsoids)

The origin of sillimanite in metamorphites is a difficult problem with many facets. It is not the purpose of this study to address the fundamental problem but some elementary conclusions relevant to the evolution of the Kinderlê Gneiss can be drawn from the field evidence cited above:

i) Sillimanite bearing nodules occur in rocks which are rich in alumina;

ii) The host rock need not necessarily be metasedimentary - granite enriched with alumina through assimilation of metapelitic country rock can be the precursor of nodular gneiss.

The Kinderlê Gneiss shares most compositional, textural and structural characteristics with the Noenoemaasberg Gneiss (except for the presence of sillimanite nodules). It is spatially associated with the Gladkop Suite on map and outcrop scale. It is therefore suggested that the Kinderlê Gneiss is part of the Gladkop Suite of metagranitoids, contaminated by alumina because of its emplacement into pelitic rocks, as is also the case with the Eyams Granite in the Eenriet Mountains and further to the north.

6 THE LITTLE NAMAQUALAND SUITE

In terms of stratigraphy, the augen gneisses (metagranitoids) of the Little Namaqualand Suite are the most typical representatives of the Namaqua Orogeny. They constitute the most voluminous group of rocks in Namaqualand, including the Copper District, and represent more than 70 percent of the upper crustal volume (see the geological cross section, Annexure 1). The Little Namaqualand Suite is interpreted to be the early syntectonic granitoids of the **Namaqua Orogeny.**

Only a relatively small body of this type of augen gneiss, the Konkyp Gneiss, is found in the north-eastern part of the mapped area. In this chapter the Konkyp Gneiss is described, the general characteristics of the augen gneiss of the Copper District is given, the evolution of the augen in terms of microstructural studies is discussed and, finally, a brief chemical comparison is made between the different gneisses.

6.1 THE KONKYP GNEISS

The first published reference to the Konkyp Gneiss is in SACS (1980) where a very brief description is given (ibid., p. 298) and reference is made to its age relationship with the Gladkop Suite (ibid., p. 293).

6.1.1 DISTRIBUTION

The distribution of the Konkyp Gneiss in the Geotraverse is shown in Figure 6.1. The correlation with augen gneisses in adjacent terranes is obscure. Significant volumes of augen gneiss is found in the Geselskapbank area to the east, but these are generally more leucocratic than the Konkyp Gneiss (Strydom, 1985).

6.1.2 GENERAL APPEARANCE AND TEXTURE

The Konkyp Gneiss can be described as a typical Namaqualand augen gneiss. It consists of large K-feldspar megacrysts (up to 40 millimetres in diameter), at some places with a rapakivi character owing to the presence of irregular, thin, plagioclase rims, (e.g. Figure 6.2). The penetrative foliation deviates around the megacrysts, with the result that the rock exhibits a typical augen structure. The matrix consists of two feldspars, quartz and biotite. The biotite content is relatively high (approximately 15 volume percent), compared to other augen gneisses in the Little Namaqualand Suite (generally less than 10 volume percent). The colour of the rock is grey on fresh surfaces and brownish where weathered.

The texture varies according to the strain state. In zones of low strain the coarse grain size of the granite precursor is retained, especially as far as the feldspar megacrysts (interpreted as relict phenocrysts) are concerned. The zones of more severe strain are characterized by more penetratively developed foliation and a significant reduction in grain size. At places of extreme strain, the rock is reduced to a fine-grained, grey gneiss, comparable to the Gladkop Gneiss. One clear distinction, however, lies in the textural characteristics of the biotite. In the highly deformed Konkyp Gneiss, the biotite flakes are large and have a tendency to cluster, compared to the more or less equidimensional, fine grain size and more uniform distribution of the biotites of the Gladkop

grey gneiss. It must be noted that the Gladkop Gneiss is generally more fine-grained than the Konkyp Gneiss and that distinction in the field is usually unequivocal.

In thin section, the quartz and feldspars exhibit deformation features such as high distribution densities of low-angle sub-grain boundaries, serrated grain boundaries and simple mineral fracturing. Replacement of biotite by muscovite (affecting about 20 percent of the biotite), is a common phenomenon. This is discussed further in Chapter 10.

6.1.3 CONTACT RELATIONS

On map scale the Konkyp Gneiss is in contact with all the major stratigraphic units of the Steinkopf Domain. At the Konkyp hill and the smaller inselberg to the north-east (localities 1 and 2, Figure 6.1), the gneiss structurally underlies metasediments of the Eenriet Subgroup (Kabina Formation). At locality 3, Figure 6.1, the Konkyp Gneiss structurally overlies the Kinderlê Gneiss, while at localities 4 (Duke's Kop), 5, 6 and 7 the augen gneiss is respectively structurally below the Kabina Formation, above the Groothoek Formation and above the Kinderlê Gneiss. The Konkyp Gneiss generally overlies the Gladkop Suite, but in the area of locality 8 (Figure 6.1), it constitutes a band of between 400 and 500 metres wide within the banded gneiss of the Gladkop Suite.

On outcrop scale the Konkyp Gneiss contains numerous xenoliths of various lithological compositions. The xenoliths are in the form of flattened lenses or bands that vary in size from a few millimetres to tens of metres. Mafic restites resulting from partial assimilation of certain xenoliths are common. Xenoliths of the following lithological types were recorded: Steinkopf Gneiss, Brandewynsbank Gneiss, Noenoemaasberg Gneiss, calc-silicate rock, biotite-sillimanite schist and thinly banded metaquartzite (the latter three types probably derived from the Kabina Formation).

The contact relationships with regard to kinematic fabrics indicate the age of the gneiss relative to different deformation events. These are described under 9.4.3.

6.2 THE AUGEN GNEISS OF THE OKIEP COPPER DISTRICT

The lithostratigraphy and petrochemistry of the augen gneiss in the Copper District are described in a number of publications, e.g. Benedict et al. (1964), Clifford et al. (1975a), Martens (1979), Marais and Joubert (1980a), Holland and Marais (1983) and Lombaard et al. (1986). In this section the salient features of these rocks are summarized and their textural development is discussed.

6.2.1 GENERAL DESCRIPTION

Nababeep Gneiss

The Nababeep Gneiss is the most common rock type in the Copper District and has to some extent become a yardstick against which the other augen gneisses can be compared. The ellipsoidal augen consist of aggregates of feldspar and quartz, which vary in size and shape depending on the strain state. In the central Copper District, the augen are flattened parallel to the penetrative regional foliation and elongated parallel to the stretching direction, imposing a well developed lineation to the rock. It must

be noted, however, that, even in the cases of the most elongated augen in the "regional foliation", the shapes of the augen still indicate plane strain (Venter, 1984). In the southern part of the Copper District, in areas of less severe regional strain, the augen are "..tennis-ball sized..." (Marais and Joubert, 1980a).

The matrix consists of biotite, plagioclase and quartz, with occasional hornblende, garnet and even hypersthene. Accessory phases include ubiquituous magnetite as well as pyrite, zircon, apatite and sphene. The difference in magnetite content between the Nababeep Gneiss and the Modderfontein Gneiss, in the central Copper District, is sufficient for it to be registered by regional magnetic surveys. This difference is less marked elsewhere, where the Modderfontein Gneiss is more biotite rich (J. A. H. Marais, pers. comm., 1980).

In the southern and less deformed areas, xenoliths of Gladkop Suite rocks exhibit an older metamorphic/kinematic fabric than the Nababeep Gneiss, indicating a similar time relationship between the Nababeep Gneiss and the Gladkop Suite as between the Konkyp Gneiss and the Gladkop Suite.

Modderfontein Gneiss

The Modderfontein Gneiss (referred to as 'unnamed gneiss at Modderfontein' in Marais and Joubert, 1980a) is generally more leucocratic than the Nababeep Gneiss. The augen rarely consist of single feldspar megacrysts, up to 4 centimetres in diameter (ibid, p. 298). The matrix also contains plagioclase, quartz and biotite, with occasional garnet, but amphibole or pyroxene has apparently never been reported. At least two compositional varieties can be distinguished, the one slightly more felsic than the other. A sharp contact between the two types was pointed out to the author by F. J. G. Schreuder on the farm Modderfontein during a field trip in 1980. The augen gneiss present in the Ratelpoort synform, i.e. the Leeupoort Gneiss, is correlated with the Modderfontein Gneiss on grounds of lithological similarity (J. A. H. Marais, pers. comm., 1980).

Areb Gneiss

The Areb Gneiss, that is the augen gneiss found in the Areb Mountains to the east of the Copper District, is lithologically very similar to the Modderfontein Gneiss. It is leucocratic, usually with less than 5 percent biotite. The augen are generally smaller than those of the Nababeep Gneiss, with which it is in contact on the farm Oranjefontein in the eastern part of the Copper District. The Areb gneiss has also been referred to as the "contorted gneiss" and correlation with the Brandewynsbank Gneiss of the Gladkop Suite has been suggested (Lombaard et al., 1986). From numerous discussions with staff of the O'okiep Copper Company, it is clear that the main distinction drawn by these geologists between the Areb Gneiss and any other augen gneiss in the area is the difference in strain state.

Contact relations between Areb Gneiss and other members of the Little Namaqualand Suite is nowhere exposed in such a way as to indicate relative ages. In terms of lithological similarity and on grounds of structural interpretation (Strydom, 1985, p. 13) the Areb Gneiss is correlated with the Modderfontein Gneiss.

6.3 PROPERTIES AND SIGNIFICANCE OF THE AUGEN

6.3.1 GENERAL

To gain insight into the evolution of the augen gneiss, an understanding of the development of the augen themselves is necessary. In the past, much attention was given to the homogeneity of the augen in a particular gneiss, in the sense that they may either consist of single feldspar megacrysts, or be composed of aggregates of feldspar and quartz (e.g. Marais et al., 1975 and Marais and Joubert,1980a, p. 298). Venter (1951) gave fairly complete descriptions of the Nababeep Gneiss and Brandberg Gneiss (at present correlated with each other). He noted that the augen of the gneiss consist of quartz and feldspar. As far as can be ascertained, however, reference to the relative abundances of the different phases within the augen is lacking in the literature and unpublished reports. During a research project on the steep structures (see Chapter 9.3.2) in the Copper District, the author had the opportunity to examine a number of gneiss specimens, both megascopically and microscopically. The samples were collected (mostly by L. C. Venter) from Nababeep Gneiss and Areb Gneiss, from both outside and within the zones of strain associated with the steep structures. In this section only the textural characteristics of the gneiss outside the zones of steep structure strain will be discussed.

6.3.2 TEXTURAL PROPERTIES OF THE AUGEN

The sizes of the augen of the Nababeep Gneiss in the Eendoorn area, to the south of the Copper District, sometimes exceed 80 millimetres in diameter. In the central Copper District they are commonly smaller than 25 millimetres in diameter. The Areb Gneiss augen are generally smaller than 25 millimetres in diameter. The state of strain in the augen gneiss vary as a result of the zonal deformation during several deformation episodes. In areas of least strain, such as on the farm Eendoorn, the distribution of the augen is generally fairly uniform, and the augen to matrix volume ratio is greater or equal to 1 (see Figure 6.4). In zones of high strain, however, the relative spatial and size distributions of the augen are irregular. It is evident that some individual augen were more resistant to deformation than others so that they were not all deformed to the same extent. In an advanced stage of deformation only a small number of more resistant augen remain. In the extreme case, the whole rock is transformed into an equidimensional fine-granoblastic gneiss.

The matrix between the augen consist of up to 50 percent quartz and more or less equal amounts of plagioclase, K-feldspar and biotite. A planar fabric is defined by the dimensional preferred orientation of the biotite and quartz and, to a lesser extent, by that of the feldspars. The quartz is commonly highly strained, exhibiting undulose extinction and a high distribution density of low angle boundaries and irregular to serrated grain boundaries. Quartz grains adjacent to augen are more severely deformed and individual grains are flattened and broken up into subgrains. The common grain size in the matrix is between 1 and 3 millimetres, but quartz aggregates up to 5 millimetres in diameter have been found. The latter type is interpreted as single grains that were broken up during deformation.

A typical auge consists of more than 75 percent microperthite and

A typical auge consists of more than 75 percent microperthite and more or less equal amounts of quartz and plagioclase (Table 6.1). Accessory phases found in the augen are biotite and an opaque mineral. A minority of plagioclase augen, that consist of more than 80 percent plagioclase, are also present in the gneiss. They are smaller than the common potash feldspar augen, which exceed them by a ratio of 10 to 1.

TABLE 6.1: MODAL COMPOSITION OF AUGEN IN NABABEEP GNEISS

	GLC219	GLC220A	GLC220B
Microperthite	80.1	74.0	77.3
Quartz	7.8	7.4	7.1
Plagioclase	6.7	11.9	14.1
Myrmekite	4.3	3.6	0.6
Biotite	1.1	1.7	0.8
Opaque minerals	0.1	1.4	nd
Total	100.1	100.0	100.0

(The data were obtained by aid of a Swift point counter, set to advance 0.2 millimetre between points. Total number of points: GLC219 - 6644, GLC220A - 1321, GLC220B - 1253)

Augen in two samples of Nababeep Gneiss from the Carolusberg Mine, outside the zone of steep structure strain, are described below as examples of the internal augen texture. Examination of twenty similar samples of Nababeep and Areb Gneiss revealed similar characteristics with only minor variations.

Sample GLC219

The thin section is cut through a large part of one K-feldspar auge, a small part of another and some matrix. The large auge is at least 40 millimetres long and 28 millimetres wide. It consists mainly of K-feldspar in the form of more or less equidimensional subgrains. The boundaries between the subgrains are high angle boundaries for most part, but low angle boundaries are also found, proving the former existence of a larger crystal (Figure 6.5). The subgrains are separated by either

(i) an irregular grain boundary,
(ii) a film of myrmekitic plagioclase, or
(iii) a "mixed zone".

"Pure" K-feldspar boundaries are scarce within the auge due to the common presence of quartz and/or plagioclase. The irregularity of the grain boundaries are partly due to the presence of these phases. The film of myrmekite, found along most of the grain boundaries, vary from very thin (<.01 millimetre) (Figure 6.5) to prominent (>1 millimetre). The thickness of the quartz veinlets within the myrmekite increases sympathetically with the thickness of the myrmekite film. The "mixed zones" are continuous zones separating more than one pair of subgrains. They consist of a mixture of small K-feldspar subgrains, plagioclase (myrmekitic for most part) and quartz. The boundaries between the "mixed zone" and the adjacent K-feldspar subgrains are usually sharp but examples exist where a subgrain is progressively broken up into yet smaller subgrains, to merge with the "mixed zone".
The geometry of the K-feldspar subgrains displays a texture somewhere between a granoblastic polygonal texture (with triple

points) and a rectangular pattern (with four phase junctions) (Figure 6.5). The quartz is present as small rounded inclusions in the K-feldspar, as independent grains in the inter-subgrain spaces and as veinlets in the myrmekite. Most plagioclase is found between the microperthite subgrains, either as myrmekite films or as apparently independent subgrains. A small number of rounded inclusions occur inside the microperthite.

Sample GLC220

This thin section contains the larger parts of two augen. They differ somewhat from the auge described above in the sense that they generally show less evidence of deformation. Serrated subgrain boundaries are perhaps the most pertinent indication of strain induced recrystallization. Plagioclase is more common than in the previously described sample as can be seen from the modal analyses (Table 6.1). It occurs as myrmekite free inclusions in the microperthite, as prominent myrmekite inter-subgrain films and as myrmekitic embayments into the microperthite (replacement texture). Quartz, biotite and opaque minerals also occur as inclusions in microperthite.

In none of the twenty samples of augen gneiss examined were any examples found of helicitic textures representing an older kinematic/tectonic fabric.

6.3.3 MODELS FOR THE EVOLUTION OF THE AUGEN GNEISSES

At this stage in our understanding of Namaqualand geology, the igneous origin of the augen gneisses of the Little Namaqualand Suite is generally accepted. The relationship between the emplacement and the main metamorphic event(s) is, however, still unclear. On the one hand the augen gneisses can be considered to be pre-tectonic in terms of the Namaqua Orogeny and are thus metamorphites. On the other hand the gneisses can be regarded as syntectonic intrusives. The two possibilities involve significantly different tectonic models.

As far as the development of the augen gneisses is concerned, different models have been proposed in the past. McCarthy (1976) developed a model based on major and trace element chemistry, in which the Nababeep type augen gneisses were considered to be metamorphites that had lost various amounts of their felsic components through partial melting. He noted that ".... the coarse texture of the residue evidently reflects prolonged solid-melt equilibrium, during which larger crystals grew at the expense of smaller ones." Reid and Barton (1983) re-interpreted McCarthy's data in terms of the clearcut evidence for the intrusive origin of the augen gneiss provided by Marais et al. (1975). They concluded that the pattern shown by the Nababeep Gneiss on a Ba-Sr-Rb variation diagram supports a model of partial melting, while the plotted positions representing the Modderfontein Gneiss suggests fractional crystallization. They also speculated on the environmental thermal conditions during emplacement of the augen gneisses.

The partial melting model suggests that the Nababeep Gneiss was emplaced into a relatively cool environment while the Modderfontein Gneiss was emplaced into a relatively hot crust, allowing sufficient time for fractional crystalization. In these terms one should take cognizance of the notion accepted by OCC geologists, that the augen gneisses were emplaced into already metamorphosed supracrustal rocks (J. A. H. Marais, personal comm., 1980).

6.3.4 DISCUSSION

Both models discussed above are compatible with the slow growth of large feldspar crystals in a melt. Such conditions existed when the gneiss precursor was still a magma. This interpretation is consistent with the interpretation that the augen represent deformed and recrystallized **primary phenocrysts.** The presence of other phases than K-feldspar in the K-feldspar augen can be explained by a combination of primary inclusions and replacement during strain-induced recrystallization.

In a comprehensive review, Vernon (1986) combined a wide spectrum of published data with his own considerable experience and concluded that '... all K-feldspar megacrysts in granitoid rocks and their enclaves are phenocrysts, not porphyroblasts..'. As far as augen gneisses are concerned '...the augen are relicts of megacrysts (i.e. phenocrysts) that have not been deformed as much as the matrix..'. This is in exact accordance with conclusions reached in this study, concerning the origin of augen both in the Little Namaqualand Suite and in the Gladkop Suite.

The development of myrmekite at the subgrain-boundaries suggests that the deformation and transformation of the original megacrysts took place under high temperature conditions. It remains to be explained whether the granite was first cooled and then re-heated during the deformation or whether the deformation took place at least partly during the emplacement. This aspect will be discussed further in Chapter 12.

6.4 CHEMICAL CORRELATION

6.4.1 GENERAL CONSIDERATIONS and SOURCES OF DATA

In this section the chemical characteristics of the Little Namaqualand Suite is briefly discussed. The aim is, mainly, to test the validity of the correlation of the Konkyp Gneiss with the rest of the Little Namaqualand Suite in the Geotraverse. The petrochemistry of these gneisses has been discussed by a number of authors such as Venter (1951), Clifford et al. (1975), McCarthy (1976) and Reid and Barton (1983). The data used here are mainly from these publications/theses. Holland and Marais (1983) used a total of 890 whole rock chemical analyses to ascertain the general chemical characteristics of the Proterozoic gneisses of Namaqualand.

The new chemical analyses of augen gneisses reported by Reid and Barton (1983), were done on samples collected for the purposes of geochronological study, as part of the Namaqualand Geotraverse IGP project. This includes five samples of Konkyp Gneiss from locality 3, Fig. 6.1. Since that time three more Konkyp Gneiss samples from different localities were analysed by A. Duncan (Dept. of Geochemistry, Univ. of Cape Town) who kindly made the results available (pers. comm. 1985).

The average composition of the Little Namaqualand Suite gneisses in the geotraverse is granitic with a relatively high potash content. The compositional variation of the well studied Vioolsdrif Suite (Reid, 1977) serves as handy reference trend for chemical characteristics of the granitoid augen gneisses. As far as the major elements are concerned, there is considerable compositional

overlap between the Little Namaqualand Suite gneisses and the Vioolsdrif Suite granitoids. On Harker variation diagrams, significant differences are detectable only for iron and titanium (Reid and Barton, 1983, p.73). In the case of trace elements, a significant difference between the strontium contents of the two suites is apparent (ibid.).

Only major element compositions are considered here. The sources of the data are listed below:

Source	Rock type	Number of analyses
McCarthy (1976)	Brandberg Gneiss	2
do.	Nababeep Gneiss	9
do.	Augen Gneiss (Leeupoort type)	6
do.	Mesocratic Nababeep Gneiss	6
do.	Modderfontein Gneiss	9
Clifford et al., (1975a)	Nababeep Gneiss	2
do.	Modderfontein Gneiss	1
Venter (1951)	Nababeep Gneiss	1
Reid and Barton (1983)	Nababeep Gneiss	4
do.	Kabis Gneiss	5
do.	Aroams Gneiss	1
do.	Konkyp Gneiss	5
A. Duncan (pers. comm. 1985)	Konkyp Gneiss	3

Because the analyses of the Konkyp Gneiss provided by A. Duncan have not been published, it is given in Appendix 3.3.

6.4.2 VARIATION DIAGRAMS

The compositions of the gneisses are compared on three ternary composition variation diagrams with the weight percentages of the element oxides as baricentric coordinates. Figure 6.6 shows that the Leeupoort Gneiss and Modderfontein Gneiss are depleted in CaO relative to the rest of the Klein Namqualand Suite. On this diagram, the Konkyp Gneiss is indistinguishable from the Kabis, Nababeep and Brandberg Gneisses. A diagram depicting the relative amounts of the oxides of sodium, potassium and calcium in igneous rocks is usefull for elucidating possible differentiation trends in granitoids. Figure 6.7 is a relevant diagram for the Little Namaqualand Suite, with the Vioolsdrif Suite differentiation trend as reference. The Modderfontein Gneiss and Leeupoort Gneiss again form a group separated from the rest of the gneisses, namely at the felsic end of an apparent differentiation trend. Figure 6.8 is the 'AFM' diagram for igneous rocks. On this diagram the Leeupoort Gneiss is separated from the Modderfontein Gneiss, the latter being more alkaline. Furthermore, it is clear that the Konkyp Gneiss is enriched in iron relative to the rest of the gneisses.

The compositions of the different samples are further compared by means of a 'QAP' diagram (Figure 6.9) found by the same technique as used for Figure 4.18 (see Chapter 4 and Appendix 1). In this diagram a significant difference between the compositions of the Konkyp Gneiss and those of the other Little Namaqualand Suite gneisses is apparent. The Konkyp Gneiss is clearly enriched in normative quartz and impoverished in normative alkali-feldspar relative to the rest of the Little Namaqualand Suite.

6.4.3 DISCUSSION

The apparently insignificant silica enrichment of the Konkyp Gneiss seen in Figure 6.6 coupled with the iron enrichment seen in Figure 6.8 cause an enrichment in normative quartz and biotite at the expense of K-feldspar. No modal analyses were done on the augen gneisses, but qualitative estimates of mineral compositions confirm a generally higher biotite content in the Konkyp Gneiss compared to other augen gneisses. Different interpretations can be made from the presentation in Figure 6.9 depending on whether one considers the composition of the granites in terms of a differentiation interpretation or a metatectic model. An important model concerning the tectonic evolution of the Geotraverse is the one suggested by Reid and Barton (1983), namely that the Little Namaqualand Suite is the product of anatexis of crust consisting essentially of the Orange River Igneous Complex (comprising the Vioolsdrif Suite and the Haib Group of calc-alkaline volcanites). In terms of such a model, the composition of the Konkyp Gneiss, as indicated on Figure 6.9, suggests a different source. Considering the relatively high normative quartz content, a metasedimentary component in the source region is probable.

From the above one can conclude that there is a fundamental compositional difference between the Konkyp Gneiss and the Nababeep Gneiss. Differences in the isotopic characteristics of the two rock types led Barton (1983) to conclude that there is also an essential difference in the times of emplacement. The Nababeep Gneiss is concluded to be not older than 1300 Ma while the Konkyp Gneiss could be as old as 1800 Ma.

The field correlation of the Konkyp Gneiss with the Little Namaqualand Suite is thus not supported by geochemical data. Although the final assessment of the isotopic data is still unclear, the difference between the Konkyp Gneiss and the Nababeep Gneiss, in terms of major element composition, probably reflects different source compositions. If the present geographical seperation between the Konkyp Gneiss and the rest of the Little Namaqualand Suite do indeed reflect spatially different source regions, an inhomogeneous lower crust model is indicated. Despite the chemical differences, the Konkyp Gneiss is interpreted to be part of the Little Namaqualand Suite on the basis of field and structural correlation and can be considered the product of anatexis of an inhomogeneous lower crust during the early stages of the Namaqua Orogeny.

7 THE SPEKTAKEL SUITE

7.1 GENERAL

The Spektakel Suite was originally defined as a suite of leucogranites with a wide distribution in the Copper District and further to the west and south in Namaqualand (Marais and Joubert, 1980b). In the Copper District the Spektakel Suite is represented by the Concordia, Rietberg and Kweekfontein Granites. Blignault et al. (1983) included the Eyams Granite, the Wyepoort Granite and the Middelplaat syenitoid dykes in the Spektakel Suite. The distribution of the different units in the study area and further west is shown in Figure 7.1. These units proved to be very important time markers in the geological history of the Geotraverse and their proper correlation and dating is fundamental for the unravelling of the complex tectonic development of the Namaqua Metamorphic Complex.

7.2 THE CONCORDIA and RIETBERG GRANITES

Volumetrically, the Concordia Granite is an important unit in the Copper District. It is described as a gneissose aplogranite consisting of microcline-microperthite, quartz and sericitized plagioclase (Marais and Joubert, 1980b).

Texturally, the Concordia Granite is intermediate between the Little Namaqualand gneisses and an undeformed coarse-grained leucogranite. To get some idea of the textural development of the granite, three samples from the vicinity of "New Prospect", east of Concordia, were examined. The gneissose texture is defined by elongated K-feldspar phenocrysts (consisting of three or more subgrains, individually up to 5 millimetres in diameter), and by a vague planar fabric in the matrix, that consists of quartz, partially saussuritized plagioclase and K-feldspar. The effects of ductile strain are undulose extinction and a high density of low angle subgrain boundaries in quartz, serrated to irregular K-felspar boundaries in the "augen" and seriate size distribution of grains in the matrix. Vague micro-zones of finer grain size are orientated parallel to the general foliation.

The essentially sheetlike form of the Concordia Granite makes it convenient to use the terms lower and upper when discussing the contacts. These contacts are actually contact zones and have remarkable properties.

The contact zone with the underlying older Nababeep Gneiss is known as the "Mixed zone" (Lombaard et al., 1986). It has a thickness of about 120 metres (ibid.) and consists of intimately interbanded sheets of the two rock types. The alternating bands vary from several metres to a few centimetres in thickness. The contact can therefore be described as interbanded-gradational. The transition to the structurally overlying Rietberg Granite is also gradational, though in a more familiar fashion. The texture of the Concordia Granite changes towards the top of the sheet (Marais and Joubert, 1980b) and the gradation to Rietberg Granite is over a relatively long distance of several metres (Martens, 1979, p. 16).

The Rietberg Granite is usually described as an undeformed leucogranite. The granite is characterized by euhedral K-feldspar

phenocrysts with conspicuous simple twinning lamellae, mostly according to the Carlsbad law, in an even-grained matrix of quartz and feldspar (Venter, 1951). It can be added that the phenocrysts generally exhibit a high distribution density and that they are equidimensional. These features contrast markedly with the textural characteristics of the Kweekfontein Granite described below. The existence of a planar fabric defined by the weak but discernible preferred orientation of feldspar phenocrysts have been ascribed to flow banding (Marais and Joubert, 1980b). Structural features that indicate significant deformation of the Rietberg Granite, are described in Chapter 9.

7.3 THE KWEEKFONTEIN GRANITE

The term Kweekfontein Granite is used to refer to a number of large and small irregular dyke-like bodies of fine-grained leucogranite, widely distributed in the Copper District. In the eastern half of the Copper District, bodies of the granite large enough to be represented on the 1:250 000 scale printed map, have been mapped by geologists of the O'okiep Copper Company. These bodies generally transgress across all other granitic rocks in the area except the Rietberg Granite (Lombaard et al., 1986). The stratigraphic relation with the Rietberg Granite is not clear.

During this study, special attention was given to the Kweekfontein Granite in the Ratelpoort Synform because of the similarity to the Eyams Granite (see below). Some of the localities described below are indicated in Figure 7.2. A considerable portion of the Kweekfontein Granite in this area shows textural deviation from the mean. It contains a varying proportion of large and small feldspar phenocrysts, giving the rock a distinctly pegmatitic appearance at some places (Figure 7.3). One can thus refer to a megacrystic type of Kweekfontein Granite and to a normal type. The latter is the most common type, especially in the southern and eastern parts of the Copper District.

In the eastern part of the Ratelpoort Synform, the Kweekfontein Granite is clearly intrusive into the Leeupoort augen gneiss (Little Namaqualand Suite) and into the grey gneisses of the Gladkop Suite. On grounds of contact relations (admittedly vague) and a more penetrative deformation imprint on the Kweekfontein Granite than on the Rietberg Granite, Martens (1979, p.14) concludes that the Rietberg Granite is younger than the Kweekfontein Granite in this area, with an intrusive relationship. East of Bulletrap (locality 2, Figure 7.2) the presence of apparently xenolithic bodies of Kweekfontein Granite in the Rietberg Granite was also noted during mapping for the present study. Dykes and sheets of leucogranite, which are practically identical to the common type of Kweekfontein Granite, cut across the Rietberg Granite in some places (Martens, 1979, p.14). It is therefore not clear whether the larger bodies of leucogranite, that are not in contact with other members of the Spektakel Suite, as for example on the farm Kweekfontein, have been emplaced before or after the Rietberg Granite.

At locality 3, Figure 7.2, the contact relations between the Rietberg Granite and the megacrystic type of Kweekfontein Granite, can be studied on a well exposed outcrop. The outcrop consists of fine-grained granite in which feldspar phenocrysts, identical to those of the Rietberg Granite, occur intermingled with the

"pegmatitic" phenocrysts of the Kweekfontein Granite. In places the Rietberg-type phenocrysts are concentrated, to the exclusion of the Kweekfontein-type. Phenocryst patches such as these have the appearance of xenoliths of typical Rietberg Granite (Figure 7.4). The transition from the mixed type of rock to these pseudo-xenoliths is gradational, in contrast to the discrete xenolith of Leeupoort augen gneiss that exhibits an abrupt contact (Figure 7.5).

The contact between grey gneiss of the Gladkop Suite and the Kweekfontein Granite is of special interest, as it indicates the mode of emplacement of the granite. It is very similar to the contacts between the grey gneisses and the Eyams Granite in the Steinkopf Domain. In one outcrop at locality 1, Figure 7.2, the fine-grained gneissic texture of the gneiss is gradually replaced by a medium-grained granitic texture, through the progressive blastesis of subhedral plagioclase and K-feldspar. As a result, the contact between the gneiss and the Kweekfontein Granite is completely gradational. Nearby, the contact is gradational in a different way. Thin sheets of the granite follow minor shear planes in the gneiss. The spacing of the shear planes become closer to each other and their widths increase towards the contact, untill the rock is an intimate mixture of granite and sheared, recrystallized gneiss. The strained forms of grey gneiss xenoliths indicate the sense of shearing. These features are demonstrated in Figures 7.6 to 7.8. The shears form part of the Skelmfontein shear system described in Chapter 9.

The feldspar megacrysts do not show signs of brittle fracture, indicating that the deformation did not take place while the granite was in the solid state. Signs of deformation of the Kweekfontein Granite subsequent to emplacement is found at locality 5, Figure 7.2, where a sill of the granite in grey gneiss is boudinaged, as shown in Figure 7.9.

7.4 THE EYAMS GRANITE IN THE STEINKOPF DOMAIN

7.4.1 INTRODUCTION

The Eyams Granite was first described as the M-3 migmatite and the Kabinaberg Granite in unpublished IGP reports. Theart (1979) reported that large areas to the west of the Geotraverse are underlain by this granite and referred to it as the migmatitic granite. Later, however, he named it after the farm Eyams where typical outcrops are to be found (Theart, 1980). In this section the salient features of the granite in the Steinkopf Domain is described. The granite is referred to in Chapter 11.

7.4.2 DISTRIBUTION

Small bodies of the granite are scattered over most of the Steinkopf Domain. The main occurrences of the Eyams Granite, as known at present, is shown in Figure 7.1. The leucogneiss immediately to the north of the metaquartzites of the Eenriet Mountains, to the west of the tarred road, was initially mapped as undifferentiated pink gneiss (see printed map), but re-examination revealed that it actually represents deformed Eyams Granite, originally texturally identical to the granite a few hundred metres to the south (see Chapter 9).

7.4.3 FIELD ASPECTS

The Eyams Granite can be described as a nebulitic migmatite with schlieric remnants of country rock. Contacts with the country rock are characterized by many of the migmatitic structures defined by Mehnert (1968). Theart (1980) describes a complete gradation over a distance of about two kilometres, from grey gneiss with a brecciated appearance impregnated by the granite (agmatitic structure) to granite with abundant large and small xenolithic rafts of the gneiss (schollen structure).

The composition, as reflected mainly by the biotite content, varies from outcrop to outcrop and depends on the composition of the host rock. Where the country rock is Steinkopf Gneiss, the granite is coloured grey with up to ten percent modal biotite. Biotite rich schlieren are common and ghost banding reflects the pre-existing structure of the gneiss. Where the Eyams Granite occurs within the Noenoemaasberg Gneiss, the composition is similar to the leucogneiss. The granite can on textural grounds be distinguished from an earlier type of mobilizate, referred to as the N2 neosomes (Chapter 11) and from the gneiss itself.

Schistose country rock near to the contact with the Eyams Granite is enriched in feldspar (K-feldspar as well as plagioclase). At some places in the Eenriet Mountains, this feldspathization is well advanced. Entire outcrop areas are compositionally and texturally more or less half-way between the schist and the granite. The subhedral plagioclase crystals of the granite matrix as well as the phenocrysts are conspicuously white (due to saussuritization), which serves to distinguish the rock in the field from other leuco-granitic types. The same observation applies to those plagioclase crystals in the country rock near to the contacts with the granite. In the field, the contact effect of the granite on the country rock can thus be traced by noting the distribution of white plagioclase. A similar situation is found at the contact between the Kweekfontein Granite and the grey gneiss in the Ratelpoort Synform described above.

The migmatization is well advanced in the biotite-sillimanite schist of the Kabina Formation over most of the Eenriet Mountain Range. Only in the western parts of the range is the schist relatively unaffected.

A compositional banding, defined by trains of feldspar phenocrysts, is found in the Eyams Granite in places. This banding is similar to that described as flow banding in the Kweekfontein Granite (Martens, 1979), but in the Eyams Granite it is only developed on a limited scale.

7.5 THE WYEPOORT GRANITE

The type locality of the Wyepoort Granite is near Safnek, at the confluence of the Wyepoort River and one of its major tributaries from the southeast (Figure 7.1). Here the river has cut through a pluton with an exposed diameter of approximately 2.5 km. The granite is leucocratic, fine-grained and homogeneous, with a foliation varying from feeble to well-developed. In the vicinity of the type locality it has been described as an aplogranitic gneiss (Ward, 1977), but the main body is penetratively foliated at its

margins only. In the central parts the foliation is hardly visible. A large number of smaller bodies and dykes of fine-grained granite, to the south of the type locality, is correlated with the Wyepoort Granite on grounds of similar composition, field appearance and structural age. In many cases the smaller bodies are, however, finer-grained and have a distinctive grey colour due to a relatively high biotite content (up to 8 volume percent). A small, but prominent outcrop of this type was first found at Vlieholteberg (see Figure 7.1) and this variety of the Kweekfontein Granite is referred to as the Vlieholteberg-type.

A number of fine-grained grey granite dykes, mostly of the Vlieholteberg-type, are scattered over the entire Steinkopf Domain. The dykes are irregularly shaped and apparently do not follow any specific structural trend. In the mapped area they attain sizes large enough to be shown on the 1:250 000 scale printed map, only in two examples from the Eenriet area.

The texture of the granite is predominantly fine-grained, but some bodies contain a low proportion of small K-feldspar phenocrysts averaging less than one centimetre in diameter. Some small outcrops of leucogranite are texturally and compositionally similar to the normal type of the Kweekfontein Granite.

In most outcrops, the granite exhibits a weakly developed foliation, difficult to discern in cases where the biotite content is low. In zones of advanced shearing in the Groothoek Thrust Zone (see Chapter 9), however, the rock is transformed into a fine-grained gneiss.

The Wyepoort granite cuts across the Eyams Granite at Vlieholteberg. A similar situation is described for the Eenriet Mountains (see Chapter 9.4.2). In addition to the foliation of variable intensity, the granite exhibits minor patchy recrystallization (flecky structures in migmatite nomenclature). In the southeastern part of the mapped area a number of thin Vlieholteberg type dykes are affected by late stage migmatization.

7.5 THE MIDDELPLAAT DYKES

The last of the igneous units grouped with the Spektakel Suite is a series of mafic to mesocratic dykes of rather peculiar syenitic composition ('lamproitic' according to Reid and Barton, 1983). The type locality is at Middelplaat (see Figure 7.1). Here one of the widest known dykes crop out reasonably well in the stream bed behind the homestead.

The dykes are vertical and trend northeasterly. They vary in width from a few centimetres to about three metres. Strain features are described in chapter 9. The dykes weather negatively, resulting in sharply defined trenches where the dykes traverse domes of resistant gneiss. Unweathered outcrops are scarce.

The bulk of the dykes consist of fine-grained mafic to mesocratic meta-syenitoid. The mineral composition varies as shown in Appendix 4.5.3. The rock is fine-grained and has a penetrative foliation, defined by the preferred orientation of hornblende and/or biotite. A pegmatitic phase, consisting almost exclusively of K-feldspar, occurs along the edges of most of the dykes and also as cross-cutting veins. In some cases the contact between the pegmatitic phase and the mesocratic rock is gradational. In such

instances the replacement of plagioclase and hornblende by K-feldspar and biotite, as seen in thin section, suggests a process of potash metasomatism.

8 THE YOUNGER INTRUSIVES

To supply a comprehensive view of the entire litho-stratigraphy of the mapped area, brief descriptions of the following units are added:

The Nariams Suite (metadolerite)
Orbicular rocks
The Gannakouriep Suite (dolerite)

The Nariams Suite consists of two major dykes and a number of small bodies of dolerite in various stages of amphibolitization. The distribution of these rocks are shown in Figure 9.14. The most prominent dyke strikes north-westerly in the area south of Nariams. It is exposed discontinuously for about 4 kilometres, the discontinuity being a strain effect due to Skelmfontein shearing. The second major dyke transects the Brandewynsbank Gneiss south of Wildehondspoort and is approximately parallel to the dyke at Nariams. It is also discontinuous, but, superficially does not show strain. In terms of their relations with the Late Namaqua thrust fabrics and similar metamorphic histories, the Nariams dykes are equivalent to the Gareskop dyke swarm of the Naab thrust sheet in the Geselskapbank Synform (Strydom and Schoch, 1983; Strydom et al., 1987). The two sets of dykes cannot be correlated, however, because the Gareskop dykes apparently originated more than 200 kilometres to the north-east and were transported to north-western Bushmanland tectonically (Strydom, 1985).

Esoteric orbicular intrusive bodies were encountered during the mapping phase of the study at two localities in the central part of the Steinkopf Domain (indicated as 'or' on the printed map). The southernmost body contains abundant spherical feldspar orbicules averaging 20 millimetres in diameter. The rock is characterized by a high alumina content and relative low silica, iron and magnesium contents (the composition is listed in Appendix 3.5, Sample SOB1). The northern body is dark grey in colour and contains irregularly shaped orbicules as much as 10 centimetres in diameter, defined by a 5 millimetres wide feldspar rim enveloping a darker centre.

The Gannakouriep Suite consists mainly of dolerite dykes, a swarm of which strikes north-easterly in the northern part of the mapped area. These dykes are more common in the northern part of the Geotraverse. Their age is bracketed by the Nama Group, that unconformably overlies the dykes, and the Blesberg Suite pegmatites (Blignault et al., 1983), that are cut by the dykes. The Gannakouriep Suite possibly symptomize extensional tectonics related to the development of the Gariep mobile belt in the western Richtersveld (e.g. Onstott et al., 1986). The Gannakouriep dykes were not petrographicaly examined during this study.

9. STRUCTURAL DEVELOPMENT

9.1 INTRODUCTION

The study area consists basically of four thrust bounded tectonic domains. The Steinkopf Domain occupies a central position and is bounded by the Richtersveld Domain to the north, the Okiep Copper District to the south and the Geselskapbank Domain to the east. The Transition Zone, as defined here, is a structurally and lithologically complex zone which separates the Steinkopf and Richtersveld Domains. The regional structural setting of the study area is shown in Figure 1.2. and the outlines of the tectonic domains are shown in Figure 1.3.

The geometric and kinematic aspects of the structural geology in the Geotraverse is the main theme of a companion study by van der Merwe (1986) and a detailed structural analysis of the Geselskapbank Domain is given by Strydom (1985). In this chapter only the general outline of the structural development is sketched and emphasis is placed on the sequence of events as deciphered by the author in the Steinkopf Domain.

Structural correlation of separated areas was mainly accomplished by utilizing the effects of particular structures on intrusives of known isotopic age. Once the structural framework was established, undated lithological units could be placed in the tectonic sequence by analyzing their contact relations with other units as well as the relations with known structures. The sequence of events is here treated from the youngest to the oldest. Localities of interest are indicated in Figures 9.1, 9.14 and 3.1.

9.2 THE VERY LATE FAULTS

The Steinkopf fault is the most prominent of the very late faults. In the Copper district the Steinkopf fault is one of several major north trending faults showing strike separations of up to 1000 metres. The actual displacement involved a major component of dip slip, as can be deduced from the way in which the subhorizontally disposed metasediments is truncated in the Jakkalswater - Mörewag area, west of Springbok (see Annexure 1). In the Copper District, the Steinkopf fault forms the contact between the Namaqua Metamorphic Complex and the Nama Group for a short distance in the area west of Nababeep.

In the Steinkopf Domain the northerly trending faults peter out. The late faults are much less prominent with strike directions of northwesterly and northeasterly, in contrast to the dominantly northerly trends in the Copper District. The Steinkopf fault now changes strike; at the transition between the Copper District and the Steinkopf Domain, the fault changes direction to northwesterly for a distance of about 12 kilometres. It then changes strike again, to mainly northeasterly. In the Steinkopf Domain, the relatively undisturbed and unmetamorphosed Nama Group sedimentary rocks and the complexly deformed and metamorphosed gneisses of the Namaqua Metamorphic Complex are juxtaposed by this fault, constituting a natural western boundary for the study area. The throw is west-down and the Nama rocks adjacent to the fault are folded to some extent in response to the drag effect. The trace of the fault is marked by vein quartz ridges as seen, for example, in

the vicinity of Besondermeid, a few kilometres southwest of Steinkopf.

The northwesterly trend of these faults coincide with the general trend of the Gannakouriep mafic dykes. The main movement along the faults are, however, clearly younger than the dykes, since they displace the Nama Group which overlies the dykes. In the north of the study area, the northwesterly trending faults displace the Gannakouriep dykes (van der Merwe, 1981).

9.3 THE LATE STRUCTURES

9.3.1 THE NORTHWESTERLY TRENDING MINOR SHEARS

The youngest of the ductile deformation structures constitute a set of north-northwesterly trending minor shears, commonly observed in the western part of the mapped area. The shears are generally filled with pegmatite up to 50 centimetres wide in the largest shears. The width of the shear zones (i.e. the width of the zones showing any shear strain effects such as rotation of fabrics) are between 1 and 10 metres. Most of these minor shears show right lateral strike separation and drag. These shears cut across the Ratelpoort and Dabbiknik shear fabrics discussed below.

Northerly trending meso-scale monoclinal structures with right lateral displacements, similar to the structures described as "F-4" folds by Joubert (1971) and which might be related to the shears described above, were observed at several places in the northwestern parts of the mapped area. Dilatation type neosomes are associated with these structures, especially where boudinage structure is developed.

9.3.2 THE LATE SHEARS

In the Steinkopf Domain the dominant fabrics are steeply inclined and a first impression is that the strata have steep dips. On a macroscopic scale however, the lithological contacts are subhorizontal. The apparent vertical attitude is the result of relatively late shearing and associated mesoscale folding. In the south the dominant strike is easterly, mainly as a result of the Ratelpoort shearing, while the western part of the area is dominated by the northeasterly trending Dabbiknik zone of shearing and folding.

The Ratelpoort shear

The transition zone between the Steinkopf Domain and the Copper district forms a prominent lineament on maps and aerial photographs and has informally been referred to as the Ratelpoort lineament. The zone contrasts against the surrounding terrane because (i) it consists of contrasting lithological types, (ii) the regional strike of the foliation/banding of the rocks remains constant for a relatively long distance, (iii) the dip of the foliation/banding is steeper than that of the adjacent areas and (iv) the rocks are extremely deformed. The high strain is not attributed to the Ratelpoort shear, but to older deformation such as that associated with the the Skelmfontein thrust zone (see below). The existence of the structure referred to as the Ratelpoort shear is recognised by the rotation of the pre-existing planar structure towards the shear plane. In the southeastern part of the mapped area two separate

shear zones are recognized namely the Ratelpoort north and Ratelpoort south shear zones. On the printed map the Ratelpoort Shear Zone is indicated by converging sets of broken lines. Only in the case of the Ratelpoort north shear is a new mineral foliation (i.e. refoliation as a result of shearing) recognised in the country rock gneiss (van der Merwe, 1981). The two zones converge and the shear strain diminishes westwards so that, in the area west of Bulletrap, the effects of the Ratelpoort shear are less prominent. The actual displacement along the Ratelpoort shear is calculated to be of the order of ten kilometres, mainly right lateral, with a lesser vertical and north-up component (ibid., p. 30).

The Dabbiknik zone of shearing and folding

The whole of the western and northern parts of the Steinkopf Domain are dominated by the northeasterly trending Dabbiknik shearing and folding. These areas are characterized by subvertical mesostructure and subhorizontal macrostructure.

The mesoscale folds (e.g. Figure 9.3a) have amplitudes and wavelengths of the order of 5 centimetres to a 100 metres and have subvertical axial planes. The plunges of the fold axes vary through the horizontal with a mean of about five degrees toward the northeast. Subvertical minor shear zones are intimately associated with the folds. The shears are either localized in the limbs of the folds (folding dominant) or the folds occur in the form of minor drag folds in penetrative shear zones (shearing dominant).

In some places the shearing is quite penetrative and pre-existing structures are either obliterated or transposed. The consequence of the shearing is obvious where lithological markers are disrupted as at locality 1, Figure 9.1 (see Figure 9.2). The total effect of the shearing is difficult to determine because of the absence of such markers in the homogeneous country rock gneisses. In zones of shearing, such as depicted in Figure 9.2. the effects of Dabbiknik shearing cannot be distinguished everywhere from the effects of older disruptions, such as the Skelmfontein shearing (see below), which had been reoriented parallel to the Dabbiknik shearing direction.

Mineral refoliation, as at locality 2, Figure 9.1 (Figure 9.3a and b), is much more common than in the case of the Ratelpoort shearing, but it is not penetrative. The new foliation is commonly defined by the flattening of flecky structures as is the case with the Ratelpoort north shear mentioned above. In those cases the refoliation apparently formed simply by the physical flattening of the pre-existing structure. In other cases, however, the refoliation is defined by the preferred orientation of individual biotite flakes and metamorphic recrystallization is indicated. In the Eenriet Hills (locality 6, Figure 2.3) one Steinkopf Gneiss outcrop represents an intermediate stage between a mineral refoliation and penetrative reconstitution of the grey gneiss foliation/banding (see Figure 9.4)

Dabbiknik deformation of the Eyams Granite and the Middelplaat dykes

The Eyams Granite is mostly very low in mica and it did not readily develop a mineral foliation. Nevertheless, at outcrop GS-1 near Witwater (see Chapter 11) and at places in the Eenriet Mountains (e.g. locality 9, Figure 2.3), a distinct mineral foliation

parallel to the Dabbiknik fabric is discernible. The younger Middelplaat dykes, on the other hand, show well developed Dabbiknik shear fabric. The dykes and the granite must therefore pre-date the Dabbiknik shearing.

At several localities, also at the type locality of the Middelplaat dykes, the northeasterly trending Dabbiknik shear fabric transects the contact between the dyke and the country rock gneiss. The deformation of the dykes include ptygmatic folding of the K-feldspar rich pegmatitic veins. Some 200 metres south of the layby at Korrogas, the contact between one of the dykes and the country rock grey gneiss is deformed into a mullion structure with the Dabbiknik shear fabric cutting across the contact, parallel to the axial plane of the structure. The dyke forms convex cusps in the gneiss (Figure 9.5), indicating that it reacted in a less viscous manner than the gneiss during the deformation. The fabric at the contact with the dyke shown on the printed map (Annexure 1) about 1.6 kilometre south-west of Paddagat (locality 3, Figure 9.1) is diffracted. The strike of the fabric in the dyke is 62° while it is close to 70° in the adjacent country rock gneiss. Since the dyke was more ductile than the gneiss (see above) one can conclude that the shear fabric in the dyke is situated closer to the non-material shear plane than is the case with the Noenoemaasberg Gneiss. The fabric configuration, as described, then suggests left lateral shear movement as seen on the horizontal plane.

Age relation between the Dabbiknik and Ratelpoort shear zones

The Ratelpoort and Dabbiknik shear zones converge in the southwestern part of the Steinkopf Domain. The age relationship between the two structures is established with the help of the Middelplaat dykes at the lower contact of the band of Steinkopf Gneiss which is folded in a small synform 2.6 kilometres south-east of Koros (locality 4, Figure 9.1). The dominant local structure has a westerly attitude, defined by the orientation of lithological contacts in the country rock as well as by an older refoliation. The older refoliation probably belongs to the Skelmfontein thrusting, which predates the Late Shears. The westerly attitude of the latter is interpreted as a manifestation of the Ratelpoort shearing. One of the dykes clearly transects the westerly trending structure. The northeasterly trending Dabbiknik shearing is in turn superimposed on the dyke. These relationships are schematically explained in Figure 9.6.

The recurrence of refoliation with a strike attitude of between 60° and 70°, observed during routine data collection in the southern part of the Steinkopf Domain, indicates that the northeasterly trending refoliation is superimposed on the westerly trending Ratelpoort shear. Figure 9.7 is an equal area hemispherical projection of the poles of foliations from the southwestern part of the Steinkopf domain. It indicates the dominance of attitudes with a northeasterly strike and the poorly defined concentration of attitudes with east-northeasterly strikes. The latter corresponds to the average orientation of foliations in the Ratelpoort north shear zone described by van der Merwe (1981).

Late Folds

Blignault et al. (1983) concluded that the Late Shears and the regional scale easterly trending open folds belong to the same broad time category. The latter were referred to as F-3 folds by Joubert (1971). One interpretation of the age relation between the

Late Shears and the open folds involve rotation of the open folds to an easterly trend by the Late Shears, from an original northeasterly strike (Blignault et al., 1983). Similar significant shearing is suggested by Strydom (1985) to have affected the very large scale Geselskapbank synform. An alternative model was suggested earlier by Joubert (1974), namely that the open folds formed as a result of the westerly shearing. Either way, the relations between the Ratelpoort shear and the Dabbiknik structures described above, suggests that the latter postdate the open folds. This conclusion is substantiated by the occurrence of northeasterly trending minor shears with associated neosomes, transecting the regional tectonic grain, in the Nariams area. Figure 9.8 shows these shears from locality 1, Figure 9.14. The foliation/banding traversed by the shears in Figure 9.8 is the Skelmfontein fabric (see below). The orientation of this older fabric is a function of the regional scale Geselskapbank synform. Actually the entire eastern part of the Steinkopf Domain forms part of the western hinge zone of this large synform (see Figure 1.2). It would therefore seem that the northeasterly trending shears post-date the macro-fold.

In terms of the above interpretation, the Dabbiknik shears could be correlated with the right lateral S-7 shears of Martens (1979) in the eastern nose area of the Ratelpoort synform. (It should be mentioned that the Ratelpoort synform, which is a Late Fold, is an F-5 structure in his sequence). Martens described the S-7 shears as being as much as 20 metres wide, with refoliation zones of up to 1 metre wide. Furthermore, he distinguished between a northerly trending set with left lateral strike separation and a northeasterly trending set with right lateral strike separation. The orientation of the right lateral shears (his Figure 3.27), are similar to that of the Dabbiknik shears.

Late shears, steep structures and the Koperberg Suite

The intimate genetic relationship between the steep structures and the Koperberg Suite is well known and had been used as an exploration aid in the past. The salient features of steep structures are elegantly described by Lombaard and Schreuder (1978). The strain history of the Koperberg Suite is, however, a subject of some dispute. The view held by O'okiep Copper Company geologists during the seventies and early eighties was that the basic bodies are post kinematic relative to the regionally significant Namaqua tectonic events (Lombaard et al., 1986, Table III). In contrast, McIver et al. (1983) suggested that the irregular forms of the basic bodies are the results of significant deformation. Conradie (1983) and Conradie and Schoch (1986a) described microscopic deformation textures in some anorthositic bodies of the Koperberg Suite. They concluded that the deformation was related to the steep structures albeit of limited extent. Venter (1984) showed that a mesoscopically observed kinematic fabric, the product of steep structure strain, is clearly superimposed on some of the basic bodies.

At the Klondike west prospect, north of Okiep, the leuco-diorite, which forms outcrops to the east of the prospecting pit, are characterized by complex structures. The rock displays a fairly penetrative planar fabric defined by the parallel orientation of the mafic phases. Under the microscope this fabric is associated with cataclastic texture in plagioclase, strongly suggesting that it is indeed a kinematic fabric and not an igneous flow structure. The igneous pyroxene in this rock is deformed and recrystallized

(see Figure 10.24). The fabric is predominantly parallel to the easterly trending steep structure fabric in the surrounding Nababeep Gneiss. At one point, however, the fabric turns towards the northeast. The rotation is accomplished over a distance of about 3 metres. The extension of the northeasterly trend is obscured owing to poor outcrop, but a few metres further to the northeast the fabric strikes easterly once again. If the return to the easterly direction is gradational in the unexposed region, a perfect S geometry would be defined, which would imply continuous steep structure deformation during development of the fabric. It is a common phenomenon that the newly formed shear fabric within a shear zone is folded during the progressive development of the shear zone (e.g. Ramsay, 1980).

From the above it can be concluded that at least some of the bodies of the Koperberg Suite show strain effects related to steep structure deformation. The absence of megascopic strain effects in most basic bodies spatially associated with steep structures does not preclude the possibility that significant deformation during and after intrusion, has taken place. One model does in fact suggests that no fabric developed because the mafic rocks were still in a magmatic state when deformed. Protoclastic textures have been recognized in some anorthosites (Conradie, 1983; Conradie and Schoch, 1986a). Alternatively, the scarcity of an internal fabric in rocks of the Koperberg Suite could be attributed to the competent nature of the rocks. In these terms one could compare the basic bodies with highly boudinaged pegmatites which, due to their competent nature, do not readily display internal fabrics.

A number of basic bodies of the Koperberg Suite are present in the Ratelpoort shear zone. For most part, no strain effects are mesoscopically observed. All of them cut across the regional fabric, which is defined mainly by the Skelmfontein refoliation. In the absence of a penetrative mineral refoliation related to the Ratelpoort shear zone, the relation of the basic rock to the Late shearing is not readily established. A kilometre north-west of Bulletrap, within the zone of intimately interbanded gneisses (see Annexure 1), a two phase intrusion of basic rock consists of a hypermelanic and a mesocratic part. The first mentioned rock exhibits a subvertical planar fabric with a strike parallel to the general trend of the Skelmfontein refoliation in the country rock gneiss. The regional fabric in the country rock has, however, a shallow dip (45° south-southeast). The steep dip of the fabric in the mafic rock is consistent with the steep dip of the new mineral refoliation associated with the Ratelpoort and Dabbiknik shear zones. Under the microscope the fabric is seen to be penetrative on millimetre scale and defined by the parallel orientation of biotite. Strain effects in the feldspar confirms the tectonic origin of the fabric.

It is unclear whether the fabric in the mafic rock described above represents the Ratelpoort or the Dabbiknik shear fabric. In general, however, one can conclude that the relations between the Koperberg Suite and the steep structures are similar to that of the Late Shears. This is then an indirect way of correlating the steep structures with the Late Shears, consistent with the interpretation given by Blignault et al. (1983).

9.4 EARLY STRUCTURES

9.4.1 INTRODUCTION

The early structures are those which occur within that enveloping surface which is deformed by the Late Structures. The most prominent of the early structures is the regional penetrative foliation. When the effects of the late structures are removed, an essentially subhorizontal macrostructure becomes apparent. This is clearly illustrated by the controlled cross section (constructed by S. W. van der Merwe) which is given with the printed map (Annexure 1). It is within this subhorizontal enveloping surface that the really significant (early) strain features are to be found. The early structures are subdivided into two main categories, namely the Skelmfontein structures and the older Namaqua structures. Relicts of a third (still older) category of structures, here referred to as the Gladkop structures, are preserved only in certain places.

The major thrust zones which separate the main tectonic domains consist of a combination of Skelmfontein and older structures. The thrust zones are themselves deformed by the Late Structures. The Groothoek Thrust is described by Blignault et al. (1983) and, in more detail, by van der Merwe (1986). The northern boundary is taken at the position where the shear fabric on the Vioolsdrif Suite granitoids becomes penetrative and the rocks distinctly gneissic. A distinct change in the weathering pattern of the granitoids, from round boulders in the north to a more platy type, can be observed from a distance at this transition. Van der Merwe (1986) considered the main locus of movement along the Groothoek Thrust Zone to be at the regional junction between recognizable Vioolsdrif Suite granitoids and schistose rocks of the Groothoek Formation. Shear strain continues into the footwall of this plane and southwards becomes indistinguishable from that of the northern extension of the Skelmfontein Thrust Zone. The cross section (Figure 1.2) shows the ramp configuration of the Groothoek Thrust Zone. The Richtersveld Domain had been transported southwards over the Steinkopf Domain along the Groothoek Thrust Zone and the northern extension of the Skelmfontein Thrust Zone.

Van der Merwe (1986) shows that the Wyepoort Granite had transgressed the Groothoek shear fabric in the northern parts of the thrust zone, but that the granite is marginally foliated. For purposes of correlation the relations between granites and shear fabrics at a number of localities in the study area are described below.

9.4.2 THE SKELMFONTEIN STRUCTURES

General

The Skelmfontein structures are a series of subhorizontal shear zones in which the strain effects range from partial refoliation to total reconstitution. They are non-penetrative in both the Steinkopf Domain and the Okiep Copper District and they culminate in the Skelmfontein Thrust Zone. The Skelmfontein structures are essential components of the thrust zones which separate the Steinkopf Domain from the Copper District in the south, the Geselskapbank Domain in the east and the Richtersveld Domain in the north.

During the regional mapping of the area, one of the most prominent of these structures was first recognised by the author as a zone of penetrative refoliation at Skelmfontein se Poort (locality 5, Figure 9.1). The refoliation is spectacular in the Gladkop Suite grey gneiss on the northern side of the poort (Figure 9.9). The Skelmfontein-type shear zones have been subdivided by Martens (1979) into his F-3 and F-4 structures, but this subdivision was rejected by Blignault et al. (1983). Martens proved that the Skelmfontein refoliation (his F-3 and F-4 structures) is indeed located within the subhorizontal enveloping surface folded by the Ratelpoort synform. Subsequent investigations by van der Merwe (1986) and Strydom (1985) led to the recognition of the Skelmfontein Thrust Zone as a macrostructure of regional significance.

The Skelmfontein Thrust Zone is a zone of penetrative refoliation and shearing which separates the Steinkopf Domain from the Okiep Copper District. The thrust is located in a planar zone of contrasting lithology and the different lithological types are intimately interbanded on centimetre to metre scale (see the "intimately interbanded" zones shown on the printed map). Most of the stratigraphic units of the Steinkopf Domain and Copper District are represented in the Skelmfontein Thrust Zone. The Ratelpoort Shear Zone is superimposed on the Skelmfontein Thrust for most part, adding to the complex structure of this zone, which constitutes the northern limb of the Ratelpoort synform.

A kilometre westward from Skelmfontein se Poort, at the structural base of the Khurisberg Subgroup (locality 6, Figure 9.1), a small lense of calc-silicate rock displays the effects of at least three deformation episodes (Figure 9.10). This demonstrates the complex structural history of the metasedimentary rocks. Although small scale interference structures such as those in Figure 9.10 are of limited use in the unravelling of the actual sequence of deformation events, the observed effects are consistent with other lines of evidence concerning the protracted tectonic history of the metasediments.

The Skelmfontein fabric in the Leeupoort augen gneiss

In the Copper District the Skelmfontein refoliation is zonally developed in the augen gneisses (van der Merwe, 1986). On the southern side of Skelmfontein se Poort (locality 7, Figure 9.1) the refoliation of the Leeupoort augen gneiss, as seen on outcrop scale, is an approximate small scale model of the relationships in the augen gneisses of the Copper District. A series of three photographs show, first of all, that the Skelmfontein fabric is zonally developed, secondly, that it is superimposed on an older foliation (i.e. a refoliation) and thirdly, that entire zones are penetratively refoliated in some places. In the latter instances the pre-existence of older fabrics is impossible to recognize (Figures 9.11a,b and c).

Effects on the Spektakel Suite in the south

The genetic relations between the Kweekfontein Granite and the Skelmfontein shearing is described in Chapter 6. Although the Kweekfontein Granite lacks mica, which precludes development of conspicuous planar fabrics, a foliation is invariably visible in the rock, albeit faintly in places. Martens (1979) described examples where the foliation in the Kweekfontein Granite is a refoliation in xenoliths of older gneiss. He concluded that the

emplacement of the Kweekfontein Granite was synkinematic with respect to his F-4 (i.e. Skelmfontein) structures (ibid., p. 80).

The Skelmfontein deformation of the Rietberg Granite can be considered in terms of three examples. In the Klipvloer area, north of the Jan Coetzee mine, in the western part of the Ratelpoort synform (locality 8, Figure 9.1), the Rietberg Granite generally lacks an obvious kinematic fabric. In zones of 2 to 3 metres in width, however, a foliation is developed, especially in the vicinity of xenolithic rafts of the pelitic metasediments described in Chapter 3.3.2. This foliation has a shallow dip towards the south. Veinlike apophyses of Rietberg Granite display small scale folds with axial planes parallel to the foliation. Approximately 2.5 kilometres west-southwest of Bulletrap (locality 9, Figure 9.1), where the Steinkopf Gneiss and the Rietberg Granite meet along a regional junction, a similar situation is found with respect to xenolithic rafts of Gladkop Suite grey gneiss. The foliation in the Rietberg Granite is generally more penetrative in this area. Apophyses of the granite into a xenolithic raft of the grey gneiss is here folded in ptygmatic fashion and a penetrative axial plane foliation is found in the hinge zones of the small scale folds. The situation is schematically illustrated in Figure 9.12. A third example is found northeast of Bulletrap. Here, a satellite body of Rietberg Granite is transformed into a fine-grained to medium-grained gneiss with a penetrative foliation. The rock is still recognized as Rietberg Granite by virtue of its characteristic grains of dark quartz interspersed with grains of nearly white feldspar, although virtually devoid of mafic phases. The gneissic granite occurs in the form of bands parallel to the foliation/banding of the country rock Gladkop Suite gneisses. On mesoscale the gneissic granite cuts across older foliation/banding in the Gladkop rocks. Smaller apophyses into the country rock are ptygmatically folded, with the Skelmfontein refoliation being axial planar to the small scale folds.

An interesting situation arises from the phenomena discussed above, because a feature that is commonly used to indicate the antiquity of the grey gneisses of the Gladkop Suite, namely the preponderance of ptygmatic folds, can, in some places, be younger than the Rietberg Granite. The latter is traditionally considered to be an essentially post-tectonic intrusive (e.g. O'okiep Copper Company, 1975; Lombaard et al., 1986.).

The relation of the Skelmfontein refoliation to the Middelplaat dykes is illustrated in Figure 9.6. If the interpretation of the easterly trending refoliation in this figure is correct, the intrusion of the Middelplaat dykes must represent a post-Skelmfontein event. The vertical attitude of the Middelplaat dykes appears to place them in a different structural category than the rest of the Spektakel Suite. This may, however, be more apparent than real, as is illustrated by the orbicular dyke found at locality 10, Figure 9.1. The northeasterly trending orbicular dyke (more or less granitic in composition) appears to cut across the Skelmfontein refoliation, locally penetratively developed in the Leeupoort augen gneiss. Closer inspection reveals that the refoliation transects the dyke and that the orbicules are flattened parallel to the trace of the refoliation (Figure 9.13). The contact between the dyke and the country rock gneiss is somewhat disturbed on decimetre scale, but on metre scale it is straight for the entire exposure (30 metres). The stratigraphic position of the orbicular dyke is unknown, but it probably belongs to the time bracket of the Spektakel Suite.

The Nariams area

The eastern part of the mapped area is characterized by two macrofolds and zones of penetrative refoliation, all attributed to Skelmfontein deformation.

Southeast from Nariams the contact between the Brandewynsbank Gneiss and the structurally overlying Steinkopf Gneiss is folded into a macroscopic tight synform (see Figure 9.14). On map scale, the limbs of the fold is characterized by penetrative refoliation. To the southeast of Nariams this refoliation is particularly well developed in a broad zone. The zone consists of all three gneiss units of the Gladkop Suite, with minor calc-silicate lenses and bands of Eyams Granite, intimately interbanded on metre scale. The origin of this intimately interbanded zone is similar to the one immediately north of Bulletrap, described above. The fact that the foliation/banding in the limbs of the macro fold is actually the result of at least a second penetrative deformation event, superimposed on the older rocks, is illustrated at locality 1, Figure 9.14. Here, thin amphibolite bands display an interference structure of the coaxial type, illustrated in Figure 9.15. The macrofold can be compared directly with the the second phase of folding in Figure 9.15. At locality 2, Figure 9.14, in the hinge zone of the large fold, older minor folds with a Z-geometry are possible correlatives of the older folds (Figure 9.16), which occur within the foliation/banding deformed by the macro structure. A mineral refoliation, axial planar to the macro fold, is inconspicuous in the hinge zone.

Younger intrusive rocks, deformed by the Skelmfontein event, serve as valuable time markers. At locality 3, Figure 9.14, outside the zone of Skelmfontein refoliation, a small body of Eyams Granite transects the regional fabric in the country rock Brandewynsbank Gneiss. Apart from some minor effects of northeasterly orientated Dabbiknik shearing, the Eyams granite is in this case undeformed. At locality 4, Figure 9.14 however, Eyams Granite is present in the form of bands, 1 or 2 metres wide, which are oriented parallel to the refoliation/banding. The schlieren in the granite are folded and the rock displays a distinct internal foliation. In this region the emplacement of the Eyams Granite can thus be bracketed by the older regional foliation and the Skelmfontein refoliation.

Another intrusive rock affected by the Skelmfontein refoliation is the Nariams metadolerite. The dolerite occurs in the form of a disrupted (boudinaged) dyke which can be followed for about 5 kilometres in a southeasterly direction across a regional contact between the Steinkopf and Brandwynsbank Gneisses (see Figure 9.14). The dolerite boudins are marginally foliated and transformed to amphibolite. At locality 5, Figure 9.14, a xenolith of Steinkopf Gneiss with N2 neosomes, representing the Namaqua fabric, indicates that the dolerite essentially belongs to the same time bracket as the Eyams Granite, in this region.

The Eenriet area

The relations between the Eyams and Wyepoort Granites and deformation in the Eenriet area, is illustrated at four localities indicated in Figure 2.3. At locality 10, the Eyams Granite is undeformed and has all the attributes of a post tectonic (migmatitic) granite. A vague northeasterly trending foliation (Dabbiknik foliation, see above), can only just be recognized in

some places. At locality 11 (Figure 2.3) a faint foliation with a shallow northerly dip is developed in a concordant band of Eyams Granite immediately below the metaquartzite. A thin dyke of Wyepoort Granite cuts across the Eyams Granite. The fabric is in fact more clearly visible in the dyke because of its finer grain size and higher biotite content. These relations are indicated in Figure 9.17.

At locality 12 (Figure 2.3) the Kabina Formation is also intruded by both the Wyepoort and Eyams Granites. Here small apophyses of the Wyepoort Granite in the schistose metasediments are folded and the granite is penetratively foliated. The Eyams Granite is also foliated but not to the same extent as the Wyepoort Granite, clearly a function of relative viscosities controlled by primary grain sizes and mica contents.

At locality 13 Figure 2.3 the country rock is a pentratively foliated, medium-grained leucogneiss, mapped as undifferentiated pink gneiss at first (see the Namaqualand Geotraverse Map, Annexure 1), because it could not be correlated with a known stratigraphic unit in the area. Subsequent detailed observations, however, revealed metre scale 'structural xenoliths' - small areas which were less affected by the penetrative deformation. In these relict areas the primary characteristics are sufficiently preserved for the rock to be recognized as Eyams Granite. On map scale the penetrative foliation of this gneissified Eyams Granite is parallel to the regional Namaqua fabric, typical of the Skelmfontein refoliation. Where this foliation is penetratively developed, it is difficult to distinguish between the Skelmfontein foliation and the older regional foliation.

The Konkyp Gneiss

The main body of Konkyp Gneiss always has a gneissic fabric, while the marginal zone is characterized by a finer grain size and generally by a more penetrative foliation. At locality 11, Figure 9.1, the regional fabric in the Konkyp transects the contact between the gneiss and a minor body of Wyepoort Granite, although the foliation in the Konkyp Gneiss is more penetratively developed than in the younger granite. This is opposite to the situation where a dyke of the Wyepoort Granite carries a more penetrative strain fabric than the surrounding older Eyams Granite, due to viscosity contrast. The Wyepoort Granite at the locality of interest here has a biotite content comparable to that of the Konkyp Gneiss. The difference in the intensities of the foliation indicates a longer history of deformation for the Konkyp Gneiss than for the Wyepoort Granite. This phenomenon is interpreted as indicative of the effects of early Namaqua deformation in the Konkyp Gneiss as well as the relatively late Skelmfontein shear strain. The Wyepoort Granite was affected by the Skelmfontein shearing only.

The Geselskapbank Area

Strydom (1983) and Strydom et al. (1987) unraveled extremely complex structures in the Geselskapbank Domain. Thrust faults of different magnitudes, imbricate structures and isoclinally folded thrust planes are common. The Skelmfontein Thrust is shown by Strydom to form the boundary between the Geselskapbank Domain to the east and the Steinkopf Domain to the west. A series of major thrust faults occur in the hanging wall of the Skelmfontein Thrust and thrust tectonics were clearly active over an extended period of

time, producing more than one set of refoliations. Strydom recognized two major phases of isoclinal folding, associated with thrusting, namely F-2 and F-3 (his terminology). The Skelmfontein structures described above, the Skelmfontein Thrust as demarcated by Strydom, and his F-3 structures are all broadly time-equivalent, being superimposed on the older Namaqua fabric.

9.4.3 EARLY AND PRE-NAMAQUA STRUCTURES

General

The close genetic association between the main phase of the Namaqua orogeny and the Little Namaqualand Suite of augen gneisses is indicated by the fact that, on a regional scale, the distribution of these gneisses corresponds closely with the highest grade metamorphic zones. In the Copper District the isotopic age of the most voluminous of the augen gneisses, namely the Nababeep Gneiss, also corresponds to the 'peak Namaqua metamorphism' (Barton, 1983; Clifford et al., 1975a). This is consistent with the interpretation that the emplacement of the augen gneisses was syntectonic with respect to the main Namaqua orogeny. The augen gneisses dominate the lithology of the Namaqua mobile belt and serve as important time markers for early structures.

The Copper District

The structural features of the gneisses and other rock types in the Copper District have been described and interpreted by several authors (e.g. Benedict et al., 1964, Marais et al., 1975, Clifford et al., 1975a and van der Merwe 1986) and only the most important features are summarized here.

In the Copper District the augen gneisses form extensive subhorizontal sheets with a penetrative foliation (commonly referred to as S-2) parallel to the contacts. This regional foliation of the augen gneisses represents the most obvious structural effect of the early deformation phase of the Namaqua orogeny. In some places the Skelmfontein refoliation is superimposed on the older fabric, complicating structural analyses. Early Namaqua isoclinal folds (commonly referred to as F-2 folds, mainly after Joubert, (1971) are characteristic of the metasedimentary rafts. These folds are recumbent and the regional foliation of the augen gneisses is axial planar to them. Thus, while the granites were being deformed to become gneisses, planar xenoliths with a favourable attitude relative to the direction of shortening, were folded.

Structures older than the augen gneisses are not easily recognized. Sub-angular xenoliths of grey gneiss (Gladkop Suite) and amphibolite are reported in less deformed parts of the Nababeep Gneiss, in the southern parts of the Copper District (Marais and Joubert 1980a). F.J.G. Schreuder (pers. comm., 1980) pointed out xenoliths of grey gneiss (correlated with Steinkopf Gneiss), in Nababeep Gneiss south of Springbok. The grey gneiss xenoliths contain leucosome bands parallel to its penetrative foliation/banding. The Nababeep Gneiss transects the neosomes and the foliation/banding of the grey gneiss, suggesting deformation and metamorphism which predate the Little Namaqualand Suite. Martens (1979, p.9) suggested the existence of schistosity earlier than Brandewynsbank Gneiss. According to him leucosomes in metasediments of the Khurisberg Subgroup in the eastern nose area

of the Ratelpoort Synform, are transected by the gneiss. Hypotheses regarding tectonic features of such antiquity are discussed in the final chapter.

The Steinkopf Domain

Apart from the effects of late shearing, the regional fabric in the Steinkopf Domain is essentially subhorizontally disposed. The flat-lying fabric consists of zonally developed Skelmfontein refoliation zones and an older fabric. The older fabric is the penetrative regional foliation/banding of the Gladkop Suite gneisses, which is geometrically indistinguishable from the S-2 fabric in the augen gneisses. Some isoclinal folds are interpreted to be pre-S2 in age. One example of a pre-S-2 structure is at outcrop GS-1 near Witwater where an isoclinal fold within the enveloping surface of the Early Namaqua regional fabric is defined, inter alia, by the geometry of a still older foliation in Noenoemaasberg Gneiss (see the description of the detailled map of outcrop GS-1 near Witwater in Chapter 11). These features imply gneissification of the Gladkop Suite prior to the development of the regional Namaqua fabric, as is also suggested by the xenoliths in the Nababeep Gneiss described above.

A similar structure, but on a different scale, is the Spitskop enclave south of Steinkopf. The macroscopic fold, defined by the enclave outline, represents the attitude of the Early Namaqua enveloping surface (see the geological section, Annexure 1). At locality 7, Figure 2.1, the northeastern limit of the Besondermeid Formation is marked by a well defined fold closure. The traces of structural grain indicated around this fold closure are as seen on an aerial photograph. An investigation of this structure during the mapping part of the project, revealed that an old foliation/banding in the Gladkop Suite gneiss can be followed around this fold nose. It is suggested that a similar situation exists at the other end of the enclave (east of locality 2, Figure 2.1), although outcrops to prove it do not exist. The Spitskop enclave thus provides at least one macroscopic example similar to the small scale fold at outcrop GS-1 at Witwater referred to above.

In the gneiss domes east of Steinkopf (Locality 8, Figure 2.1) banded metasedimentary rocks within the Brandewynsbank Gneiss show small scale folding which might mirror the Spitskop structure in diminutive form. A flattened domal structure is folded by Dabbiknik deformation. The domal structure either represents an interference of two non-coaxial and non-coplanar fold phases, or the outcrop surface represents a section through a small sheath fold, normal to the stretcing direction (Figure 9.18). If the suggested fold hinge exists in the vicinity of locality 2, Figure 2.1, then the Spitskop enclave could be the macroscopic version of the structure depicted in Figure 9.18.

A peculiar phenomenon in the gneisses of the Gladkop Suite is the presence, in some places, of mafic rods. In addition to normal amphibolite bands and lenses, which are tabular bodies, these mafic rods are linear. On the smooth domal gneiss outcrops it is often difficult to ascertain the three dimensional shapes of mafic 'bands'. At many places, however, it was noted that the mafic 'bands' do not extend far into depth. In some cases, the rods at the plane of the outcrop surfaces, can be followed for several metres (Figure 9.19). Statistically, the probability that such a linear body will appear at the outcrop surface is rather remote and therefore one can conclude that many such rods are distributed

through the volume of the Gladkop Suite gneisses. Lithologically the mafic rods vary from amphibolite to biotite-plagioclase rock. It is suggested that they developed through repeated and extreme deformation of once planar bodies (sills or dykes), consistent with the notion that the Gladkop Suite gneisses went through several penetrative deformation events.

The Konkyp Area

At Locality 11, Figure 9.1, small scale xenoliths of Brandewynsbank Gneiss are tightly folded with axial planes parallel to the regional foliation of the Konkyp Gneiss. The internal foliation of the xenoliths follow the fold curvature and thus pre-dates the Konkyp Gneiss (Figure 9.20). Further to the east (Locality 12, Figure 9.1) the foliation/banding of a metasedimentary xenolith is transected by the Konkyp Gneiss. Microscopic examination confirmed the existence of a metamorphic/kinematic fabric, defined by the orientation of biotite flakes parallel to the banding of the xenolith. The regional foliation of the gneiss is parallel to a faint new foliation developed along the axial plane of a small fold in the xenolith (Figure 9.21). These occurrences indicate that the Konkyp Gneiss has intruded previously tectonised rocks, as is the case with the augen gneisses of the Copper District.

The odd occurrence of small scale folding of the gneiss foliation near the margins of the main body and the intensification of the foliation as described in the previous section, are considered to be the effects of superimposed Skelmfontein thrusting.

9.5 STRUCTURAL SEQUENCE

A brief summary of the structural sequence is given below. The entire tectonic history is interpreted in Chapter 12. The symbols D_1, D_2 signify sequential deformation stages.

Structure	Comment
D_1	Minor remnants in the pre-Little Namaqualand Suite rocks.
D_{2a}	The most important phase of deformation producing the principal part of the gneissic foliation in the augen gneisses. The primary horizontal disposition reflects early thrust tectonics.
D_{2b}	The Skelmfontein and related refoliations were produced during relatively late thrusting.
D_{3a}	Late open folds.
D_{3b}	Late Shears with an easterly orientation.
D_{3c}	Steep structures.
D_{3d}	Dabbiknik folding and refoliation.
D_4	Northwesterly trending minor shears.

The D_4 shears are considered to be the youngest significant structures associated with the Namaqua mobile belt. Major late faulting affected the cover rocks as well and are not directly related to the Namaqua Orogeny.

10 METAMORPHISM

10.1 INTRODUCTION

The highest grade zones in the eastern parts of the Namaqua mobile belt, of which the study area represents a small portion, strike northwesterly parallel to the 'Namaqua Front' (Figure 1.1). The high grade rocks follow the general trend of the mobile belt, reflecting the PT-gradient of the Namaqua tectogenesis. In the western region however, (Namaqualand sensu stricto) similar northwesterly trends of the metamorphic zones (Joubert, 1971) are considered to be the result of reworking during the later Gariep tectogenesis (e.g. Zelt, 1980a and 1980b). In the study area (the Geotraverse), the metamorphic zonation follows the outline of the Richtersveld Domain with the result that the metamorphic zones strike easterly. The Richtersveld Domain represents an island of relatively low grade rocks (upper greenschist to lower amphibolite facies) in a sea of high grade rocks (middle and upper amphibolite to granulite facies).

In the paragraphs below the salient metamorphic characteristics of key parts of the study area are discussed in terms of the prevalent metamorphic assemblages. Where applicable, reference is also made to variations in mineral chemistry. Geothermometry and geobarometry are dealt with at the end of this chapter.

10.2 THE RICHTERSVELD DOMAIN

10.2.1 PETROGRAPHY

The metavolcanites in the Richtersveld Domain are very fine-grained. Incomplete metamorphic reconstitution is indicated by pristine plagioclase phenocrysts and amygdaloidal structures in the metavolcanites, as well as by relict pyroclasts in the metavolcaniclastic rocks. In general, the mineral assemblages in these rocks indicate metamorphic conditions near the transition between the greenschist facies and the amphibolite facies.

With the exception of the Late Shears, Namaqua kinematic fabrics (attributable to the Namaqua tectogenesis) are not developed in the core zone of the Richtersveld Domain. The prograde mineral assemblages define the axial plane foliation of macroscopic isoclinal folds of pre-Vioolsdrif Suite age (van der Merwe, 1986), suggesting regional metamorphism in the time bracket 2 000 Ma to 1750 Ma, i.e. the Orange River Orogeny. Namaqua mineral ages reported by Reid (1977), however, reflect thermal overprinting as is also apparent from textures described below. The Late Shears produced new mineral schistosities defining greenschist metamorphic conditions.

The Vioolsdrif Granitoids are themselves zonally affected by the pre-Namaqua Tsams Thrust (Blignault et al., 1983) and they also display progressive strain and mineralogical reworking of Namaqua age towards the Groothoek Thrust Zone. With standard optical techniques, no mineralogical evidence of regional metamorphism related to the Orange River Orogeny is discernible in the granitoids.

The mineral assemblages and brief petrographic descriptions of selected specimens from that part of the Richtersveld Domain

included in the study area, are given in Appendix 4.1. One sample (SK070) is from a mafic dyke which transects Vioolsdrif Granite near Bitterfontein (see Annexure 1 and Figure 10.1). The rest are all metavolcanite samples from the Haib Subgroup and range in composition from basaltic to rhyodacitic. Sampling sites of the metavolcanites are limited by the outcrop pattern of the kilometre scale metavolcanite rafts in Vioolsdrif granitoids. The boundary between the Richtersveld Domain and the Transition Zone is taken where regional Namaqua fabrics becomes conspicuous in the field; the position of the boundary is therefore not clearcut or marked by lithological changes. Several metavolcanite samples from within the Groothoek Thrust Zone are actually included in Appendix 4.1. Sample localities are shown in Figure 10.1.

Parageneses typical of both upper greenschist and amphibolite facies occur; detailed observations for the mafic and intermediate rocks lead to a threefold classification of assemblage types. Type (i) represents prograde upper greenschist facies assemblages, type (ii) prograde lower amphibolite assemblages and type (iii) retrogressive greenschist parageneses. While the relation between the first mentioned two types of assemblages and tectonism is difficult to interpret, the retrogression which yielded type (iii) assemblages is fairly clearly associated with the late Namaqua Nous Shears described by van der Merwe (1986).

Quartz and plagioclase are common to all samples except the ultrabasic rock (SK043). Type (i) assemblages are characterized by actinolite of bimodal size distribution and associated greenish biotite; relict igneous plagioclase and quartz phenocrysts and amygdales are common. The type (ii) assemblages contain blue-green hornblende and/or brown biotite as main mafic phase(s); epidote is usually present but no prograde chlorite was found. In some cases a distinct compositional zonation is evident in the type (ii) amphibole, namely pale to colourless (actinolitic) in the centre and bluish-green (hornblendic) at the rim. This aspect is discussed in greater detail below.

The type (iii) assemblages are characterized by chlorite as the main mafic phase, which have partially or completely replaced biotite and/or hornblende. The plagioclase in these samples are extensively saussuritized. In the metavolcanites of intermediate composition (dacitic), skeletal muscovite porphyroblasts are found in addition to the sericite in the plagioclase. The presence of white mica ranging in grain size from minute sericite flakes (in the plagioclase) to skeletal porphyroblasts, indicates a probable genetic relation between the plagioclase breakdown and the muscovite growth.

The metavolcanite sample with the best preserved igneous attributes (SK400) is a quartz porphyry with perfectly preserved plagioclase phenocrysts. A few of these phenocrysts show undulose extinction and kinked twin lamellae. Most of the quartz phenocrysts are recrystallized, resulting in granoblastic interlobate quartz aggregates. The random orientation of relict igneous plagioclase crystals (see Figure 10.2) in a very fine-grained matrix, reflects the original igneous texture. No primary dark minerals are preserved. The greenish biotite and the epidote are evenly distributed through the matrix, but also forms a few coarse-grained aggregates in some places. The preferred orientation of the biotite define a faint foliation which is superimposed on the relict igneous texture.

10.2.2 MINERAL CHEMISTRY

The results of all mineral analyses are listed in Appendix 5. Fairly extensive electron microprobe analyses of minerals in the volcanites and intrusives of the Richtersveld Domain were reported by Reid (1977). He listed many calcic amphibole analyses with hornblende compositions; most of the amphiboles examined are of igneous origin. The metamorphic amphiboles have compositions on either side of the actinolite - hornblende miscibility gap suggested by Miyashiro (1973). The prevalent typomorphic mineral assemblages and compositions were interpreted by Reid to represent the products of upper greenschist facies metamorphism. Van Zyl (1986) reported additional mineral analyses of four mafic metavolcanite samples from Reid's original collection and found essentially similar amphibole compositions. The sample localities of the specimens investigated by Van Zyl in the Richtersveld Domain (identified by the code DRL) are also shown in Figure 10.1.

The calcic amphibole in one of the metavolcanite samples (DRL099 - see Figure 10.1) consists of green hornblende rims mantling cores of light-coloured amphibole, originally thought to be actinolite. Similarly mantled amphiboles are found in sample SK043 (see Appendix 4.1). As part of a joint investigation, DRL099 was analyzed once again by the present author. One particular mantled grain was analyzed along two traverses, each traverse approximately 0.5 mm long across the entire grain with one hundred spot analyses per traverse (Figure 10.3). The pale centre turned out to be 'normal' magnesio-hornblende, somewhat more silica-rich and alumina-poor than the green rim. The centre is not homogeneous and, especially along the one traverse, 'lamellae' of the rim type were found. Most of the transitions from the one compositional type to the other are sharp, but, in some cases, the transitions appear to be gradational over 0.05 mm. These relations are shown graphically in Figures 10.4a and 10.4b. In Appendix 5.1 most of the more than two hundred full analyses which were obtained from DRL099 (i.e. all of the analyses used in Figure 10.4) are given.

One other specimen was investigated by electron microprobe, namely SK394 from the Koubank River gorge (see Appendix 4.1 for petrographic description and Figure 10.5). In this sample, the amphibole is true actinolite. Chemical classification of calcic amphiboles from the Richtersveld Domain, as obtained by the present study and by Van Zyl (1986), are compared in Figure 10.6. From this figure it can be seen that no amphiboles from the present study, other than those from SK394, can be classified as actinolite. Similarly, none of the calcic amphiboles analyzed by Reid in the Richtersveld Domain could be classified as actinolites, not even as 'actinolitic hornblendes' according to the nomenclature of Leake (1978) (see Van Zyl, 1986, p. 175).

The coexisting typomorphic plagioclase in SK694 is albite. Both albite and oligoclase were found as typomorphic phases in DRL099. Reid reports albite and oligoclase in DRL042. Judging from the andesine composition, Van Zyl (1986, his Appendix 2) analyzed only a relict igneous grain in that specimen.

In DRL154 the hornblende composition deviates from the 'trend' displayed by those from the other three samples in Figure 10.6. The typomorphic plagioclase in DRL154 has an anorthite content of more or less 22 percent (van Zyl, 1986).

The composition of the plagioclase in some of the other

metavolcanite samples from the Richtersveld Domain, outside the core zone, were estimated with the Michel-Lèvy method and they are all estimated to be oligoclase. The amphiboles in all of these samples outside the core zone are deeply coloured pleochroic hornblendes.

10.2.3 DISCUSSION

The variation in mineralogical characteristics shown by the Haib metavolcanites and the one mafic dyke investigated in that part of the Richtersveld Domain included in this study, is shown in Figure 10.7. The mineral assemblages and mineral chemistry of the Koubank River gorge area have been shown above to represent greenschist facies metamorphism in the classic sense, as described by most textbooks. In mafic and intermediate metavolcanites, the key mafic phases are actinolite and/or green biotite while the plagioclase is albite. In the least deformed parts of this core zone, relict igneous features in even the very fine-grained matrix of porphyritic metalava indicates incomplete metamorphic reconstitution.

Outside the core zone, the calcic amphibole is hornblende; both albite and oligoclase occur as typomorphic phases. These features were discussed at length by Van Zyl (1986). He concluded (ibid., p. 289) that the two amphibole - two plagioclase assemblage of DRL099 represents an equilibrium paragenesis near the boundary between the greenschist facies and the amphibolite facies. A survey of the literature on this particular subject reveal different opinions concerning the existence of a miscibility gap between actinolite and hornblende (e.g. Mongkoltip and Ashworth, 1986). The features found in DRL099 could alternatively be interpreted as a disequilibrium texture, the result of a lower amphibolite phase of metamorphism superimposed on a greenschist assemblage. The acceptance of either interpretation would, however, make little difference to the tectonic implications (see below).

South of the intermediate zone the assemblages and mineral compositions indicate epidote-amphibolite facies metamorphism. This includes a large part of the Richtersveld Domain adjacent to the Groothoek Thrust Zone. Thus, a distinct metamorphic zonation is apparent in the part of the Richtersveld Domain studied, starting with greenschist facies in the core zone, followed by an intermediate zone and ending in epidote - amphibolite facies near the Groothoek Thrust zone. This zonation was previously unknown (e.g. Blignault et al., 1983). Due to the lack of continuous outcrop the locations of specific iso-reaction lines are not known.

According to the petrographical evidence, most of the chlorite can be classified as retrograde although the existence of some prograde typomorphic chlorite cannot be excluded.

Some reflection on the significance of the above in terms of tectonic modelling is opportune. On grounds of detailed structural analyses, van der Merwe (1986) concluded that the kinematic fabric in most of the Haib metavolcanites of the Richtersveld Domain is of pre-Vioolsdrift Suite age and thus a product of the Orange River orogeny. Namaqua mineral ages reported by Reid (1977) in the Richtersveld Domain, however, indicate thermal overprinting. The question therefore arises whether the mineral assemblages represent Orange River orogeny metamorphism or whether they reflect Namaqua metamorphism, with the Namaqua age phases mimetically following the pre-Namaqua kinematic fabric. The solution to the problem can most

likely be found in the properties of post-Vioolsdrif mafic dykes, here represented by specimen SK070. This dyke was metamorphosed to epidote-amphibolite facies in a static environment (no discernible fabric in thin section or hand specimen). Since the dyke post-dates the Vioolsdrif granitoids which, in turn, post-date the Orange River kinematic fabrics, one may conclude that the dykes reflect the thermal effects of Namaqua metamorphism. It would therefore seem that the mineral assemblages under discussion reflect Namaqua metamorphism; the observed foliation is related to the pre-Vioolsdrif fabric merely because of mimetic new mineral growth.

10.3 THE GROOTHOEK THRUST ZONE

10.3.1 GENERAL

The term Groothoek Thrust Zone as used here is synonymous with the 'Transition Zone' of Van der Merwe (1986). It covers the area between the Richtersveld Domain in the north and the interpreted trace of the Groothoek Thrust Fault. Lithologically the zone is dominated by the mica schists of the Groothoek Formation and various granite gneisses. Sillimanite and muscovite are common phases in the schists and in many of the gneisses. A few small outcrops of aluminous metapelitic rocks in the northern part of the Transition Zone exhibit interesting mineral assemblages referred to by Ward (1977). The sample distribution in the Groothoek Thrust Zone is shown in Figure 10.1 and the mineral assemblages found in some of these are given in Appendix 4.2.

10.3.2 THE GNEISSES

The Vioolsdrif Suite

Textural changes in the Vioolsdrif Suite granitoids from the Richtersveld Domain into the Groothoek Thrust Zone, serve as the single most important criterion for demarcating these tectonic domains. In the field the increasing development of a gneissic fabric is reflected by the mode of weathering, entailing a gradual change from prominent woolsack-type outcrops to negative flaky-type outcrops. The fabric change involves a reduction in grain size and the warping of typomorphic biotite and/or hornblende around flattened relict feldspar phenocrysts, to produce an augen texture. In local extreme cases the granitoids are transformed into very fine-grained gneisses, consisting virtually completely of typomorphic phases. Granodioritic gneiss in the Groothoek Thrust Zone is characterized by prismatic hornblende porphyroblasts which, in some places, are randomly oriented. Leucogranite is transformed into muscovite-bearing gneiss; one body in the region of Groothoek is particularly muscovite-rich. In the latter rocks replacement of biotite by muscovite is common.

The leuco-gneisses

South of the Groothoek Thrust, leucocratic metagranites of different ages, together with leuco-gneiss of uncertain origin, constitute the Kinderlê (pink gneiss) metamorphic complex of Van der Merwe, 1986. These gneisses are characterized by granoblastic textures with or without domainal fabrics. Sillimanite is a common minor phase in some varieties of the 'pink gneiss', it is generally present in the form of nodules (see discussion of the Kinderlê Gneiss in Chapter 6). Typical 'granitic' mineral assemblages characterize these rocks. In addition to K-feldspar, oligoclase and quartz, one or more of the following phases are normally present in

minor amounts, mentioned here in decreasing order of abundance: muscovite, biotite, sillimanite and garnet. The mere presence of sillimanite in a granitic gneiss implies the coexistence of K-feldspar and sillimanite. In most cases studied, however, it was found that while the sillimanite included in quartz is intact, only pseudomorphous white mica is in contact with or included in K-feldspar. Descriptions of a few representative samples are given in Appendix 4.2.3.

10.3.3 THE CALC-SILICATE ROCKS

Calc-silicate rocks are here defined as rocks consisting essentially of plagioclase and quartz with lesser quantities of the Ca-rich phases hornblende and epidote. They are generally considered to be of sedimentary origin and occur as minor layers within the Groothoek Formation. Mineralogically they differ from the amphibolites in the relative quantities of the different phases. The rocks are characterized by fine-granoblastic to medium-granoblastic textures, in some cases with hornblende porphyroblasts. Epidote is present as a prograde phase and, with white mica, as a retrograde breakdown product of plagioclase. Sphene is abundant in some cases.

10.3.4 THE AMPHIBOLITES

The amphibolites described here (see Appendix 4.2.2) generally occur as minor bands with an obscure origin. One sample (SK059) is from a thin apophysis of a major dyke which can be correlated with the post-Vioolsdrif Suite dykes described above (SK070). About half of the samples can be described as epidote-amphibolites, i.e. they contain prograde epidote. Hornblende colour (as seen in thin section) is blue-green in all of the samples. Plagioclase is almost completely saussuritized and biotite is replaced by chlorite and white mica in all samples. In one case (SK134) the retrogression is complete and the rock consists of chlorite, epidote, white mica and accessory opaque minerals. The prograde portion of the assemblages is typical of the lower parts of the amphibolite facies while the retrograde portion reflect greenschist facies conditions.

10.3.5. THE MICA SCHISTS

In terms of pre-tectonic rocks, the Groothoek Thrust Zone is dominated by the mica schists of the Groothoek Formation. Mineral assemblages and petrographic descriptions are given in Appendix 4.2.4. Quartz, muscovite, biotite and plagioclase are the major phases in almost all of the samples investigated. Sillimanite, both as fibrolite and discrete prismatic needles, are found in about a third of the specimens.

Minor lenses of muscovite-cordierite-sillimanite schist within the Groothoek Formation are described by Van der Merwe (1986). His Figure 2.10 depicts an andalusite porphyroblast which has grown over the regional penetrative schistosity, although some bending of the foliation had taken place around the crystal.

Tourmaline (schorlite) is found in some of the schist samples as interstitial grains. It is a common phase in pegmatites in the Groothoek Thrust Zone.

Saussuritization of plagioclase varies from complete to slight. In some cases the saussuritization advanced to the stage where discrete epidote grains form part of the mineral assemblage.

Chlorite occurs exclusively as a retrograde replacement of biotite.

The absence of K-feldspar is significant in terms of metamorphic conditions, while the absence of garnet is regarded as a function of bulk chemistry. It should be noted that garnet is present in some of the massive aluminous rocks.

The schistosity defined by the biotite and muscovite is a kinematic fabric which reflects a protracted history of deformation, culminating in the Skelmfontein thrusting. In general the fabric is defined by both micas, but the detailed textural relations vary. The biotite appears for most part to be syn-kinematic with respect to the local penetrative fabric-producing deformation. A major part of the muscovite is intimately associated with the biotite and decussate intergrowths between the two micas are a common feature, although some replacement of the biotite by late growth of muscovite is also common. In the process of replacement, opaque material, representing the excess iron from the original biotite, which could not be accommodated by muscovite, was either concentrated along cleavage planes or disseminated through the muscovite flakes. This caused the muscovite to have a murky appearance under the microscope. The late phase muscovite is post-kinematic relative to the main fabric-forming deformation. The muscovite is either randomly oriented or follows the existing fabric mimetically. Small scale folding in some of the specimens however, postdate the muscovite blastesis.

Texturally, the muscovite is of a somewhat later age than the biotite and certainly younger than the sillimanite, hence, in the strict sense, these three phases should not be listed as part of an equilibrium paragenesis. The significance of such textural interrelationships between metamorphic phases is, however, difficult to interpret. Readjustments of grain boundaries upon cooling, of the less refractory phases, should not be taken as evidence of retrograde metamorphism. The presence of significant amounts of tourmaline in a number of the schist samples suggests the presence of volatile components, which would promote grain boundary readjustments. One possibility is that the 'hydrothermal' action is part of a regional penetrative retrograde event which produced the muscovite-biotite-sillimanite assemblage. Mesoscopically the andalusite appears to be texturally of the same age as the muscovite, thus possibly post-dating the sillimanite. Late retrograde metamorphism of the schists is represented by the chloritization of biotite and sericitization in general.

10.3.6 THE MASSIVE ALUMINOUS ROCKS.

The sample localities are shown in Figure 10.1 and the mineralogy is given in Appendix 4.2.5. The cordierite schist unit in the Tsams/Hom metavolcanites south of Safnek are marked by the ubiquitous presence of cordierite-rich nodules in a muscovite-bearing matrix. Decimetre-scale zones consist almost exclusively of cordierite. Andalusite is the most abundant phase in some of the samples collected, while orthoamphibole dominates the mineralogy in a minority of cases.

On outcrop scale, the cordierite schist unit is penetratively foliated, but sampling bias towards the more resistant lithological varieties resulted in a collection of samples which are rather more massive than the norm. The rocks are generally porphyroblastic, the porphyroblasts consisting of cordierite and/or andalusite or, in a few cases, orthoamphibole. The matrix is generally composed of

quartz, plagioclase, biotite, muscovite and opaque minerals, although, in various combinations, all of these phases also occur as chadacrysts in the poikiloblasts.

Micro-structural relations indicate a protracted kinematic history. An early planar fabric is preserved as helicitic inclusions in the cordierite and andalusite porphyroblasts. In some cases the internal fabric is rotated relative to the matrix foliation while in other cases the porphyroblasts themselves are flattened together with the included fabric. In the latter instance the elongate shapes of the porphyroblasts and the matrix foliation are parallel. In most cases the regional foliation of the Groothoek Thrust Zone warps around the porphyroblasts.

Plagioclase varies from unaltered to completely saussuritized. Together with quartz it forms the bulk of the matrix of most specimens studied.

Cordierite is pinitized in most cases. This alteration appears to coincide with the saussuritization of the plagioclase and is later than the patchy replacement by retrograde chlorite. The most common inclusions in the porphyroblasts are elongate opaque grains. Other chadacrysts are quartz, plagioclase, biotite and muscovite.

Biotite is partially replaced by retrograde chlorite in most samples. This breakdown process appears to be of a later age than the muscovitization described below.

As in the case with the mica schists, the textural relations involving muscovite are complex. Where muscovite is included in cordierite, embayed forms indicate replacement of muscovite t cordierite. On the other hand, there is muscovite associated th clearly retrograde chlorite which replaced bi :ite and cordierite in patches. The bulk of the muscovite can be classified between the two extremes. It is spatially associated with biotite which it partially replaces leaving dark ferromagnesian remnants along cleavage traces.

In the cases where sillimanite and andalusite occur together in the same assemblage, some sillimanite are included in the andalusite porphyroblasts wh le most are interstitial and not preferentially associated with any particular phase. Most of the grain boundaries between sillimanite and andalusite show no evidence of reaction. Some contacts however, are marked by the presence of a thin film of quartz separating the two phases.

Porphyroblasts of orthoamphibole are present in two of the specimens examined and garnet in only one. Neither alumina silicate nor cordierite are present in the three samples, although it is admitted that saussuritized plagioclase is difficult to distinguish from some types of pinitized cordierite. Both garnet and orthoamphibole are partially replaced by bright green retrograde chlorite along cracks.

Staurolite was found in one sample only. It occurs as inclusions in cordierite and andalusite and is not found in contact with other phases. The grains have embayed and irregular boundaries suggesting partial replacement. On grounds of these relations, staurolite is considered to be a relict of an earlier stage of metamorphism.

Accessory tourmaline occurs interstitially in some samples. A few rounded zircon grains, included in the porphyroblasts as well as

occurring interstitially were also noted.

From the descriptions in Appendix 4.2.5 one can deduce the following sets of prograde parageneses for the dominant metamorphic stage in the Groothoek Thrust Zone:

qtz + plg + crd + bi
qtz + plg + crd + bi + ms
qtz + plg + crd + bi + ms + and
qtz + plg + crd + bi + ms + and + sil
qtz + plg + bi + ms + and
qtz + plg + bi + ms + sil
qtz + plg + bi + ms + and + sil
qtz + crd + and + sil
qtz + plg + bi + grt
qtz + plg + bi + ged

Apart from the orthoamphibole in one particular rock type, the mineral assemblages in the massive aluminous rocks can be adequately represented by the composition-assemblage diagram shown in Figure 10.8. This diagram also represents a reasonable model for the mineral assemblages in the mica schists. The frequent absence of sillimanite in the latter can possibly be explained in terms of the degeneracy created by the compositional colinearity between plagioclase, muscovite and sillimanite in the AFMK compositional space.

10.3.7 DISCUSSION

The assemblage diagram in Figure 10.8 is typical of the sillimanite zone of the Buchan type of metamorphic sequence. In the Dalradian Supergroup of Scotland and Ireland a distinction is made between an early Barrow-type metamorphic sequence, representing a medium pressure (kyanite) environment, and the later, low pressure type of sequence typical of the Buchan county in Scotland (e.g. Mason, 1978, p. 142).

Further confirmation of the low pressure environment of metamorphism in the Transition Zone is, of course, the presence of andalusite in the massive aluminous rocks of the Tsams/Hom Formation and in the cordierite-bearing schists of the Groothoek Formation. The coexistence of sillimanite and andalusite in a few cases show that the PT path passed below the aluminium-silicate triple point.

Textural relations between the andalusite and sillimanite are not clearcut. In the mica schists the sillimanite is aligned parallel to the regional penetrative foliation. In the same stratigraphic unit, the andalusite appears structurally younger, though not entirely post-tectonic. In the massive aluminous rocks, an extended structural record was preserved because the core zones of mesoscopic boudins escaped the final structural reworking during Skelmfontein thrusting (see Chapter 9). The textural relations described above suggest that the andalusite is a late kinematic phase and, in terms of the structural history, formed during the period of Skelmfontein thrusting. The 'andalusite out' line shown on the printed map (Annexure 1) therefore probably reflects metamorphic conditions during this late stage of Namaqua metamorphism.

10.4 THE KONKYP AREA

10.4.1 GENERAL

On map scale, the Konkyp Area is the easterly extension of the Transition Zone. This area is, however, isolated from the other domains by relatively large sand covered areas. Lithologically it resembles a mixture of the Copper District and the Steinkopf Domain in the sense that an augen gneiss similar to the Nababeep Gneiss, together with gneisses of the Gladkop Suite, dominate the stratigraphy.

The petrographic features of the important rock types are summarized in the paragraphs below while descriptions of some individual samples are given in Appendix 4.3. The positions of samples studied are shown in Figure 10.1.

10.4.2. THE CALC-SILICATE ROCKS.

Calc-silicate rocks occur as metre-scale bands and lenses in the gneisses. They consist mainly of plagioclase and quartz, with variable volumes of K-feldspar, diopside, hornblende and epidote. Grossularite is present in a few cases as well. Sphene is present in relatively high volumes in all samples studied, estimated at between 1 and 3 percent. The sphene occurs as individual crystals or groups of anhedral grains and as rims around opaque grains.

The hornblende is blue-green in thin section in all cases. Where in contact with diopside some replacement of the pyroxene by the hornblende is evident in every case and it is not settled whether hornblende was indeed part of the prograde assemblage.

The replacement features indicate that most of the epidote is of late retrograde origin. It occurs in minor amounts, having replaced diopside, hornblende or plagioclase.

Prograde parageneses (with sphene and an ubiquitous opaque phase) are:

pl + qtz + di (+ hbl ?)
pl + qtz + di + grs (+ hbl ?)

The lower stability limit of grossularite-rich garnet, in calc-silicate rocks, according to Liou (1973) is probably given by reactions such as

$$zo + qtz = grs + an + H_2O$$

which proceed towards the right above 620° C at a fluid pressure of 5 kb. Diopside can form at temperatures well below 600°C according to

$$tr + cal + qtz = di + CO_2 + H_2O$$

(Metz, 1970), but, since neither tremolite nor calcite are found in the calc-silicate rocks under consideration, it is not likely that the diopside developed according to this reaction. Although several references to the stability of diopside and of grossularite in metamorphites can be found in literature, the significance of parageneses where these two phases are found together is unclear (see further discussion under 10.6.2 below).

Gradational contacts between gneiss of the Gladkop Suite and

calc-silicate lenses indicate assimilation of the supracrustal rock by the intrusive gneiss precursor; the intervening rock type can be described as granitized calc-silicate rock. Another form of metasomatic alteration of these rocks, is represented by neosomes superimposed on the early fabrics of the grey gneiss. In the Konkyp area a variety of migmatitic features are developed (see Chapter 11); one of these involves the total recrystallization (melting?) of calc-silicate-rich parts of the grey gneiss. The products of this process are bodies several metres across in which a meduim-granoblastic texture (with no apparent foliation) is developed, superimposed on the normal fine-grained and foliated texture of the gneiss. Skeletal porphyroblasts of either diopside, grossularite or hornblende comprise the ferromagnesian phase (Figure 10.9). In thin section specimens from such metasomatized bodies show variable volumes of K-feldspar. Small-scale replacement of plagioclase by a micrographic to **symplektic intergrowth of K-feldspar and epidote** suggests

$$4(CaO.Al_2O_3.2SiO_2) + H_2O + K_2O \rightarrow$$
anorthite

$$4CaO.3Al_2O_3.6SiO_2.H_2O + K_2O.Al_2O_3.SiO_2$$
epidote K-feldspar

Whether such metasomatism was part of the formation of the granoblastic neosomes or part of late retrogression is unclear. Textural relations between diopside, hornblende, epidote and actinolite (the latter phase was found in one case) suggest two stages of retrogression, the first involving the development of hornblende at the expense of diopside and the second the development of epidote, chlorite and actinolite at the expense of both hornblende and diopside. One possibilty is that the formation of the large skeletal porphyroblasts of diopside, grossularite and hornblende, the growth of hornblende at the expense of diopside, the development of the granoblastic areas ('neosomes') and the metasomatism described above are all part of one high grade metamorphic stage and that the retrogression involving the rest of the epidote, the chlorite and the odd actinolite is part of a later retrograde event. Further discussion of these features is deferred until Chapter 12.

10.4.3 AMPHIBOLITES

The amphibolite samples investigated (Appendix 4.3.2) have normal amphibolite assemblages (quartz + plagioclase + hornblende) with the development of retrograde chlorite and epidote prominent in one case. The hornblende colour is bluish green in thin section.

10.4.4 GNEISSES

The three units of the Gladkop Suite, Kinderlê Gneiss and the Konkyp Gneiss are here included. As far as the felsic components are concerned and apart from relative grain sizes, the different varieties of gneiss are mineralogically similar. K-feldspar displays pronounced tartan twinning. Retrograde muscovite growth, at the expense of biotite and, in some cases at the expense of K-feldspar and sillimanite, characterize these rocks. In the case of the Konkyp Gneiss, the replacement of biotite by muscovite with resultant stringers of opaque ferromagnesian material within the newly formed muscovite, is especially notable.

10.4.5 METAPELITES

Biotite-sillimanite schist occurs as minor xenolithic bands in the Konkyp Gneiss and the Gladkop Suite gneisses. More prominent pelitic schist associated with metaquartzite structurally overlies the main body of Konkyp Gneiss.

Compositionally similar to mica schists in the Transition Zone, one important petrographic difference, namely the presence of K-feldspar, sets the pelitic schists of the Konkyp area in a different metamorphic class. The prograde assemblage K-feldspar + sillimanite is common in the samples studied, although, in most cases, the sillimanite in contact with K-feldspar has been replaced by sericite.

Retrogression with muscovite growth at the expense of biotite and sillimanite is also common. Some spectacular examples of muscovite-quartz micrographic intergrowths replacing K-feldspar + sillimanite associations were found. This is clear evidence of the retrograde reaction

$$kfs + sil + H_2O \rightarrow ms + qtz.$$

10.4.6 METAMORPHIC HISTORY OF THE KONKYP AREA

In the paragraphs above and in Appendix 4.3 evidence is given that high grade metamorphism was followed by a phase of retrogression involving extensive muscovitization of alumina-rich rocks and the development of epidote, some chlorite and, in one case, actinolite, in the calcic metamorphites. The high grade metamorphism post-dates that phase of deformation which produced the fine-grained foliated character of the Gladkop Suite gneisses, as indicated by the skeletal growth of diopside and grossularite in 'neosomes' superimposed on this fabric. The time relations between the emplacement of the Konkyp Gneiss and this phase of high grade metamorphism is obscure; the well developed neosome-features of the Gladkop Suite gneisses are absent in the Konkyp Gneiss. The metapelite xenoliths in the Konkyp Gneiss exhibit high grade assemblages which could conceivably predate the emplacement of the augen gneiss granite precursor.

10.5 THE EENRIET AREA

10.5.1 GENERAL

Aspects of the lithostratigraphy of the Eenriet area are discussed in Chapter 2.2.1. The rock types petrographically investigated are amphibolite, ultramafic rock, schistose metamorphite and massive cordierite-rich rock. Amphibolite and schist samples show pronounced retrograde effects while high grade assemblages are found in the garnetiferous metapelites and ultramafic rock. A number of representative rock samples are described in Appendix 4.4 and their field localities are shown in Figure 10.10.

10.5.2 AMPHIBOLITE

All of the amphibolite samples collected show retrograde effects to some extent. Plagioclase is largely saussuritized, in most cases with the development of distinctive epidote grains. In one sample retrograde clinozoisite is abundant. In another sample additional epidote have been introduced along veins. In a third of the

specimens studied, the hornblende is partially or completely replaced by chlorite. For the rest, the hornblende is unaltered even though the coexisting plagioclase may be totally replaced by epidote and white mica. The colour of the hornblende is blue-green in thin section. Biotite, present in five specimens, is partially or completely replaced by chlorite.

10.5.3 THE ULTRAMAFIC ROCK

The ultramafic rock referred to in Chapter 2.2.1 consists of large orthopyroxene grains and light-green hornblende. Ore and green spinel are accessory phases. The amphibole has partially replaced the pyroxene. The orthopyroxene is pleochroic in pink and forms a major component of the rock. Another pyribole was identified as a second orthopyroxene by electron microprobe analysis (see Appendix 5), but represents a minor phase. It is colourless and forms relatively small, elongate grains. Textural characteristics give no indication of the genetic relation between the two pyroxenes, apart from the fact that they are clearly separate phases.

The compositional difference between the two pyroxenes is subtle, but may be important in terms of origin. According to the scheme of Bhattacharyya (1971), orthopyroxenes with weight percentages

$$((MgO + FeO + Fe_2O_3) + 0.775Al_2O_3) < 44.304$$

are classified to be of igneous origin. In terms of the chemical compositions (Appendix 5.3), both orthopyroxenes in the ultramafic rock under consideration could thus be classified as igneous phases. Bhattacharyya does, however, note that the ionic redistribution in igneous orthopyroxene may, under certain conditions of metamorphism, not be sufficient to shift the composition of the pyroxene into the accepted metamorphic field (ibid., p. 504). The dominant orthopyroxene in the ultramafic rock from Eenriet could be considered as marginal in terms of his classification, since the composition plots near the line separating igneous from metamorphic orthopyroxenes on the graphical presentation; the composition of the second (minor) orthopyroxene is clearly 'igneous' (Figure 10.11). Because igneous rocks with more than one variety of orthopyroxene and no clinopyroxene are rare, the dominant orthopyroxene is interpreted to be a metamorphic phase. The minor orthopyroxene could then be igneous in origin, representing relict grains.

The chemical composition of the green spinel is listed in Appendix 5 (sample S765). The spinel can be classified as pleonaste on grounds of its relatively high magnesian content (e.g. Haggerty, 1976).

10.5.4 THE SCHISTOSE METAPELITES

The structural/stratigraphic distribution of the schistose metapelites are described in Chapter 2 and petrographic descriptions of seven representative samples are given in Appendix 4.4.3. The rocks typically contain retrograde muscovite which partially or completely replaced sillimanite, plagioclase and biotite. Quartz-muscovite micrographic intergrowths, similar to those described for the Transition Zone and the Konkyp area, represent the retrogression common to these schistose rocks. The most significant prograde assemblage found is

bt + Kfs + sil + pl + qtz

in specimen S745, indicating upper amphibolite facies metamorphism.

10.5.5 THE MASSIVE ALUMINA-RICH ROCKS

Garnetiferous metapelite occurs in isolated enclaves in the Gladkop Suite or Kinderlè Gneiss where the rocks were shielded from late shear strain and accompanying muscovitization. They are typically dark-coloured rocks which behaved in a more competent manner than the surrounding rocks during late shear deformation, even where the rock contains up to 30 percent biotite, resulting in boudins. Common parageneses are:

bt + alm + crd + qtz + pl

and

bt + alm + crd + ged + qtz + pl

Note the absence of K-feldspar and sillimanite. The chemistry of some of the constituent phases and the corresponding whole rocks are given in Appendices 3 and 4 respectively. The compositional relations between the ferromagnesian phases and whole rocks for four of the samples of interest are diagrammatically illustrated in a stereopair ACFM diagram (Figure 10.12).

Specimen SK297 fits well into the category of K-poor aluminous metasedimentary rocks discussed by Hudson and Harte (1985). They constructed a useful petrogenetic grid (ibid., p 246), according to which the paragenesis

grt + crd + ged

requires a metamorphic temperature of at least 600° C. The rest of the garnetiferous rocks contain biotite in addition to the above assemblage, reflecting a higher potassium content.

Chemically the garnets are zoned. A garnet porphyroblast in specimen SK296 was analyzed in some detail and contour maps of the Mn/(Mn+Mg+Fe) and Mg/(Mn+Mg+Fe) ratios are shown in Figures 10.13a & b. The contours show distinct prograde zoning with Mg content relative to Fe and Mn increasing from centre to rim. Such zoning is also evident from the core and rim analyses available for specimens SK387 and S752. The garnet in SK297 is practically unzoned while in S752 the garnets show retrograde zoning, with the cores richer in Mg.

The cordierite-garnet-biotite assemblages lend themselves to standard metapelite geothermometry (see Chapter 10.9). The temperatures obtained for the Eenriet area are summarized in Table 10.1 below.

The temperatures reflect the garnet zoning in all samples except in SK297 where the garnet is homogeneous and for which no analysis for contact cordierite could be obtained. The specimens with SK numbers are from localities 6 and 8 and S752 is from locality 5, Figure 10.10.

TABLE 10.1 GEOTHERMETRIC RESULTS FOR THE EENRIET METAPELITES

Each number (e.g. grt-1) refers to a particular spot analysis. c - grain centre; r - grain rim; cr - adjacent to chadacryst; inc - chadacryst; f - not touching another ferromagnesian phase.

No.	Mineral pair		T(°C)	Remarks
SK387	grt-2 c	crd-2 c	534	crd isolated from bt & grt
SK387	grt-2 r	crd-1 r	574	The two grains are in contact
SK387	grt-2 c	bt-1 c	538	bt isolated from crd & grt
SK387	grt-1 r	bt-2 r	638	The two grains are in contact
SK297	grt-r	crd-1 r	615	Rim of zoned grt-porphyroblast touching crd
SK297	grt-1 r	crd-1 r	548	The two grains are in contact
SK297	grt-2 c	crd-2 c	595	crd isolated from bt and grt
S752	grt-1 c	crd-1 c	659	Centres of two large porphyroblasts in contact
S752	grt-3 r	crd-2 c	638	The two grains are touching, the crd rim too pinitized to be analyzed
S752	grt-1 c	bt-1 c	658	grt- porphyroblast, bt isolated
S752	grt-2 r	bt-2 r	588	Same grt as above, near rim, touching bt

10.5.6 DISCUSSION

The high grade nature of the rocks building the Eenriet Mountains are indicated by the Kfs + sil and the alm + ged + crd parageneses in the metapelites. The maximum metamorphic temperature estimated by means of geothermometry is above 650° C. The virtually identical temperatures indicated by both the biotite-garnet- and the cordierite-garnet geothermometers in the case of S752 lends credibility to these numbers. Such a temperature is probably sufficient to stabilize metamorphic orthopyroxene in an ultramafic rock. The gedrite-bearing assemblages furthermore indicate a relatively low pressure since, at medium pressure (> 4 kb) the parageneses sil + ged would have become stable (Hudson and Harte, 1985, Figure 9).

Retrogression involved mainly the muscovitization of the aluminous schist and the development of epidote and chlorite in amphibolite. As in the Groothoek Thrust Zone in general, the retrogression is correlated with the latest thrusting, namely the Skelmfontein event.

The geothermometric values suggested by the observed compositional zoning in garnet, reflect prograde metamorphism during garnet growth in one locality (specimen numbers starting with SK) and diffusion zoning due to retrogression in the other locality (S752). The structural setting of the respective sampling sites are of

interest. The Eenriet Mountains consist of prominent metaquartzite beds with an associated banded metasedimentary sequence. The supracrustal units are all structurally duplicated and intersheeted with gneisses of the Gladkop Suite owing to thrust faulting and isoclinal folding, which took place during early subhorizontal Namaqua deformation, i.e. prior to the Skelmfontein event. The effects of the Skelmfontein event are most pronounced immediately above the structural top of the metasedimentary units. These effects diminish structurally downwards. The fabric in the gneisses below the metasedimentary sequence (the position of S752) is considered to be unaffected by Skelmfontein shearing. The prograde zoning in SK387 and SK296 shows that these rocks escaped retrogression during Skelmfontein deformation, despite their location above the structural top of the metasedimentary sequence. The retrograde zoning in S752 is probably not the result of the Skelmfontein tectonic event either, since the structural setting is outside the local Skelmfontein Thrust Zone. In terms of the early Namaqua thrusting, the SK samples are situated in the hanging wall and S752 in the foot wall of local thrust faults, suggesting that, if the retrogression in S752 was coeval with the progression in the SK samples, the hanging wall was heated while the foot wall was cooled during early Namaqua tectonism.

10.6 THE STEINKOPF DOMAIN

10.6.1 GENERAL

The Steinkopf Domain is not richly endowed with metapelites, the petrography of which forms the most important basis for metamorphic characterization in other parts of Namaqualand. Small outcrops of calc-silicate rocks are numerous and widespread, but these rocks are mineralogically monotonous and give no clues to possible metamorphic zonation in the Domain. A widespread distribution of amphibolites makes it possible to deduce metamorphic zonation, by taking cognisance of variation in hornblende colour as observed in thin section. The characteristics of mafic and mesocratic dykes give insight into the variation of metamorphism with time. An attempt to delineate metamorphic zonation in the Steinkopf Domain by means of grey gneiss petrology proved unsuccessful.

10.6.2 THE CALC-SILICATE ROCKS

The petrography of a number of individual specimens of calc-silicate rock is given in Appendix 4.5.1. and their geographical distribution indicated in Figure 10.4a. The rock type resists weathering and fresh material is readily available. The common prograde assemblage is

qtz + pl + grs + di

Epidote/clinozoizite is a common retrograde phase, clearly replacing plagioclase and the ferromagnesian phases. In one specimen, however, epidote appears to be in textural equilibrium with garnet. The particular sample does not contain diopside and a possible prograde paragenesis is

qtz + pl + grs + ep

Diopside can form in calcareous rocks at a lower temperature than grossularite (Chapter 10.4.2). The fact that, in a number of

samples studied, garnet occurs as a rim around the diopside, or forms porphyroblasts with diopside inclusions, indicate that the diopside formed earlier than the garnet. These textures also indicate some reaction involving both ferromagnesian phases; such a reaction is not described in standard texts.

Scapolite can coexist with plagioclase under amphibolite facies metamorphic conditions (e.g. Turner, 1981, p. 318 - 319). Pure meionite requires an extreme temperature (about 900° C) to form according to

an + cal = meionite

(Goldsmith and Newton, 1977). These authors showed, however, that, for coexisting plagioclase and scapolite, a decrease in temperature is accompanied by an increase in the sodium content of the scapolite. The relatively high marialite content (25 percent marialite, 75 percent meionite) of the scapolite in specimen S404B (see Appendix 4.5.1 and Appendix 5) is consistent with upper amphibolite facies metamorphic conditions.

10.6.3 THE AMPHIBOLITES

The amphibolite samples from the Steinkopf Domain differ from those from the domains to the north mainly in the pleochroism colour of the Z-direction of hornblende, this colour varying from blue-green in the north to olive-green in the south. A few samples contain diopside in addition to the normal plagioclase + hornblende + quartz assemblage.

The amphibolite is generally fine-granoblastic polygonal with a small variation in grain size. The orientation of hornblende and biotite (where present) defines a continuous foliation in most samples, the foliation being parallel to the dominant local foliation in the country rock. Descriptions of individual samples are given in Appendix 4.5.2.

The following prograde assemblages (with or without quartz) occur in the amphibolites of the Steinkopf Domain:

pl + hbl
pl + hbl + bi
pl + hbl + bi + kfs
pl + hbl + di
pl + hbl + di + kfs

Winkler (1979, p. 172) considered the presence of diopside in amphibolite to reflect 'high grade' or, at least, the higher temperature part of his 'medium grade'. This would indicate metamorphic temperature of around 600° C at least (ibid., p. 5).

Sphene is conspicuous in four samples studied while the opaque phase observed in a number of polished thin sections consists of magnetite-ilmenite composite grains. The presence of these Ti-rich accessory minerals suggests that the hornblende should be saturated with Ti, the component dominantly responsible for the colour changes which occur in hornblende with increasing metamorphic grade (e.g. Jackson, 1976). Distinction was made between blue-green, intermediate and olive-green to describe the pleochroic colour of the Z-direction of the hornblendes (see Appendix 4.5.2); the relevant geographical distribution is shown in Figure 10.14b. The hornblende in the southern part of the Steinkopf Domain is

olive-green while it is blue-green in the north. The presence of intermediate hornblende in the intervening area suggests a gradual increase in metamorphic grade from the north to the south.

10.6.4 THE METAPELITES

General

Metapelites in the Steinkopf Domain are restricted to the Spitskop metasedimentary enclave and minor bands and lenses in the gneisses. Sillimanite-bearing nodules are found widespread in the outcrops of Kinderlê Gneiss (see Chapter 5). Eleven of the metapelite specimens, described in Appendix 4.5.5, represent xenolithic (mostly schlieric) bands in the Kinderlê Gneiss from the eastern and central parts of the Steinkopf Domain, namely from Nariams (S261B, S261C, SK360), from the area north of Wildehondspoort (S023C, S023D, S146, SK160D, S260H, SK344), from north-west of Wildehondspoort (S705) and from east of T'Gybiekop (S713). Two samples from the Dabbiknik pelitic granulite (S579A, S579B) and two from the retrograde schists of the Spitskop enclave (S522, S535) complete the list. Figure 10.14c shows the sample distribution.

Minor occurrences in the Kinderlê Gneiss

Significant prograde assemblages in metapelitic samples from the eastern and central parts of the Steinkopf Domain are:

qtz + pl + kfs + sil + bt
qtz + pl + kfs + sil + bt + grt

Retrograde muscovite occurs as minor replacement of biotite. The modal volume of such muscovite nowhere exceeds 3 percent. Some of the specimens represent aluminous restite parts of migmatitic rock. The absence or low percentage of feldspars in these samples is interpreted to reflect the removal of the granitic component as the result of anatexis. A number of the specimens are completely free of muscovite, a feature nowhere found in biotite-sillimanite bearing metapelites of the northern domains.

Minor metapelitic bands in small outcrops of Kinderlê Gneiss, on the plain north-northwest of Kinderlê, contain significant volumes of retrograde muscovite, similar to the schistose rocks of the adjacent Eenriet Mountains. The description of a specimen from this locality was included in Appendix 4.4

The retrograde schist of the Spitskop enclave

The schists from the Spitskop enclave are penetratively retrogressed. Small sillimanite needles are preserved in quartz grains, but interstitial sillimanite is replaced by sericite. Biotite is largely replaced by chlorite. Garnet is preserved in some places (e.g. Figure 2.2), but, for most part, it is replaced by a fine-grained decussate aggregate of chlorite and sericite. The petrographical analysis shows that the prograde assemblages included biotite, sillimanite, garnet, quartz and plagioclase. An unequivocal prograde paragenesis-list is, however, impossible to deduce due to the penetrative effects of the retrogression.

There are no structural phenomena with which the retrogression can be associated. The retrograde phases either define a random fabric or an old fabric through mimetic blastesis.

The Dabbiknik metapelitic granulite

The most unique metapelitic rock from the Steinkopf Domain is the Dabbiknik pelitic granulite (S579A, S579B). The metamorphic paragenesis is not repeated elsewhere in the study area:

qtz + pl + bt + grt + ged + opx

with a minor volume of opaque minerals completing the mineral assemblage. The whole rock composition is given in Appendix 3.1 and analyses of most of the typomorphic phases are given in Appendix 5. The compositional relations of the constituent phases and the whole rock is shown in Figure 10.15.

The Fe:(Fe+Mg) ratios of the orthopyroxene and biotite are 0.395 and 0.310 respectively (two analyses of each of these phases are given in Appendix 5; in each case the two compositions are practically identical). These ratios suggest an equilibrium temperature of about 790° C according to the calibration of Fonarev and Konilov (1986). Fe-Mg distribution between biotite and garnet suggests a metamorphic temperature of about 700° C.

10.6.5 THE NARIAMS DOLERITE SUITE

The general stratigraphic and structural relations of the Nariams Metadolerite Suite are described in Chapter 8 and 9.4.2 respectively. The petrography of 11 samples are described in Appendix 4.5.4, the mineral chemistry of three samples is given in Appendix 5.

In the Nariams area a dyke is boudinaged on a macroscopic scale, due to Skelmfontein shearing, and marginally amphibolitized. Another dyke which cuts across all local fabrics in the Brandewynsbank Gneiss immediately southwest of Wildehondspoort (Figure 9.14) appears to be undeformed. The progressive transformation of the dykes to deformed metamorphites is observeable in outcrop. Three different sample sites are represented by the selected petrographic descriptions given in Appendix 4.5.4. In each of these localities transformation is evident over distances of one to five metres. The samples under discussion are the following (with arrows indicating the transformation):

SK245 -> SK246, SK249 -> SK251 -> SK252 and SK338 -> SK339. Specimen SK337 is from a different part of the body represented by SK338 and SK339. The stages of increasing transformation can be described as follows:

Stage 1

Metadolerite. The original dolerite texture is perfectly preserved with partial replacement of both orthopyroxene and clinopyroxene by olive-green to brown hornblende. The plagioclase grains are not recrystallized and original igneous forms are retained. The hornblende forms granoblastic polygonal aggregates with perfect triple junctions reflecting typomorphism (Figure 10.16a).

Stage 2

Similar to stage 1, but in this case the remaining pyroxenes are recrystalized to form granoblastic polygonal aggregates. Minute anhedral diopside grains occur inside relict igneous plagioclase crystals in elongate clusters parallel to the feldspar edges (Figure 10.16b).

Stage 3

Pyroxene amphibolite; the pyroxenes are recrystallized and display granoblastic forms. A few large plagioclase laths remain as igneous relicts.

Stage 4a

Amphibolite, indistinguishable from amphibolite in the country rock (Figure 10.16c).

Stage 4b

A fine-granoblastic two-pyroxene hornblende granulite, indistinguishable from such granulites in the Ratelpoort shear system, except for the presence of some minute diopside grains in plagioclase as described under 2 above. Such products may form instead of those diagnostic of stage 3.

It is interesting to note the progressive change in hornblende colour in the case of SK249 to SK252. In the first stage the modal volume of hornblende is small, the colour (in thin section) is brown and no conspicous sphene grains are present. In the second stage, all pyroxene is already replaced by hornblende, but the rock retained an igneous texture in the sense that the plagioclase is almost intact. Minute sphene grains then appear and the hornblende colour is olive-green. The final step is an amphibolite with prominent sphene grains and with hornblende colour intermediate between blue-green and olive-green (in terms of the hornblende colour classification applied to the amphibolites described above). This confirms the prominent role of Ti in the colour of metamorphic hornblende and suggests that the ability of hornblende to accommodate Ti increases with metamorphic grade. This is in contrast to the notion that, as the modal volume of hornblende decreases with increase in grade, the Ti in the hornblende simply becomes concentrated and that the compositional change does not necessarily reflect a change in response to grade (e.g. Albat, 1984, p.77).

The metamorphic development of the Nariams Dolerite Suite clearly demonstrates the often described phenomenon that granulite metamorphism is controlled less by temperature than by availability of water. The development of both amphibolite and granulite from the same body, in places a few metres apart, can be explained by local variation in the water content of the fluid phase during metamorphism.

Two-pyroxene geothermometry applied to the recrystallized pyroxenes indicate a temperature of metamorphism of the order of 700° C. The application of geothermometry to these rocks are justified in terms of the fact that the recrystallized pyroxenes appear to be in textural equilibrium (triple points) and chemical equilibrium (no crossing tielines on a composition-paragenesis diagram, see Figure 10.30); note that the one tieline that crosses all the rest does not belong to the population considered here. According to the classification of Bhattacharyya (1971), most orthopyroxenes in the metadolerites are of metamorphic origin (Figure 10.11).

The relatively high temperature indicated by the geothermometry and the fact that the final amphibolite product of the dolerites cannot be distinguished from amphibolites in the country rock, show that metamorphism which accompanied Skelmfontein shearing, in the eastern part of the Steinkopf Domain, was of similar grade to the older 'Early Namaqua' metamorphism, or that the prevalent

metamorphic character of the country rock reflect penetrative reworking during Skelmfontein times.

10.6.6 THE MIDDELPLAAT DYKES

The Middelplaat Dykes in the southwestern part of the Steinkopf Domain cut across the dominant subhorizontal strain fabric of the gneisses, but are penetratively deformed by the Dabbiknik event of subvertical refoliation. The dykes therefore recorded effects of metamorphism subsequent to the main Namaqua Metamorphism.

The Middelplaat Dykes have anomalous but variable compositions. The largest dykes are sodium-poor syenitic and the metamorphic petrography of these can therefore not be directly compared to that of the amphibolites or metadolerites discussed above. Many dykes are, however, lithologically composite and the collected specimens vary from 'normal' amphibolite to pure K-feldspar pegmatite (the latter not included in Appendix 4.5.3). No igneous textures are recognized and hand specimens vary from schistose to gneissic.

K-felspar, where present in the specimens described in Appendix 4.5.3, appears to have infiltrated and replaced plagioclase to a large extent. Different stages of plagioclase replacement are: (i) irregular microveins of microcline microperthite in plagioclase, (ii) microcline microperthite crystals with large, irregular plagioclase inclusions and (iii) microcline microperthite in which it is difficult to distinguish between exsolved and included plagioclase patches. Symplectic intergrowths between microcline and epidote, which replaced plagioclase, are similar to those described for the calc-silicate rocks of the Konkyp area. The relation between the metasomatism and the prograde metamorphism described below is unclear from petrographical observations, but field relations suggest the former to be part of the igneous process. The breakdown of poikiloblastic inclusions and exsolved patches of plagioclase in microcline to epidote, white mica and calcite indicates that retrogression took place after the K-feldspar infiltration.

The dykes exhibit two phases of metamorphism, a prograde phase followed by a retrograde phase. The prograde assemblages (with or without quartz) are:

hbl + bt + pl
hbl + bt + pl + kfs

The hornblende colour in thin section varies from blue-green to intermediate between blue-green and olive-green (colour classification as in the case of the amphibolites and metadolerites discussed above). Sphene is an ubiquitous minor phase and apatite a notable accessory phase in most specimens.

The prograde assemblage define a penetrative continuous foliation owing to the preferred orientation of biotite and hornblende. In some specimens a second fabric is superimposed on the amphibolite grade foliation. This produced a crenulation cleavage, with minor accompanying cataclastesis in some cases.

Retrogression includes the replacement of hornblende and biotite by chlorite and/or epidote and the replacement of plagioclase by epidote. In one sample the hornblende is partially replaced by light green actinolite and in another it is completely replaced by green biotite. The retrogression is found in samples with or

without the second strain fabric.

It can be concluded that the first metamorphic phase affecting the Middelplaat dykes was of amphibolite facies. This serves as a minimum estimate for the metamorphic conditions which reigned during Dabbiknik refoliation as is shown by the fact that the amphibolite assemblage define this fabric in the dykes. The blue-green to intermediate colours of the hornblende in the different samples, in an area where the country rock amphibolites have predominantly olive-green hornblende, suggest a somewhat lower grade than the main Namaqua event. The role of the whole rock compositions to buffer the hornblende composition (as reflected by the colour in thin section) is, however, not understood in this case and no firm conclusion regarding the relative metamorphic grades between the dykes and the country rock can be made.

10.6.7 GREY GNEISS BIOTITES

Introduction

The grey gneisses are the most common rocks in the Steinkopf Domain. The monotonous granitic composition render the mineral parageneses useless as metamorphic grade indicators. Routine petrographic investigation revealed an areal variation in the modal volumes of biotite and the opaque phases. An attempt to correlate this variation in mineral content with metamorphic zonation is described below.

Sample selection

Sixty samples were chosen with the following characteristics in common: fine-granoblastic foliated texture, no leucosomes and a biotite-granitic composition (between 5 and 10 modal percent biotite, no hornblende), i.e. representing the most prevalent grey gneiss of the Steinkopf Domain. Minimum variation in bulk chemical composition was, to a large extent, ensured by the use of specimens for which analyses are available (compare Appendices 3.2 and 6). Figure 10.17 shows that the selected samples cover a sample strip from the southern half of the Transition Zone, across the Steinkopf Domain to the southern part of the Copper District.

Laboratory methods

Fist-sized and compositionally homogeneous samples were crushed by jaw crusher and sieved. The fraction between 100 mesh and 170 mesh was then further treated. The majority of magnetic grains were first removed by a specially constructed electromagnet. This instrument allows a layer of constant thickness of material to pass along a polished aluminium furrow at a constant distance below a 10 mm diameter, flat ended, stainless steel rod which is magnetized by an electric coil. Since the electric current can be controlled, an optimum magnetic strength could be selected for the removal of the bulk of the magnetic particles from each sample, leaving all biotite behind. After each sample was passed underneath this electromagnet, the current was switched off and all the magnetic particles were caught in a clean glass jar. Since the stainless steel does not retain magnetism and because the rod is machined to a smooth finish, all of the magnetic particles were released as soon as the electric current was interrupted and recovery was virtually complete. The remainder of the material was then twice passed through a Franz magnetic separator. During the first run, a

low current setting (0.25 Ampere) was used and the remaining opaque grains were removed. This concentrate was added to the magnetic grains removed by special electromagnet. During the second run the current was set at 0.6 Ampere and all biotite was removed. The end product was a magnetite-rich concentrate, an almost pure biotite concentrate and a felsic remainder. Microscopic analysis showed that the opaque concentrate consisted of more than 95 percent opaque grains (magnetite with ilmenite exsolution lamellae, pure magnetite grains and, less commonly, pure ilmenite grains), with up to five percent biotite or felsic grains adhering to some of the larger opaque grains. The biotite concentrate was also at least 95 percent pure while the felsic remainder contained no dark coloured grains.

The concentrates were weighed on an electronic balance to four decimal places. The results are given in Appendix 6.

Small samples from the biotite concentrates were mounted on glass in clear epoxy (normally used to fix thin sections to glass plates) by sprinkling the biotite onto drops of the glue. In this way up to eight samples could be mounted on one glass plate. After 24 hours, the epoxy was hard and careful polishing could commence. Microprobe analysis of at least two biotite grains of each of the samples were obtained.

Results

Figure 10.18a shows a general increase in the (magnetite + ilmenite) : biotite ratio with increasing distance southwards from the Transition Zone. Considering the Steinkopf Domain on its own (i.e. the data between the two broken lines, Figure 10.18a), no such trend is, however, discernible because of the large scatter of data.

Surprisingly, the chemical composition of the biotite appears not to be related to metamorphic grade in this case. Figures 10.18b and 10.18c show the variation in titanium content and magnesium:iron ratio of the biotite with distance from the Transition Zone.

Conclusions

In the Gladkop Suite grey gneisses, the magnetite:biotite ratios increase with increasing metamorphic grade. Large scatter in the data and the fact that the major element biotite chemistry does not correlate with this observed trend, do, however, prohibit the demarcation of metamorphic zones within the Steinkopf Domain.

10.6.8 DISCUSSION

Metamorphic parageneses in the Steinkopf Domain reflect metamorphic conditions ranging from granulite to greenschist facies. Rocks representing these extremes are, however, uncommon and the general metamorphic character belongs to the upper amphibolite facies.

The metamorphic history of the Nariams metadolerite Suite plus the similarity between their amphibolite end products and the regionally distributed amphibolites indicate that the prevalent metamorphic character of the Steinkopf Domain was established as a result of tectonic reworking during Skelmfontein times. Two-pyroxene granulite products of the dolerite transformation show that granulite assemblages could have developed in the Steinkopf Domain during this period, depending on local compositions of the

fluid phase. The metamorphic temperatures indicated by the two-pyroxene pairs in the metadolerite and by the orthopyroxene-biotite pairs in the Dabbiknik pelitic granulite, agree to some extent, although little significance can be attached to the biotite-orthopyroxene temperatures at this stage (see Chapter 10.10.3). An upper temperature of about 750° C is indicated by the two-pyroxene geothermometer while biotite-garnet pairs in the pelitic granulite indicate an upper temperature of 696° C. It is therefore not necessary to explain the Dabbiknik pelitic granulite as a relict from an earlier metamorphic event, as was previously proposed by the author and co-workers (Blignault et al., 1983).

Late retrogression, reflected by mineralogical aspects of the Middelplaat Dykes, took place under greenschist facies conditions. The reason for the dykes to have undergone significant retrogression not shown by the petrography of the country rocks nor by that of the Nariams metadolerites can possibly be explained as follows. The dykes are vertical, subparallel to the locally well developed Dabbiknik refoliation. They are thus ideally oriented to absorb strain associated with the rejuvenation of subvertical shear, for example during isostatic adjustments. The vertical posture, if continuous for a significant distance makes the dykes ideal conduits for the metamorhic plumbing system active during the late stages of the Proterozoic crustal procedures.

10.7 THE COPPER DISTRICT

10.7.1 GENERAL

Clifford et al. (1975a, 1975b, 1981) suggested that the peak P and T conditions of the main metamorphism in the Copper District were in the order of 6 to 8 kb and 800° C. They correlated the main metamorphic event with Joubert's (1971) M2 tectonic event. The main regional foliation in the gneisses, here classified as 'early Namaqua' in age, formed during this event.

Typomorphic orthopyroxene characterizes mafic metamorphites. Although the metamorphites along the northern limb of the Ratelpoort synform have been reworked in a complex fashion due to the superimposition of the Skelmfontein Thrust Zone and the Ratelpoort Shear on the early Namaqua strain, they share a common metamorphic history with the rocks of the rest of the Copper District; the Skelmfontein shears are zonally developed in the Copper District and the steep structures apparently correlate with the Late Shears. Petrographic descriptions of a number of metamorphite specimens are given in Appendix 4.6 and their geographical distribution is shown in Figure 10.19.

10.7.2 THE CALC-SILICATE ROCKS

Calc-silicate rocks are scarce in the Copper District and petrographic descriptions of four specimens only are given in Appendix 4.6.1. They consist of plagioclase and diopside, with or without quartz and grossularite. In one specimen from within the Ratelpoort Synform (S230B), the garnet forms thin rims around diopside grains, suggesting that grossularite formed at the expense of pyroxene. This is the case in some samples from the Steinkopf Domain as well.

10.7.3 THE MAFIC METAMORPHITES

Mafic metamorphites occur mainly (i) as disrupted bands in the northern limb of the Ratelpoort Synform, part of the supracrustal sequence, and (ii) as part of the 'hornblende gneiss'. The latter is a stratiform unit within the Nababeep Gneiss. Lithologically it varies from a two-pyroxene granulite to a hornblende-rich granitic gneiss. This gradational aspect could reflect contamination of the enveloping gneiss, consistent with the interpretation that the hornblende gneiss is a raft of a pre-existing sill or dyke, engulfed during the original magmatic emplacement of the Nababeep Gneiss.

Mafic orthopyroxene-bearing varieties of the Koperberg Suite are not regarded as metamorphites. Certain mineralogical features which evince partial metamorphic reconstitution of these rocks are discussed under 10.7.5.

Two-pyroxene granulite - Carolusberg

The six specimens with numbers starting with GLC described in Appendix 4.6.2 are from the Carolusberg Mine. They represent different parts of the same two-pyroxene granulite body (part of the 'hornblende gneiss') from different mine levels, the deepest approximately 1000 m below surface. GLC020 represents the largest part of the granulite body and displays regional foliation of the Copper District. The rest of the specimens illustrate subtle petrographical deviations, some with strain effects related to the major Carolusberg steep structure.

The granulite is generally medium-granoblastic with a weak foliation defined by the pyroxenes and prominent red-brown biotite. Pyroxene porphyroblasts are poikiloblastic to skeletal, the inclusions being almost exclusively plagioclase. In most cases, the skeletal porphyroblasts are optically continuous, reflecting low strain subsequent to textural equilibrium. The long axes of the porphyroblasts are parallel to the regional foliation. Olive-green to brown hornblende generally constitutes a minor phase. In one specimen more abundant hornblende is concentrated in pyroxene-free micro-bands (2 millimetre wide). Microcline-microperthite was found in two specimens. The first (GLC025) was taken from a metre-scale xenolithic lense in Nababeep Gneiss, while the second (GLG055) is from the main granulite body, some 10 metres from the contact with the gneiss. Antiperthitic exsolution patches characterize the larger plagioclase grains in these K-feldspar-bearing specimens. Specimen GLC059 was taken from within the zone of intense steep structure refoliation on 39 level. The rock displays significant ductile strain. Skeletal pyroxene porphyroblasts are recognized under the microscope as elongate clusters of small grains, each with its own orientation. On textural grounds it is unclear whether the subgrains of the original porphyroblasts recrystallized or whether the they were physically disturbed only. The unstrained nature of the individual brown mica flakes, which define the penetrative steep structure refoliation, suggests recrystallization of this phase.

The chemical compositions of the pyroxenes, the biotite and the plagioclase for two samples from the Carolusberg-mine are given in Appendix 5. In these samples, at least ten spot analyses were performed on each analyzed grain. In each case the two pyroxenes analyzed are in mutual contact and appears to be in textural equilibrium. The compositional relations between the pyroxenes are

shown in Figures 10.30. Peak metamorphic temperatures of 850° C and 800° are indicated for GLC053 and GLC059 respectively.

Application of the Fonarev and Konilov (1986) geothermometer indicates a larger temperature difference between the two Carolusberg granulite samples than that suggested by two pyroxene geothermometry. The difference between GLC053 and GLC059 lies mainly in the annite contents of the brown mica (34.5 percent and 26.0 percent respectively). This suggests that the brown mica composition was adjusted during the recrystallization referred to above. If the orthopyroxene did not partake in such compositional adaptations, the two phases would not be in equilibrium and the relative temperatures indicated by Figure 10.31 would be meaningless.

Two-pyroxene granulite and amphibolite from the Ratelpoort lineament.

Amphibolite constitute distinct bands in a mafic unit of the Khurisberg Subgroup. Both diopside-bearing and diopside-free varieties are found. Hornblende colour in thin section is olive-green throughout. The amphibolites were not considered to be informative as far as metamorphic indicators are concerned and little petrological examination of these rocks were done. The mere presence of the amphibolites, however, is signficant in terms of metamorphic conditions in a granulite terrane and some interpretations are given below.

Varieties of two-pyroxene granulite occur along the northerm limb of the Ratelpoort Synform as discontinuous bands and lenses within the banded sequence of the Khurisberg Subgroup. Associated rock types include metapelite and amphibolite. Petrographical descriptions of a number of representative samples are given in Appendix 4.6.2. Hornblende and/or biotite are present in most samples studied, but two-pyroxene granulite devoid of volatile-bearing phases forms part of many granulite outcrops. Texturally the granulite varies from very coarse-granoblastic to very fine-granoblastic. The most common type consists of skeletal porphyroblasts of pyroxene in a fine-granoblastic polygonal matrix dominated by plagioclase. The individual grains, whether large or small, display stable grain shapes.

The outcrops east-northeast of Skelmfontein se Poort display a variety of lithological and structural relations. The local penetrative Skelmfontein foliation is defined by all index minerals. The association of two-pyroxene granulite with amphibolite is found on both mesoscopic and microscopic scale. In outcrop, two-pyroxene granulite forms decimetre to centimetre-wide bands, lenses and boudins within amphibolite. Transitions are generally sharp. Millimetre-wide bands of amphibolite within banded granulite are described in Appendix 4.6.2 for specimen SK222. Specimen SK227 consists of amphibolite with granulite nodules, four to seven millimetres across.

A thinly banded variety of two-pyroxene granulite in the same area display small-scale isoclinal Skelmfontein folds. No axial plane foliation is discernible. The ductile nature of the deformation is indicated by isoclinal folding of individual, elongate quartz grains, with no more discernible internal strain than slight undulose extinction (see Appendix 4.6.2). The elongate forms of the quartz grains suggest that the banding is in the first place of structural origin (e.g. the Rooiberg-type banding of the

Noenoemaasberg Gneiss, Chapter 4.4.1).

In the banded metapelite unit west of Skelmfontein se Poort (structurally above the mafic unit described in Chapter 3), diopside-plagioclase veins cut across the penetrative foliation of biotite bearing two-pyroxene granulite. A sample was collected specifically to include such a vein and is described in Appendix 4.6.2 (SK493). The vein pyroxene is not skeletal as is the case with the pyroxene in the country rock granulite. Very small, pale-green hornblende patches replaced approximately 20 percent of the vein clinopyroxene. This type of replacement hornblende was not found in the adjacent granulite clinopyroxene. The vein plagioclase is slightly more anorthitic than the country rock plagioclase. Slight kinking of vein plagioclase indicates minor strain. In the same area, centimetre-scale two-pyroxene granulite veins (coarse-granoblastic to medium-granoblastic) cut across the penetrative foliation of fine-granoblastic amphibolite, e.g. SK408 (see Appendix 4.6.2).

The results of two-pyroxene geothermometry on granulite samples from the northern limb of the Ratelpoort Synform are given in Figure 10.30. A peak metamorphic temperature of between 750° and 800° C is indicated. Crossing tie-lines on the pyroxene quadrilateral and relatively low temperatures indicated by orthopyroxene suggest disequilibrium. The only pyroxene pair for which the orthopyroxene indicates a high temperature similar to that suggested by the clinopyroxene composition is from SK408, discussed above. One could interpret this as suggesting that the orthopyroxene in the granulite veins was not as susceptible to compositional alteration during later retrogression as was the orthopyroxene in the rest of the two-pyroxene granulites. Only one spot analysis on each pyroxene in question is, however, available and the hypotheses cannot be tested.

The structural relations between the granulite assemblages and the Skelmfontein fabric is significant and is referred to again under 10.10.

Ultramafic metamorphite

The ultramafic band found east of Skelmfontein se Poort consists of typomorpic orthopyroxene, othoamphibole, hornblende and small quantities of biotite and plagioclase (see descriptions of SK203 and SK204 in Appendix 4.6.3). On the classification diagram of Bhattacharyya (1971), the orthopyroxene plot well into the metamorphic field, in contrast to the comparable rocks from the Eenriet Mountains (Figure 10.11). The whole rock and mineral chemistry of the two ultramafic metamorphites are compared in Figure 10.20a, 10.20b and 10.20c. It shows that whole rock compositions of the two specimens from the south are close to that of the constituent ortho-amphibole. The whole rock compositions plot just outside the triangle formed by the pyroxene and the two ampiboles testifying to the relative aluminous and calcium-rich nature. This explains the presence of plagioclase in these rocks. The Eenriet Mountain specimen is more magnesian than those from the south, however. The whole rock composition is nearly colinear with the tie-line connecting orthopyroxene and hornblende, explaining the absence of additional ferromagnesian silicates in that rock. The variance in whole rock composition is also reflected by the more Mg-rich compositions of the pyroxene and hornblende in the Eenriet Range rock relative to those from the Skelmfontein se Poort area. The difference in amphibole compositions are well illustrated

on the 'S-A-NCFM' classification diagram (Figure 10.21). The mineralogical differences between the two groups can be explained fully by the difference in whole rock chemistry. No conclusions regarding relative possible differences in metamorphic grade can be inferred.

The textural relations of the orthopyroxene in SK204 suggest that the pyroxene is a late phase mineral, post-dating the penetrative fabric defined by the amphiboles and spinel. Low-angle boundaries in the skeletal pyroxene indicates some late deformation.

10.7.4 THE METAPELITES

Metasedimentary rocks form a small portion of the stratigraphical succession in the Copper District and potential sample sites are limited. A representative selection of specimens are described in Appendix 4.6.4. and the sample distribution is shown in Figure 10.19. Two uncommon rock types, an orthopyroxene-cordierite rock and a sapphirine-bearing rock are described in Appendix 4.6.5.

Petrography

The rocks vary from fine-granoblastic to coarse-granoblastic and from non-foliated to schistose. The schistose rocks are, however, scarce. Outside zones of Skelmfontein refoliation, the metapelitic rocks are commonly unfoliated, exhibiting only compositional banding. In some places the banding appears to be primary with the quartz content the main compositional variable. At other places the banding is migmatitic in the sense that medium-granoblastic to coarse-granoblastic quartzo-feldspathic bands, usually garnet-rich, alternate with metapelitic bands.

As far as can be established on textural grounds, the assemblages listed in Appendix 4.6.4 represent the metamorphic parageneses for most part. The following parageneses occur:

qtz		+ kfs	+ sil	+ bi		+ crd				1
qtz	+ plg		+ sil	+ bi	+ grt	+ crd				2
qtz	+ plg	+ kfs	+ sil	+ bi		+ crd				3
qtz		+ kfs	+ sil	+ bi		+ crd	+ green spinel			4
qtz			+ sil	+ bi	+ grt					5
qtz	+ plg			+ bi	+ grt	+ crd				6
qtz	+ plg		+ sil	+ bi		+ crd				7
				bi	+ grt	+ crd				8
qtz	+ plg	+ kfs	+ sil	+ bi	+ grt	+ crd				 9
qtz			+ sil	+ bi						10
	plg		+ sil	+ bi						11

The paragenesis kfs + crd + grt is considered to reflect granulite grade metamorphic conditions, the responsible reaction being

$$bt + sil + qtz = grt + crd + kfs + H_2O$$

Where anatexis is indicated by the presence of granitic neosomes, the reaction is probably

$$bt + sil + qtz = grt + crd + kfs + melt$$

(Waters, 1986).

Assemblage 9 above, found in at least three specimens from different localities, is unlikely to be a stable paragenesis (e.g.

Winkler, 1979, p. 233). Since the assemblage appears stable, texturally, the conditions during formation could not have been too far removed from the equilibrium conditions of the appropriate reactions.

Compositional control over the assemblages in the metapelites is illustrated in Figure 10.22. In the figure, the compositions of some metapelitic rocks from the Copper District are projected into an AFMK tetrahedron (A = Al_2O_3, F = FeO, M = MgO and K = K_2O). Within this tetrahedron, a smaller tetrahedron is defined by the compositions of sillimanite, cordierite, biotite and garnet. The compositions of these phases as reference points were taken from the mineral chemical data for specimen SK231A. All whole rock iron was expressed in terms of FeO and 75 percent of this was used. This generalization is bound to introduce serious errors in cases where the $Fe^{+++}:Fe^{++}$ ratio of a metapelitic sample deviates significantly from the assumed value. Viewing Figure 10.22 in stereoscopic perspective one can, however, visualize the effect of such variation. Only in a minority of cases would a small variation in the iron oxidation ratio move the rock composition with respect to the sil-crd-grt-bt tetrahedron and, generally, the results of the projection do explain the observed assemblages:

SK267 contains no cordierite because the whole rock composition plots on the Fe-rich side of the sil-bt-grt plane.

S231A contains no sillimanite because its composition plots on the alumina-poor side of the crd-bt-grt plane.

S193 and S194A contain no garnet since their compositions plot on the MgO side of the sil-bt-crd plane.

GNA002 contains garnet, biotite, cordierite and sillimanite since its compositions plots within the tetrahedron defined by the compositions of these phases.

S207 also contains all four phases of interest, but its composition plots just outside the inner tetrahedron, on the Fe-poor side of the grt-crd-sil plane. This is one case where a slight deviation from average $Fe^{+++}:Fe^{++}$ ratio could be the cause of an apparent discrepancy. Alternatively, the three ferromagnesian phases could be more magnesian than the reference sample, which would move the appropriate tetrahedron away from the F corner to include the whole rock composition.

Figure 10.23 is a similar projection of the whole rock and mineral compositions of SK322. In this case, the rock composition plots virtually on the opx-crd-bt plane, just on the alumina-poor side, explaining both the paragenesis and the magnesian composition of the brown mica. The same type of projection for the sapphirine-bearing rock from Leeupoort illustrates the extreme magnesian composition.

The petrogenesis of orthopyroxene-cordierite and sapphirine-bearing rocks of the Copper District were considered in some detail by Clifford et al. (1981). It is generally accepted that these rock types reflect high metamorphic temperatures, consistent with the suggested thermal peak of 800° C or higher for the Copper District. Whether the magnesian rocks represent the residue after the removal of a granitic melt from a greywacke type metasediment (ibid., 1981) or whether they are simply the metamorphic products of specific altered volcanic rocks (e.g. Vallance, 1967, Waters, 1986) would make little difference to the PT implications of the existing parageneses. The lack of any leucosome veins within the few square metres of outcrop of both the sapphirine-bearing rock and the

cordierite-orthopyroxene rock support the latter interpretation. For the present study, the age relations of these very high grade parageneses, relative to the different fabrics, are important. The textural characteristics of specimen SK322 indicates that the growth of orthopyroxene was late or post-kinematic with respect to the local Skelmfontein shear fabric (see description, Appendix 4.6.5).

Clifford et al. (1981) described anthophyllite as retrograde product in cordierite-orthopyroxene rocks, while they considered gedrite in some such rocks as part of the prograde assemblage. No details are given concerning structures associated with the retrogression. In the more common cordierite-rich metapelitic rocks, retrogression involving the breakdown of cordierite to produce biotite and sillimanite in specimens SK479, SK481 and SK485 is described in Appendix 4.6.4. No garnet is involved here. The metapelitic rocks where these samples were taken are migmatitic. In terms of the probable hydrothermal effect during the solidification of the granitic leucosomes, with which the local metapelitic rock is riddled, the retrogression could have taken place according to

$$crd + \text{Fe-rich bt} + K^{+} + H_2O = sil + \text{Mg-rich bt} + qtz$$

Garnet-biotite and garnet-cordierite geothermometry

From the relevant results reported under 10.9, the temperatures obtained through garnet-biotite and garnet-cordierite geothermometry is summarized in Table 10.2.

In general the mineral pairs show retrograde diffusion zoning with closing temperatures around 500 ° C. The maximum temperature obtained (780 ° C) was from a biotite and a garnet which is not in contact with each other or any other ferromagnesian phase (SK453B). It is possible that chemical equilibrium could have been reached between two separated phases owing to optimal diffusion during the metamorhic peak ('through-the-matrix' diffusion), which became less efficient during subsequent cooling and loss of volatiles. The highest temperature calculated for touching grains is 735 ° C in the case of S231A.

The field location of SK490, in the zone of prominent Skelmfontein refoliation, and the temperature of above 700° C indicated by a cordierite-garnet pair, is consistent with the suggested high grade conditions in this region during the late thrusting. In the case of the other two high temperature specimens referred to above (S231A and SK453B) the relation to Skelmfontein fabric is not clear.

TABLE 10.2 GEOTHERMOMETRIC RESULTS FOR COPPER DISTRICT METAPELITES

r = rim, c = core, cr = adjacent to chadacryst, inc = chadacryst, f = not touching any other ferromagnesion phase.

Nr.	Mineral pair	Temperature	Remarks
S231A	grt-1 r bt-1 r	611	rims of touching grt and bt
S231A	grt-2 cr bt-2 inc	586	rim of a biotite inclusion and the immediately adjacent garnet
S231A	grt-1 c crd-1	735	centres of touching grains
S378	grt-1 c crd-1 c	683	centres of touching grains
S378	grt-1 r crd-1 r	601	rims of the above
S381	grt-1 c crd-1 c	691	centres of touching grains
S381	grt-1 r crd-1 r	568	rims of touching grains
SK453B	grt-1 r bt-1 r	588	rims of touching grains
SK453B	grt-2 r bt-2 r	578	rims of touching grains
SK453B	grt-1 c bt-3 f	781	centres of non-touching grains
SK490	grt-1 cr bt-1 inc	670	bt inclusion and adjacent grt
SK490	grt-2 r bt-2 c	635	centre of small bt, rim of grt where it touches the bt
SK490	grt-1 c crd-1 c	713	centres of touching grains
GNA002	grt-1 p bt-2 c	583	centre of a bt in contact with a grt porphyroblast
GNA002	grt-1 cr bt-inc	552	bt included in grt porphyroblast
GNA002	grt-3 bt-3	511	bt in contact with grt
GNA002	grt-4 bt-4	494	bt in contact with grt
GNA022	grt-1 r bt-1 r	459	rims of touching grains
GNA022	grt-c bt-c	542	centres of touching grains

10.7.5 METAMORPHIC FEATURES OF THE STEEP STRUCTURES AND KOPERBERG SUITE.

At Carolusberg mine, an outcrop of metapelite several hundred metres in diameter, is correlated with compositionally similar rocks some 1000 m directly underground. The surface body is interpreted to have been forcefully removed from its stratigraphic position in the deepest part of the mine, as a result of diapiric steep structure deformation. Careful study of the outcrops showed that sillimanite has grown across the steep structure shear fabric and a number of samples from here is described in Appendix 4.6.4 (GLC 002 - GLC008). The common assemblage in these schistose rocks

is

qtz + bt + sil.

The garnet found in GLC012 is deformed and new biotite has grown in the resulting pressure shadows. The stratigraphically equivalent but non-dislocated metapelitic rocks in the mine, as much as 1000 metre below surface, have retained the high grade assemblage

kfs + sil + crd + grt

for most part (only one such specimen is described in Appendix 4.6.4, but five more have been inspected in a reconnaisance fashion, to test the above statement). The lower grade sillimanite assemblage in the surface schist is interpreted to reflect metamorphic conditions during steep structure development.

Specimens GNA001 and GNA002, described in Appendix 4.6.4, are penetratively deformed in a zone of steep structure refoliation at, Nababeep mine. Both specimens contain the assemblage

grt + crd + kfs + bt + sill + qtz

but the cordierite is pinitized and it is difficult to assess on textural grounds whether the assemblage was an equilibrium paragenesis during steep structure development or not. Relatively low temperatures are indicated by geothermometry for GNA002 (Table 10.2). Similar low temperatures are obtained for biotite-garnet pairs in GNA022 from Wheal Heath (west of Okiep). GNA022 is not as deformed as the Nababeep mine samples and the relatively low temperatures indicated for the latter need thus not necessarily reflect the conditions during steep structure development.

At the northern contact between the anorthositic body at Klondike central, the Nababeep Gneiss foliation is folded as a result of steep structure deformation. In the hinge zone of the meso-scale synform, of which the southern limb is replaced by the anorthositic body, an axial planar foliation is defined by deeply coloured (in thin section) hypersthene. The normally biotite-rich gneiss contains virtually no biotite in the hinge zone. Two metres removed from the small fold under discussion the rock is typical Nababeep Gneiss with about 10 modal percent biotite and no pyroxene. This phenomenon probably indicates a form of synkinematic contact metamorphism. It is known that the intrusive bodies of the Koperberg Suite had some thermal imprint on the country rock gneisses (Prins, 1970 and Venter, 1970). The granulite assemblage could have formed as a result of heating at the contact and/or through the dehydration of already hot gneiss by the water undersaturated anorthosite magma. It is doubtful whether the granulite assemblage in the gneiss could have formed as a purely contact metamorphic effect on a cool country rock, corroborating the model according to which the Koperberg Suite was emplaced into a crust which was still at an elevated temperature (Conradie and Schoch, 1986b).

Certain intrusive bodies of the Koperberg Suite show clear evidence of steep structure strain (McIver et al., 1983; Venter, 1984; Conradie, 1983, Conradie and Schoch, 1986a). The body at Klondike Central, described in Chapter 9 and referred to above, shows microtextural evidence of metamorphic recrystallization. Most plagioclase grains are recrystallized along the edges to form fine-granoblastic polygonal aggregates, depicting a mortar texture.

Biotite define the steep structure foliation owing to preferred orientation. Pyroxene is also affected by the steep structure deformation and some grains are recrystallized to form polygonal subgrains with perfect triple junctions; accessory clinopyroxene is similarly recrystallized and forms polygonal aggregates with orthopyroxene (Figure 10.24). The results of two-pyroxene geothermometry for this rock is shown in Figure 10.30; the fact that the pyroxenes of the Klondike body are similar to all the other pyroxenes of granulites and metadolerites suggests a common cooling history. This is perhaps the strongest evidence of a hot crustal host for the Koperberg Suite.

The geothermometric results from the Nababeep mine steep structure and the assemblage

qtz + bt + sil

found at Carolusberg, provide a minimum temperature of 500 ° C during steep structure development. These relatively low temperature features have developed during a late stage along the structures favourably oriented (reminiscent of the greenschist assemblages in the Middelplaat dykes, Chapter 10.6.6). Metamorphic features of the Klondike anorthosite suggest conditions near the thermal peak during emplacement, consistent with migmatitic features associated with steep structures elsewhwere in the Copper District (Venter 1984).

10.8 THE GESELSKAPBANK DOMAIN

10.8.1 GENERAL

The Geselskapbank Domain was mapped and structurally analyzed in detail by Strydom (1985). Further accounts of the geological intricacies of the area are given in Colliston and Strydom (1985), Strydom and Visser (1986), Van Aswegen et al., (1987) and Strydom et al., (1987). The area is characterized by four major and several smaller thrust faults. Starting from the bottom, the major thrusts are (i) the Skelmfontein Thrust (juxtaposing the Geselskapbank Domain and the Steinkopf Domain), (ii) the Groothoek Thrust, (iii) the Geselskapbank Thrust and (iv) the Naab Thrust (see Figures 1.2 and 10.25). The intervening nappes are named after the subjacent thrust faults.

The thrusting introduced granulite grade rocks into a region at present characterized by amphibolite grade (Van Aswegen, 1981); non-penetrative retrograde metamorphism is associated with the thrust shear fabric. A number of samples were selected to illustrate the different metamorphic features and are described in Appendix 4.7; some mineral analyses are given in Appendix 5. The petrography of the rocks investigated is summarized below and the significance of mineral compositions is evaluated.

10.8.2 THE SKELMFONTEIN AND GROOTHOEK NAPPES

Metapelitic rocks

Metapelitic rocks from these nappes are characterized by ubiquitous muscovite, generally oriented parallel to the regional foliation; porphyroblasts of the white mica display a random orientation (Figure 10.26). Although the muscovite appears to be late to

post-kinematic for most part, some late shearing, interpreted as rejuvenation of the thrusting, deformed the muscovite in some places.

The late to post-kinematic muscovite is of retrograde origin. Textural relations, similar to those described for the schistose rocks of the Konkyp area, are typical of these rocks. K-feldspar porphyroblasts with inclusions of sillimanite, are replaced by micrographic intergrowths of muscovite and quartz (e.g. Figure 10.27), indicating the retrograde reaction

$$kfs + sil = ms + qtz$$

A large number of schistose specimens from the collection of D. Strydom were examined on a reconnaissance basis (not described in Appendix 4.7.1). It was not possible, however, to establish whether the rocks were muscovite-free prior to the retrogressive metamorphic event.

Amphibolites

Although the supracrustal rocks of the Skelmfontein and Groothoek nappes are dominantly of sedimentary origin, minor amphibolite bands are widespread. A large number of amphibolite specimens from the collection of D. Strydom were examined for comparison with the amphibolites of the Steinkopf Domain to the west.

The amphibolite samples investigated were all hornblende-plagioclase rocks with minor quartz and opaque grains. The hornblende is blue-green (in thin section) and is further characterized by a high distribution density of quartz inclusions. The orientation of the hornblende crystals vary from parallel to the penetrative foliation, to random. The plagioclase is generally saussuritized.

10.8.3. THE GESELSKAPBANK AND NAAB NAPPES

Stratigraphically, the rocks of the Geselskapbank and Naab nappes can be considered as exotic to the local terrane (Strydom, 1985). The Geselskapbank nappe consists for most part of the Geselskapbank Formation which is characterized by dark coloured cordierite-garnet-sillimanite rocks. Lithologically equivalent rocks are absent in the lower nappes, but similar cordierite-rich rocks occur as minor lenses in the Eenriet Mountain Range and in the Ratelpoort Synform.

The Geselskapbank nappe is cut by numerous small thrust planes as part of imbricate sets. Specimens from within such zones are foliated milonitic to schistose, while the country rock is hardly foliated in some cases.

The Naab nappe is dominated by granitic gneiss of the Naab Suite (Strydom et al., 1987). The latter is intruded by dolerite dykes of the Gareskop dyke swarm which are amphibolitized in the Naab thrust zone, the thrust zone being as much as one km wide at some places (Schoch and Strydom, 1987).

The Geselskapbank Formation metapelites

Samples from the Geselskapbank Formation are described in Appendix 4.7.2 and the sample sites are shown in Figure 10.25. The most typical rock type is a cordierite rock; it consists of a

fine-granoblastic polygonal matrix of cordierite with interstitial and included sillimanite and widely spaced garnet porphyroblasts. Biotite, quartz and plagioclase are additional phases in most of the specimens investigated. Prograde assemblages are

						sil	+	crd	+	grt
					bt	+ sil	+	crd	+	grt
qtz				+	bt	+ sil	+	crd	+	grt
qtz	+	plg		+	bt	+ sil	+	crd	+	grt
qtz	+	plg	+ kfs	+	bt	+ sil	+	crd		
qtz	+	plg	+ kfs	+	bt	+ sil				
qtz				+	bt					+grt
qtz	+	plg	+ kfs	+	bt	+ sil	+	crd		

Retrogression produced muscovite, chlorite and andalusite. The muscovite and chlorite occur as large and small grains, the white mica replacing feldspars and biotite, and the chlorite replacing biotite and cordierite. The andalusite occurs as poikiloblastic porphyroblasts of irregular shape, surrounded by chlorite. Sillimanite is generally included in the porphyroblasts. In specimens not penetratively refoliated during late thrust deformation, the retrograde minerals appear to be post-kinematic.

Specimens taken from minor thrust zones are foliated milonitic or schistose (micaceous), the origin possibly depending on the relative availability of water during deformation. In one example (NMG012 in Appendix 4.7.2) the relatively high grade assemblage of

kfs + sil + bt (+ plg + qtz)

is milonitized in the sense that all the mineral grains, except for a number of feldspar porphyroclasts, are recrystallized to a reduced grain size of around .03 millimetre. New quartz and biotite grew in the pressure shadows. From the same small thrust zone, a few metres away from the first example, a metapelitic rock with an apparently similar whole-rock composition, is transformed into a muscovite-chlorite schist with a median grain size of .15 mm (NMG013 in Appendix 4.7.2)

TABLE 10.3 GEOTHERMOMETRIC RESULTS FOR THE GESELSKAPBANK FORMATION METAPELITES

Each number (e.g. grt-1) refers to a particular spot analysis.
c - grain centre; r - grain rim; cr - adjacent to chadacryst;
inc - chadacryst.

No.	Mineral pair		T (° C)	Remarks
DST7	grt-1 r	bt-1	568	Grt rim touching bt-1
DST7	grt-5 r	crd-1	564	Grt rim touching crd-1
DST7	grt-cr	bt-inc	641	Grt centre touching bt inclusion
NMG031	grt-1	bt-1	583	Grt1 rim touching bt-1
NMG031	grt-cr	crd-inc	600	Grt centre touching crd inclusion
SK323	grt-c	crd-inc	536	Grt centre touching crd inclusions
SK323	grt-1 r	crd-1 r	510	Grt rim touching crd rim

Mineral compositions from the cordierite-garnet rocks apparently reflect re-equilibration during the retrogression because

temperatures of around 550 ° C are indicated by geothermometry. Results from geothermometric determinations (Chapter 10.9) is summarized in Table 10.3 above. It shows that the temperatures obtained for mineral grains which are in contact are lower than those determined for the centres of mineral grains or inclusions, indicating retrograde zoning and a minimum temperature of 500° C. This is consistent with the development of andalusite porphyroblasts in some places.

The two-pyroxene granulite

Occurring as minor bands in the metapelitic rocks of the Geselskapbank Formation, two-pyroxene granulite probably represents metamorphosed dykes or sills. Descriptions of specimens are given in Appendix 4.7.3. These specimens are all from one area, the structural position being ten to thirty metres above the Naab thrust (Figure 10.25). Some of the specimens show strain which is related to the thrusting; retrograde hornblende (bluish-green) replaced pyroxene along cracks (see Figure 10.28). It is possible to distinguish retrograde hornblende and pre-existing hornblende on textural grounds (see Appendix 4.7.3). As in the case with the granulites of the northern limb of the Ratelpoort synform, amphibolite is interbanded with granulite on centimetre-scale. This situation predates the thrust-induced strain and probably reflects small-scale compositional heterogeneities, such as the water content during the metamorphic peak.

Geothermometry applied to the pyroxenes is discussed in Chapter 10.9. The results listed in Table 10.4 indicate lower temperature conditions for the Geselskapbank granulite samples than for those from the Copper District.

The Gareskop dolerite

Dolerite dykes of the Gareskop dyke swarm are deformed in the Naab thrust zone (see Figure 10.25 and 10.29). Samples of these deformed rocks show textural development similar to that found in the Nariams dolerite dykes of the Steinkopf Domain. Descriptions are given in Appendix 4.7.4. Progressive transformation, from virtually intact dolerite to amphibolite, can be observed over tens of metres.

As in the case of the Nariams metadolerites, the pyroxenes were analyzed and, in terms of geothermometry, these minerals appear to have undergone compositional adaptations under metamorphic conditions. The pyroxenes are recrystallized, as in the case of some of the Nariams dolerite samples, in one of the samples studied only (NNB027, Appendix 4.7.4). The correct tectonothermal interpretation of the temperatures given in Table 10.4 is not yet apparent but it is possible that the orthopyroxene composition was re-equilibrated to a greater extent than the clinopyroxene during the metamorphic cooling phase.

10.9 GEOTHERMOMETRY AND GEOBAROMETRY

The concept of geothermometry and geobarometry appeals to geologists since it provides quantitative answers to the most basic questions about the PT conditions of metamorphism. Unfortunately the accuracy of most methods is not very good (e.g. Hodges and Crowley, 1985) and often the best one can expect from such studies

are indications of the relative variations in conditions from place to place. In this study reasonable success was achieved with biotite-garnet, cordierite-garnet and two-pyroxene geothermometry, while cordierite-garnet geobarometry indicated metamorphic pressures consistent with interpretations based on petrography.

10.9.1 TWO-PYROXENE GEOTHERMOMETRY

Methods

The main approaches to two-pyroxene geothermometry are based on (i) the Mg-Fe distribution between the two pyroxenes and (ii) the pyroxene solvus. Regular recalibrations reflect a growing experimental database and more sophisticated thermodynamic calculations.

Stephenson (1984) tested ten different variations of the thermometer on ten two-pyroxene granulite samples from a 1.5 km long sample strip in an extensive granulite terrain. The bulk chemistry of his ten samples cover a significant part of the compositional range of two-pyroxene rocks in general. The average temperatures obtained by Stephenson from the different methods vary from 683° to 893° C as follows:

Geothermometer	Average temp	Variation (° C)
Lindsley (1983; opx version)	683	11
Kretz (1982; Kd version)	705	19
Ross and Huebner (1975)	709	30
Kretz (1982, solvus version)	735	24
Fonarev & Graphchikov (1982, opx)	<750	
Lindsley (1983, cpx version)	784	40
Fonarev & Graphchikov (1982, cpx)	820	30
Wood & Banno (1973)	849	16
Powell (1978)	854	23
Wells (1977)	893	10

The above averages are based on between 6 and 21 spot analyses of several grains in each case. Temperatures derived from single spot analysis pairs vary between 670° and 1020° C.

In Namaqualand, the Wood and Banno (1973) and Wells (1977) methods were applied in two recent metamorphic studies (Zelt, 1980 and Albat, 1984). Waters and Moore (1985) preferred the method of Lindsley (1983).

In the present study the methods of Lindsley (1983), Kretz (1982) and Wood and Banno (1973) were applied to pyroxene pairs from mafic granulites and from metadolerites. The relevant calculations and graphic applications were also performed on data from Zelt (1980), Albat (1984) and Stephenson (1984) for comparison. Data from these publications/theses were selected in such a way as to include the whole range of temperatures found by each. The method of Lindsley (1983) involves the projection of pyroxene compositions onto the Di-En-Hd-Fs quadrilateral according to a specific scheme based on statistical analyses (Lindsley and Anderson, 1983, as quoted by Lindsley, 1983). The scheme, as described by Lindsley (1983, p. 485 - 486) was implemented by means of the following practical algorithm:

Clinopyroxene:

```
 1  Calculate cation proportions on the basis of 6 oxygens.
 2  Al(iv) = 2 - Si
 3  Al(vi) = Al(total) - Al(iv)
 4  Fe3+   = Al(iv) + Na - Al(vi) - 2Ti
 5  Fe2+   = Fe(total) - Fe3+
 6  Xfe    = Fe2+/(Fe2+ + Mg)
 7  Ac     = smallest of Fe3+ and Na
 8  Fe3+   = Fe3+ - Ac
 9  Na     = Na - Ac
10  Jd     = smallest of remaining Na or Al(vi)
11  Na     = Na - Jd
12  Al(vi) = Al(vi) - Jd
13  FeCaTs = remaining Fe3+
14  AlCaTs = remaining Al(vi)
15  Wo     = (Ca + Ac - AlCaTs - FeCaTs)/2
16  En     = (1 - Wo) * (1 - Xfe)
17  Fs     = (1 - Wo) * Xfe
```

Orthopyroxene:

```
 1  to 6: the same as for clinopyroxene
 7  R3           = Al(vi) + Fe3+
 8  NaR3Si2O6    = smallest of Na or R3
 9  Na           = Na - NaR3Si2O6
10  R3           = R3 - NaR3Si2O6
11  NaTiAlSi2O6  = smallest of Ti, Na or Al(iv)
12  Ti           = Ti - NaTiAlSi2O6
13  Na           = Na - NaTiAlSi2O6
14  Al(iv)       = Al(iv) - NaTiAlSi2O6
15  R2TiAl2O6    = smallest of Ti or (Al(iv)/2)
16  Al(iv)       = Al(iv) - 2 * R2TiAl2O6
17  px           = R2TiAl2O6/(Mg * (1 - Xfe) + Fe * Xfe)
18  Mg           = Mg - Mg * px
19  Fe2+         = Fe2+ - Fe2+ * px
20  R2R3AlSiO6   = R3 or Al(iv) ... since these are now equal
21  px           = R2R3AlSiO6/(Mg * (1 - Xfe) + Fe * Xfe)
22  Mg           = Mg - Mg * px
23  Fe2+         = Fe2+ - Fe2+ * px
24  Wo           = Ca/(Ca + Fe2+ Mg)
25  Ens          = Mg/(Ca + Fe2+ Mg)
24  Fs           = Fe2+/(Ca + Fe2+ Mg)
```

The projections are then graphically compared to isotherms which have been mapped on the pyroxene quadrilateral (e.g. Figure 10.30).

The methods of Kretz (1982) and Wood and Banno (1973) involve the application of formulae and are straightforward. The method of Wood and Banno and the solvus method of Kretz (1982) were applied, using Fe^{++} as calculated above (up to step 5). In the case of the Wood and Banno method, the resulting temperatures show less variation and a slight increase in temperature (average 8° C) is discernible if compared to the results when all Fe is taken as Fe^{++}. The Kretz Kd method is very sensitive in this regard and if all Fe is taken as Fe^{++}, temperatures up to 200° C higher are obtained.

Results

Figures 10.30a and 10.30b show the application of the Lindsley (1983) graphical method to metadolerite samples from the Steinkopf Domain and from the Geselskapbank Thrust Sheet, as well as to the two-pyroxene granulite samples from the Copper District, the

Geselskapbank thrust sheet, the Swartlintjiesrivier traverse (Zelt, 1980), the Kliprand area (Albat, 1984) and Cape Rich area, Western Australia (Stephenson 1984). The temperatures derived from this graphical analysis and by the application of the Wood and Banno (1973) and Kretz (1982) methods are listed in Table 10.4.

TABLE 10.4 RESULTS OF TWO-PYROXENE GEOTHERMOMETRY

METHOD	1	2	3	4	5	
						METADOLERITE
NMG005	600	810	806	709	898	Geselskapbank
NNB027	620	710	645	550	744	,,
SK467	620	712	736	636	797	Steinkopf
SK337.1	620	750	753	736	812	,,
SK337.2	620	770	747	645	777	,,
SK338	690	760	722	748	833	,,
						KOPERBERG SUITE
GLK001	610	760	644	788	826	Klondike central
						TWO-PX. GRANULITE
SK289.1	600	710	745	612	834	Ratelpoort
SK289.2	600	770	753	884	852	,,
SK289.3	610	810	756	875	863	,,
S965.1c	650	805	754	687	824	,,
S965.1r	650	740	721	620	794	,,
S965.2	650	750	767	764	848	,,
S969.1	620	795	763	750	889	,,
S969.2	620	805	796	802	905	,,
SK406	650	800	751	756	829	,,
SK420	600	800	799	902	873	,,
GLC053	610	850	680	760	826	Carolusberg
GLC059	610	800	752	762	798	,,
CEA16	600	850	791	750	804	Okiep area
GEA17	600	710	683	770	848	,,
CEA36	600	790	642	782	842	,,
CEA37	600	780	538	749	834	,,
DGE76.1	610	730	653	551	825	Geselskapbank
DGE76.2	600	730	702	598	816	,,
DGE20.1	600	730	691	597	765	,,
DGE20.2	600	750	704	583	765	,,
DGE61	600	650	672	394	830	,,
GZ1.1	600	800	748	621	842	Buffelsrivier
GZ1.2	620	740	639	781	805	,,
GZ2.1	650	700	748	765	846	,,
GZ2.2	620	830	837	795	882	,,
GZ3.1	650	850	805	862	869	,,
GZ3.2	680	900	825	933	885	,,
GZ6.1	650	790	721	662	841	,,
GZ7.1	630	790	762	725	857	,,
GZ7.2	750	710	708	655	808	,,
GZ9.1	600	900	896	889	914	,,
GZ9.2	680	810	775	780	860	,,

Table 10.4 continued

METHOD	1	2	3	4	5	
HA1025	650	720	743	746	858	Kliprand
HA1050	800	720	726	823	825	,,
HA725	600	700	790	671	847	,,
HA472	700	760	790	1033	847	,,
HA239	650	850	778	806	915	,,
HA939	700	720	695	706	833	,,
HA269R	650	760	711	819	825	,,
HA269C	850	890	794	765	859	,,
STE305	650	805	827	601	866	Cape Rich
STE301	660	790	827	753	845	,,
STE298	640	770	819	762	838	,,
STE293	600	695	739	782	808	,,

1. Lindsley (1983) orthopyroxene
2. Lindsley (1983) clinopyroxene
3. Kretz (1983) solvus
4. Kretz (1983) Kd
5. Wood and Banno (1973)

The above results are disappointing because of the large variation in calculated temperatures between different samples from the same rock type and region. The Wood and Banno temperatures are regarded as too high (e.g. Bohlen and Essene, 1979). The Lindsley (1983) opx method consistently appears to yield temperatures which are too low, while the Kretz (1982) Kd method gives erratic results. The Lindsley (1983) cpx and Kretz (1982) 'solvus' methods are both based on the composition of the cpx alone (accepting that it is in equilibrium with coexisting opx) and the two methods give comparable and reasonably consistent results. The differences between opx and cpx temperatures (Lindsley, 1983 method) and the erratic Kd results (Kretz, 1982) reflect either (i) disequilibrium between the two pyroxenes in most of the samples, or indicate (ii) poor calibration of the geothermometers.

Davidson and Lindsley (1985) presented an update on two-pyroxene geothermometry, based on a thermodynamic analysis of the latest experimental data. Their method involves solving a system of equations in which the variables are P, T and the enstatite and wollastonite components of the pyroxenes (in the case of natural systems they use the components as calculated according to the projection method of Lindsley and Anderson, 1983). As with the Lindsley (1983) method, only the composition of one pyroxene is necessary; if the composition of the other pyroxene is added, the system is overdetermined and the precision of the calculated temperatures can be estimated. When applied to granulites, this latest pyroxene thermometer was found to give temperatures approximately 25°C higher than those generated by the method of Lindsley (1983). It is also sensitive for cases where the two coexisting pyroxenes are not in equilibrium. The projected compositions of the pyroxenes used in this study were compared to Figure 7a of Davidson and Lindsley (1985) and the temperatures thus obtained are slightly higher than those obtained by the Lindsley (1983) method for clinopyroxene. According to the positions of orthopyroxenes on that same graphical presentation, none of the

pyroxene pairs used are in equilibrium, supporting option (i) above.

One interpretation of the results is that post-equilibrium readjustment of the pyroxene compositions took place. In such a case any geothermometer based on distribution coefficients would be worthless. Solvus methods, however, will give minimum temperatures since the compositions of both pyroxenes can be considered as an intermediate stage, trending to the new, low temperature equilibrium composition. The solvus methods depend heavily on the Ca contents of the pyroxenes. The error which results from a minor change in the Ca content will be more severe in the case of the ferromagnesian pyroxene than in the case of the calcic pyroxene, as indicated by the close spacing of opx isotherms on the quadrilateral. In terms of this interpretation, one can conclude that the temperatures yielded by the Lindsley (1983) method for clinopyroxene and the Kretz (1982) solvus method reflect a minimum temperature of metamorphism and, barring analytical bias, the clinopyroxene composition yielding the highest temperature should be closest to the composition which coexisted in equilibrium with orthopyroxene during metamorphism. Where sufficient analyses are available and where a range of temperatures is indicated a **group of highest** temperatures would probably most closely approximate the thermal peak. The significance of the lower orthopyroxene temperatures is uncertain. Stephenson tentatively suggested that the temperatures yielded by the rims of orthopyroxenes in the Cape Rich area reflect the same metamorphic conditions as indicated by the rim compositions in metapelite garnets from the same region. The compositions of most orthopyroxenes in Namaqualand were apparently adjusted during a cooler period after the metamorphic peak, but the actual temperatures are probably not meaningful because of the large departure from equilibrium compositions.

The Cape Rich results show a notable correlation between the obtained temperatures and Fe:Mg ratios in the clinopyroxenes, i.e. the composition range graphically transect the isotherms (see Figure 10.30). In the present study area this effect is minimized by the relatively small compositional range of the clinopyroxenes among the rocks used and the temperatures obtained from the different domains are considered to be directly comparable.

Considering the relative temperatures indicated by the Lindsley (1983) method for clinopyroxene (Table 10.4), interesting comparisons can be drawn between the different areas considered here. The temperature indicated for the Ratelpoort lineament is at least 50°C higher than that for the Geselskapbank thrust sheet. Temperatures from the Cape Rich granulites compare well with those from the study area. Significantly higher maximum temperatures (as high as 900°C) are indicated for the region south of the Copper District and for southern Namaqualand.

Despite the fact that the metadolerite bodies escaped complete metamorphic reconstitution, the pyroxenes analyzed are of metamorphic origin. The Lindsley (1983) method indicates metamorphic temperatures similar those experienced by the granulites.

10.9.2 ORTHOPYROXENE-BIOTITE GEOTHERMOMETRY

In their experiments, Fonarev and Konilov (1986) showed that the distribution of Fe and Mg between coexisting biotite and orthopyroxene depends on the temperature at equilibrium. Their Figure 5 shows isotherms mapped on the $X^{Fe}_{biotite}$ / $X^{Fe}_{orthopyroxene}$ plane. Although not calibrated for natural systems, application of this geothermometer could indicate relative metamorphic temperatures. For all the cases where analyses of brown mica and orthopyroxene from the same specimen are available, the relevant Fe/(Fe + Mg) ratios are plotted on the abovementioned figure, here depicted as Figure 10.31. The rock types represented are metapelite, metadolerite, leucodiorite and two-pyroxene granulite. The metamorphites, with no relict primary mineralogical features, generally plot along one isotherm (800° C). On the other hand, the igneous rocks with variable metamorphic imprints plot amongst isotherms applicable to the igneous environment (1000 ° C and higher).

Generally the relative temperatures obtained for each of the samples represented in Figure 10.31 are consistent with the interpreted metamorphic developments - the metadolerite and the leucodiorite retained imprints of their magmatic history. Amongst themselves, the different granulites experienced equivalent peak metamorphic conditions, except for the specimen from the zone of advanced steep structure strain, which is interpreted to have been retrogressed. The results are, however, inconsistent with two-pyroxene geothermometry. The relatively high temperature indicated by the hypersthene and biotite of GLC053 on the Fonarev and Konilov diagram contrasts with the low temperature suggested by the low wollastonite content of the same hypersthene in terms of the two-pyroxene geothermometer (Figure 10.30). Present results include too few examples to draw valid conclusions regarding the general applicability of the biotite-orthopyroxene geothermometer.

10.9.3 BIOTITE-GARNET GEOTHERMOMETRY

The garnet-biotite geothermometer is based on the exchange reaction:

phlogopite + almandine = annite + pyrope

with the distribution of Fe and Mg between the biotite and the garnet being mainly a function of temperature. Several calibrations for the geothermometer have been published before the 1980's (e.g. Perchuk, 1969, 1970; Thompson, 1976; Holdaway and Lee, 1977; Goldman and Albee, 1977). In the lower temperature range (below 650 ° C), the Ferry and Spear (1978), Perchuk (1970) and the Thompson (1976) calibrations agree closely. Essene (1982) concluded that the biotite-garnet geothermometer is the 'thermometer of choice' for medium grade regional metamorphic rocks, using the experimental calibration of Ferry and Spear (1978). This calibration does not, however, work well in high grade rocks, since it generally yields temperatures which are too high. Compensation for the non-ideal mixing of Fe, Mg and Mn in garnet (Hodges and Spear, 1982) worsened the case (see Table 10.5 below). For high grade rocks, all other calibrations, including the recent experimental calibration by Perchuk and Lavrent'eva (1983), yield significantly lower temperatures than that of Ferry and Spear. Indaras and Martignole (1985) addressed this problem and proposed a new formulation of the biotite-garnet geothermometer taking into account the influence of Ti and Al in biotite. They applied their formula to high grade

rocks and found good correspondence with the empirical calibration of Thompson (1976).

TABLE 10.5 RESULTS OF BIOTITE-GARNET GEOTHERMOMETRY

Each number (e.g. grt-1) refers to a particular spot analysis.
c - grain centre; r - grain rim; cr - adjacent to chadacryst;
inc - chadacryst; f - not touching another ferromagnesian phase;
myr - biotite which forms a symplektic intergrowth with quartz.

No.	Garnet	Biotite	Kd	1	2	3	4	5	6	7	8
S579	grt-1	bt-1	.265	739	766	869	747	706	674	675	696
S579	grt-2	bt-1	.252	716	741	831	719	683	663	659	679
S579	grt-3	bt-2	.258	727	759	855	740	697	668	666	687
S752	grt-1	bt-1	.251	714	754	817	730	706	662	658	678
S752	grt-1	bt-3	.230	674	710	768	684	665	642	630	648
S752	grt-2	bt-2	.198	614	646	721	643	607	612	588	604
SK453B	grt-1c	bt-1c	.186	549	614	648	565	558	600	572	588
SK453B	grt-1c	bt-f	.332	860	898	957	815	805	728	756	781
SK453B	grt-2r	bt-2r	.180	580	605	641	560	548	593	562	578
S231A	grt-1c	bt-3	.311	822	846	886	755	756	712	731	755
S231A	grt-1r	bt-1r	.202	624	639	668	579	576	617	594	611
S231A	grt-2cr	bt-2inc	.182	586	599	622	518	521	596	566	582
SK387	grt-1r	bt-2myr	.236	685	723	804	714	682	648	638	657
SK387	grt-2c	bt-1f	.162	548	582	670	593	546	675	538	553
DST7	grt-1r	bt-1	.172	567	594	627	549	558	586	552	568
DST7	grt-3cr	bt-inc	.224	664	696	737	652	659	638	623	641
SK490	grt-1c	bt-1c	.246	703	716	732	654	655	657	651	670
SK490	grt-2c	bt-2c	.220	655	663	683	604	607	633	617	635
NMG032	grt-1	bt-1	.183	586	614	650	575	581	596	567	583
GNA002	grt-c	bt-inc	.162	546	550	557	462	474	574	537	552
GNA002	grt-cr	bt-inc	.168	557	559	569	470	480	580	546	561
GNA002	grt-4	bt-4	.126	473	475	484	425	435	530	481	494
GNA002	grt-3	bt-3	.135	494	496	502	438	447	543	496	511
GNA022	grt-1r	bt-1r	.105	430	441	467	402	389	503	446	459
GNA022	grt-c	bt-c	.155	534	552	584	501	485	567	527	542

1. Ferry and Spear (1978)
2. Hodges and Spear (1982) - adaption of the calibration of Ferry and Spear (1978), in this case asuming Margule's parameter = 0.
3. Hodges and Spear (1982) - adaption of the calibration of Ferry and Spear (1978), in this case asuming Margule's parameter = 3300 - 1.5T(° K).
4. Indaras and Martignole (1985), formula 1.
5. Indaras and Martignole (1985), formula 2.
6. Perchuk and Lavrent'eva (1983).
7. Thompson (1976).
8. (1 + 6 + 7)/3.

In the present study the geothermometer of Ferry and Spear (1978), the two modifications suggested by Hodges and Spear (1982), the calibrations of Indaras and Martignole (1985), Perchuk and Lavrent'eva (1983) and Thompson (1976) were applied to specimens from different localities in the study area. The results are given in Table 10.5. As found by Indaras and Martignole (1985), temperatures calculated by their calibration agree well with those according to Thompson's (1976) calibration for high grade rocks. At

lower temperatures, however, the Indaras and Martignole calibration yield temperatures which are too low. It appears that the calibration of Thompson (1976) is the most generally applicable biotite-garnet geothermometer, although it does not take into account the role of pressure or non-ideality of mixing in the two participating phases. To take into account the most popular experimental calibration, the most recent experimental calibration and the most popular empirical calibration, the average temperature found by aid of the methods of Ferry and Spear (1978), Perchuk and Lavrent'eva (1983) and Thompson (1976) respectively is here taken as a reasonable approximation, applicable over the whole of the study area.

10.9.4 GARNET-CORDIERITE GEOTHERMOMETRY

As a result of the continuous reaction

1/2 Mg-crd + 1/3 alm = 1/2 Fe-crd + 1/3 pyr

the distribution of Fe and Mg between garnet and coexisting cordierite is temperature sensitive, rendering it a suitable basis for a practical geothermometer. In this study three calibrations were used, namely those of

Thompson (1976) - T1
Holdaway and Lee (1977) - T2
Perchuk and Lavrent'eva (1983) - T3

These calibrations, with temperatures in degrees C, can be expressed as follows:

T1 = (2724.948 + 0.0155P)/(ln Kd + 0.896) - 273
T2 = (6150 + 0.0303P)/(2.69 - 1.98717 ln Kd) - 273
T3 = (3020 - 0.018P)/(ln Kd + 1.287) - 273

In the case of T2, Kd is the inverse of the Kd in the other two cases (see Albat, 1984).

One advantage of this geothermometer is that volatiles probably do not play any important role and it should be useable under both 'dry' and 'wet' conditions. Mineral pairs suitable for the application of the garnet-cordierite geothermometer are present in samples from three tectonic domains and results are given in Table 10.6 below.

TABLE 10.6 RESULTS OF GARNET-CORDIERITE GEOTHERMOMETRY

c - grain centre; r - grain rim; cr - adjacent to chadacryst; inc - chadacryst.

No.	Garnet	Cordierite	T1	T2	T3	Area
S752	grt-1	crd-1	679	659	607	Eenriet
SK387	grt-2c	crd-2f	535	534	488	,,
SK387	grt-2r	crd-1r	580	574	526	,,
SK297	grt-1c	crd-1	627	615	565	,,
SK297	grt-1r	crd-1r	550	548	501	,,
SK297	grt-c	crd-2f	604	595	546	,,
S378	grt-1c	crd-1c	708	683	631	Copper District
S378	grt-1r	crd-1r	611	601	553	,,
S381	grt-1c	crd-1c	717	691	639	,,
S381	grt-1r	crd-1r	573	568	520	,,
SK490	grt-1c	crd-1c	743	713	660	,,
DST7	grt-5r	crd-1	569	564	516	Geselskapbank
SK323	grt-1c	crd-inc	536	536	489	,,
SK323	grt-1r	crd-1r	507	510	464	,,
NMG031	grt-1cr	crd-inc	610	600	551	,,

10.9.5 GARNET-CORDIERITE GEOBAROMETRY

The continuous reaction

3 crd = 2 grt + 4 sil + 5 qtz

is sensitive to variations in pressure and such variations are reflected by the distribution of Fe and Mg between the two ferromagnesian phases. Calibrations of a geobarometer based on this reaction include those of Currie (1974), Weisbrod (1973), Holdaway and Lee (1977) and Martignole and Sissi (1981). Albat (1984) showed that a geobarometer for conditions of $P_{H_2O} = 0$ can be written as

$$P\ (bar) = 5206.423 + 2.976*T*\ln(Xg/Xc) - 2.6335*T$$

for

T = temperature (° K),
Xg = almandine component in garnet
Xc = Fe-cordierite component in cordierite.

He further elaborated a method for taking into account the role of water in the composition of cordierite and applied this method to rocks in the southern part of the Namaqua mobile belt (ibid., p. 213). The difference in pressure calculated for the two extreme cases of $P_{H_2O} = 1.0$ and 0.0 was found to be more or less 1kb, the lower pressure applicable to 'dry' conditions. The equation above can thus be used as an estimate of the minimum pressure, assuming that some water would always have been present during metamorphism.

Application of the above equation to specimens from the study area are listed in Table 10.7. The pressure minimum of between 5.1 kb and 5.5 kb for samples from the Copper District is lower than the pressure inferred by Clifford et al. (1981) for the Copper District's metamorphic peak. In the case of the Geselskapbank domain, where compositional adaptions of biotite, garnet and cordierite accompanied retrogression, the calculated pressure of around 5 kb is not consistent with the presence of andalusite as retrograde product in these rocks. Because the third term in the equation above largely cancels the contribution of the second term (the second term is a function of the mineral compositions), the equation tends to yield values close to that of the large first term, i.e. near 5 kb. It is insensitive to small variations in mineral compositions.

During recent experimental work, Aranovich and Podlesskii (1983) found a positive slope for the Fe end member reaction

alm + sil + qtz = Fe-crd

at variance with the results of Richardson (1968), Weisbrod (1973) and Holdaway and Lee (1977), who found positive slopes for the Mg end member reaction, but negative slopes for the Fe end member reaction. Martignole and Sissi (1981) argued that the negative slopes for the Fe end member reactions are at variance with calorimetric and field data. Aranovich and Podlesskii (ibid.) explain the contradiction in terms of probable non-equilibrium in those experiments which yielded the negative slopes.

Aranovich and Podlesskii (1983) mapped compositional isopleths for garnet and cordierite (which coexist with sillimanite and quartz) on the PT plane yielding an easy-to-use geothermobarometer. The relevant figure is given here as Figure 10.32. The positions of those samples in the study area with the correct assemblage and for which mineral compositions are available are plotted on Figure 10.32.

TABLE 10.7 RESULTS OF CORDIERITE-GARNET GEOBAROMETRY

c - grain centre; r - grain rim; cr - adjacent to chadacryst; inc - chadacryst; the calculated pressures are given in kilobars.

No.	Mineral pair	Albat (1984)	Aranovich & Podlesskii (1983)
S378	grt-cr crd-inc	5.7	5.3
S378	grt-r crd-r	5.3	5.0
S381	grt-cr crd-inc	5.7	6.0
S381	grt-r crd-r	5.1	4.8
SK323	grt-c crd-inc	5.3	3.2
SK323	grt-r crd-r	5.0	2.9
DST7	grt-r crd-r	5.1	3.3
NMG031	grt-cr crd-inc	5.3	3.2

10.10 DISCUSSION

Although structural evidence indicates that two orogenies have affected the Proterozoic rocks of the study area (Chapter 9), the metamorphic mineralogy can be explained mainly in terms of the effects of the Namaqua orogeny. The main metamorphic features of the different tectonic domains are as follows:

1. The Richtersveld Domain: Except for localized shear zones, the core zone displays structural features of the Orange River Orogeny. The metamorphic mineralogy, though defining the older fabrics mimetically, are the products of thermal metamorphism of the Namaqua Orogeny. Metamorphic grade increases from greenschist facies (actinolite and albite) to lower amphibolite facies (blue-green hornblende and oligoclase) from north to south. Neither of the two orogenies transformed the core zone sufficiently to obliterate certain primary igneous textures in metavolcanites. Retrogression is limited to the Late Shears.

2. The Groothoek Thrust Zone: The presence of sillimanite and cordierite in metapelitic rocks and the absence of K-feldspar + sillimanite assemblages reflect middle amphibolite metamorphic grade for the metamorphic peak. Penetrative retrogression during Skelmfontein thrusting involved the partial replacement of sillimanite and biotite by muscovite and the growth of andalusite porphyroblasts, late-kinematic relative to the Skelmfontein fabric. A low pressure environment is indicated by the andalusite, at least for the late stage of the Namaqua tectogenesis.

3. The Konkyp area: The same retrogression as in the Transition Zone is superimposed on the upper amphibolite assemblage K-feldspar + sillimanite.

4. The Eenriet Mountains: High temperature (metamorphic peak > 650° C) and low pressure (< 4kb) are indicated by mineral assemblages and mineral compositions. Mineral zoning tentatively suggest that a cool Transition Zone was thrust over a hot Steinkopf Domain during the early stage of the Namaqua Orogeny. Muscovite developed mainly during late (Skelmfontein) thrusting.

5. The Steinkopf Domain: Hornblende colours in amphibolites suggest a metamorphic zonation with the grade increasing from north to

south. The central and southern parts were subjected to upper amphibolite grade metamorphism during Skelmfontein reworking, as reflected by the amphibolitization of the Nariams dolerite dykes. Very late retrogression under greenschist facies conditions affected mainly the Middelplaat dykes and the Besondermeid metasedimentary enclave due to the relatively favourable permeability. This retrogression is possibly post-Namaqua in age.

6. The Copper District: Granulite facies metamorphism, with the temperature peak in the order of 800 ° C, is indicated by mineral assemblages (e.g. sapphirine-parageneses) and mineral compositions. Two-pyroxene assemblages define the Skelmfontein fabric along the northern limb of the Ratelpoort Synform. The development of orthopyroxene porphyroblasts superimposed on the Skelmfontein fabric and veins of two-pyroxene granulite which cut across the same fabric, show that these high grade conditions prevailed during and after the Skelmfontein thrusting in this area. Although new sillimanite grew during and/or after steep structure development, it appears as if the assemblage K-feldspar + sillimanite did not survive metamorphic transformation in zones penetratively affected by steep structure deformation.

7. The Geselskapbank Domain: The uppermost nappes contain stratigraphic units with a granulite metamorphic imprint. The highest grade reached by these rocks appear to be slightly lower than that reached in the Copper District (no Kfs + grt + crd, two-pyroxene geothermometry indicate a 50° C difference). If structural correlations, which place all the major thrusts in the same time category, are correct, the Geselskapbank granulites are clearly of an older (early Namaqua?) age than the syn-Skelmfontein granulites of the Copper District. Pro-grade and retrograde characteristics of the lower nappes are similar to those in the Konkyp area, while the andalusite in the upper nappes appears to be of the same structural age as the andalusite of the Groothoek Trust Zone.

11 MIGMATITES

11.1 GENERAL

Migmatitic rocks are widely distributed in the study area. This prominence renders the migmatitic phenomena useful for the assessment of the metamorphic evolution of the study area by making use of field observations only. The paleosome (average Gladkop Suite grey gneiss) invariably exhibits a fine-grained texture, continuous foliation (in the sense of Powell, 1979) and homogeneous composition, supplying an ideal reference framework. In this chapter the migmatitic features are classified into different types, site descriptions are given, to demonstrate geographical variation (Figure 11.1) and the implications with regard to the tectonic history of the study area are discussed. Finally the selected representative outcrop, GS-1 near Witwater, is described in detail.

11.2 CLASSIFICATION OF MIGMATITIC FEATURES

In terms of Mehnert's (1968) structural classification, stromatic, flecky and nebulitic types are the most common varieties of migmatitic rocks in the study area. Different ages of neosomes are distinguished on grounds of relations with fabrics and structures described in Chapter 9. A shorthand nomenclature system is used whereby N2s denotes a stromatic neosome of the second age class and N5n refers to a nebulitic neosome of the fifth age class.

The oldest neosomes (N1) are recognized as compositional banding parallel to the oldest fabric in the grey gneiss. The bands vary in width from a millimetre to several centimetres (e.g. Figure 4.11). The composition is granitic and a mafic selvage is discernible. The texture in the neosome is generally fine-granoblastic and equidimensional, similar to that of the paleosome (except for the effect of biotite in the latter). Where advanced levels of early Namaqua strain is present in gneiss with an augen texture, the distinction between N1 neosomes and elongate augen is not clearcut (e.g. Figure 4.13).

The characteristics of the N1 texture contrasts with the inequidimensional medium-grained to pegmatitic nature of stromatic leucosomes in general (e.g. Mehnert, 1968, Chapter 3). This textural peculiarity of the N1 leucosomes can be explained by metamorphic recrystallization. Should the N1 neosomes represent a metamorphic phenomenon older than the main Namaqua metamorphic event, the rock can be interpreted as a metamigmatite (metamorphosed migmatite).

Stromatic neosomes of the second age class (N2s) are concordant to the regional foliation for most part and, in many instances, ptygmatically folded where they deviate from this general orientation (e.g. Figure 11.2). Texturally they vary from medium-granoblastic inequigranular to pegmatitic. Flecky neosomes also occur in this structural class (N2f, Figure 11.3). In the Gladkop grey gneiss the melanosome of the latter is hornblende in most cases, but biotite or hypersthene constitute the mafic part of the neosomes in some places.
In some places along Skelmfontein shear zones N3s neosomes are very prominent. In the Ratelpoort synform, such neosomes grade inperceptibly into Kweekfontein Granite (Chapter 7). Similarly the

Eyams Granite can be classified as N3n. Flecky neosomes of this structural category (N3f) are superimposed on the early Namaqua regional fabric (Figure 11.4) and are deformed by the Skelmfontein refoliation (Figure 11.5). The distinction between N2f and N3f is possible only where distinction can be made between the early Namaqua regional foliation and the Skelmfontein shear fabric. In many cases the latter is not clearcut.

Minor neosome development along the Dabbiknik shears (N4s) and flecky neosomes (N4f) transect the Skelmfontein shear fabric. The N4f neosomes are mineralogically indistinguishable from the N3f neosomes.

Pegmatitc features associated with younger structures are not considered here. The classification scheme outlined above is of little use, of course, on outcrops where the local fabrics cannot be readily correlated with the established structural framework.

11.3 FIELD DESCRIPTIONS

In order to elucidate the manifestation of the different migmatitic phenomena in the study area, the migmatitic features of twelve example sites are briefly described below (the locations of the example sites are shown in Figure 11.1). Next, the observed distribution of key types are discussed.

11.3.1 EXAMPLE SITES

Site I The Steinkopf Gneiss at this locality is fine-granoblastic with a continuous foliation. The gneiss is compositionally heterogeneous because it contains thin (< 20 cm) discontinuous biotite-rich bands. Fine-granoblastic flecky neosomes occur as irregular patches and zones (Figure 11.6), some of which transect the compositional banding. The neosomes consist, in decreasing order of abundance, of plagioclase, quartz, blue-green hornblende and K-feldspar . Small anhedral sphene grains and relict biotite patches are associated with the hornblende. The hornblende crystals, together with the rest of the neosomes, are elongated to define an L-tektonite (Turner and Weiss, 1963). The outcrop surface seen in Figure 11.6 is oblique to the stretching direction. The flecky neosome at this site is unique because of the fine-granoblastic equidimensional texture and can be compared to the more general early stromatic N1s neosomes.

Minor N2s type leucosomes are also found at site I. They are also unique in the sense that they lack mafic selvages, indicating a totally arteritic origin.

Site II The country rock at this site is Steinkopf Gneiss and Brandewynsbank Gneiss, the latter structurally overlying the former in this particular case. No N1 neosomes are apparent in the gneisses. N2 stromatic type neosomes are present but scarce (< 1 percent of the outcrop area).

Medium-grained to coarse-grained pegmatitic veins transect the N2 veins and are folded where oriented at a high angle to the local foliation (Figure 11.2). The mafic selvage along the pegmatitic vein edges remain the same width (approximately 1 mm) despite significant variation in the width of the veins themselves. The younger veins increase in abundance towards a sheet of Eyams

Granite; a three metre wide contact zone between the gneiss and the granite can be described as a nebulitic migmatite.

Site III The Steinkopf Gneiss at this locality is structurally overlain by Konkyp Gneiss. N1s, i.e. early stromatic neosomes are abundant. A detailed traverse of 5 metres across strike yielded 57.44 percent N1s and 11.5 percent N2s by surface area (Figure 11.7). Such measurements have limited value, however, because some fifty metres from where the traverse was measured, another outcrop consists almost entirely of nebulous N1 migmatite (Figure 11.8). Flecky neosomes of the N3 class occur as small isolated patches.

A small body of Wyepoort Granite transects the grey gneiss locally and carries xenoliths of the gneiss with N2 neosomes. The age relations with the N3 neosomes could not be established at this site.

Site IV The Steinkopf Gneiss in this area apparently contains no significant N1 neosomes. Stromatic N2 neosomes constitute an estimated 15 percent of the gneiss. Flecky neosomes occur in patches and cover approximately 2 percent of the outcrop area. An advanced form of this type of flecky neosome development, where it affects calc-silicate rich parts of the gneiss, is described in Chapter 10.4.2. The regional fabric is common to the grey gneisses and the adjacent Konkyp Gneiss, therefore the flecky neosomes are classified as N3.

All metamorphic hornblende in the Konkyp is blue-green in thin section (Chapter 10.4). This includes the hornblende in the N2f neosomes.

Site V Dabbiknik deformation locally 'shortened' a portion of Steinkopf Gneiss and a refoliation normal to the foliation/banding of the gneiss developed. In the latter process the foliation/banding was unstrained to some extent and the distribution density of N1s is approximately 50 percent. Some of the wider N1 leucosomes exhibit a new Rooiberg-type banding (cf. Chapter 4.4.1). A photograph of the grey gneiss at site V is presented as Figure 9.4.

N2s and N3s together constitute less than 5 percent of the outcrop area at this site.

Site VI This site, the type locality of Eyams Granite in the Steinkopf Domain, is characterized by schlieric to nebulitic migmatite within which remnants of the country rock, in various stages of transformation, abound. The subtle nature of the emplacement (in situ development?) of the Eyams Granite is exemplified by the way in which a small body sharply cuts across N1s and N2s neosomes in the country rock grey gneiss at one place and, within a few centimetres, fades away (Figure 11.9).

In the Kinderlê Gneiss nearby, minor N3 flecky neosomes contain sillimanite and biotite as part of the melanosome.

Site VII At this site (Korrogas) several stratigraphic, structural and migmatitic features of the Gladkop gneisses can be demonstrated (e.g. Figure 4.13). At one locality, where non-domainal Steinkopf Gneiss and an augen-bearing variety of the Brandewynsbank Gneiss are in contact, the development of N1 stromatic neosomes can be examined in both gneisses. Although, at first glance, the N1s neosomes appear to be confined to the Steinkopf Gneiss, closer

inspection reveals that similar neosomes are present in the augen gneiss as well, albeit less ubiquitous and of more limited individual continuity; some N1s neosomes appear to be the extensions of flattened augen (Figure 11.10). An N1s distribution density of up to 50 percent is developed at some places at Korrogas, but, in general, does not exceed 30 percent of the outcrop area. N2s neosomes, ptygmatically folded in some places, constitute a measured 5 percent of the outcrop area. Advanced N2 neosomes, with a schlieric to nebulous appearance, grades almost imperceptably into the paleosome. It is prominently developed at one occurrence, covering about 30 percent of the outcrop area, but is poorly developed elsewhwere. Small N3f neosomes cover less than 2 percent of the outcrop area.

Both N1s and N2s neosomes are more prominently developed in the Steinkopf Gneiss than in the Noenoemaasberg Gneiss. The difference is especially notable where the two orthogneiss units are interbanded on metre scale at the nothwestern limit of the Korrogas outcrops.

Site VIII Site VIII is in an area of zonal development of Skelmfontein shearing. The status of N1 neosomes are unclear. N2 stromatic neosomes are poorly developed (< 5 percent of the outcrop areas). N2f neosomes constitute some 30 percent of the grey gneiss outcrops. Areas as large as 500 m² can be described as metatexites (migmatite with no paleosome remaining). The hornblende colour in thin section is olive green. The superimposition of N3f on N2s is shown in Figure 11.11.

Site IX Advanced Skelmfontein refoliation renders N1s and N2s neosomes in this region to be indistinguishable from each other. N3f is well developed, preferentially along particular bands in the grey gneiss. Flecky neosomes of the N4 category cut across all the older features and reaches its most prominent development in this area (Figures 9.8 and 11.12).

Site X Some two kilometres to the north of site IX the Brandewynsbank Gneiss shows relatively low strain. N2f neosomes are superimposed on the augen texture of the gneiss and the stages of the process is illustrated in Figure 11.13.

Site XI At site XI a twenty metre wide band of Steinkopf Gneiss occurs within augen gneiss of the Little Namaqualand Suite. The normal neosomes in the grey gneiss are not clearly discernible because of advanced strain. The contact zone between the grey gneiss and the Nababeep Gneiss is locally characterized by apophyses of the Nababeep Gneiss and younger pegmatitic veins. Advanced deformation of this zone yielded a mixture of rock types (Figure 11.14).

Site XII This site is in the southeastern part of the Copper District. N1 neosomes are not recognised. Pegmatitic N2s neosomes (< 2 percent of the outcrop area) range in width from a few millimetres to several decimetres, in some cases as part of single continuous bodies (Figure 11.15). N2f neosomes are well developed (<= 30 percent of the outcrop surface) and pre-date the pegmatitic neosomes. The N2f melanosomes contain biotite and hornblende, the latter olive-green to brownish in thin section. A few patches of N3 flecky neosome contain hornblende only as melanosome (Figure 11.4)

11.3.2 DISTRIBUTION OF KEY MIGMATITE-TYPES

11.3.2 DISTRIBUTION OF KEY MIGMATITE-TYPES

During routine mapping, the estimated volumes of the different migmatites at each investigated outcrop were noted. An attempt to quantitatively map out the different features proved impractical due to the seemingly random variations on outcrop and regional scale. The geographical distribution of some features which are significant in terms of the metamorphic evolution of the study area can, however, be considered.

The best development of N1 neosomes are found at the northernmost outcrop of Steinkopf Gneiss (Example site II). This is in direct contrast to the metamorphic zonation which confirms to maximum metamorphic grade in the south.

The best development of N2 flecky neosomes are found in the area shown in Figure 11.1. Neosome areas of up to 10000 m² are found in this zone, although they are still haphazardly distributed (Figure 11.16). N2 flecky textures with orthopyroxene in the melanosome were found at isolated localities in the Copper District. These localities are also shown in Figure 11.1.

Flecky neosomes are developed in Leeupoort augen gneiss in the Ratelpoort Synform, as reported by Martens (1979). His descriptions fit the characteristics of the N3f neosomes.

Remobilization of Brandewynsbank Gneiss during Dabbiknik shear deformation caused a 'Sederholm effect' in the sense that a mafic dyke intrusive into the gneiss is cut by the remobilized gneiss along shear zones (Figure 11.17).

11.4 THE GEOLOGY OF OUTCROP GS-1 NEAR WITWATER

11.4.1 INTRODUCTION

Outcrop GS-1 represents the geology of the Steinkopf Domain to a large extent. The outcrop is situated some 10 km from Steinkopf, 20 m south of the road to Nigramoep (see Figure 11.1). The outcrop consists essentially of highly migmatized gneisses, small granite bodies, pegmatities and minor lenses of interpreted supracrustal rocks. Many of the important structural, igneous and metamorphic aspects of the area can be studied on this one domal outcrop. Part of the outcrop was mapped in great detail. The map (given here as Annexure 2) is in two parts and a total of 400 m² is covered. An alphabetic/numeric coordinate system is convenient for describing specific localities and is referred to in the descriptions (see Annexure 2).

11.4.2 THE SUPRACRUSTAL ROCKS

In the region of N-34 a nine metre long lense interpreted as a metavolcanite (with a rhyodacitic composition) is apparent. The texture is not gneissic and it includes a thin quartz band which could be of sedimentary origin. Although no age relations relative to the Gladkop gneisses can be established on this outcrop, minor xenolithic lenses of similar 'pretectonic' grey gneiss are found in some places in the Steinkopf Domain, e.g. east of Middelplaat.

11.4.3 STEINKOPF GNEISS

11.4.3 STEINKOPF GNEISS

The major part of the paleosome in the outcrop consists of Steinkopf Gneiss. It displays the typical penetrative foliation/banding with stromatic leucosomes (mm to cm scale). At a few places K-feldspar megacrysts (interpreted as relict phenocrysts - see Chapter 4) are preserved, for example just north of the pegmatite dyke at J-32.5. In the northernmost extension of the map, isoclinally folded mafic bands are shown. Such mafic bands are widespread in the Steinkopf Domain and are commonly found in all three of the gneiss units of the Gladkop Suite. They range in composition from normal amphibolite, through biotite amphibolite to biotite-feldspar rock devoid of amphibole. No clearcut indication of the age relations are apparent at outcrop GS-1.

11.4.4 NOENOEMAASBERG GNEISS

Bands of Noenoemaasberg Gneiss are shown in the northwestern portion of both mapped blocks. It is fine-grained, penetratively foliated to thinly banded and contains only minor leucosomes. In the northernmost extension of the map (from Y-37 to B-31) vague assimilation effects (schlieric remains of the Steinkopf Gneiss in the Noenoemaasberg Gneiss) are consistent with numerous other field observations in the Steinkopf Domain, indicating that the Noenoemaasberg Gneiss has intruded into the Steinkopf Gneiss.

11.4.5 GREY METAGRANITOID

The grey metagranitoid (mineralogically adamellitic to granodioritic in composition), which crops out in the southern parts of the map, cannot be correlated with any major lithological unit of the Steinkopf Domain. It clearly crosscuts the penetrative foliation/banding of the Steinkopf Gneiss (south of U-6), but is in turn cut by neosomes which are concordant with the planar fabric in the gneiss (T-9, Figure 11.18). In the southwestern parts, the granitoid is dissected into lenticular rafts by the migmatitic granite.

11.4.6 SYNTECTONIC PEGMATITE

Small sheets and pods of the 'syntectonic pegmatite' are confined to the northern parts of the map. Relative to the fabrics in the gneisses, this pegmatite belongs to the same age bracket as the grey granitoid.

11.4.7 NEOSOMES AND THE EYAMS MIGMATITIC GRANITE

Although no attempt was made to depict leucosomes of different ages in different ways, at least three groups with distinctly different structural styles are apparent on the map. The first group is concordant with the foliation and individual veins vary in width from 1 to 300 mm. Thus the leucosomes merge with the fabric at one extreme, representing the microlithon part of the disjunctive foliation. These leucosomes are generally medium-grained and the wider ones, at some places, cut across the foliation at a low angle. They are therefore classified as N2s, i.e. part of the second generation stromatic neosomes. Possible relict N1s leocosomes are found at L.5-37.5 (i.e. 50 centimetres south of the L coordinate and 37.5 metres west of the numeric origin). At this locality relatively wide N1s leucosomes cut across the foliation and are in turn transected by the Eyams migmatite (Figure 11.19).

The Eyams granite, as elsewhere, has all the characteristics of an in situ metatexite and descriptive terms such as schlieric, nebulitic and nebulous (Mehnert 1968) are applicable (e.g. Figure 11.20). At some places the geometry of schlieren and ghost banding reflect the paleosome structure to a large extent, indicating passive emplacement or granitization. However, the migmatite has its own zonally developed planar fabric, which dips towards the north-northwest at a shallow angle. It could be described as flow banding, but the shear effects at the contacts with the paleosome indicate a kinematic origin (e.g. D-36 and L-35).

Flecky neosomes (stichtolithic structure) cuts clearly across the stromatic leucosomes and are associated with northwesterly trending minor shears. These migmatitic structures are grouped as N4f. The flecky neosomes are restricted to areas in which the more biotite-rich Steinkopf Gneiss paleosome occurs. The melanosome flecks are themselves biotite concentrations and the texture of the leucosome is medium-granoblastic and sugary. The shearing associated with the flecky neosomes is of a later generation than the Skelmfontein shearing associated with the Eyams migmatitic granite, hence the N4f classification.

11.4.8 LATE GRANITE AND LATE PEGMATITES

A 40 cm wide northeasterly trending granite dyke in the southeastern corner of the western map portion is fine-grained and leucocratic and probably correlateable with the Wyepoort Granite (Chapter 7). Two northeasterly trending dykes (10 to 40 cm wide) and a two to three metre wide irregular body of pegmatite cut across all the abovementioned lithological types in the mapped area.

11.4.9 STRUCTURE

Isoclinal folds involving mafic bands in the northernmost extention of the map have axial planes parallel to the penetrative foliation of the gneiss. An older fabric similar to the penetrative foliation of the gneisses is folded around the hinge zone of one of the isoclines. These folds and the foliation of the gneiss thus represent the oldest structures in the map area. Except for local zones of disturbance, these planar structures generally have mild dips in the order of 20°. The strike and direction of dip vary as a result of younger deformation.

The shear fabric associated with the Eyams migmatitic granite also dips at low angles (20° or less) and is subhorizontally disposed for most part. In the area of the GS-1 outcrop the general strike of the shear fabric is east-northeasterly while that of the older foliation/banding is north-northwesterly, resulting in the two sub-parallel fabrics to appear orthogonal when viewed in plan (e.g. in the region of F-36).

Two sets of steep northeasterly trending shears cut across the shallow dipping structures, namely an older, minor set with left lateral separation which strikes at about 40 degrees and a second, more prominent set, striking at 65 degrees. At G-29 the separation along one of these shears is clearly right lateral, but, for most part, there is no shear displacement visible, suggesting that the movement was mainly in a direction normal to the plane of outcrop, i.e. close to vertical. These shears are considered to be minor structures resulting from an important deformation event, seen regionally as a set of subvertical mesoscopic to macroscopic

northeasterly trending folds. The open folds such as at K-35 and G-28 are minor examples of the meso-scale folds. A mineral refoliation which accompanies the folds is well developed at places on the GS-1 outcrop, for example at L-37 where it clearly cuts across the shear fabric of the Eyams migmatitic granite. Areas devoid of such refoliation suggests heterogeneous strain on outcrop scale.

One of the late pegmatite dykes are located in a right lateral shear zone which caused rotation of all the abovementioned structures over a shear zone width of at least 5 metres, as can be seen in the region of K-11. It demonstrates the ductile nature of deformation at a late stage in the tectonic evolution of the Steinkopf Domain.

11.4.10 CONCLUSIONS

The geology of outcrop GS-1 reveals a complex history of tectonic development of a small part of the Steinkopf Domain. Two major subhorizontal deformation events and associated recrystallization and/or migmatization were responsible for the basic geometric and lithologic characteristics of the rocks. Later northeasterly trending folding, refoliation and shearing contributed to minor alterations.

11.5 DISCUSSION

The migmatitic development of the grey gneisses indicates a complex metamorphic history. Because the separation of components caused by migmatization is largely preserved during subsequent tectonism, the principal attributes of the migmatitic history is reflected by observable outcrop features. In contrast, the mineral assemblages and/or mineral compositions of metapelitic and mafic paleosome (non-migmatic metamorphites) usually reflect the last major metamorphic event only.

The N1 neosomes are interpreted as the products of the Orange River Orogeny because they are deformed and recrystallized; they do not appear in augen gneisses (Little Namaqualand Suite) and their maximum development bears no geographic relation to the Namaqua metamorphic zonation. The Vioolsdrif Suite granitoids were migmatized during the Namaqua Orogeny in the eastern extension of the Orange River igneous belt (Blignault et al., 1983). These rocks lack N1 type neosomes, but are characterized by N2-neosomes of the flecky and stromatic type (according to field observations during visits to the area between Goodhouse and Pella drif, on either side of the Orange River). Although the Gladkop Suite and the older parts of the Vioolsdrif Suite are of similar emplacement age, that part of the latter granitoids which are exposed at present, escaped the high grade effects of the Orange River Orogeny.

The advanced development of N2 flecky neosomes (no paleosome remaining in relatively large areas) in an easterly trending zone adjacent to the granulite terrane of the Copper District, indicate large scale anatexis. The melanosome in this flecky migmatite is mainly composed of hornblende while the paleosome is grey gneiss with the chemical and mineralogical composition of biotite granite. This indicates a metamorphic temperature of more than 700° C for PH_2O = Ptot $\geq$ 4 kb (Bösch et al., 1974). The N2f neosomes with orthopyroxene in the melanosome, found in the Copper District, indicate local conditions of $PH_2O \leq$ Ptot (ibid., p. 360).

The occurrence of prominent N2 flecky neosomes in the Konkyp area (with hornblendic melanosomes) is noteworthy. The proximity of the Konkyp Gneiss to these can be compared with the proximity of the Copper District augen gneisses to the flecky neosomes in the south. These features are consistent with the observed spatial association of the highest grade metamorphism with augen gneisses (e.g. Blignault, 1977). Although these flecky migmatites from both regions are mineralogically similar, the hornblende colours, as observed in thin section, differ; those of the Konkyp area are blue-green and those in the south are olive-green. This is interpreted to reflect compositional adaptation of the hornblende to prevalent metamorphic conditions during late Namaqua tectonism (Skelmfontein thrusting).

The question of whether a stromatic leucosome is a venite (developed in situ) or an arterite (introduced) is difficult to resolve and requires extensive petrological analyses, which need not necessarily provide conclusive results (e.g. White, 1966; Hedge, 1972; Ashworth, 1976). The presence of a mafic selvage to a leucosome vein are considered by some to prove the venitic origin (e.g. Amit and Eyal, 1976, p. 109), but, in fact, it probably only indicates that some of the leucocratic components of the paleosome were incorporated in the leucosome, whether the leucosome originated in situ or not. If the mafic selvages developed only along in situ leucosomes, their widths should vary sympathetically with those of the veins - obviously not the case in many pegmatitic veins in the study area. On the other hand, a cm wide arterite would not contain enough energy to actively assimilate the country rock and a melanosome along such a vein would indicate that metamorphic conditions were favourable for the migmatic process of the separation of leucocratic and mafic phases, regardless of the origin of the vein itself. The next question then is whether this migmatitic process involved melting. Where the metamorphic assemblages in the paleosome indicate upper amphibolite facies metamorphism and the leucosome's composition is reasonably close to the granite eutectic, it is most probable that the migmatite originated through partial melting. The latter argument is applicable to obviously in situ migmatites (the flecky migmatites) as well. The absence of an obvious magmatic source, the ubiquitous melanosomes and their generally narrow widths, indicate that the N2 stromatic neosomes were of metatectic origin.

Flecky neosomes of the N3 age category appear to be associated in time with the development of the migmatitic Kweekfontein and Eyams Granites and Skelmfontein shear deformation. The development of N3 neosomes in augen gneiss of the Little Namaqualand Suite, superimposed on the early Namaqua regional fabric of the gneiss, is consistent with high grade conditions indicated by the pelitic and mafic metamorphites during Skelmfontein deformation for the Copper District.

It is generally observed that migmatitic features are more prominently developed in the Steinkopf Gneiss than in the more leucocratic Brandewynsbank Gneiss (e.g. Chapter 4.4.4). This is interpreted as resulting from the greater availability of water, emanating from the larger volume of biotite in the Steinkopf Gneiss, relative to the Brandewynsbank Gneiss. The Noenoemaasberg Gneiss composition is close to that of the granite eutectic, apparently allowing large scale re-melting of this unit in some places (see Chapter 4.4.1, the N2-type of Noenoemaasberg Gneiss).

Sustained elevated temperatures during the Late Shearing (Dabbiknik and Ratelpoort Shears) are indicated by the development of N4s and N4f neosomes over the whole of the Steinkopf domain.

12 CONCLUSIONS

One of the most important results of the UOFS Geodynamics Project was the provision of a stratigraphic classification of the major lithological units in the Namaqualand Geotraverse, much of which were previously unknown. This applies particularly to the Steinkopf Domain which was not mapped before.

The grey and pink gneisses of the Steinkopf domain have the appearance of a basement complex while the banded varieties were formerly considered part of a metasedimentary sequence, but it is now established that those gneisses in fact represent an orthogneiss unit, i.e. the Gladkop Suite. The Gladkop Suite intruded the Bushmanland Group sedimentary rocks more or less at the same time that the Vioolsdrif Suite was emplaced into the Haib Subgroup volcanites. Deformation, metamorphism and migmatisation transformed the granitoids into fine-granoblastic gneisses with strongly developed secondary banding in some places. Sufficient primary characteristics were retained, however, to indicate the origin and relative age.

The plausible tectonic models for the Namaqua Geotraverse are constrained by the stratigraphic peculiarities. All supracrustal rocks are older than the Gladkop Suite; no supracrustal rocks are associated with the Namaqua Orogeny. The rocks associated with the Vioolsdrif Suite are mainly of volcanic origin (Haib Subgroup) and together they define a major calc-alkaline igneous complex - the igneous products of the Orange River orogeny. The metasedimentary units (Khurisberg Subgroup, Eenriet Subgroup) are possibly the geosynclinal accumulations of the Orange River orogeny. Deep water sediments may be represented by the Grünau Subgroup of the Korannaland Sequence while a shallower basin contained the more psammitic sediments of the Khurisberg - and Eenriet Subgroups.

The geographical association of the Eenriet and Khurisberg Subgroups with the Gladkop Suite (by analogy of the spatial association between the Vioolsdrif Suite and the Haib Subgroup), together with the compositional peculiarities of the Gladkop Suite, indicate different tectonic environments for the two time-equivalent intrusive suites during the Orange River orogeny. One model suggests that the Gladkop Suite developed oceanward of a continental or near-continental arc environment represented by the Vioolsdrif Suite and Haib Subgroup.

The isotopic age of about 1800 Ma (Barton, 1983) for the Gladkop Suite was retained throughout the Namaqua Orogeny because of high grade metamorphism soon after emplacement. This metamorphism probably coincided with the anatexis which produced the younger phase of the Vioolsdrif Suite at more or less 1750 Ma (Reid, 1977); the 1800 Ma age possibly representing a mixed age between the age of emplacement (contemporaneous with the older Vioolsdrif intrusives) and the time of metamorphism (e.g. Loock, 1984). The main remnant of this first metamorphic event in the Gladkop Suite is the presence of the N1 neosomes. Those parts of the Vioolsdrif Suite presently exposed did not suffer the high grade effects of the Orange River orogeny. Where these gneisses were penetratively involved in the Namaqua orogeny (in the easternmost extension of the Orange River Igneous belt), migmatitic effects of the N2 age and younger, developed.

The prominent development of N1 neosomes near the present junction between the Steinkopf Domain and the Richtersveld Domain and the

low grade character of the core zone of the Richtersveld Domain are the only indications of metamorphic zonation during the Orange River Orogeny. The northeasterly tectonic transport of pre-Namaqua age indicated by the geometry of the Tsams Thrust (Blignault et al., 1983) possibly reflect the direction of main tectonic transport during the Orange River Orogeny. The anomalous situation of low grade rocks having been thrust across high grade rocks along the Groothoek Thrust (Figure 1.2) could conceivably be attributed to a reverse situation inherited from the early orogeny whereby the Steinkopf Domain structurally overlaid the Richtersveld Domain.

In terms of the above model, the Gladkop Suite was involved in thrust deformation during two orogenies, explaining the extreme strain and resultant textural properties of the grey gneisses.

The early Namaqua metamorphic zonation apparently involved equally high grade metamorphism in the whole of the Steinkopf Domain as well as the Konkyp area of the Transition Zone. The distribution of the the most significant early Namaqua migmatite is consistent with the spatial association of the Little Namaqualand Suite with the highest grade metamorphites in the Geotraverse and beyond (e.g. Blignault, 1977). This supports the model according to which the early Namaqua metamorphism was mainly controlled by the syntectonic distribution of large volumes of silicic magma - the Little Namaqualand Suite. Under the force of gravity, the magma spread from a topographical high (a magmatic arc) in the form of hot and ductile thrust sheets. The Koras-Sinclair arc, as the magmatic source, fits this model in terms of the kind of magmatism involved (silicic), the age (1100 - 1200 Ma) and the location (the thrust movement was from the northeast toward the southwest, the Koras-Sinclair arc is situated northeast of the Geotraverse) (Blignault et al., 1983). The thrusting was deep seated for most part and, at the crustal levels now exposed for the augen gneiss domains, cooling took place at a very slow rate. This allowed prolonged interaction between crystàls and melt in the granites and the growth of megacrysts, subsequently and/or simultaneously deformed to augen. Richtersveld Domain was heated from above and below as it was first overridden by the Grünau thrust sheet, then undercut by the Groothoek Thrust and driven across the Steinkopf Domain in the west and the Bushmanland crustal segment (dominated by augen gneisses) in the east (Figure 12.1). For ease of discussion and in line with nomenclature used in the foregoing chapters, the Bushmanland crustal segment will be referred to as the Bushmanland domain.

The present metamorphic zonation in the study area is largely the product of metamorphism during the late stage of the Namaqua tectogenesis during which the Skelmfontein thrusting took place and the Spektakel Suite was emplaced. The relatively low metamorphic pressures indicated by the metamorphic petrology implies a high geothermal gradient, probably sustained by the addition of the Spektakel Suite magmas (and fluids ?). The pressure estimates of up to 8 kb for the Copper District, (Clifford et al., (1975a, 1975b, 1981)) are not consistent with petrological data for the common metamorphites; an upper pressure limit of 6 kb, as reported from the south, is favoured (e.g. Waters, 1986, Zelt, 1980 and Albat, 1984). It must be pointed out, however, that the pressure estimates apply only to the late Namaqua tectogenesis and very little indications exist as to the pressure conditions during early Namaqua times.

The Skelmfontein thrusting imparted a retrograde metamorphic fabric

on the rocks of the Transitiion Zone and the northern Steinkopf Domain. The metamorphic grade associated with this late kinematic fabric increases towards the south and very high grade conditions are indicated by the development of granulite veins (melts?) near Skelmfontein se Poort. The area where cooling took place is where the hanging wall of the Skelmfontein thrust was dominated by the cool extension of the Rictersveld Domain. Where the hanging wall was dominated by augen gneisses and the granites of the Spektakel Suite, the high grade metamorphic conditions, which reigned during the early Namaqua tectogenesis, were retained. This tectonic model is schematically explained in Figure 12.1.

Note that the model requires the Copper District to be underlain by components of the Steinkopf Domain plus more augen gneisses. Gladkop Suite gneisses occur as relatively small slivers within the Copper District and possibly reappears in significant volumes, as part of the gneisses grouped together as the Garies Subgroup (Joubert et al., 1980), further toward the south.

The scheme described above and depicted in Figure 12.1 does not satisfactorily resolve the relationship between the Bushmaland crustal segment and the Copper District. Lithological differences between the two augen gneiss domains include the following: the Bushmanland domain contains a higher volume of supracrustal rocks (mainly metasedimentary) than the Copper District; the Spektakel Suite is confined to the region of the Copper District and further to the south and west and only minor correlatives occur in the Bushmanland domain; the Koperberg Suite is confined to the Copper District. Furthermore, the Bushmanland domain is characterized by amphibolite facies metamorphism in contrast with the Copper District's established granulite facies imprint (note that the granulite rocks of the Geselskapbank area were tectonically introduced and are of an older age than the Copper District granulites). It is thus apparent that the Copper District represents a deeper crustal level than the Bushmanland domain; the junction between the two crustal segments is possibly defined by as yet unmapped thrust faults.

Although most of the Spektakel Suite rocks were involved in late Namaqua thrusting and their place of origin therefore undetermined, indications are that these intrusives did not experience the same horizontal displacements as is suggested for the augen gneisses. The vertical attitude of the Middelplaat dykes and the fact that they transect the Skelmfontein fabric indicate that at least this unit of the Spektakel Suite originated in the deeper parts of the crust now exposed in the region of the Copper District. The Koperberg Suite similarly cuts across all subhorizontal fabrics and the associated deformation processes involved material movement in the vertical (steep structures), indicating an origin somewhere directly below the present exposures. The described attributes of the Spektakel and Koperberg Suites suggest that Copper District represent the source area for Late Namaqua magmatism. This could be the result of local crustal thickening due to the primary tectonic style of thick skinned thrust tectonics which characterized the Namaqua tectogenesis.

ACKNOWLEDGEMENTS

I am grateful to the following persons/institutions for generous assistance and support:

Dr. H. J. Blignault skillfully led the UOFS-NGP project.

Prof. A. E. Schoch supervised the thesis and guided me past scientific and grammatical pitfalls.

Other friends at the UOFS contributed in their different ways: Dr. S. W. van der Merwe (companion in the field), Dr. D. Strydom (Geselskapbank data and samples), Dr. H. de Bruiyn (electron microprobe analyses), Dr. W. A. van der Westhuizen and Prof. L. D. C. Bok (XRF analyses) and Messrs. A. Felix and J. Stallenberg (draughting).

The Geological Survey of South Africa in Pretoria provided whole rock chemical analyses and electron microprobe analyses and here Dr. G. du Plessis was both helpful and hospitable.

The Dept. of Geochemistry, University of Cape Town allowed the use of their electron microprobe and Mr. R. S Rickard instructed me.

The O'okiep Copper Company provided logistical support and staff members like Messrs. J. A. H. Marais, G. H. F. Schreuder, A. Louw and B. de V. Packham joined our research team in numerous fruitful field excursions and discussions.

My wife, Marie, assisted in numerous ways.

REFERENCES

Albat, H.M. (1984). The Proterozoic granulite facies terrane around Kliprand, Namaqualand Metamorphic Complex. Bull. Precambr. Res. Unit, Univ. Cape Town, 33, 382 pp.

Amit, O. and Eyal, Y. (1976). The genesis of Wadi Magrish migmatites (N-E Sinai). Contrib. Mineral. Petrol., 59, p. 95-110.

Aranovich, L.Ya. and Podlesskii, K.K. (1983). The cordierite-garnet-sillimanite-quartz equilibrium: Experiments and applications. Advances in physical geochemistry, 3, p. 173-198.

Ashworth, J.R. (1976). Petrogenesis of migmatites in the Huntly-Portsoy area, northeast Scotland. Mineralogical Magazine, 40, p. 661-682.

Babuska, I. (1972). Numerical stability in problems of linear algebra. SIAM J. Numer. Anal., 9, p. 53-77.

Barton, E.S. (1983). Reconnaissance isotopic investigations in the Namaqua mobile belt and implications for Proterozoic crustal evalution - Namaqualand geotraverse. Spec. Publ. geol. Soc. S. Afr., 10, p. 45-66.

Benedict, P.C., Wiid, D. De N., Cornelissen, A.K. and Staff (1964). Progress report on the geology of the O'okiep Copper District. In: Haughton, S.H. (ed.), The geology of some ore deposits of Southern Africa. Geol. Soc. S. Afr., 2, p. 239-302.

Beukes, G.J., van Zyl, V.C., Schoch, A.E., de Bruiyn, H., van Aswegen, G. and Strydom, D. (1986). A högbomite-spinel-gedrite paragenesis from northern Bushmanland, Namaqua mobile belt, South Africa. Neues Jb. Mineral. Abh., 155, p. 53-66.

Bhattacharyya, C. (1971). An evaluation of the chemical distinctions between igneous and metamorphic orthopyroxenes. Amer. Mineral., 56, p. 499-506.

Blignault, H.J. (1977). Structural-metamorhic imprint on part of the Namaqua mobile belt in South West Africa. Bull. Precambr. Res. Unit, Univ. Cape Town, 23, 197 pp.

----, Van Aswegen, G., Van der Merwe, S.W. and Colliston, W.P. (1983). The Namaqualand geotraverse and environs; part of the Proterozoic Namaqua mobile belt., 1-29. In: B.J.V Botha (ed.), Namaqualand Metamorphic Complex. Spec. Publ. geol. Soc. S. Afr., 10, 198 pp.

Bogdanova, S.V. (1979). Grey gneisses and problems of the growth of the oldest crust of the earth. Geotectonics, 13, 501-502.

Bohlen, S.R. and Essene, E.J. (1979). A critical evaluation of two-pyroxene thermometry in Adirondack granulites. Lithos, 12, p. 335-345.

Brun, J.P., and Cobbold, P.R. (1980). Strain heating and thermal softening in continental shear zones: a review. J. Struct. Geol., 2, p. 149-158.

Bus , J.C.P. (1977). Convergence of Newton-like methods for solving systems of nonlinear equations. Numer. Math., 27, p.271-281.

Büsch, W., Scnheider, G. and Mehnert, K.R. (1974). Initial melting at grain boundaries. Part II. Melting in rocks of granodioritic, quartzdioritic and tonalitic composition. Neues Jb. Mineral. Mh., 8, p.345-370.

Clifford, T.N., Gronow, J., Rex, D.C. and Burger, A.J. (1975a). Geochronolocical studies of high-grade metamorphic rocks and intrusives in Namaqualand, South Africa. J. Petrol., 16, p. 154-188.

----, Stumpfl, E.F. and McIver, J.R. (1975b). A sapphirine - cordierite - bronzite - phlogopite paragenesis from Namaqualand, South Africa. Mineral. Mag., 40, p. 347-356.

----, Stumpfl, E.F., Burger, A.J., McCarthy, T.S. and Rex, D.C. (1981). Mineral-chemical and isotopic studies of Namaqualand granulites, South Africa: A Grenville Analogue. Contrib. Mineral. Petrol., 77, p. 225-250.

Cobbold, P.R. (1977). Description and origin of banded deformation structures - II. Rheology and the growth of banded perturbations. Can. J. Earth Sci., 14, p. 2510-2523.

----, and Quinquis, H. (1980). Development of sheath folds in shear regimes. J. Struct. Geol., 2, p. 119-126.

Colliston, W.P. (1983). Sratigraphic and depositional aspects of the Proterozoic metasediments of the Aggeneys subgroup at Pella and Dabenoris. Spec. Publ.Geol. Soc. S. Afr., 10, p. 101-110.

----, and Strydom, D. (1985). Guide book - Contribution from the Bushmanland Research Project to Copper '85. (Ed: A. E. Schoch), Geol. Dept. Univ., Orange Free State, Bloemfontein, 40 pp.

Conradie, J.A. (1983). Petrological and petrochemical aspects of the Koperberg Suite, Namaqualand. M.Sc. thesis (unpubl.), Univ. Orange Free State, Bloemfontein, 136 pp.

----, and Schoch, A.E. (1986a). Petrographical characteristics of the Koperberg Suite South Africa - an analogy to massif-type anorthosites? Precambrian Res., 31, p. 157-188.

----, and Schoch, A.E. (1986b). Iron-titanium oxide equilibria in copper-bearing diorites, Namaqualand. Trans. geol. Soc. S. Afr., 89, p. 29-34.

Currie, K.L. (1974). A note on the calibration of the garnet - cordierite geothermometer and geobarometer. Contrib. Mineral. Petrol., 44, p. 35-44.

Davidson, P.M. and Lindsley, D.H. (1985). Thermodynamic analysis of quadrilateral pyroxenes. Part II: Model calibration from experiments and applications to geothermometry. Contrib. Mineral. Petrol., 91, p. 390-404.

De Bruiyn, H., van der Westhuizen, W.A. and Schoch, A.E. (1983). The estimation of FeO, F and H_2O^+ by regression in microprobe analyses of natural biotite. J. Trace and microprobe

techniques., 1, p. 399-413.

de La Roche, H., Leterrier, J., Grandclaude, P., and Marchal, M. (1980). A classification of volcanic and plutonic rocks using the R_1R_2-diagram and major element analyses - its relationships with current nomenclature. Chem. Geol., 29, p. 183-210.

Dunn, E.J. (1872). On the country traversed by the "Gold Prospecting Expedition", Namaqualand. Parliamentary Report No. G 21, Cape of Good Hope, 11 pp.

Essene, E.J. (1982). Geologic thermometry and barometry. In: Ferry, J.M. (ed.). Reviews in Mineralogy, 10: Characterization of metamorphism through mineral equilibria. Mineral. Soc. Amer., Washington DC, p. 153-206.

Ferguson, C.C., Harvey, P.K., and Lloyd, G.E. (1980). On the mechanical interaction between a growing porphyroblast and its surrounding matrix. Contrib. Mineral. Petrol., 75, p. 339-352.

Ferry,J.M. and Spear, F.S. (1978). Experimental calibration of Fe and Mg between biotite and garnet. Contrib. Mineral. Petrol., 66, p.113-117.

Fonarev, V.I. and Graphchikov, A.A. (1982). Experimental study of Fe-, Mg- and Ca-distribution between coexisting ortho- and clinopyroxenes at P=294 MPa, T=750 and 800°C. Contrib. Mineral.Petrol., 79, p. 311-318.

---- and Konilov, A.N. (1986). Experimental study of Fe-Mg distribution between biotite and orthopyroxene at P=490 MPa. Contrib. Mineral. Petrol., 93, p. 227-235.

Gevers, T.W., Partridge, F.C. and Joubert, G.K. (1937). The pegmatite area south of the Orange River in Namaqualand. Mem. geol. Surv. Un. S. Afr., 31, 180 pp.

Goldman, D.S. and Albee, A.L. (1977). Correlation of Fe-Mg partitioning between garnet and biotite with $18_O/16_O$ partitioning between quartz and magnetite. Amer. J. Sci., 277, p.750-767.

Goldsmith, J.R. and Newton, R.C. (1977). Scapolite-plagioclase stability relations at high pressures and temperatures in the system $NaAlSi_3O_8$ - $CaAl_2Si_2O_8$ - $CaCO_3$ - $CaSO_4$. Amer. Mineral., 62, p. 1063-1081.

Golub, G.H. and Reinsch, C. (1970). Singular value decomposition and least squares solutions. Numer. Math., 14, p. 403-420.

Green, T.H. (1980). Island arc and continent-building magmatism - a review of petrogenetic models based on experimental petrology and geochemistry. In: Banks, M.R. and Green, D.H., (eds.), Orthodoxy and Creativity at the Frontiers of Earth Sciences (Carey Symposium). Tectonophysics, 63, p. 367-385.

Greenwood, H.J. (1975). Thermodynamically valid projections of extensive phase relationships. Amer. Mineral., 60, p. 1-8.

Haggerty, S.E. (1976). Opaque mineral oxides in terrestrial igneous rocks, in Rumble, D.(ed.): Reviews in mineralogy 3, Oxide Mineralogy. Mineral. Soc. Amer. p. 101-300.

Hedge, C.E. (1972). Source of leucosomes of migmatites in the front range, Colorado. geol. Soc. Amer.,135, p. 65-72.

Higgens, M.W. (1971). Cataclastic rocks. Prof. Paper, U.S. geol. Surv., 687, 96 pp.

Hodges, K.V. and Crowley, P.D. (1985). Error estimation and empirical geothermobarometry for pelitic systems. Amer. Mineral., 70, p. 702-709.

----, and Spear, F.S. (1982). Geothermometry, geobarometry and the Al_2SiO_5 triple point at Mt. Moosilauke, New Hampshire. Amer. Mineral., 67, p. 1118-1134.

Holdaway, M.J. and Lee, S.M. (1977). Fe-Mg cordierite stability in high-grade pelitic rocks based on experimental, theoretical, and natural observations. Contrib. Mineral. Petrol., 63, p. 175-198.

Holland, J.G. and Marais, J.A.H. (1983). The significance of the geochemical signature of the Proterozoic gneisses of the Namaqualand Metamorphic Complex with special reference to the Okiep Copper District. In Botha, B.J.V., Ed., Namaqualand Metamorphic Complex, Spec. Publ. geol. Soc. S. Afr., 10, p. 83-89.

Hudson, N.F.C. and Harte, B. (1985). K_2O-poor, aluminous assemblages from the Buchan Dalradian, and the variety of orthoamphibole assemblages in aluminous bulk compositions in the amphibolite facies. Amer. J. Sci., 285, p. 224-266.

Indaras, A. and Martignole, J. (1985). Biotite - garnet geothermometry in the granulite facies: the influence of Ti and Al in biotite. Amer. Mineral., 70, p.272-278.

Jackson, M.P.A. (1976). High grade metamorphism and migmatization of the Namaqua Metamorphic Complex around Aus in the southern Namib desert, South West Africa. Bull. Precambr. Res. Unit, Univ. Cape Town, 18, 299 pp.

Joubert, P. (1971). The regional tectonism of the gneisses of part of Namaqualand. Bull. Precambr. Res. Unit, Univ. Cape Town, 3, 322 pp.

----, (1974). The gneisses of Namaqualand and their deformation. Trans. geol. Soc. S. Afr., 77, p. 339-345.

----, Marais, J.A.H., Van Aswegen, G., and Van der Merwe, S.W. (1980). Okiep Group. In: (Compiler, L.E. Kent) SACS. Stratigraphy of South Africa, Part 1. Handb. geol. Surv. S. Afr., 8, p. 275-281.

Kretz, R. (1982). Transfer and exchange equilibria in a portion of the pyroxene quadrilateral as deduced from natural and experimental data. Geochim. Cosmochim. Acta, 46, p. 411-421.

---- (1983). Symbols for rock forming minerals. Amer. Mineral., 68, p. 277-279.

Leake, B.E. (1978). Nomenclature of amphiboles. Amer. Mineral., 63, 1023 - 1059.

Le Maitre, R.W. (1976). Some problems of the projection of chemical data into mineralogical classifications. Contrib. Mineral. Petrol., 56, p. 181-189

Lindsley, D.H. (1983). Pyroxene thermometry. Amer. Mineral., 68, p. 477-493.

---- and Anderson, D.J. (1983). A two-pyroxene thermometer. Proceedings of the Thirtheenth Lunar and Planetary Science Conference, Part 2. J. Geophys. Res., 88, supp. a887-a906.

Liou, J.G. (1973). Synthesis and stability relations of epidote, $Ca_2Al_2FeSi_3O_{12}(OH)$. J. Petrology, 14, 381-414.

Lipson, R.D. (1978). Some aspects of the geology of part of the Aggeneysberge and surrounding gneisses, Namaqualand. M.Sc. thesis (unpubl.), Univ. Witwatrsrand, Johannesburg, 100 pp.

Lombaard, A.F. and Schreuder, F.J.G. (1978). Distribution pattern and general geological features of steep structures, megabreccias and basic rocks in the Okiep Copper District, In: Verwoerd, W.J. (ed.), Mineralization in metamorhic terranes. Spec. Publ. geol. Soc. S. Afr., 4, p. 269-275.

---- and the exploration Department staff of the O'okiep Copper Company Ltd. (1986). The copper deposits of the Okiep district, Namaqualand. In: Anheausser, C.R. and Maske, S. (eds.), Mineral Deposits of South Africa, 2, p. 1421-1445.

Loock, J.C. (1984). Zircons from the granites and gneisses of the Namaqua mobile belt and the interpretation of radiometric ages. Twentieth Congress, Geol. Soc. S. Afr. (Potchefstroom), Abstracts, p. 77-79.

Losert, J. (1968). On the genesis of nodular sillimanitic rocks. Proc. 13th Int. geol. Congress, 4, Praque, p. 109-122.

Marais, J.A.H., Packham, B. de V. and Schreuder, F.J.G. (1975). Regional geology of the O'okiep Copper District. Abstracts 16th Congress geol. Soc. S.Afr., p.88-89.

---- and Joubert, P. (1980a). Little Namaqualand Suite. In: (Compiler, L.E. Kent) SACS. Stratigraphy of South Africa, Part 1. Handb. geol. Surv. S. Afr., 8, p. 294-301.

---- and Joubert, P. (1980b). Spektakel Suite. In: (Compiler, L.E. Kent) SACS. Stratigraphy of South Africa, Part 1. Handb. geol. Surv. S. Afr., 8, p. 314-316.

Martens. F. (1979). A sequence of deformational events in the Ratelpoort Fold area, Namaqualand. M.Sc. thesis (unpubl.), Univ. Orange Free State, Bloemfontein, 84 pp.

Martignole, J. and Sissi, J.C. (1981). Cordierite - garnet-H_2O equilibrium, geological thermometer, barometer and water fugacity indicator. Contrib. Mineral. Petrol., 77, p. 38-46.

Mason, R. (1978). Petrology of the metamorphic rocks. George Allen & Unwin Ltd., Londen, 254 pp.

Mathias, M. (1941). A comparitive study of the Namaqualand

granites. Trans. geol. Soc. S. Afr., 43, p. 175-203.

McCarthy, T.S. (1976). Chemical interrelationships in a low-pressure granulite terrain in Namaqualand, South Africa, and their bearing on granite genesis and the composition of the lower crust. Geochim. et Cosmochim. Acta, 40, p. 1057-1068.

McIver, J.R., McCarthy, T.S. and Packham, B. de V. (1983). The copper-bearing basic rocks of Namaqualand. Mineral. Deposita, 18, p. 135-160.

Mehnert, K.R. (1968). Migmatites and the origins of granitic rocks. Elsevier Publishing Company, Amsterdam., 405 pp.

Metz, P. (1970). Experimentalle Untersuchung der Metamorphose von kieselig dolomitischen Sedimente. II. Die Bildungsbedingungen des Diopsids. Contrib. Mineral. Petrol., 28, p. 221-250.

Miyashiro, A. (1973). Metamorphism and metamorphic belts. John Wiley and Sons, New York, 492 pp.

Mongkoltip, P. and Ashworth, J.R. (1986). Amphibolization of metagabbros in the Scottish Highlands. J. Metamorphic Geol., 4, p. 261-283.

Moore, A.C. Descriptive terminology for the textures f rocks in granulite facies terrains. Lithos, 3, 123-127.

Moore, J.M. (1977). The geology of Namiesberg, Northern Cape. Bull. Precambr. Res. Unit, Univ. Cape Town, 20, 69 pp.

Myers, J.S. (1978). Formation of banded gneisses by deformation of igneous rocks. Precambr. Res. Unit, Univ. Cape Town, 6, p. 43-64.

Onstott, T.C., Hargraves, R.B. and Reid, D.L. (1986). Constraints on the tectonic evolution of the Namaqua Province III: paleomagnetic and $^{40}Ar/^{39}Ar$ results from the Gannakouriep dyke swarm. Trans. geol. Soc. S. Afr., 89, p. 171-183.

O'okiep Copper Company Limited (1975). In Precongress excurison guide book No. 1, 16th Geocongress, geol. Soc. S. Afr., Stellenbosch, 73 pp.

Paizes, P.E. (1975). The geology of an area between Vaalkop and Aggeneys in the vicinity of Pofadder, north-western Cape Province. M.Sc. thesis (unpubl.), Univ. Witwatersrand, Johannesburg, 220 pp.

Perchuk, L.L. (1969). The effect of temperature and pressure on the equilibrium of natural iron-magnesium minerals. Int. Geol. Rev.,11, p. 875-901.

---- (1970). Equilibrium of biotite with garnet in metamorphic rocks. Geochim Int., 7, p. 157-179.

---- and Lavrent'eva, I.V. (1983). Experimental investigation of exchange equilibria in the system cordierite - garnet -biotite. Advances in physical geochemistry, 3, Springer Verlag, p. 199-239.

Prins, P. (1970). Geochemical and mineralogical variations in the

wall rocks of copper-bearing bodies, Namaqualand. M.Sc. thesis (unpubl.), Univ. Stellenbosch, 40 pp.

Powell, C.M (1979). Morphological classification of rock cleavage. Tectonophysics, 58, p. 21-34.

Powell, R. (1978). The thermodynamics of pyroxene geotherms. Phil. Trans. R. Soc. London. A, 288, p. 457-469.

Ramsay, D.M. (1980). Shear zone geometry: a review. J. Struct. Geol., 2, p. 83-99.

Reid, D.L. (1977). Geochemistry of Precambrian igneous rocks in the lower Orange River region. Bull. Precambrian. Res. Unit, Univ. Cape Town, 22, 397 pp.

---- and Barton, E.S. (1983). Geochemical characterisation of granitoids in the Namaqualand geotraverse. Spec. Publ. geol. Soc. S. Afr., 10, p. 67-82.

Richardson, S.W. (1968). Staurolite stability in a part of the system Fe - Al - Si - O - H. J. Petrology, 9(3), p. 467-488.

Robin, P.Y.F. (1979). Theory of metamorphic segregation and related processes. Geochim. Cosmochim. Acta, 43, p. 1587-1600.

Robinson, P., Spear, F.S., Schumacher, J.C., Laird, J., Klein, C., Evans, B.W. and Doolan, B.L. (1982). Phase relations of metamorphic amphiboles: natural occurrence and theory. In: Veblen, D.R. and Ribbe, P.H. (eds.). Reviews in Mineralogy, volume 9b. Amphiboles: petrology and experimental phase relations. Mineral. Soc. Amer., Washington D C, p. 1-227.

Rogers, A.W. (1915). The geology of part of Namaqualand. Trans. geol. Soc. S. Afr., 18, p. 72-101.

Ross, M. and Heubner, J.S. (1975). A pyroxene thermometer based on temperature-composition relationships of naturally occuring orthopyroxene, pigeonite, and augite (extended abstract). International Conference on Geothermometry and geobarometry, Penn. State Univ., Oct. 5-10,1975.

Rozendaal, A. (1975). The geology of Gamsberg, Namaqualand, South Africa. M.Sc. thesis (unpubl.), Univ. Stellenboch, 109 pp.

---- (1982). The petrology of the Gamsberg zinc deposit and the Bushmanland iron formations with special reference to their relationships and genesis. Ph.D. thesis (unpubl.), Univ. Stellenboch, 349 pp.

SACS (1980). Stratigraphy of South Africa, Part 1 (Comp. L.E. Kent). Handb. geol. Surv. S. Afr., 8, 690 pp.

Schoch, A.E. and Strydom, D. (1987). Moegabees (detailed map of the Naab thrust zone, 1:2000). In: Strydom, D. (Ed.) The tectonic units of part of Namaqualand, Busmanland and southern Southwest Africa/Namibia. Dept. Geol. Univ. Orange Free State, Printpak, Cape Town. 1 Sheet printed on both sides.

Spear, F.S. (1980). Plotting stereoscopic phase diagrams. Amer. Mineral., 65, p. 1291-1293.

----, Rumble, D. and Ferry, J.M. (1982). Linear algebraic manipulation of n-dimensional composition space. In: Ferry, J.M. (ed.). Reviews in mineralogy, 10, Characterization of metamorphism through mineral equilibria. Mineral. Soc. Amer., Washington DC, p. 53-104.

Spry, A.H. (1969). Metamorhic textures. Pergamon Press, London., 350 pp.

Streckeisen, A. (1976). To each plutonic rock its proper name. Earth Sci. Rev., 12, p. 1-33.

Stephenson, N.C.N (1984). Two-pyroxene thermometry of Precambrian granulites from Cape Riche, Albany-Fraser Province, Western Australia. J. Metamorphic Geol., 2, p. 297-314.

Strydom, D., (1985). 'n Struktureel-stratigrafiese studie van die metasedimente en ander metamorfiete van noordwestelike Boesmanland, Suid-Afrika. Unpubl. Ph.D. thesis, Univ. Orange Free State, Bloemfontein, 172 pp.

---- and Schoch, A.E. (1983). Die Naab-suite p. 74-75. In Schoch, A.E. (ed.), Boesmanland projek-jaarverslag (Unpubl.), Univ. O.F.S., Bloemfontein, 3, 108 pp.

---- and Visser, J.N.J. (1986). Nappe structures in highly deformed Proterozoic metasedimentary Aggeneys-type sequence of western Bushmanland, South Africa. Precambrian Res., 33, p. 177-187.

---- (Ed.), Colliston, W.P., Praekelt, H.E., Schoch, A.E., van Aswegen, G., Prwetorius, J.J., Beukes, G.J., Cilliers, B., Watkeys, M.K. and Botes, F.J. (1987). The tectonic units of part of Namaqualand, Busmanland and southern Southwest Africa/Namibia. Dept. Geol. Univ. Orange Free State, Printpak, Cape Town. 1 Sheet printed on both sides.

Theart, H.F.J. (1979). Preliminary report on the geology of an area in western Namaqualand. Ann. Rep. Precambr. Res. Unit, Univ. Cape Town, 16, p. 58-72.

Theart, H.F.J. (1980). The geology of the Precambrian terrane in parts of western Namaqualand. Bull. Precambr. Res. Unit, Univ. Cape Town, 30, 103 pp.

Thompson, A.B. (1976). Mineral reactions in pelitic rocks. II. Calculation of some P - T - X (Fe - Mg) phase relations. Amer. J. Sci., 276, p.425-454.

Thompson, J.B. (1957). The graphical analysis of mineral assemblages in pelitic schists. Amer. Mineral., 42, 842-858.

Turner, F.J. and Weiss, L.E. (1963). Structural analysis of metamorhic tectonites. McGraw Hill, New York, 543 pp.

---- (1981). Metamorphic petrology: mineralogical, field and tectonic aspects. Second edition. McGraw-Hill Book Co., 524 pp.

Vallance, T.G. (1967). Mafic rock alteration and isochemical development of some cordierite - anthophylite rocks. J. Petrology, 8, p. 84-96.

Van Aswegen, G. (1980a). Gladkop Suite, 291-293. In: (Compiler,

L.E. Kent) SACS. Stratigraphy of South Africa, Part 1. Handb. geol. Surv. S. Afr., 8, 690 pp.

---- (1980b). The grey gneisses of the Gladkop Suite. In: (Compiler, H.J. Blignault), Namaqualand Excursion, S.A. Geodynamics Project, Geol. Soc. S. Afr., 50 pp.

---- (1982). Petrografiese studie van die Geselskapbank metamorfiete. In: Progress Reports 1982, National Geoscience Programme, NGP Secretariat, CSIR, Pretoria. 105-109

---- (1983a). The Gladkop Suite - the pink and grey gneisses of Steinkopf. Spec. Publ. geol. Soc. S. Afr., 10, p. 31-44.

---- (1983b). Die Aggeneysberge - Eerste vorderingsverslag. Jaarverslag Boesmanland-Navorsingsprojek, Univ. Oranje Vrystaat, Bloemfontein, p. 11-24.

----, Strydom, D., Colliston, W.P., Praekelt, H.E., Schoch, A.E., Blignault, H.J., Botha, B.J.V. van der Merwe, S.W. (1987). The structural-stratigraphic development of part of the Namaqua Metamorphic Complex - an example of proterozoic major thrust tectonics. Proterozoic Lithospheric Evolution, Amer. Geophys. Union Geodynamics Ser., 17, p. 207-216.

Van Biljon, W.J. and Legg, J.H. (1983). The Limpopo belt. Spec. Publ. geol. Soc. S. Afr., 8, pp. 203.

Van der Merwe, S.W. (1981a) Section through the Bleskop shear in the Kosies river. In: (Compiler, H.J. Blignault), Namaqualand Excursion, S.A. Geodynamics Project, Geol. Soc. S. Afr., 50 pp.

---- (1981b) The Ratelpoort north shear at Koegas. In: (Compiler, H.J. Blignault), Namaqualand Excursion, S.A. Geodynamics Project, Geol. Soc. S. Afr., 50 pp.

---- (1986). The structural development of part of the Namaqua Mobile Belt, in an area between Springbok and Vioolsdrif, South Africa. Ph.D. thesis, Univ. Orange Free State, Bloemfontein, 373 pp.

Van Zyl, V.C. (1986). Metamorphic studies in the Proterozoic rocks of parts of northern Bushmanland. M.Sc. thesis (unpubl.), Univ. Orange Free State, Bloemfontein, 317 pp.

Venter, J.P. (1970). Trace element dispersion in wall rocks of copper-bearing bodies, Namaqualand. M.Sc. thesis (unpubl.), Univ. Stellenboch, 72 pp.

Venter, L.C., (1984). Geometriese en vervormingsanalises op enkele steilstrukture van die Okiep-Koperdistrik. M.Sc. thesis (unpubl.), Univ. Orange Free State, Bloemfontein, 191 pp.

Venter, P.P. (1951). The petrology of the Nababeep and Brandberg gneisses. M.Sc. thesis (unpubl.), Univ. Pretoria, 74 pp.

Vernon, R.H. (1976). Metamorphic processes. George Allen & Unwin Ltd., Londen, 274 pp.

---- (1986). K-feldspar megacrysts in granites - phenocruysts, not porphyroblasts. Earth-Science Reviews, 23, 1-63.

Ward, J.H.W. (1977). The geology of the area south of Vioolsdrif, Cape Province. Rep. S. Afr. Atomic Energy Board, PEL-257, 48 pp.

Watkeys, M.K. (1986). The Achab gneiss: a "floor" in Busmanland or a flaw in Namaqualand? Trans. geol Soc. S. Afr., 89, p. 103-116

Waters, D.J. (1986). Metamorphic zonation and thermal history of pelitic gneisses from western Namaqualand, South Africa. Trans. Geol. Soc. S. Afr., 89, p.97-102.

---- and Moore, J.M. (1985). Kornerupine in Mg-Al-rich gneisses from Namaqualand, South Africa: mineralogy and evidence for late-metamorphic fluid activity. Contrib. Mineral. Petrol., 91, p. 369-382.

Weisbrod, A. (1973). Cordierite-garnet equilibrium in the system Fe-Mn-Al-Si-O-H. Carnegie Inst. Washington, Yearbook, 72, p. 515-523.

Wells, R.A. (1977). Pyroxene thermometry in simple and complex systems. Contrib. Mineral. Petrol., 62, p. 129-139.

White, A.J.R. (1966). Genesis of migmatites from the Palmer region of South Australia. Chem. Geol., 1, p. 165-200.

Winkler, H.G.F. (1979). Petrogenesis of metamorphic rocks. Springer Verlag New York Inc., USA. 348 pp.

Wood, B.J. and Banno, S. (1973). Garnet-orthopyroxene and othopyroxene-clinopyroxene relationships in simple and complex systems. Contrib. Mineral. and Petrol., 42, p. 109-124.

Wyley, A. (1857). Report upon the mineral and geological structures of South Namaqualand and the adjoining mineral districts. Parliamentary Rep. No. 36, Cape Good Hope, 55 pp.

Wynne-Edwards, H.R. (1969). Tectonic overprinting in the Grenville Province, southwestern Quebec. In: Wynne-Edwards, H.R., Ed., Age relations in high-grade metamorphic terrains. Spec. Pap., Geol. Ass. Can., 5, 163-182 pp.

Zelt, G.A.D. (1980a). A geotraverse across Namaqualand, South Africa: the petrology, geochemistry, and structural relations of a Proterozoic high-grade metamorphic terrain. Ph.D. thesis (unpubl.), Univ. Natal, Pietermaritzburg, 203 pp.

---- (1980b). Granulite facies metamorphism in Namaqualand, South Africa. Precambrian Research, 13, p. 253-274.

THE EVOLUTION OF THE PROTEROZOIC GNEISSES AND OTHER METAMORPHITES BETWEEN SPRINGBOK AND VIOOLSDRIF, SOUTH AFRICA

APPENDIX

APPENDIX I: FIGURES

(See list of figures on pages 0-1 to 0-11)

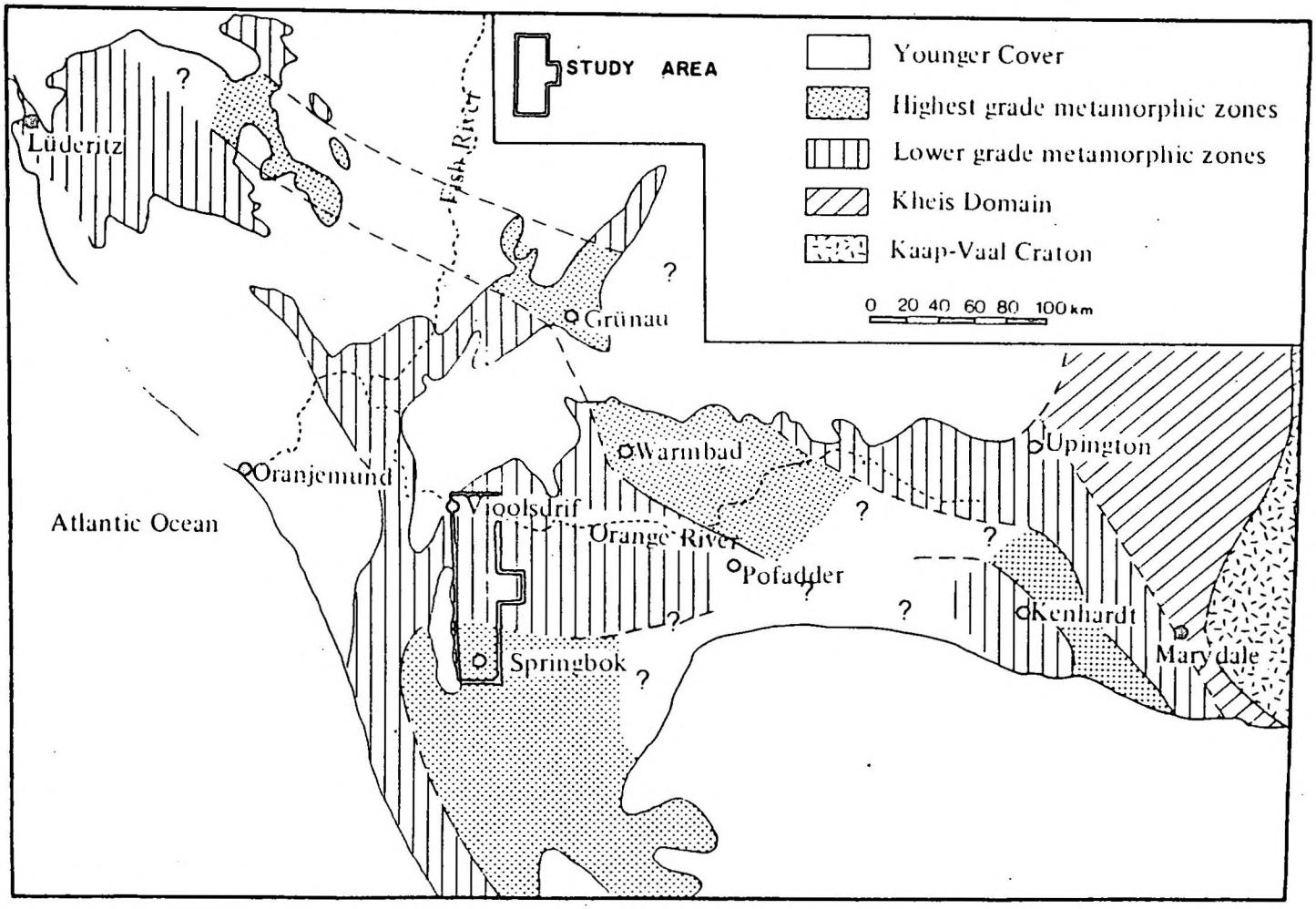

FIGURE 1.1 The regional setting of the study area and the distribution of the high grade metamorphic zones in the Namaqua Metamorphic Complex

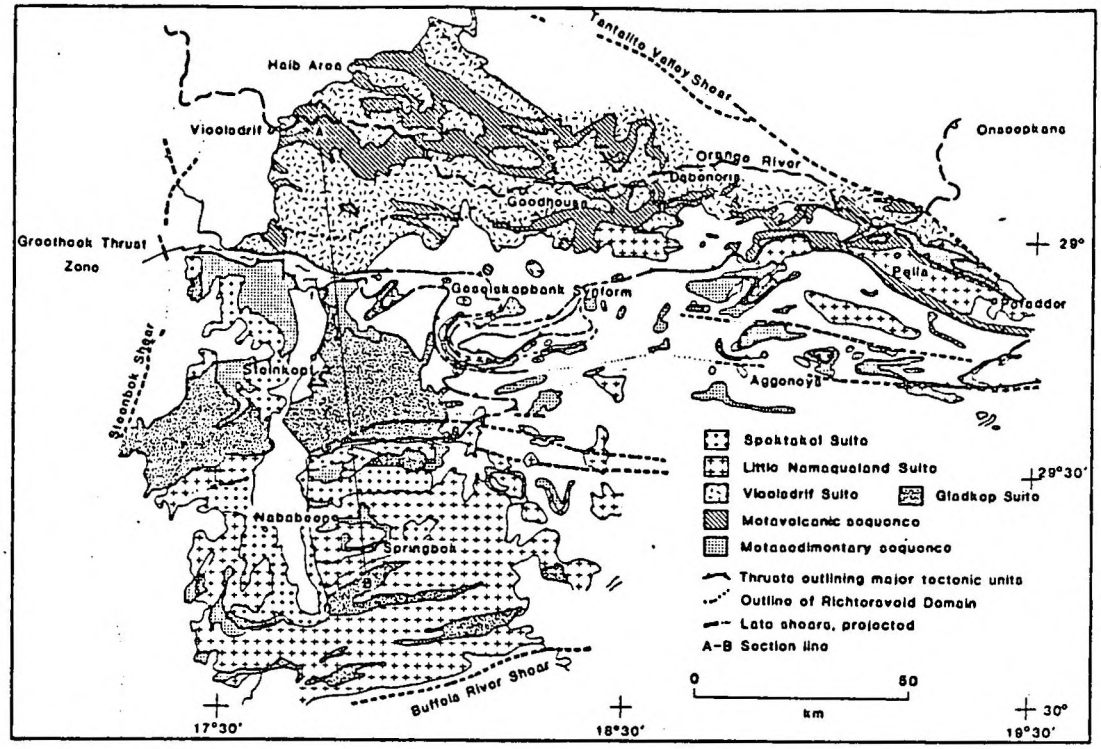

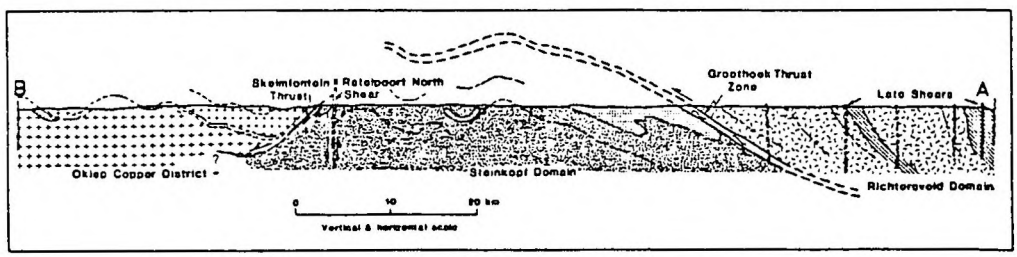

FIGURE 1.2 Generalized tectonostratigraphy of the Namaqua Metamorphic Complex in northern Namaqualand, northern Bushmanland and a small part of southern Namibia. The section AB runs more or less down the middle of the study area.

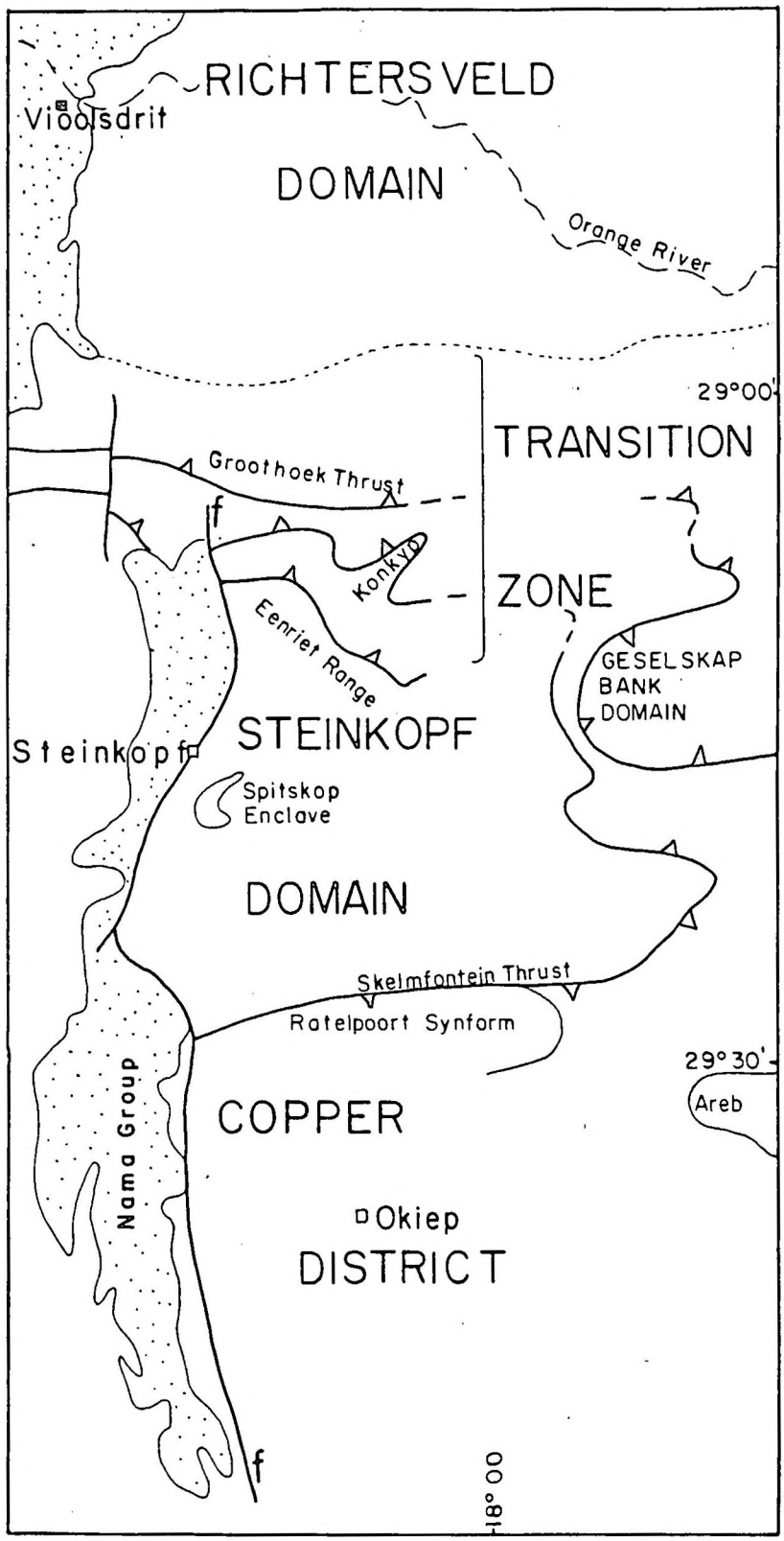

FIGURE 1.3 The tectonic domains of the study area.

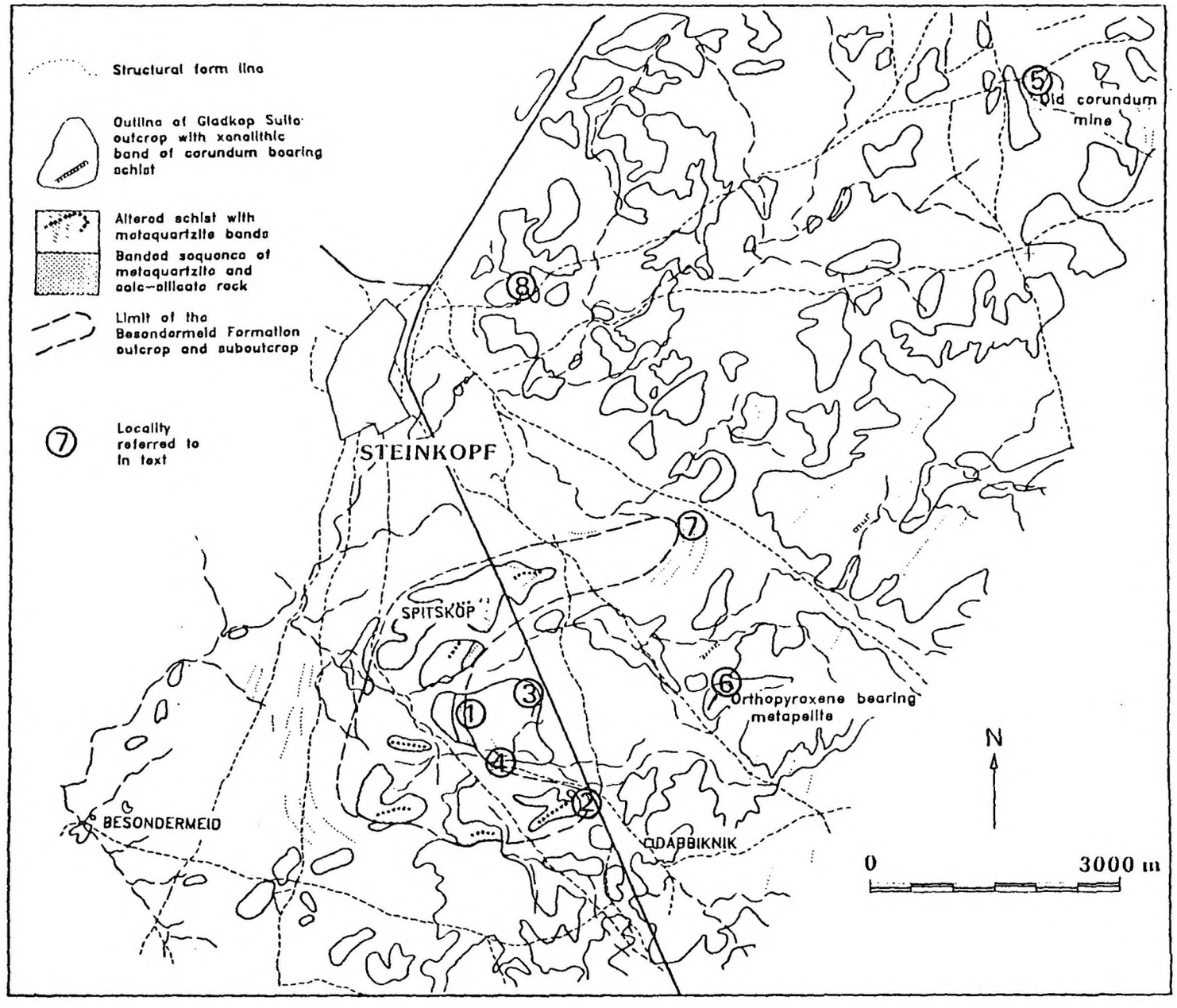

FIGURE 2.1 Map showing the distribution of outcrops of the Besondermeid Formation and the positions of localities referred to in the text.

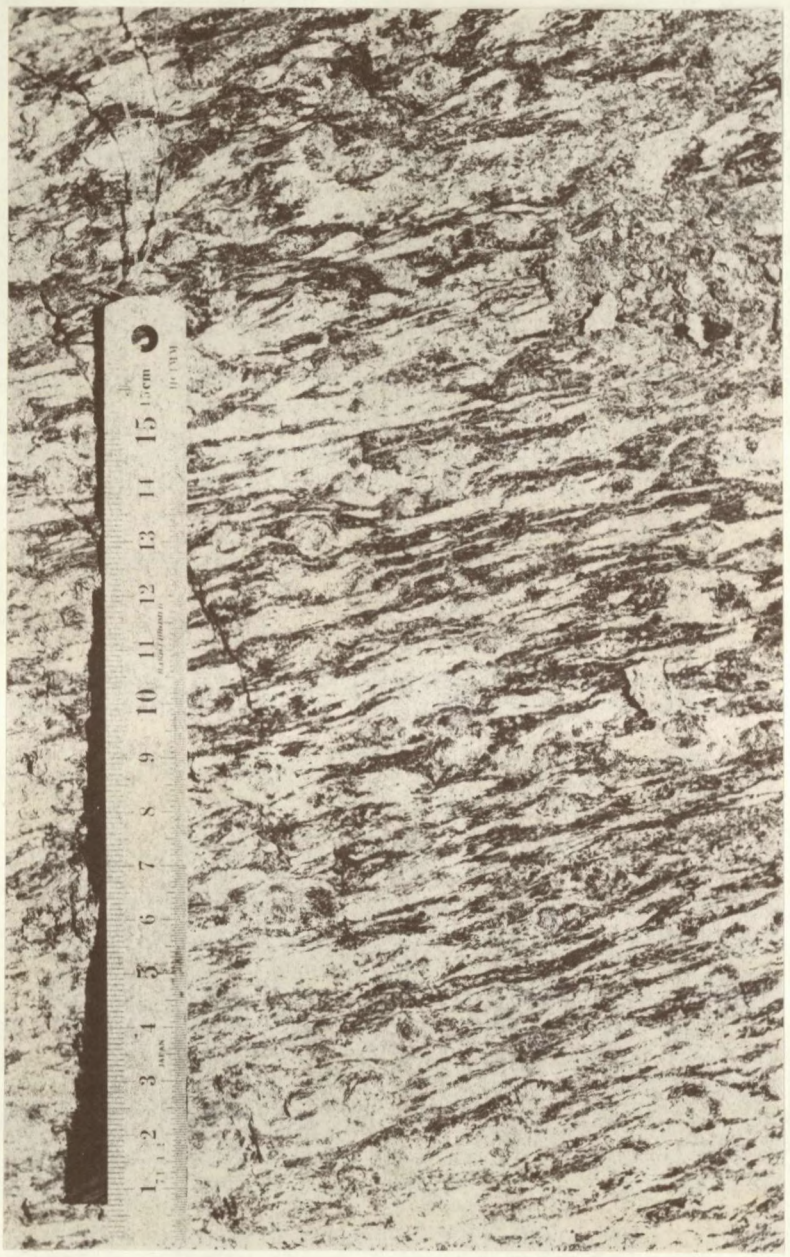

FIGURE 2.2 Garnet-sillimanite-biotite schist in a quarry at locality 2, Figure 2.1

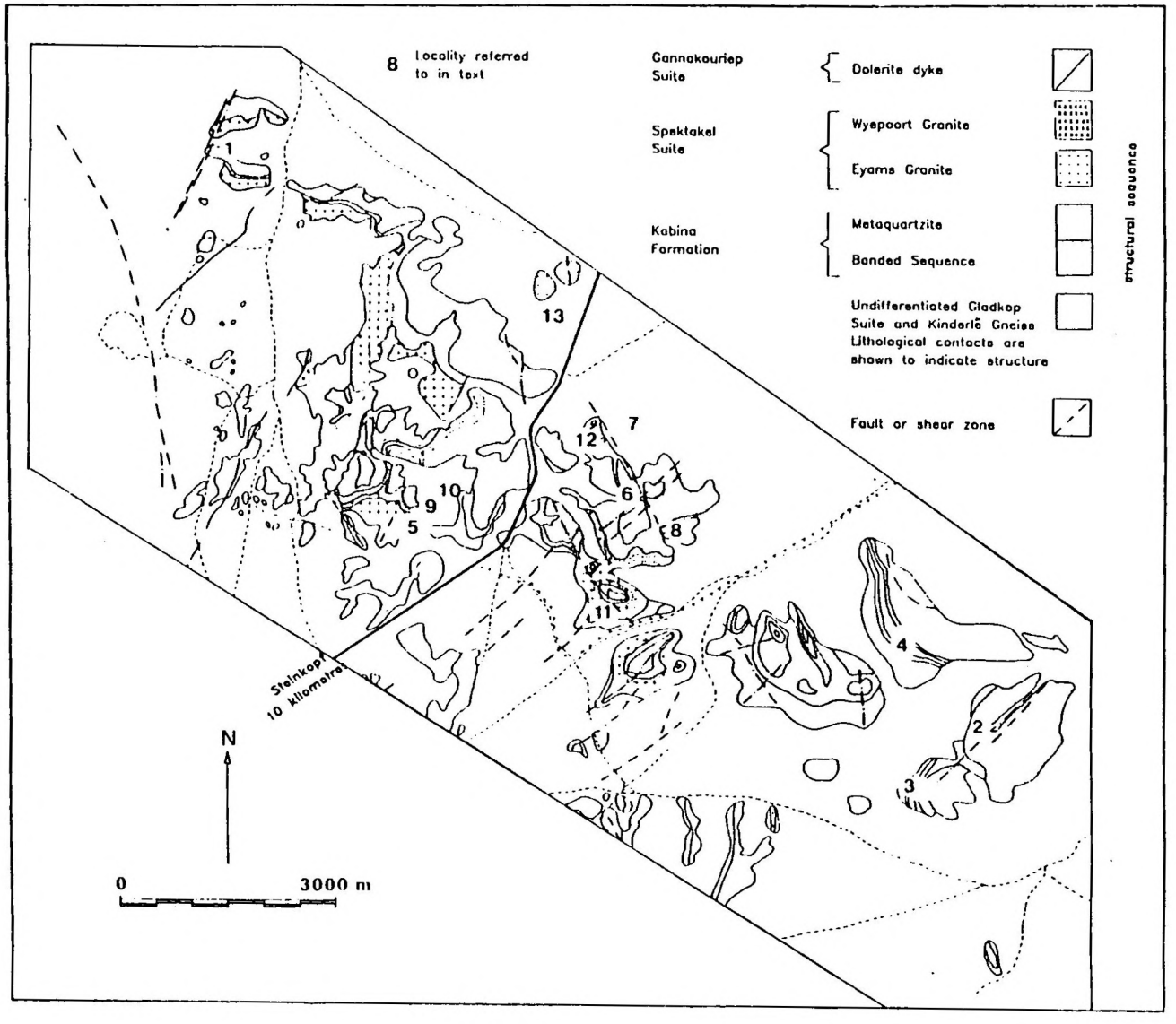

FIGURE 2.3 A simplified geological map of the Eenriet Mountain Range with the positions of localities referred to in the text.

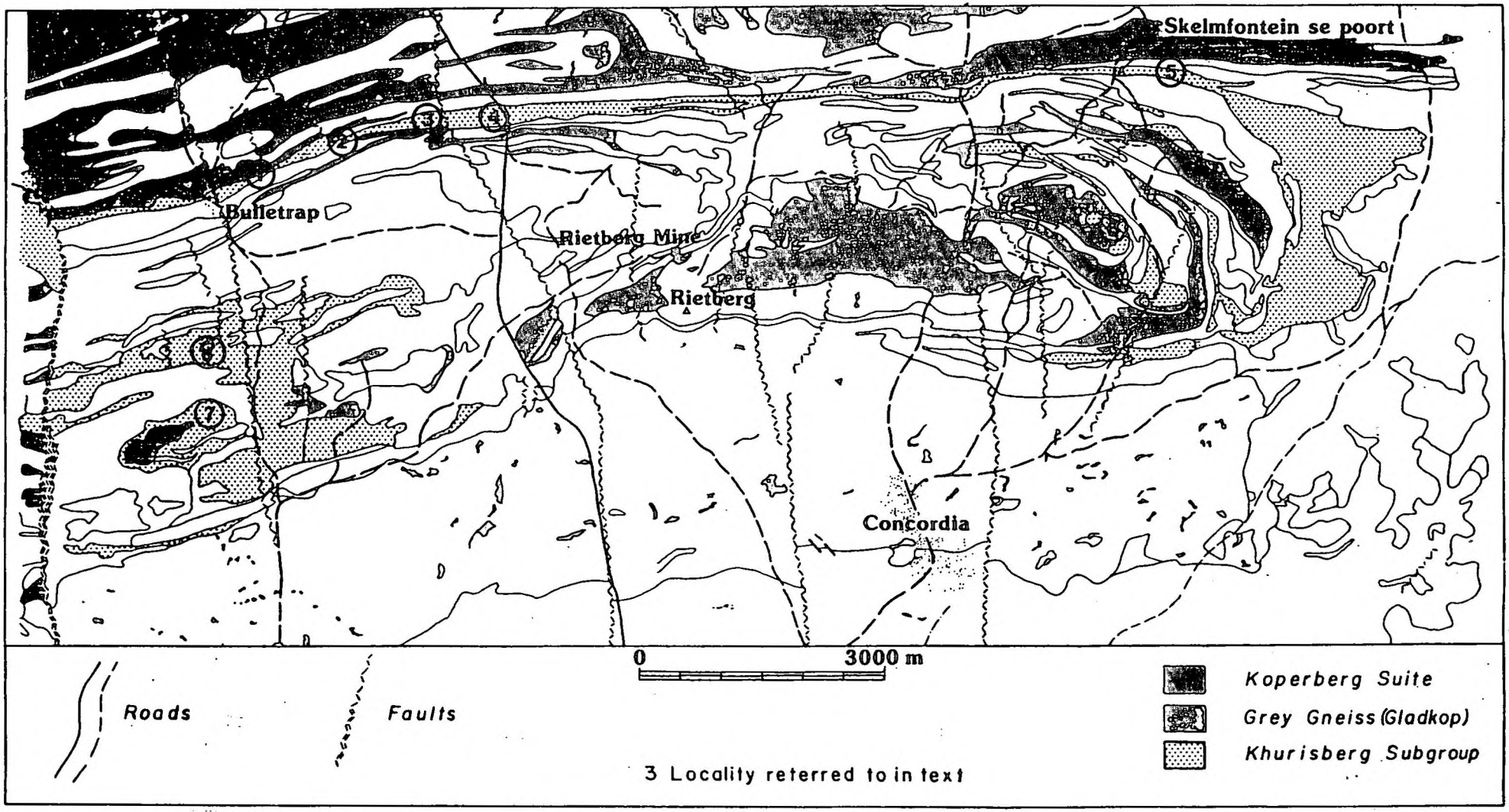

FIGURE 3.1 Simplified geological map of the Ratelpoort Synform with the positions of localities referred to in the text

FIGURE 3.2 Radial aggregates of sillimanite in a fine-granoblastic crd-sil-bt-kfs-qtz rock, one of the varieties of metapelite in the Khurisberg Subgroup (near Klipvloer).

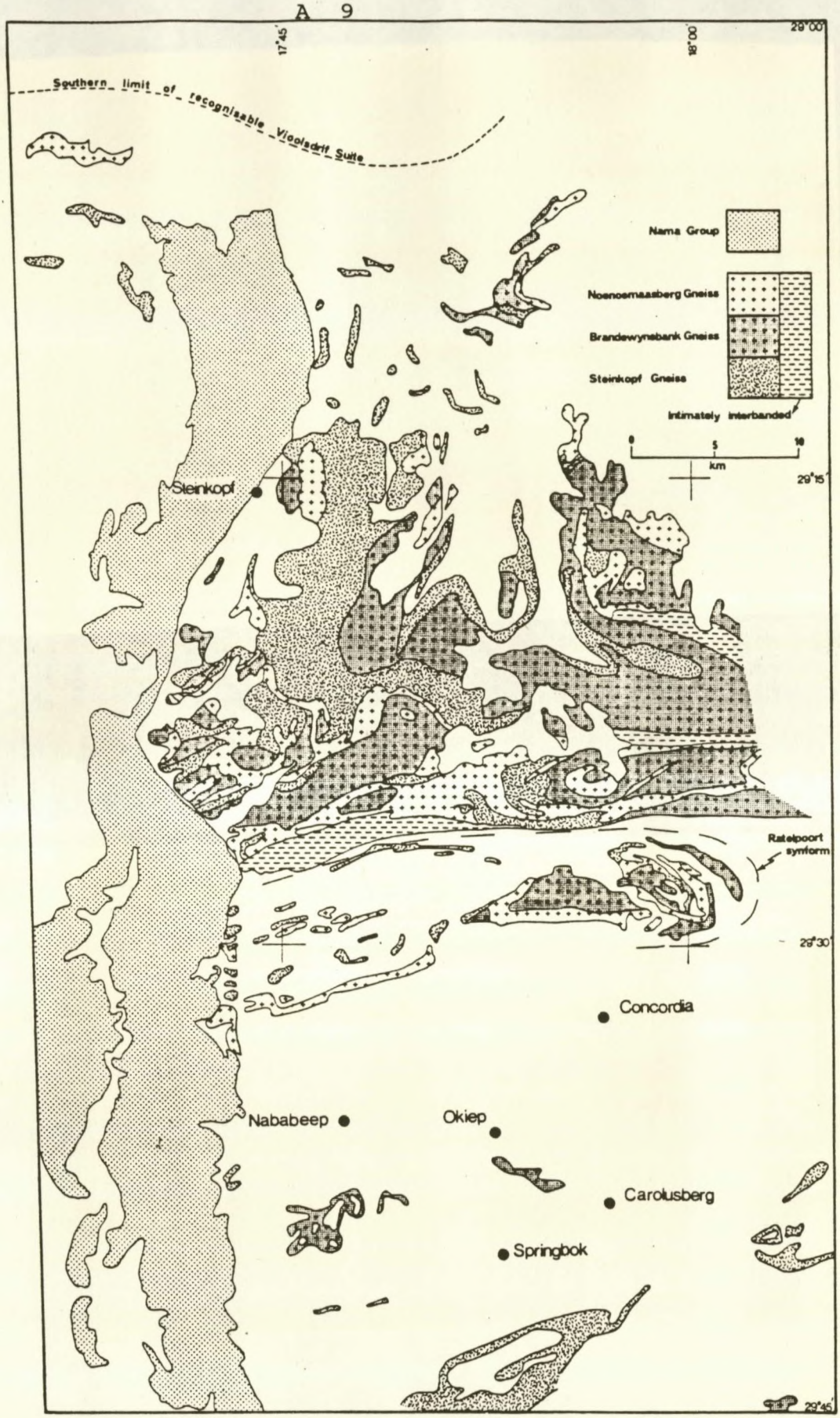

FIGURE 4.1 The distribution of the gneisses of the Gladkop Suite

FIGURE 4.2 Rafts of Brandewynsbank Gneiss (outlined) within Noenoemaasberg Gneiss against the eastern slope of Gladkop. The long dimension of the outcrop shown is approximately 600 metres.

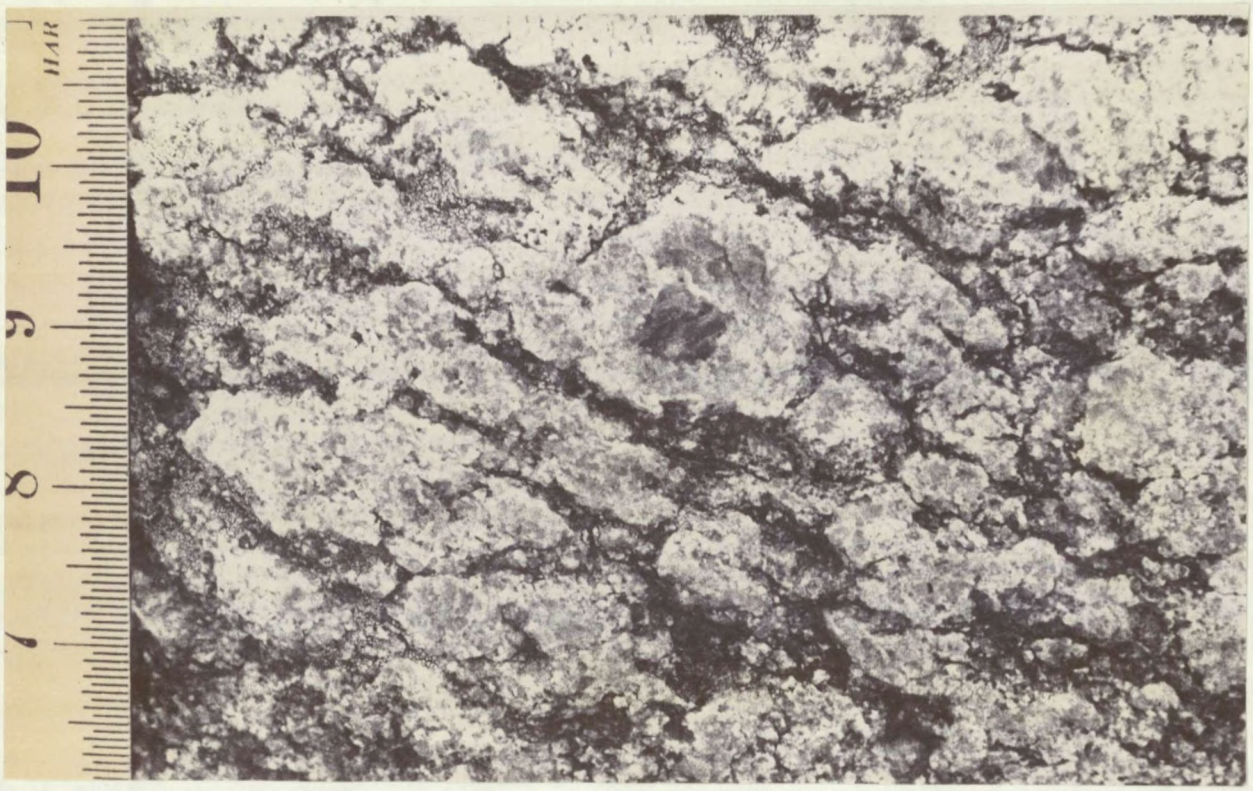

FIGURE 4.3 Relict augen structure in Noenoemaasberg Gneiss. The particular stage of weathering permits the recognition of the augen outlines. In the general case, only the fine-granoblastic texture, resulting from strain induced recrystallization, is visible. The smallest unit on the scale is 0.5 mm.

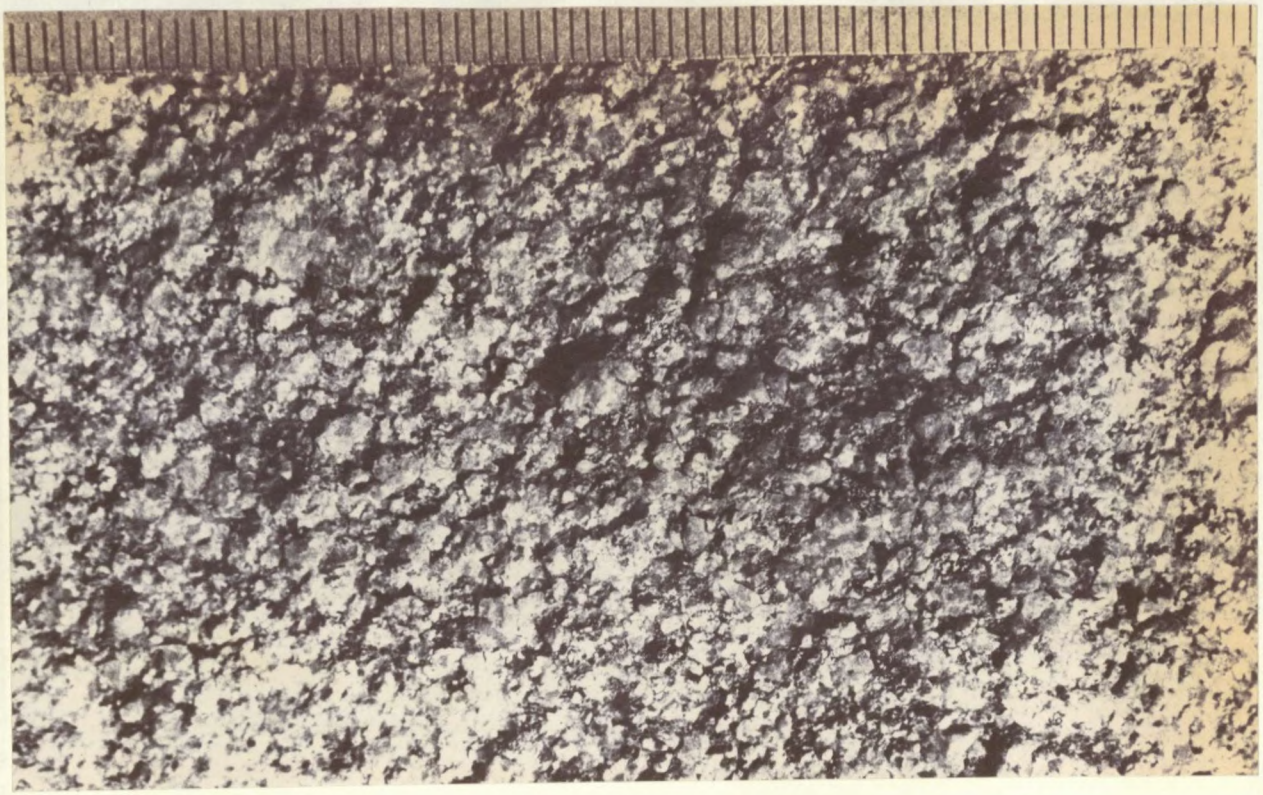

FIGURE 4.4 Fine-granoblastic texture of the Noenoemaasberg Gneiss as seen on a relatively fresh surface, a few metres away from where the photograph in Figure 4.2 was taken. The same ruler as in Figure 4.2 was used here for scale.

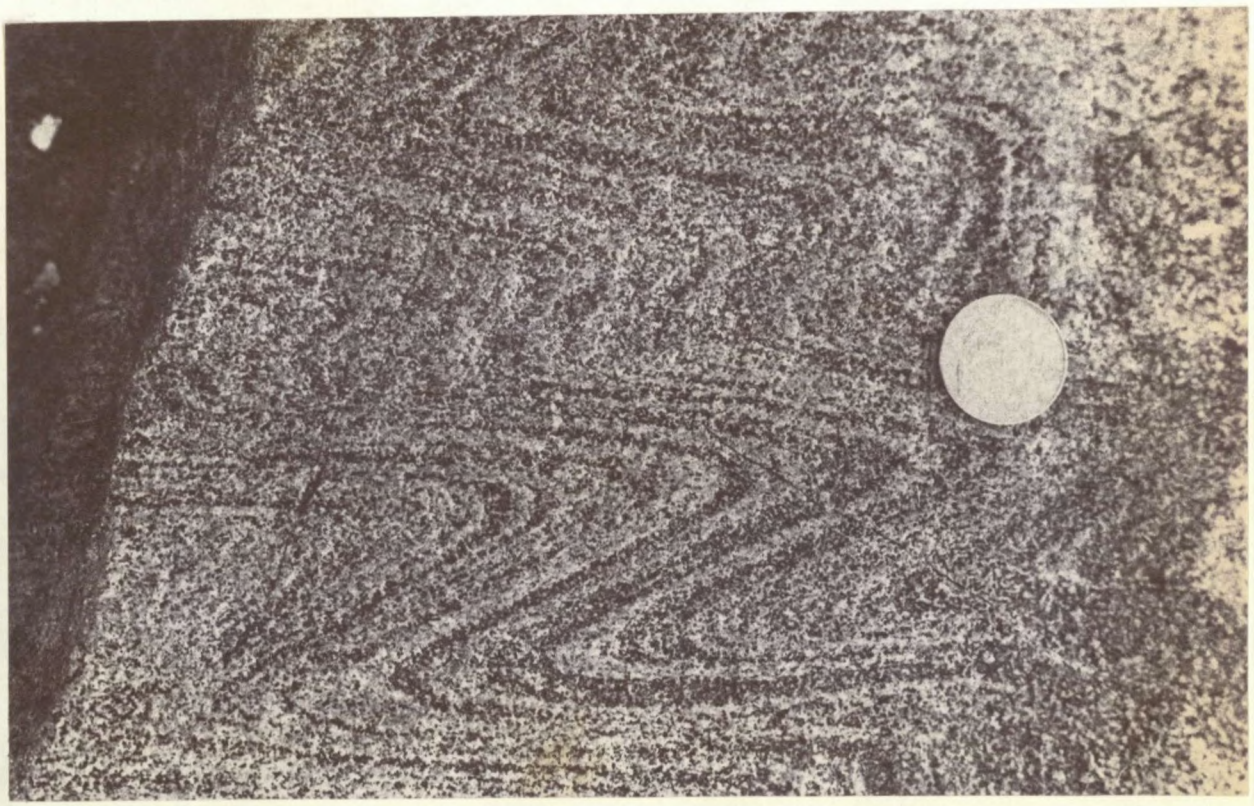

FIGURE 4.5 Secondary banding in the Noenoemaasberg Gneiss at Coetzeesbank, folded during the Ratelpoort shearing event. The coin used for scale has a diameter of 25 mm.

FIGURE 4.6 Intrusive relations between the banded variety of Noenoemaasberg Gneiss and Steinkopf Gneiss (west of Brandewynsbank). Thin xenolithic bands of the Steinkopf Gneiss can be seen above and to the right of the hammer.

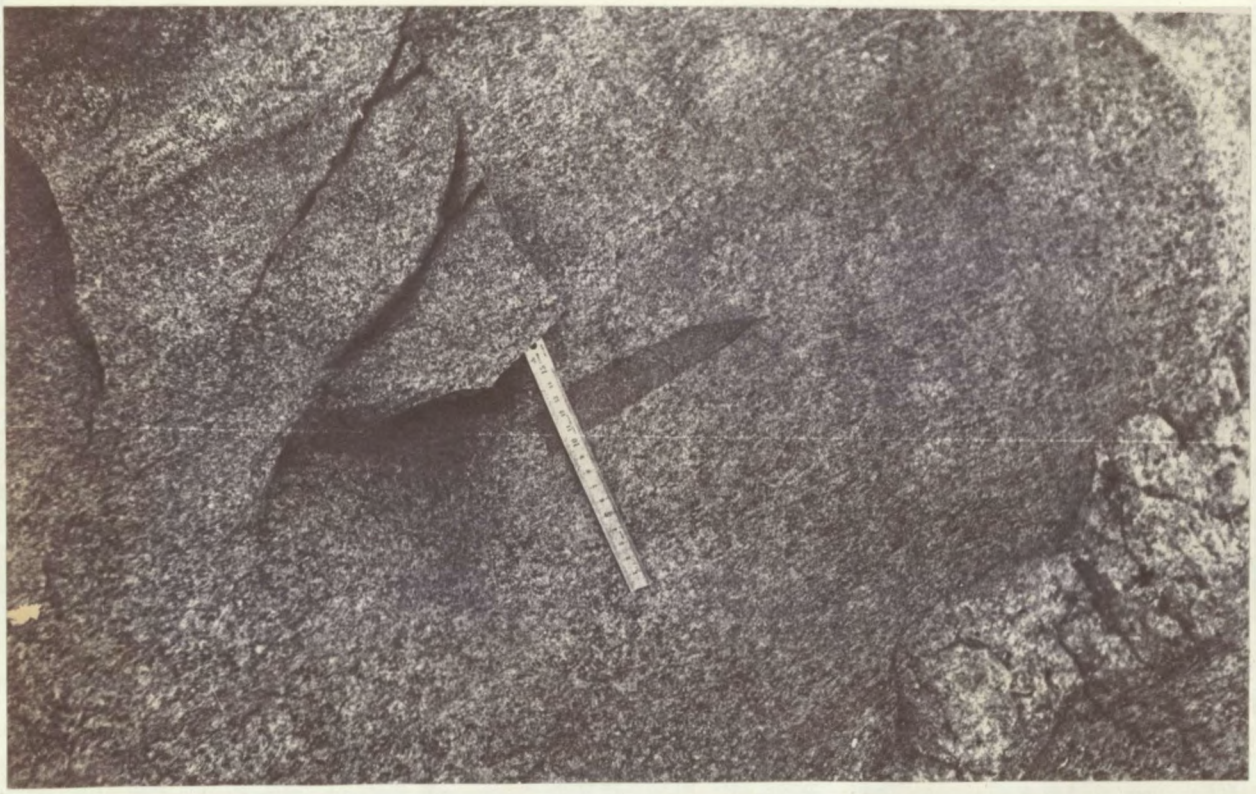

FIGURE 4.7 A discrete xenolith of calc-silicate rock in Brandewynsbank Gneiss, near Konkyp.

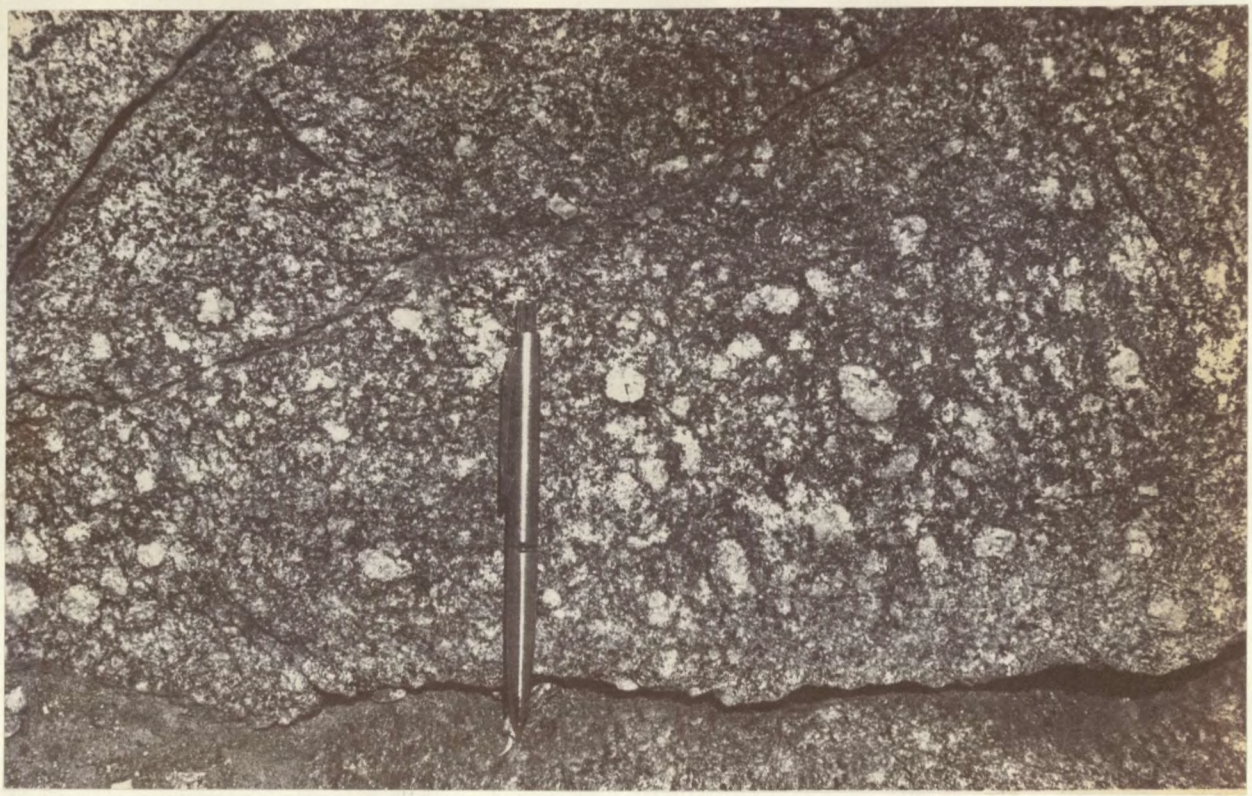

FIGURE 4.8 Rounded K-feldspar megacrysts in the Brandewynsbank Gneiss near Sabies (section normal to the stretching lineation).

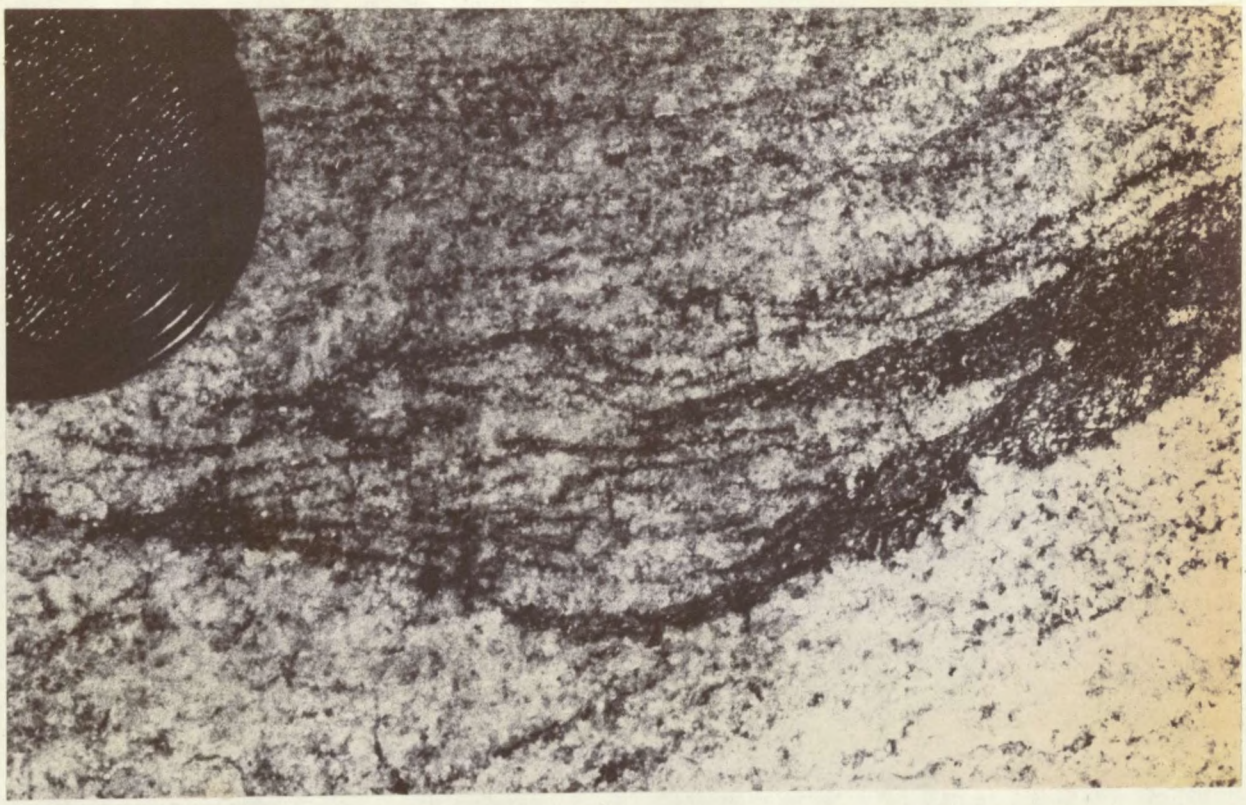

FIGURE 4.10 The appearance of the end of a small mafic lense in grey gneiss at Korrogas is suggestive of partial assimilation by the gneiss. The diameter of the camera lense-cap is approx. 60 mm.

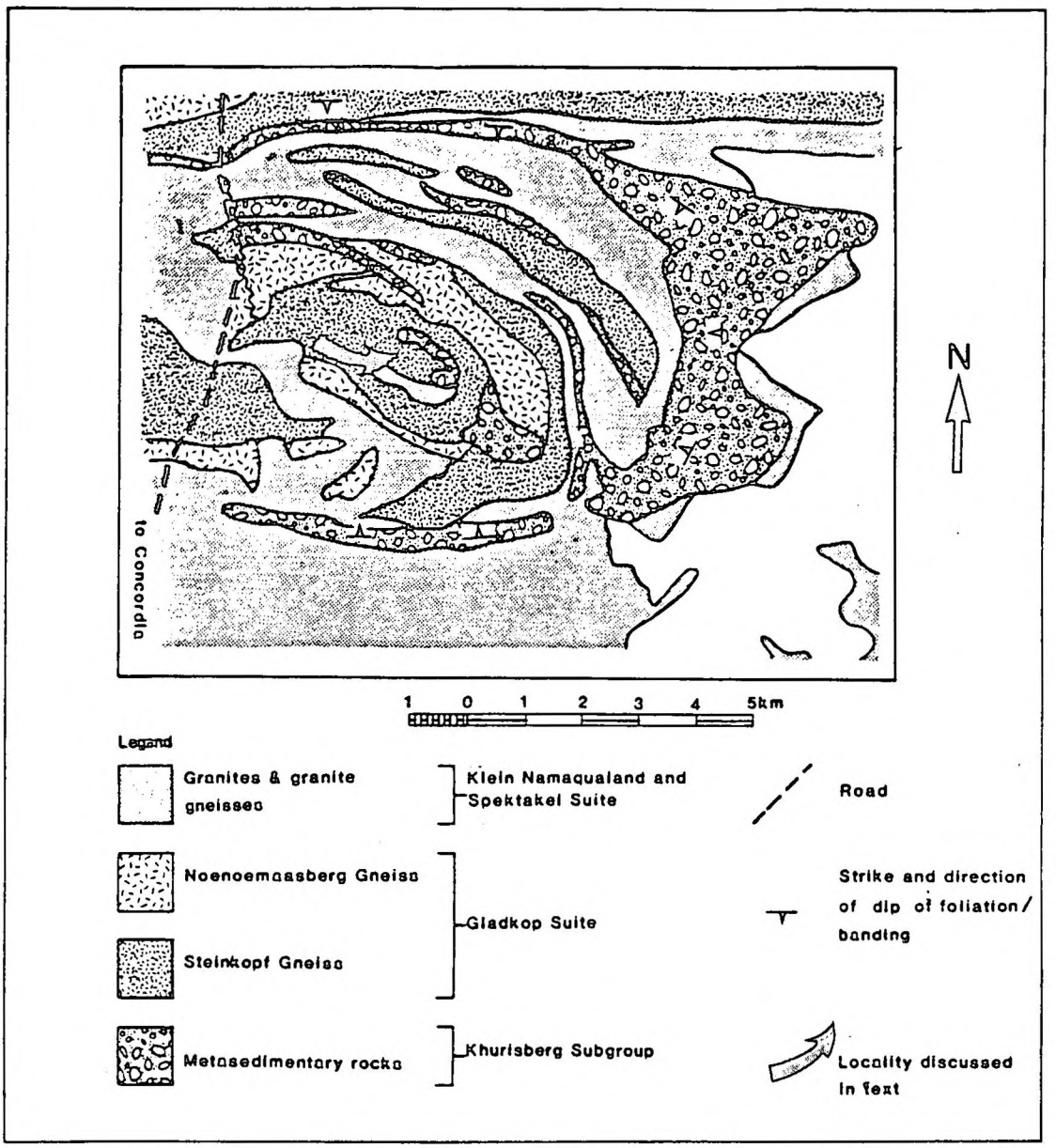

FIGURE 4.9 The geology of the eastern nose area of the Ratelpoort Synform and the location of clear-cut intrusive relations between Steinkopf Gneiss and Khurisberg Subgroup metasediments.

(Note: Figure 4.10 is on page A 13)

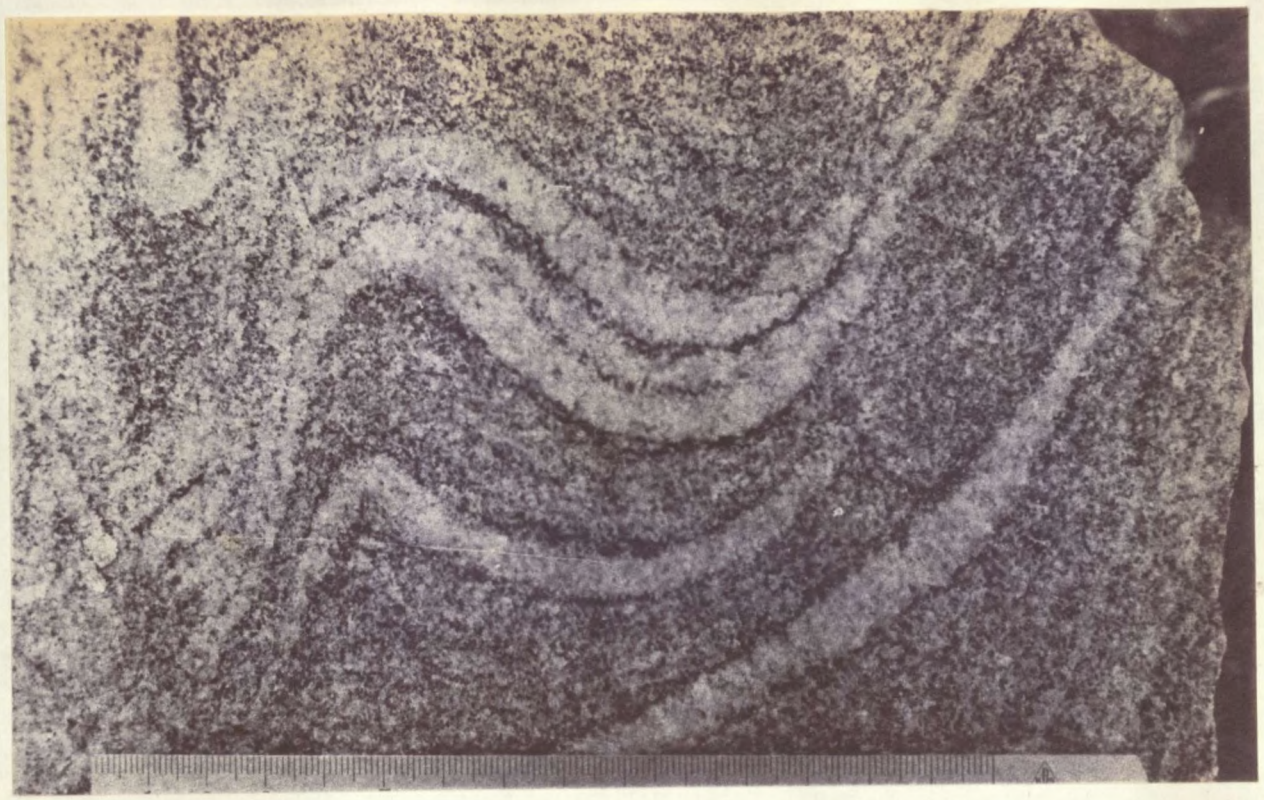

FIGURE 4.11 Two sets of secondary banding in the Steinkopf Gneiss from Dabbiknik. The first set is defined by N1s neosomes and the second by N4s neosomes (N1s and N4s as used in Chapter 11).

FIGURE 4.12 A small domal structure in Brandewynsbank Gneiss, interpreted as a sheath fold, near Sabies. The section is normal to the stretching lineation.

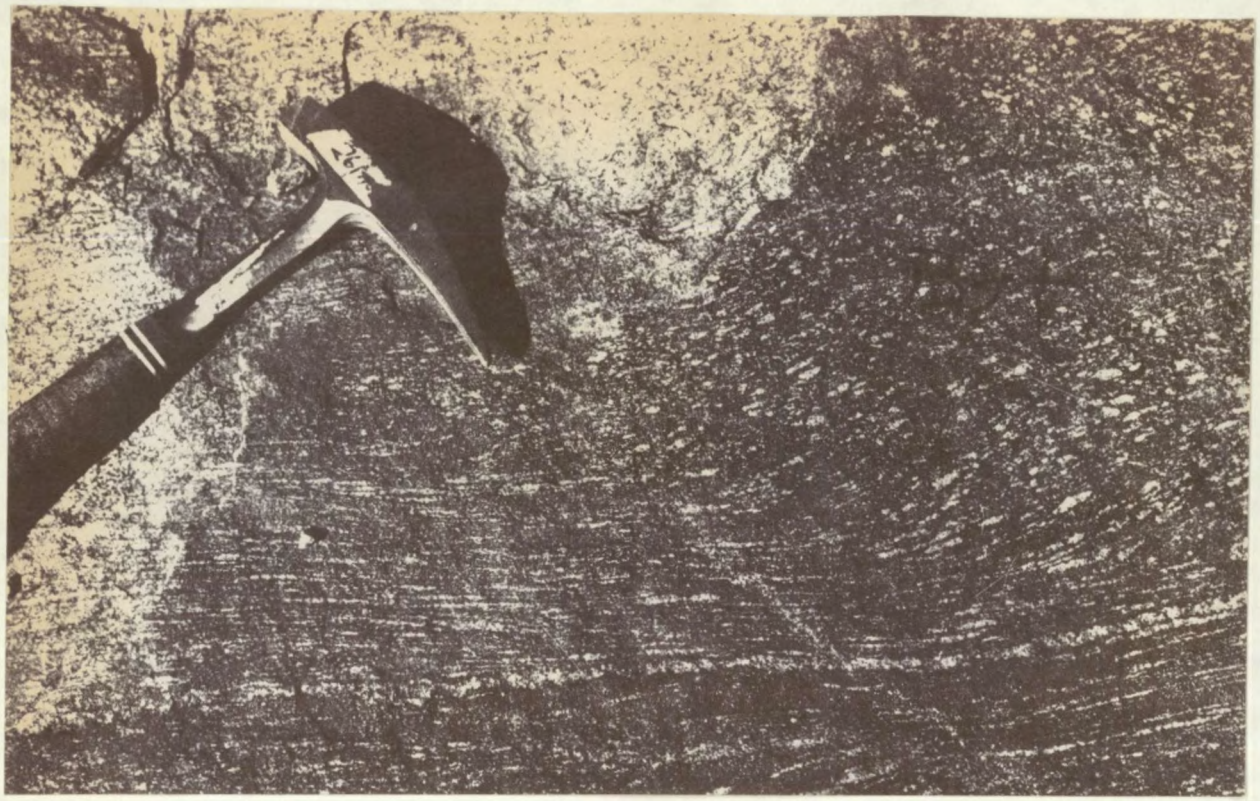

FIGURE 4.13 The formation of a banded grey gneiss through shearing of megacrystic Brandewynsbank Gneiss (at Korrogas).

FIGURE 4.14 N1s neosomes enhance the banding shown in Figure 4.13. The symbol N1s is used as in Chapter 11.

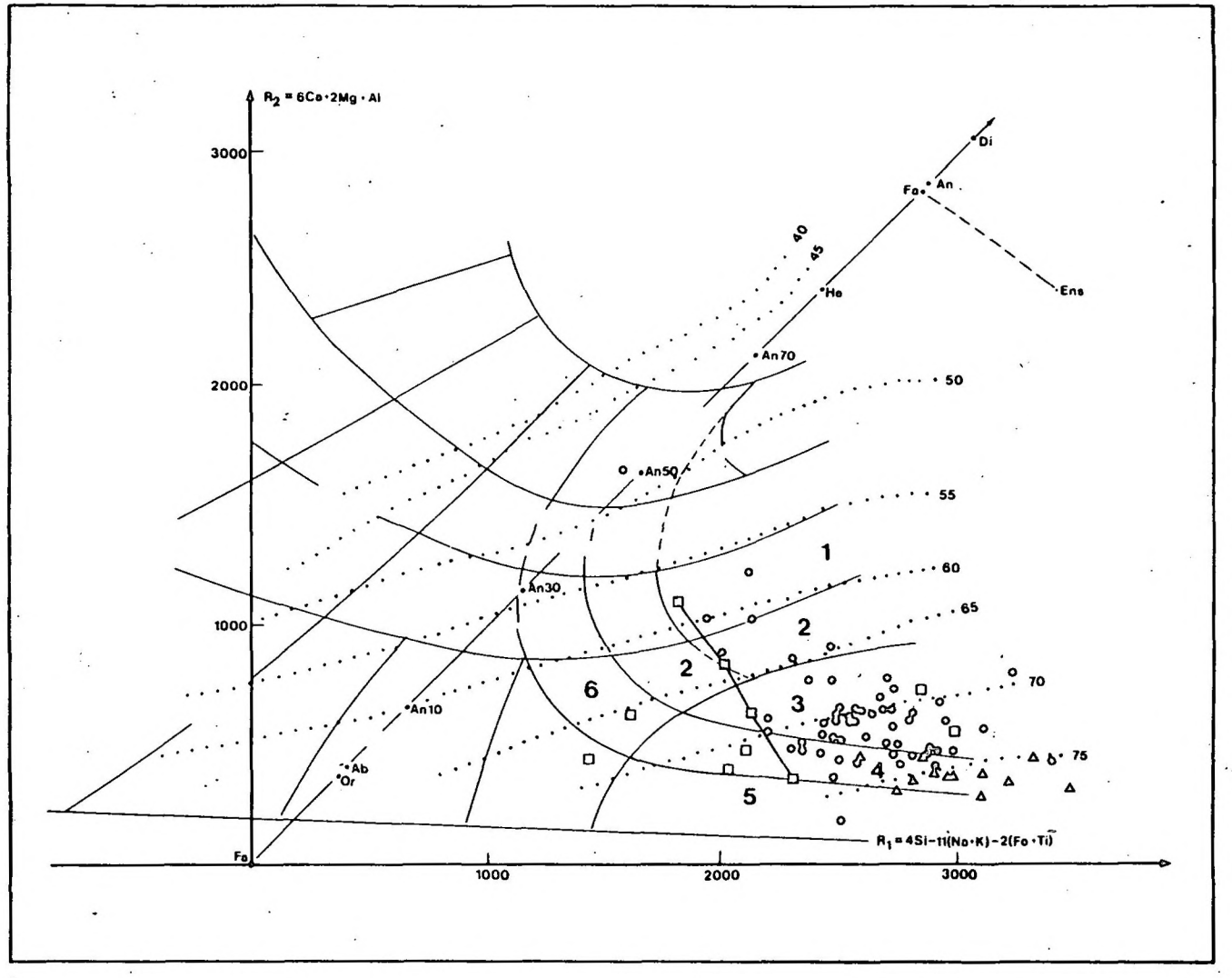

FIGURE 4.15 R1/R2 composition variation diagram (de La Roche et al., 1981) for the Gladkop Suite (solid circles). Other rock types represented are: solid squares - the average compositions of tonalite, granodiorite, adamellite and leucogranite of the Vioolsdrif Suite; open squares - gneissic Vioolsdrif granitoid from the Groothoek Thrust Zone; solid triangles - Noenoemaasberg Gneiss. The numbers indicate plutonic fields: 1 - diorite; 2 - tonalite; 3 - granodiorite; 4 - granite; 5 - alkali granite; 6 - quartz monzonite

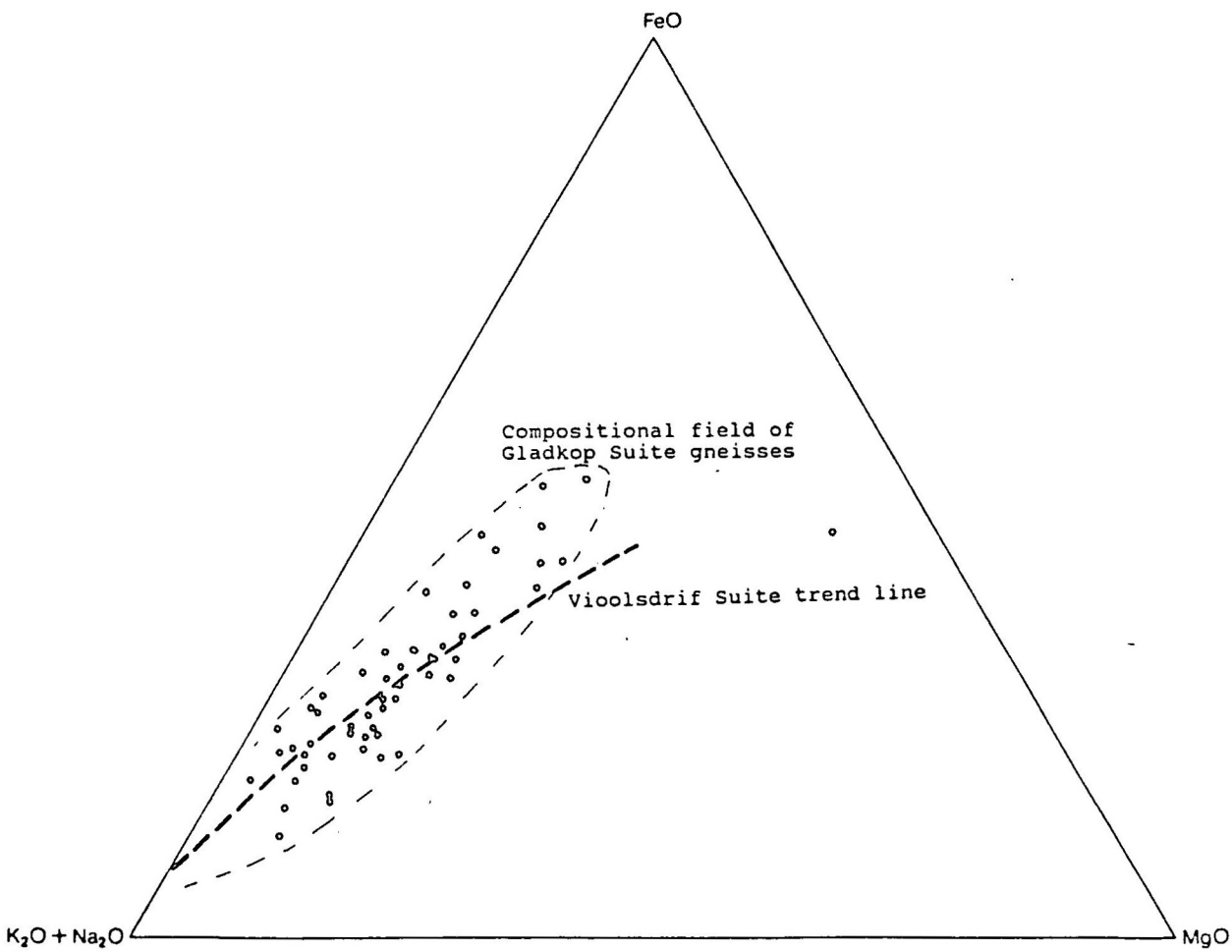

FIGURE 4.16 'AFM' plot of the grey gneisses of the Gladkop Suite (solid circles) compared with the Vioolsdrif Suite trend.

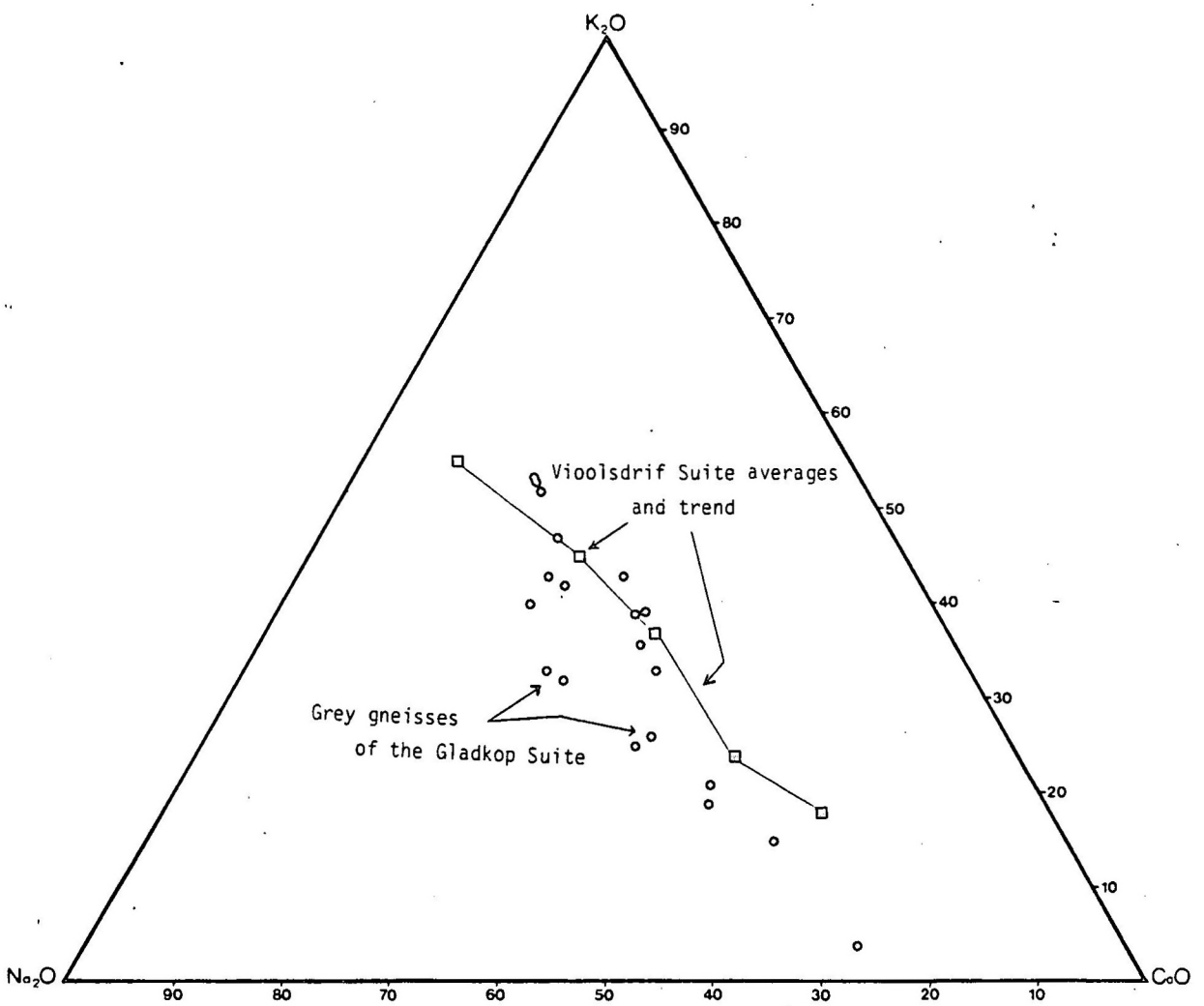

FIGURE 4.17 Ca-Na-K plot of Gladkop Suite grey gneisses (solid circles) compared to the Vioolsdrif Suite averages (solid squares) and trend.

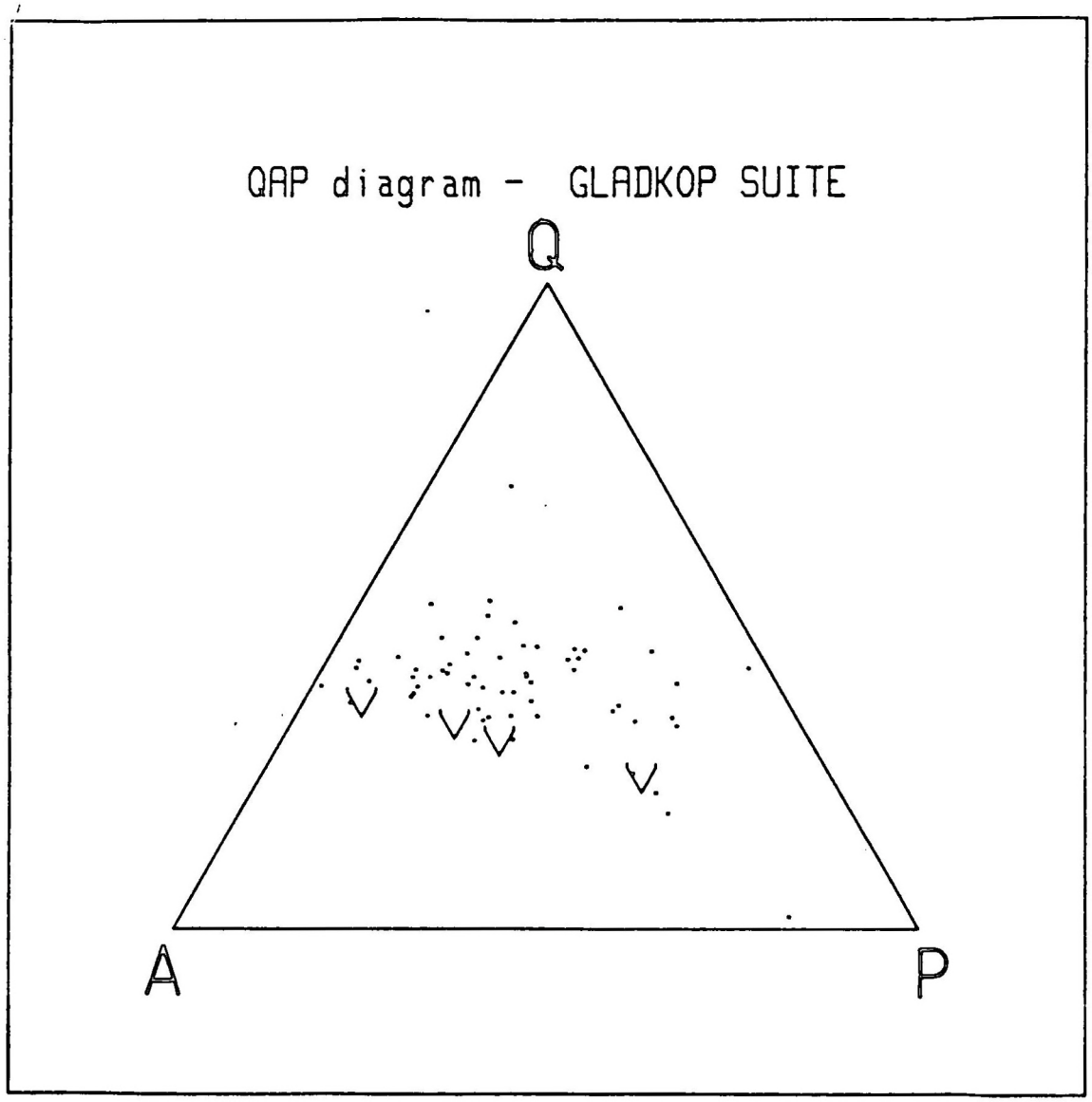

FIGURE 4.18 'QAP' diagram of Gladkop Suite grey gneisses compared with the Vioolsdrif Suite trend (V). See the text for the methods of projection involved.

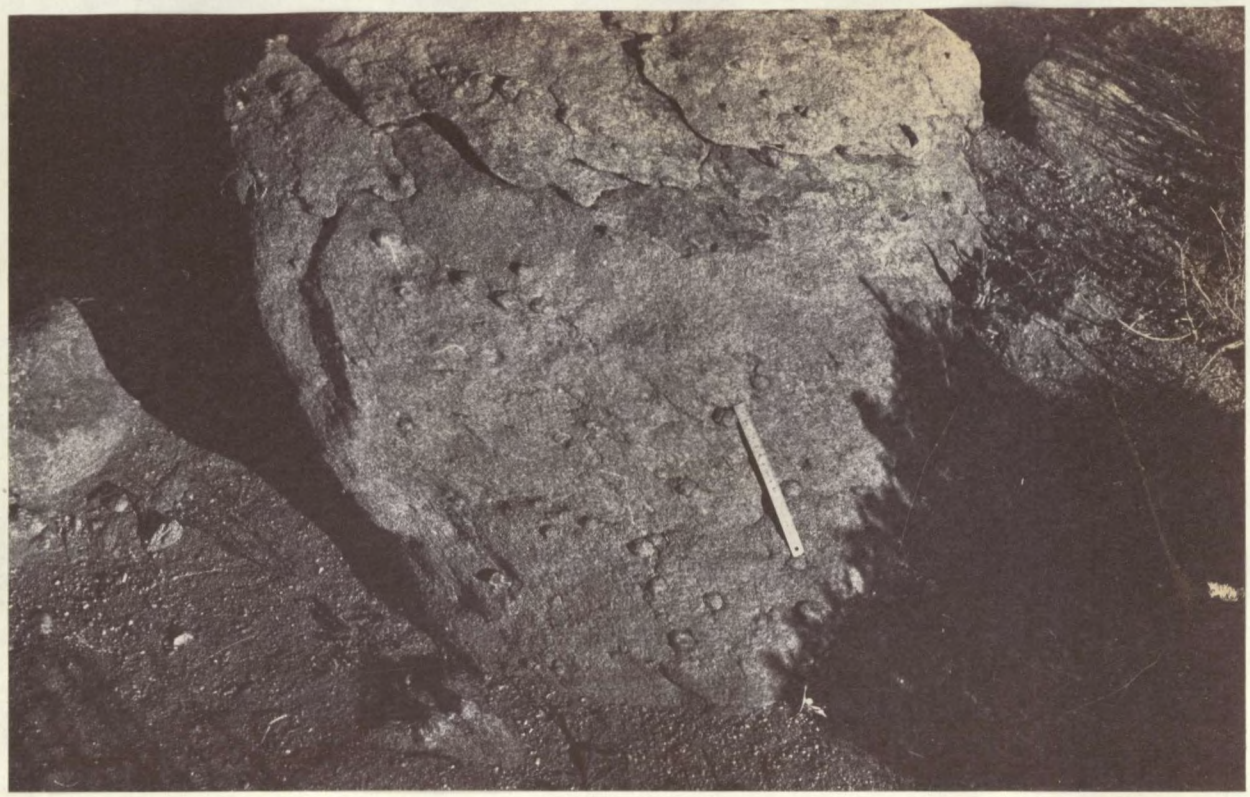

FIGURE 5.1 Kinderlê Gneiss near Konkyp with a relatively high sillimanite nodule content. The scale ruler is 16 cm long.

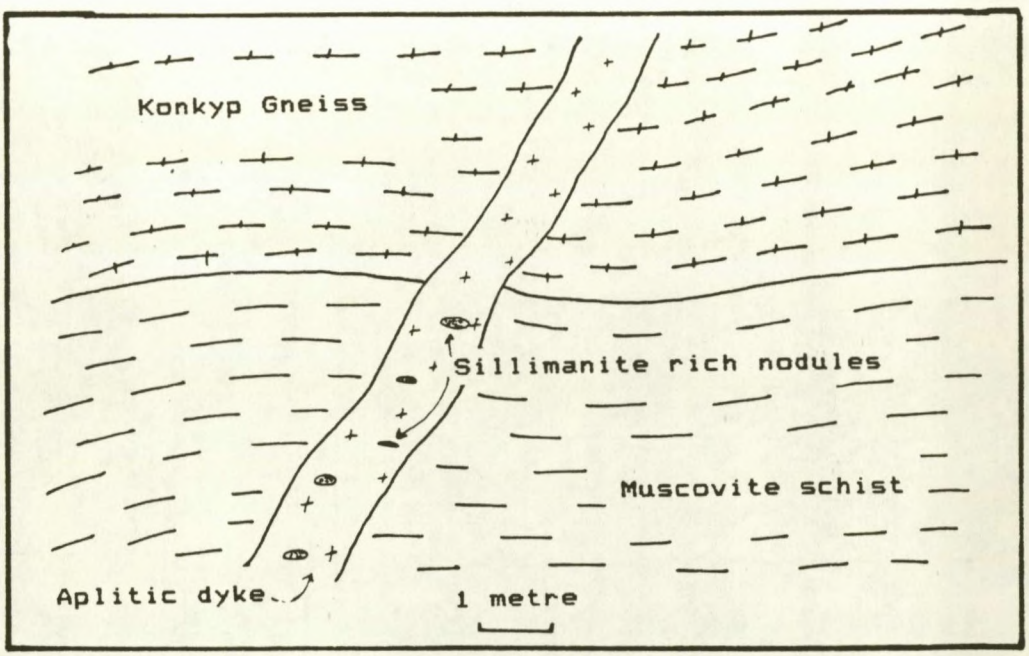

FIGURE 5.2. Field sketch of an aplitic dyke which transects the contact between Konkyp Gneiss and mica schist. Sillimanite nodules are confined to that part of the dyke in contact with the aluminous metasediment. The sizes of the nodules are exaggerated.

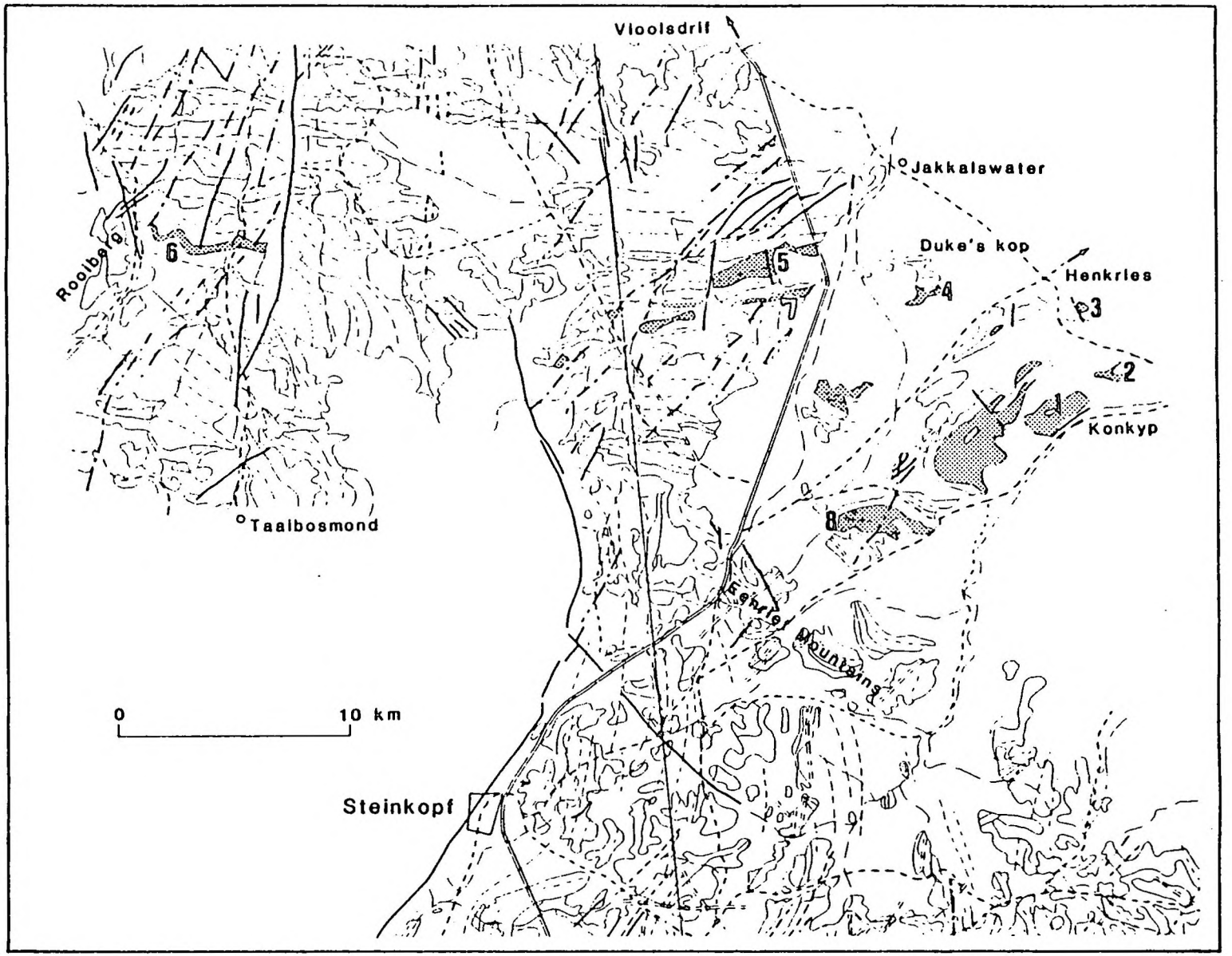

FIGURE 6.1 The distribution of the Konkyp Gneiss (shaded areas on the map). The numbers refer to localities mentioned in the text.

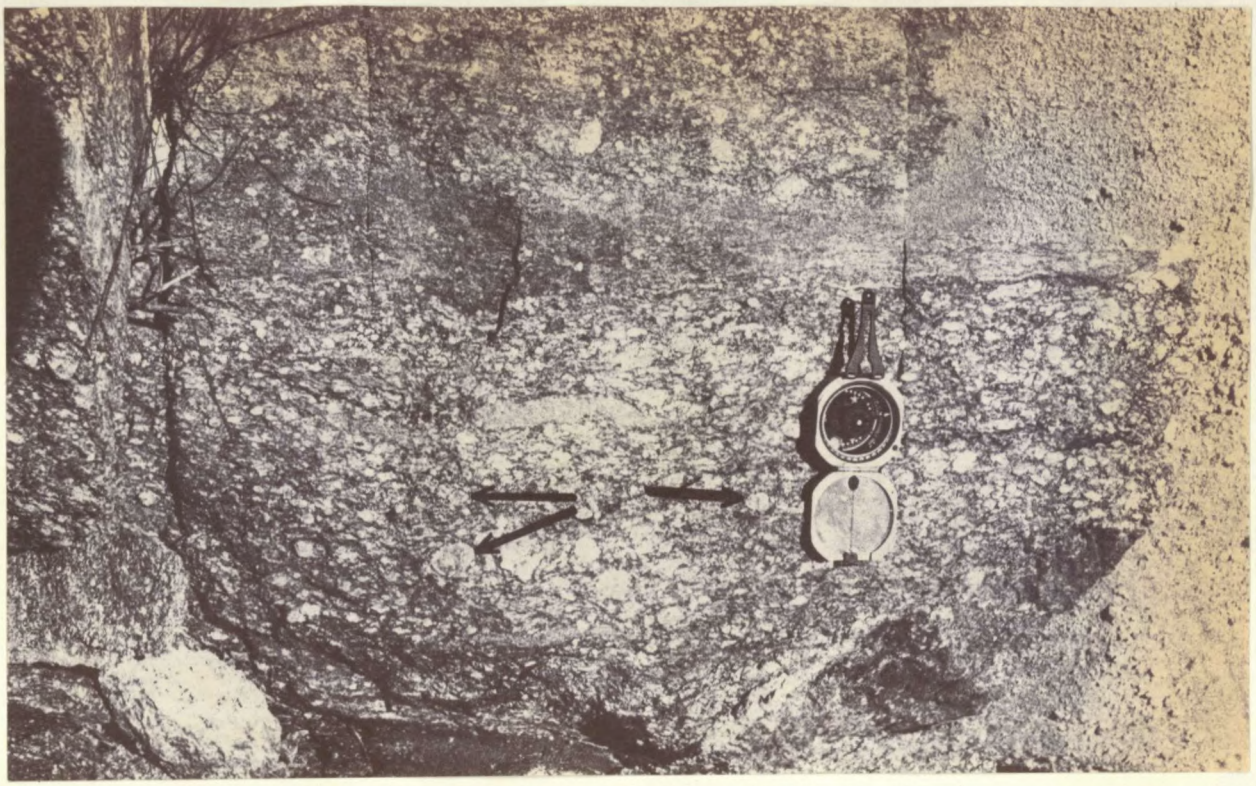

FIGURE 6.2 Outcrop appearance of the Konkyp Gneiss on the plain west of the Konkyp hill. Note the elongate xenoliths. The arrows point to feldspars with rapakivi texture.

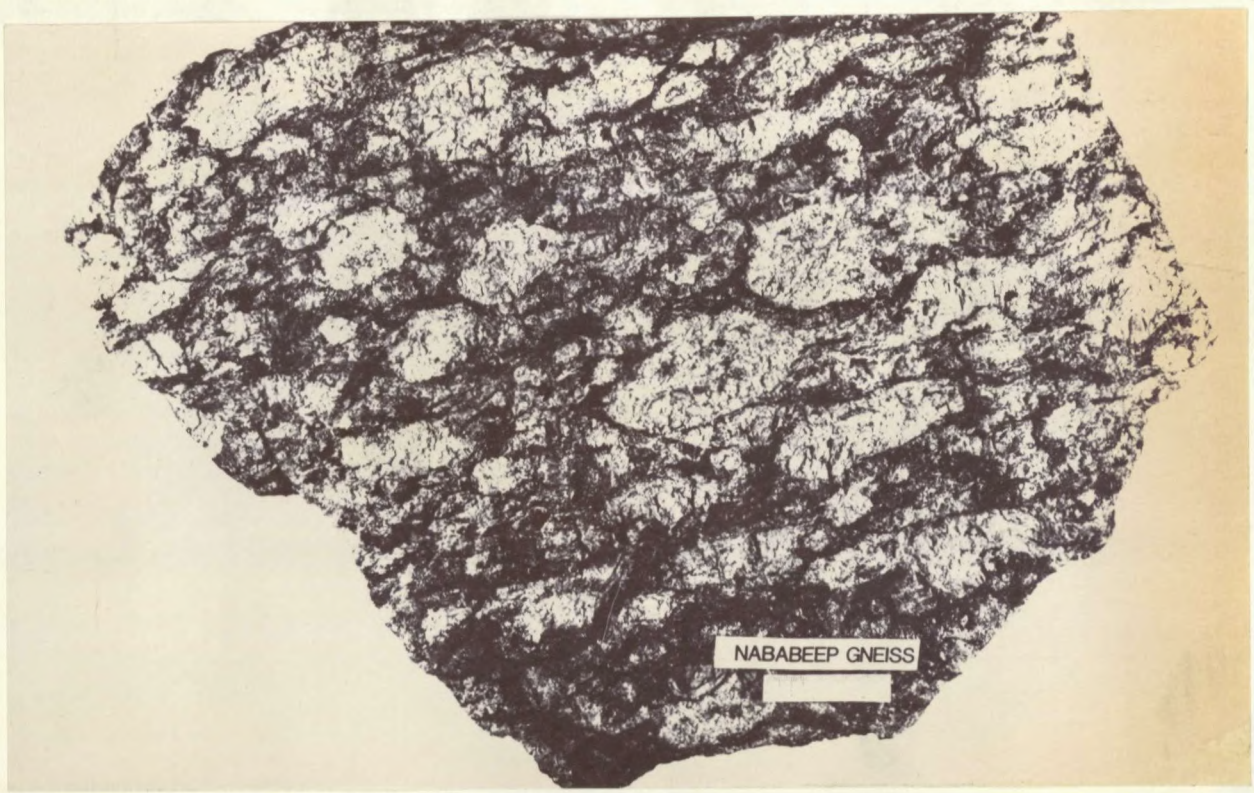

FIGURE 6.3 Nababeep Gneiss from the farm Eendoorn south of Springbok. The scale is 5 cm long.

FIGURE 6.4 A single auge from the specimen shown in Figure 6.3. The smallest unit on the scale is 1 mm.

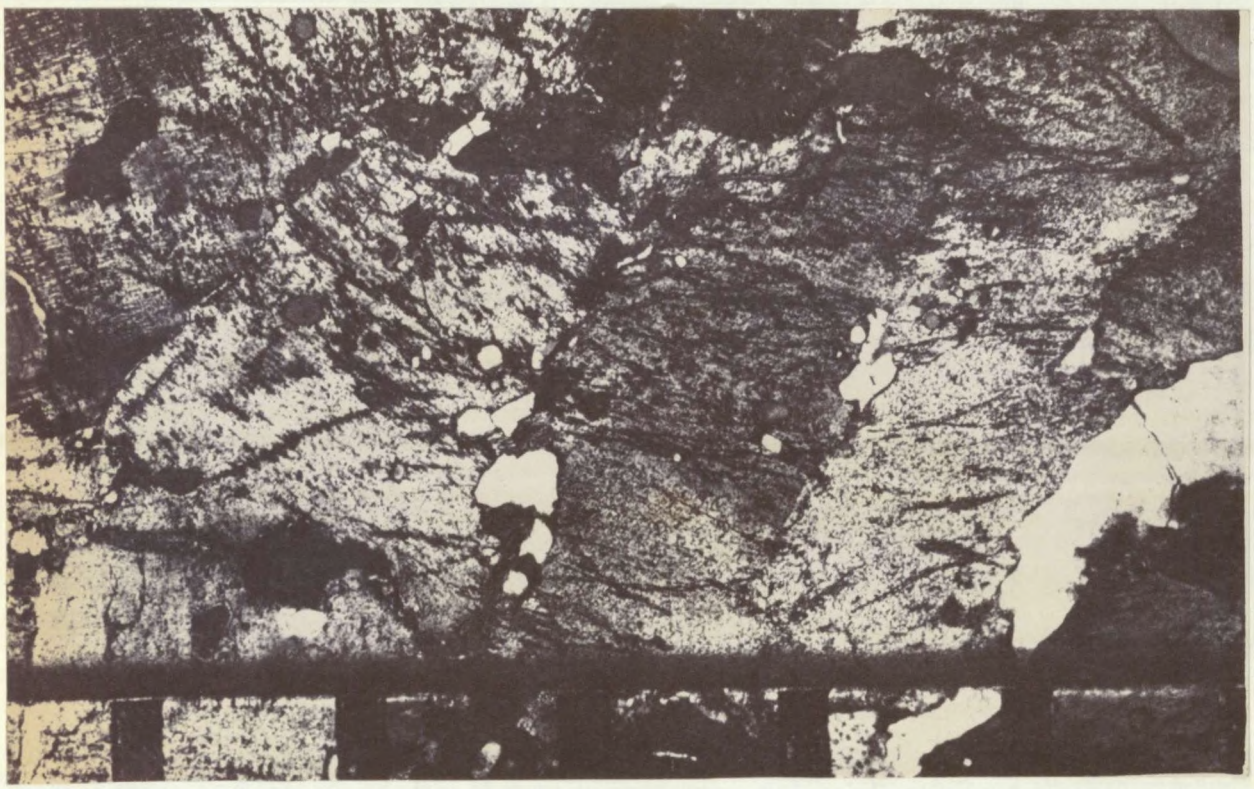

FIGURE 6.5 Photomicrograph of part of a K-feldspar auge in specimen GLC219. See full description in the text. The scale units along the top of the picture are 1 mm apart.

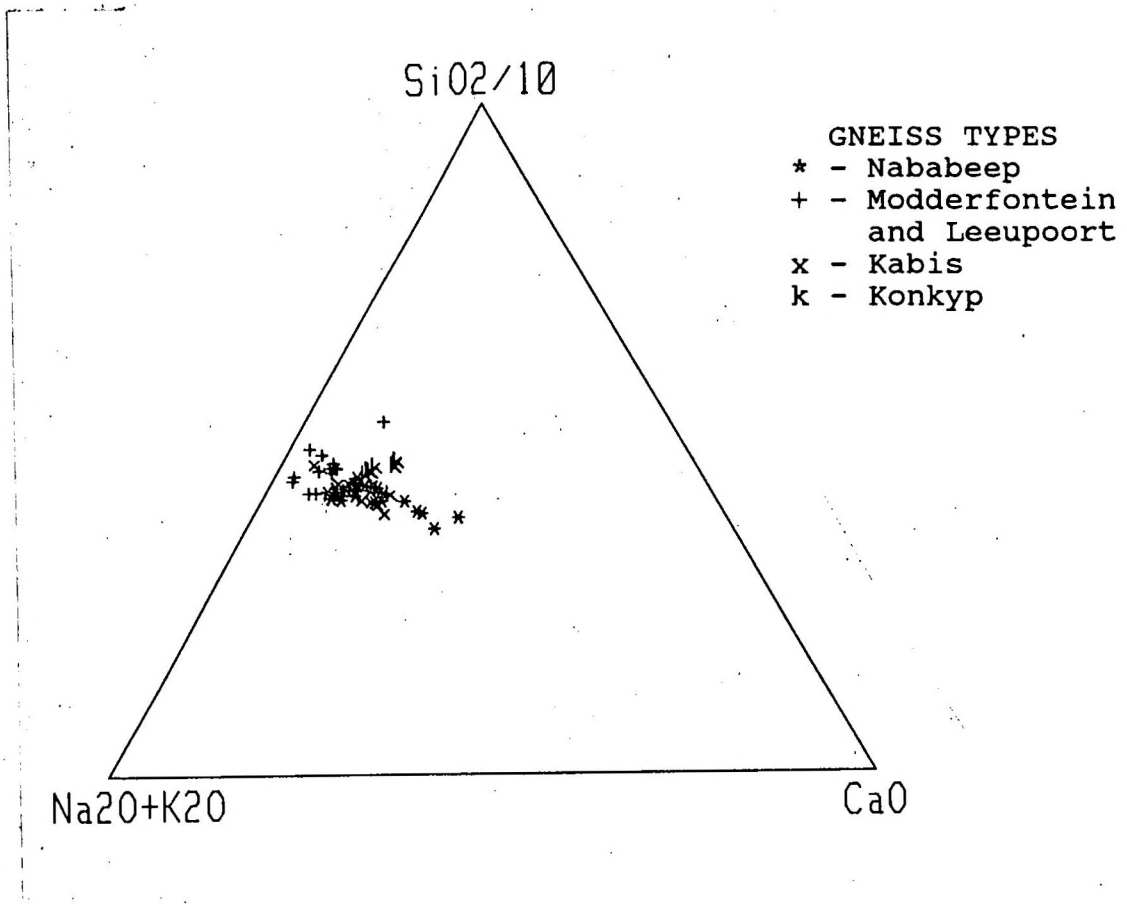

FIGURE 6.6 SiO_2-(K_2O+Na_2O)-CaO plot of Little Namaqualand Suite gneisses.

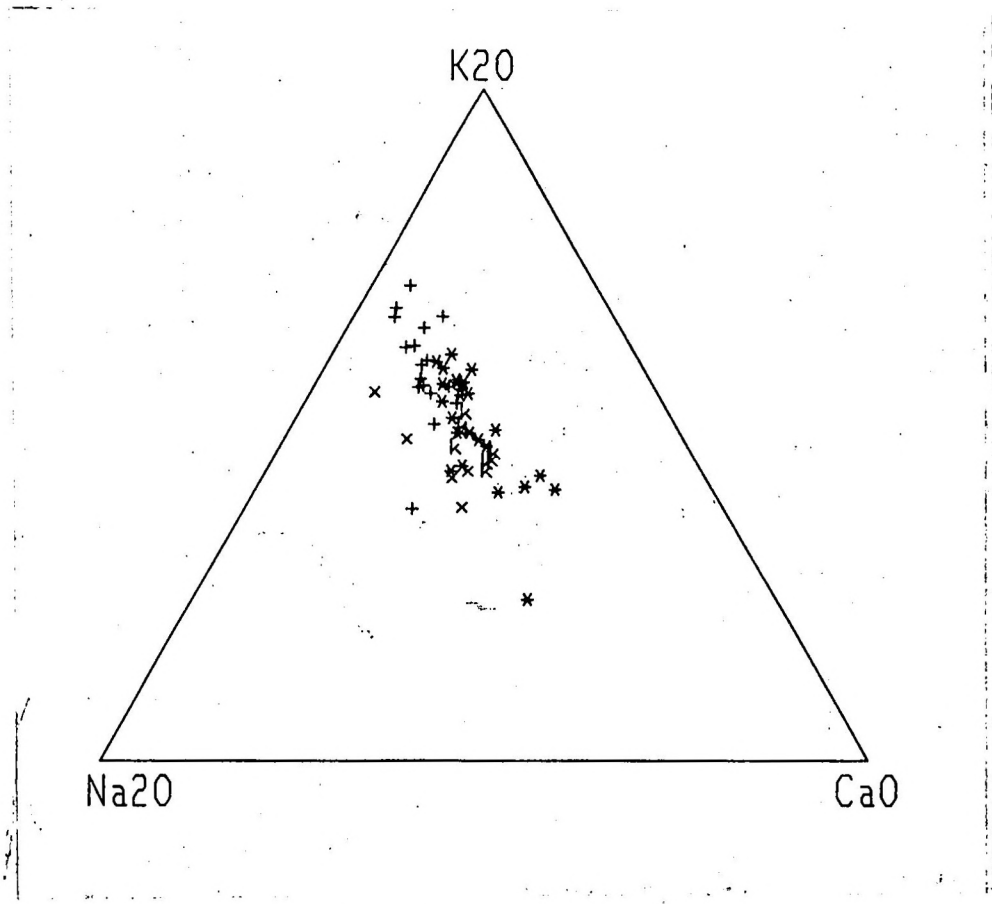

FIGURE 6.7 K_2O-Na_2O-CaO plot of Little Namaqualand Suite gneisses. (Symbols as in Figure 6.6)

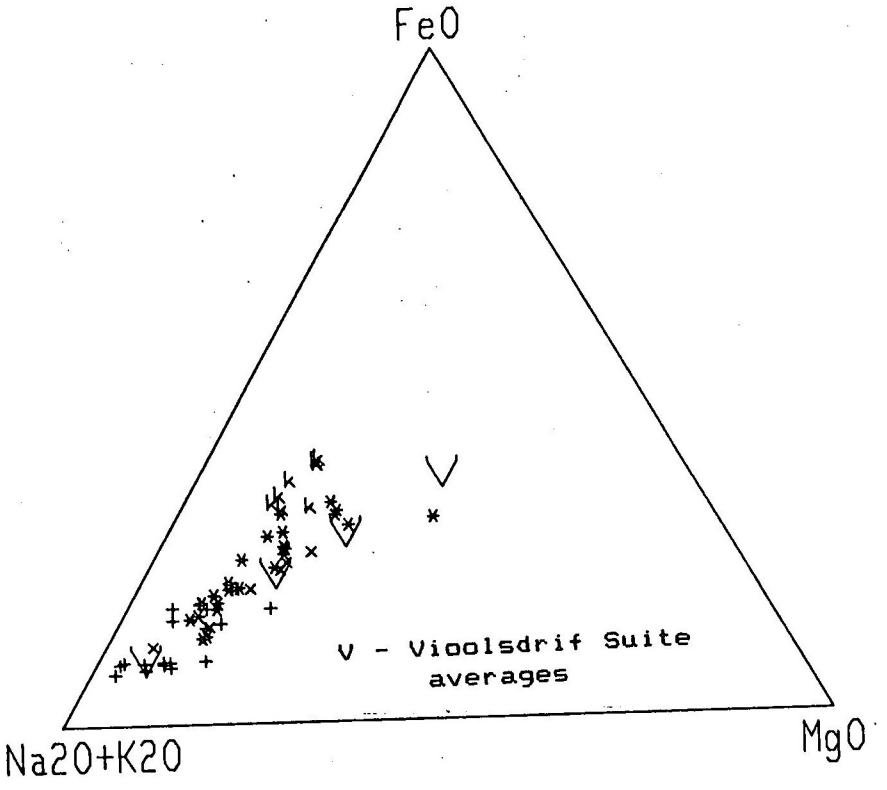

FIGURE 6.8 'AFM' plot of Little Namaqualand Suite gneisses. (Symbols as in Figure 6.6)

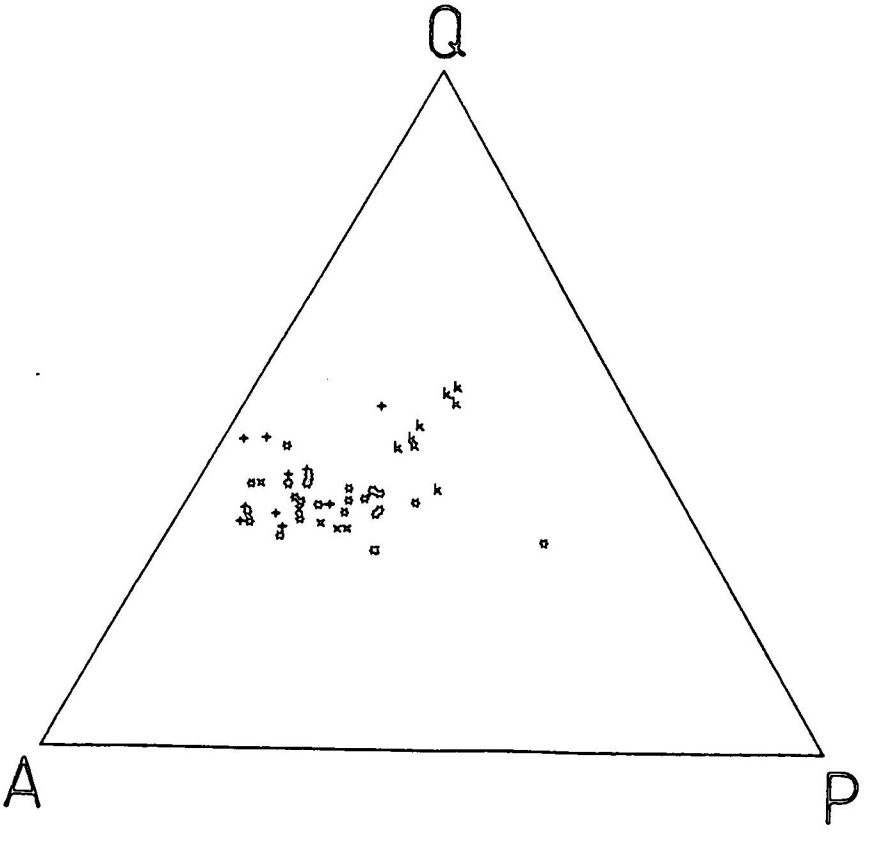

FIGURE 6.9 'QAP' diagram of Little Namaqualand Suite gneisses The same calculation method as for Figure 4.18 was used. (Symbols as in Figure 6.6)

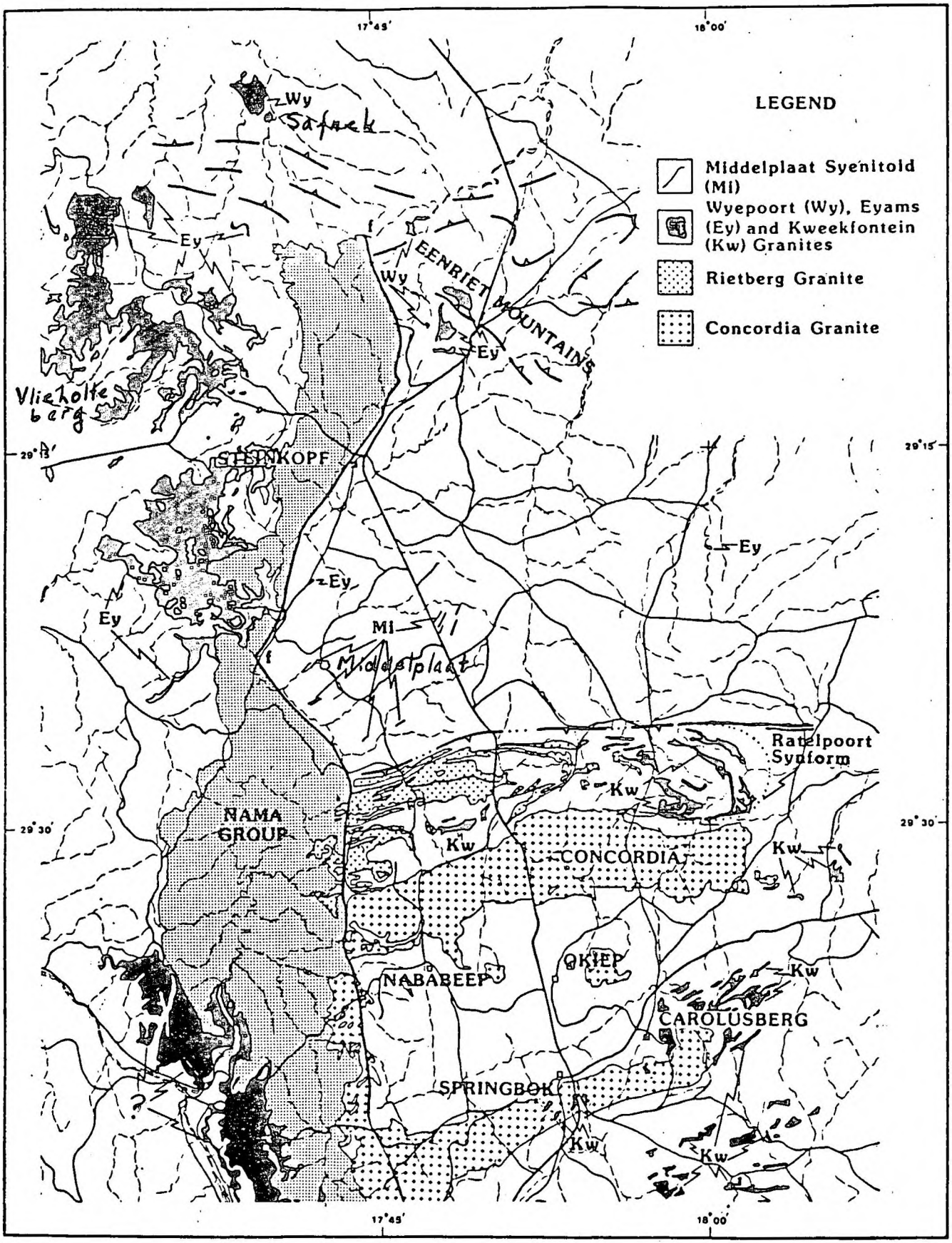

FIGURE 7.1 The distribution of different Spektakel Suite units in the study area and further toward the west.

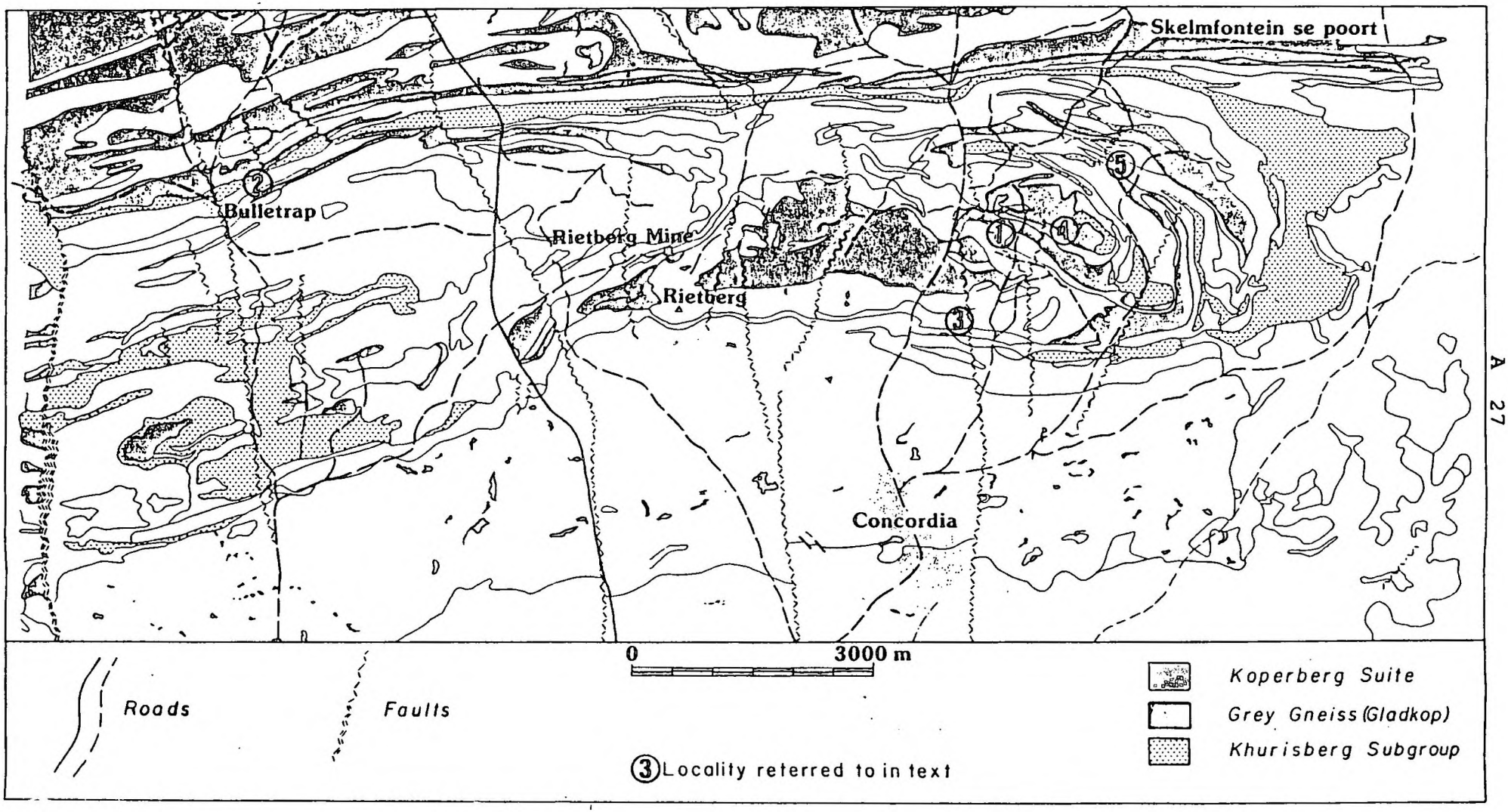

FIGURE 7.2 Map of the Ratelpoort Synform indicating the positions of some of the localities referred to in the text.

FIGURE 7.3 The megacrystic type of Kweekfontein Granite as found at locality 1, Figure 7.2.

FIGURE 7.4 Kweekfontein Granite with concentrations of Rietberg-type phenocrysts. The patch at the centre of the photograph appears to be a xenolith of Rietberg Granite (locality 3, Figure 7.2).

FIGURE 7.5 A discrete xenolith of Leeupoort augen gneiss in the Kweekfontein Granite (locality 3, Figure 7.2)

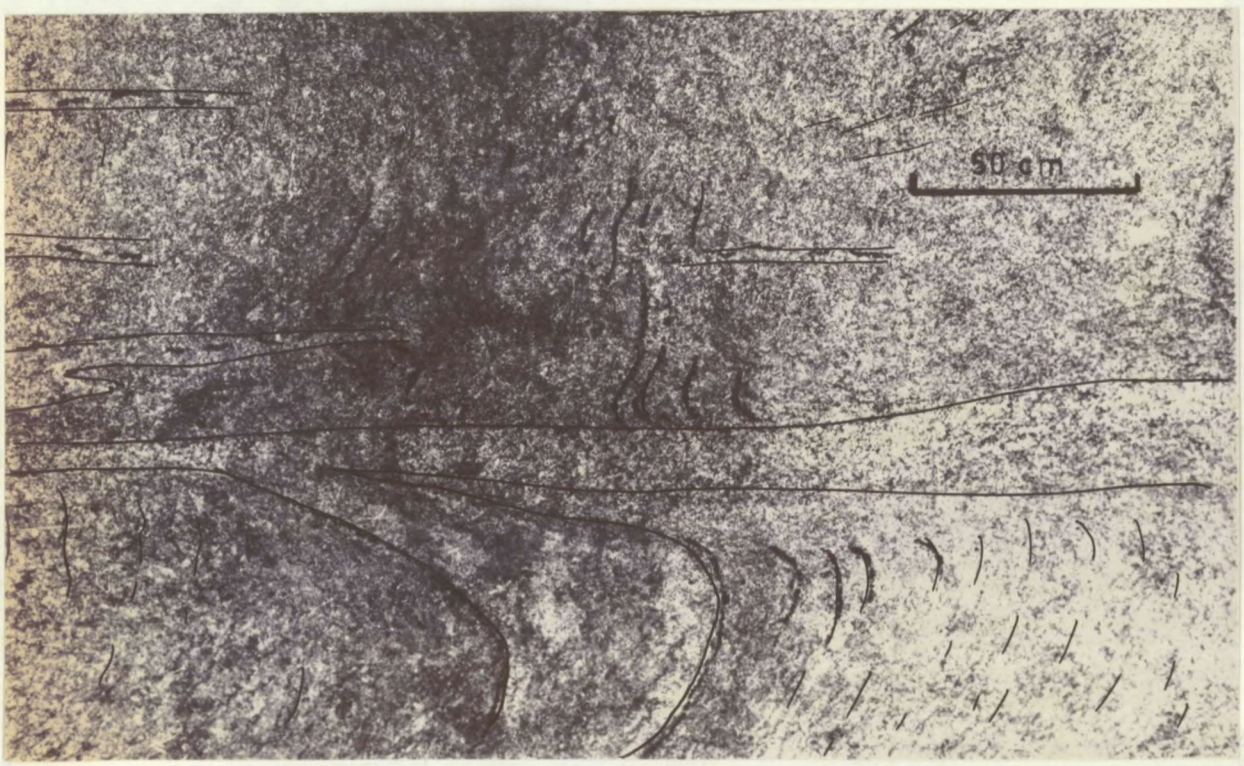

FIGURE 7.6 Kweekfontein Granite along minor Skelmfontein shears. Some of the features are accentuated by marker pen: broken lines trace very thin (2 - 4 mm) granite stringers; solid lines follow the older fabric in the country rock (locality 1, Figure 7.2).

FIGURE 7.7 Granite-filled shears (Kweekfontein Granite) in Steinkopf Gneiss. The photograph was taken few metres from the locality of Figure 7.6 and the salient features were accentuated by marker pen.

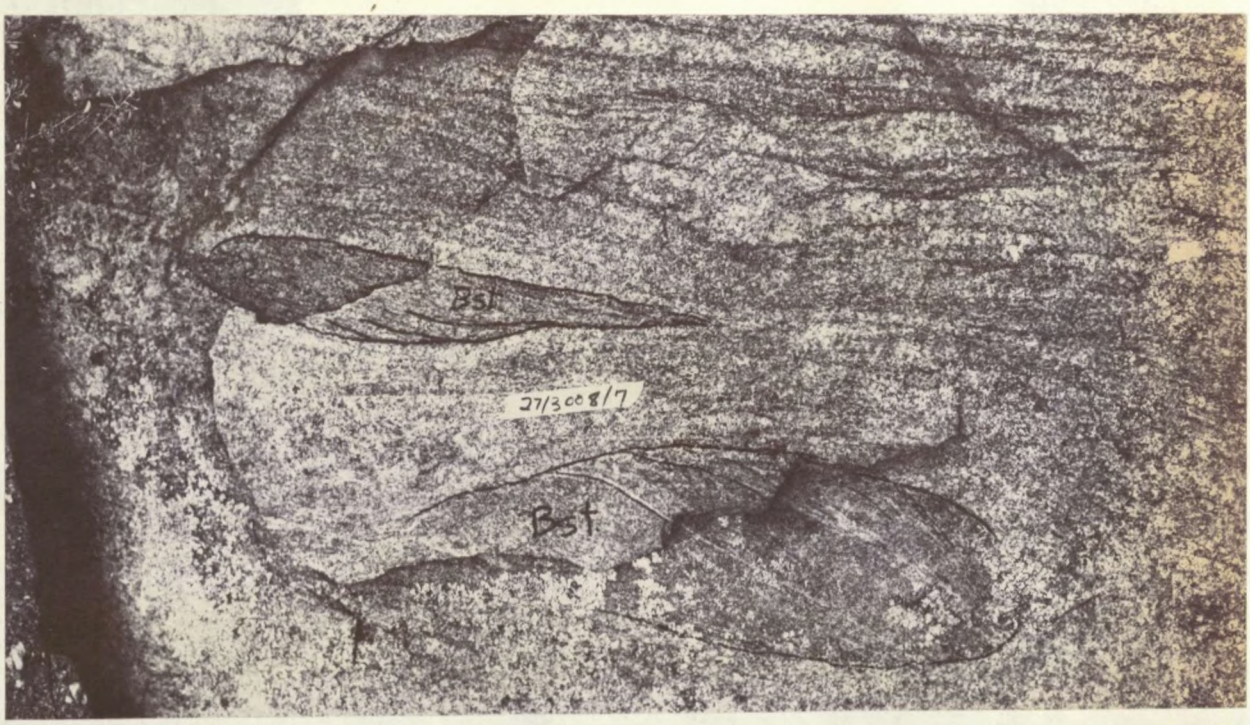

FIGURE 7.8 Kweekfontein Granite with the schlieric remains of the country rock defining a kinematic flow banding. The strain on two xenoliths indicate left lateral shear. The masking tape with reference number is 20 mm wide. Some features are accentuated by marker pen.

FIGURE 7.9 Boudinaged form of a Kweekfontein Granite sheet indicates deformation subsequent to emplacement. Note the neosome development in the dilatation zone.

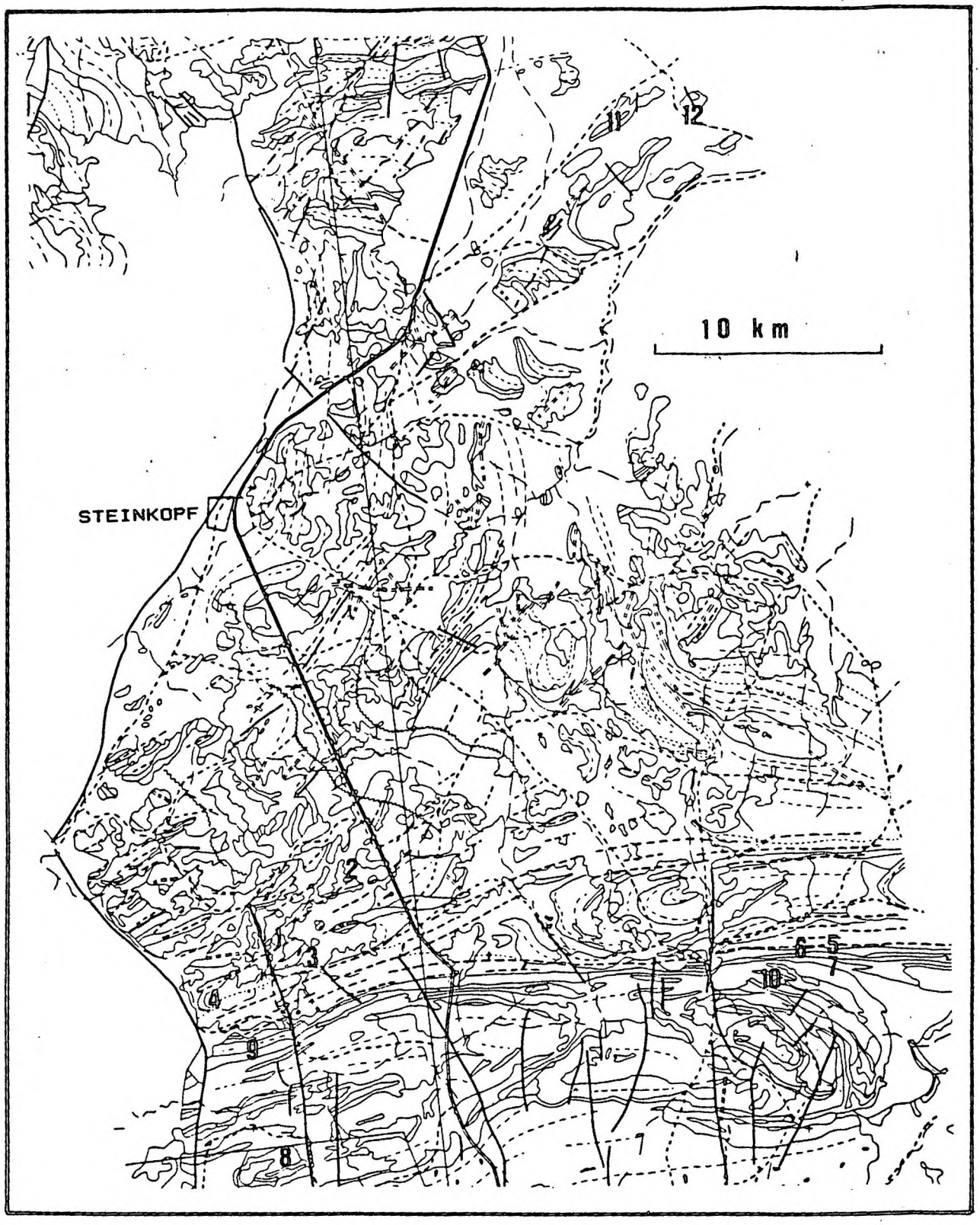

FIGURE 9.1 Map showing the positions of some localities described in the text. Compare with the printed map (Annexure 1) for explanation of line types.

FIGURE 9.2 Disrupted amphibolite band within Brandewynsbank Gneiss (locality 1, Figure 9.1). The disruption is caused by Dabbiknik shearing.

FIGURE 9.3a Typical mesoscale folds in the Dabbiknik zone of refoliation. Note the shearing along the fold limbs (above the hammer head). The box indicates the area covered by Figure 9.3b.

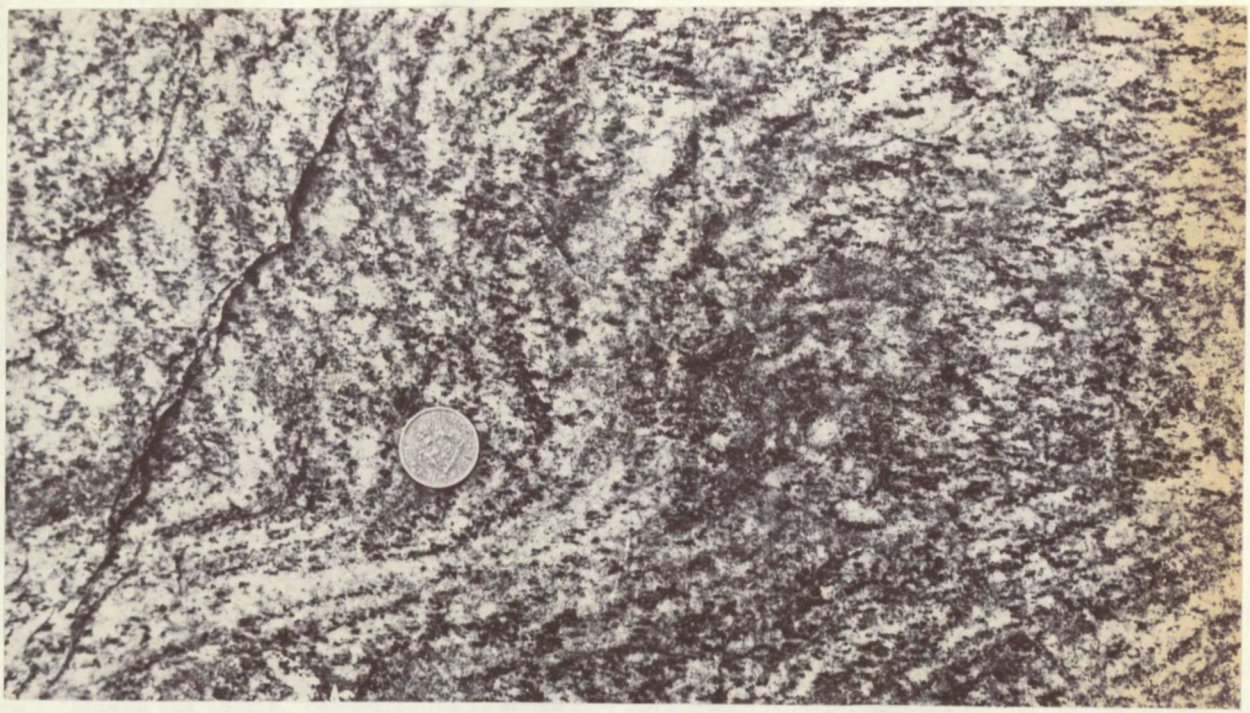

FIGURE 9.3b Mineral refoliation in the hinge zone of the larger fold (the area within the box) shown in Figure 9.3a.

FIGURE 9.4 Two ages of secondary banding in Steinkopf Gneiss in the Eenriet Mountain Range. The boudinaged felsic band (N1s leucosome) to the right of the the scale ruler, displays thin banding (mm scale) which developed during Dabbiknik deformation. This new banding, together with a mineral refoliation, defined by the orientation of biotite flakes (not visible in the photograph), is axial planar to the folds depicted by the cm scale banding (N1s).

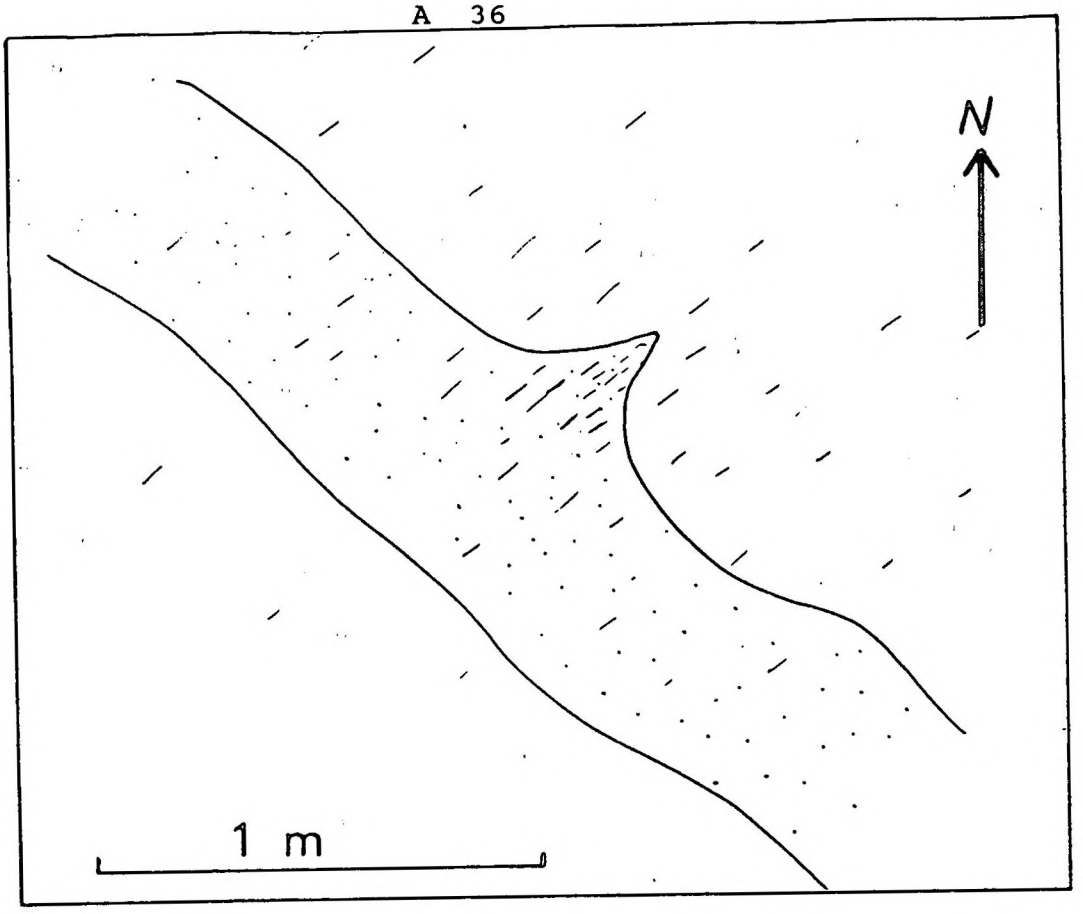

FIGURE 9.5 Sketch map showing mullion structure developed at the contact between a thin Middelplaat dyke (stippled) and Steinkopf Gneiss, near Korrogas. As indicated, the Dabbiknik refoliation is best developed in the hinge zone of the structure.

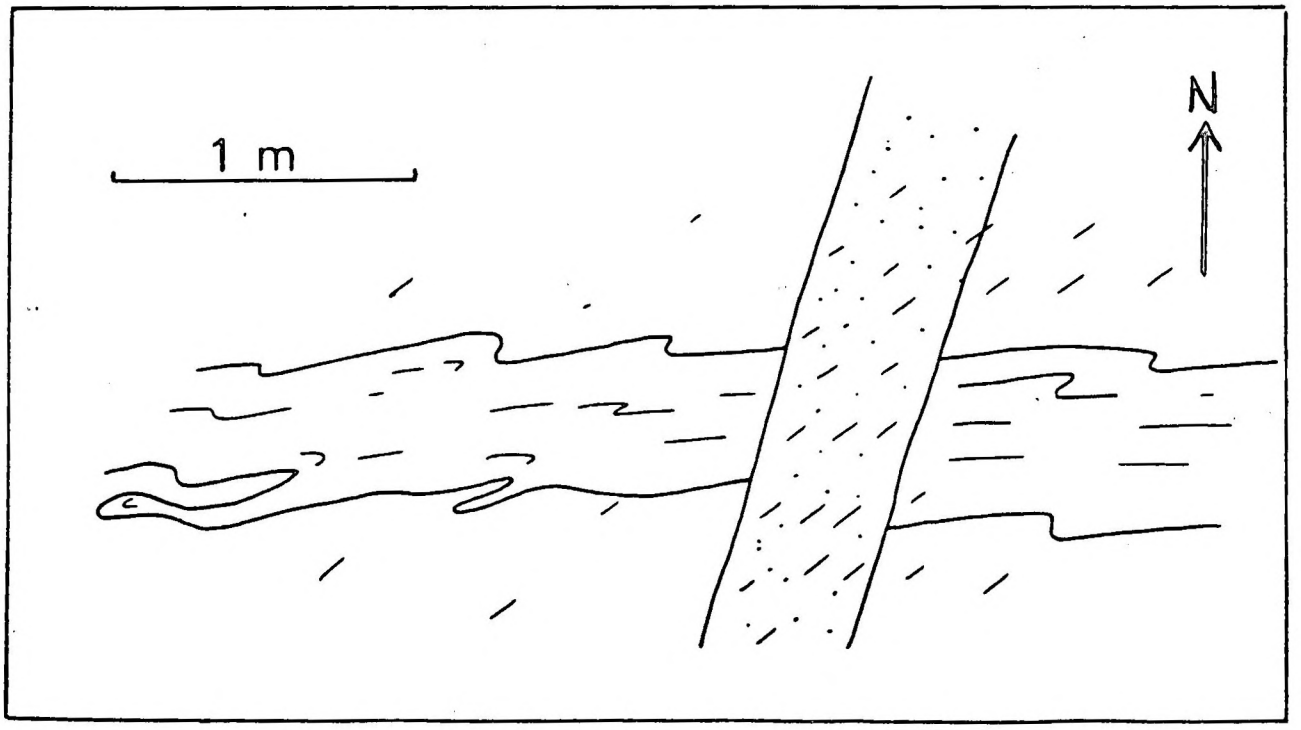

FIGURE 9.6 Sketch map showing age relations between a thin Middelplaat dyke (stippled) and two refoliation events. The dyke transects foliation/banding as well as an old, westerly trending refoliation, the latter associated with the minor S-folds. The Dabbiknik refoliation is superimposed on the dyke.

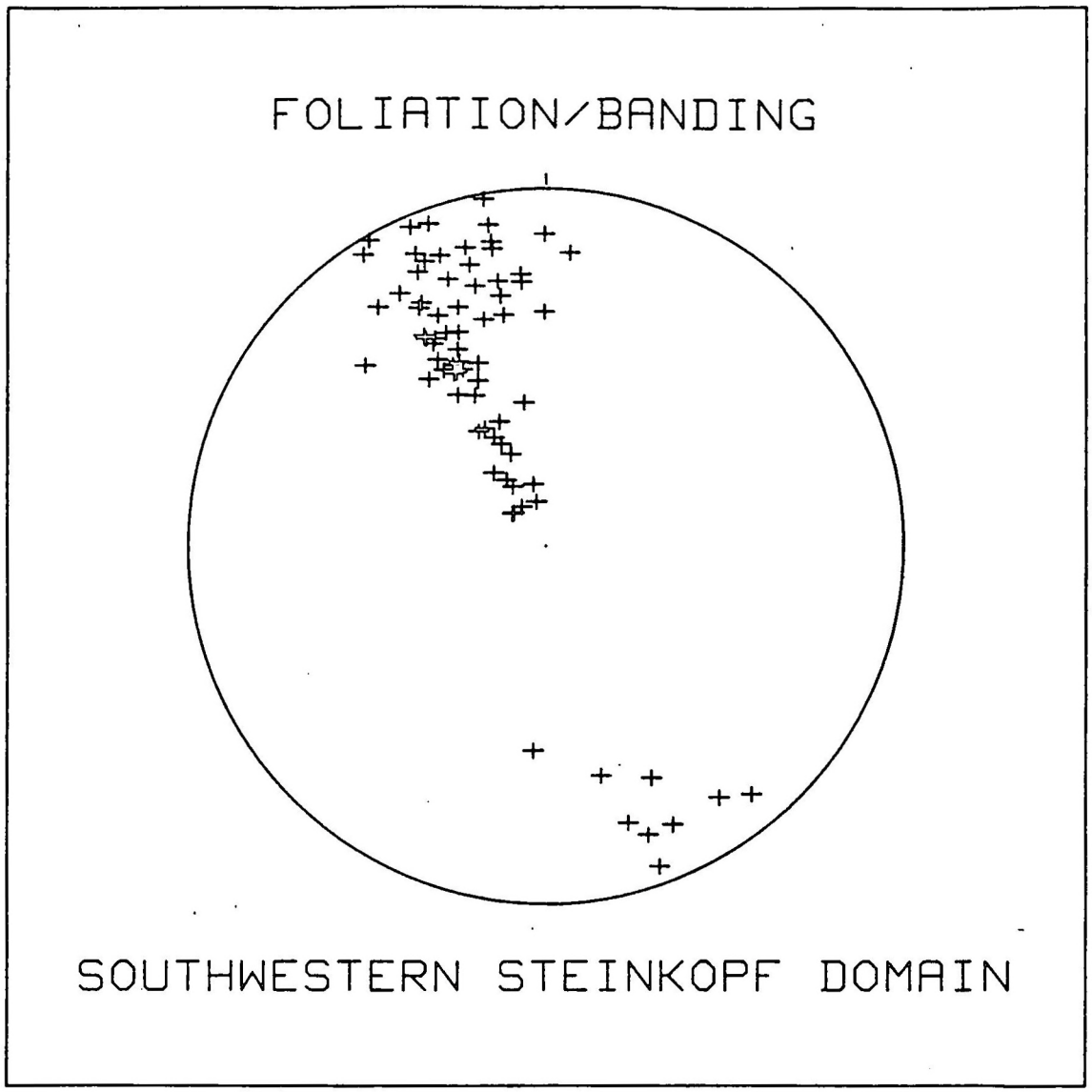

Figure 9.7 Equal area projection of poles to foliation/banding in the southwestern part of the Steinkopf Domain.

Figure 9.8 Dabbiknik shears assosiated with numerous N4f neosomes, in the Nariams area (the symbol N4f is used as in Chapter 11).

Figure 9.9 Skelmfontein refoliation in Steinkopf Gneiss at the northern end of Skelmfontein se Poort.

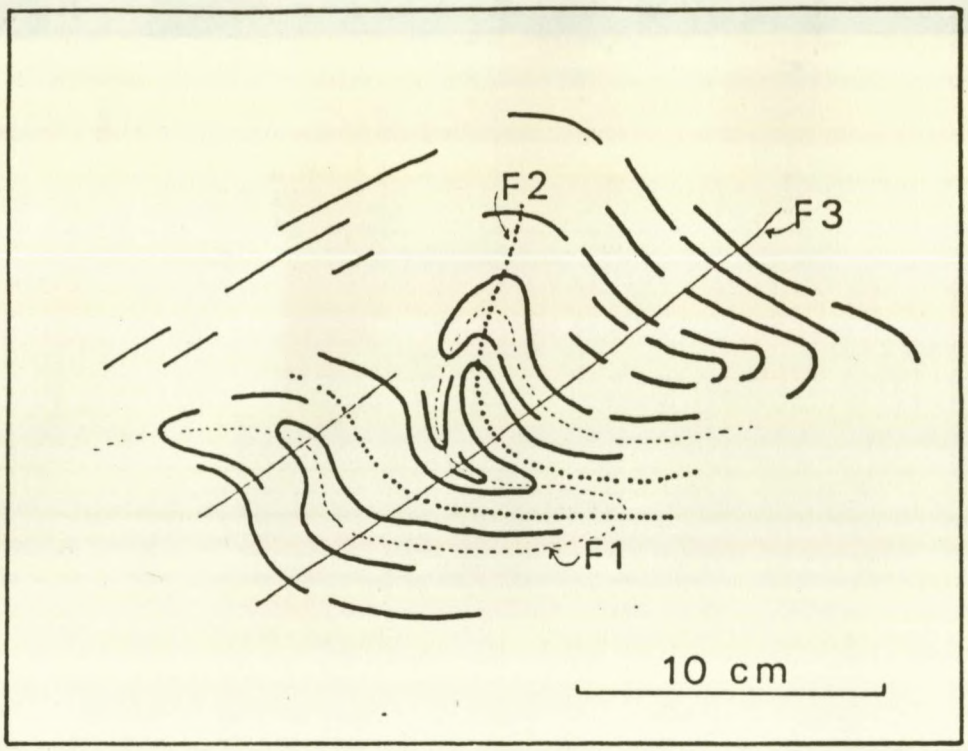

Figure 9.10 Field sketch illustrating three phases of folding in metasedimentary rock,west of Skelmfontein se poort.F1, F2 and F3 denote the traces of axial planes.

Figure 9.11a Zonally developed Skelmfontein .refoliation [nearly perpendicular to the shaft of the hammer] in Leeupoort Gneiss,south of Skelmfontein se Poort. The boxes indicate the areas shown in greater detail in Figures 9.11b and 9.11c.

Figure 9.11b The appearance of the Leeupoort Gneiss at the position indicated by box I in Figure 9.11a. The original augen texture is largely retained.

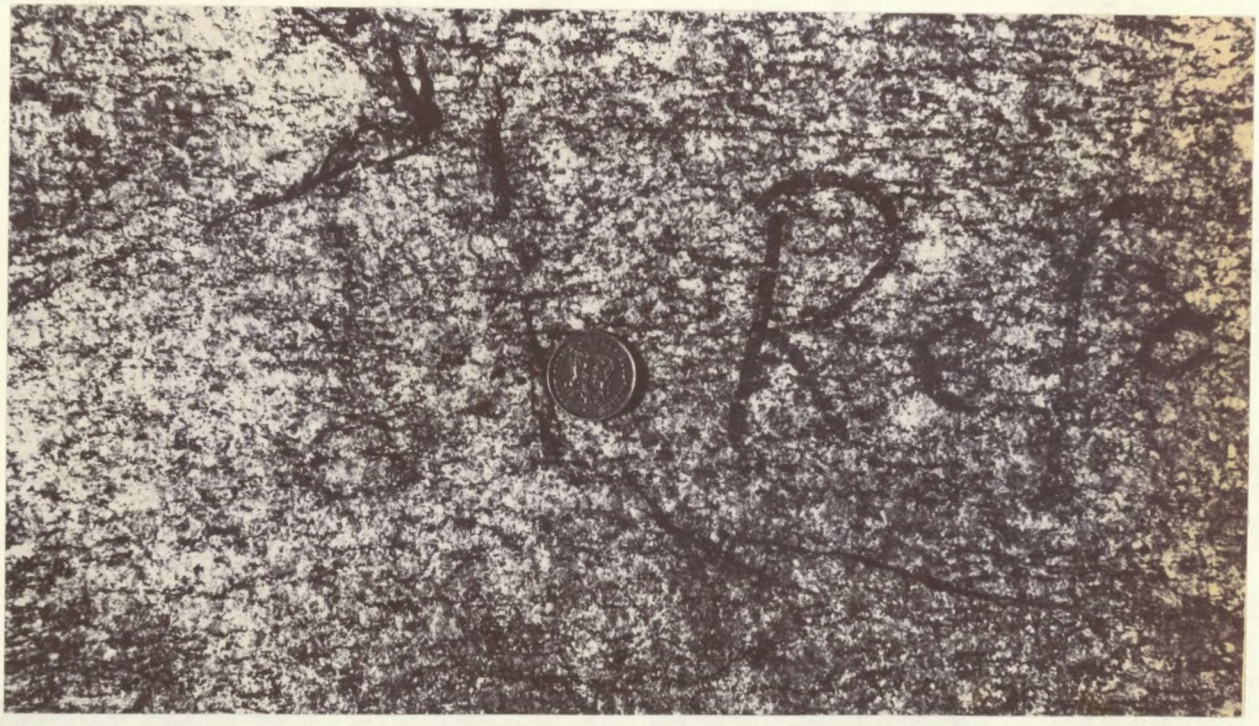

Figure 9.11c The appearance of the Leeupoort Gneiss at the position indicated by box II in Figure 9.11a. The entire area is penetratively refoliated and the rock has a fine-grained, gneissic texture.

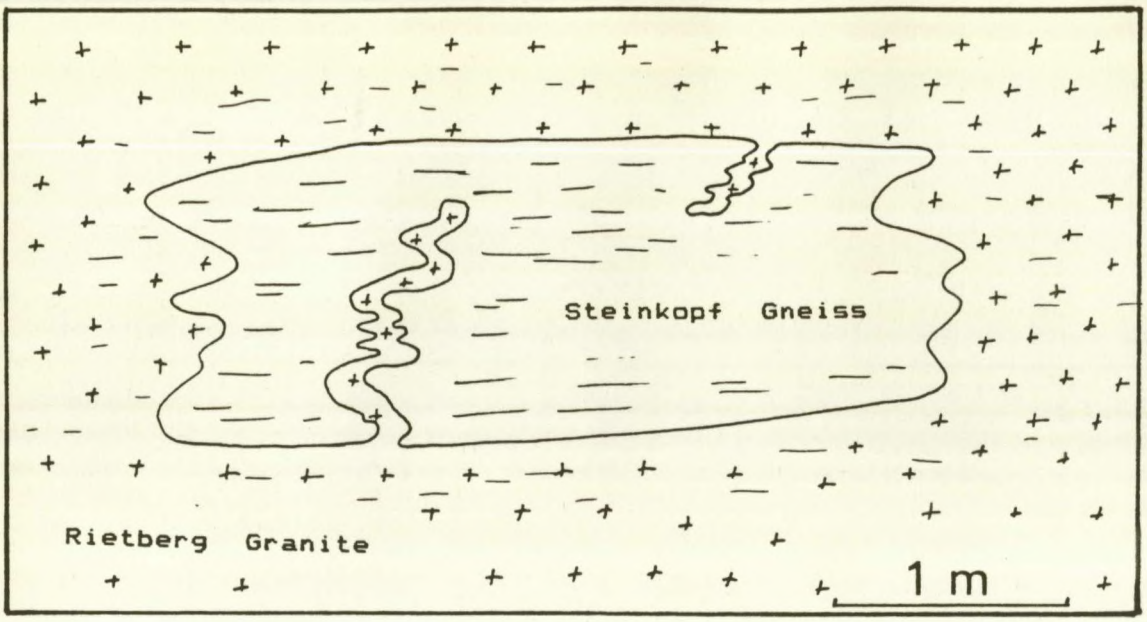

Figure 9.12 Field sketch demonstrating folded apophyses of Rietberg Granite in a Steinkopf Gneiss raft, west of Bulletrap.

Figure 9.13 Skelmfontein refoliation transects the contact between an orbicular dyke and Leeupoort augen gneiss (locality 10, Fig. 9.1).

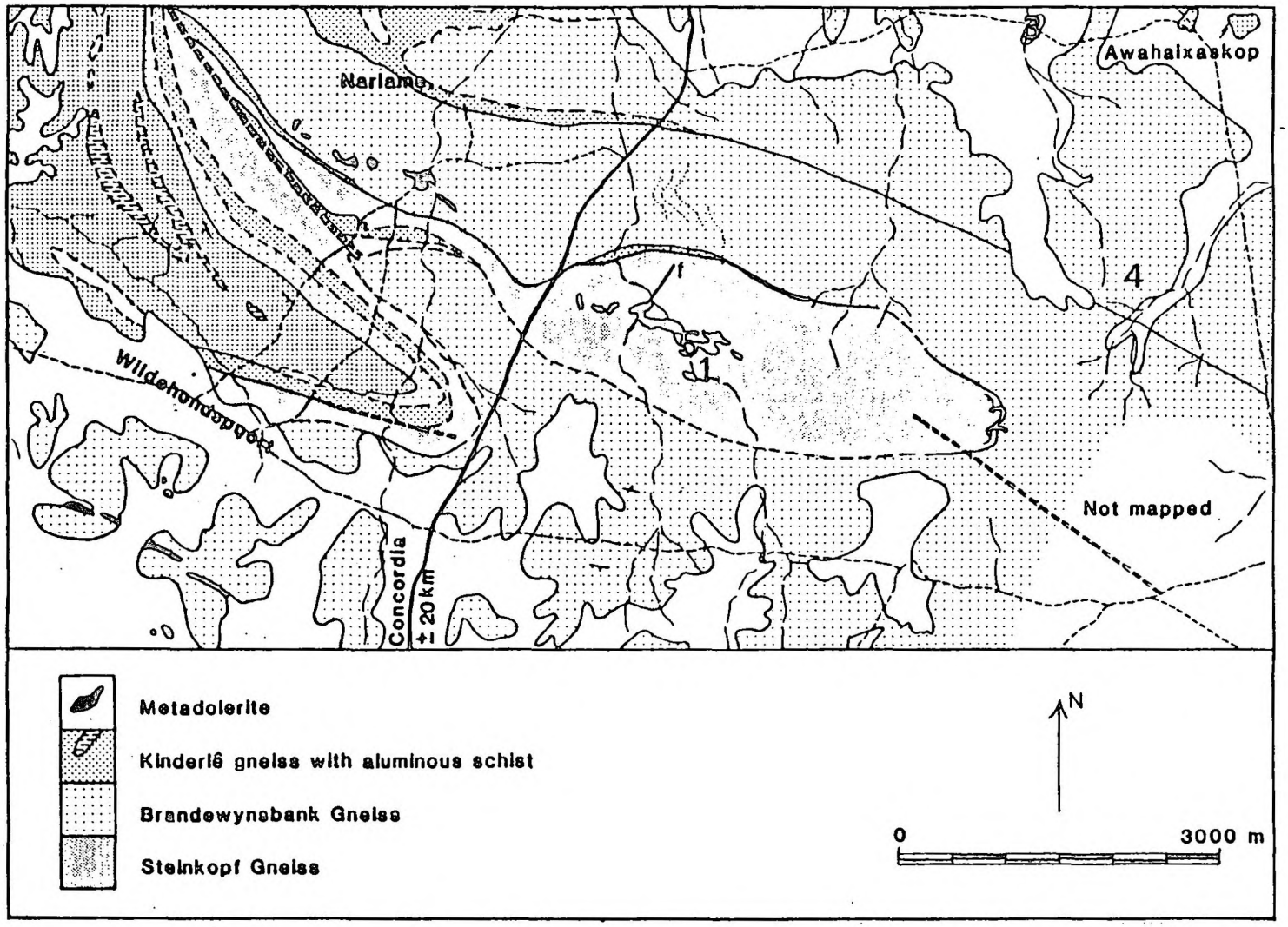

FIGURE 9.14 Map of the Nariams area showing the positions of some of the localities referred to in the text.The macroscopic folds are isoclinal and are interpreted to be Skelmfontein age structures. They occur within the enveloping surface which is folded around the Geselskapbank Synform to the east.

Figure 9.15 Coaxial interference structures resulting from the superimposition of Skelmfontein age refoliation on older fabrics (locality 1, Figure 9.14).

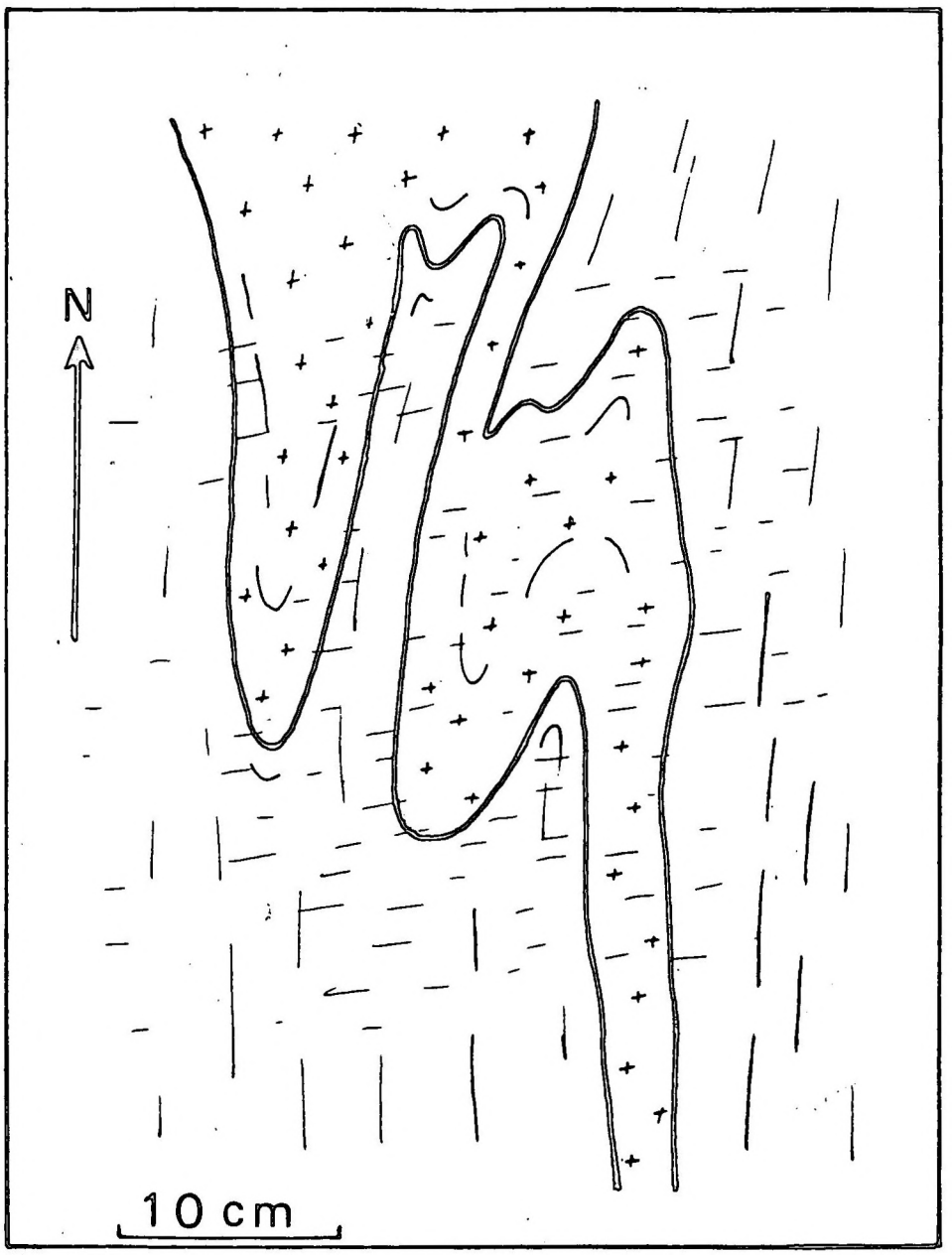

Figure 9.16 Sketch map showing minor Z-folding associated with an early refoliation at locality 2, Figure 9.14. The rock is Steinkopf Gneiss, with a leucosome band [+]. A weak easterly trending fabric, superimposed on the older refoliation, appears to be axial planar to the macrofold and is interpreted to be of Skelmfontein age.

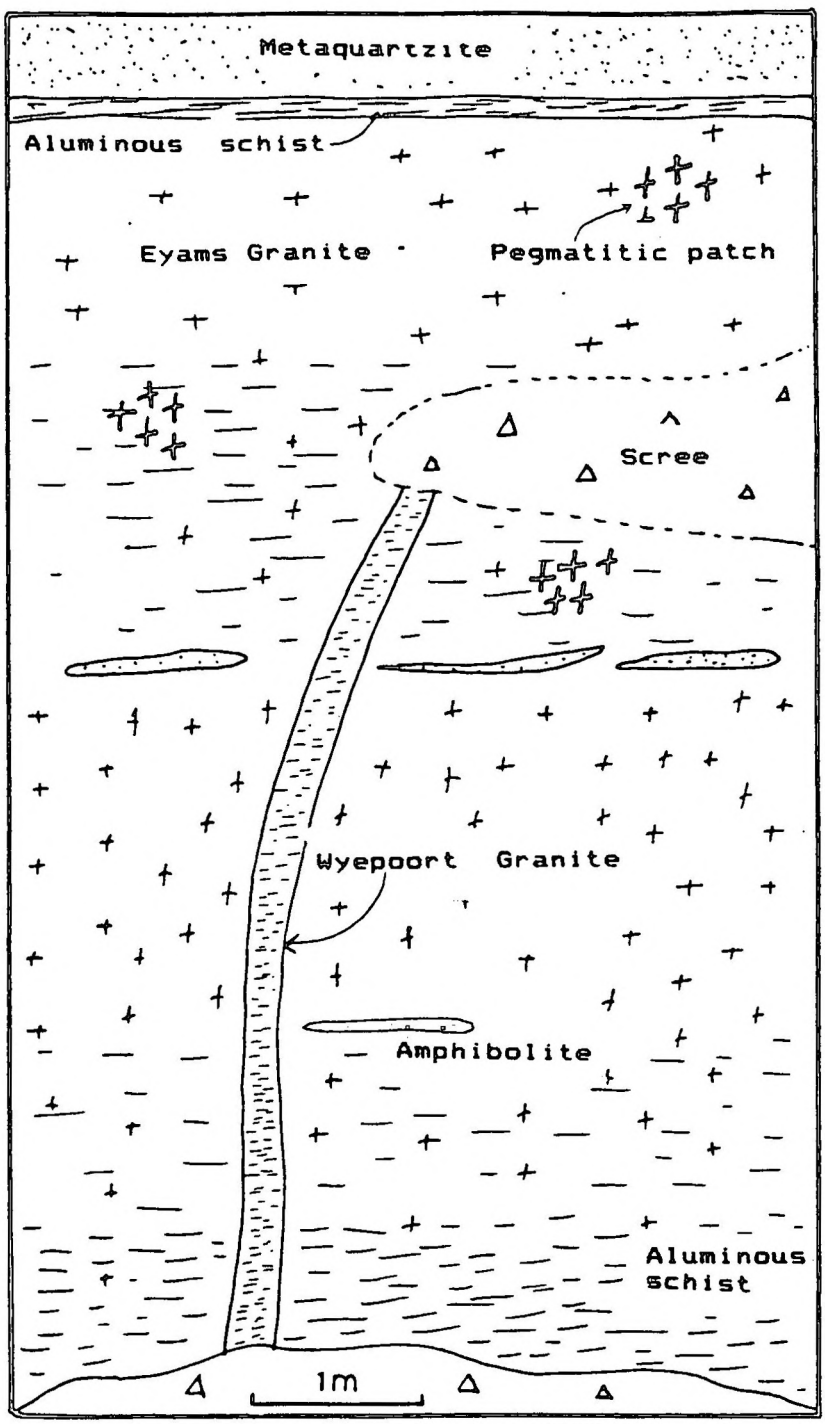

Figure 9.17 Contact - and structural relations in the Eenriet Mountains. The field sketch depict gradational contacts between migmatitic Eyams Granite (+) and aluminous schist (-). The Eyams Granite appears undeformed while a dyke of the younger Wyepoort Granite displays a pronounced foliation (Skelmfontein fabric).

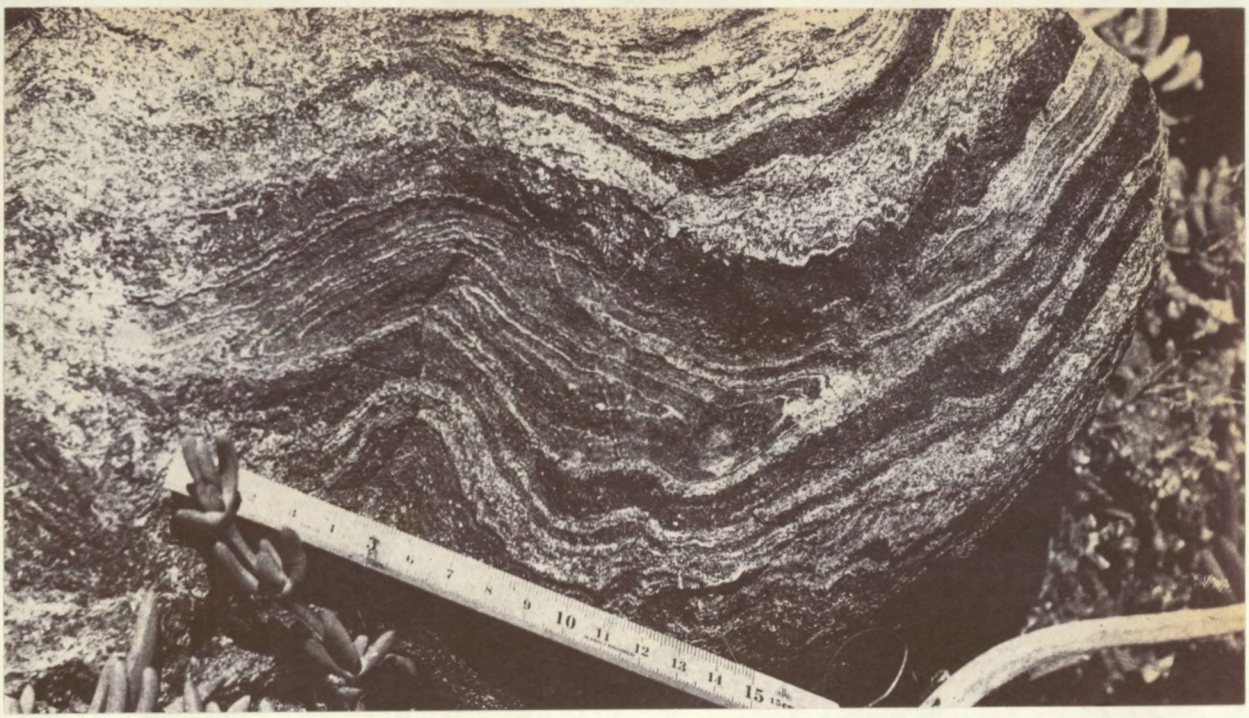

FIGURE 9.18 Folded domal structure possibly reflect three phases of folding in calc-silicate rock, east of Steinkopf.

FIGURE 9.19 A folded amphibolite rod in Brandewynsbank Gneiss, east of Steinkopf. Because the mafic rock has limited dip continuation, the outcrop ceases along strike where the topography changes.

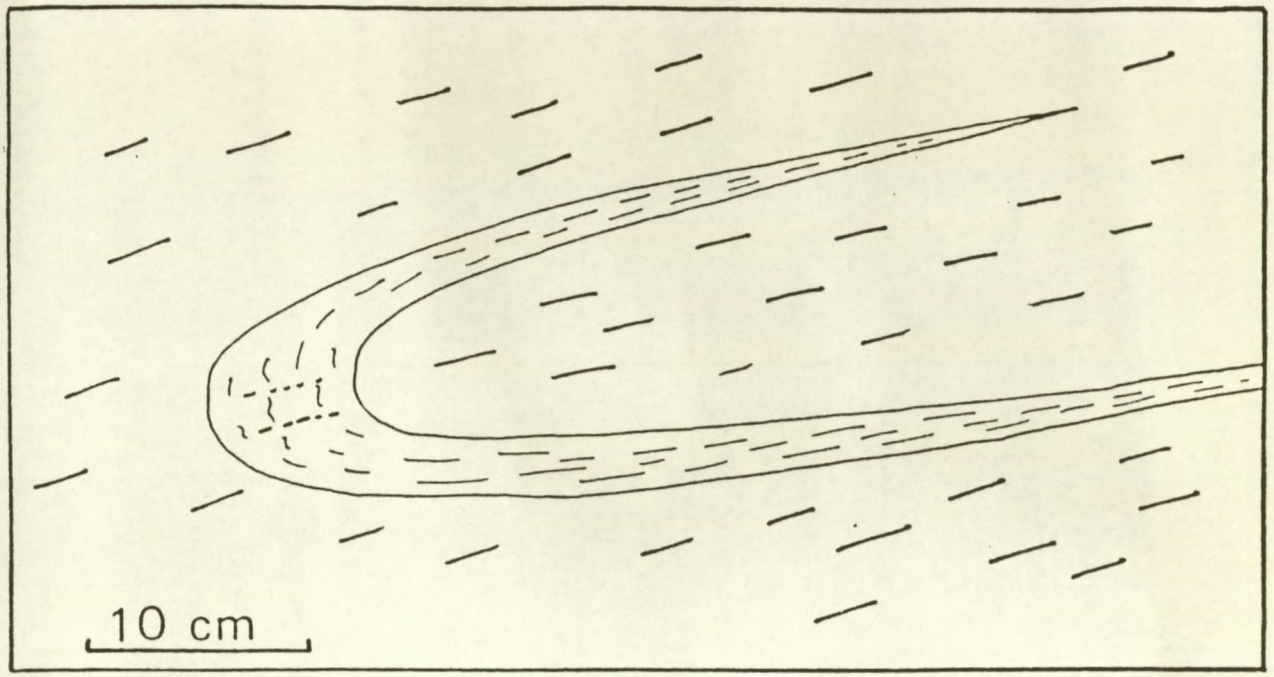

FIGURE 9.20 Field sketch of a small, folded Brandewynsbank Gneiss xenolith within Konkyp Gneiss (locality 11, Figure 9.1). The regional fabric of the Konkyp gneiss is axial planar to the small fold and superimposed on the older fabric of the Brandewynsbank Gneiss.

FIGURE 9.21 Tectonic fabric (which predates the Little Namaqualand Suite), preserved in a metasedimentary xenolith within Konkyp Gneiss (locality 12, Figure 9.1). Note the angular relation between the Namaqua fabric of the gneiss and the older foliation in the xenolith.

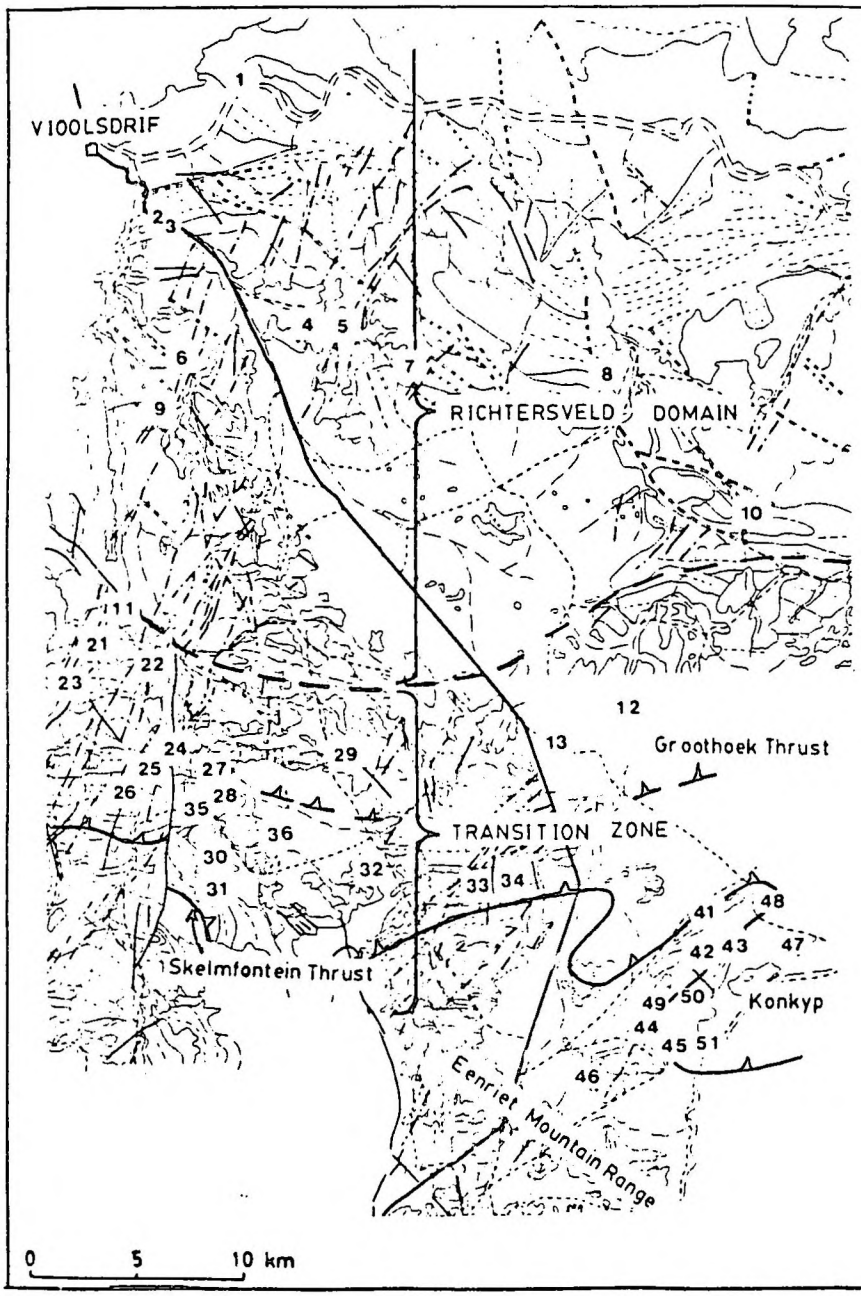

THE SAMPLES:

1	DRL040
2	SK057, 060
3	SK391 - 400
4	SK064
5	SK065
6	SK063
7	SK070
8	DRL099
9	SK061, 062
10	DRL140
11	SK071 - 073
12	SK055
13	SK040 - 043, SK045 - 049
21	SK075, 079, 090
22	SK017
23	SK082
24	SK140
25	SK001 - 003, SK084, 086, 089
26	SK007, 008
27	SK107
28	SK100 - 106, SK108, 111
29	SK138, 187
30	SK325, 326
31	
32	SK151, 154, 155 SK159, 160
33	SK145
34	SK141
35	SK115
36	SK133
41	S854H, 857A
42	S854
43	S782, 783
44	S787, 789, 826
45	S817, 822, 823, 796
46	S792
47	S839
48	S842, 843, 846, S848, 850, 852 SK518
49	S812, 810
50	S799, 800, 808, 899
51	S830, 832, 834, 835

FIGURE 10.1 Sample localities in the Richtersveld Domain and Transition Zone (Groothoek Thrust Zone and Konkyp area), described in Appendices 4.1 and 4.2.

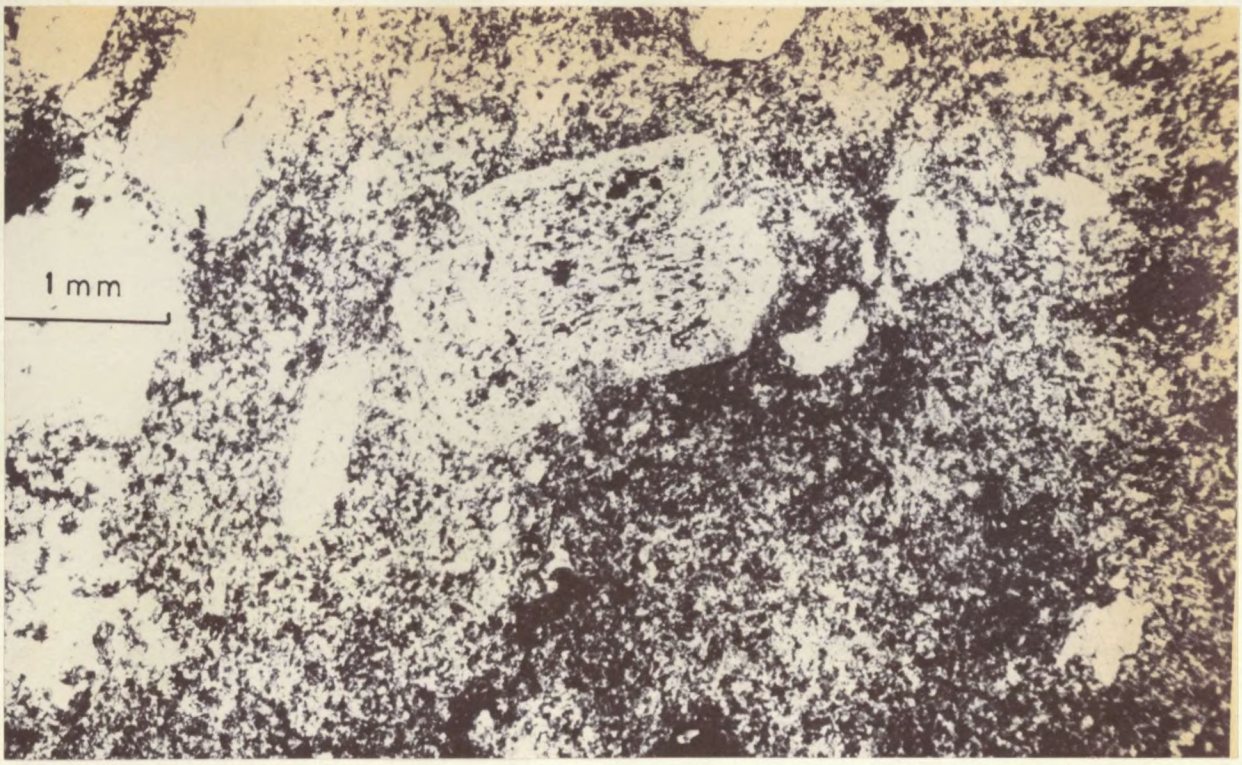

FIGURE 10.2 Photomicrograph of relict plagioclase phenocrysts in porphyritic meta-andesite (the Koubank River gorge).

FIGURE 10.3 Photomicrograph showing part of the thin section from specimen DRL099 examined by electron microprobe. The lines I and I indicate two probe traverses, each approx. 0.5 mm long, across an amphibole grain.

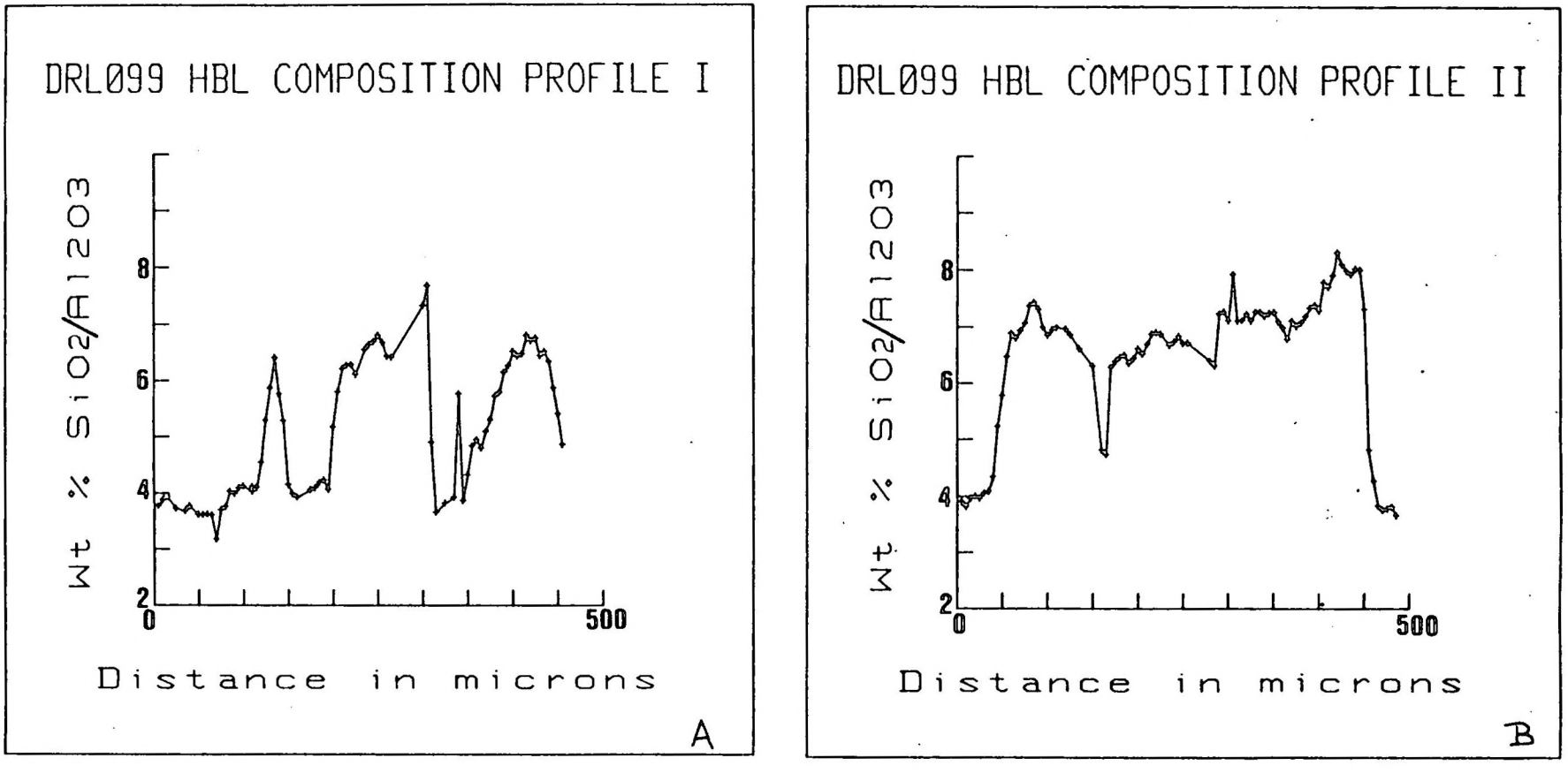

FIGURE 10.4 Compositional variation along two traverses across an amphibole grain in specimen DRL099 (see Figure 10.3).

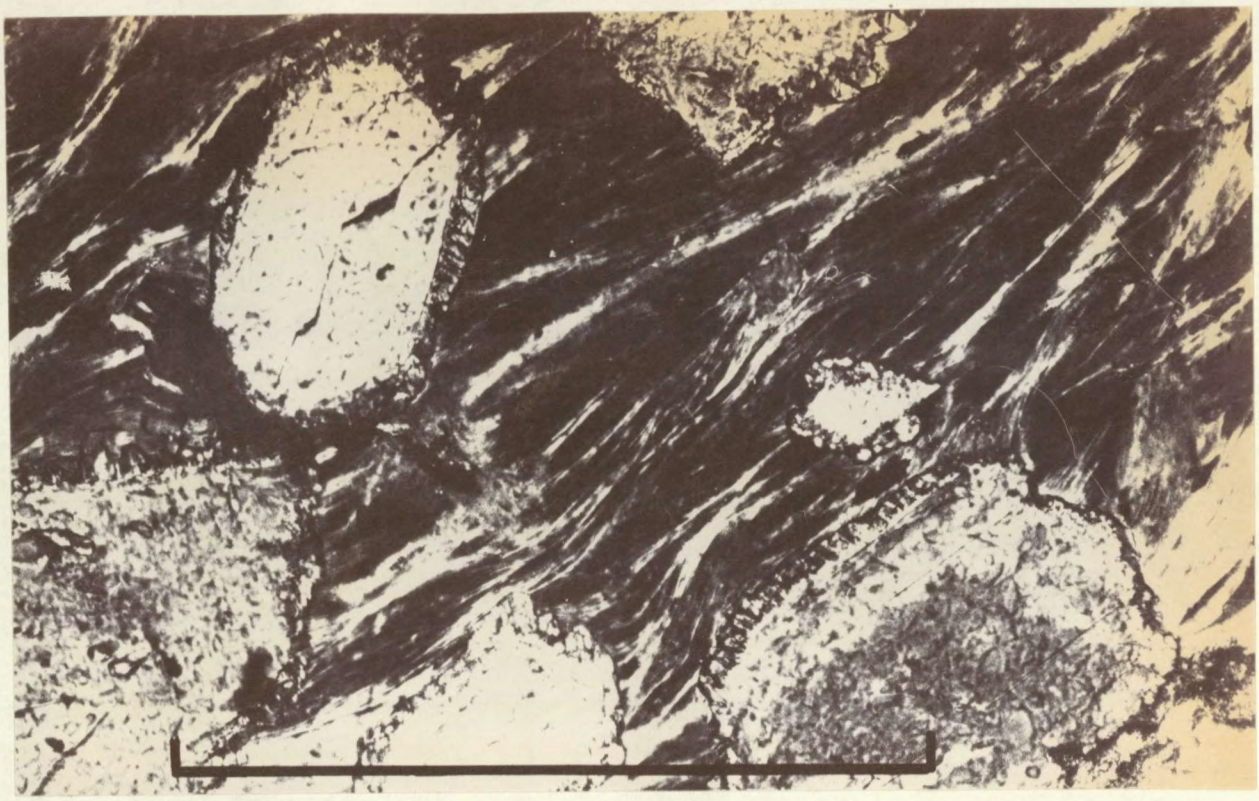

FIGURE 10.5 Actinolite porphyroblasts in a schistose metavolcanite from the core zone of the Richtersveld Domain. The scale bar is 4 mm long (from the Koubank River gorge).

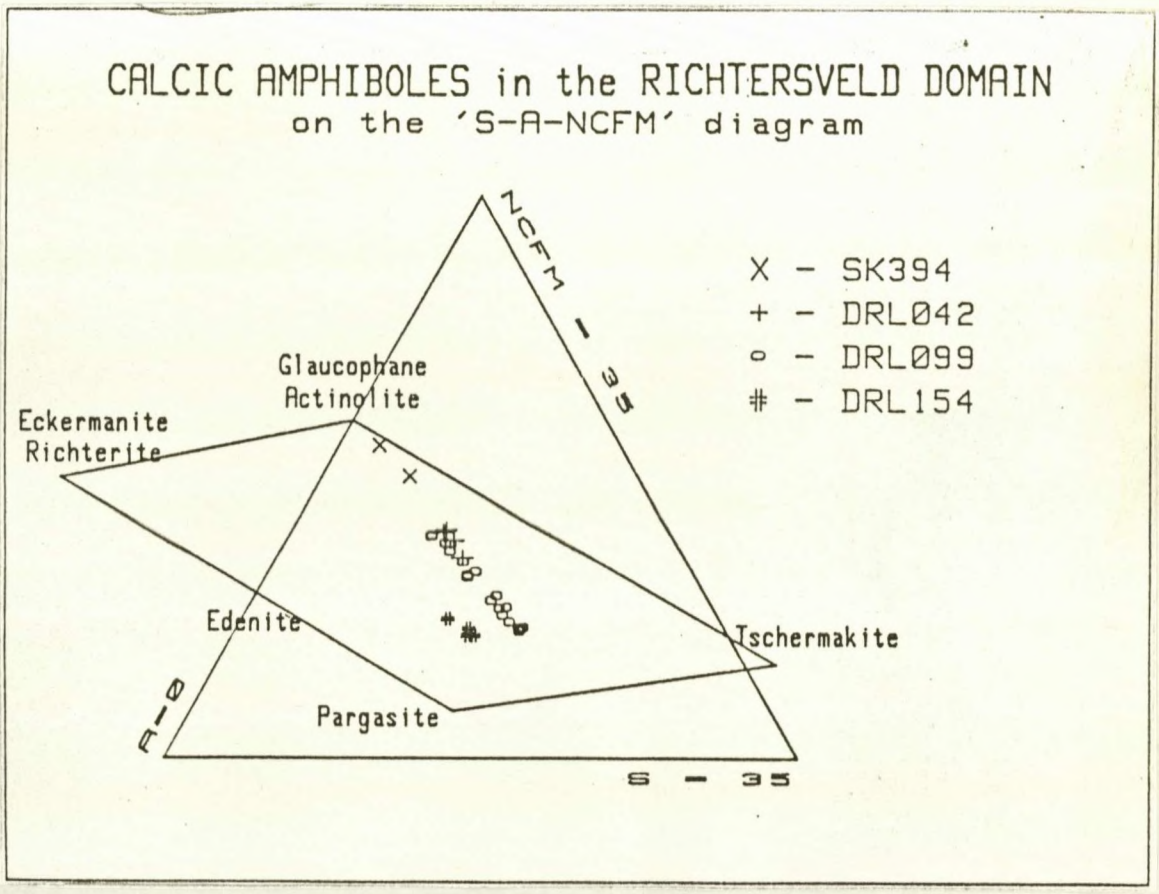

FIGURE 10.6 A graphical classification of calcic amphiboles (Robinson et al., 1982) from the Richtersveld Domain. Note the apparent miscibility gap between actinolite and hornblende and the wide range of compositions from in one grain (DRL099).

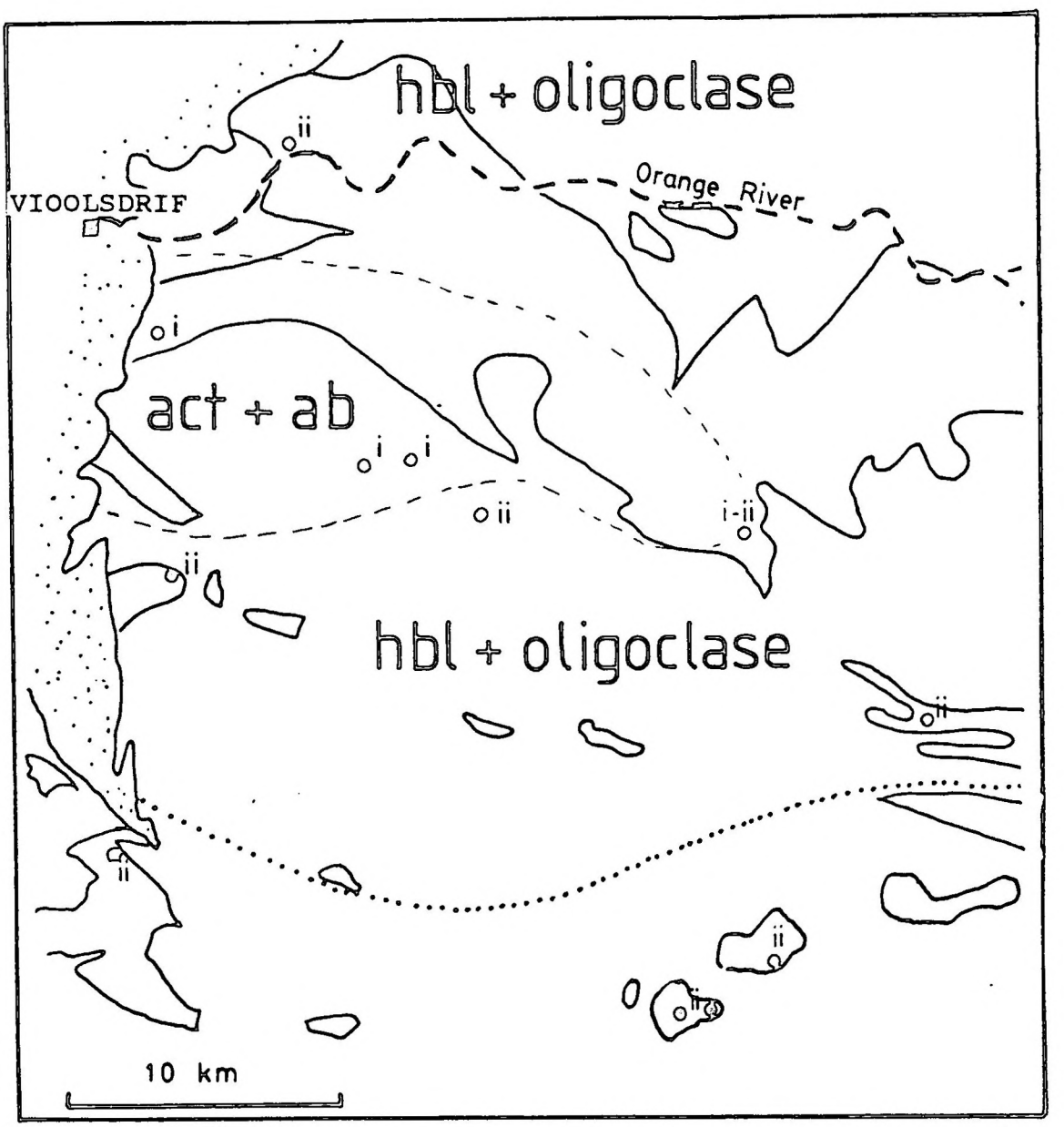

FIGURE 10.7 The mineralogical variation in metavolcanites in that part of the Richtersveld Domain covered by this study (prograde assemblages only). The symbols i and ii indicate assemblage types described in the text. The dotted line in the south depict the interpreted boundary with the Transition Zone.

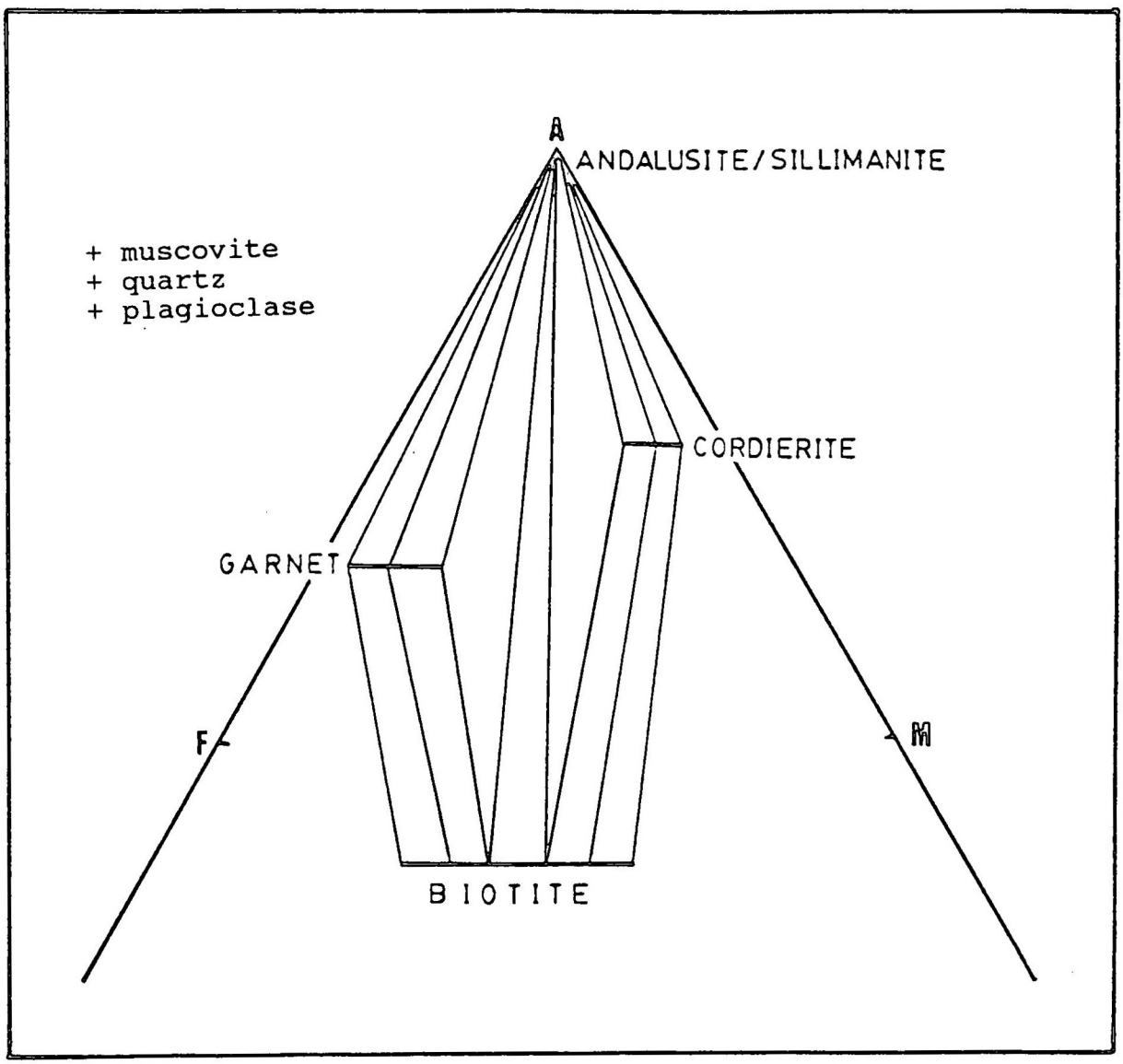

FIGURE 10.8 Schematic AFM diagram (Thompson, 1957) illustrating the stable parageneses in the Groothoek Thrust Zone.

FIGURE 10.9 Skeletal porphyroblasts of hornblende in granoblastic quartzofeldpathic neosome in Steinkopf Gneiss (Konkyp area).

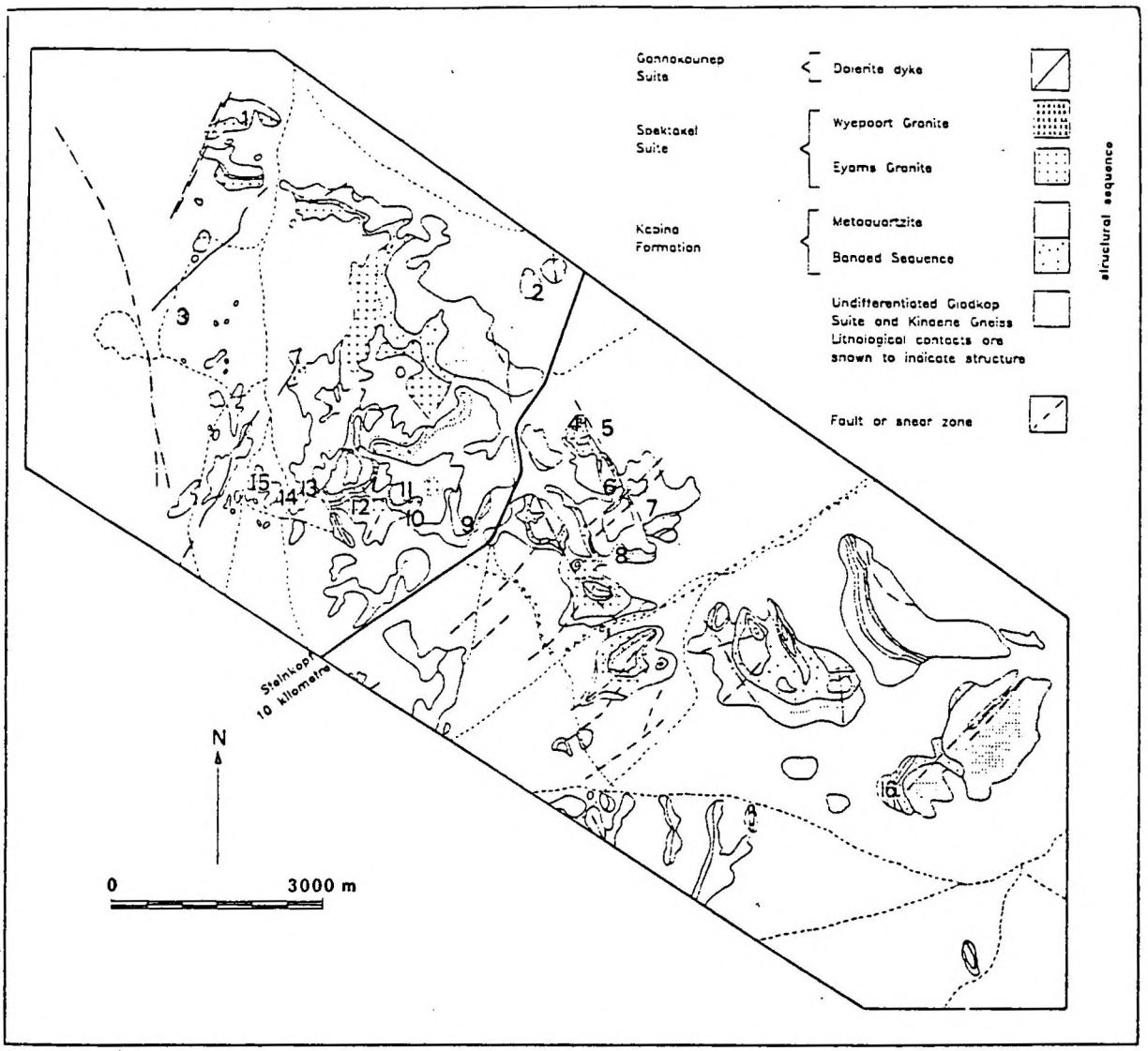

FIGURE 10.10 The distribution of rock samples from the Eenriet Mountains described in Appendix 4.4. The numbers in the figure correspond to sample numbers as follows: 1 - S767C, SK014; 2 - SK470; 3 - S682; 4 - S760, S761; 5 - SK387, SK295, SK296, SK297, SK300; 6 - S765, SK419; 7 - S290A, S290B, S290C; 8 - S283A; 9 - S689; 10 - S749, S751, S752, S753; 11 - S740; 12 - S736, S745; 13 - S756; 14 - S757; 15 - S680; 16 - S661, S662

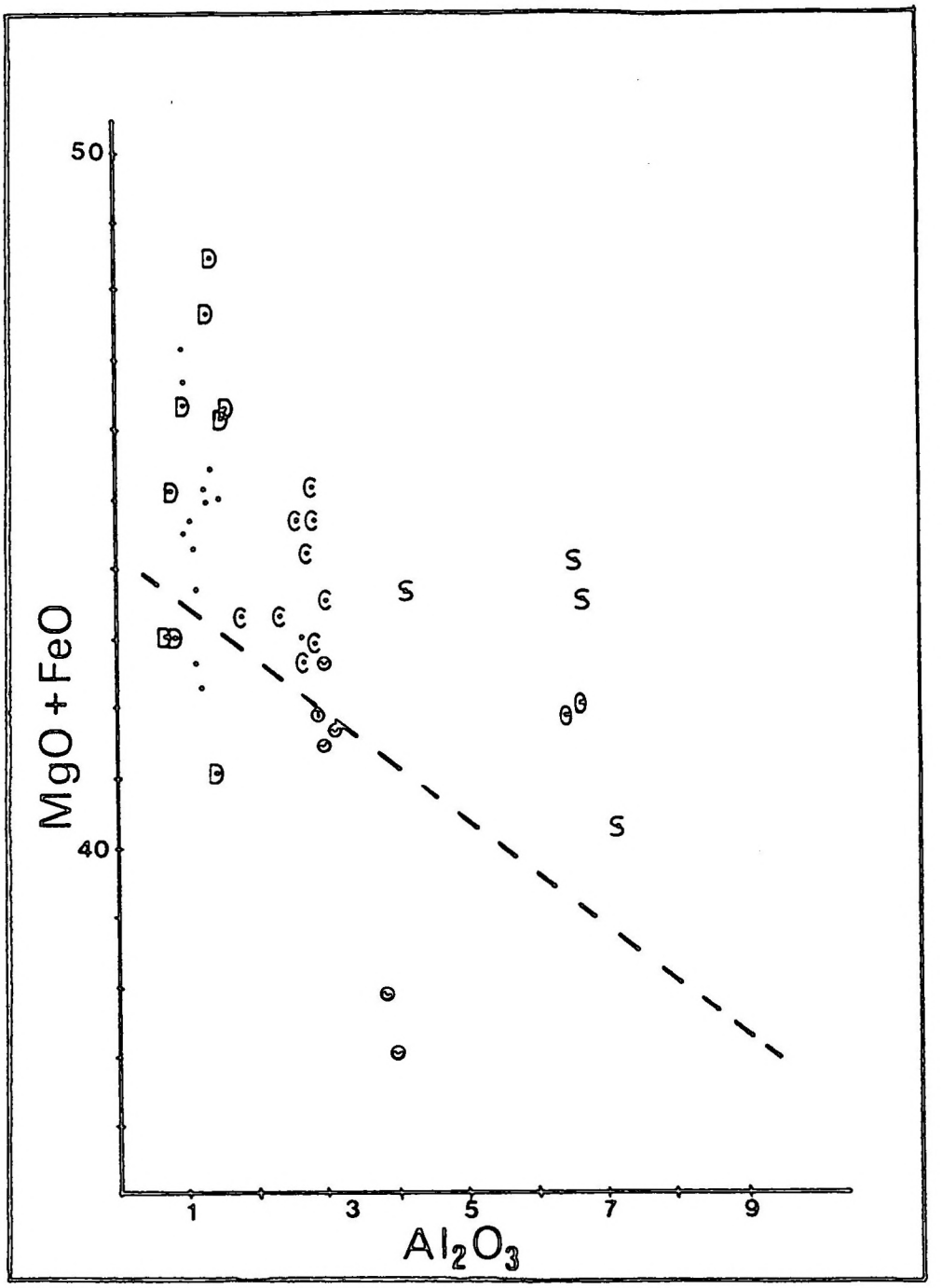

FIGURE 10.11 Classification of orthopyroxenes according to the scheme of Bhattacharyya (1971). In this application the Y-axis represent MgO + FeO without Fe2O3, because electron microprobe analyses yield all Fe as FeO. Metamorphic pyroxenes plot above the broken line and igneous ones below. Symbols: D - metadolerite; C - Koperberg Suite; S - metasedimentary rocks; and O - ultramafic metamorphites from the Eenriet Mountains and the Skelmfontein se Poort area respectively; • - two-pyroxene granulites.

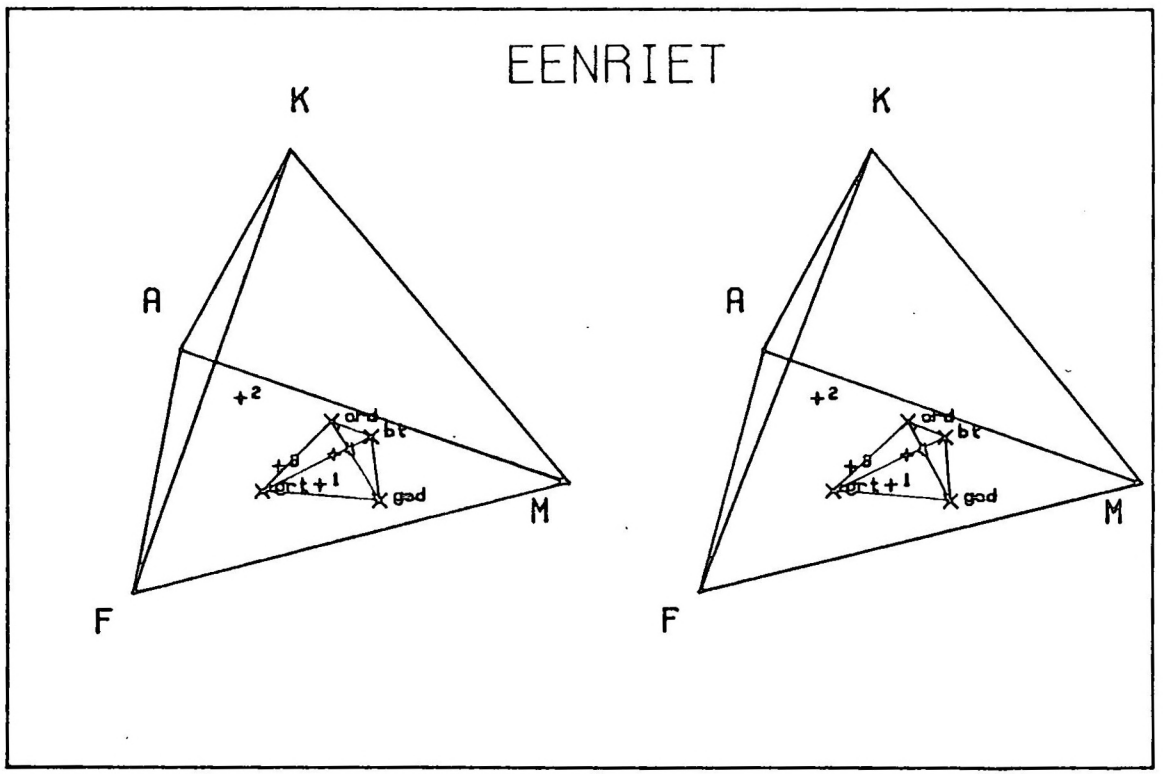

FIGURE 10.12 Whole rock compositions of metapelites from the Eenriet Mountains in the AFMK tetrahedron. The small reference- tetrahedron is defined by the compositions of biotite, garnet, cordierite and gedrite from specimen SK387. The numbers refer to different specimens: 1 - SK387; 2 - S747; 3 - S752; 4 - S290C.

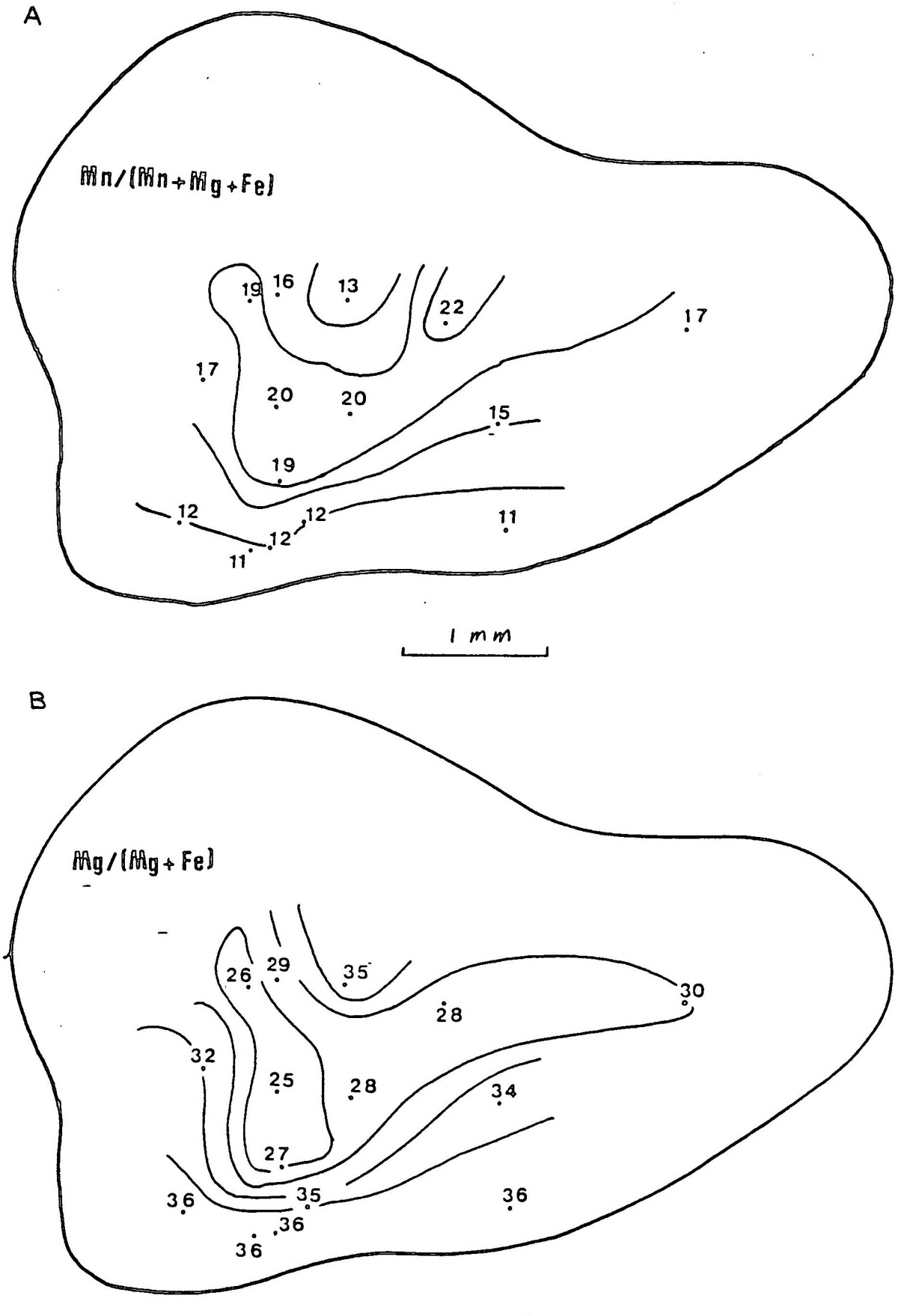

FIGURE 10.13 Compositional zoning in garnet from the Eenriet Mountains (specimen S296).

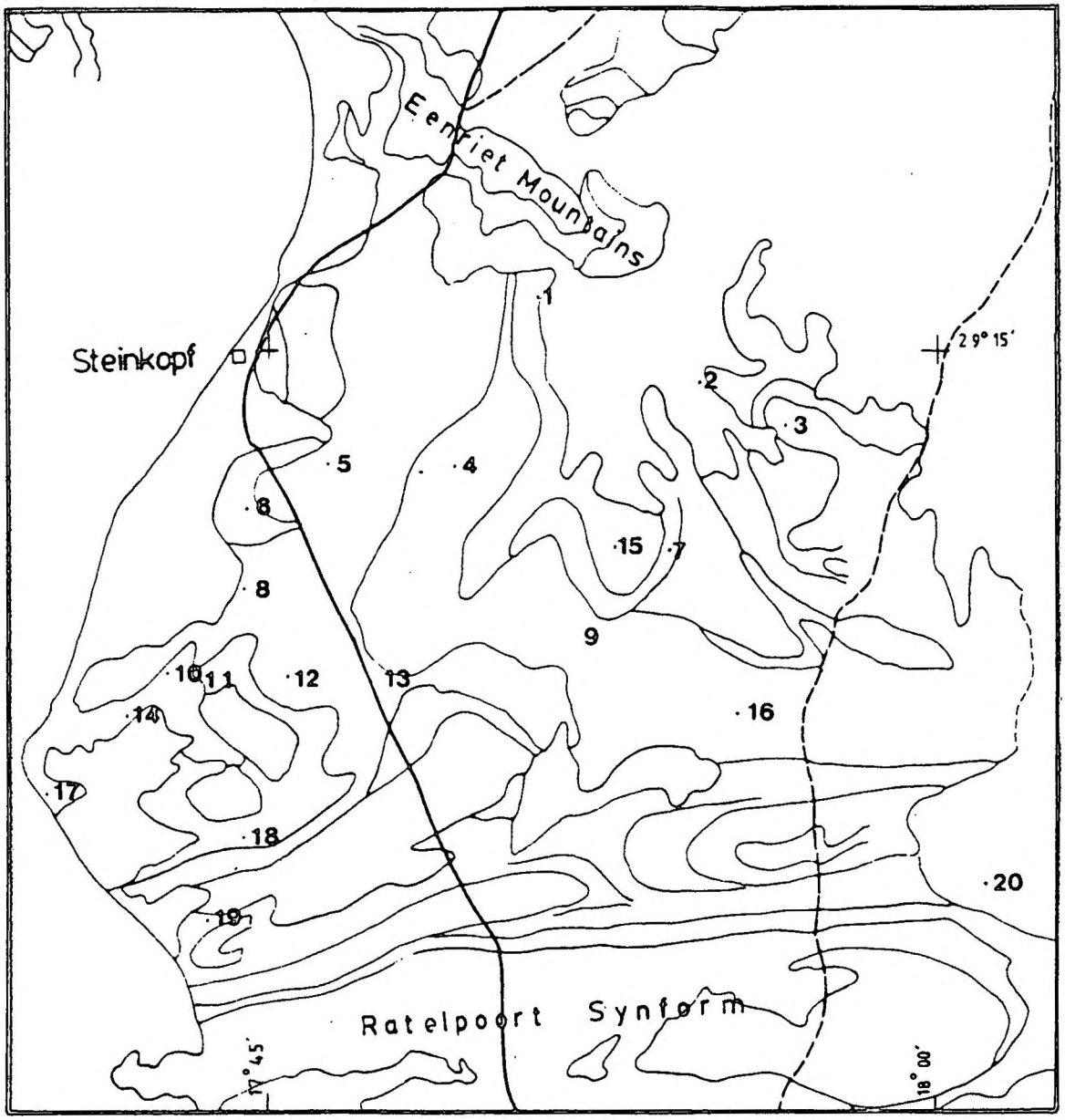

FIGURE 10.14a The distribution of samples of calc-silicate rock, from the Steinkopf Domain, described in Appendix 4.5.1. The numbers in the figure correspond to the sample numbers as follows: 1 - S671; 2 - S946; 3 - S897; 4 - S618A; 5 - SK167B; 6 - S538; 7 - S721; 8 - S521; 9 - S723; 10 - S458, S460; 11 - S452; 12 - 6513; 13 - S570, S571; 14 - S465; 15 - S709; 16 - S006; 17 - S437; 18 - S421, S422; 19 - S404; 20 - SK208, SK284.

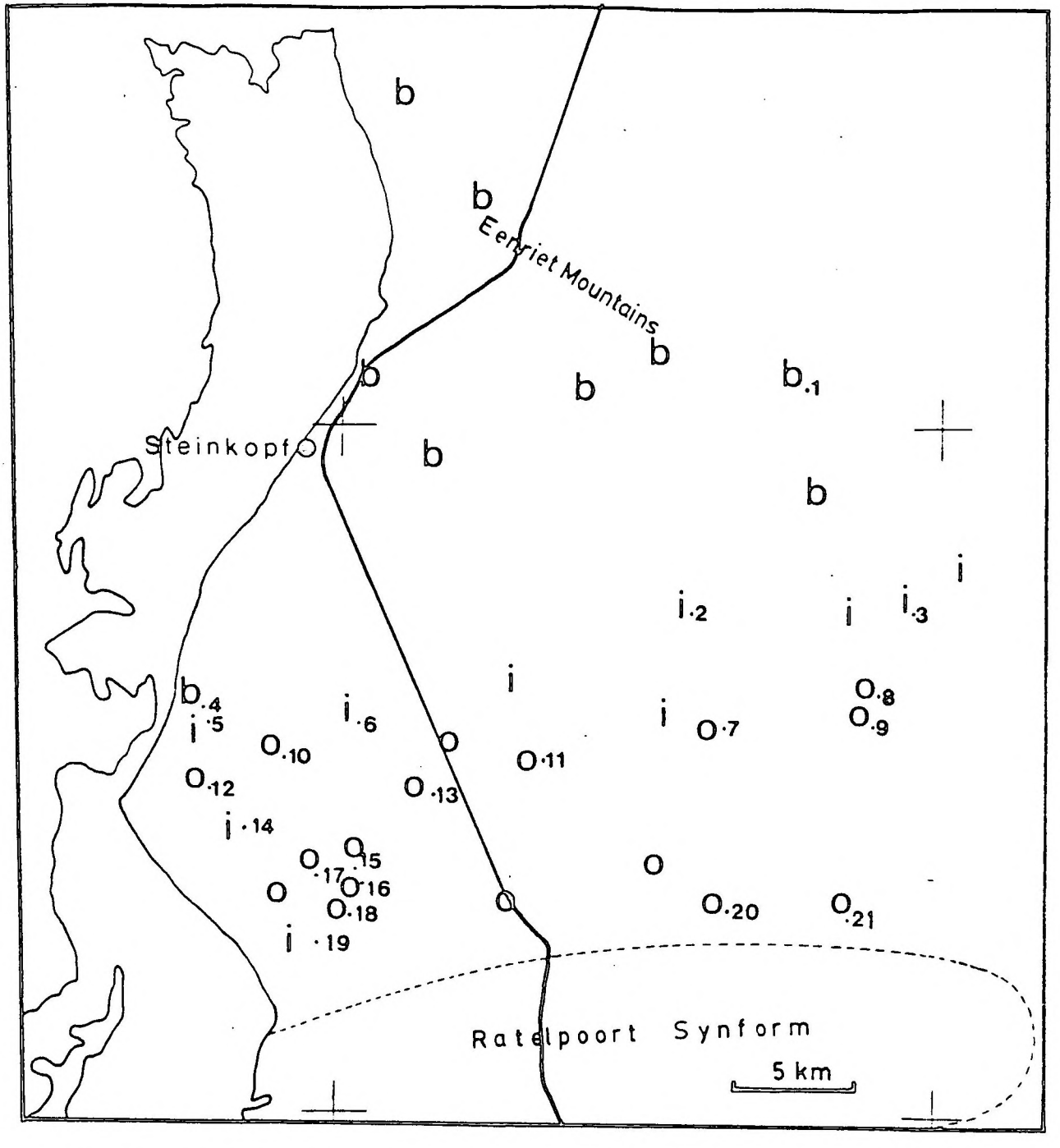

FIGURE 10.14b The distribution of samples of amphibolite, from the Steinkopf Domain, described in Appendix 4.5.2. The numbers in the figure correspond to the sample numbers as follows: 1 - S672; 2 - S722; 3 - S125; 4 - S456; 5 - S453; 6 - S507; 7 - S268; 8 - S093; 9 - S036; 10 - S496; 11 - SK240; 12 - S464; 13 - S731; 14 - S432; 15 - S396; 16 - S401; 17 - S420; 18 - S388; 19 - S415, S418; 20 - S281; 21 - S278D. The symbols b, o and i represent the colour of the hornblende as seen in thin section (b = blue-green, i = intermediate and o = olive-green). Where these hornblende colour symbols are not associated with one of the listed sample numbers, the specimen was examined under the microscope, but the description was not added to Appendix 4.5.2.

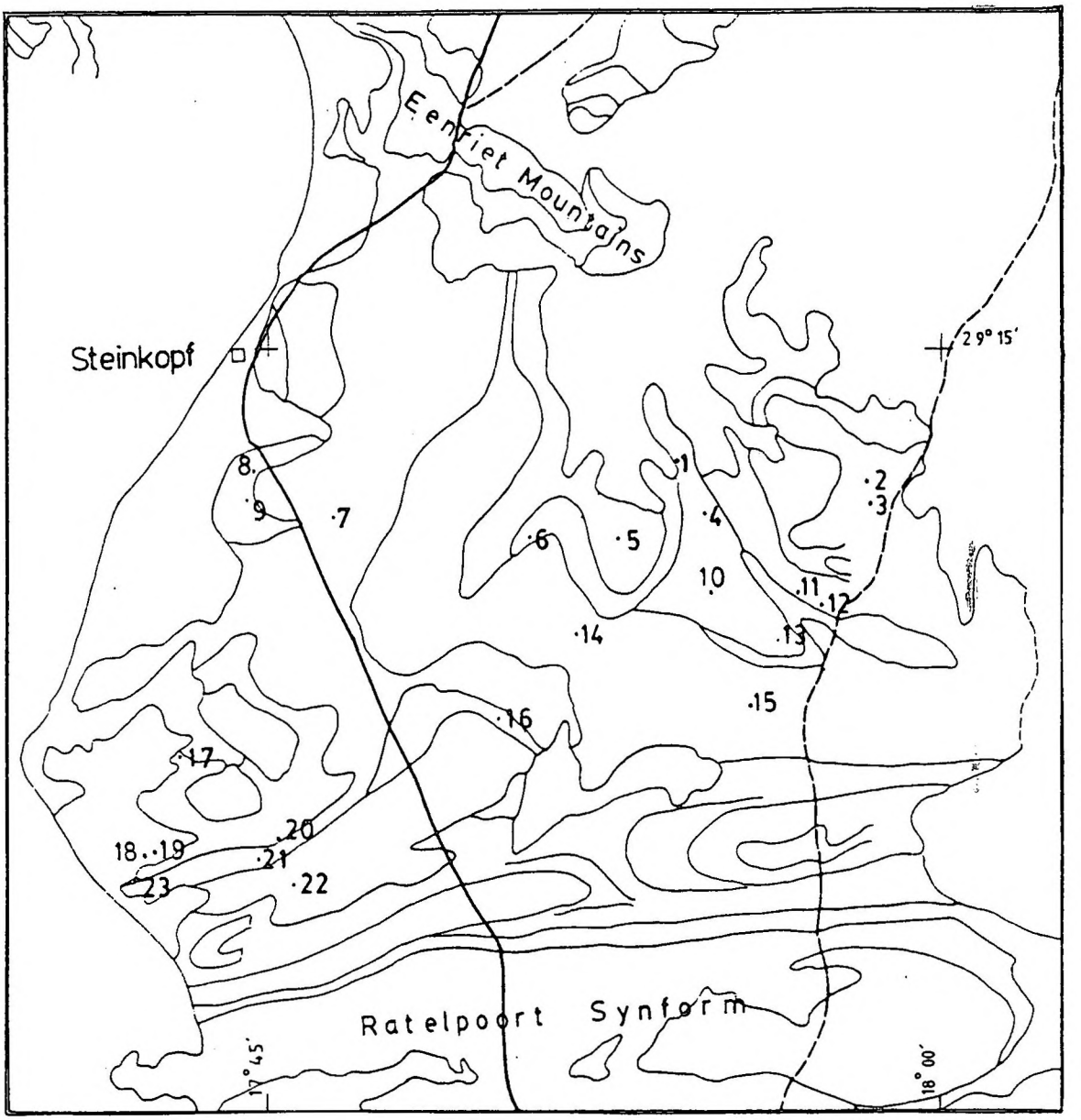

FIGURE 10.14c The distribution of samples of metapelite, metadolerite and the Middelplaat dykes, from the Steinkopf Domain, described in Appendices 4.5.3, 4.5.4 and 4.5.5 respectively. The numbers in the figure correspond to the sample numbers as follows: 1 - S713; 2 - S261B, S261L; 3 - SK360; 4 - S023C, S023D; 5 - S705; 6 - S693, S694; 7 - S579A, S579B; 8 - S525; 9 - S522; 10 - SK260D, SK260H, SK344; 11 - SK249, SK251, SK252; 12 - SK245, SK246; 13 - S146; 14 - SK337, SK338, SK339; 15 - S005B; 16 - SK243; 17 - SK413; 18 - S276; 19 - SK216, SK219; 20 - SK401, SK403, SK212; 21 - S420; 22 - S397.

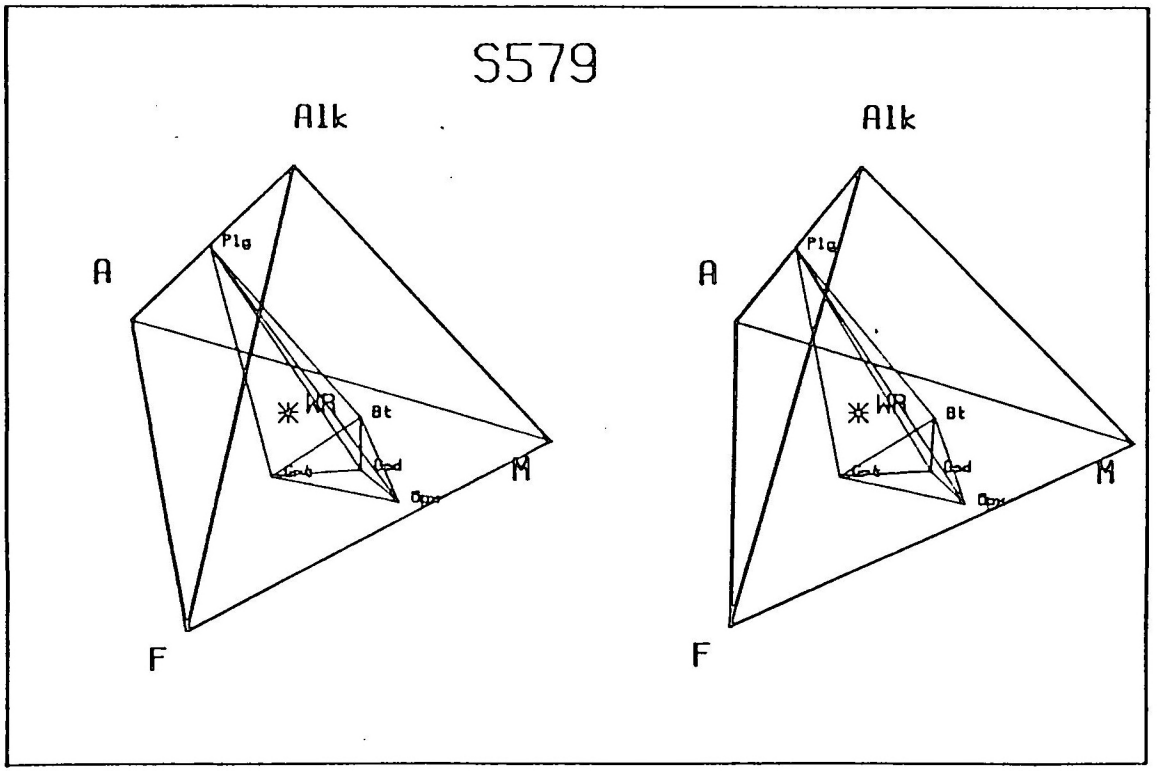

FIGURE 10.15 The mineral and whole rock compositions of the Dabbiknik pelitic granulite, projected into the AFM-Alk tetrahedron (AFM as in Thompson, 1957; Alk = molecular ratios of K2O + Na2O + CaO).

FIGURE 10.16a Relict igneous texture in metadolerite from the Nariams area. The pyroxenes are largely replaced by hornblende.

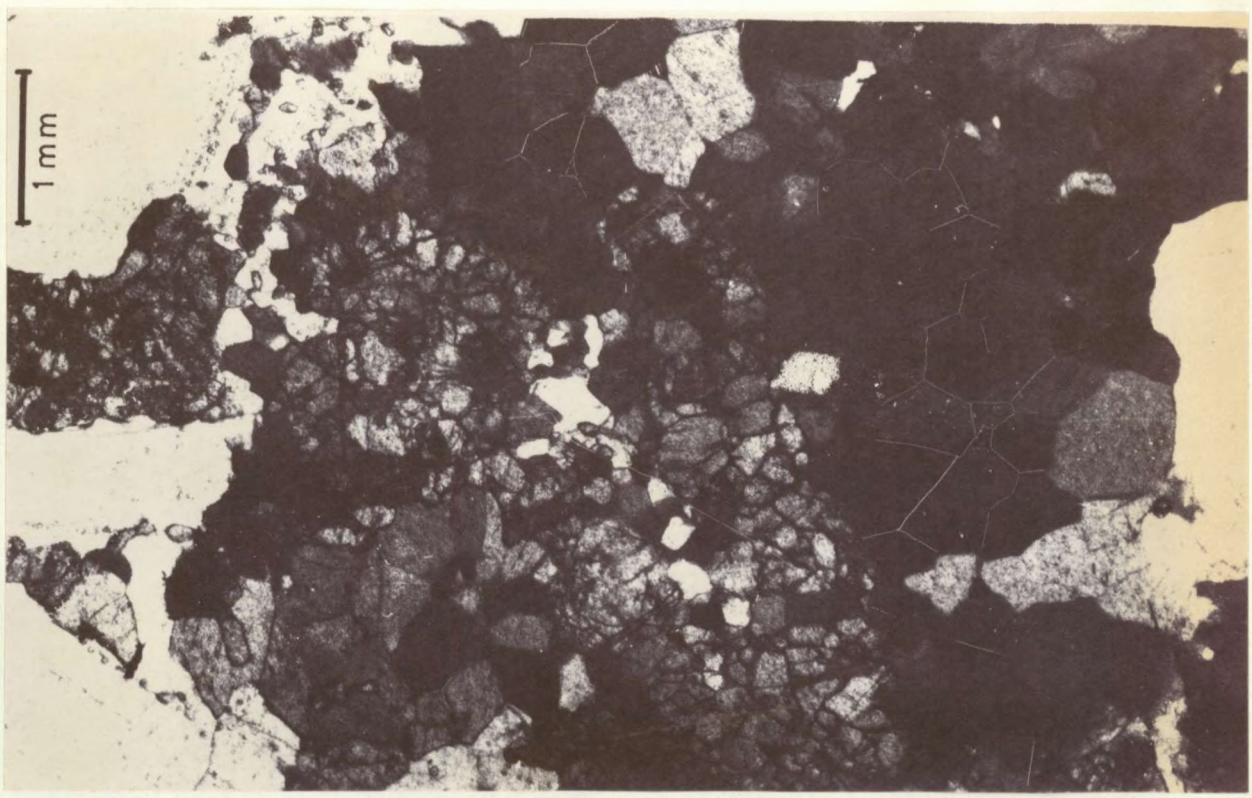

FIGURE 10.16b Granoblastic polygonal aggregates of pyroxene have replaced the original igneous pyroxene in metadolerite from the area south of Wildehondspoort. Note the larger (dark) hornblende grains with triple junctions (emphasized in some cases). Small diopside chadacrysts in the plagioclase increase in size and abundance toward the plagioclase crystal boundaries.

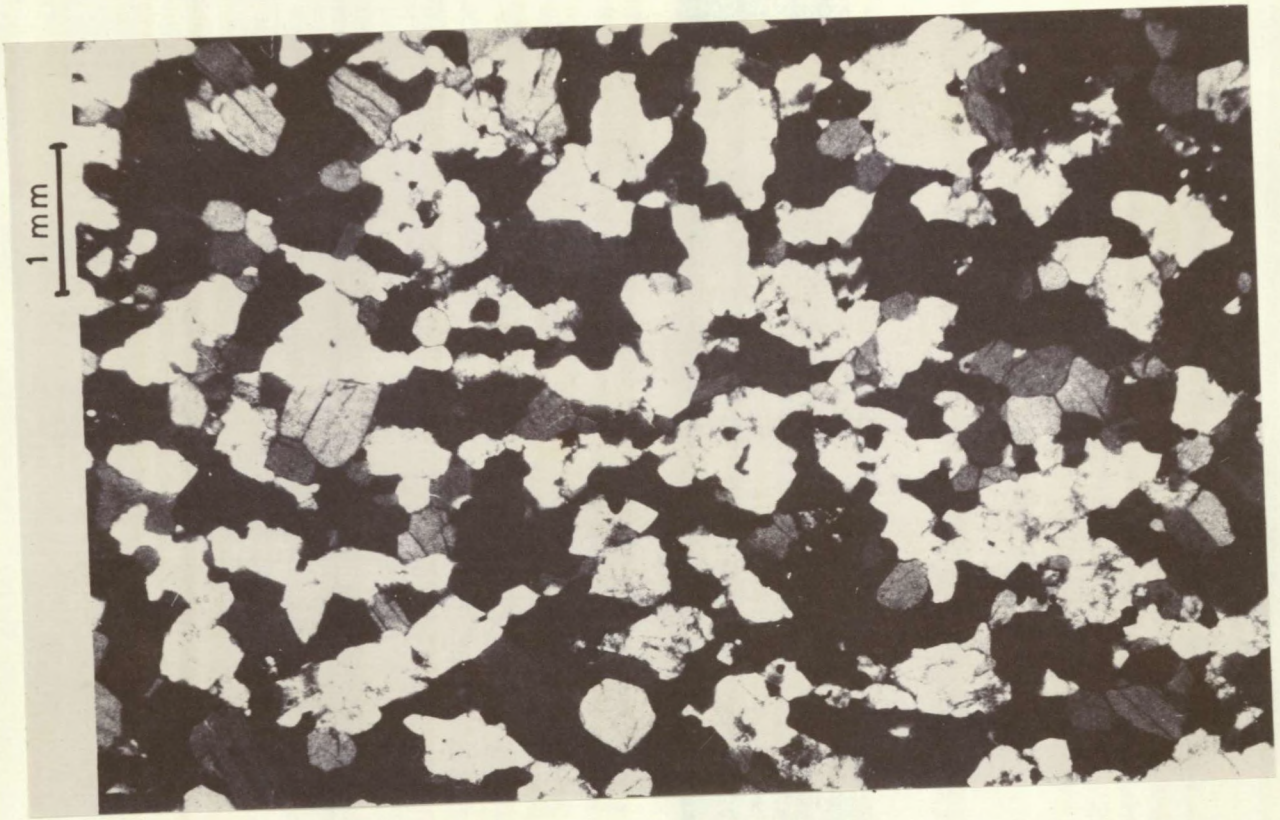

FIGURE 10.16c Photomicrograph showing the texture of fine-granoblastic amphibolite, the ultimate product of the amphibolitization of the Nariams metadolerite.

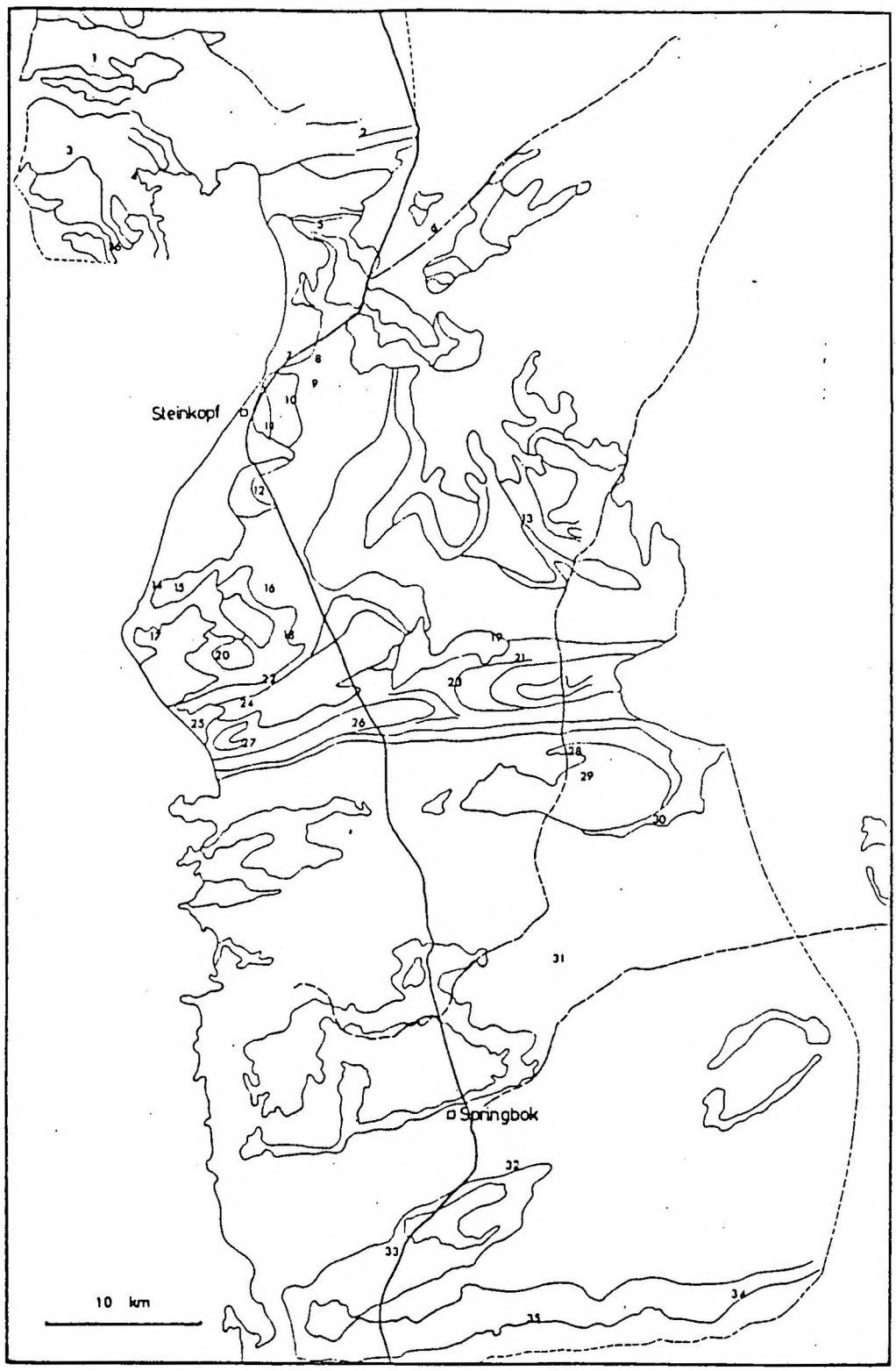

FIGURE 10.17 The distribution of samples used for the grey gneiss biotite study. The the numbers correspond to the samples listed in Appendix 6 as follows: 1 - S1479; 2 - S242C; 3 - S1408A; 4 - S1414; 5 - SK015; 6 - S780B, S776E, S776B; 7 - S765J; 8 - S641B; 9 - S645B; 10 - S601; 11 - S605B, S505E, S605, S595B; 12 - S553; 13 - S024A; 14 - S451, S452; 15 - S552C; 16 - S515, S505; 17 - S469D; 18 - S500; 19 - S010; 20 - S426; 21 - S014A, S014; 22 - S398, S399B, S518C; 23 - S982B, S982; 24 - S416, S470A, S415; 25 - S405; 26 - S237C; 27 - S373C; 28 - S226; 29 - S209A, S217; 30 - SK020; 31 - SK185; 32 - S180; 33 - SK194, SK193; 34 - SK254; 35 - S188; 36 - S1424

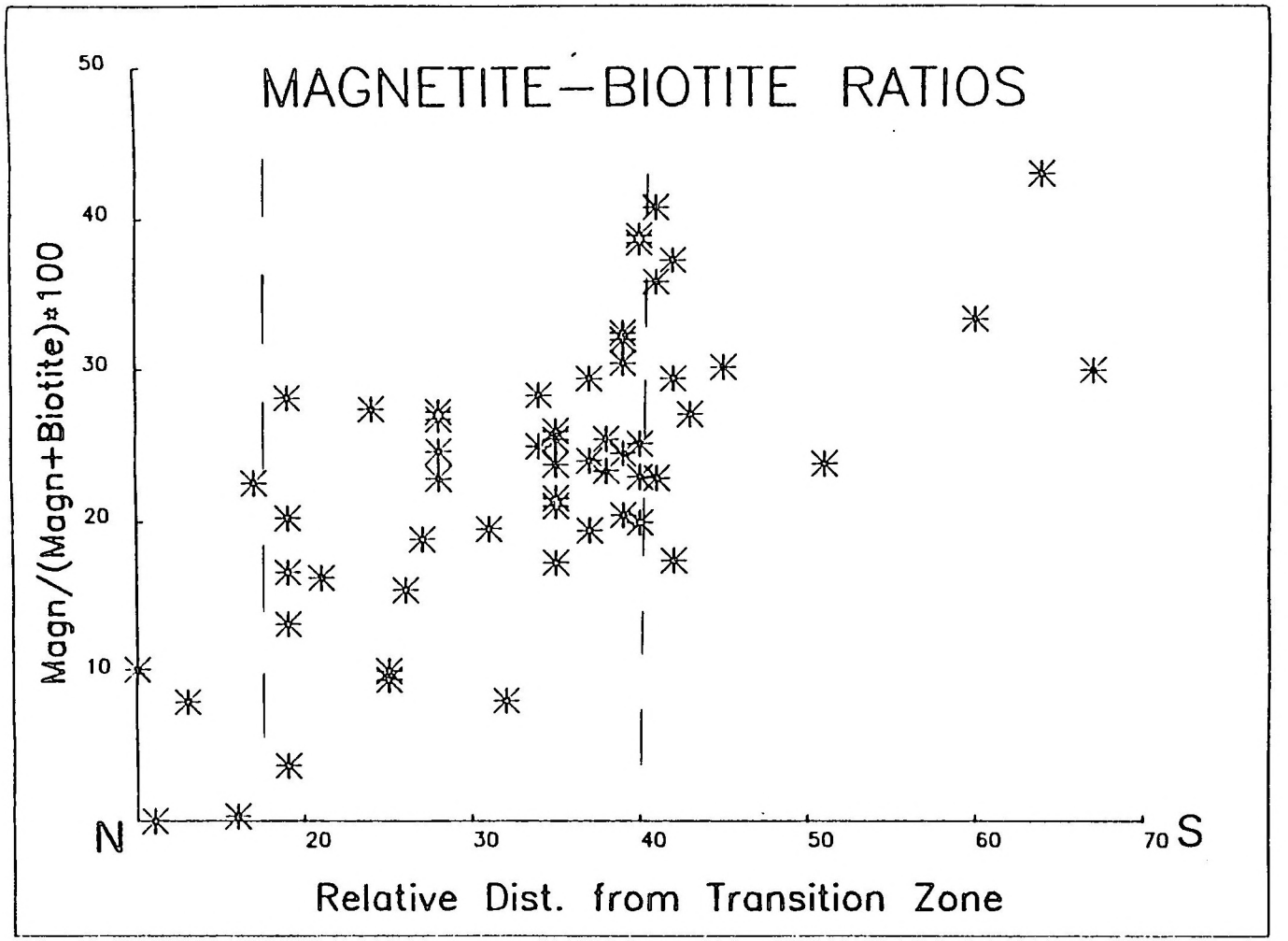

FIGURE 10.18a The variation of the magnetite:biotite ratio with distance from the Transition Zone in grey gneiss samples from the study area. Each unit of distance represents 1.25 km.

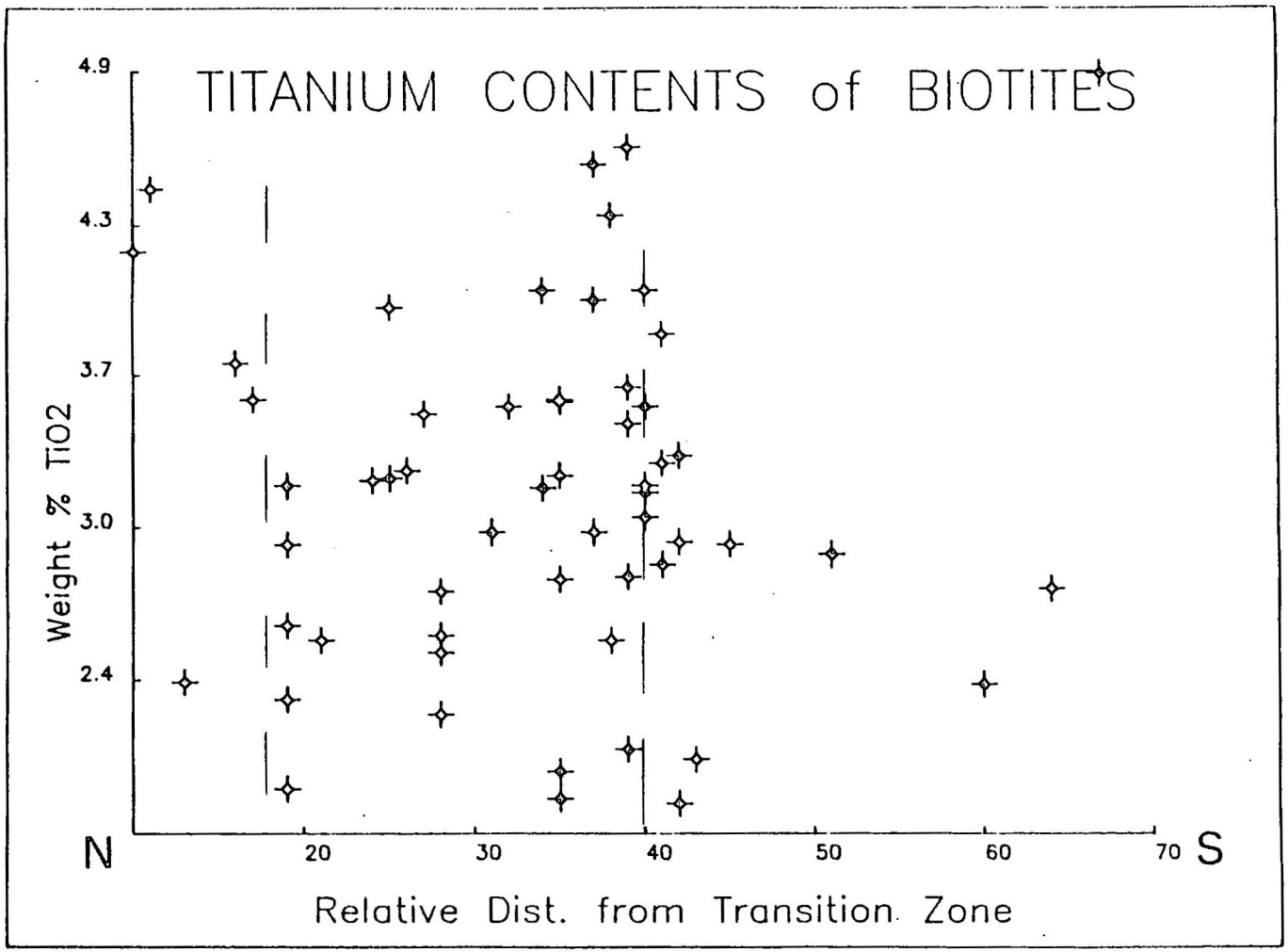

FIGURE 10.18b The variation of the titanium contents of biotite with distance from the Transition Zone, for grey gneiss samples from the study area (distance scale same as for Figure 10.18a).

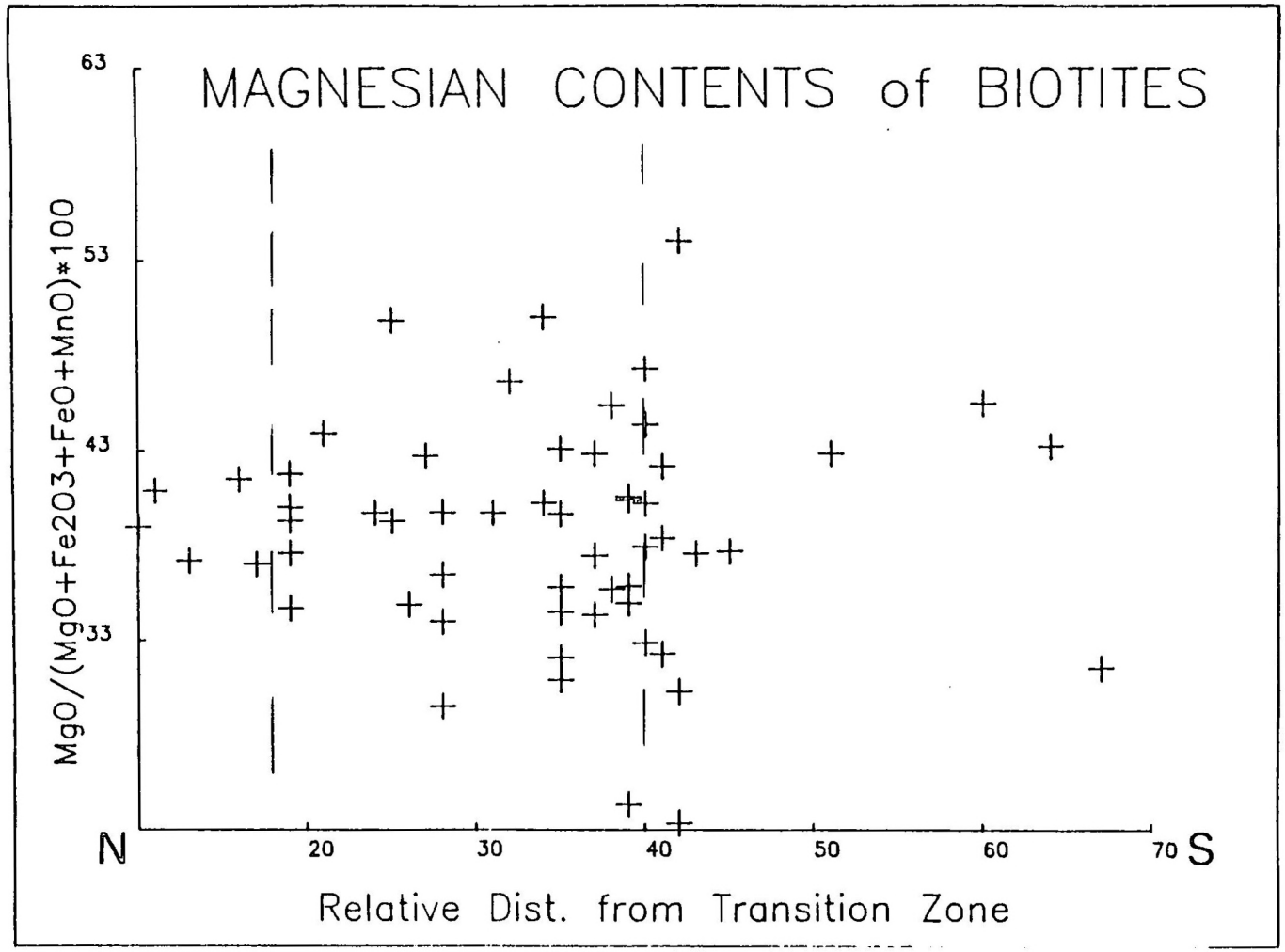

FIGURE 10.18c The variation of the magnesian contents of biotites with distance from the Transition Zone, for grey gneiss samples from the study area (distance scale same as for Figure 10.18a).

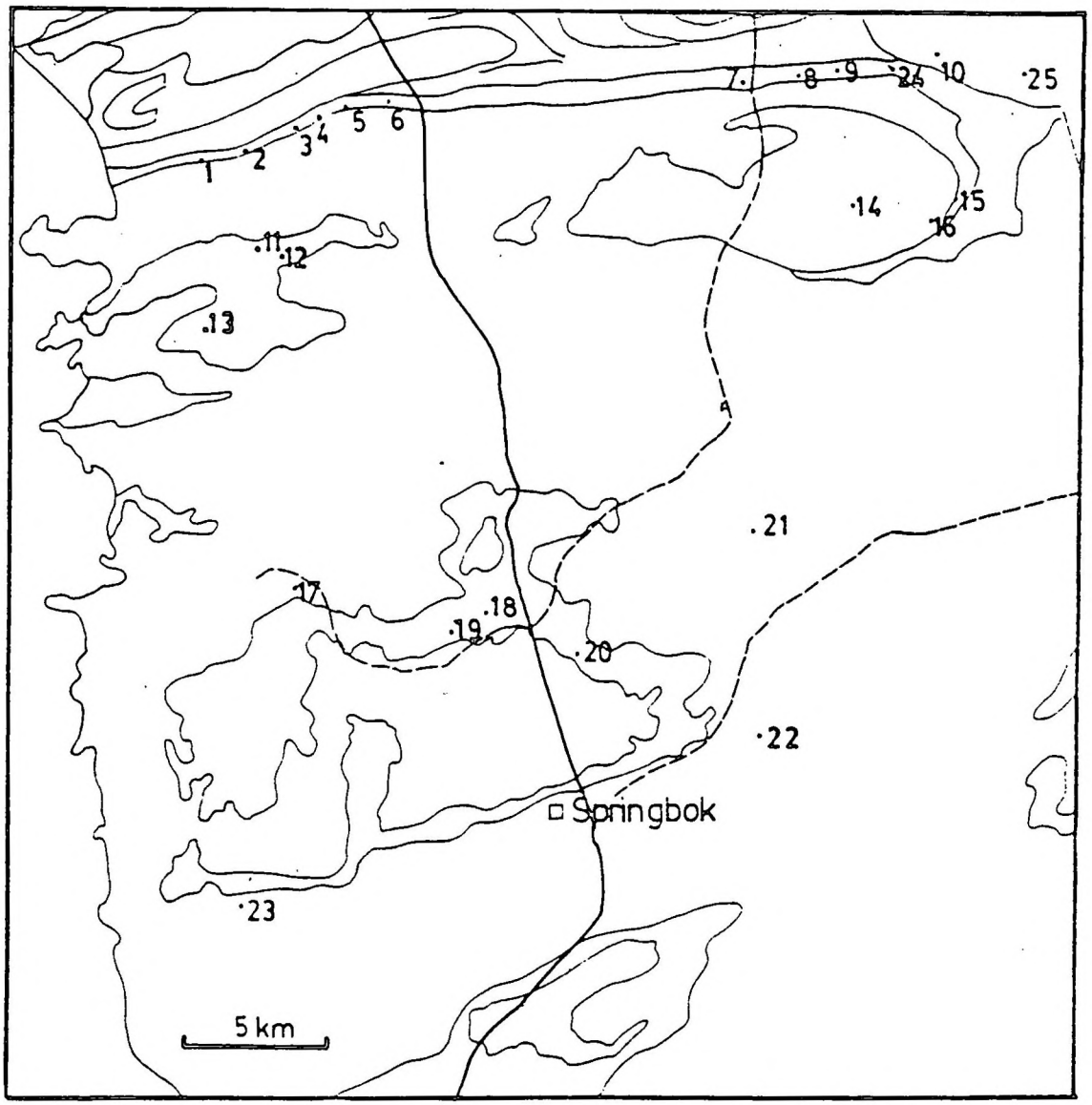

FIGURE 10.19 The distribution of samples from the Copper District described in Appendix 4.6. The numbers correspond to the samples described in Appendix 4.6 as follows: 1 - S378, S381; 2 - S350; 3 - 6969; 4 - S964, SK485, SK489, SK490; 5 - SK453B; 6 - S312; 7 -S069, S065C; 8 - S058, S059, S060, S061; 9 - SK406, SK408A, SK408B; 10 - SK203, SK204, SK205, SK208, SK284, SK222, SK223, SK493; 11 - SK479, SK481; 12 - S194A, S194B; 13 - S193; 14 - S267; 15 - S231A, S231B; 16 - S230B, S230C; 17 - GNA002, GNA001; 18 - GNA022, GNA023; 19 - S200, S202; 20 - S207, S208; 21 - SK184; 22 - all samples with prefix GLC; 23 - SK233, 24 - SK022, SK406, SK408; 25 - SK227

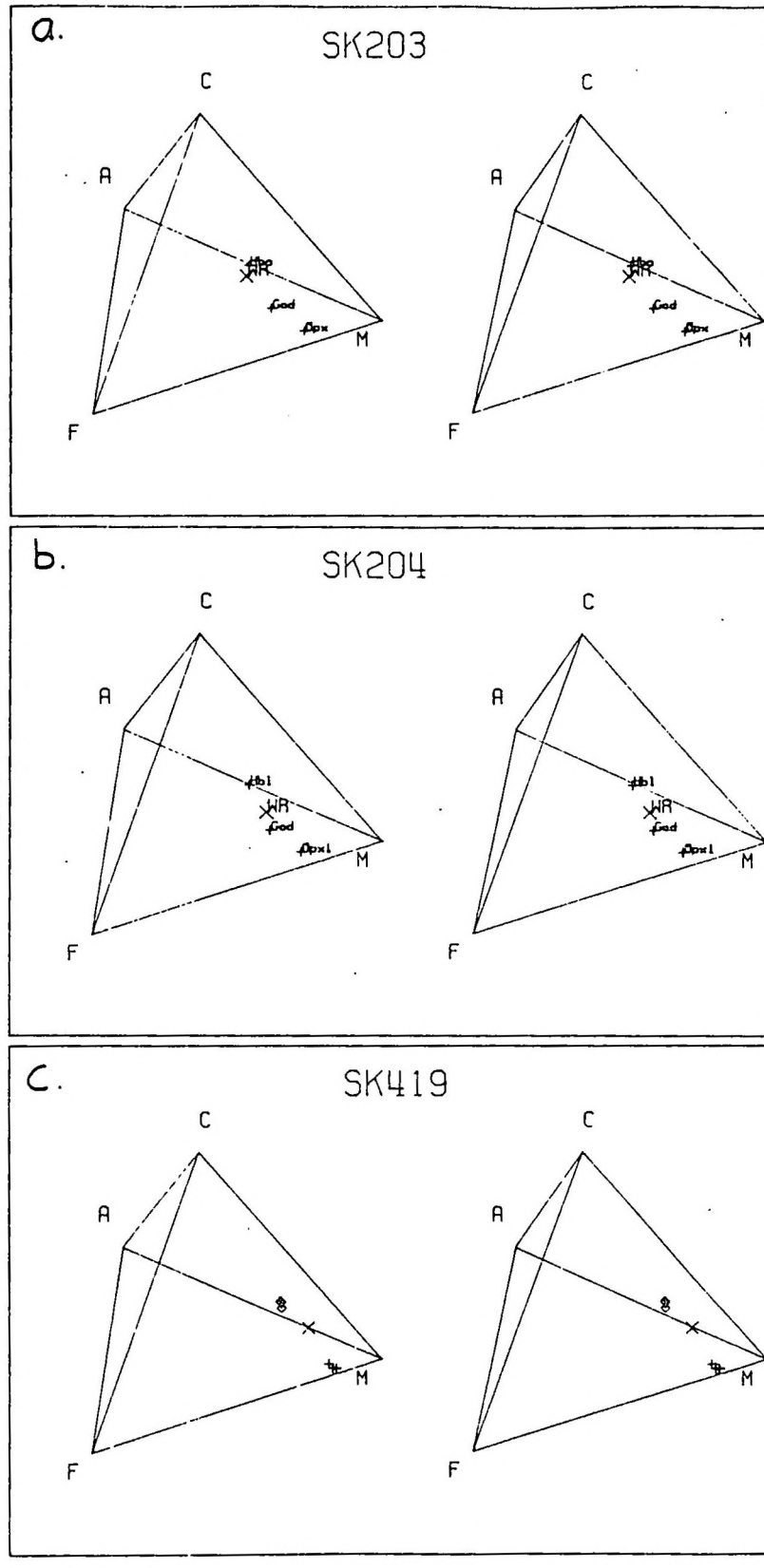

FIGURE 10.20 The compositions of constituent phases and the whole rocks (X) of three ultramafic metamorphites, projected into the ACFM tetrahedron. SK203 and SK204 are from the Skelmfontein se Poort area (Copper District) and SK419 is from the Eenriet Mountains.

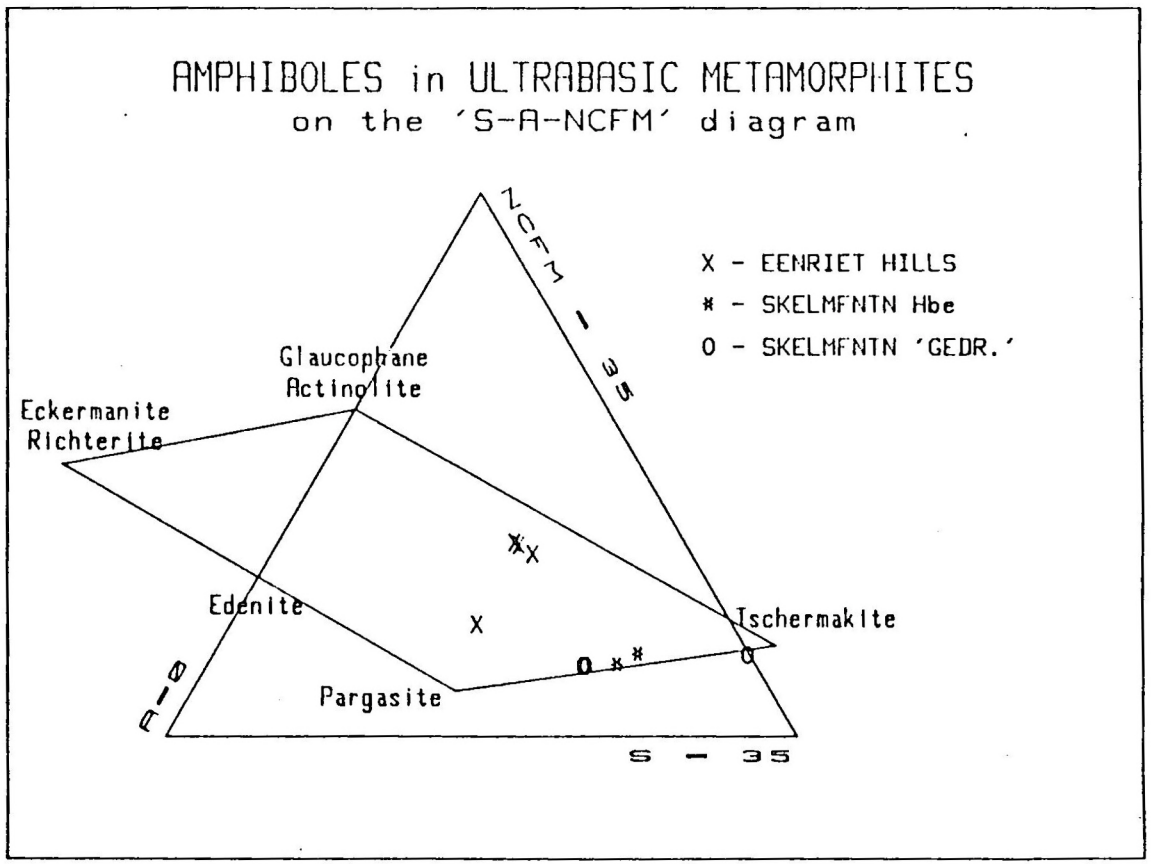

FIGURE 10.21 Graphical classification of the amphiboles from the ultramafic metamorphites (S-A-NCFM diagram of Robinson et al., 1982)

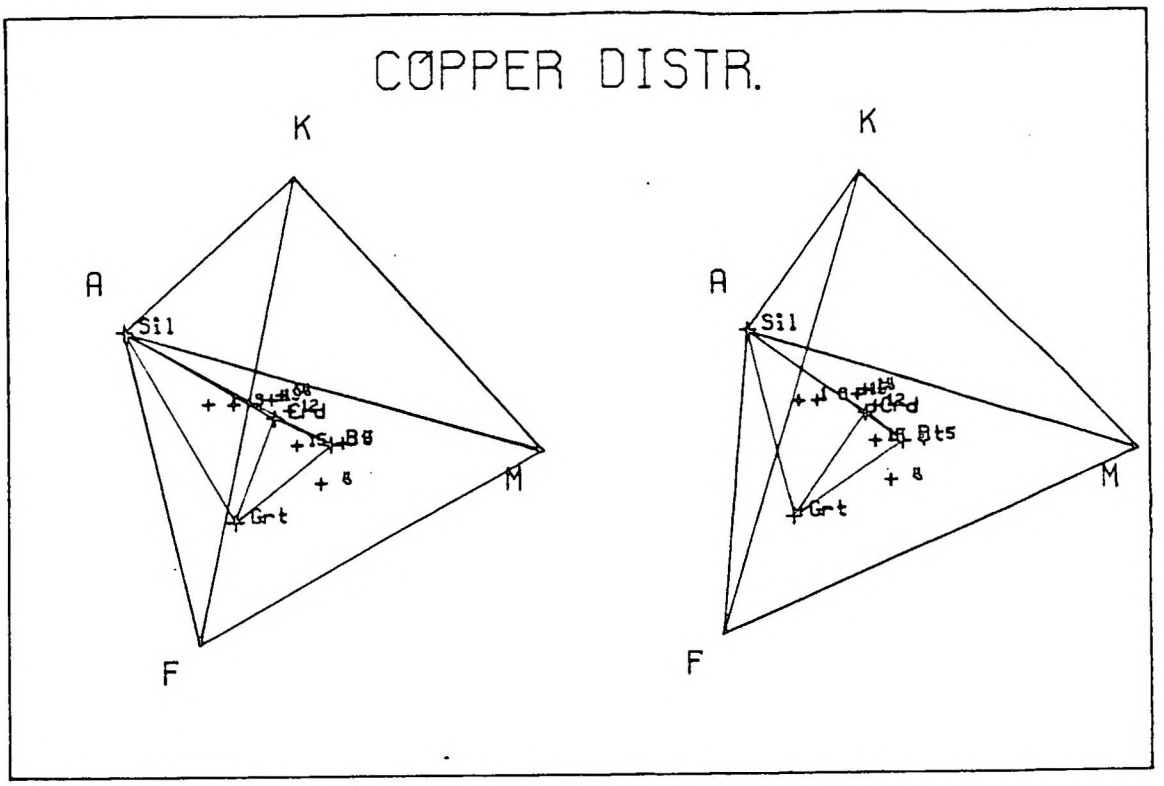

FIGURE 10.22 Whole rock compositions of metapelites from the Copper District projected into the AFMK tetrahedron (A = [Al2O3], F = [FeO], M = [MgO] and K = [K2O]). A reference tetrahedron inside the projection represents the compositions of biotite, garnet and cordierite from SK231A and the composition of sillimanite. The numbers in the figure correspond to metapelite samples as follows: 1 - GNA002; 3 - SK267; 4 - SK387; 5 - SK321; 12 - S207; 13 - S194A; 14 - S193; 15 - S231A.

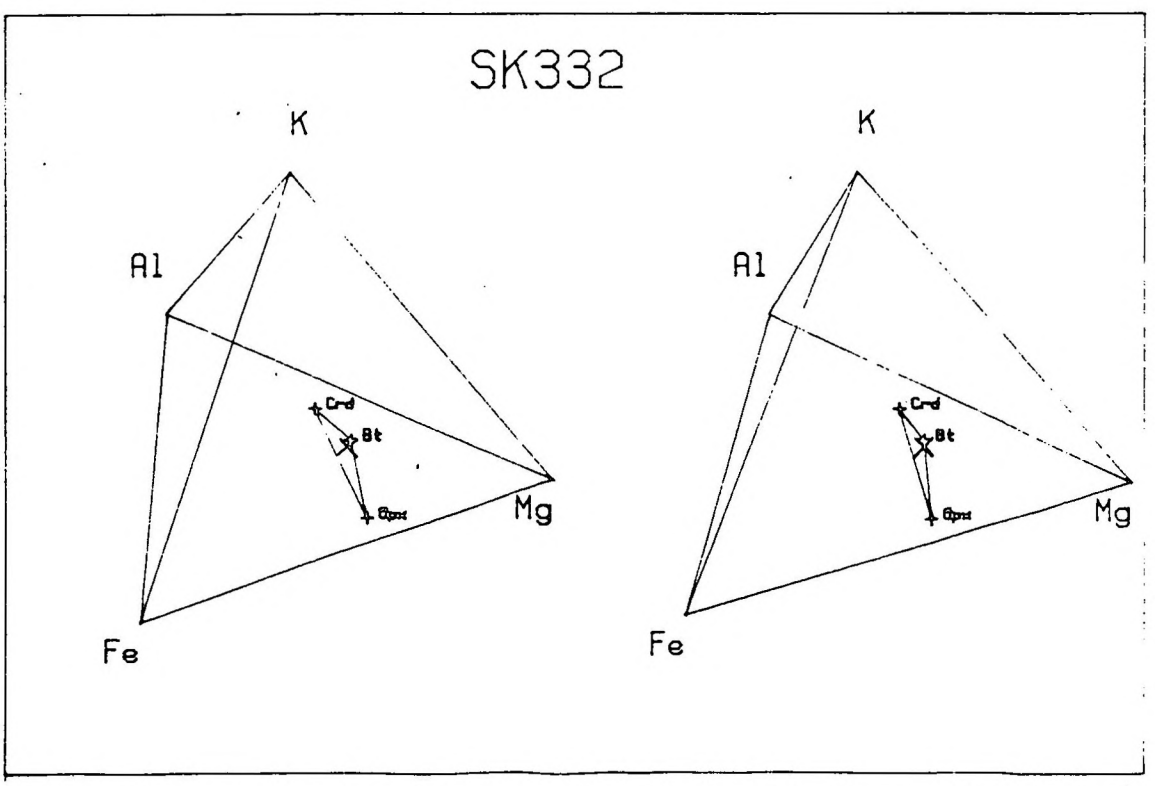

FIGURE 10.23 The same projection as in Figure 10.22, applied for the whole rock and mineral compositions of the orthopyroxene-cordierite rock from the Skelmfontein se Poort area.

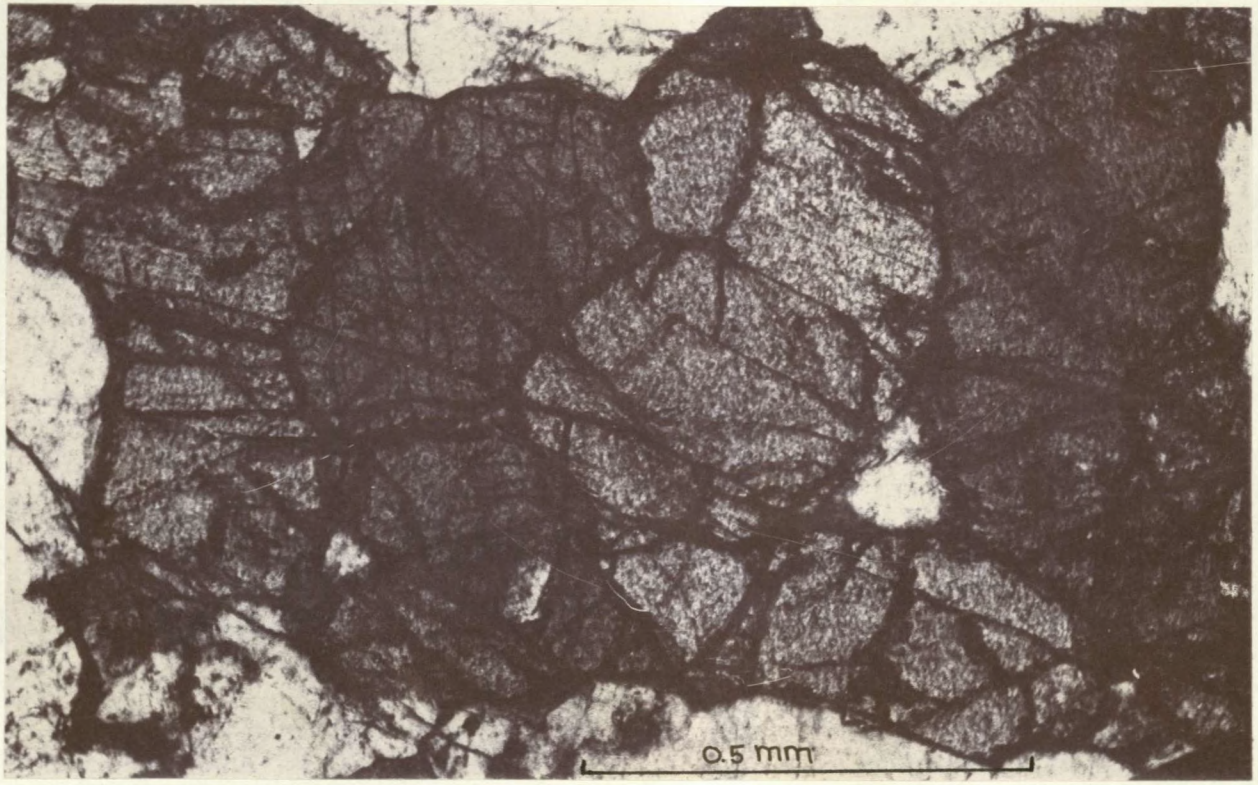

FIGURE 10.24 Metamorphic texture displayed by pyroxenes in leucodiorite from Klondike central prospect, north of Okiep.

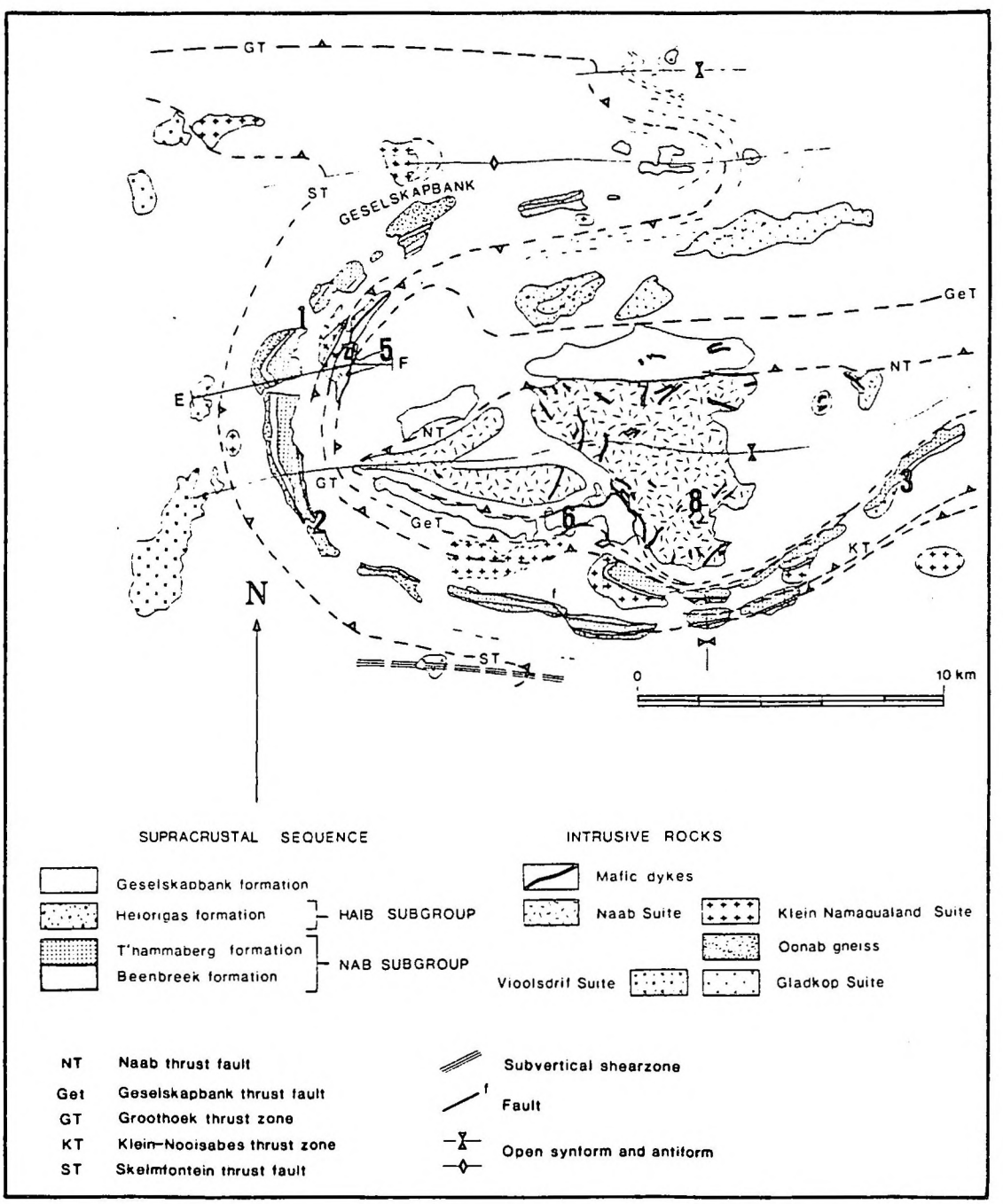

FIGURE 10.25 The geology of part of the Geselskapbank Synform, showing the localities of the samples. The numbers correspond to the samples described in Appendix 4.7 as follows: 1 - DST1, DST20; 2 - DST18; 3 - DNA3; 4 - DST7, DST67, SK323, SK324, NMG029, NMG030, NMG034; 5 - NMG006, NMG013, DGE14; 6 - DGE16, DGE18, DGE20, DGE61, DGE76; 7 - NMG002, NMG003, NNB027; 8 - NMG001

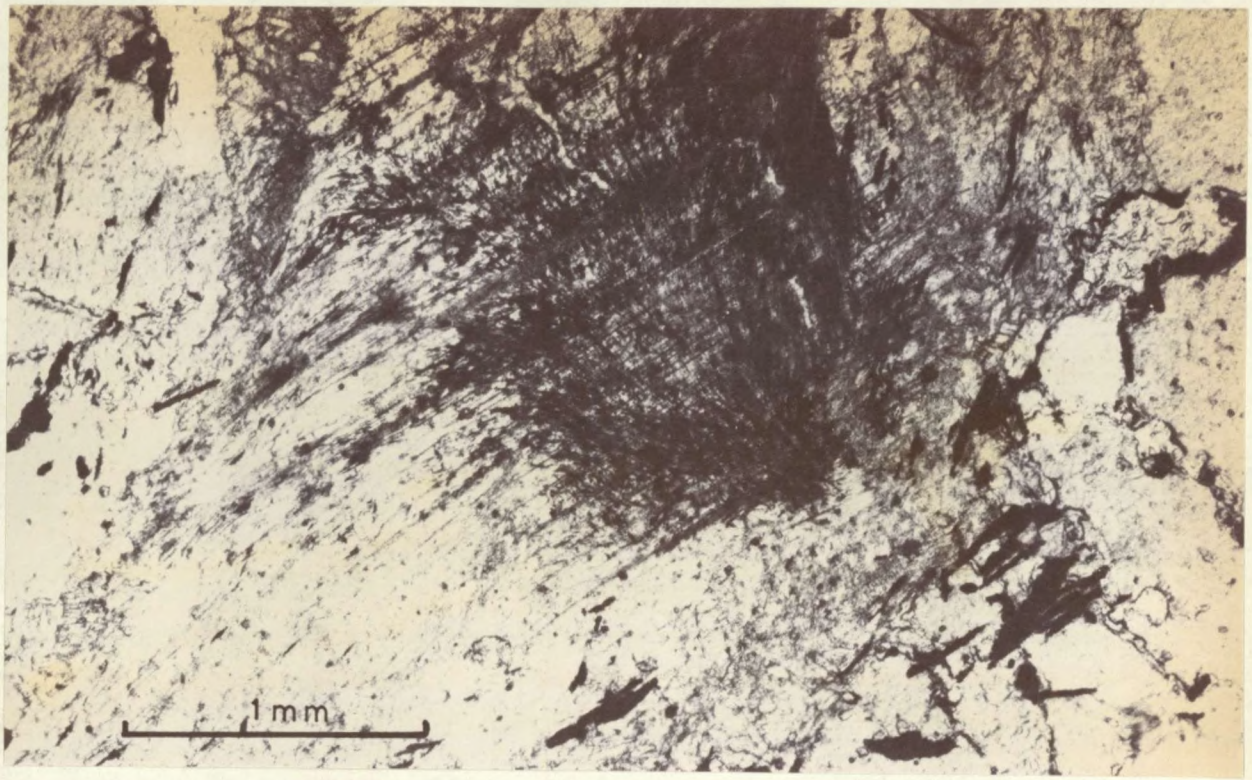

FIGURE 10.26 Photomicrograph of post-kinematic muscovite (it is the mica cleavage which appears as parallel lines running diagonally across the picture) which has overgrown a radial cluster of sillimanite in metapelite from the Skelmfontein nappe, Geselskapbank Domain.

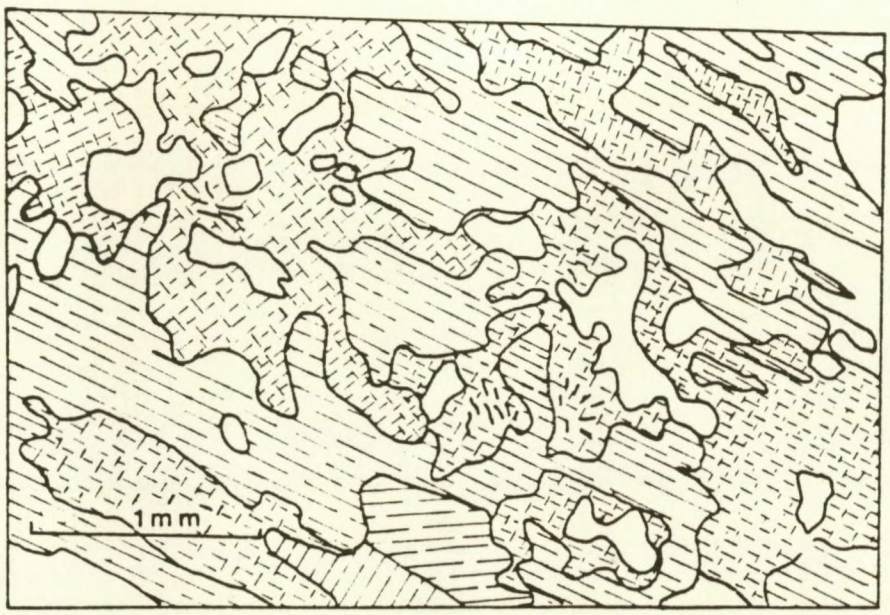

FIGURE 10.27 Sketch of replacement texture in metapelite from the Skelmfontein nappe, Geselskapbank Domain. The different phases are depicted as follows: quartz - clear; muscovite - parallel cleavage; K-feldspar - cross hatched; sillimanite - small needles in K-feldspar.

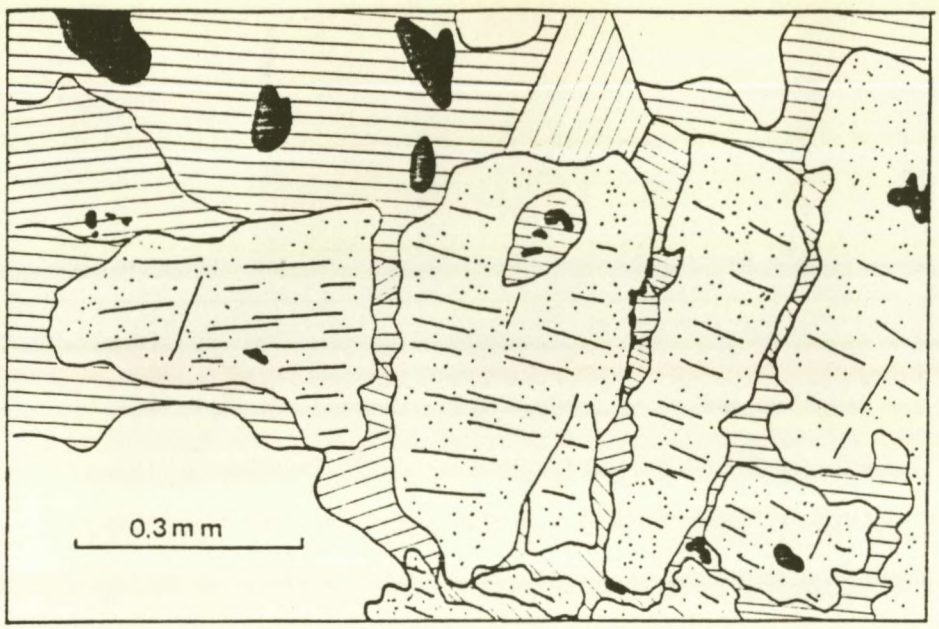

FIGURE 10.28 Retrogressive replacement of orthopyroxene (stippled) by hornblende (parallel lines) in two-pyroxene granulite from the Geselskapbank nappe, Geselskapbank Domain. The black areas depict opaque grains, the clear areas plagioclase.

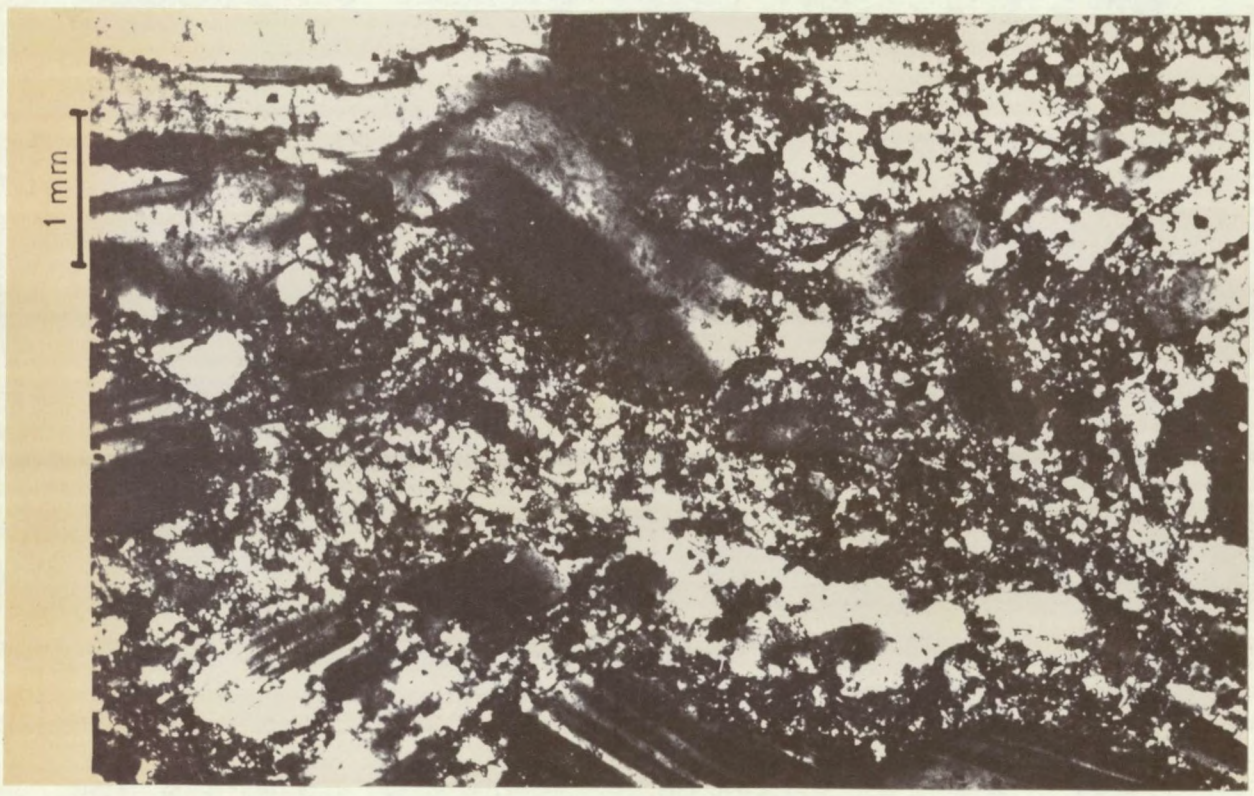

FIGURE 10.29 Photomicrograph of cataclastic texture in a sample of Gareskop dolerite, from the Naab thrust zone. Note the bending of plagioclase twin lamellae

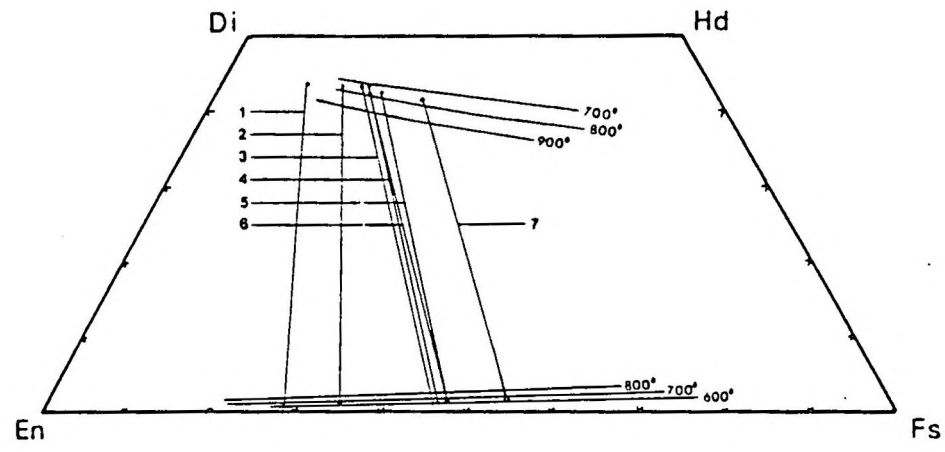

Metadolerites and leucodiorite

1	-	NMG005 (Gareskop)	2	-	SK338 (Nariams)
3	-	NNB027 (Gareskop)	4	-	SK467 (Nariams)
5	-	SK337(2) (Nariams)	6	-	SK337(1) (Nariams)
7	-	GLK001 (Leucodiorite, Koperberg Suite)			

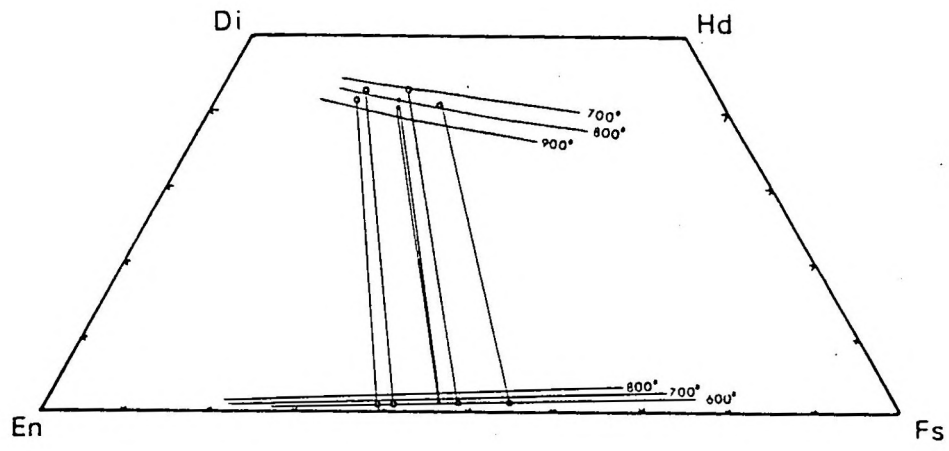

Specimens of the 'hornblende gneiss' of the Copper District.

1 - GLC059 (Carolusberg mine)
2 - GLC053 (Carolusberg mine)
3 to 6 Surface samples, from Clifford et al., 1981

FIGURE 10.30a The compositions of coexisting clinopyroxenes and orthopyroxenes projected onto the pyroxene quadrilateral according to the method of Lindsley (1983) - metadolerites, leucodiorite and two-pyroxene granulite of the 'hornblende gneiss' unit, Copper District.

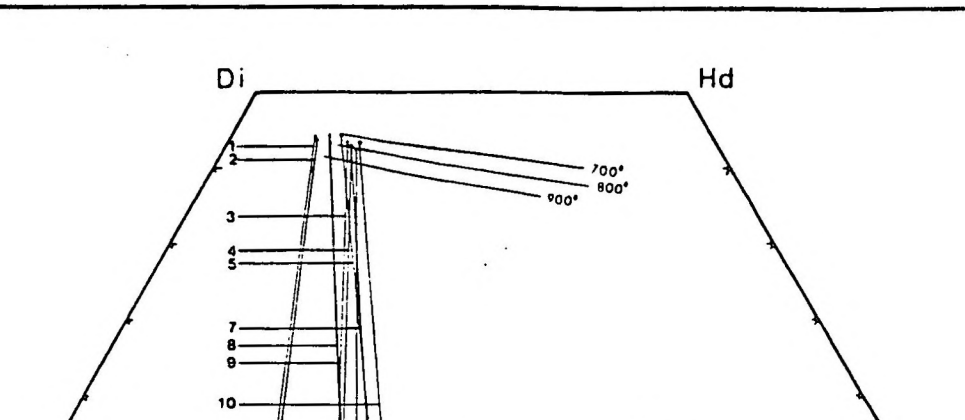

Two-pyroxene granulite samples from the northern limb of the Ratelpoort synform.

1 - S969(1) 2 - S969(2) 3 - SK289(2)
4 - SK420 5 - SK289(1) 7 - SK289(3)
8 - S965(1-r) 9 - S965(1-c) 10 - S965(2)
11 - SK406

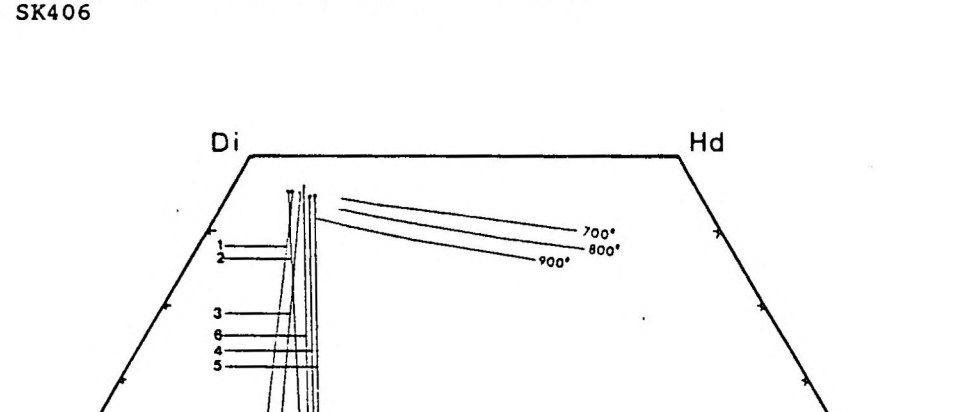

Two-pyroxene granulite samples from the Geselskapbank Nappe, Geselskapbank Domain.

1 - DGE20(1) 2 - DGE20(3) 3 - DGE20(2)
4 - DGE76(1) 5 - DGE76(2) 6 - DGE61

FIGURE 10.30b The compositions of coexisting clinopyroxenes and orthopyroxenes projected onto the pyroxene quadrilateral according to the method of Lindsley (1983) - two-pyroxene granulite from the northern limb of the Ratelpoort Synform and from Geselskapbank.

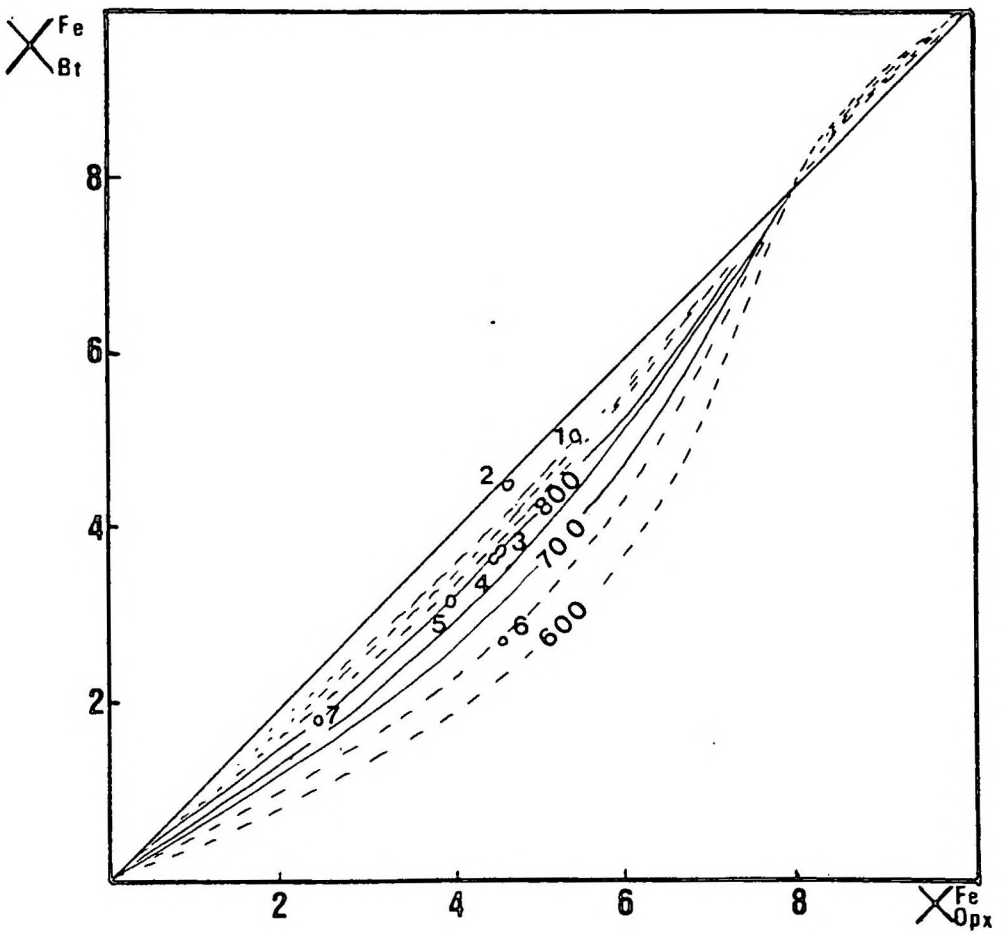

FIGURE 10.31 Application of the Fonarev and Konilov (1986) experimental orthopyroxene-biotite geothermometer. The curves are isotherms, drawn solid where found by experiment and drawn as broken lines where extrapolated. The numbers 600, 700 and 800 indicate the temperatures for the different isotherms. The samples plotted on the diagram are: 1 - GLK001 (leucodiorite) ; 2 - NNB027 (metadolerite); 3 - GLC053 (two-pyroxene granulite); 4 - SK332 (cordierite-orthopyroxene rock); 5 - S579 (Dabbiknik pelitic granulite); 6 - GLC059 (two-pyroxene granulite); 8 - S069 (saphirine-cordierite rock).

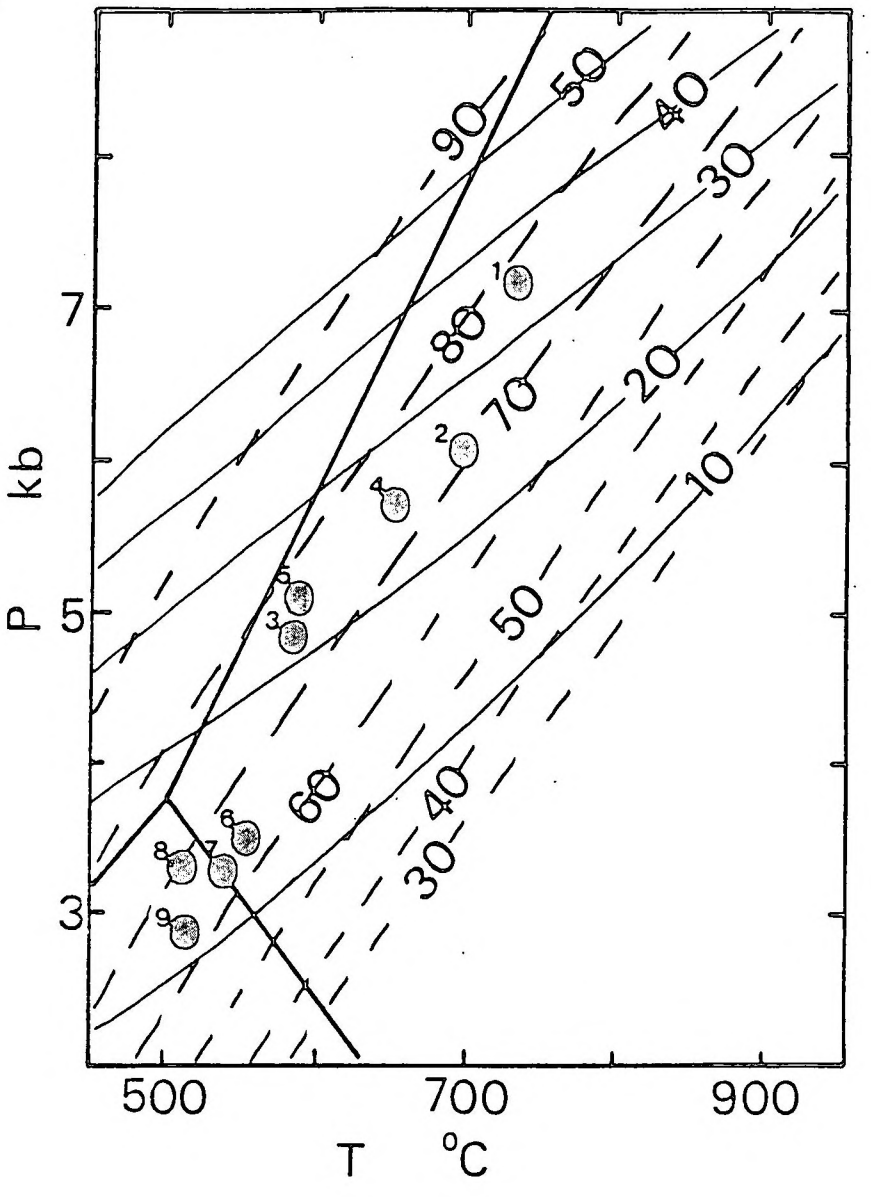

FIGURE 10.32 Application of the garnet-cordierite geothermo- barometer proposed by Aranovich and Podlesski (1983) to specimens from the Copper District and the Geselskapbank Domain. The steep broken lines represent the Mg content of cordierite (the numbers refer to the value Mg/(Mg + Fe) * 100) while the shallower solid lines represent similar values for garnet. The solid ovals depict the positions of samples as follows:

1 - SK490 (cordierite inclusion in garnet)
2 - S381 (cordierite inclusion in garnet)
3 - S381 (rims of touching grains)
4 - S378 (cordierite inclusion in garnet)
5 - S378 (rims of touching grains)
6 - DST7 (rims of touching grains)
7 - NMG031 (rims of touching grains)
8 - SK323 (rims of touching grains)
9 - SK323 (rims of touching grains)

Samples 1 - 5 Copper District; 6 - 9 Geselskapbank Domain.

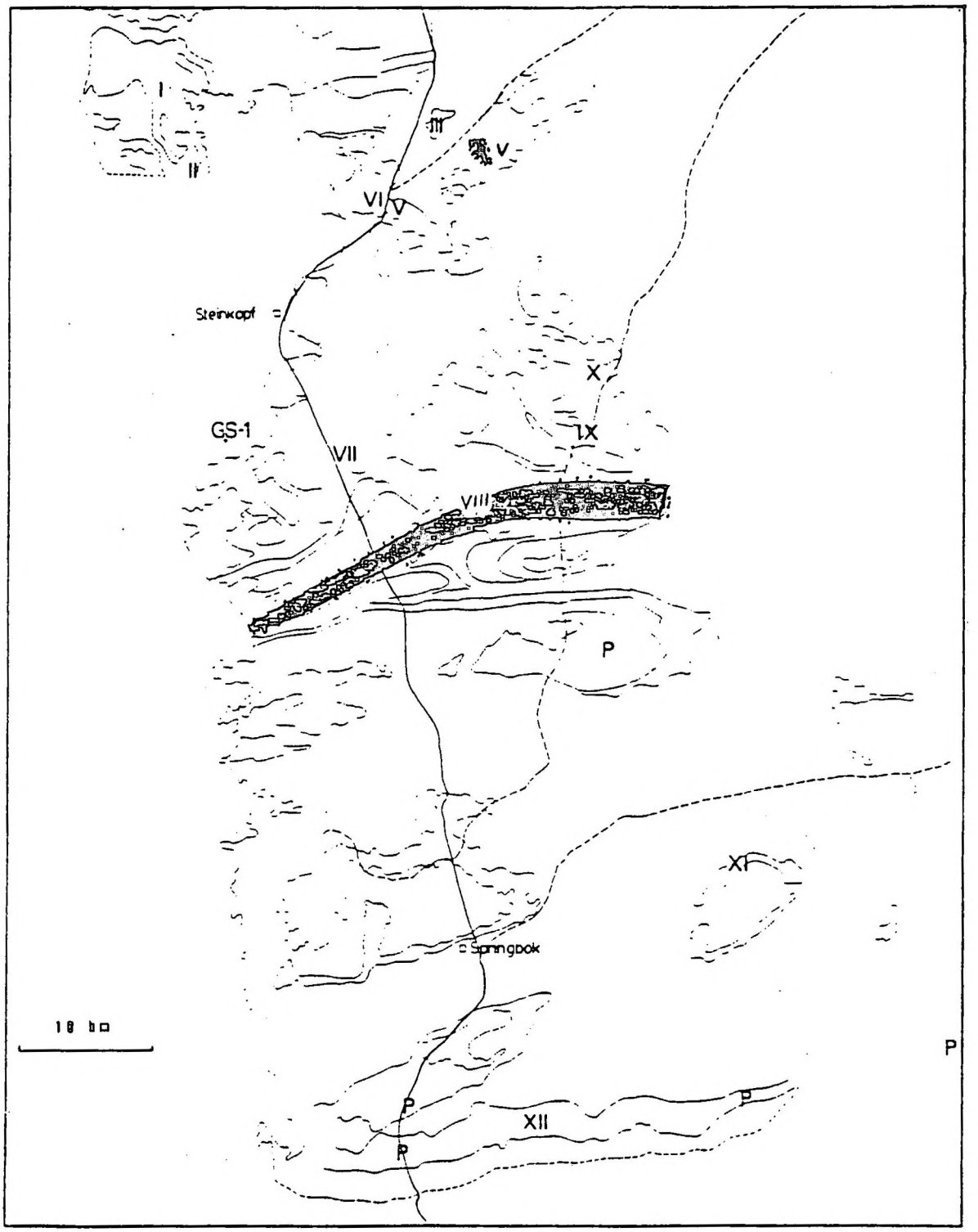

FIGURE 11.1 Map showing the locations of the example sites of migmatitic features described in the text (e.g. VI), the distribution of significant flecky neosome development (dark shading), the occurrences of flecky neosomes with orthopyroxene in the melanosome (P) and the location of outcrop GS-1.

FIGURE 11.2 Stromatic neosomes, ptygmatically folded in some places. The paleosome is Steinkopf Gneiss and the locality is Example site II (Figure 11.1).

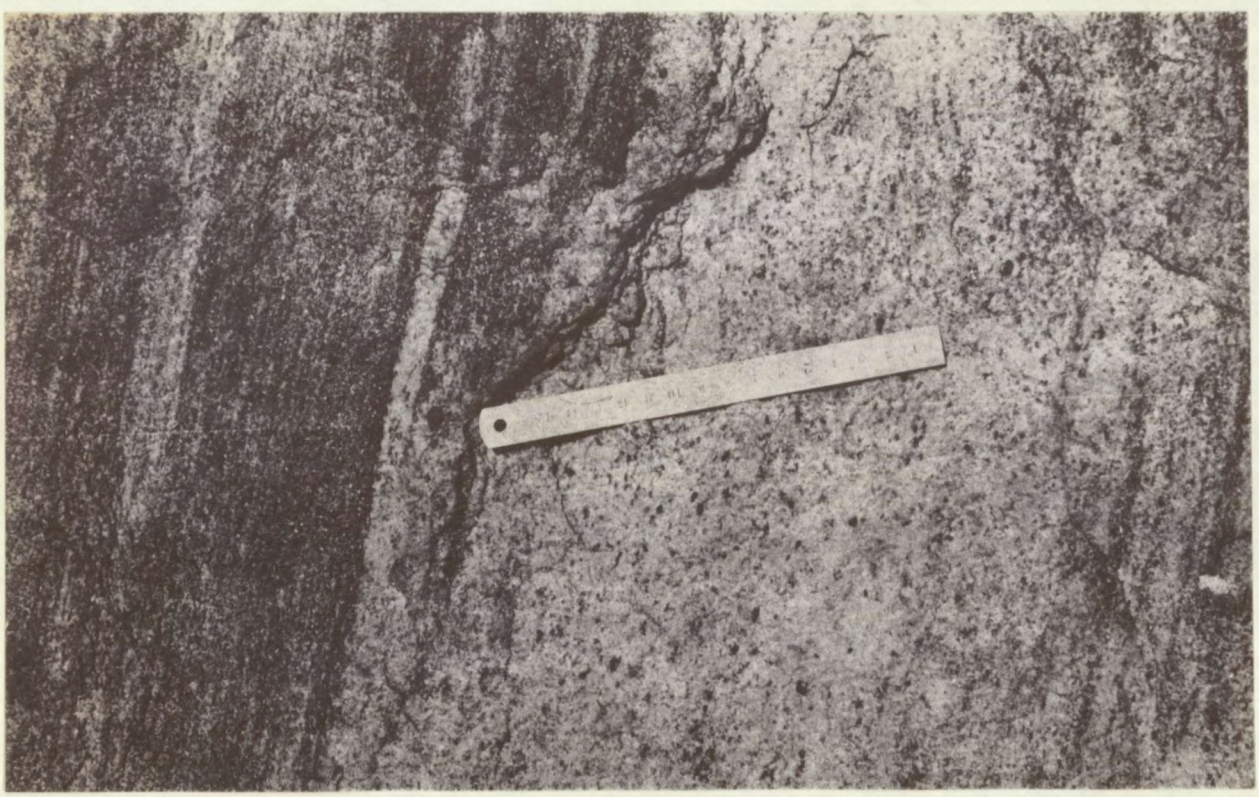

FIGURE 11.3 N2 flecky neosome in Steinkopf Gneiss in the Konkyp area. The melanosome is hornblende (site V, Figure 11.1)

FIGURE 11.4 N3f neosome in Steinkopf Gneiss at Example Site XII (Figure 11.1). The melanosome is hornblende. The width of the masking tape used as marker is 1 cm.

FIGURE 11.5 N3f neosomes in the area west of Ratelpoort. The neosomes transect the old foliation/banding in the grey gneiss and is deformed by the Skelmfontein shearing.

FIGURE 11.6 Early flecky neosomes in Steinkopf Gneiss at Example Site I (Figure 11.1).

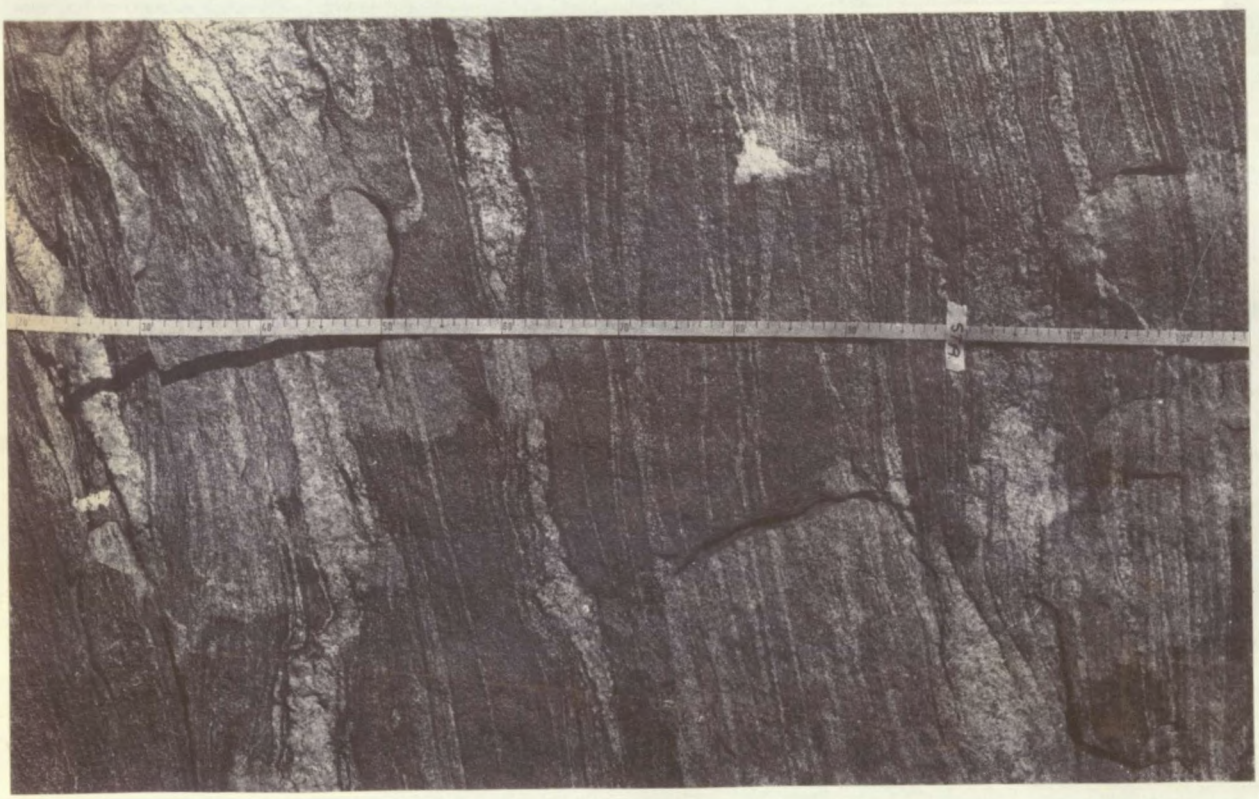

FIGURE 11.7 N1s and N2s neosomes seen on the surface of a vertical outcrop at Example Site III (Figure 11.1).

FIGURE 11.8 Advanced N1s neosome development at Example Site III (Figure 11.1).

FIGURE 11.9 A small body of Eyams Granite sharply transects N1s and N2s neosomes at one place in the Steinkopf Gneiss and fades away into the paleosome a few centimetres further (site VI, Figure 11.1).

FIGURE 11.10 N1s neosomes in Brandewynsbank Gneiss (Bst on the photograph) are not as continuous as in Steinkopf Gneiss (GGn in photograph), possibly due to the interference of augen (Example Site VII, Figure 11.1).

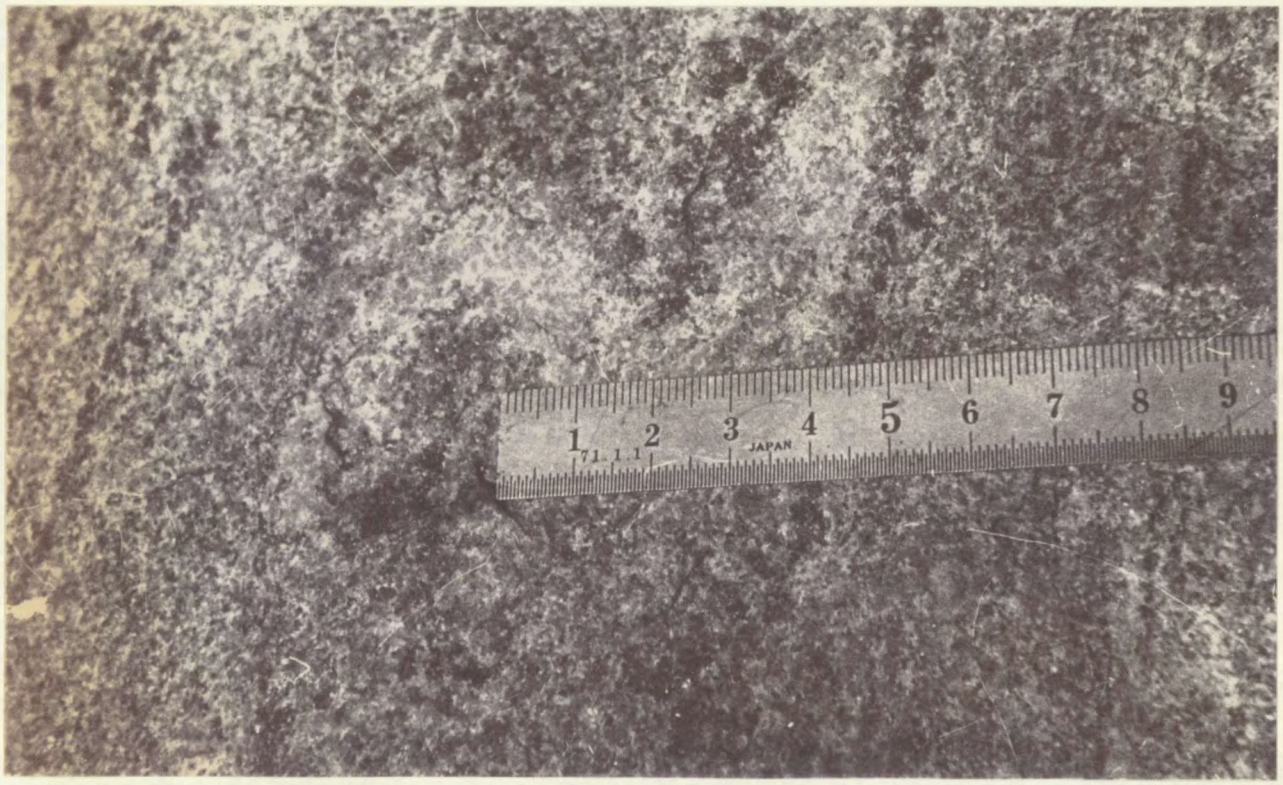

FIGURE 11.11 N3f neosome superimposed on the N2s melanosome caused a flecky structure to replace the normal mafic salvage (Example Site VIII, Figure 11.1).

FIGURE 11.12 N1s and N2s neosomes are difficult to distinguish in this zone of Skelmfontein shearing. N3f neosome bands are subconcordant to the older foliation/banding. N3f neosomes transect all older structural and migmatitic phenomena (Example Site IX, Figure 11.1).

FIGURE 11.13 N2f superimposed on an augen texture in Brandewynsbank Gneiss at Example Site X (Figure 11.1).

FIGURE 11.14 Migmatite formed as a result of the intrusion of Nababeep Gneiss as well as younger pegmatite into Steinkopf Gneiss, followed by deformation (Example Site XI, Figure 11.1).

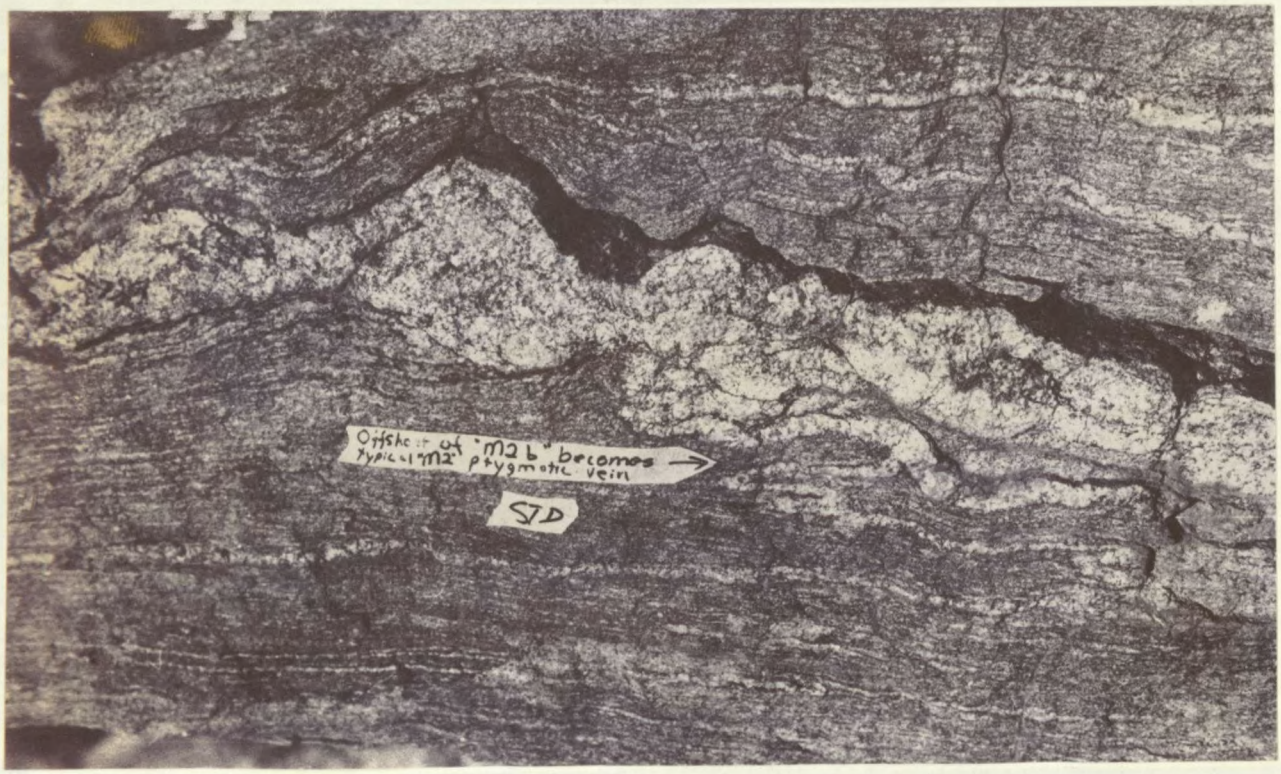

FIGURE 11.15 A small apophysis from a boudinaged pegmatite forms a typical 'N2s' neosome at Example Site XII (Figure 11.1).

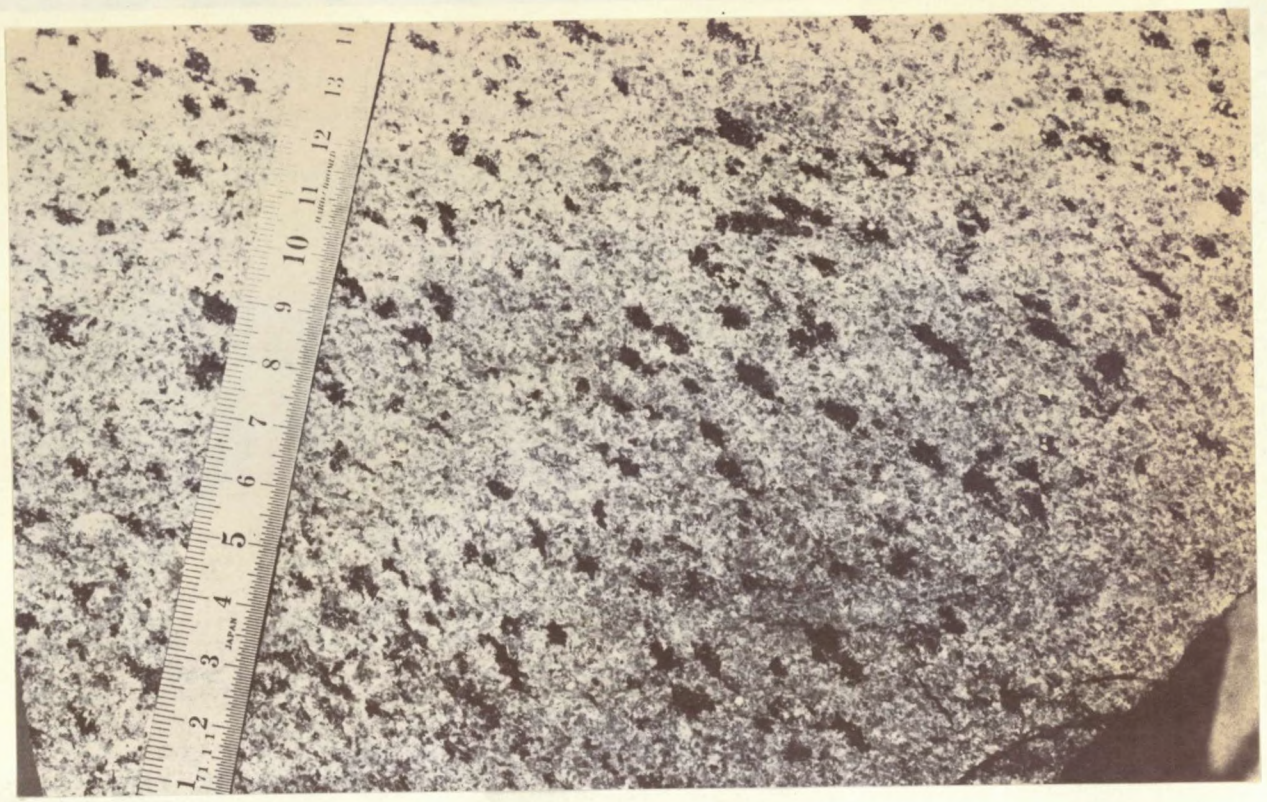

FIGURE 11.16 Advanced N2f neosome development in Brandewynsbank Gneiss (east of Example Site VIII, Figure 11.1).

FIGURE 11.17 Mobilization of Brandewynsbank Gneiss during the Dabbiknik phase of shearing produced a form of the 'Sederholm-effect' (west of Korrogas).

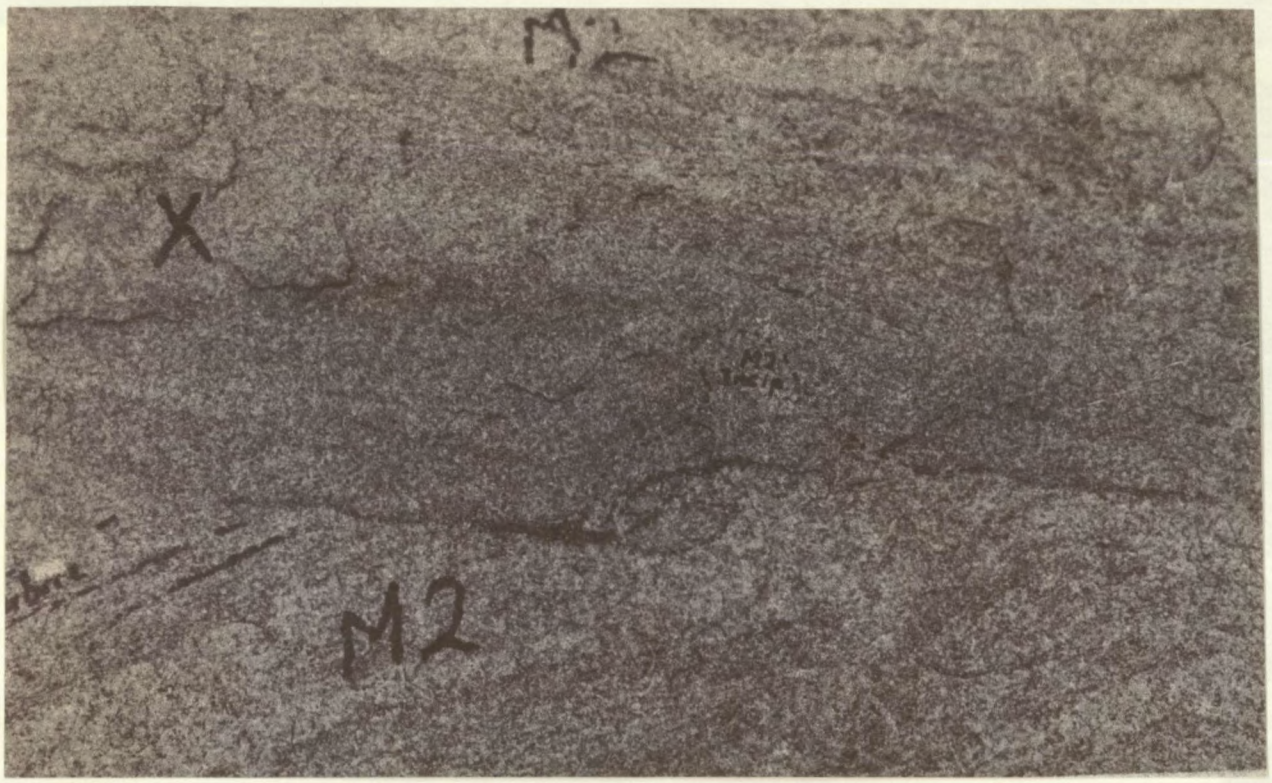

FIGURE 11.18 N2s neosome (M2 on photograph) is concordant to the foliation/banding of Steinkopf Gneiss, but is clearly younger than a dyke of grey granite which cuts across the old fabric (outcrop GS-1).

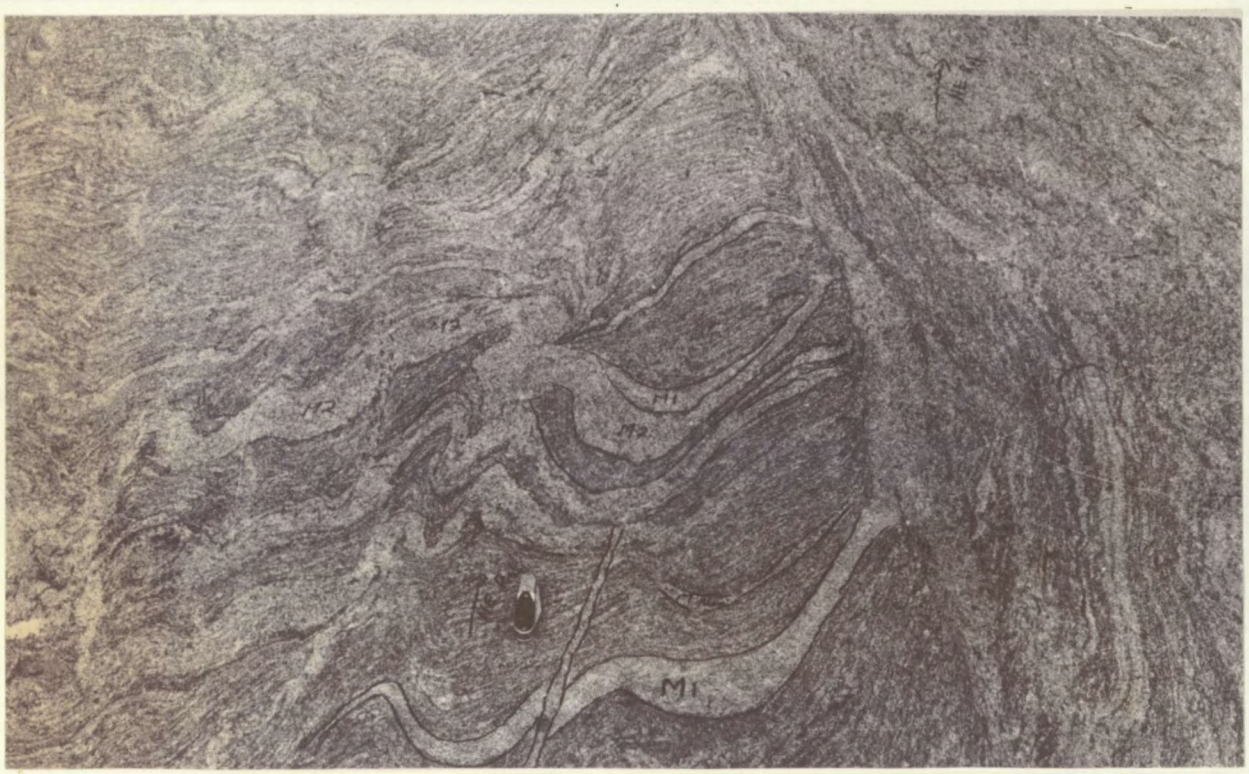

FIGURE 11.19 Schlieric migmatite (Eyams migmatitic granite) transects N1s and N2s neosomes at outcrop GS-1.

FIGURE 11.20 A close-up view of the schlieric to nebulitic structure characteristic of the migmatitic Eyams Granite at outcrop GS-1.

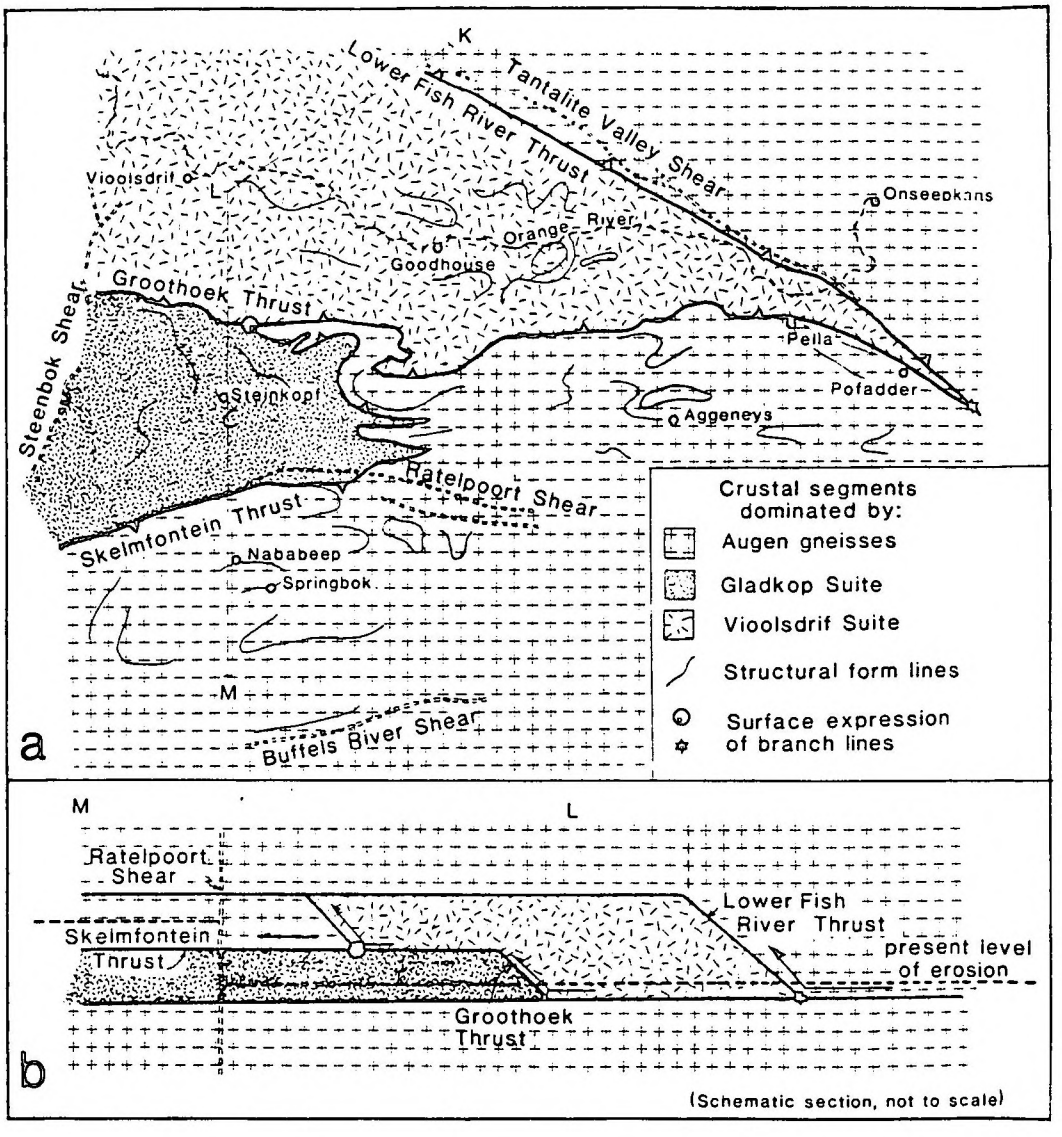

FIGURE 12.1 A sketch map of the Namaqualand Geotraverse and surrounding area showing the different tectonic domains separated by major thrust faults. A schematic cross section illustrates the tectonic development prior to late folding and shearing (van Aswegen, et al., 1987)

APPENDIX 2

PROJECTION OF CHEMICAL COMPOSITIONS.

In this appendix the methods used to produce the QAP classification diagram for igneous rocks and the stereopair tetrahedron plots are briefly described.

The chemical components of a rock or mineral is usually expressed as weight percentages of the element oxides or some derivation thereof (e.g. molecular proportions). The list of components can be considered as an n-element vector representative of the total composition. One way to graphically illustrate the composition is to use ternary diagrams. The composition of the mixture is expressed in terms of a barycentric coordinate system and the sum of the coordinates is always one (or 100%). Only the relative amounts of the three components are seen. However, a three component system can accurately be illustrated on the two dimensional plane of a piece of paper. In the case of a four component system, the composition of a mixture can be shown as a position in the volume of a tetrahedron. The composition of the rock (or mineral) of interest is commonly shown as the projection from the apex onto the base of the tetrahedron. The choice of the component at the apex is arbitrary, and four projections can be generated. In the case of an n-component system projections to any n - m (m greater or equal to zero) component coordinate system is possible through the application of simple linear algebra techniques. It generally involves the transformation of composition coordinate axes from an old coordinate set to a new coordinate set. Application in the production of thermodynamically valid projections of phase compositions is given by Greenwood (1975) and an explanation of the manipulation of n-dimensional composition space in petrology is given by Spear et al. (1982).

The techniques described in literature can be applied to the development of unique composition variation diagrams, the calculation of norms of rocks using very specific mineral compositions, the calculation of end member mineral compositions, the balancing of metamorphic reactions and more. To calculate, for example, the position of a particular phase on a diagram such as the well known Thompson's AFM diagram, the following steps are followed:

1. Express the composition of the phase in terms of the molecular ratios of the components of the model pelitic system (the 'old' composition coordinate set) SiO_2, Al_2O_3, FeO, MgO, K_2O and H_2O by deviding the weight percentage of each element oxide by the molecular weight of that element oxide.

2. Do the same with the compositions of the components of the new coordinate system, namely those components which define the projection plane: 'Al_2O_3', 'FeO' and 'MgO', and those components from which the projection is made: quartz, muscovite and water.

3. Find the inverse of the matrix of molecular ratios of new components - the columns are the composition vectors of the new components in terms of the molecular ratios of the old components.

4. Multiply this inverse with the column vector of the molecular ratios of the phase of interest - the product is a composition vector of the phase of interest in terms of the molecular ratios of the new components.

5. Delete from this vector the elements of the components from which the projection is made (in this case water, quartz and muscovite) and normalize the rest of the elements - these normalized elements are the barycentric coordinates of the phase of interest on the AFM diagram.

The procedure can be generalized to start with the standard composition vector of any mineral or rock and express its composition in terms of any combination of new components, provided that the matrix of new components is non-singular. Modern inverse theory enables one to find the inverse (more correctly, the pseudo-inverse) of non-square matrices by means of singular value decomposition. This allows one to start with the full composition of a sample (rock or mineral, for example, as a 10 element vector) and express this composition in terms of less than 10 components. Say the new components are represented by a 10 X 6 matrix (e.g. 6 minerals, each of their compositions expressed in terms of a 10 weight percentages of element oxides). The pseudo-inverse of this is a 6 X 10 matrix, which, multiplied with the 10 element sample vector, gives a 6 element vector, the composition vector of the sample in terms of the six new components. The stability of the mathematical experiment is reflected by the 'condition number' (the inverse of the smallest eigen value). The larger this number, the easier the results will change with small perturbations in the data (Babuska, 1972; Bus, 1976). Computer programs to solve such inversions and which run on micro-computers, are available in literature (Golub and Reinsch, 1970).

The normative mineral compositions for use in the QAP diagrams in Chapters 4 and 6 were calculated using the method described above. The list of minerals chosen as the new components are given in Chapter 4. The plots were made using the method suggested by Le Maitre (1976), who showed that the normative mineral compositions can be used on the QAP diagram of Streckeisen (1976) by application of the following adaption: Q = qtz; A = or x T; P = an x T; T = (or + ab + an)/(or + an).

The graphical visualization of relative compositions can be extended by projection into a four component system which, in terms of barycentric coordinates, yield a three dimensional picture. This, in turn, can be projected from any angle onto a two dimensional plane. A further extention is the simultaneous projection of the same picture from two sligtly different angles (generally 6 degrees relative rotation) to produce a stereographic pair. For this purpose, Spear (1980) presented an algorithm converting four-component barycentric coordinates into spatial Cartesian coordinates. The stereo pair can be viewed either by means of a stereoscope or, with a bit of practice, with unaided eyes, allowing each eye to view the appropriate picture of the stereo pair independently. Modern micro computers are ideal for the calculations involved and, since the stereographic images can be projected onto the graphics console, 'projective analysis' of complex systems becomes a quick and practical tool in metamorphic petrology.

APPENDIX 3

THE CHEMIAL COMPOSITIONS OF SOME ROCK SPECIMENS

The analyses presented here were, for most part, provided by the Geological Survey in Pretoria, as a service to the National Geodynamics Project. Analyses carried out at the Department of Geology, UOFS, are characterized by zero values for FeO - all iron is expressed in terms of Fe_2O_3.

APPENDIX 3.1 THE METAPELITES

	S837	S846	S207	S194A	S193	S201	S231A
SiO2	46.670	59.650	74.220	54.080	57.840	68.930	68.860
TiO2	2.180	1.020	0.590	1.100	1.470	0.800	0.650
Al2O3	13.960	21.110	11.820	21.610	17.650	16.390	11.770
Fe2O3	6.740	1.510	1.720	1.550	2.920	1.780	4.700
FeO	9.700	5.350	3.240	7.060	5.100	3.070	4.350
MnO	0.450	0.020	0.040	0.150	0.250	0.020	0.110
MgO	7.780	2.300	3.680	5.300	5.000	3.300	4.580
CaO	4.830	0.580	0.220	0.290	0.900	0.080	1.050
Na2O	0.510	0.870	0.750	2.410	1.620	1.010	1.490
K2O	3.390	2.860	2.140	5.330	6.460	2.660	1.250
P2O5	0.600	0.040	0.090	0.120	0.280	0.070	0.060
H2O+	1.050	2.890	0.740	0.670	1.280	1.000	0.990
H2O-	0.000	0.000	0.100	0.200	0.100	0.100	0.300
TOTAL	97.860	98.200	99.350	99.870	100.870	99.210	100.160

	S641C	S162	S535	S539	S961	S069	S067B
SiO2	70.080	68.040	58.850	56.110	54.860	36.730	38.830
TiO2	0.400	0.650	1.050	0.940	0.970	1.290	1.310
Al2O3	14.110	12.300	22.250	22.740	23.710	21.540	18.740
Fe2O3	0.370	1.850	2.320	1.740	6.400	11.430	12.270
FeO	1.610	7.170	5.000	8.150	4.000	0.000	0.000
MnO	0.010	0.120	0.100	0.060	0.210	0.050	0.060
MgO	3.090	4.560	1.800	1.980	2.960	20.950	20.420
CaO	1.000	1.060	0.290	0.380	0.920	0.860	0.450
Na2O	4.130	1.430	0.700	0.930	1.600	0.000	0.300
K2O	5.130	1.110	3.740	3.450	3.830	2.990	1.700
P2O5	0.110	0.070	0.050	0.050	0.050	0.110	0.100
H2O+	0.360	1.040	4.750	4.170	0.400	2.290	2.170
H2O-	0.100	0.800	0.000	0.000	0.300	0.040	0.170
TOTAL	100.500	100.200	100.900	100.700	100.210	98.280	96.520

	S579A	S579B	S747	S752	S290D	S290C	S378	S379	S538	S750
SiO2	54.53	54.21	69.63	46.61	47.21	43.46	60.97	57.86	55.22	76.86
TiO2	2.07	2.12	0.83	2.15	0.95	0.99	1.17	0.95	0.48	0.38
Al2O3	13.53	13.61	15.87	15.48	16.38	17.62	18.43	20.65	14.35	14.11
Fe2O3	4.59	2.38	1.18	7.47	18.34	18.76	3.00	4.20	1.14	0.96
FeO	10.60	12.60	4.00	13.15	0.00	0.00	5.70	4.05	16.60	2.15
MnO	0.61	0.65	0.05	0.50	0.54	0.52	0.14	0.22	0.16	0.07
MgO	5.80	5.78	1.71	6.10	9.60	10.87	3.47	2.82	1.59	1.33
CaO	3.06	3.13	1.55	2.60	2.02	1.63	1.21	0.89	7.65	0.59
Na2O	2.56	2.68	1.77	1.01	0.15	0.13	2.32	1.94	0.44	1.02
K2O	0.88	0.78	1.94	2.46	1.94	3.49	2.54	4.47	0.33	1.07
P2O5	0.56	0.56	0.06	0.55	0.19	0.19	0.12	0.08	0.39	0.04
LOI	0.40	0.30	0.96	1.19	3.32	4.07	1.17	0.97	0.41	0.76
H2O-	0.00	0.00	0.00	0.00	0.11	0.01	0.00	0.00	0.00	0.00
TOTAL	99.19	98.80	99.55	99.27	100.74	101.72	100.24	99.10	98.76	99.34

APPENDIX 3.2.1 THE STEINKOPF AND BRANDEWYNSBANK GNEISSES

	S430 b	S605B b	S490 b	S768E sb	S491 b	S469B b	S123 sb	S813 b	S605 b	SK358 b	S014 b	S014 b	S259 sb	S426 b	S010 b
SiO2	75.37	75.33	75.27	74.62	74.61	74.47	74.21	74.08	74.06	73.56	72.81	72.49	72.72	72.61	72.40
TiO2	0.21	0.25	0.36	0.28	0.31	0.37	0.28	0.34	0.40	0.01	0.38	0.42	0.43	0.60	0.47
Al2O3	12.45	11.60	12.43	12.67	12.62	13.19	13.67	13.33	13.20	13.67	12.12	13.57	14.45	12.62	12.33
Fe2O3	0.58	1.79	0.92	0.00	0.71	1.27	0.01	0.75	1.06	1.28	2.43	1.59	2.66	1.58	2.78
FeO	0.55	0.00	0.80	1.48	0.80	0.80	1.78	1.30	1.00	1.52	0.00	0.85	0.00	1.55	0.00
MnO	0.03	0.05	0.02	0.01	0.21	0.03	0.01	0.05	0.01	0.07	0.04	0.02	0.08	0.04	0.07
MgO	0.78	0.27	1.16	0.77	1.09	0.50	1.02	0.95	1.50	0.51	1.10	0.65	0.86	1.45	0.26
CaO	1.77	1.51	1.36	1.23	1.51	1.68	1.11	1.39	2.17	1.82	1.96	2.16	1.41	2.41	1.72
Na2O	2.80	2.71	3.43	2.59	3.09	3.21	2.48	3.09	2.69	3.65	2.87	2.92	2.43	2.54	2.93
K2O	4.58	4.75	4.05	5.39	3.73	3.33	2.66	3.88	3.48	3.14	4.35	3.68	4.39	3.15	5.17
P2O5	0.04	0.07	0.03	0.08	0.04	0.07	0.07	0.05	0.08	0.01	0.11	0.09	0.07	0.14	0.10
H2O+	0.00	0.00	0.00	0.00	0.00	0.50	0.65	0.00	0.00	0.60	0.00	0.64	0.00	0.00	0.00
H2O-	0.00	0.02	0.00	0.00	0.00	0.32	0.13	0.00	0.00	0.11	0.02	0.40	0.03	0.00	0.03
TOTAL	99.16	98.35	99.83	99.12	98.72	99.74	98.08	99.21	99.65	99.95	98.19	99.48	99.53	98.69	98.26

	S490B b	S582 s	S765J s	S690 s	S013 b	S013 b	SK366 s	SK366 s	S723B b	S49 s	S305P1 s	S195 s	S605C bs	S605C bs	S024A s
SiO2	69.04	70.48	70.39	70.21	70.02	68.58	69.94	69.01	69.91	69.76	69.51	69.44	69.34	69.91	69.29
TiO2	0.47	0.56	0.43	0.60	0.41	0.44	0.60	0.29	0.59	0.62	0.58	0.67	0.51	0.53	0.51
Al2O3	14.58	13.78	15.34	14.39	14.23	16.52	15.31	16.13	13.81	14.23	13.47	15.22	13.77	14.63	13.39
Fe2O3	1.67	1.37	0.30	1.18	2.47	1.64	3.59	1.97	0.22	1.93	4.27	4.98	3.51	2.20	3.75
FeO	1.15	1.80	2.21	1.90	0.00	0.95	0.00	1.60	2.89	1.70	0.00	0.00	0.00	1.35	0.00
MnO	0.05	0.30	0.05	0.07	0.07	0.04	0.08	0.09	0.01	0.05	0.10	0.09	0.09	0.09	0.08
MgO	0.77	1.39	1.31	1.23	0.51	0.78	0.84	0.01	1.32	1.56	1.36	1.46	1.10	1.02	1.11
CaO	2.76	2.38	2.13	2.34	2.61	2.46	4.05	4.05	1.60	3.27	3.32	2.99	2.93	2.80	3.15
Na2O	3.63	3.18	3.52	3.70	3.41	3.14	3.55	3.75	2.67	3.36	2.59	2.43	3.69	3.41	2.66
K2O	3.36	3.88	3.77	3.33	4.42	4.45	2.50	1.98	5.42	2.89	2.88	3.04	3.09	2.27	3.79
P2O5	0.11	0.10	0.12	0.12	0.15	0.10	0.15	0.01	0.13	0.15	0.12	0.12	0.15	0.13	0.15
H2O+	0.82	0.00	0.41	0.00	0.00	0.42	0.00	0.56	0.63	0.00	0.00	0.00	0.00	0.60	0.00
H2O-	0.52	0.00	0.01	0.00	0.03	0.27	0.01	0.11	0.17	0.00	0.06	0.03	0.01	0.37	0.00
TOTAL	98.93	99.22	99.99	99.07	98.33	99.79	100.62	99.56	99.37	99.52	98.26	100.47	98.19	99.31	97.88

	S024A s	S087C s	S776C s	S150B s	S429 s	S498 s	SK254 s	S855 s	S595E bs	S505 s	S413F s	S518B s	S575B s	S601 sm	SK331 sm
SiO2	69.12	69.26	68.45	68.29	68.29	68.27	68.08	67.85	67.73	67.41	65.02	64.79	63.66	62.78	60.48
TiO2	0.55	0.46	0.45	0.58	0.77	0.70	0.84	0.80	0.33	0.69	0.84	0.73	0.91	1.06	0.26
Al2O3	14.70	14.58	14.70	14.57	14.48	14.07	12.39	14.26	17.38	14.97	14.97	14.79	15.85	16.39	14.47
Fe2O3	1.48	0.01	1.70	2.48	1.81	1.72	5.34	2.50	1.19	2.03	3.01	5.25	3.72	3.44	8.41
FeO	1.64	2.79	1.10	2.12	2.55	2.05	0.00	1.80	0.80	2.00	2.70	0.00	2.47	2.89	1.67
MnO	0.01	0.01	0.05	0.05	0.06	0.10	0.09	0.08	0.40	0.07	0.10	0.11	0.07	0.12	0.10
MgO	1.47	1.14	1.03	1.15	1.78	1.63	1.41	1.58	0.75	1.93	1.68	1.14	1.51	2.19	9.15
CaO	3.07	1.73	2.82	1.75	3.36	2.76	2.93	2.57	1.77	3.10	3.74	4.51	4.43	4.55	0.55
Na2O	2.55	3.15	3.15	3.27	2.98	2.88	2.52	2.74	3.16	3.63	3.37	3.63	3.34	2.81	0.55
K2O	4.14	4.87	2.74	4.41	2.72	3.62	4.03	3.52	4.81	3.03	2.13	2.88	2.43	2.22	1.48
P2O5	0.15	0.82	0.13	0.16	0.18	1.15	0.26	0.20	0.07	0.15	0.22	0.25	0.27	0.21	0.01
H2O+	0.47	0.36	0.00	0.64	0.00	0.00	0.00	0.00	0.93	0.00	0.41	0.00	0.33	0.89	2.23
H2O-	0.04	0.00	0.00	0.11	0.00	0.00	0.11	0.00	0.62	0.00	0.26	0.01	0.23	0.17	0.01
TOTAL	99.39	99.18	96.32	99.58	98.98	98.95	98.00	97.90	99.94	99.01	98.45	98.09	99.22	99.72	99.38

APPENDIX 3.2.1 continued

	S010	S001	S373D	SK988	S691	S982	S982	S776C	S373	S765D	S776B	S469	S550	SO12P2	S460B	SK452	SK450	S765K	SK178	SK180
	b	b	s	s	sb	b	b	b	b	s	b	b	s	bs	bb	sm	sm	sm	sm	sm
102	68.50	72.21	72.14	72.08	71.57	71.52	70.83	71.17	71.13	70.74	70.73	70.70	70.69	70.64	70.60	61.08	59.50	58.92	57.82	49.42
102	0.49	0.53	0.40	0.35	0.66	0.35	0.40	0.67	0.47	0.50	0.66	0.48	0.37	0.58	0.47	0.74	0.83	1.18	0.80	0.93
1203	14.22	12.93	14.26	13.01	14.65	13.00	14.45	13.06	14.59	14.32	12.72	13.89	13.95	14.95	13.31	15.54	15.82	17.18	15.20	19.68
e203	1.36	1.50	1.65	2.26	1.81	2.52	0.27	1.78	2.11	2.64	2.05	1.32	1.16	3.93	2.96	6.02	6.55	4.85	6.51	8.06
eO	1.25	1.20	0.75	0.00	1.55	0.00	2.09	1.95	0.90	1.05	1.45	1.45	1.30	0.00	0.00	0.00	0.00	3.27	0.00	0.00
nO	0.04	0.00	0.04	0.08	0.01	0.10	0.03	0.07	0.09	0.02	0.08	0.06	0.01	0.08	0.08	0.12	0.15	0.09	0.13	0.16
gO	0.62	0.58	0.70	0.41	1.38	0.57	1.18	1.45	0.70	1.27	0.90	1.17	1.36	0.95	0.47	2.71	2.85	2.23	2.59	2.60
aO	1.58	1.68	1.69	2.25	2.27	2.17	2.11	2.56	2.34	2.68	2.23	2.55	1.91	2.65	2.86	5.52	7.31	4.15	5.64	10.73
a20	2.87	2.94	3.09	3.56	4.13	3.37	3.05	2.52	3.40	3.42	2.82	2.72	3.18	2.41	3.95	3.38	3.40	3.57	3.48	3.82
20	4.85	4.12	4.14	3.84	2.71	4.23	4.43	3.36	3.07	3.23	4.22	3.73	4.29	3.96	3.33	2.43	1.94	1.81	2.14	0.65
205	0.10	0.10	0.06	0.08	0.06	0.10	0.11	0.14	0.09	0.09	0.15	0.10	0.11	0.12	0.13	0.21	0.23	0.24	0.23	0.28
20+	1.43	1.23	0.45	0.00	0.00	0.00	0.48	0.00	0.56	0.00	0.62	0.00	0.00	0.00	0.00	0.00	0.00	0.78	0.19	0.11
20-	0.90	0.83	0.28	0.01	0.00	0.00	0.07	0.00	0.37	0.00	0.40	0.00	0.00	0.04	0.00	0.08	0.08	0.20	2.31	0.84
TOTAL	98.21	99.85	99.65	97.93	100.80	97.93	99.50	98.73	99.82	99.96	99.03	98.17	98.33	100.31	98.16	97.83	98.66	98.47	97.04	97.28

* The symbols below the sample numbers indicate the field classification when the sample was collected: s - Steinkopf Gneiss; b - Brandewynsbank Gneiss; bs - 'mafic' Brandewynsbank Gneiss'; sb - leucocratic Steinkopf Gneiss; sm - mesocratic Steinkopf Gneiss.

APPENDIX 3.2.2 THE NOENOEMAASBERG GNEISS

	S821F	S790	S373B	S540	S324B	S780E	S640B	S947	S583B	S812F	S518C	S549B	S987
SiO2	78.34	77.80	77.75	77.29	76.14	76.04	75.95	75.63	75.55	74.67	73.23	74.20	71.00
TiO2	0.14	0.14	0.20	0.14	0.28	0.20	0.29	0.34	0.13	0.15	0.22	0.74	0.30
Al2O3	11.66	11.77	11.12	11.91	12.63	12.01	12.07	11.86	12.49	12.66	15.14	12.58	15.32
Fe2O3	0.58	0.47	0.37	0.43	0.34	0.71	0.37	0.83	0.03	0.25	0.65	4.03	0.91
FeO	0.30	0.20	0.50	0.40	0.91	0.40	1.00	0.65	0.40	0.07	0.45	0.00	0.60
MnO	0.03	0.01	0.02	0.02	0.04	0.02	0.01	0.02	0.01	0.01	0.02	0.04	0.03
MgO	0.21	0.71	0.22	0.68	0.28	0.32	0.37	0.85	0.15	0.78	0.50	0.71	0.44
CaO	0.67	0.86	0.74	0.73	0.98	1.19	1.09	0.94	0.60	0.43	1.26	1.53	1.16
Na2O	2.34	2.77	3.32	2.88	2.84	2.67	2.38	2.54	2.56	3.01	2.83	2.86	2.86
K2O	3.89	4.64	4.98	3.81	4.88	4.86	4.56	4.77	5.77	5.26	4.20	4.37	5.47
P2O5	0.02	0.02	0.03	0.03	0.04	0.03	0.05	0.04	0.01	0.04	0.04	0.19	0.52
H2O+	0.86	0.00	0.51	0.00	0.27	0.49	0.62	0.00	0.70	0.46	0.53	0.67	0.51
H2O-	0.55	0.00	0.36	0.00	0.61	0.32	0.39	0.00	0.46	0.14	0.63	0.41	0.32
TOTAL	99.59	99.39	100.12	98.32	100.24	99.26	99.15	98.47	98.86	97.93	99.70	102.33	99.44

APPENDIX 3.3 THE KONKYP GNEISS

KONKYP	S851K	S851A	S851C	S851H	S851G	MF-52	NF-53	NF-54
SiO2	68.54	69.02	69.35	69.28	69.47	69.88	70.56	67.80
TiO2	0.82	0.87	0.88	0.68	0.62	0.66	0.64	0.75
Al2O3	14.02	13.37	13.68	13.40	13.73	13.73	13.98	14.39
Fe2O3	5.89	6.03	6.05	5.61	5.22	5.24	4.65	5.16
FeO	0.00	0.00	0.00	0.00	0.00	0.00	0.00	0.00
MnO	0.10	0.10	0.11	0.11	0.11	0.11	0.10	0.14
MgO	1.16	1.20	1.24	0.96	0.87	0.85	0.84	1.28
CaO	2.28	2.27	2.25	1.94	1.88	1.89	1.98	2.73
Na2O	2.16	2.05	1.98	2.18	2.22	2.29	2.55	2.61
K2O	3.58	3.54	3.62	4.01	4.45	4.20	4.00	4.09
P2O5	0.19	0.20	0.20	0.23	0.24	0.25	0.20	0.32
H2O+	0.78	0.73	0.57	0.66	0.58	0.68	0.61	0.75
H2O-	0.05	0.04	0.08	0.40	0.09	0.15	0.13	0.12
TOTAL	99.57	99.42	100.01	99.46	99.48	99.93	100.24	100.14

APPNDIX 3.4 MAFIC METAMORPHITES

	SK093	S964	S965	S968	S969	S479	SK203	SK204	SK419
SiO2	43.12	52.66	45.32	50.46	48.83	41.69	36.04	37.60	46.66
TiO2	0.19	0.86	0.72	1.36	0.85	2.26	1.98	1.49	0.50
Al2O3	3.21	17.00	11.81	16.22	12.27	20.61	20.85	17.51	8.50
Fe2O3	14.23	4.01	5.04	6.41	2.89	16.52	19.20	18.95	11.88
FeO	0.00	7.25	12.15	8.20	7.35	1.00	0.00	0.00	0.00
MnO	0.22	0.19	0.69	0.39	0.24	0.26	0.40	0.50	0.19
MgO	33.50	6.70	11.47	6.60	13.35	4.96	14.69	17.36	24.62
CaO	1.83	9.77	10.52	9.11	11.37	6.15	6.16	3.55	6.71
Na2O	0.00	0.47	0.85	0.80	0.56	1.44	0.96	0.15	0.48
K2O	0.01	0.48	0.41	0.38	0.68	3.19	0.44	0.10	0.08
P2O5	0.03	0.18	0.04	0.13	0.22	0.52	0.19	0.09	0.07
H2O+	1.48	0.53	0.69	0.32	0.35	0.00	0.92	0.85	0.21
H2O-	0.09	0.33	0.49	0.21	0.23	0.00	0.05	0.00	0.07
TOTAL	97.92	100.43	100.20	100.59	99.19	98.60	101.89	98.14	99.96

APPENDIX 3.5 OTHERS

	Orbicular rock	Kinderlê Gneiss	
	SOB1	S686	S654
SiO2	54.39	74.18	74.72
TiO2	0.61	0.28	0.23
Al2O3	24.02	13.12	11.86
Fe2O3	5.75	1.01	0.31
FeO	0.00	nd	0.71
MnO	0.05	0.04	0.04
MgO	1.84	2.15	2.84
CaO	6.81	0.80	0.56
Na2O	3.02	3.01	2.69
K2O	2.43	5.49	5.41
P2O5	0.48	0.06	0.05
H2O+	0.93	0.21	0.31
H2O-	0.00	0.10	0.28
TOTAL	100.09	100.50	100.04

APPENDIX 4: PETROGRAPHICAL DESCRIPTIONS

In this Appendix, a number of metamorphite samples from each tectonic domain is described. The mineral assemblages found in each of the specimens are first tabulated and this is followed by brief descriptions. In some of the cases only one particular aspect of the petrography is mentioned. The relative abundances of the different phases are indicated as follows:

*	= major phase, >10%
+	= minor phase, 1% < + < 10%
-	= accessory phase
R	= major phase of retrograde origin
r	= minor phase of retrograde origin
'*'	= only pseudomorphs of this once major phase is left
Hbc	= colour of the Z-direction of hornblende B - blue-green; I - intermediate; O - olive-green
?	= minor presence inferred but not proven
blank	= not detected.

In the tables, the mineral abbreviations suggested by Kretz (1983) are used, the term 'Ore' (used in the tables and in the descriptions) indicates opaque phases. In the case of the Richtersveld Domain only, the table includes an assemblage-type column ('Ass'). The number in the 'Ass' column indicates to which assemblage-type the sample belongs, according to the classification system used in Chapter 10.2.1.

Where hornblende colour is given in the descriptions, it always refers to the colour of the amphibole in the Z-direction, as observed in thin section.

'Gr. size' indicates grain size distribution. The minimum and maximum values (in millimetres) for the grain sizes are used as follows: the maximum grain size is as measured in thin section or hand specimen, the minimum grain size indicates the lower limit of the grain size distribution which occurs with a frequency such that 90 % of the rock volume is represented by grains of that minimum size or greater, i.e. the small percentage of very small grains normally found, are not considered. The minimum and maximum grain sizes are separated by a minus sign ('-') indicating a seriate grain size distribution. The ampersand ('&') indicates a bimodal grain size distribution and here the median values for the two size populations are given. A single value for the grain size indicates an equidimensional texture.

Where a grain was recrystallized to form a granoblastic polygonal aggregate, the term 'polygonised' is used.

APPENDIX 4.1 THE METAVOLCANITES OF THE RICHTERSVELD DOMAIN

In Appendix 4.1 metavolcanite specimens of the Nous and Tsams Formations are described, mainly from the Richtersveld Domain, but including a few samples from within the Transition Zone (see Figure 10.1). Specimen SK070 described here represents a mafic dyke which transects the Orange River kinematic fabric (Chapter 9) and appears to be undeformed.

	Qtz	Kfs	Plg	Act	Hbe	Bi	Ms	Chl	Ep	Cc	Ore	Ass	Gr. size
SK040	+	*	*			+	+				-	iii	0.2 & 0.6
SK042	*						+	*				iii	1.8
SK043				?	*	+					-	ii	0.6
SK045	+		*		*				+		-	ii	0.5 & 2.5
SK046	+	*	*		-		+	+	+		-	iii	0.2 & 0.5
SK047	*	*	*				+	+		-	-	iii	0.5
SK048	*	-	*		*	*					-	ii	0.3 - 0.6
SK049	*	-	*		*				+		-	ii	0.5 - 1.0
SK055			+		*						-	ii	0.5 - 1.0
SK057	*		+				*	*	*		-	i	.05 - 0.1
SK060	*		+				*	*	+		+	i	.05 - 0.1
SK061	*		*			*			*			ii	0.3 - 0.1
SK062	*	+	*			*			*	-		ii	0.2 & 1.5
SK063	*	+	*				+	*	*		-	iii	0.2 & 2.5
SK064	*		*	+				*			-	iii	0.2 & 1.0
SK065	*		*	+				*	+		-	iii	0.2 & 0.5
SK070	*		*		*			+	+	-	-	ii	0.1 - 0.3
SK072	*		*		*	-	-	-	-		-	ii	0.5 - 1.0
SK073	*		*			*		-	+		+	iii	0.2 & 1.2
SK391	*		?				*	+		+	+	i	.005 & 0.2
SK392	*		*				*			+	-	i	.005 & 1.7
SK393	*		*			+	*			+	-	i	.005 & 1.0
SK394	+	?	*	*		*			+		-	i	.005 -.02 & .06
SK395	*	?	+			*					-	i	.02 - .04
SK396	*		?			+		+	-			i	.005 - .30
SK397	+		*	*		*			+		-	i	.005 - .02
SK398						*	+				-	i	.002 - .01
SK399	*		?			*	*	*			+	i	.002 & 0.2
DRL040	*		*		*	*			+		+	ii	
DRL099	*	-	*		*	*			*		+	ii	
DRL140	*		*		*	*			+		+	ii	
DRL154	*		*		*			+	+		+	ii	

SK040 Metarhyodacite, contains prograde brown biotite and two feldspars, with skeletal retrograde muscovite.

SK042 Retrograde chlorite mimetic after biotite.

SK043 Hornblende zonation: pale centres, green rims.

SK045 Skeletal hornblende, apparently in equilibrium with Ep.

SK046 Skeletal muscovite in fine-grained metatuff.

SK047 Plagioclase partially saussuritized.

SK048 "Normal" amphibolite.

SK049 Fine-grained, quartz rich biotite gneiss.

SK055 "Normal" amphibolite.

SK057 Very fine-grained metadacite. Chlorite is concentrated in clusters while the other phases are uniformly distributed. All phases are randomly oriented. A faint centimetre scale banding is defined by the spatial distribution of the phases.

SK060 Mineralogically similar to SK057, but with a penetrative foliation defined by the preferred orientation of muscovite and flattened chlorite clusters.

SK061 Quartz in relict amygdales underwent strain induced recrystallization.

SK062 Relict quartz & plagioclase phenocrysts show strain induced recrystallization and neomineralization.

SK064 Actinolite is broken down to chlorite; the actinolite grains have thin irregular reaction rims where in contact with the chlorite. Quartz is highly strained. Chlorite shows slight discolouration in crenulation cleavage traces.

SK065 Similar to SK064.

SK070 The mineral assemblage is dominated by hornblende with a blue-green colour similar to other samples of assemblage type (ii). The plagioclase is partially saussuritized. Some of the larger grains have hypidiomorphic forms typical of igneous plagioclase. Internally they are largely replaced by a granoblastic aggregate of quartz and new plagioclase. Chlorite occurs as a fine micaceous replacement product of an unidentified phase (pyroxene?) which had apparently been largely replaced by hornblende at an earlier stage. The general texture of the rock is fine-granoblastic and no strain effects are apparent.

SK072 A quartz rich amphibolite. The hornblende is blue-green and defines a continuous foliation. Prograde epidote forms relatively large (0.2 millimetre) grains associated with the hornblende. Plagioclase is partially saussuritized, yielding a second generation of very fine-grained (0.002 millimetre) epidote and somewhat coarser (0.1 millimetre) white mica. Chlorite occurs as a retrograde replacement product of biotite.

SK073 Characterized by porphyroblasts of ore. Foliation is defined by the distribution of biotite clusters rather than orientation of individual grains. Minor replacement of biotite by chlorite.

SK391 Similar to SK392 but more deformed. Chlorite occurs as small porphyroblasts; relict quartz phenocrysts are deformed; relict plagioclase (e.g. phenocrysts) are replaced by muscovite and calcite.

SK392 This is a sample of quartz porphyry which shows relatively little strain effects. Centimetre scale primary banding is defined by differences in mica content associated with slight differences in general grain size (the bands with a lower distribution density of mica are slightly coarser-grained). The rock consists for most part of a very fine-granoblastic (about 0.005 millimetre) matrix of white mica (about 30% by volume) and quartz. Some albitic plagioclase may also be

present (the felsic crystals are cryptocrystalline). Small phenocrysts (0.8 to 1.3 millimetre in diameter) of quartz and plagioclase are, for most part, physically intact and undulose extinction is the only indication of strain. Advanced deformation of a minority of the phenocrysts caused recrystallization of the quartz and fracturing of the plagioclase. Dimensional preferred orientation of the white mica in the matrix defines a penetrative continuous foliation which is oriented at a relatively large angle to the compositional banding. On thin section scale, the strain is heterogeneous and a 2 millimetre wide zone of high strain is marked by discoid quartz phenocrysts, arranged in en echelon style to produce a nearly continuous band of recrystallized quartz with a granoblastic texture and an average grain size of 0.1 millimetre. Some of the plagioclase phenocrysts are partially replaced by white mica and calcite. The typomorphic phases in and immediately surrounding the relict phenocrysts are much coarser-grained (0.1 to 0.6 millimetre) then their counterparts in the matrix. While the phenocrysts consist largely of relict igneous phases, the matrix represents complete metamorphic reconstitution.

SK393 High strain and alteration precludes feldspar identification. Biotite forms clusters. Ellipsoidal quartz aggregates (relict phenocrysts ?) impart a domainal foliation.

SK394 This sample is characterized by centimetre scale compositional banding defined by the relative abundances of the different constituent phases. Penetrative continuous foliation is defined by the dimensional and crystallographic preferred orientation of matrix biotite and actinolite. Porphyroblasts of actinolite and megacrysts of plagioclase (relict phenocrysts ?) show various stages of strain. The actinolite porphyroblasts (light green, non pleochroic, composition confirmed by electron micro probe) are generally intact and the foliation is warped around them. Plagioclase megacrysts are, for most part, recrystallized to form a fine-granoblastic texture with irregular grain boundaries. Pressure shadows consist of unstrained quartz with minor amounts of 'new' biotite and actinolite.

SK395 Very fine-grained mica schist, similar to SK393.

SK396 Seriate grain size distribution and irregular grain boundaries indicate a state of high strain.

SK397 Mineralogically the same as SK394. Pronounced crenulation cleavage indicates prolonged shear deformation. Differentiation accompanying crenulation involved mainly the redistribution of quartz. Small actinolite porphyroblasts have grown across the crenulation cleavage.

SK398 A virtually monomineralic, fine-grained biotite schist. The biotite has a light green colour.

SK399 Mafic metatuff (?), characterized by millimetre to centimetre scale compositional banding. Very fine-grain size prevents the recognition of feldspar. Ore forms small porphyroblasts (0.2 millimetre) while aggregates of biotite and muscovite attain the same grain size. A penetrative continuous foliation, defined by the very fine-grained phases, is

oriented at an angle to the primary banding.

SK400 See description in Chapter 10.2.1

APPENDIX 4.2 GROOTHOEK THRUST ZONE

APPENDIX 4.2.1 CALC-SILICATE ROCKS

	Qtz	Kfs	Plg	Act	Hbe	Bi	Ms	Chl	Ep	Cc	Ore	Gr. size
SK001	*		*						*		+	0.1 - 2.5
SK086	*		*		*				+		+	0.1 - 1.0
SK115	-		*		*		'*'		'*'		+	0.4 & 2.5 - 12
SK133	*	-	*		*				-		-	0.1 - 1.0
SK086	*		*		*				+		+	0.1 - 1.0

SK001 Banded (quartz bands alternating with epidote - plagioclase bands) on millimetre scale; large and small magnetite grains are randomly distributed.

SK086 Fine-granoblastic texture; the epidote forms crystal clusters.

SK115 Large poikiloblastic porphyroblasts of blue-green hornblende in a fine-granoblastic polygonal matrix of plagioclase. The plagioclase is approximately 50% replaced by clinozoizite and white mica. The opaque phase forms subhedral grains up to 2.5 millimetre in diameter.

SK133 Fine-granoblastic hornblende (blue-green) plagioclase rock. The rock is further characterized by the presence of K-feldspar and a significant volume of sphene.

APPENDIX 4.2.2 AMPHIBOLITES

	Qtz	Plg	Hbe	Bi	Ms	Chl	Ep	Ore	Gr. size
SK006	+	*	*	'+'		+	*	-	0.2 - 1.2
SK092	+	*	*	+				-	0.2 - 2.0
SK098		*	*				-	+	.02 & 0.4
SK114	+	*	*				r	+	0.1 - 1.2
SK134					+	*	*	+	0.1 - 1.2
SK144	*	*	*	'+'	r	r	r	*	0.1 - 1.5
SK147		*	*	'*'		r	r		1.0 & 20.0
SK159	+	*	*	'+'	-	-	+	+	0.1 - 0.3
SK329		*	*	'-'	-		-	-	0.2 - 0.5
SK330	*	*	*	'+'	-	+	+	-	0.2 - 2.5

SK006 Epidote amphibolite (blue-green hornblende; epidote occurs as relatively large, elongated grains) in which minor biotite is virtually completely replaced by retrograde chlorite. The plagioclase is almost completely replaced by sericite.

SK092 Mafic amphibolite; blue-green hornblende constitutes more than 80% of the volume and defines a continuous foliation because of its dimensional preferred orientation. The hornblende contains inclusions of all the other phases. The

biotite is partially replaced by white mica and chlorite and the plagioclase is virtually completely saussuritized.

SK098 Small porphyroblasts of hornblende set in a very fine-granoblastic matrix of hornblende, saussuritized plagioclase and ore. Epidote occurs as a single discrete grains.

SK114 Amphibolite with largely saussuritized plagioclase. Epidote occurs only as part of the breakdown products of plagioclase.

SK134 A retrograde schistose mafic metamorphite, presumably a metabasite, which consists virtually only of chlorite and epidote. Minor white mica also forms part of the retrograde paragenesis.

SK144 Fine-granoblastic amphibolite with porphyroblasts of quartz, ore and biotite. The colour of the hornblende is blue-green. The plagioclase is completely broken down to discrete epidote and white mica grains and the biotite to chlorite and epidote.

SK147 Porphyroblastic amphibolite (blue-green hornblende porphyroblasts with abundant rounded plagioclae inclusions); biotite is nearly completely replaced by chlorite and epidote. Plagioclase is approximately 50% saussuritized. The opaque phase is partially replaced by chlorite. Sphene is an ubiquitous accessory phase.

SK159 Fine-granoblastic amphibolite with blue-green hornblende. Biotite is replaced by chlorite, plagioclase by discrete epidote and fine-grained sericite.

SK329 Mafic amphibolite with fine-granoblastic polygonal texture. The hornblende colour is intermediate between blue-green and olive-green. Most plagioclase grains are fresh, but complete saussuritization with the development of discrete white mica flakes is found in one zone. Single porphyroblasts of biotite are completely replaced by epidote and chlorite. Sphene is a more abundant accessory phase than ore.

SK330 Although gradational with SK329 in outcrop, SK330 is texturally quite different. Hornblende forms porphyroblasts with rounded quartz inclusions. Quartz also occurs interstitially and as microveins. Total saussuritization of the plagioclase produced discrete epidote and white mica grains of up to 1.5 by 0.5 millimetre in size.

APPENDIX 4.2.3 GNEISSES

	Qtz	Kfs	Plg	Sil	Bi	Ms	Grt	Hbe	Chl	Ep	Ore	Gr. size
SK009	*	*	*		-	+	-				-	1.0 - 3.0
SK010	*		*		*						-	0.6 - 1.2
SK011	*	*	*	-	-	-	-				-	0.5 - 1.2
SK134				-	+	-					-	0.4 - 1.3
SK034	*	*	*		+	-					-	0.4 - 1.3

SK009 Granitic gneiss with medium granoblastic texture. The minor biotite is altered and, together with K-feldspar, partially

replaced by muscovite, resulting in quartz-muscovite micrographic intergrowths. The K-feldspar is characterized by pronounced tartan twinning. The plagioclase (oligoclase according to the Michel Levy method) shows reaction rims of slightly different composition where in contact with K-feldspar. The reaction rim is less saussuritized. Polysynthetic twinning is continous from the core zone into the reaction rim. Garnet occurs as small rounded grains.

SK010 Granodioritic grey gneiss, fine-granoblastic with continuous foliation defined by preferred orientation of biotite. Plagioclase composition is oligoclase (as determined by the Michel Levy method).

SK011 Fine-granoblastic granitic gneiss with accessory sillimanite and garnet. The sillimanite is replaced by muscovite for most part, especially where it was in contact with K-feldspar. A few sillimanite needles are preserved intact as inclusions in quartz. The garnet occurs as a few isolated rounded grains. The biotite is largely replaced by chlorite and white mica. The plagioclase is unaltered for most part. It shows reaction rims with K-feldspar, observed under crossed nicols as thin rims with extinction angles which differ from that of the rest of the plagioclase grains. Twinning lamellae continue from the central parts of the grains into the reaction rims. Minute myrmekitic intergrowths are common on the reaction zones. The K-feldspar displays pronounced tartan twinning.

APPENDIX 4.2.4 THE MICA SCHISTS OF THE GROOTHOEK FORMATION

	Qtz	Plg	Bi	Ms	Sil	Chl	Ep	Ore	Trm	Gr. size
SK002	*	-	*	*				-	-	0.4 - 1.3
SK003			?	*						0.001-0.1
SK007	*	*	*	*				-		0.2 - 3.0
SK008	*	*	*	*				-		0.2 - 3.0
SK078	*	*	+	*				+		0.3 - 2.2
SK107	*	*	*				+	+		0.1 - 1.2
SK128	*	*	*	*				+		0.5 - 1.0
SK137	+	*	*	*				+		0.1 - 2.5
SK138			*	*	*				-	0.1 - 1.2
SK141	-			+						up to 0.3 x 1.2
SK145	*	*	+	-	-			-		0.1 - 1.2
SK151			+	*	*			*		0.1 - 0.8
SK154	*	+	*	*	+			-		0.4 - 2.0
SK155	*	+	*	*	*			-		0.2 - 5.0
SK158			*					+	+	0.5 - 3.0
SK160	*	?	*	*				+		0.5 - 5.0
SK325	*	*	*	*				-		0.2 - 1.4
SK326	*	*	*	-				-		0.2 - 1.4

SK002 Biotite is 90% altered and, in some places, replaced by fresh, randomly oriented muscovite. The plagioclase is completely replaced by sericite. Quartz embayments characterize quartz-mica grain boundaries. The sericitization also affected the 'new' muscovite and is clearly related to some later retrogression.

SK003 Completely sericitized rock.

SK007 Medium-grained mica schist. The biotite is 50% altered and 50% replaced by muscovite. Sericitization clearly post dates muscovitization and is virtually complete in plagioclase.

SK008 Same as SK007.

SK078 Muscovite 'metaquartzite'; fine-granoblastic texture defined by quartz and plagioclase (the latter largely saussuritized), with the foliation defined only by the orientation and distribution of the muscovite. Biotite is partially broken down, probably to very fine-grained chlorite, and partially replaced by the muscovite.

SK107 Biotite-plagioclase-quartz schist with centimetre scale banding defined mainly by grain size. A penetrative fabric is defined by the preferred orientation of biotite in the finer-grained bands. In the coarser-grained bands (+/- 1 millimetre) the biotite is randomly oriented. A relict fabric, parallel to that of the first mentioned bands, is defined by helicitic inclusions of small elongated opaque grains within all three major phases.

SK128 Quartz-muscovite schist with lesser volumes of biotite and plagioclase. The biotite and muscovite are intimately intergrown parallel to the cleavage; decussate texture is developed in small elongate aggregates. The biotite is partially replaced by muscovite and, in a few places, younger muscovite crystal transect older biotite-muscovite intergrowths. Quartz embays both micas. Biotite is further partially replaced by accessory chlorite. Minor kinking of the mica flakes is common.

SK137 Plagioclase-muscovite-biotite schist. Elongate monomineralic quartz aggregates help define the planar fabric. The biotite is partially replaced by muscovite with resultant decussate intergrowth. A second phase of retrogression is represented by sericite replacing both abovementioned micas and by internal alteration of the biotite.

SK138 Sillimanite-mica schist; the sillimanite forms discrete crystals. Two phases of retrogression are recognized: (i) The biotite and muscovite forms patches and veins of decussate intergrowth which transect lenticular sillimanite grains as well as the penetrative fabric defined by the sillimanite and the opaque phase, (ii) sericitization postdates the sillimanite as well as the micas.

SK141 Sample from a massive sillimanite body, similar to those economically exploited in Bushmanland. It consists almost completely of fibrolite.

SK145 Fine-granoblastic quartz-plagioclase schist with up to 10% biotite and minor sillimanite clusters and muscovite. The latter occurs as a replacement product of biotite and sillimanite. An opaque phase concentrated at the contacts between muscovite and biotite grains and fine opaque specks distributed through the muscovite indicates that the iron (and/or magnesium) components of the biotite could not be accommodated by the muscovite.

SK151 Muscovite schist with relatively high opaque mineral content. The muscovite includes sillimanite and is intergrown in a

decussate fashion with lesser biotite. Late sericitization cuts across all other phases.

SK154 Quartz-mica schist; the biotite and muscovite are concentrated in irregular bands where they form decussate texture. Sillimanite is also concentrated in these bands and is transected by muscovite. Discrete inclusions are intact, but interstitial sillimanite is broken down to sericite. Plagioclase is partially saussuritized.

SK155 Similar to SK154, but in this case the schistosity defined by biotite, sillimanite, opaque grains and, to a lesser extent, muscovite, is folded on the scale of the thin section. The individual mica crystals are kinked in the fold hinges. The effects of the folding appears to be less severe in the muscovite and first impressions are that the white mica is post-kinematic with respect to this deformation. Closer examination reveals, however, that, although the white mica is randomly oriented with respect to the schistosity, it is internally strained, and, where it is properly oriented within fold hinges, it is folded as well. Some chloritization of biotite and sericitization of sillimanite superseded the muscovite blastesis.

SK158 Muscovite schist. Dark brown staining along the cleavage traces of some muscovite grains indicate that biotite was replaced. The muscovite is folded with the fabric defined by the elongate opaque grains and was annealed after folding to produce subgrains which follow the micro-fold traces in a stepwise fashion. The muscovite is replaced for approximately 30% by sericite. Tourmaline occurs as isolated porphyroblasts, partially replaced by late sericite.

SK160 Coarse-granoblastic quartz-biotite rock which had undergone retrogression in two stages namely (i) muscovitization and (ii) sericitization.

SK325 Quartz-mica schist with micro folding defined by the distribution and orientation of the mica flakes. The individual grains are undeformed. The biotite and muscovite are intergrown in parallel fashion. Some replacement of biotite by muscovite is indicated by opaque concentrations at the muscovite rims. Accessory amounts of chlorite replaced biotite in places.

SK326 Biotite schist with an accessory amount of muscovite. The latter occurs in the form of small replacement patches (with a murky appearance due to very fine-grained opaque residual material), as well as in the form of clear flakes coexisting with biotite with no signs of replacement.

APPENDIX 4.2.5 MASSIVE ALUMINA-RICH ROCKS

	Qtz	Plg	Crd	Ged	Stt	Bi	Ms	And	Sil	Grt	Chl	Ore	Grain size
SK017	-	*	*	+	*	+	*			+	*		0.1 & 2 - 6
SK075	-		*		+	-	*	+		-	*		0.1 & 2 - 6
SK079	*	+	*		+	+				-	+		< 1 & 3 - 6
SK080	*	+	*		*	*				-	+		0.3 - 3 & >10
SK082	*	-	*		+	+				+	+		0.2 - 6
SK090	*	*	*		+	*				-	+		0.2 - 2.5
SK100	*	*	*		-	-	+			-	+		1.0 & > 10
SK102	+	-			*	+	*	-			+		0.2 & > 20
SK103	*				*	-	*	+			+		0.1 - 12
SK104	*	*			'*'	+		+		*	+		0.1 - 15
SK105	*	*	*			-	*	-		-	*		0.5 & 2 - 20
SK106	-	?	?		'*'	r			*	*	+		0.5 & 2.5
SK108	*		+				*	+			*		0.2 - >15
SK111	*	*		*	+					+	+		0.2 - .5 &>20
SK121		*	?	*						+	+		0.2 - .5 & 3
SK123	*	*	*		*					-	-		0.2 - 10.0
SK140	+	*	*		+					-	*		0.05 - 10.0

SK017 Coarse-grained, dark coloured rock with no obvious foliation. The cordierite and andalusite are the dominant phases, followed by biotite and plagioclase. The biotite is dark brown. The staurolite occurs as small grains included in cordierite and andalusite. The opaque phase is mainly magnetite. Muscovite and chlorite are associated in patches which replace biotite and cordierite. The cordierite, andalusite and plagioclase are furthermore partially replaced by sericite and other fine-grained secondary products.

SK075 Massive cordierite rich rock with lesser quantities of sillimanite (fibrolitic), andalusite (small rounded grains included in cordierite), ore (mainly magnetite), biotite (1 millimetre sized interstitial grains) and quartz (small interstitial grains). Accessory muscovite and chlorite of retrograde origin, are concentrated in clusters.

SK079 A fine-granoblastic quartz rich rock with skeletal porphyroblasts of cordierite. Evenly distributed plagioclase and opaque grains form part of the granoblastic texture. Lesser biotite and accessory muscovite define a vague foliation owing to their distribution and orientation. The biotite and muscovite are spatially associated and form a decussate intergrowth. The muscovite, however, partially replaced the biotite as described below for SK080. The cordierite is virtually completely replaced by fine-grained chlorite and other unidentified retrograde products. The plagioclase is partially saussuritized. The biotite has a murky appearance due to internal alteration. In some places biotite and the opaque phase are partially replaced by discrete chlorite grains.

SK080 Medium-grained quartz-muscovite-biotite schist with large (> 12 millimetre) cordierite porphyroblasts. Plagioclase and an opaque phase are present in lesser quantities. The matrix foliation, defined mainly by muscovite, wraps around the cordierite porphyroblasts and, to a lesser extent, around larger quartz and biotite grains. The cordierite

porphyroblasts contain a helicitic fabric oriented at a large angle to the matrix schistosity. The included fabric is largely defined by the forms and orientations of opaque grains, but included muscovite grains are aligned parallel to the helicitic fabric as well. The included muscovite grains have rounded and embayed forms indicating that the cordierite partially replaced the muscovite. The matrix muscovite is intergrown with biotite and with itself in a decussate fashion. Minute biotite flakes are present along cleavage planes in the muscovite. All gradations between these small biotite flakes and stringers of opaque material are found, indicating that some replacement of the biotite by the muscovite has taken place. The cordierite is almost completely pinitized, the plagioclase partially saussuritized. In places biotite is replaced by discordant patches of chlorite while in other cases the retrograde chlorite forms pseudomorph after the biotite. An unidentifined red-brown by-product of the breakdown process is concentrated in small clusters within the chlorite. Chlorite-muscovite age relations are complex; at some places in the matrix and in the retrograde patches the two phases are intergrown in a decussate fashion, while, generally, the muscovitization of the biotite appears to have preceded the retrograde replacement of the biotite by chlorite.

SK082 Coarse-granoblastic cordierite-quartz-muscovite schist. Completely pinitized cordierite grains of variable size are rich in poikiloblastic inclusions of all other phases. Muscovite rich stringers anastomose around porphyroblasts to yield a vague foliation. Biotite-muscovite-chlorite relations are as in SK080.

SK090 A medium-granoblastic quartz-muscovite-schist with evenly distributed plagioclase (only slightly saussuritized, An 20 - An 30), cordierite (completely pinitized) and biotite. Textural relations between muscovite, biotite and chlorite as in SK080.

SK100 Pinitized cordierite porphyroblasts (> 70 % per volume) and a few andalusite porphyroblasts are contained in a quartz - plagioclase (An 30 - 40) matrix with accessory micas and chlorite concentrated in layers. The orientation and distribution of opaque grains define a penetrative planar fabric, helicitically included by all the major phases. Breakdown of andalusite to sericite is dominant around such inclusions.

SK102 The thin section studied is cut through one large porphyroblast of andalusite which contains the rest of the listed phases, except for cordierite, as poikiloblastic inclusions. Matrix cordierite was identified in hand specimen. The distribution and orientation of the opaque grains define a helicitic fabric.

SK103 Elongate andalusite porphyroblasts include biotite, quartz and opaque grains. The form and distribution of the andalusite together with the opaque grains define a penetrative foliation. The biotite grains included in the andalusite are randomly oriented, but those in the matrix tend to be aligned parallel to the foliation. Sillimanite occurs in the form of small clusters, fibrolitic in places. Such small clusters occur within andalusite porphyroblasts,

but most are part of the matrix. The sillimanite shows no spatial association with any particular phase. The muscovite occurs as single grains, intergrown with biotite in a decussate fashion and as flakes parallel to the biotite cleavage, where residual opaque material indicates that the biotite is partially replaced by the muscovite.

SK104 Highly retrogressed quartz-plagioclase-biotite rock; virtually all biotite replaced by chlorite; plagioclase about 75% saussuritized, the resultant epidote and white mica forming grains > 0.1 millimetre.

SK105 Elongate andalusite and cordierite porphyroblasts include a large volume of small opaque grains, collectively defining a penetrative foliation. Quartz and plagioclase form a granoblastic polygonal matrix. Sillimanite occurs as small prismatic grains, both included in andalusite and as part of the matrix. Muscovite is associated with retrograde chlorite which replaced cordierite in places. The cordierite is only partially pinitized and the plagioclase is generally fresh. In places, however, the plagioclase is completely replaced by relatively coarse-grained white mica flakes and epidote. Accessory tourmaline is present in the matrix.

SK106 The specimen consists of subhedral garnet porphyroblasts (partially replaced by chlorite along fractures) set in a matrix of completely broken down plagioclase (?) now represented by white mica and relatively large epidote grains. Biotite is virtually completely replaced by chlorite in a pseudomorph fashion.

SK108 An andalusite-quartz-sillimanite-ore rock with accessory cordierite (completely pinitized) and tourmaline. A few small rounded zircon grains were also noticed. The total absence of mica is notable. A penetrative planar fabric is defined by the forms and orientations of all the phases: large porphyroblasts of andalusite have elongated forms and they include elongate quartz and opaque grains; interstitial quartz, sillimanite grains and fibrolitic clusters are all elongate and aligned parallel to each other. The sillimanite and andalusite are in direct contact in many places, although commonly some quartz is present between the two aluminium silicates. No indication of reaction between the aluminium silicates was observed and no age relations are apparent.

SK111 Euhedral orthoamphibole (gedrite) porphyroblasts are set in a granoblastic polygonal quartz-plagioclase matrix. Minor biotite and opaque grains define a foliation helicitically enclosed by the amphibole. Large and small grains of chlorite have partially replaced the amphibole and almost all of the biotite. Undulose extinction and slight kinking of the chlorite suggests late deformation.

SK121 A granoblastic polygonal plagioclase matrix with porphyroblasts of orthoamphibole, the latter almost completely replaced by bright green chlorite.

SK123 Pinitized skeletal cordierite porphyroblasts in a plagioclase-quartz-biotite matrix. Minor retrograde chlorite replaced biotite in some places.

SK140 A continuous mass of pinitized cordierite (original grain

boundaries cannot be distinguished) enclosing opaque grains; plagioclase and quartz constitute the matrix. A few biotite porphyroblasts are partially replaced by retrograde chlorite. Strain induced recrystallization reduced the grain size of the plagioclase.

APPENDIX 4.3 THE KONKYP AREA

APPENDIX 4.3.1 CALC-SILICATE ROCKS

	Qtz	Kfs	Plg	Cpx	Hbl	Bt	Grs	Chl	Ep	Clz	Cc	Ore	Gr. size
S787	*	*	*	-	+				-			+	1.1 & 0.4
S789A	*	*	*	-			*		-				2.0 - 1.0
S783	*		*	-	+		-	+	*	*		+	4.0 & 0.5
S817			*				*		+				3.0 & 0.5
S822	*	-	*	*	-				-			-	2.5 - 0.5
S823	*	-	*	*	-				-			-	4.5 - 0.5
S854	-	*	*	-	+				-			-	2.0 - 0.5
S854H	-	-	*	+	-				*			-	2.0 - 0.5
S857A	*		*	+	+							-	1.1 - 0.5

The calc-silicate rock specimens listed above have some common features which need not be repeated in each description below: the plagioclase is generally fresh or only slightly saussuritized. Sphene is relatively abundant (between 1% and 3% per volume) and occurs as small anhedral scattered grains and in clusters. The opaque phase is commonly partially rimmed by sphene. The hornblende colour in thin section is blue-green.

S787 K-feldspar rich calc-silicate rock. The texture is fine-granoblastic with a few porphyroblasts (up to 1.2 mm in diameter) of the hornblende and ore. Diopside occurs as extremely skeletal grains i.e. groups of small grains, which barely touch, but which are optically continuous, define porphyroblasts. Epidote occurs as small scattered grains as well as in the form of small replacement clusters around diopside and hornblende.

SK789A 'Granitized' (?) calc-silicate rock. Skeletal light brown garnets occur in a granoblastic granitic matrix. Diopside occurs as small scattered anhedral grains, at places surrounded by allanite. K-feldspar is microperthitic while the plagioclase is antiperthitic. In isolated cases, small epidote grains are micrographically intergrown with K-feldspar, the intergrowth replacing plagioclase. This K-feldspar is optically continuous with adjacent grains which belong to the rock forming population. Lobate myrmekite is common in the thin section.

S783 Centimetre scale, coarse quartzose lenses alternate with fine-grained mafic streaks forming an anastomosing fabric. The ferromagnesian phases consist of light brown garnet (assumed to be grossularite), hornblende and diopside, all in variable stages of replacement by chlorite and epidote/clinozoizite.

S817 Fine-granoblastic polygonal plagioclase rock with numerous skeletal garnet porphyroblasts. Epidote is evenly distributed through the matrix and many grains have allanite cores.

S822 A fine-granoblastic to medium-granoblastic plagioclase-quartz rock with diopside and accessory hornblende. Epidote occurs as isolated skeletal grains, in some cases associated with K-feldspar, replacing diopside and plagioclase.

S823 Similar to S822 but coarser-grained. The diopside occurs as skeletal porphyroblasts. In extreme cases, individual 'skeletons' are up to 10 mm across, enclose plagioclase, quartz and ore and consisting of less than 20% diopside by volume. Accessory hornblende had partially replaced diopside. Most plagioclase grains show antiperthitic exsolution patches while accessory amounts of K-feldspar are present interstitially, in some cases associated with epidote, having replaced plagioclase.

S854 In the field it is difficult to categorize this rock as either an amphibolite or a metaquartzite. The origin may be complex since the high K-feldspar content suggests metasomatism. The prograde assemblage included diopside, plagioclase, hornblende and K-feldspar. Uncertainty surrounds the status of the hornblende because, to some extent, it replaced the diopside. Retrogression produced interesting features: epidote occurs as thin irregular rims around hornblende and diopside and also in the form of micrographic intergrowths with K-feldspar. These intergrowths are located between plagioclase grains, the plagioclase apparently having been replaced by the intergrowth. Small euhedral grains of a pale, non-pleochroic amphibole, identified as actinolite, is developed at the expense of hornblende.

S854H Fine-granoblastic plagioclase-diopside-epidote rock. The diopside occurs as small randomly distributed grains and as small porphyroblasts virtually completely broken down to epidote. Hornblende occurs as minor patches partially replacing diopside. Epidote is concentrated around the diopside porphyroblasts and is characterized by minute symplektic intergrowths with a leucocratic phase too small to positively identify. Antiperthite patches are common in the plagioclase and presents the only positively identified occurence of K-feldspar

S857A A fine-granoblastic plagioclase-quartz rock with centimetre scale banding defined by the relative abundance of diopside or hornblende. In this specimen none of the retrograde features common to the previously described samples are present.

APPENDIX 4.3.2 AMPHIBOLITES

	Qtz	Kfs	Plg	Cpx	Hbl	Bt	Grs	Chl	Ep	Clz	Cc	Ore	Gr. size
S792	*		'*'		?	?		R	R			+	0.1 - 0.4
S796	*	*	*		*				-			-	0.1 - 0.4
S826	*		*		*				r			-	0.2 - 1.5
S839	*		*		*							+	0.1 - 0.4
S839	*		*		*							+	0.1 - 0.4
S850	*		*		*			+	+			-	0.1 - 0.5

S792 A quartz-rich rock with plagioclase completely replaced by white mica and epidote and the ferromagnesian phase (unclear whether it was biotite or hornblende) completely replaced by chlorite and epidote.

S796 A granoblastic K-feldspar bearing amphibolite with accessory

retrograde epidote.

S826 Fine-granoblastic quartz-rich amphibolite with an accessory amount of cummingtonite. Foliation defined by dimensional preferred orientation of the hornblende. Accessory epidote appears to be related to the epidote product of saussuritization of the plagioclase.

S839 Fine-grained amphibolite with bluish-green hornblende. The plagioclase is completely replaced by sericite. The opaque grains are subhedral.

S850 Fine-grained amphibolite with a penetrative schistosity defined by elongate bluish-green hornblende. Chlorite and epidote are clearly retrograde and partially replace hornblende and plagioclase. The rest of the plagioclase is completely saussuritized.

APPENDIX 4.3.3 GNEISSES

	Qtz	Plg	Kfs	Sil	Bi	Grt	Ms	Chl	Ep	Ore	Gr. size
S781	*	*	*		*	-	-			+	2.5 - 0.2
S782	*	*	*		*	-	-			+	1.0 - 0.2
S812	*	*	*	-	'+'		-	-		-	6.0 - 1.0
S842	*	*	*	-	+		+				4.0 - 1.0
S843	*	*	*	+	-		+				4.0 - 1.0
S851	*	*	*		*		+			-	5.0 - 2.0
S852	*	*	*		*		+			-	5.0 - 2.0

S861 Konkyp Gneiss with relatively small grain size and a seriate grain size distribution. The distribution and orientation of the biotite and the felsic phases define a penetrative anastomosing foliation. Quartz grains are deformed (low angle subgrain boundaries), but the rest of the phases are essentially strain free. K-feldspar displays pronounced tartan twinning. Plagioclase is only slightly saussuritized. Approximately 5% of all biotite is replaced by muscovite, the latter containing opaque stringers, the excess mafic component of the replaced biotite.

S782 Fine-grained biotite gneiss, a xenolith in the Konkyp Gneiss. The texture is fine-granoblastic with a poorly developed foliation defined by the orientation of biotite grains. Mineralogically the same as S861.

S812 Coarse-grained sillimanite-bearing quartzofeldspathic gneiss ('pink gneiss'). The sillimanite occurs as minor fibrolite concentrations. Where it is in contact with K-feldspar, it is replaced by sericite. The biotite is almost completely replaced by chlorite. Large K-felspar grains are partially replaced by muscovite.

S842, S843 & S844 The three specimens are similar except for a higher sillimanite content of the S843. K-feldspar is the most abundant phase in these muscovite bearing gneisses. It displays pronounced tartan twinning. The sillimanite is included in K-feldspar, also in quartz. Fibrolitic interstitial concentrations are totally replaced by muscovite which had overgrown all other phases and displays symplektic

intergrowths with quartz. Biotite is partially replaced by muscovite.

S851 & S852 Coarse biotite granite with examples of muscovite having replaced biotite with resultant opaque stringers along the new muscovite cleavage.

S840 The specimen is coarse-granoblastic, consisting of >50% K-feldspar (pronounced tartan twinning), saussuritized plagioclase (in many cases with a film of quartz between it and the K-feldspar), quartz, minor garnet (anhedral, skeletal) and muscovite.

APPENDIX 4.3.4 METAPELITES

	Qtz	Plg	Kfs	Sil	Bt	Grt	Ms	Ore	Gr. size
S799	*	*		+	*		+	+	2.5 & 0.5
S808	*	*	*	+	*		+	-	2.5 - 1.0
S809		*		*	*				1.5 - 0.5
S810	+	*		+	*		+	-	0.5
S830	*			+	-		+		4.0 - 1.0
S831	*	-	-	+	-		+	+	3.0 - 1.0
S832	*	-	*	+	-		*	-	7.0 - 1.0
S834	*			*	-		-	*	2.0 - 1.0
S835	*	*	*	*	+		-	*	3.0 - 1.0
S846	*	*	-		*		+	-	1.0 - 0.5
S848	*	-		+	+		-	-	10.0 - 4.0
S800	+	with about 20% graphite							1.5 - 0.5

S799 Fine-grained biotite sillimanite schist with a penetrative high strain planar fabric; skeletal opaque porphyroblasts are flattened. Late retrograde muscovite porphyroblasts, which replaced biotite, are superimposed on the schistosity.

S808 Medium-granoblastic biotite sillimanite gneiss with retrograde muscovite porphyroblasts. Strain effects on the muscovite indicate late deformation.

S809 Sillimanite-biotite-plagioclase rock with no retrograde effects.

S810 Biotite-sillimanite schist with a high plagioclase content. Sillimanite occurs as prismatic needles and fibrolite mats and is partially replaced by sericite. It is spatially associated with the biotite and, together, these two phases define a penetrative schistosity. Skeletal muscovite porphyroblasts have overgrown all other phases and the schistosity.

S830 Metapsammite consisting of elongate quartz grains with needle-like sillimanite, interstitial for most part, but also included in the quartz, together defining a penetrative schistosity. Quartz self-boundaries are serrated, indicating late adjustments. Muscovite has overgrown some patches of sillimanite; quartz-muscovite symplektite is common.

S831 Similar to S830, but with some plagioclase and K-feldspar. Sillimanite was not found in contact with K-feldspar.

S832 Coarse-grained muscovite schist with pronounced micrographic

quartz-muscovite intergrowths. The muscovite forms large porphyroblasts with inclusions of sillimanite. Quartz-muscovite intergrowths range from minute symplektic to the form of skeletal muscovite grains. K-feldspar shows pronounced tartan twinning. Where fibrolite mats are in direct contact with K-feldspar, the sillimanite is replaced by sericite. Biotite is included in and partially replaced by muscovite.

S834 Sillimanite schist with a relatively high ore content.

S835 Sillimanite schist; discrete sillimanite needles occur across K-feldspar-quartz grain boundaries with no signs of alteration where in contact with the feldspar. Muscovite porphyroblasts include all other phases and form symplektic intergrowths with quartz.

S846 A fine-grained biotite schist with advanced sericitization.

S848 A coarse-granoblastic metaquartzite with minor biotite-sillimanite clusters which occur interstitially. Some sillimanite is also included in the coarse quartz grains. In some of the sillimanite-biotite clusters zircon is concentrated and in one case twenty rounded zircon grains were counted, being on average 0.05 millimetre in diameter.

S800 Quartz-graphite schist; the quartz grains are flattened and forms part of a penetrative planar fabric.

APPENDIX 4.4 THE EENRIET MOUNTAINS

APPENDIX 4.4.1 AMPHIBOLITES

	Qtz	Kfs	Plg	Cpx	Hbe	Bi	Grs	Chl	Ep	Clz	Cc	Ore	Gr. size
S283A	*		*		*	-		+				-	0.1 - 0.9
S290b	*		'*'		'*'			*	*			+	0.4 - 1.1
S736	-		*		*							+	0.3 - 1.5
S757	*		'*'			*		*	+			+	0.2 - 1.3
S661	*		'*'		*	*		+				+	0.5 - 1.1
S662	*		*		*							*	0.5 & 2.5
S689	+		*		*							+	0.1 - 0.7
S760	*		'*'		'*'			*				-	0.3 - 1.0
S761	*		'*'		*	+						-	0.2 - 1.0
S767c	*		*		*	'+'		+				-	0.2 - 1.3
SK014	*		'*'		*				*			-	0.2 - 1.2
SK295	*		*		*					+		*	0.3 - 0.6
SK470	*		'*'		*	'+'		-	+			+	0.1 - 0.8

S283A Fine-granoblastic polygonal quartz amphibolite. Advanced saussuritization produced discrete epidote and white mica grains. A penetrative foliation is defined mainly by the dimensional preferred orientation of the hornblende.

S290b Retrogressed amphibolite; the hornblende is completely replaced by chlorite, the plagioclase by epidote and white mica. Additional prominent epidote grains are associated with the retrograde chlorite.

S736 A fine-granoblastic amphibolite with a relatively high ore content. The hornblende is blue-green. Sphene is an accessory phase which occurs as small scattered grains. The plagioclase is slightly saussuritized.

S757 Mafic schist with plagioclase completely saussuritized and biotite largely replaced by chlorite.

S661 Schistose amphibolite in which the plagioclase is completely saussuritized, the biotite and blue-green hornblende is partially replaced by chlorite.

S662 Amphibolite with prominent magnetite porphyroblasts. The porphyroblasts are surrounded by leucocratic halos. Hornblende is blue-green. Plagioclase is largely saussuritized.

S689 Fine-granoblastic amphibolite with more than 70% hornblende and subhedral opaque grains.

S760 Completely chloritized amphibolite - all hornblende is replaced by chlorite.

S761 Fine-granoblastic amphibolite with blue-green honrblende. Plagioclase is completely saussuritized and biotite almost completely replaced by white mica. Quartz is concentrated in microveins.

S767C Fine-granoblastic amphibolite with blue-green hornblende. Plagioclase is partially saussuritized and individual epidote grains are prominent. Biotite is almost completely replaced by chlorite.

SK014 Retrogressed amphibolite. All plagioclase is replaced by epidote and white mica. Epidote is concentrated in one zone, suggesting the introduction of epidote along veins. The hornblende is blue-green and unaltered. Sphene is a prominent accessory phase.

SK295 Fine-granoblastic amphibolite (the hornblende is blue-green in thin section) with an estimated 15 volume percent magnetite-dominant opaque grains. Sphene is slightly more than an accessory phase and occurs as randomly distributed anhedral crystals and as rims on some opaque grains. Plagioclase is partially replaced by white mica and clinozoizite (anomolous blue colour under crossed nicols).

SK470 Fine-granoblastic amphibolite (blue-green hornblende) largely retrogressed. The plagioclase is largely replaced by epidote and white mica, the biotite is completely replaced by chlorite and white mica and the hornblende is partially replaced by chlorite.

APPENDIX 4.4.2 ULTRAMAFIC ROCK

	Opx	Cum	Hbe	Ple	Ore	Gr. size
S765	*	*	*	+	+	0.5 - 5.0

S765 A coarse grained ultramafic rock consisting of orthopyroxene and, apparently, two species of clinoamphibole. The orthopyroxene is light pink pleochroic and optically positive! In one thin section a completely colourless amphibole (optically negative) and one which shows a faint green colour (optically positive) are present. The same observations with regard the optic signs could not be repeated in either of two more thin sections from the same outcrop. Large orthopyroxene grains are embayed and partially replaced by the amphibole. In some cases remnants of pyroxene included in the amphibole are in optical continuity, suggesting a passive mode of replacement. Pleonaste and 0.3 millimetre size opaque inclusions are abundant in the pyroxene grains while 0.1 millimetre size opaque inclusions characterize the amphiboles.

APPENDIX 4.4.3 SCHISTOSE METAPELITES

	Qtz	Plg	Kfs	Sil	Bi	Grt	Ms	Ore	Gr. size
S680	*	'*'		'*'	'+'		*	+	0.5 - 2.5
S828		'*'		'*'	'+'		*	-	2.5 - 1.0
S740	*			*				-	1.0 - 2.5
S745	*	*	*	*	+		-	-	0.5 - 1.5
S750	*	+		*	+		'-'	'-'	0.3 - 2.0
S749	*	*		*	+		-	-	0.2 - 1.5
S753	*	*		*	+	-		-	0.2 - 2.0
S756							*	+	.001 & 1.5

S680 Medium-grained quartz-muscovite rock with a random fabric. Patterns formed by sericite reflect pseudomorphic replacement of sillimanite and plagioclase respectively. All size variations exist between fine-grained sericite flakes and muscovite porphyroblasts. The muscovite porphyroblasts are all micrographically intergrown with quartz. Biotite is completely replaced by muscovite; the original biotite outlines are defined by opaque remnants.

S682 Muscovite-sericite schist, similar to S680, but with no quartz. In addition to the pseudomorphs after sillimanite and plagioclase, a very fine-grained and light green compact form of sericite possibly represent replaced cordierite.

S740 Medium-grained sillimanite-quartz schist with an anastomosing foliation; single quartz grains or aggregates of two to five grains have elongate lense shapes and are separated from each other by sillimanite mats.

S745 Sillimanite-biotite gneiss. The feldspar is unaltered. The K-feldpar exhibits pronounced tartan twinning. The sillimanite and the biotite grains are partially replaced by muscovite.

S749 Sillimanite-biotite-quartz schist. The sillimanite occurs in disk shaped clusters which define an anastomosing foliation. About half of the biotite grains are partly replaced by muscovite + ore while in few isolated cases they are altered to chlorite. Accessory zircon grains are spatially associated with biotite and, where they occur as inclusions, the biotite is darkened for about 0.1 millimetre around each inclusion.

S750 Sillimanite-quartz rock, consisting of radial sillimanite clusters in a fine-granoblastic interlobate matrix of quartz, minor plagioclase and biotite. Accessory muscovite and opaque grains are the products of partial biotite breakdown.

S753 Similar to S749, with no muscovite except for minor sericitization of the plagioclase.

S756 Sericite schist; the rock represents total sericitization of a sillimanite-rich schist. The muscovite and ore occur as porphyroclasts. The muscovite is embayed and clearly predates the sericitization.

APPENDIX 4.4.4 MASSIVE ALUMINA-RICH ROCKS

	Qtz	Plg	Kfs	Sil	Bi	Grt	Crd	Ged	Ms	Ore	Gr. size
S290c	+	'?'			*		'*'	*		+	0.5 - 1.0
S290d	-	'?'			+	*	'*'	*		-	0.9 & 5.0
S751	+	+			*	*	*			+	0.5 - 5
S752	+	-			*	*	*			+	0.5 - 7
SK296	-				-	*	*	+		*	0.8 & 20.0
SK297		-				*	*	*		*	1.0 & 20.0
SK300	*	+			*	*	+	+		-	0.5 * 10.0
SK387		-			*	+	*	*		*	0.3 - 0.8

S290b Non-foliated cordierite-gedrite rock with biotite and lesser quartz. The cordierite is completely pinitized and the biotite and gedrite partially replaced by chlorite.

S290d Cordierite-gedrite rock with garnet porphyroblasts. A weak foliation is defined by the dimensional preferred orientation of biotite and gedrite. Concentrations of epidote and white mica suggest the former existence of plagioclase.

S751 Poorly foliated biotite-garnet-cordierite rock. The cordierite is completely pinitized. The garnet occurs as porphyroblasts of up to 5 millimetre across with inclusions of all the other phases. In some porphyroblasts the biotite and opaque inclusions define a helicitic fabric. Most of the biotite grains contain symplectic quartz intergrowths. The plagioclase is unaltered and identified as andesine (Michel-Levy method).

S752 Biotite-garnet-cordierite schist. The foliation is defined by the orientation of biotite and it warps around the garnet to yield an augen texture. The garnet contains many large and small inclusions of all other phases. About 80 % of the cordierite is pinitized.

SK296 Large garnet porphyroblasts in a matrix of fine-granoblastic cordierite with lesser gedrite, biotite and ore.

SK297 A fine-grained to medium-grained anthophyllite rock (displaying decussate texture) with poikiloblastic garnet porphyroblasts. Cordierite is restricted to thin bands (veins?) consisting of one third ore and the rest cordierite. Accessory green spinel (probably pleonaste) and a brown anisotropic phase, too small to optically identify, but similar in appearance to the högbomite found in similar rocks at Dabenoris (Beukes et al., 1986). Plagioclase (partially replaced by white mica) occurs mainly as inclusions in garnet, but a few small grains are present amongst the matrix gedrite.

SK300 Quartz-rich metapelite with a 5 millimetre scale banding defined by variable concentrations of the ferromagnesian phases. All the ferromagnesian phases, quartz and plagioclase are found in contact with each other, but for plagioclase-gedrite. This is probably a question of statistics rather than equilibrium because both latter phases are relatively scarce and some separation is caused by the concentration of phases in bands.

SK387 Fine-grained cordierite gedrite rock with more than 10 volume percent each of biotite and opaque. Garnet forms widely separated porphyroblasts (although they are ubiquitous in hand specimen, only one garnet porphyroblast was found in the thin section). Cordierite grains are only marginally pinitized.

APPENDIX 4.5 THE STEINKOPF DOMAIN

APPENDIX 4.5.1 THE CALC-SILICATE ROCKS

	Qtz	Kfs	Plg	Cpx	Hbe	Grs	Chl	Ep	Clz	Cc	Sph	Ore	Gr. size
S404			*	+		*						-	0.5 - 3.0
S421	*		*	+		+		r					0.1 - 1.0
S422			*			*		r	r			+	0.1 - 0.8
S437	*		*	-		*		r			-	-	0.1 - 1.3
S458			*			*		r	r		-	-	0.1 - 0.5
S460			*	+		*		r	r		-	-	0.1 - 1.0
S465			*	-		*		r	r		-	-	0.1 - 1.0
S513	*		*			*					-		0.1 - 3.0
S521	*		*	*		*		r	r		-	-	0.1 - 0.8
S538	*		-	-	*	*		r	r			-	0.2 - 7.0
S542			*			*		r	r			-	0.1 - 0.8
S570			*	-		*		r	r		+	+	0.1 - 0.5
S571	-		*	*							+	+	0.1 - 0.7
S575	*		*	+		+					-	-	1.0 - 2.5
S618A			*			*					+		1.0 - 2.6
S671			*			*		*			-	-	0.5 - 1.5
S709	*		*	*		*		r	r		-	-	0.1 - 0.8
S721			+	*		*					-		0.1 - 0.8
S723	*		*	-		*		r	r		+	-	0.2 - 1.3
S897	*		*	*		*		r	r		-	-	0.1 - 2.0
S946	*		*			*					-	-	0.1 - 1.2
S006			*	*		*					+		0.1 - 1.5
SK167B	*		*			*		r			-	+	0.1 - 1.2
SK208	+		*	*		*					+		0.2 - 1.7
SK284	*		*	*				r			-	-	0.1 - 1.2

S404 Medium-granoblastic garnet-plagioclase rock with green diopside, partially enclosed by the garnet. Scapolite forms subhedral grains and, texturally, appears to be in equilibrium with plagioclase.

S421 Fine-granoblastic rock with centimetre scale banding. Garnet grains of irregular shape envelop dark green diopside. Epidote occurs as a retrograde product of plagioclase.

S422 Fine-granoblastic plagioclase-garnet rock with distinct opaque grains. Epidote forms coronas around some garnet grains. Clinozoizite occurs as retrograde product along irregular patches.

S437 Similar to S421, with distinct anhedral sphene grains and more advanced retrogression (epidote replaced plagioclase).

S458 Very fine-granoblastic plagioclase-grossular rock with retrograde effects as in S422, but in a more advanced state of retrogression.

S460 Fine-granoblastic plagioclase-grossular rock. The garnet envelops diopside. Minor retrograde epidote and clinozoizite as in S422.

S465 Fine-granoblastic plagioclase-garnet rock. Epidote occurs as retrograde coronas around some garnet grains and as

replacement patches in plagioclase grains, immediately adjacent to the affected garnet grains.

S513 Garnet forms elongate continuous masses, enveloping subhedral plagioclase. Quartz occurs mainly as rounded inclusions in plagioclase.

S521 Fine-granoblastic rock. Green diopside and garnet are not spatially related as in most other cases, but rather define a centimetre scale banding by preferred concentration. Retrograde clusters of epidote and clinozoizite replace plagioclase.

S538 Coarse-grained garnet-quartz rock with olive-green hornblende and relicts of very light green diopside. Minor plagioclase and parts of the pyriboles are replaced by epidote/clinozoizite. The large garnet blasts are poikiloblastic with mainly quartz inclusions.

S542 Fine-granoblastic plagioclase-grossularite rock with minor retrograde epidote

S570 Very fine-granoblastic grossular-plagioclase rock with a relatively high sphene content, mainly associated with the garnet. Diopside grains are bright green. The sample displays a very thin (1 millimetre scale) banding defined by the preferred distribution of the constituent phases. Single aggregates of retrograde epidote and clinozoizite are up to 2 millimetre in diameter and are superimposed on the banding.

S571 Very fine-granoblastic plagioclase-diopside rock with prominent minor ore and sphene. Minor saussuritization of plagioclase. Thin banding is defined by the preferred distribution of the phases.

S575 Medium-granoblastic plagioclase-quartz rock with lesser diopside, grossular and conspicuous sphene and ore.

S618A Coarse-granoblastic plagioclase-grossular rock with conspicuous sphene.

S671 Medium-granoblastic plagioclase-grossular-epidote rock. The epidote is subhedral and many grains have allanite cores. The epidote appears to be in textural equilibrium with garnet and not a retrograde phase. Sphene occurs as small scattered grains with rounded forms.

S709 Fine-granoblastic plagioclase-grossular-quartz-diopside rock with minor retrograde epidote/clinozoizite.

S721 Fine-granoblastic diopside-grossular rock with lesser plagioclase. Continuous masses consisting of about 90% diopside grains, with minor sphene and plagioclase, form irregular bands, alternating with grossular-rich bands.

S723 Medium-granoblastic plagioclase-grossular-quartz rock with distinct subhedral sphene and accessory green diopside, the latter partially enveloped by the garnet. Accessory retrograde epidote.

S897 Fine-granoblastic plagioclase-grossular-diopside rock with minor quartz in the form of a few large grains. The diopside

forms elongate clusters with some individual grains up to 2 millimetre in diameter. Retrograde epidote and muscovite form a few subhedral grains.

S947 Fine-granoblastic to medium-granoblastic plagioclase-grossular-quartz rock.

S006 Medium-granoblastic plagioclase-grossular-diopside rock. The diopside is enveloped or rimmed by garnet. A few grains of an unknown phase is completely replaced by retrograde white mica and some epidote. The adjacent plagioclase, like all the plagioclase, is completely unaltered.

S015 Fine-granoblastic to medium-granoblastic grossular-plagioclase rock with minor sphene. Larger garnet grains are surrounded by garnet free halos, suggesting the growth of larger grains at the expense of others.

SK167B Fine-granoblastic plagioclase-quartz-grossular rock with accessory epidote, apparently of retrograde origin, forming rims around some garnet grains.

SK208 Medium-granoblastic plagioclase-grossular-diopside rock with lesser quartz and conspicuous anhedral sphene grains showing twinning. The diopside is generally enveloped by garnet.

SK284 Fine-granoblastic plagioclase-quartz-diopside rock with distinct anhedral sphene grains randomly distributed.

APPENDIX 4.5.2 THE AMPHIBOLITES

	Qtz	Kfs	Plg	Cpx	Hbe	Bi	Chl	Ep	Clz	Sph	Ap	Ore	Hbc	Gr. size
S036	*		*		*	*				-		-	O	0.2 - 0.6
S093			*		*	+						-	O	0.1 - 0.4
S125			*		*	-						-	LO	0.1 - 0.5
S268	+	+	*		*	+				-		-	O	0.3 - 1.5
S278D			*	-	*							-	O	0.2 - 1.3
S281			*		*	+						-	O	0.6 - 2.0
S396	+	+	*	+	*							+	O	0.2 - 1.2
S388	-		*	*	*							-	O	0.2 - 1.1
S415			*	-	*							-	I	0.1 - 1.1
S418		-	*		*								I	0.1 - 0.9
S432			*		*			-					I	0.1 - 0.9
S453	+		*		*	-		-				-	I	0.5 - 1.5
S456	*	*	*		*	*							B	0.2 - 2.5
S464			*		*							-	O	0.1 - 0.6
S496			*	*	*							-	O	0.2 - 1.3
S507			*		*					-		-	I	0.4 - 2.5
S672	*		*		*	*		*				+	B	0.1 - 1.5
S722			*		*					-		+	I	0.2 - 1.2
S731	-		*		*	-	r	r				-	I-O	0.4 - 1.3
SK210			*		*	*					-		I	0.4 - 1.5
SK240	+		*	+	*							-	O	0.3 - 1.2

S036 Fine-granoblastic biotite-quartz amphibolite. A continuous foliation is defined mainly by the dimensional preferred orientation of the biotite. About one quarter of the plagioclase is saussuritized.

S093 Very fine-granoblastic polygonal amphibolite with slender biotite flakes defining a continuous foliation.

S125 Fine-granoblastic polygonal amphibolite. Single large biotite grains are largely replaced by secondary products.

S268 Fine-granoblastic to medium-granoblastic polygonal amphibolite with no apparent kinematic fabric. Abundant apatite is associated with the mafic phases.

S278D Fine-granoblastic polygonal amphibolite with accessory diopside. Plagioclase is partially saussuritized.

S281 Medium-granoblastic polygonal amphibolite with minor biotite. A foliation is defined by the dimensional preferred orientation of the mafic phases. Apatite is a notable accessory phase.

S396 Fine-granoblastic amphibolite with lesser quartz, diopside and K-feldspar.

S401 Medium-granoblastic biotite amphibolite. A foliation is defined by preferred orientation of mafic phases.

S388 Fine-granoblastic diopside amphibolite with weak foliation defined by hornblende orientation.

S415 Fine-granoblastic polygonal amphibolite with accessory diopside. One occurrence of a very small scale symplectic intergrowth between plagioclase and hornblende was observed.

S418 Fine-granoblastic polygonal amphibolite with a few small diopside relicts surrounded by the amphibole.

S432 Fine-granoblastic polygonal amphibolite with minor saussuritization, in some cases culminating in discrete epidote clusters.

S453 Medium-granoblastic quartz amphibolite. Accessory biotite nearly completely replaced by retrograde chlorite. Small epidote clusters are associated with an opaque phase.

S456 Coarse-grained hornblende-biotite schist with decussate texture, interbanded on centimetre scale with fine-granoblastic granitic rock.

S464 Very fine-granoblastic polygonal amphibolite.

S496 Fine-granoblastic diopside amphibolite; the plagioclase is antiperthitic.

S507 Medium-granoblastic amphibolite with a foliation defined by elongate hornblende clusters. Sphene occurs as discrete grains and as rims around the opaque grains.

S672 Fine-granoblastic to medium-granoblastic quartz-biotite amphibolite with a seriate grain size distribution. Quartz occurs interstitially and as rounded inclusions in plagioclase.

S722 Fine-granoblastic to medium-granoblastic amphibolite with conspicuous opaque grains, rimmed by sphene and surrounded

by leucocratic halos.

S731 Medium-granoblastic amphibolite. Accessory quartz occurs as small rounded inclusions in plagioclase, as part of small patches of myrmekite and, together with chlorite, as replacement product of biotite.

SK210 Fine-granoblastic to medium-granoblastic biotite amphibolite.

SK240 Fine-granoblastic to medium-granoblastic interlobate diopside amphibolite.

APPENDIX 4.5.3 THE MIDDELPLAAT DYKES

	Qtz	Kfs	Plg	Hbe	Bi	Chl	Ep	Clz	Sph	Ap	Cc	Ore	Hbc	Gr. size
S276	+	*	+	+	*	r	r		+	-		-	B	0.1 - 1.8
S392	*	*	*		*	R			+	-		-		0.05- 1.2
S401			*	*	*					-			B	0.5 - 1.4
S403	+	*	+	*	*	r	r		+	-		+	B	0.5 - 2.0
S420			*	*	+								B	0.3 - 1.4
SK212	+	*	*		*		r		+			-		0.2 - 1.2
SK216	+	*	*	*	*		r		+	-	-	-	I-O	0.1 - 1.4
SK218	+	*	*	+	*		R			-	-	-	I-O	0.1 - 1.3
SK219	+	*	*	+	*		r			-	+	-	I	0.1 - 1.2
SK243	+	*	*	+	*		r		+	-		-	?	0.2 - 1.3
SK413	+	*	+	*	*		r		+	-		-	I	0.3 - 1.6
SK502	*	*	+	'*'	R		r		+	-	-	-		0.2 - 1.3

S276 Fine-grained to medium-grained rock with a penetrative foliation defined by the preferred orientation of biotite, hornblende and elongate quartz and feldspar grains. The K-feldspar is perthitic, minor myrmekite is developed on interstitial plagioclase. Epidote is concentrated in clusters, replacing plagioclase.

S392 Fine-grained K-feldspar-plagioclase-quartz-biotite rock with prominent chlorite patches, apparently in place of prograde hornblende. The specimen is refoliated, i.e. it carries two strain fabrics. Relicts of the first foliation, defined mainly by biotite orientation, are preserved in lense shaped microlithons, separated by anastomosing cleavage planes, the latter characterized by mild cataclastesis.

S401 Medium-granoblastic biotite amphibolite with a penetrative foliation defined by the preferred orientation of the mica and the amphibole. Where the mafic phases cluster, decussate texture is developed, with biotite transecting the amphibole. Generally, the hornblende grains meet at triple points.

S403 Medium-grained feldspar-hornblende-biotite-quartz rock. A poor fabric is defined by the distribution and orientation of the mafic phases. The K-feldspar has replaced different plagioclase grains to different extents, beginning with replacement along irregular 'veins' and ending with microcline blasts with irregular plagioclase inclusions. Minor retrograde chlorite replaced parts of the biotite and hornblende. Epidote occurs as irregular clusters. Subhedral sphene and apatite is notable, associated with the mafic

phases.

S420 Medium-granoblasic biotite amphibolite with a penetrative foliation defined by the preferred orientation of the hornblende.

SK212 Fine-granoblastic gneiss with irregular grain size distribution.

SK216 Fine-grained to medium-grained mesocratic rock with a continuous foliation defined by biotite and hornblende. Replacement of hornblende by biotite and by epidote and of plagioclase by epidote, is common. K-feldspar grains contain irregular veins and patches of perthite, partially replaced by epidote and white mica.

SK218 Similar to SK216 with less hornblende and more biotite. K-feldspar-plagioclase relations are of interest: the K-feldspar contains irregularly shaped inclusions of plagioclase and, in some cases, the distinction between plagioclase inclusions and perthitic exsolutions is not obvious. Replacement of the included/exsolved plagioclase leaves K-feldspar blasts with calcite and epidote 'inclusions'.

SK219 Fine-grained to medium-grained amphibolite with replacement effects: small patches of plagioclase are replaced by K-feldspar-epidote micrographic intergrowths; hornblende is replaced by biotite along cleavage traces and by epidote in irregular patches; K-felsdpar embays biotite.

SK413 Medium-grained feldspar-biotite-hornblende rock with a penetrative foliation defined by the preferred orientation of the mafic phases and the elongated forms of the feldspars and quartz. Ubiquitous rounded sphene grains occur interstitially as well as included in the major phases. Epidote occurs as subhedral grains, replacing plagioclase as well as the mafic phases. A number of hornblende grains are altered to a light green mineral, tentatively identified as actinolite.

SK243 Fine-grained to medium-grained gneiss with a penetrative foliation defined by biotite flakes.

SK502 Fine-grained to medium-grained gneiss. Hornblende grains (recognized by its form) are completely replaced by green biotite and minor epidote. The plagioclase is saussuritized. K-feldspar contains plagioclase as poikiloblastic inclusions as well as patch and vein perthite; all partly replaced by epidote, calcite and fine white mica.

APPENDIX 4.5.4 THE NARIAMS METADOLERITES

	Qtz	Plg	Opx	Cpx	Hbe	Bi	Chl	Ep	Clz	Sph	Ap	Ore	Hbc	Gr. size
S005B		*	*	*	*	-						+	O	0.2 - 3.5
S694	-	*	+		*	+						-	O	0.2 - 1.5
S692	-	*	+		*	+					-	-	O	0.2 - 1.1
SK246	-	*	*	*	*							+	O	0.2 - 2.2
SK245	+	*		+	*							+	O	0.2 - 1.6
SK249	-	*	*		*							+	B	0.1 - 1.2
SK251	-	*			*							+	O	0.1 - 2.2
SK252	-	*			*					-		-	I	0.3 - 1.5
SK338		*	*	*	*							+	O	0.1 - 1.5
SK339	-	*	*	*	*						-	+	O	0.4 - 1.4
SK337		*	*	*	*							-	O	0.1 - 1.1
SK464		*	*	*	*	-						+	O	0.2 - 17.0

S005B Medium-grained metadolerite with original igneous texture mainly defined by plagioclase laths. Some pyroxene cores survived, surrounded by hornblende. Most pyroxenes are completely replaced by a granoblastic polygonal aggregate of hornblende with an opaque grain at the centre. Small opaque grains are also concentrated at the boundaries between adjacent hornblende grains. Some hypersthene grains have recrystallized to join the hornblende in equidimensional polygonal aggregates. The plagioclase contains numerous small inclusions, ranging from very small small (.002 millimetre to .05 millimetre). The largest ones were determined by microprobe to be diopside (see SK464 below).

S694 Medium-grained metadolerite, the igeneous texture preserved mainly by plagioclase laths. Pyrooxenes are replaced by hornblende in which relicts of orthopyroxenes are found. Some amphibole grains contain rounded inclusions of quartz, while, in one case at least, the quartz is micrographically intergrown with the hornblende. Reddish-brown typomorphic biotite appears not to be associated with any particular phase.

S692 Similar to S694 but finer-grained.

SK246 Similar to S005B, except for an accessory amount of quartz. The metamorphic hornblende, which replaces the pyroxenes, forms continuous grains instead of aggregates.

SK245 Pyroxene amphibolite with irregular grain size. Except for a few relatively large plagioclase grains and possibly the diopside (amoeboid grains), all phases are typomorphic.

SK249 Fine-grained metadolerite with about half of all igneous pyroxene replaced by brownish hornblende. Quartz occurs as small rounded grains or as occasional symplectic intergrowths with both hornblende and plagioclase.

SK251 Medium-grained metadolerite; the igneous texture still preserved by the plagioclase. Minor typomorphic plagioclase occurs as small rounded inclusions in hornblende. The hornblende, in the form of polygonal aggregates with a seriate size distribution, occupy the areas previously held by the pyroxenes.

SK252 Medium-granoblastic polygonal amphibolite with a foliation defined by the preferred orientation of hornblende and slightly elongate plagioclase. Sphene occurs as conspicuous rounded inclusions in hornblende and as interstitial grains.

SK338 Similar to SK005 but medium-grained. Both pyroxenes have largely recrystallized to form polygonal aggregates with hornblende. The diopside inclusions in the plagioclase laths are conspicuous.

SK339 Medium-granoblastic interlobate amphibolite. A few small K-feldspar grains are also present.

SK337 Fine-granoblastic two-pyroxene hornblende granulite; the rock is essentially indistinguishable from hornblende bearing two-pyroxene granulite specimens from the Ratelpoort Lineament. Only the presence of small diopside inclusion groups in plagioclase is common between SK337 and the other metadolerite samples of the area.

SK464 Apart from grain size, very similar to S005B. The small diopside inclusions in plagioclase are notable; they tend to be aligned parallel to the albite twin lamellae. Some smaller ones obviously amalgamated, leaving halos devoid of inclusions. Toward some grain boundaries, the inclusions increase in size and abundance, in one instance culminating in a graphic intergrowth with the plagioclase host. The inclusion there has the same appearance as adjacent diopside and probe analysis confirm the inclusions to be diopside.

APPENDIX 4.3.3 THE METAPELITES

	Qtz	Plg	Kfs	Sil	Bi	Grt	Crd	Opx	Ged	Ms	Ore	Gr. size
S023C	*	*	+	*	*					r	+	0.1 - 1.9
S23D	-	+		*	*					+	+	0.2 - 2.5
S146	*	*	*	*	*						-	0.3 - 7.0
S260D	*			*	-							0.1 - 3.0
S260H	*	*	*	*	*					-	+	0.1 - 2.3
S261B				*	*						+	0.1 - 1.2
S261L	*	*	*	+	-	-					-	0.1 - 1.1
S522	*				*	*				R		1.0 & 3.7
S535	*	'*'		'*'	'*'	'*'				R	+	1.5 & 4.0
S539	*	'+'		'*'	*	*				R	+	1.5 & 4.5
S579A	*	*			*	*		*	*		+	1.1 & 3.7
S579B	*	*			*	*		*	*		+	1.0 & 2.5
S705	*	*		+	*						-	0.1 - 1.0
S713	*			*	+						-	0.1 - 2.6
SK344	*	*		*	*					-	-	0.1 - 1.1
SK360				*	*					-	+	0.2 - 2.1

S023C Medium-grained sillimanite-biotite schist. The sillimanite forms elongate clusters of discrete needles. The muscovite replaces small patches of the biotite. Sphene is an ubiquitous accessory phase.

S023D Medium-grained sillimanite schist (about 70% modal

sillimanite). Muscovite partially replaces biotite. Opaque porphyroblasts have frayed edges.

S146 Migmatitic rock with coarse-grained granitic leocosomes and sillimanite-biotite schist restites, the latter with complex microstructure. Note the absence of muscovite.

S260D Medium-grained quartz-sillimanite schist with an anastomosing foliation. The sillimanite needles are up to 0.1 millimetres thick.

S260H Medium-grained biotite-sillimanite schist, interbanded on centimetre scale with fine-granoblastic interlobate granitic gneiss. Biotite is partially replaced by elongate patches of ore + muscovite.

S261B Fine-grained biotite-sillimanite schist. Individual sillimanite grains are up to 0.5 millimetres thick.

S261L Fine-granoblastic interlobate granitic gneiss with 0.5 millimetre thick stringers of biotite and sillimanite and a few rounded garnet grains in the 'matrix'.

S322 Retrograde schist in which only quartz, a few garnet porphyroblasts and biotite grains are recognized, the rest is replaced by sericite.

S535 Retrograde schist, minerals listed above inferred from form and mineral characteristics of replacement products, i.e. plagioclase replaced by white mica + epidote, stringers of sericite represent altered fibrolite (small sillimanite needles are preserved in quartz), biotite is (not completely) replaced by chlorite and rounded porphyroblasts of presumably garnet are replaced by a fine-grained and decussate aggregate of chlorite and white mica.

S539 Retrograde schist in which the former existence of plagioclase is deduced from the forms of white mica pseudomorphs. Garnet porphyroblasts are largely intact; their cores are rich in quartz inclusions. The schistosity warps around the porphyroblasts. Biotite is altered and appears green in hand specimen. Under the microscope it is unnaturally dark. Along cleavage traces it is replaced by white mica. White mica, pseudomorph after sillimanite, define an anastomosing schistosity.

S579A Medium-granoblastic interlobate quartz-biotite-hypersthene-gedrite-plagioclase gneiss with garnet porphyroblasts. All phases are in contact and no replacement features are apparent, suggesting that all constitute a single paragenesis.

S579B Mineralogically the same as S579A; a penetrative fabric is defined by the preferred orientation of elongate quartz and plagioclase grains as well as all ferromagnesian phases, except for garnet, the latter apparently resisted flattening and the foliation is bent around the porphyroblasts.

S705 Fine-granoblastic interlobate biotite gneiss with minor fibrolite.

S713 Medium-grained quartz sillimanite schist.

SK344 Fine-grained sillimanite-biotite schist with complex microstructure. Accessory muscovite replaces biotite in small patches.

SK360 Medium-grained sillimanite-biotite schist, the melanosome component of migmatitic metapelite. Opaque grains are conspicuous. Small accessory muscovite grains replace biotite.

APPENDIX 4.6 THE COPPER DISTRICT

APPENDIX 4.6.1 CALC-SILICATE ROCKS

	Qtz	Kfs	Plg	Cpx	Hbe	Bi	Grs	Chl	Ep	Clz	Cc	Sph	Ore	Gr. size
S230B			*	*			-							1.0 - 3.5
S230C			-	*			*							1.0 - 3.5
SK233	*	-	*	*								+	-	0.1 - 0.8
SK401	*		*	*					r			-	+	0.6 & 2.0

S230A Coarse-grained diopside-plagioclase-grossular rock. The garnet forms thin rims around some of the pyroxene grains.

S230B Coarse-granoblastic diopside-grossular rock with accessory plagioclase.

SK233 Fine-granoblastc plagioclase-diopside rock with minor ore and sphene. The diopside is light green. Sphene rims some opaque grains while other anhedral sphene grains are surrounded by radial cracks indicating radio active emission.

SK401 Fine-granoblastic-plagioclase-diopside rock. An opaque phase forms oval shaped porphyroblasts with sphene rims. Individual sphene grains are subhedral. Minor retrograde epidote replaced plagioclase.

APPENDIX 4.6.2 MAFIC METAMORPHITES

	Qtz	Kfs	Plg	Cpx	Opx	Hbe	Oam	Bi	Sph	Ap	Spl	Ore	Hbc	Gr. size
S059	*		*	*	*							+		0.1 - 0.8
S060	*		*	*	*	+		+				+	O	0.2 - 1.1
S061	*		*	*	*	+						+	O	0.3 & 1.3
S267	-		*			*		-				-	LO	0.5 - 1.5
S350			*	*	*	*						-	O	0.3 - 2.0
S351			*	*	*							+		0.1 - 0.3
S964			*	+	*	+		+				+	O	0.1 - 0.8
S965			*	*	*							+		0.1 - 0.4
S969			+	*	*	*		-				+	B	1.0 - 3.0
SK022			*	*		*			-			+	BO	0.4 - 1.6
SK184	*	*	*		'+'	*		*		-		-	B	0.8 - 3.0
SK203			-		+	*	*	+			-	+	O	0.2 - 1.1
SK204			+		*	*	*	-			*	+	L	1.0 & 3.5
SK205			*	+		*							I	0.8 - 1.3
SK222	+		*	*	*	+						+	O	0.2 - 3.5
SK223	*		*	*	*							-		0.1 - 3.5
SK227			*	*	*	*					-	+	O	0.1 - 2.5
SK406			+	*	*	*						-	I	0.3 - 5.0
SK408p			*			*						+	O	0.3 - 0.9
SK408n			*	*	*			+				+		0.4 - 3.5
SK493	-		*	*	*			*				+		0.3 & 15.0
GLC020			*	*	*			*				+		0.2 - 2.8
GLC025		-	*	*	*			+				+		0.3 - 2.7
GLC034			*	*	+	+		*				-	O-B	0.3 - 2.8
GLC051		-	*	*	*			*				*		0.3 - 2.5
GLC055			*	*	*	*		*				+	O-B	0.2 - 2.0
GLC059			*	*	*	+		*				+	O-B	0.2 - 0.5

S059 Quartz-rich, fine-granoblastic two-proxene granulite with nearly 10 modal percent ore.

S060 Fine-granoblastic interlobate two-pyroxene granulite. Pyroxene forms large skeletal porphyroblasts broken up into subgrains which deviate slightly from optical continuity. These skeletal porphyroblasts are elongated and oriented, defining a foliation. The minor red-brown biotite is apparently not associated with any particular phase while the olive-green hornblende has grown at the expense of pyroxene.

S061 Very fine-granoblastic interlobate two-pyroxene granulite with skeletal pyroxene porphyroblasts up to 1.4 millimetre long. Within the micro-domain of the skeletal porphyroblast, the plagioclase inclusions constitute about 60 modal percent and are the same size as the matrix plagioclase. The skeletal porphyroblasts are recognized as such because of the optical continuity of the subgrains. Quartz is concentrated in microveins with diffuse boundaries. Hornblende occurs in millimetre wide bands of amphibolite, i.e. fine-granoblastic hornblende-plagioclase rock with no pyroxene.

S267 Medium-granoblastic hornblende-plagioclase rock with minor biotite and quartz. A penetrative foliation is defined by the dimensional preferred orientation of the hornblende and the biotite.

S350 Medium-granoblastic interlobate hornblende two-pyroxene granulite. The plagioclase constitutes a fine-granoblastic polygonal matrix for poikiloblastic pyroxene blasts of variable size. Hornblende has partially replaced diopside in a minority of cases; for most part the hornblende appears to be in textural equilibrium with the pyroxenes as indicated by numerous pyroxene-hornblende triple junctions.

S351 Very fine-granoblastic polygonal two-pyroxene granulite with about equal volumes of the three major phases.

S964 A fine-granoblastic interlobate matrix of plagioclase with elongate skeletal to poikiloblastic pyroxene blasts. All hornblende blasts observed have apparently grown at the expense of diopside. Red-brown biotite show no preferential association with any particular phase. A penetrative foliation is defined by the dimensional preferred orientation of the mafic phases.

S965 Fine-granoblastic interlobate two-pyroxene granulite.

S969 Medium-granoblastic mafic to ultra-mafic hornblende two-pyroxene granulite with less than 5 modal percent plagioclase. Hornblende occurs as rounded 'inclusions' in some diopside grains, while, in others, the 'inclusions' have amalgamated to form continuous blasts. Plagioclase have embayed forms against the other phases.

SK022 Medium-granoblastic diopside amphibolite.

SK184 Coarse granitic gneiss with brown hornblende and redbrown biotite as mafic phases. Plagioclase is antiperthitic and microcline is perthitic (small patches in each case). Myrmekite is common.

SK205 Fine-granoblastic diopside amphibolite with a penetrative foliation defined by the preferred orientation of all three major phases. The normal accessory phases are not apparent in the thin section studied.

SK222 The specimen is banded on millimetre to centimetre scale. The dominant bands consist of a fine-granoblastic polygonal plagioclase matrix in which pyroxene grains in groups up to 10 millimetre across are optically continuous. The second type of band consists of about 90 modal percent plagioclase (medium-granoblastic polygonal) with lesser quartz and ore. The third type of band consist of hornblende and plagioclase only.

SK223 Quartz-rich thinly banded two-pyroxene granulite. Two millimetre wide pure quartz bands (consisting of a few elongate individual grains) alternate with 5 - 10 millimetre wide bands consisting of fine-granoblastic polygonal quartz-bearing two-pyroxene granulite. Spectacular isoclinal micro-folding lacks axial planar fabric. Individual elongate quartz grains in the hinge ones are folded, but, apart from some undulose extinction, show no internal strain.

SK227 A medium-granoblastic polygonal amphibolite with about 40 volume percent two-pyroxene granulite 'nodules'. Each 'nodule' measures about 7 by 4 millimetres and consists of

two or three skeletal pyroxene porphyroblasts in a fine-granoblastic polygonal plagioclase matrix. Ore grains associated with hornblende are larger than those associated with pyroxene. Accessory green spinel is found with the opaque grains in the granulite 'nodules'. A foliation is defined by the preferred orientation of all mafic phases and the alignment of the elongate granulite 'nodules'.

SK403 Medium-grained mafic to ultramafic hornblende-two-pyroxene granulite. Micrographic intergrowths between both pyroxenes and plagioclase can be compared to the skeletal pyroxene porphyroblasts in the other specimens. The pyroxene in SK403 has the same form, but the plagioclase 'matrix' is a single continuous grain. Hornblende-orthopyroxene relations vary from micrographic to polygonal with clearcut triple junctions.

SK408p Fine-granoblastic polygonal amphibolite with a fairly strong foliation defined by the preferred orientation of the hornblende.

SK408n A vein which transects the foliation in SK408p: Medium-granoblastic polygonal plagioclase-rich biotite-two-pyroxene granulite. A transition zone between the vein (SK408n) and the amphibolite (SK408p) of approximately 1 millimetre wide contains both pyroxene and hornblende.

SK493 Fine-granoblastic to medium-granoblastic biotite two-pyroxene granulite with a diopside-plagioclase vein. In the vein, diopside grains are up to 5 millimetre across, some with small hornblende grains developed along cleavage traces. Vein plagioclase are slightly anti-perthitic (about 2 modal percent exsolution patches). Quartz occurs interstitially as small irregular grains.

GLC020 Medium-granoblastic interlobate two-pyroxene granulite with approximately 15 modal percent red-brown biotite and nearly 10 percent ore. Larger pyroxene grains are surrounded by areas poor in mafic phases, lending the rock a 'flecky'appearance in hand specimen.

GLC025 Similar to GLC020 with the addition of a few grains of microcline. The larger plagioclase grains are antiperthitic, containing a few exsolution patches. The biotite is concentrated directly adjacent to a 5 millimetre wide zone of coarser grain size.

GLC034 Medium-granoblastic interlobate biotite-hornblende two-pyroxene granulite, the orthopyroxene constituting only about 5 modal percent. Slight kinking and bending of twin lamellae and one observed small polygonized patch reflect minor deformation.

GLC051 Similar to GLC025. The microcline grains are more prominent and the opaque content is about 15 modal percent.

GLC055 Banded granulite; centimetre wide two-proxene granulite alternate with 2 millimetre wide discontinuous hornblende-rich bands. Biotite is only partially concentrated into bands.

GLC059 Compositionally similar to GLC034 and GLC055, this granulite

sample is fine-grained and schistose: a penetrative foliation is defined by the alignment of all the constituent phases. Apart from one observed plagioclase grain which is partly 'polygonized', the texture does not reflect any strain induced recrystallization. Indirect evidence of deformation is the fact that groups of pyroxene grains, similar to the groups which define optically continuous skeletal blasts in the other samples, are recognized, but in this sample each small grain is uniquely oriented.

APPENDIX 4.6.3 ULTRAMAFIC ROCKS

	Qtz	Kfs	Plg	Cpx	Opx	Hbe	Oam	Bi	Sph	Ap	Spl	Ore	Hbc	Gr. size
SK203			-		+	*	*	+			-	+	O	0.2 - 1.1
SK204			+		*	*	*	-			*	+	L	1.0 & 3.5

SK203 Fine-granoblastic polygonal two-amphibole rock with lesser biotite and minor hypersthene. Green spinel is conspicuous and occurs randomly distributed.

SK204 Fine-granoblastic polygonal two-amphibole rock with skeletal hypersthene porphyroblasts and abundant green spinel. The hornblende is very pale green while the orthoamphibole is colourless in thin section. Plagioclase is spatially associated with the orthopyroxene and, to a lesser extent with the spinel. A penetrative fabric is defined by the preferred orientation of the amphiboles and the spinel. The hypersthene porphyroblasts appear unaffected by the foliation-forming deformation.

APPENDIX 4.6.4 METAPELITES

	Qtz	Plg	Kfs	Sil	Bi	Grt	Crd	Ore	Gr. size
S058	*		*	+	-		*	+	0.3 - 2.2
S065C	*	*		*	+	*	*	+	0.2 - 1.9 & 10.0
S193	*	+	*	+	+		*	*	0.1 - 0.4
S194A	*		*	+	+		*	*	0.1 - 0.3
S194B	*		*	+	+		*	*	0.1 - 0.5
S200	+			+	*	*		-	1.0 - 12.0
S202	*	*	*	*	*	*	*	+	0.2 - 10.0
S207	*		*	+	+	+	*	-	0.1 - 1.5
S208	*		+	+	+	*	*	*	0.2 - 3.5
S231A	*	*			*	*	*	+	0.3 - 0.6 & 4.0
S231B	*	*		*	+		*	+	0.2 - 0.9
S312	+		*	-	+		*	+	0.2 - 4.0
S378	*	*	*	*	+	*	*	+	0.2 - 3.5
S381	*	*	*	+	-	*	*	+	0.5 & 10.0
SK453B	+	*		-	*	*		+	0.5 & 10.0
SK481	*	+	*	+	+		*	+	0.1 - 0.5
SK479	*	+	*	+	+		*	+	0.1 - 0.9
SK485	*	+	*	+	*		+	+	0.1 - 2.1
SK489	*	*			+	*	*	+	0.2 - 1.5 & 5.0
SK490					*	*	*	+	0.2 - 5.0
GLC002	*			*	*			-	0.2 - 0.9
GLC003	*			*	*			-	0.3 - 1.6
GLC008		*		*	*			+	0.2 - 2.2
GLC012		+		*	*	*		*	0.3 - 10.0
GLC036	*		*	*	-	*	+	+	0.2 - 4.0
GLC040	*		*	*	+	*	+	+	0.2 - 5.0
GNA001	*		+	*	+	*	+	*	0.3 - 0.9 & 5.0
GNA002	*		+	*	+	*	+	+	.05 - 1.0
GNA022	*	*	-	+	+	*		-	0.5 - 7.0
GNA023	*		-	-	*	*		-	0.8 - 8.0

S058 Migmatitic metapelite (stromatic). The leucosome consists of microcline, quartz and minor plagioclase. Myrmekite has replaced small parts of the K-feldspar. The melanosome consists mainly of cordierite with minor biotite and sillimanite, the latter in the form of inclusions and as interstitial grains. A penetrative foliation in the melanosome is defined by the alignment of elongate cordierite blasts and sillimanite laths, parallel to the leucosome,

S065 Garnet porphyroblasts in a sillimanite-plagioclase-cordierite matrix, with clusters of biotite randomly distributed. The garnet contains numerous sillimanite needles and rounded inclusions of cordierite. The sillimanite laths in the matrix are up to 0.5 millimetre thick and 2 millimetre long. The cordierite is partially pinitized. In terms of grain contacts, all the major phases (including biotite) forms a stable paragenesis.

S193 Fine-granoblastic metapelite with interlobate grain boundaries. The K-feldspar is microcline-microperthite. The hand specimen contains radial sillimanite clusters.

S194A Very fine-granoblastic K-feldspar-quartz-cordierite-ore rock

with minor sillimanite and biotite; the rock does not exhibit any tectonic fabric. Accessory green spinel is associated with the ore.

S194B Similar to S194A with elongate quartz-sillimanite clusters, bordered by zones rich in biotite.

S200 Coarse-grained biotite-garnet schist with minor sillimanite laths and accessory ore and green spinel.

S202 Banded metapelite: coarse-granoblastic quartz-plagioclase bands alternate with aluminous schist. The paragenesis in the latter is quartz + sillimanite + microperthite + garnet + cordierite + biotite. The cordierite is pinitized.

S207 Medium-granoblastic quartz-rich metapelite. Quartz self-boundaries are serrated. Cordierite is completely pinitized. The listed phases form a single paragenesis.

S208 Similar to S207, but the cordierite is unaltered for most part. Green spinel is associated with and replaced by ore.

S231A Fine-granoblastic interlobate plagioclase-quartz-cordierite-biotite rock with garnet porphyroblasts. The garnet porphyroblasts are skeletal, the included phase being mostly quartz.

S231B Fine-granoblastic polygonal quartz-plagioclase-cordierite rock with aligned sillimanite laths defining a penetrative foliation. Opaque grains are elongated parallel to the foliation.

S312 Medium-granoblastic K-feldspar-cordierite rock with lesser quartz, sillimanite, ore and accessory biotite. The feldspar is perthitic. Myrmekite is developed on some of the larger exsolved perthite patches.

S378 Medium-grained, penetratively foliated metapelite, with an unusually large number of components as listed above, all seemingly in textural equilibrium. The ferromagnesian phases tend to concentrate in irreglar zones, but clearcut contacts, with no indications of reactions, are found between each phase and each of the other phases. Some cordierite blasts are riddled with sillimanite laths. Sillimanite also occurs as groups of inclusions in garnet, K-feldspar and quartz and as trains of interstitial grains parallel to the foliation. Some sillimanite needles, oriented parallel to the foliation, transect grain boundaries between quartz and feldspar.

S381 Similar to S378, but with biotite not part of the paragenesis; it occurs as an apparent replacement product around ore and along cracks in the garnet.

SK453B Garnet porphyroblasts in a plagioclase-biotite schistose matrix with lesser quartz. Minute sillimanite needles occur as inclusions in the garnet.

SK481 Fine-granoblastic interlobate K-feldspar-quartz-cordierite rock with lesser biotite, sillimanite, plagioclase and ore. Thin banding (average 5 millimetres wide) is defined by variable concentrations of opaque grains and quartz. Biotite quartz symplectite and sillimanite-quartz micrographic

intergrowths indicate late reactions with these phases as products.

SK479 Similar to SK481. The sillimanite-quartz and biotite-quartz intergrowths form patches, apparently superimposed on a matrix consisting of K-feldspar, quartz, cordierite, biotite and ore.

SK485 Migmatitic metapelite; in the thin section leucosome, paleosome, and melanosome components are recognized. The leucosome consists of medium-granoblastic interlobate quartz, microcline-microperthite and antiperthitic plagioclase. Myrmekite is found at some plagioclase-K-feldspar junctions. The paleosome is fine-granoblastic and contains quartz, K-feldspar, plagioclase, biotite and minor sillimanite. The melanosome consists of medium-granoblastic cordierite, partially replaced by biotite and sillimanite, the latter two phases micrographically intergrown with quartz. Opaque blasts are common in both the melanosome and paleosome parts.

SK489 Elongate garnet porphyroblasts in a medium-granoblastic interlobate matrix. The cordierite is completely pinitized and the plagioclase partially saussuritized. A foliation is defined by the dimensional preferred orientation of all phases.

SK490 Coarse garnet-cordierite-biotite rock. The cordierite is unaltered and displays pronounced twinning. The cordierite is internally strained (undulose extinction and low-angle boundaries) and one grain observed is 'polygonized'. Garnet is partially broken up to form subgrains and biotite has apparently grown in resultant openings.

GLC002 Fine-granoblastic biotite-sillimanite schist. The foliation is penetrative and continuous. Quartz grains are elongated parallel to the foliation.

GLC003 Similar to GLC002, but coarser-grained and less penetratively foliated. Some biotite flakes are oriented at an angle to the foliation.

GLC008 Medium-grained biotite-sillimanite schist. Individual sillimanite laths are broken up into smaller subhedral grains with little disturbance of the smaller grains from their original positions.

GLC012 Coarse-grained garnet-biotite-sillimanite schist with approximately 15 volume percent ore. A penetrative foliation is defined by the preferred orientation of all phases (the garnet and opaque grains have elongate forms), although a few biotite and sillimanite grains are not aligned parallel to the rest. Sillimanite occurs as inclusions in garnet as well as interstitially. Between garnet porphyroblasts, biotite and sillimanite are concentrated as decussate clusters (sillimanite transects biotite).

GLC036 Sheared quartzose metapelite. Elongate garnet grains are folded in microlithons, but not broken up. Cordierite (pinitized) are elongated parallel to the shear fabric. Sillimanite grains included in garnet are folded together with the host, but interstitial laths are broken up into subhedral subgrains. Quartz exhibit low-angle boundaries

internally and irregular boundaries externally.

GLC040 Quartz-rich metapelite with a penetrative strain fabric; the quartz grains are elongated and exhibit all of the following strain features: undulose extinction, low-angle boundaries and serrated boundaries between original grains. The garnet grains exhibit strain ratios of at least 6 to 1. Sillimanite laths are orientated parallel to the foliation and/or 'polygonized'.

GNA001 Fine-granoblastic sillimanite-garnet schist with a high ore content. Quartz and feldspar grains are internally strained and have irregular grain boundaries. Sillimanite, biotite and elongate garnet porphyroblasts are aligned to define a penetrative foliation, although some sillimanite laths are orientated at high angles to this fabric. Individual sillimanite laths are broken up into subgrains with low angle boundaries. The garnet porphyroblasts contain numerous small sillimanite needles and many irregularly shaped quartz inclusions. Cordierite is pinitized. The opaque phase consists of a minute regular intergrowth of green spinel and ore.

GNA002 Fine-grained sillimanite schist; the rock is penetratively sheared as indicated by flattened K-feldspar and garnet porphyroblasts (strain ratio at least 6 to 1) and internal strain in quartz, sillimanite and feldspar. Some quartz grains are partially 'polygonized', but genuine mylonitic textures (such as extremely small grain size) are absent. In the case of some garnet porphyroblasts, breakup occurred with the growth of new biotite in the pressure shadows between the subgrains.

GNA022 Coarse-granoblastic quartz-plagioclase-garnet rock with minor sillimanite, biotite and K-feldspar concentrated in zones. Strain features include low-angle subgrain boundaries in quartz and plagioclase and complete 'polygonization' of plagioclase (breakup of grains 5 millimetres in diameter, to a polygonal aggregate of high-angle subgrains, each about 0.3 millimetre across). Most garnet grains appear undeformed (they are subhedral), but those in zones of higher strain are elongate and partially broken up. Some K-feldspar grains are partially replaced by myrmekite.

GNA023 Coarse-grained quartz-garnet-biotite rock with accessory sillimanite, K-feldspar and ore. The biotite (red-brown) is spatially associated with the garnet. Most garnet blasts are broken up into a few smaller grains with biotite filling gaps. There is no apparent difference in colour or structural age between the biotite in the matrix and that amongst garnet subgrains. The quartz is internally highly strained. Subgrains with low-angle boundaries as well as with high-angle boundaries are common. About 10 percent of the garnet and biotite is replaced by chlorite with a slight tendency for radial growth. Individual chlorite blasts of up to 1 millimetre in length are present. Accessory retrograde muscovite occurs as small flakes accompanying chlorite and as a replacement product of sillimanite.

APPENDIX 4.6.5 CORDIERITE-ORTHOPYOXENE ROCKS

	Qtz	Plg	Sil	Bi	Grt	Crd	Opx	Ged	Sap	Sp	Ore	Gr. size
S069				*		*	*		*	-	-	1.5 & 20.0
SK332	*	+		*		*	*				-	0.3 - 0.8 & 12

S069 A medium-grained, 'ultramafic' rock (all constituent phases are ferromagnesian) with a decussate texture due to the transecting nature of the brown mica. Sapphirine forms large porphyroblasts.

SK332 Fine-granoblastic interlobate quartz-cordierite-biotite rock with skeletal hypersthene porphyroblasts. Relatively large plagioclase grains are associated with the pyroxene and few small grains occur in the matrix. A penetrative continuous foliation is defined by the preferred orientation of biotite and elongated cordierite and quartz. This foliation is continuous through the skeletal pyroxene porphyroblasts and is rotated. The rotation of the helicitic fabric gradually increases towards the centre of the porphyroblast - the beginning of a snowball structure.

APPENDIX 4.7 THE GESELSKAPBANK DOMAIN

APPENDIX 4.7.1 METAPELITES OF THE LOWER NAPPES

	Qtz	Plg	Kfs	Stt	Bi	Ms	Sil	Grt	Chl	Grp	Ore	Grain size
DST1	*		*		*	+	*				-	0.2 - 2.
DNA3	*					*	*			*	-	0.2 - 5
DST18	*			+		*				+		0.5 - 3.0
DST20	*				*	*					-	0.3 - 2.0

DST1 Medium-grained K-feldspar bearing biotite-sillimanite schist with retrograde muscovite. Sillimanite occurs also as inclusions in the K-feldspar. Muscovite and quartz replaced K-feldspar grains resulting in a micrographic intergrowth of K-feldspar, sillimanite quartz and muscovite (see Figure 10.27).

DNA3 Graphite bearing muscovite-sillimanite schist; the graphite traces define an anastomosing foliation. The muscovite forms porphyroblasts which preferentially developed across radial clusters of sillimanite (Figure 10.26)

DST18 Graphite-muscovite schist with 2 millimetre sized staurolite grains. The staurolite is anhedral and contains small rounded quartz inclusions. The staurolite grains do not appear to be deformed; their micro-structural relations are, however, difficult to evaluate due to their relatively small sizes.

DST20 Deformed schist; porphyroblasts of both micas are cut by micro shears along which retrograde sericite and fine-grained, unidentified dark material are developed.

APPENDIX 4.7.2 METAPELITES OF THE UPPER NAPPES

	Qtz	Plg	Kfs	Crd	Ged	Bi	Ms	And	Sil	Grt	Chl	Ore	Grain size
DST67	*					*				*		+	3 - 5
DST7				*				-	+	+	-	+	.2 & > 5
SK323				*					+	*	+	+	.2 & > 5
SK324	+			*		+	-		*	*	-	-	.2 & > 5
NMG025	+	-	*	+		+			*			+	.2 - 3.0
NMG029				*		-	-	-	*	+	+	+	.2 & > 3
NMG030		*		*		-		-	*	+	-	-	.2 - 2.0
NMG034		*		*		+	-	+	*		+	-	.3 - 1.3
NMG012	+	+	*			*			*			-	.03 & .2 - 1.2
NMG013	*	+					*		-		*	+	.1 - 1.3
DGE14	+	+	*	*		+			*			+	.05-.1 & 1-2.5

DST67 Porphyroblasts of inclusion-rich garnet are set in a matrix of medium-granoblastic quartz and biotite.

DST7 Fine-granoblastic cordierite-rich rock; sillimanite and ore grains occur both interstitially and as chadacrysts in the cordierite grains. A few small patches, in which the cordierite grains are larger than the common size, causes some textural variation. A poorly developed foliation is defined by the sillimanite needles. Garnet porphyroblasts contain numerous sillimanite inclusions as well as a few small quartz inclusions. A single andalusite porphyroblast (diameter 5 millimetre) is skeletal and includes the matrix cordierite and a few small sillimanite grains. An irregular halo of chlorite surrounds the andalusite. Chlorite is also present at two more retrograde patches with no associated andalusite.

SK323 Same as DST7, but no andalusite in this specimen. Chlorite forms radial clusters in the matrix.

SK324 Fine-granoblastic cordierite-sillimanite rock with a penetrative foliation/banding defined by the distribution and orientation of the sillimanite. Garnet porphyroblasts include this fabric. Subsequent crenulations affected both the foliation and the garnet porphyroblasts - some porphyroblasts are dislocated along the included sillimanite bands. Minor biotite is present in areas where the cordierite forms medium-granoblastic patches. Accessory retrograde chlorite and muscovite is spatially confined to the biotite.

NMG025 Gneissic rock with the foliation mainly defined by sillimanite stringers. Sillimanite also occurs as porphyroblasts with inclusions consisting mainly of quartz. Biotite is fine-grained. Cordierite is partially pinitized.

NMG029 Similar to DST7, but with a less regular grain size distribution. Sillimanite forms a few porphyroblasts. Accessory biotite is evenly distributed in the cordierite matrix. Muscovite is associated with retrograde chlorite. The andalusite occurs in the same way as in DST7.

NMG030 Similar to NMG029 with plagioclase confined to one third of the thin section (in hand specimen a vague centimetre scale banding is discernible). The cordierite in the plagioclase

bearing band is pinitized while, in the rest of the thin section, it is only slightly altered at the grain boundaries.

NMG034 Fine- to medium-granoblastic cordierite-sillimanite-plagioclase-biotite rock with minor retrograde chlorite, andalusite and muscovite.

NMG012 Pelitic milonite. Porphyroclasts of K-feldspar and plagioclase (some polygonized) are set in an equidimensional fine-granoblastic (.05 millimetre) matrix of quartz, sillimanite and biotite. Medium-grained biotite and quartz occupy some pressure shadows.

NMG013 Muscovite-chlorite schist. 'Augen' of quartz-muscovite aggregates with irregular grain shapes and sizes, are set in a muscovite-chlorite-quartz schist matrix. The schistose fabric is defined more by the distribution of the mica than by the orientation of individual flakes. In areas of high mica density, the texture is decussate.

DGE14 Coarse-grained, cataclastic gneiss. The feldspars are marginally polygonized and a typical mortar structure resulted. The grain size of the granoblastic polygonal feldspar aggregates are between .05 and 0.1 millimetre. Cordierite is similarly deformed. Minor new biotite is developed in pressure shadows.

APPENDIX 4.7.3 MAFIC GRANULITE

	Qtz	Plg	Opx	Cpx	Hbe	Bi	Ore	Hbc	Gr. size
DGE16		*	*	*	*		+	B	.5 - 3 & .04
DGE18		*	*	*	*		+	G	.7 & <2.6
DGE20		*	*	*	*		+	O	.3 - 16.0
DGE61	-	*	*	*	*	+	-	G	.1 - 1.0
DGE76		*	*	*	*		+	B	.05 & 1 - 4

DGE16 Medium-granoblastic two-pyroxene granulite in the first stage of cataclastesis. Plagioclase grains are polygonized at the edges and pyroxene grains are bent, fractured and partly replaced by a fine-granoblastic aggregate of blueish-green hornblende (see Fig. 10.28)

DGE18 Two-pyroxene-hornblende granulite. The rock is banded on centimetre scale, alternating bands consisting of amphibolite and granulite. Minor hornblende grains do, however, occur within the granulite bands, in contact with the pyroxenes. The hornblende colour is pale green. The amphibole and pyroxene grains are elongate and reach lengths up to 2.5 millimetre, set in a fine-granoblastic polygonal matrix of plagioclase. The plagioclase grains are slightly elongate and, together with the ferromagnesian phases, define a penetrative continuous foliation. Some minor buckling and undulose extinction of all the phases reflects slight deformation related to the cataclastesis shown by DGE16.

DGE20 Coarse-granoblastic hornblende two-pyroxene granulite with embayed grain boundaries and a seriate grain size

distribution.

DGE61 Hornblende two-pyroxene granulite with minor quartz and biotite. Skeletal pyroxene porphyroblasts (up to 1 millimetre long) are set in fine-granoblastic, plagioclase dominated matrix with embayed grain boundaries and irregular size distribution.

DGE76 Medium-granoblastic hornblende two-pyroxene granulite showing minor cataclastic strain. Pre-existing hornblende is polygonized and new, fine-granoblastic polygonal aggregates of hornblende rim and fill cracks in pyroxene. All hornblende is light bluish-green. Approximately 5% of plagioclase is polygonized.

APPENDIX 4.7.4 THE GARESKOP DOLERITES

	Qtz	Plg	Ol	Opx	Cpx	Hbe	Bi	Sph	Scp	Ore	Hbc	Gr. size
NMG001		*	+		*	*			-	+	B	0.2 - 0.5
NMG002		*			*	*			-	+	B-O	.005 - 3.2
NMG005		*		+	*	*	-			-	O	.05 & .1 - 1.5
NMG006	+	*				*			+	+	O	.1 - .3 & >1
NNB027	-	*		+	*	+	+			+	O	.1 - 4.5

NMG001 Fine-grained olivine dolerite. Approximately half of the pyroxene grains are replaced by brown hornblende which constitute minute granoblastic polygonal subdomains. Diopside inclusions in plagioclase vary from very small (they render a dusty appearance to parts of plagioclase crytals) to .01 millimetre; the larger ones are concentrated at the grain boundaries.

NMG002 Cataclastic dolerite, the grain size varies from very small (.005 millimetre) to more than 3 millimetre (relict plagioclase) with a seriate size distribution. Strain features in plagioclase include bent and broken laths and subgrain development of different stages. Diopside 'inclusions' in plagioclase are concentrated at subgrain boundaries and grain boundaries and attain sizes up to .01 millimetre. Opaque grains and hornblende fill advanced cracks in the deformed feldspar grains. Some of the larger plagioclase grains are remarkably intact, showing slight bending of twin lamallae and a rounding off of the edges. Some plagioclase grains are partly replaced by irregular patches of scapolite. A few relict diopside cores are surrounded by a granoblastic mass of hornblende of variable grain size. Where the hornblende grains are small and especially where it surrounds opaque grains, the colour is brownish-green. Larger grains are olive-green to light olive-green. Some of the larger hornblende grains show pronounced undulose extinction.

NMG005 Transformed dolerite. Pyroxene and plagioclase relicts of up to 1.5 millimetre in diameter are surrounded by smaller grains in various stages of deformation. At the edges, the large relicts are rounded off and recrystallized to form very fine-granoblastic polygonal aggregates. Continuous bands, up to 1 millimetre wide, consist of very fine-granoblastic polygonal masses of hornblende and

recrystallized plagioclase and pyroxene. The grain size is bimodal, with approximately 30% of the volume consisting of more or less equal size (.002 millimetre). For the rest, the grain size depends on the state of strain of each grain and the size varies between .1 and 1.5 millimetre in diameter.

NMG006 Amphibolite (hornblende-plagioclase rock) with a few igneous plagioclase relicts. The texture is fine-granoblastic, polygonal to embayed, with a penetrative foliation defined mainly by the hornblende. Relict plagioclase grains form pophyroclasts around which the foliation is warped. Internally, the porphyroclasts are polygonised and partly saussuritized. Quartz is found in poorly defined pressure shadows. Scapolite occurs as independant grains, part of the granoblastic texture.

NNB027 Texturally similar to NMG002. The pyroxenes are internally altered, but replaced by discrete hornblende to a limited extent only. Approximately 30% of the pyroxene volume is recrystallized to a fine-granoblastic polygonal aggregate which includes some hornblende. Some plagioclase grains are broken up into subgrains with stringers of small diopside grains and minor biotite grains developed along the subgrain boundaries.

APPENDIX 5 MINERAL ANALYSES

TRAVERSE OVER A HORNBLENDE IN DRL099

	1	2	3	5	7	8	10	11	12	13	14	15	16	17	18	19	20
SiO2	43.34	43.89	43.85	42.84	43.34	42.79	44.18	42.81	43.25	43.65	43.96	43.67	44.07	44.68	44.49	45.22	44.9
TiO2	0.37	0.38	0.35	0.37	0.41	0.42	0.41	0.39	0.37	0.43	0.36	0.40	0.44	0.38	0.42	0.39	0.4
Al2O3	11.50	11.33	11.14	11.51	11.79	11.87	12.22	11.85	11.95	12.11	13.87	11.80	11.74	11.10	11.16	11.06	10.9
FeO	15.60	15.87	15.08	15.36	15.73	16.21	15.90	15.68	15.85	16.41	15.19	16.21	16.10	15.94	15.60	15.56	15.5
MnO	0.39	0.32	0.32	0.34	0.31	0.41	0.39	0.35	0.34	0.37	0.34	0.34	0.39	0.40	0.38	0.33	0.3
MgO	10.94	11.09	10.82	10.97	10.56	10.24	10.73	10.17	10.87	10.85	10.27	11.04	10.96	11.14	11.20	11.17	11.1
CaO	12.20	12.02	12.06	11.78	11.34	11.71	11.50	11.82	11.97	12.04	10.31	12.00	11.90	11.78	12.08	11.92	12.0
Na2O	1.33	1.27	1.29	1.25	1.31	1.33	1.27	1.26	1.33	1.28	1.20	1.24	1.32	1.11	1.18	1.16	1.1
K2O	0.41	0.42	0.39	0.38	0.38	0.41	0.44	0.46	0.47	0.48	0.63	0.48	0.48	0.47	0.49	0.49	0.4
TOTAL	96.07	96.60	95.29	94.80	95.18	95.40	97.05	94.80	96.41	97.63	96.14	97.18	97.39	97.00	97.00	97.30	97.0

	21	22	23	24	25	26	27	28	29	30	31	32	35	36	37	38	40
SiO2	44.52	43.87	44.43	45.63	46.76	47.85	48.64	47.89	47.06	44.34	44.49	44.82	44.78	44.50	44.78	44.61	46.5
TiO2	0.40	0.43	0.42	0.43	0.40	0.35	0.32	0.38	0.35	0.46	0.51	0.50	0.47	0.49	0.50	0.55	0.4
Al2O3	11.06	10.68	10.84	10.06	8.84	8.16	7.60	8.31	8.90	10.69	11.16	11.42	11.04	10.88	10.69	10.55	9.0
FeO	15.20	15.65	15.34	15.28	14.12	14.24	13.20	14.10	14.58	15.57	16.26	15.77	15.45	15.43	15.65	15.45	15.0
MnO	0.41	0.38	0.35	0.31	0.38	0.38	0.38	0.35	0.34	0.40	0.34	0.39	0.37	0.36	0.38	0.33	0.3
MgO	11.04	10.76	11.19	12.01	12.82	13.36	13.87	13.29	12.85	11.17	10.82	11.02	11.20	11.02	10.97	11.11	11.9
CaO	11.95	12.05	12.19	12.08	12.12	12.08	11.86	11.91	12.02	11.89	11.75	11.90	11.85	11.72	12.07	11.99	12.0
Na2O	1.14	1.04	1.10	1.08	0.95	0.94	0.83	0.95	1.05	1.14	1.11	1.02	1.15	1.22	1.12	1.12	1.0
K2O	0.48	0.49	0.48	0.42	0.35	0.34	0.26	0.29	0.38	0.53	0.59	0.50	0.48	0.52	0.51	0.52	0.4
TOTAL	96.20	95.35	96.33	97.30	96.74	97.71	96.96	97.48	97.53	96.20	97.02	97.35	96.79	96.14	96.66	96.23	96.8

	41	42	43	44	45	47	48	49	50	51	52	53	60	61	62	63	65
SiO2	47.40	47.97	47.97	48.53	7.54	48.48	48.10	48.51	48.32	48.57	48.02	47.54	48.02	48.16	45.39	42.66	43.0
TiO2	0.50	0.48	0.53	0.62	0.59	0.63	0.66	0.69	0.68	0.68	0.65	0.59	0.43	0.36	0.39	0.46	0.3
Al2O3	8.18	7.73	7.64	7.73	7.79	7.41	7.25	7.26	7.11	7.28	7.47	7.42	6.56	6.28	9.27	11.67	11.2
FeO	13.85	13.90	13.83	13.50	13.69	13.49	13.44	12.97	13.14	13.20	13.41	13.29	12.63	12.51	14.29	16.04	15.4
MnO	0.40	0.38	0.40	0.33	0.37	0.44	0.35	0.33	0.48	0.36	0.32	0.35	0.35	0.44	0.31	0.31	0.3
MgO	12.74	13.09	12.38	13.18	13.22	13.55	11.49	13.57	13.50	13.56	13.49	13.41	14.02	14.30	12.28	10.34	10.8
CaO	12.25	12.13	12.18	12.10	11.81	12.14	11.83	11.88	12.06	11.93	11.84	11.97	12.03	12.10	11.98	11.93	12.0
Na2O	0.88	0.80	0.79	0.73	0.76	0.65	0.71	0.69	0.72	0.67	0.73	0.74	0.71	0.65	0.97	1.15	1.1
K2O	0.38	0.41	0.47	0.47	0.47	0.52	0.54	0.54	0.49	0.55	0.54	0.56	0.37	0.29	0.41	0.61	0.5
TOTAL	96.59	96.90	96.19	97.19	56.23	97.31	94.37	96.44	96.49	96.80	96.46	95.87	95.11	95.10	95.29	95.16	95.0

TRAVERSE OVER A HORNBLENDE IN DRL099 (cont.)

	66	67	68	69	70	71	72	73	74	75	76	77	78	79	80	81	82
SiO2	42.58	43.01	47.20	42.93	44.44	45.21	45.40	45.31	46.19	46.76	47.24	47.28	46.98	47.31	47.79	47.58	47.9
TiO2	0.40	0.37	0.29	0.34	0.32	0.26	0.31	0.29	0.30	0.30	0.28	0.32	0.41	0.43	0.47	0.48	0.5
Al2O3	11.21	10.97	8.20	11.11	10.29	9.37	9.19	9.46	9.08	8.83	8.27	8.17	7.65	7.56	7.34	7.41	7.4
FeO	15.38	15.77	13.83	15.69	15.05	14.61	14.35	14.66	14.23	14.05	13.79	13.61	12.99	12.91	12.75	13.14	13.2
MnO	0.34	0.37	0.28	0.28	0.30	0.38	0.29	0.31	0.40	0.31	0.32	0.35	0.33	0.39	0.36	0.28	0.3
MgO	10.99	10.98	12.78	11.42	11.64	12.34	12.38	12.11	12.49	12.47	12.93	13.08	13.46	13.36	13.74	13.62	13.4
CaO	12.11	12.13	11.72	11.90	12.06	12.04	11.74	11.69	11.76	11.74	11.81	11.85	11.97	11.91	11.96	11.98	11.9
Na2O	1.18	1.18	0.82	1.23	1.19	1.13	1.08	1.05	1.05	0.99	0.84	0.82	0.79	0.82	0.78	0.78	0.8
K2O	0.53	0.52	0.37	0.52	0.41	0.39	0.37	0.39	0.38	0.38	0.39	0.43	0.48	0.42	0.48	0.47	0.5
TOTAL	94.72	95.31	95.49	95.42	95.72	95.74	95.12	95.28	95.88	95.84	95.88	95.92	95.06	95.11	95.67	95.75	96.1

	83	84	85	86	87	88	89	90	91	103	104	105	106	107	108	109	110
SiO2	48.44	48.41	48.50	48.12	48.32	48.15	47.77	47.09	46.22	43.79	43.92	44.12	43.67	43.95	44.11	44.49	44.8
TiO2	0.48	0.48	0.46	0.40	0.38	0.36	0.32	0.31	0.33	0.42	0.49	0.42	0.42	0.46	0.49	0.50	0.4
Al2O3	7.12	7.22	7.19	7.48	7.42	7.59	8.13	8.71	9.52	11.26	11.53	11.15	10.93	11.11	10.89	10.91	10.3
FeO	12.97	12.91	12.96	12.97	13.36	13.15	13.39	13.65	14.11	15.18	15.08	14.80	14.96	15.34	15.03	15.26	15.1
MnO	0.29	0.35	0.33	0.37	0.37	0.40	0.35	0.30	0.33	0.34	0.41	0.28	0.30	0.31	0.36	0.32	0.3
MgO	13.41	13.35	13.37	13.33	13.29	13.29	12.82	12.42	12.19	10.81	10.79	11.03	11.19	11.17	11.18	11.20	11.5
CaO	11.89	11.86	11.76	11.90	12.04	12.05	12.23	12.06	12.03	11.78	11.86	11.98	11.93	11.98	11.93	12.18	11.8
Na2O	0.79	0.76	0.73	0.77	0.79	0.78	0.85	0.92	1.05	1.16	1.14	1.10	1.10	1.16	1.11	1.14	1.1
K2O	0.46	0.50	0.51	0.49	0.46	0.42	0.41	0.43	0.42	0.47	0.49	0.44	0.46	0.48	0.47	0.48	0.4
TOTAL	95.85	95.85	95.81	95.82	96.44	96.20	96.26	95.89	96.21	95.22	95.71	95.31	94.96	95.95	95.57	96.48	95.9

	111	112	113	114	115	116	117	118	119	120	121	122	123	124	126	127	129
SiO2	47.02	47.61	48.18	48.75	48.40	48.49	48.37	48.58	48.44	48.39	48.43	48.24	48.40	48.42	48.22	48.41	47.6
TiO2	0.39	0.49	0.26	0.30	0.30	0.36	0.57	0.83	0.82	0.82	0.70	0.71	0.66	0.76	0.79	0.76	0.7
Al2O3	9.00	8.24	7.45	7.08	7.12	6.99	6.85	6.59	6.52	6.61	6.93	7.05	6.97	6.93	6.93	7.06	7.2
FeO	14.21	13.35	12.66	12.79	13.02	12.18	12.63	12.18	12.43	12.33	12.91	12.97	12.70	12.84	12.66	12.41	12.4
MnO	0.30	0.25	0.40	0.32	0.40	0.30	0.36	0.31	0.32	0.39	0.30	0.32	0.40	0.36	0.32	0.35	0.3
MgO	12.56	12.97	13.41	13.65	13.79	13.79	13.72	13.78	13.73	13.50	13.54	13.42	13.41	13.53	13.47	13.48	13.4
CaO	11.85	11.95	12.11	12.21	12.13	12.13	12.06	12.13	11.96	11.87	12.05	11.92	11.75	11.81	11.48	11.76	11.8
Na2O	0.92	0.86	0.79	0.73	0.76	0.72	0.69	0.65	0.67	0.67	0.71	0.67	0.69	0.65	0.65	0.69	0.7
K2O	0.37	0.31	0.32	0.27	0.33	0.34	0.47	0.52	0.52	0.54	0.50	0.52	0.47	0.49	0.51	0.55	0.5
TOTAL	96.62	96.02	95.57	96.10	96.25	95.29	95.70	95.58	95.42	95.11	96.08	95.84	95.45	95.78	95.04	95.48	94.8

TRAVERSE OVER A HORNBLENDE IN DRL099 (cont.)

	131	132	134	135	136	137	138	139	140	141	142	143	144	145	146	147	149
SiO2	47.64	47.53	45.68	45.60	47.87	47.80	47.70	47.91	47.57	47.43	47.60	47.25	47.74	47.88	47.85	47.72	48.0
TiO2	0.57	0.45	0.35	0.36	0.46	0.53	0.47	0.52	0.52	0.60	0.72	0.62	0.77	0.87	0.91	0.80	0.7
Al2O3	7.20	7.53	9.50	9.65	7.62	7.49	7.38	7.37	7.49	7.37	7.20	7.25	7.14	6.97	6.94	6.95	7.2
FeO	12.52	12.69	14.39	14.37	13.02	12.78	12.96	12.81	12.92	12.49	12.54	12.78	12.62	12.44	12.44	12.75	12.8
MnO	0.35	0.32	0.33	0.31	0.35	0.28	0.33	0.27	0.34	0.33	0.37	0.32	0.30	0.35	0.36	0.29	0.3
MgO	13.41	13.32	11.79	11.66	12.97	12.99	13.09	13.15	13.27	13.29	13.52	13.53	13.46	13.40	13.53	13.39	13.3
CaO	11.70	11.96	11.88	11.92	11.97	11.91	12.24	12.09	12.02	12.12	12.19	11.94	11.86	11.89	11.93	11.71	11.6
Na2O	0.74	0.70	1.00	0.96	0.75	0.70	0.72	0.67	0.79	0.75	0.69	0.72	0.70	0.67	0.68	0.70	0.7
K2O	0.49	0.45	0.35	0.40	0.50	0.54	0.52	0.51	0.43	0.48	0.57	0.57	0.56	0.57	0.58	0.56	0.5
TOTAL	94.61	94.95	95.27	95.24	95.52	95.03	95.41	95.30	95.35	94.87	95.42	94.98	95.14	95.04	95.23	94.88	95.4

	150	151	152	153	154	155	156	157	158	159	160	161	162	163	164	165	166
SiO2	47.80	47.81	47.33	47.81	47.55	47.09	47.30	47.35	47.66	47.84	48.63	48.50	48.48	49.06	48.32	48.03	48.0
TiO2	0.85	0.78	0.77	0.68	0.77	0.70	0.74	0.69	0.65	0.63	0.73	0.73	0.60	0.37	0.69	0.95	0.9
Al2O3	7.10	7.00	7.06	7.12	6.96	7.36	7.05	7.11	7.45	7.57	6.73	6.67	6.68	6.19	6.80	6.75	6.6
FeO	12.35	12.70	12.61	12.69	12.57	12.75	12.73	12.64	12.84	13.13	12.58	12.28	12.20	12.12	12.50	12.52	12.5
MnO	0.29	0.30	0.32	0.29	0.31	0.31	0.31	0.40	0.33	0.32	0.36	0.39	0.30	0.34	0.26	0.26	0.3
MgO	13.42	13.31	13.48	13.43	13.36	13.05	13.52	13.21	13.27	12.18	13.63	13.47	13.81	14.28	13.58	13.60	13.4
CaO	11.86	11.88	11.93	11.99	12.03	12.04	11.87	11.89	12.06	12.12	11.78	12.13	12.06	12.16	12.05	11.91	11.9
Na2O	0.64	0.67	0.76	0.70	0.74	0.74	0.74	0.70	0.77	0.79	0.68	0.71	0.68	0.64	0.68	0.74	0.7
K2O	0.60	0.58	0.59	0.55	0.56	0.58	0.58	0.59	0.44	0.43	0.50	0.48	0.36	0.24	0.45	0.58	0.5
TOTAL	94.92	95.03	94.85	95.28	94.86	94.62	94.84	94.58	95.47	94.99	95.64	95.36	95.18	95.40	95.33	95.34	95.1

	167	168	169	170	171	172	173	174	175	176	177	178	179	180	181	182	183
SiO2	47.77	47.83	47.80	47.89	48.46	48.29	48.45	48.56	48.12	49.09	48.58	48.73	48.75	48.79	48.58	48.44	48.8
TiO2	0.98	1.03	0.97	0.94	0.96	0.90	0.97	0.79	0.65	0.37	0.43	0.53	0.71	0.91	0.97	0.98	0.9
Al2O3	6.72	6.58	6.59	6.66	6.69	6.65	6.83	6.95	7.10	6.91	6.93	6.89	6.78	6.65	6.58	6.65	6.2
FeO	12.56	12.98	13.08	12.95	12.95	12.93	12.79	12.81	12.82	12.54	12.67	12.52	12.84	12.71	12.83	12.82	12.7
MnO	0.34	0.34	0.37	0.36	0.30	0.37	0.37	0.36	0.35	0.31	0.32	0.32	0.34	0.35	0.31	0.37	0.3
MgO	13.61	13.39	13.64	13.24	13.35	13.37	13.34	13.15	13.06	13.24	13.22	13.52	13.39	13.60	13.62	13.49	13.5
CaO	11.70	11.67	11.60	11.64	11.68	11.36	11.37	11.89	12.02	11.93	12.14	12.02	11.97	12.05	12.03	11.83	11.9
Na2O	0.74	0.69	0.74	0.70	0.76	0.72	0.71	0.71	0.74	0.81	0.80	0.77	0.71	0.71	0.75	0.71	0.7
K2O	0.59	0.54	0.55	0.57	0.58	0.54	0.58	0.51	0.52	0.34	0.34	0.42	0.49	0.52	0.56	0.56	0.5
TOTAL	95.01	95.06	95.33	94.95	95.73	95.13	95.41	95.72	95.38	95.55	95.44	95.72	95.98	96.28	96.23	95.86	95.8

TRAVERSE OVER A HORNBLENDE IN DRL099 (cont.)

	183	184	185	186	187	188	189	190	191	193	194	195	196	197	198	199	200
SiO2	48.86	48.81	49.14	49.42	49.29	49.10	49.15	49.56	49.59	45.23	44.48	43.81	43.54	43.54	43.92	43.41	43.3
TiO2	0.90	0.83	0.88	0.82	0.79	0.86	0.85	0.83	0.77	0.50	0.47	0.45	0.47	0.44	0.40	0.38	0.4
Al2O3	6.28	6.63	6.22	5.95	6.09	6.15	6.20	6.18	6.20	9.40	10.41	11.44	11.60	11.52	11.51	11.87	11.8
FeO	12.72	12.81	12.71	12.52	12.69	12.80	12.91	12.49	12.28	13.87	14.30	14.81	14.86	15.23	15.31	15.43	15.2
MnO	0.34	0.32	0.35	0.36	0.37	0.37	0.31	0.43	0.38	0.36	0.30	0.30	0.29	0.32	0.30	0.34	0.3
MgO	13.56	13.53	13.74	13.81	13.74	13.66	13.66	13.83	13.78	12.07	11.55	10.82	10.77	10.83	10.89	10.65	10.6
CaO	11.92	11.93	11.59	11.57	11.76	11.69	11.68	11.44	11.71	11.73	11.55	11.87	11.75	11.90	11.91	11.91	12.0
Na2O	0.74	0.69	0.71	0.67	0.64	0.69	0.69	0.68	0.67	0.92	1.00	1.18	1.22	1.20	1.12	1.16	1.2
K2O	0.52	0.50	0.55	0.47	0.49	0.48	0.50	0.49	0.49	0.43	0.41	0.48	0.47	0.43	0.38	0.43	0.4
TOTAL	95.84	96.05	95.88	95.59	95.86	95.80	95.96	95.92	95.88	94.50	94.46	95.16	94.99	95.43	95.75	95.57	95.5

SK394	Alb	Amp1	Amp2	Amp3	Bte
SiO2	66.71	54.28	53.10	54.21	39.25
TiO2	0.13	0.15	0.15	0.16	1.41
Al2O3	20.55	2.66	2.87	2.31	15.32
FeO	0.16	7.03	7.36	5.83	11.16
MnO	0.11	0.30	0.23	0.26	0.23
MgO	0.10	17.92	18.35	19.20	17.60
CaO	0.99	12.19	12.32	12.45	0.14
Na2O	10.50	0.37	0.47	0.36	0.18
K2O	0.09	0.17	0.44	0.14	9.99
TOTAL	99.35	95.07	95.29	94.91	95.28
Si	11.750	7.810	7.674	7.782	5.749
Ti	0.018	0.016	0.017	0.017	0.156
Al	4.271	0.451	0.490	0.392	2.648
Fe2+	0.024	0.845	0.889	0.700	1.367
Mn	0.017	0.037	0.029	0.032	0.029
Mg	0.028	3.843	3.952	4.106	3.842
Ca	0.187	1.880	1.908	1.915	0.023
Na	3.584	0.104	0.131	0.099	0.051
K	0.020	0.031	0.081	0.025	1.866
TOTAL	19.899	15.016	15.170	15.068	15.729

ACTINOLITE SCHIST
(Richtersveld Domain)

METAPELITE SPECIMENS, EENRIET MOUNTAINS

S752	PLG1	PLG2	Grt1	Grt2	Grt3
SiO2	56.34	54.07	38.56	38.37	37.30
TiO2	0.00	0.00	0.15	0.15	0.15
Al2O3	26.60	27.79	21.55	21.39	21.95
FeO	0.16	0.20	27.07	28.42	26.98
MnO	0.00	0.00	2.41	3.53	3.13
MgO	0.00	0.00	7.98	6.59	7.54
CaO	8.72	10.28	2.19	2.08	2.26
Na2O	6.64	5.66	0.00	0.00	0.00
K2O	0.11	0.09	0.00	0.00	0.00
TOTAL	98.57	98.09	99.91	100.53	99.31
Si	10.259	9.941	2.997	2.997	2.934
Ti	0.000	0.000	0.009	0.009	0.009
Al	5.715	6.029	1.976	1.971	2.037
Fe2+	0.024	0.031	1.759	1.856	1.775
Mn	0.000	0.000	0.159	0.234	0.209
Mg	0.000	0.000	0.924	0.767	0.884
Ca	1.701	2.025	0.182	0.174	0.190
Na	2.344	2.017	0.000	0.000	0.000
K	0.026	0.021	0.000	0.000	0.000
TOTAL	20.069	20.064	8.006	8.008	8.038

S752	Crd1	Bt1	Bt2	Bt3
SiO2	49.24	36.93	36.95	37.72
TiO2	0.08	2.04	2.04	1.99
Al2O3	33.36	17.59	17.64	17.85
FeO	4.57	13.06	13.61	12.49
MnO	0.22	0.12	0.12	0.14
MgO	10.04	15.66	15.96	16.04
CaO	0.06	0.05	0.07	0.07
Na2O	0.28	0.62	0.63	0.64
K2O	0.05	8.87	8.87	9.11
TOTAL	97.90	94.94	95.89	96.05
Si	5.008	5.463	5.427	5.496
Ti	0.006	0.227	0.225	0.218
Al	4.003	3.070	3.057	3.069
Fe2+	0.389	1.615	1.671	1.522
Mn	0.019	0.015	0.015	0.017
Mg	1.522	3.452	3.493	3.483
Ca	0.007	0.008	0.011	0.011
Na	0.055	0.178	0.179	0.181
K	0.006	1.673	1.661	1.693
TOTAL	11.015	15.701	15.740	15.689

SK387	Grt1	Grt2	Grt3	Crd1	Crd2	Amph1	Bt1	Bt2
SiO2	38.76	38.06	38.12	49.83	48.86	48.19	38.53	38.11
TiO2	0.03	0.04	0.03	0.00	0.00	0.23	2.05	1.59
Al2O3	22.46	21.63	21.97	34.20	33.72	10.04	17.93	17.81
FeO	25.53	26.94	24.67	3.95	4.11	19.20	12.36	12.35
MnO	3.23	4.59	5.32	0.20	0.23	1.59	0.14	0.13
MgO	8.09	5.90	7.17	10.78	10.60	17.62	16.65	16.61
CaO	2.19	2.62	2.17	0.00	0.00	0.64	0.00	0.01
Na2O	0.00	0.00	0.00	0.09	0.12	1.04	0.19	0.19
K2O	0.00	0.00	0.00	0.00	0.00	0.01	8.88	9.04
TOTAL	100.29	99.78	99.46	99.06	97.64	98.56	96.73	95.84
Si	2.985	2.996	2.984	4.988	4.970	6.933	5.540	5.542
Ti	0.002	0.002	0.002	0.000	0.000	0.025	0.222	0.174
Al	2.041	2.009	2.029	4.039	4.047	1.705	3.042	3.057
Fe2+	1.644	1.773	1.614	0.331	0.350	2.310	1.486	1.501
Mn	0.210	0.306	0.353	0.017	0.020	0.194	0.017	0.016
Mg	0.929	0.692	0.837	1.608	1.608	3.779	3.568	3.600
Ca	0.181	0.221	0.182	0.000	0.000	0.099	0.001	0.001
Na	0.000	0.000	0.000	0.018	0.023	0.291	0.053	0.055
K	0.000	0.000	0.000	0.000	0.000	0.001	1.628	1.677
TOTAL	7.992	7.998	8.000	11.001	11.018	15.336	15.557	15.622

METAPELITE EENRIET MOUNTAINS

SK296	Grt1	Grt2	Grt3	Grt4	Grt5	Grt6	Grt7	Grt8
SiO2	37.84	37.35	37.37	37.37	37.42	37.16	37.93	37.20
TiO2	0.18	0.11	0.17	0.17	0.18	0.15	0.16	0.17
Al2O3	21.85	20.98	22.15	21.68	21.37	20.67	21.98	21.70
FeO	24.85	24.91	24.79	24.65	24.53	24.01	24.48	25.11
MnO	4.63	5.05	4.55	4.93	7.35	9.37	5.74	7.86
MgO	7.70	7.72	7.86	7.51	6.01	5.20	7.49	4.99
CaO	2.10	2.18	2.14	2.36	2.51	2.30	2.42	2.77
Na2O	0.17	0.13	0.15	0.16	0.18	0.17	0.19	0.18
K2O	0.06	0.06	0.07	0.08	0.08	0.08	0.08	0.07
TOTAL	99.37	98.48	99.25	98.91	99.61	99.11	100.46	100.05
Si	2.963	2.966	2.931	2.949	2.963	2.981	2.950	2.950
Ti	0.011	0.006	0.010	0.010	0.011	0.009	0.009	0.010
Al	2.019	1.966	2.050	2.019	1.997	1.957	2.017	2.030
Fe2+	1.627	1.654	1.626	1.626	1.624	1.611	1.591	1.665
Mn	0.307	0.340	0.302	0.330	0.493	0.637	0.378	0.527
Mg	0.898	0.914	0.919	0.883	0.709	0.622	0.867	0.590
Ca	0.176	0.185	0.180	0.199	0.213	0.198	0.202	0.235
Na	0.025	0.021	0.023	0.025	0.028	0.027	0.028	0.028
K	0.006	0.006	0.007	0.008	0.008	0.008	0.008	0.007
TOTAL	8.032	8.057	8.049	8.048	8.045	8.049	8.051	8.042

SK296	Grt9	Grt10	Grt11	Grt12	Grt13	Grt14	Grt15	Crd1
SiO2	37.74	36.66	37.37	37.65	37.78	37.43	37.31	47.71
TiO2	0.15	0.18	0.17	0.19	0.19	0.15	0.17	0.13
Al2O3	21.88	21.38	21.61	22.34	21.55	21.88	21.55	32.46
FeO	24.38	24.47	24.23	24.86	25.16	25.07	25.07	4.05
MnO	6.32	8.32	7.27	5.01	6.86	8.48	7.86	0.31
MgO	6.92	5.28	6.52	7.86	5.76	4.79	5.10	10.45
CaO	2.23	2.48	2.45	2.03	2.17	2.42	2.54	0.07
Na2O	0.17	0.17	0.16	0.06	0.12	0.06	0.09	0.22
K2O	0.06	0.07	0.08	0.07	0.06	0.09	0.07	0.05
TOTAL	99.85	99.01	99.87	100.08	99.65	100.37	99.77	95.46
Si	2.959	2.939	2.946	2.931	2.984	2.959	2.963	6.081
Ti	0.009	0.011	0.010	0.011	0.011	0.009	0.010	0.013
Al	2.023	2.022	2.010	2.052	2.009	2.041	2.020	4.881
Fe2+	1.598	1.641	1.597	1.618	1.662	1.657	1.665	0.432
Mn	0.420	0.565	0.486	0.330	0.459	0.568	0.528	0.034
Mg	0.808	0.631	0.766	0.912	0.678	0.565	0.604	1.985
Ca	0.188	0.213	0.207	0.169	0.184	0.205	0.216	0.010
Na	0.026	0.026	0.025	0.009	0.019	0.010	0.015	0.053
K	0.006	0.007	0.008	0.007	0.006	0.009	0.007	0.009
TOTAL	8.036	8.056	8.055	8.040	8.012	8.022	8.028	13.497

METAPELITE (with MnO-rich garnet)

STEINKOPF DOMAIN

S254	Grt1	Grt2	Grt3	Bt1	Bt2	Bt3
SiO2	36.84	37.13	37.20	34.92	35.01	35.07
TiO2	0.04	0.03	0.05	2.11	2.27	1.75
Al2O3	21.31	21.60	21.46	20.79	20.26	20.10
FeO	24.80	25.40	25.55	20.68	21.47	20.45
MnO	12.80	10.11	10.39	0.50	0.53	0.36
MgO	2.21	3.35	3.21	8.57	8.68	10.34
CaO	1.48	1.58	1.62	0.04	0.02	0.04
Na2O	0.00	0.04	0.00	0.21	0.18	0.10
K2O	0.00	0.04	0.04	9.70	9.66	9.54
TOTAL	99.48	99.27	99.51	97.53	98.10	97.75
Si	2.989	2.989	2.993	5.236	5.240	5.235
Ti	0.003	0.002	0.003	0.238	0.256	0.196
Al	2.040	2.052	2.037	3.678	3.577	3.541
Fe2+	1.682	1.710	1.718	2.592	2.687	2.552
Mn	0.880	0.689	0.708	0.064	0.067	0.045
Mg	0.268	0.401	0.385	1.914	1.936	2.300
Ca	0.129	0.137	0.139	0.007	0.004	0.006
Na	0.000	0.007	0.000	0.061	0.053	0.029
K	0.000	0.004	0.004	1.855	1.844	1.815
TOTAL	7.989	7.989	7.988	15.645	15.664	15.720

DABBIKNIK METAPELITIC GRANULITE
STEINKOPF DOMAIN

S579	Plg1	Opx1	Opx2	Ged1	Ged2
SiO2	59.33	49.74	49.58	45.32	45.29
TiO2	0.00	0.19	0.22	0.66	0.59
Al2O3	24.77	4.15	4.00	12.29	12.47
FeO	0.14	23.57	23.51	19.18	19.66
MnO	0.00	1.12	1.05	1.07	1.03
MgO	0.00	20.06	20.33	15.66	16.21
CaO	6.28	0.14	0.14	0.45	0.41
Na2O	7.82	0.00	0.00	1.45	1.34
K2O	0.11	0.00	0.00	0.07	0.06
TOTAL	98.45	98.97	98.83	96.15	97.06
Si	10.727	1.891	1.888	6.699	6.644
Ti	0.000	0.005	0.006	0.073	0.065
Al	5.284	0.186	0.180	2.144	2.159
Fe2+	0.021	0.749	0.749	2.371	2.412
Mn	0.000	0.036	0.034	0.134	0.128
Mg	0.000	1.137	1.154	3.450	3.544
Ca	1.216	0.006	0.006	0.071	0.064
Na	2.741	0.000	0.000	0.416	0.381
K	0.025	0.000	0.000	0.013	0.011
TOTAL	20.015	4.010	4.016	15.370	15.408

S579	Grt1	Grt2	Grt3	Bt1	Bt2
SiO2	37.58	37.71	37.86	37.70	37.54
TiO2	0.16	0.16	0.16	3.02	3.12
Al2O3	22.23	22.28	21.80	16.87	16.19
FeO	25.55	26.79	26.37	12.59	12.73
MnO	3.71	3.52	3.61	0.13	0.15
MgO	8.43	8.40	8.37	15.66	15.66
CaO	1.48	1.51	1.85	0.07	0.08
Na2O	0.00	0.00	0.00	0.44	0.47
K2O	0.00	0.00	0.00	9.51	9.26
TOTAL	99.14	100.37	100.02	95.99	95.20
Si	2.940	2.927	2.948	5.517	5.544
Ti	0.009	0.009	0.009	0.332	0.346
Al	2.052	2.040	2.003	2.913	2.821
Fe2+	1.671	1.739	1.717	1.541	1.572
Mn	0.246	0.231	0.238	0.016	0.019
Mg	0.983	0.972	0.971	3.415	3.446
Ca	0.124	0.126	0.154	0.011	0.013
Na	0.000	0.000	0.000	0.125	0.135
K	0.000	0.000	0.000	1.775	1.744
TOTAL	8.025	8.044	8.041	15.644	15.639

METAPELITE - NABABEEP MINE
COPPER DISTRICT

GNA002	Bt1	Bt2	Bt3	Bt4	Grt1	Grt2	Grt3	Grt4
SiO2	37.70	37.17	37.65	37.59	38.55	38.81	38.01	38.14
TiO2	5.63	5.90	3.83	3.23	0.05	0.02	0.00	0.02
Al2O3	16.84	16.32	16.46	16.65	22.52	22.84	22.45	22.18
FeO	10.68	11.25	10.92	10.86	31.85	31.30	31.97	32.15
MnO	0.00	0.06	0.00	0.04	0.51	0.51	0.48	0.51
MgO	15.74	15.01	16.81	16.71	7.13	7.47	6.66	6.23
CaO	0.03	0.10	0.01	0.02	0.17	0.21	0.18	0.19
Na2O	0.13	0.13	0.09	0.09	0.02	0.01	0.00	0.00
K2O	9.77	10.13	10.30	10.17	0.04	0.00	0.01	0.00
TOTAL	96.52	96.07	96.07	95.36	100.84	101.17	99.76	99.42
Si	5.441	5.429	5.484	5.509	2.985	2.985	2.981	3.004
Ti	0.611	0.648	0.419	0.356	0.003	0.001	0.000	0.001
Al	2.868	2.813	2.829	2.879	2.058	2.072	2.077	2.061
Fe2+	1.289	1.374	1.330	1.331	2.062	2.013	2.096	2.117
Mn	0.000	0.007	0.000	0.005	0.033	0.033	0.032	0.034
Mg	3.385	3.267	3.649	3.649	0.823	0.856	0.778	0.731
Ca	0.005	0.016	0.002	0.003	0.014	0.017	0.015	0.016
Na	0.036	0.037	0.025	0.026	0.003	0.001	0.000	0.000
K	1.798	1.887	1.913	1.901	0.004	0.000	0.001	0.000
TOTAL	15.432	15.478	15.651	15.659	7.986	7.979	7.981	7.964

METAPELITE SPECIMENS - COPPER DISTRICT

GNA022	Bt1	Bt2	Grt1	Grt2	Grt3	Grtt1	Grtt2	Grtt3
SiO2	38.57	38.51	38.33	39.06	39.05	39.39	38.88	39.16
TiO2	4.96	4.74	0.01	0.03	0.00	0.02	0.04	0.02
Al2O3	16.32	16.19	22.65	22.98	22.96	22.65	22.23	22.59
FeO	11.06	10.84	32.29	31.52	31.52	30.28	29.83	29.26
MnO	0.04	0.07	2.02	1.92	2.04	1.98	1.74	1.91
MgO	16.17	16.46	5.17	6.20	6.19	5.85	5.68	6.23
CaO	0.01	0.02	1.21	1.34	1.38	1.41	1.50	1.55
Na2O	0.20	0.20	0.06	0.00	0.00	0.03	0.02	0.03
K2O	10.41	10.18	0.03	0.00	0.01	0.00	0.01	0.01
TOTAL	97.74	97.21	101.77	103.05	103.15	101.61	99.93	100.76
Si	5.521	5.532	2.976	2.976	2.975	3.027	3.036	3.024
Ti	0.534	0.512	0.001	0.002	0.000	0.001	0.002	0.001
Al	2.756	2.744	2.075	2.066	2.064	2.054	2.048	2.058
Fe2+	1.324	1.302	2.096	2.008	2.008	1.946	1.948	1.889
Mn	0.005	0.009	0.133	0.124	0.132	0.129	0.115	0.125
Mg	3.449	3.523	0.598	0.704	0.703	0.670	0.661	0.717
Ca	0.002	0.003	0.101	0.109	0.113	0.116	0.125	0.128
Na	0.055	0.056	0.009	0.000	0.000	0.004	0.003	0.004
K	1.900	1.865	0.003	0.000	0.001	0.000	0.001	0.001
TOTAL	15.545	15.545	7.992	7.989	7.994	7.947	7.940	7.948

GNA022	Grtt4	Grtt5	Grtt6	Grtt7	Grtt8	Grtt9	Grtt1	Grtt1
SiO2	39.32	39.18	39.19	39.33	38.94	38.65	38.08	37.76
TiO2	0.04	0.06	0.03	0.06	0.04	0.04	0.09	0.07
Al2O3	22.43	22.63	22.58	22.72	22.63	22.44	22.59	22.60
FeO	28.86	28.84	29.02	28.51	28.85	29.12	29.55	29.90
MnO	1.74	1.80	1.77	1.94	1.96	1.89	1.95	2.10
MgO	6.51	6.71	6.84	6.78	6.55	6.80	6.66	6.78
CaO	1.46	1.44	1.43	1.40	1.40	1.42	1.42	1.40
Na2O	0.01	0.02	0.02	0.03	0.01	0.01	0.02	0.04
K2O	0.01	0.00	0.00	0.01	0.01	0.00	0.00	0.02
TOTAL	100.38	100.68	100.88	100.78	100.39	100.37	100.36	100.67
Si	3.039	3.020	3.017	3.024	3.014	2.998	2.965	2.941
Ti	0.002	0.003	0.002	0.003	0.002	0.002	0.005	0.004
Al	2.045	2.058	2.051	2.061	2.067	2.054	2.076	2.077
Fe2+	1.865	1.859	1.868	1.833	1.867	1.889	1.924	1.947
Mn	0.114	0.117	0.115	0.126	0.128	0.124	0.129	0.139
Mg	0.750	0.771	0.785	0.777	0.755	0.786	0.773	0.787
Ca	0.121	0.119	0.118	0.115	0.116	0.118	0.118	0.117
Na	0.001	0.003	0.003	0.004	0.002	0.002	0.003	0.006
K	0.001	0.000	0.000	0.001	0.001	0.000	0.000	0.002
TOTAL	7.938	7.949	7.958	7.945	7.952	7.973	7.993	8.020

GNA022	Grtt12	Grtt13	Grtt14	Grtt15	Grtt16	Grtt17	Grtt18
SiO2	38.92	36.66	36.20	35.31	35.39	34.27	38.88
TiO2	0.04	0.00	0.06	0.05	0.06	0.02	0.03
Al2O3	23.16	22.13	22.47	22.14	22.04	21.83	22.85
FeO	29.77	29.98	29.35	29.94	29.94	30.15	30.73
MnO	1.89	2.03	1.93	2.12	2.14	2.06	2.11
MgO	6.95	6.70	6.87	6.57	6.46	6.19	6.42
CaO	1.45	1.45	1.35	1.38	1.43	1.44	1.36
Na2O	0.01	0.01	0.02	0.02	0.00	0.02	0.03
K2O	0.00	0.01	0.01	0.00	0.02	0.00	0.00
TOTAL	102.19	98.97	98.26	97.53	97.48	95.98	102.41
Si	2.969	2.917	2.893	2.863	2.871	2.837	2.976
Ti	0.002	0.000	0.004	0.003	0.004	0.001	0.002
Al	2.085	2.077	2.119	2.118	2.110	2.132	2.064
Fe2+	1.899	1.994	1.961	2.030	2.031	2.087	1.967
Mn	0.122	0.137	0.131	0.146	0.147	0.144	0.137
Mg	0.790	0.794	0.818	0.794	0.781	0.764	0.732
Ca	0.119	0.124	0.116	0.120	0.124	0.128	0.112
Na	0.001	0.002	0.003	0.003	0.000	0.003	0.004
K	0.000	0.001	0.001	0.000	0.002	0.000	0.000
TOTAL	7.987	8.046	8.046	8.076	8.071	8.097	7.993

Grtt - analyzed along a traverse

SK490	Grt1	Grt2	Grt3	Crd1	Bt1	Bt2
SiO2	38.28	38.86	37.64	48.52	34.19	37.05
TiO2	0.16	0.18	0.11	0.07	3.75	3.47
Al2O3	22.76	22.21	23.16	34.69	17.78	17.22
FeO	28.38	28.74	29.63	5.05	12.81	13.56
MnO	0.94	0.73	0.98	0.10	0.10	0.09
MgO	9.50	9.23	7.58	10.73	16.72	15.78
CaO	0.71	0.72	0.39	0.05	0.12	0.06
Na2O	0.08	0.08	0.08	0.05	0.31	0.19
K2O	0.09	0.07	0.04	0.02	9.23	9.54
TOTAL	100.90	100.83	99.61	99.28	95.00	96.96
Si	2.932	2.978	2.935	4.880	5.100	5.396
Ti	0.009	0.010	0.007	0.005	0.420	0.380
Al	2.057	2.008	2.131	4.118	3.128	2.958
Fe2+	1.818	1.842	1.932	0.425	1.598	1.651
Mn	0.061	0.047	0.065	0.009	0.012	0.011
Mg	1.085	1.054	0.881	1.608	3.715	3.425
Ca	0.059	0.059	0.033	0.005	0.019	0.010
Na	0.012	0.012	0.012	0.009	0.091	0.054
K	0.008	0.007	0.004	0.003	1.756	1.771
TOTAL	8.040	8.017	8.000	11.062	15.839	15.657

METAPELITE SPECIMENS - COPPER DISTRICT

SK453	Grt1	Grt2	Grt3	Grt4	Bt1	Bt2	Bt3
SiO2	37.85	37.63	38.05	37.78	36.52	36.76	37.27
TiO2	0.06	0.06	0.05	0.04	4.11	3.73	3.70
Al2O3	21.92	21.84	22.01	21.96	17.59	17.51	17.79
FeO	31.87	31.20	30.28	29.68	17.66	16.09	12.76
MnO	1.86	1.81	1.71	1.70	0.06	0.03	0.03
MgO	4.86	5.83	6.26	6.74	12.01	13.66	15.58
CaO	1.73	1.59	1.65	1.56	0.03	0.03	0.02
Na2O	0.00	0.00	0.00	0.00	0.15	0.18	0.27
K2O	0.00	0.00	0.00	0.00	9.56	9.18	8.38
TOTAL	100.14	99.98	100.00	99.46	97.69	97.15	95.80
Si	2.990	2.970	2.984	2.973	5.380	5.391	5.426
Ti	0.003	0.003	0.003	0.002	0.455	0.411	0.405
Al	2.043	2.034	2.037	2.040	3.058	3.030	3.056
Fe2+	2.105	2.059	1.986	1.953	2.175	1.973	1.553
Mn	0.124	0.121	0.113	0.113	0.007	0.004	0.003
Mg	0.572	0.686	0.732	0.791	2.636	2.985	3.379
Ca	0.146	0.135	0.139	0.132	0.005	0.004	0.003
Na	0.000	0.000	0.000	0.000	0.043	0.052	0.075
K	0.000	0.000	0.000	0.000	1.795	1.716	1.555
TOTAL	7.985	8.009	7.994	8.005	15.555	15.567	15.456

S378	Grt1	Grt2	Crd1	Crd2
SiO2	38.26	38.00	49.13	48.83
TiO2	0.04	0.03	0.00	0.00
Al2O3	22.31	22.08	34.32	34.01
FeO	29.24	29.99	5.18	6.02
MnO	2.04	2.15	0.07	0.11
MgO	6.72	6.26	9.90	9.34
CaO	0.94	0.93	0.01	0.00
Na2O	0.06	0.00	0.12	0.12
K2O	0.01	0.00	0.00	0.01
TOTAL	99.62	99.44	98.73	98.44
Si	2.995	2.993	4.961	4.965
Ti	0.002	0.002	0.000	0.000
Al	2.060	2.052	4.089	4.080
Fe2+	1.913	1.976	0.438	0.512
Mn	0.135	0.144	0.006	0.009
Mg	0.784	0.735	1.489	1.415
Ca	0.079	0.078	0.001	0.000
Na	0.010	0.000	0.023	0.025
K	0.001	0.000	0.001	0.001
TOTAL	7.979	7.979	11.007	11.007

S231	Grt1	Grt2	Grt3	Crd1	Crd2	Bt1	Bt2	Bt3
SiO2	37.86	37.96	38.05	47.39	48.24	36.83	36.96	36.24
TiO2	0.08	0.05	0.07	0.00	0.00	3.98	5.53	4.31
Al2O3	22.12	22.24	22.17	34.18	34.02	17.51	19.11	17.52
FeO	33.02	31.49	30.98	7.61	7.59	17.05	12.59	18.07
MnO	1.41	1.31	1.16	0.06	0.05	0.03	0.03	0.04
MgO	5.06	6.20	6.72	8.69	8.61	12.90	14.99	11.45
CaO	1.02	1.04	1.06	0.01	0.01	0.02	0.03	0.01
Na2O	0.00	0.00	0.00	0.04	0.00	0.03	0.24	0.00
K2O	0.00	0.00	0.00	0.00	0.01	9.09	9.58	9.58
TOTAL	100.56	100.30	100.20	97.98	98.54	97.43	99.06	97.23
Si	2.981	2.974	2.975	4.883	4.935	5.402	5.235	5.376
Ti	0.005	0.003	0.004	0.000	0.000	0.439	0.589	0.481
Al	2.055	2.056	2.045	4.156	4.107	3.030	3.194	3.067
Fe2+	2.174	2.063	2.026	0.656	0.649	2.091	1.490	2.242
Mn	0.094	0.087	0.077	0.005	0.004	0.004	0.004	0.005
Mg	0.594	0.724	0.783	1.334	1.313	2.821	3.163	2.531
Ca	0.086	0.088	0.089	0.001	0.001	0.003	0.004	0.002
Na	0.000	0.000	0.000	0.007	0.000	0.007	0.066	0.000
K	0.000	0.000	0.000	0.000	0.001	1.701	1.731	1.812
TOTAL	7.988	7.995	7.998	11.042	11.012	15.498	15.477	15.516

S381	Grt1	Grt2	Crd1	Crd2
SiO2	37.81	38.11	48.75	47.93
TiO2	0.06	0.04	0.00	0.00
Al2O3	21.73	21.89	33.58	33.20
FeO	29.63	31.40	6.11	5.42
MnO	2.73	3.18	0.17	0.10
MgO	6.73	5.38	9.02	9.60
CaO	0.74	0.74	0.00	0.00
Na2O	0.00	0.00	0.03	0.07
K2O	0.00	0.00	0.00	0.00
TOTAL	99.43	100.73	97.65	96.33
Si	2.983	2.993	4.996	4.969
Ti	0.004	0.002	0.000	0.000
Al	2.023	2.028	4.060	4.061
Fe2+	1.955	2.063	0.523	0.470
Mn	0.183	0.212	0.015	0.009
Mg	0.791	0.630	1.377	1.483
Ca	0.062	0.062	0.000	0.000
Na	0.000	0.000	0.006	0.014
K	0.000	0.000	0.000	0.000
TOTAL	8.001	7.990	10.977	11.007

METAPELITE SPECIMENS - COPPER DISTRICT

S069	Crd1	Crd2	Opx1	Opx2	Opx3
SiO2	49.34	49.25	49.97	51.18	51.28
TiO2	0.13	0.10	0.24	0.22	0.27
Al2O3	33.79	33.79	7.28	7.14	7.28
FeO	2.16	2.29	14.15	13.71	14.38
MnO	0.09	0.10	0.20	0.20	0.18
MgO	11.71	11.58	26.85	26.55	26.28
CaO	0.07	0.08	0.15	0.16	0.17
Na2O	0.10	0.28	0.00	0.00	0.00
K2O	0.05	0.04	0.00	0.00	0.00
TOTAL	97.44	97.51	98.84	99.16	99.84
Si	4.983	4.978	1.813	1.842	1.838
Ti	0.010	0.008	0.007	0.006	0.007
Al	4.027	4.030	0.312	0.303	0.308
Fe2+	0.182	0.194	0.429	0.413	0.431
Mn	0.008	0.009	0.006	0.006	0.005
Mg	1.762	1.744	1.452	1.424	1.404
Ca	0.008	0.009	0.006	0.006	0.007
Na	0.020	0.055	0.000	0.000	0.000
K	0.006	0.005	0.000	0.000	0.000
TOTAL	11.006	11.030	4.024	4.000	4.000

S069	Bt1	Bt2	Spr1	Spr2	Spr3
SiO2	37.60	37.54	13.77	13.99	13.04
TiO2	2.99	3.79	0.16	0.15	0.20
Al2O3	17.07	17.07	61.87	61.24	62.96
FeO	7.28	7.35	7.27	7.08	7.84
MnO	0.11	0.11	0.10	0.14	0.08
MgO	19.14	18.58	17.18	16.94	16.07
CaO	0.06	0.05	0.06	0.07	0.06
Na2O	0.50	0.47	0.00	0.00	0.00
K2O	9.58	9.73	0.00	0.00	0.00
TOTAL	94.33	94.69	100.41	99.61	100.25
Si	5.468	5.447	0.814	0.833	0.774
Ti	0.327	0.413	0.007	0.007	0.009
Al	2.929	2.922	4.317	4.302	4.410
Fe2+	0.885	0.892	0.359	0.352	0.389
Mn	0.014	0.014	0.005	0.007	0.004
Mg	4.148	4.017	1.514	1.503	1.422
Ca	0.009	0.008	0.004	0.004	0.004
Na	0.141	0.132	0.000	0.000	0.000
K	1.777	1.800	0.000	0.000	0.000
TOTAL	15.699	15.645	7.020	7.009	7.012

SK332	Pl1	Pl2	Pl3	Pl4	Opx1	Opx2	Opx3	Opx4
SiO2	61.38	61.47	61.26	60.64	46.32	47.58	47.51	46.79
TiO2	0.14	0.16	0.13	0.29	0.16	0.27	0.50	0.50
Al2O3	24.02	24.40	24.81	24.15	6.84	6.66	6.56	5.85
FeO	0.18	0.12	0.16	0.18	24.99	25.38	24.86	27.40
MnO	0.15	0.08	0.10	0.09	0.37	0.37	0.25	0.24
MgO	0.07	0.06	0.07	0.06	18.96	18.18	19.25	19.39
CaO	5.11	5.55	5.43	5.97	0.14	0.13	0.16	0.13
Na2O	8.17	8.00	7.67	7.26	0.09	0.10	0.06	0.08
K2O	0.16	0.14	0.17	0.17	0.07	0.08	0.05	0.06
TOTAL	99.38	99.97	99.80	98.80	97.94	98.76	99.22	100.44
Si	10.951	10.904	10.872	10.883	1.796	1.827	1.812	1.789
Ti	0.019	0.021	0.017	0.039	0.005	0.008	0.014	0.014
Al	5.056	5.107	5.195	5.113	0.313	0.302	0.295	0.264
Fe2+	0.027	0.018	0.024	0.027	0.810	0.815	0.793	0.876
Mn	0.023	0.012	0.015	0.014	0.012	0.012	0.008	0.008
Mg	0.018	0.015	0.018	0.017	1.096	1.040	1.094	1.104
Ca	0.977	1.055	1.033	1.147	0.006	0.005	0.007	0.005
Na	2.825	2.750	2.639	2.526	0.006	0.008	0.005	0.006
K	0.037	0.031	0.038	0.039	0.004	0.004	0.003	0.003
TOTAL	19.933	19.912	19.852	19.805	4.048	4.020	4.030	4.070

SK332	Crd1	Crd2	Crd3	Bt1	Bt2
SiO2	47.28	48.74	48.74	35.12	34.88
TiO2	0.17	0.16	0.14	3.62	4.29
Al2O3	32.59	33.10	32.95	16.91	15.91
FeO	5.15	5.10	4.55	14.18	15.09
MnO	0.08	0.10	0.03	0.10	0.02
MgO	10.35	10.18	10.60	15.40	15.11
CaO	0.09	0.09	0.08	0.09	0.07
Na2O	0.17	0.16	0.20	0.29	0.24
K2O	0.05	0.06	0.05	9.32	9.40
TOTAL	95.92	97.69	97.34	95.03	95.02
Si	4.931	4.982	4.986	5.262	5.262
Ti	0.013	0.012	0.011	0.408	0.486
Al	4.011	3.992	3.978	2.990	2.832
Fe2+	0.449	0.436	0.389	1.777	1.904
Mn	0.007	0.008	0.002	0.012	0.003
Mg	1.608	1.551	1.615	3.438	3.397
Ca	0.010	0.010	0.009	0.015	0.012
Na	0.035	0.031	0.040	0.085	0.069
K	0.007	0.008	0.007	1.781	1.809
TOTAL	11.071	11.030	11.038	15.768	15.775

METAPELITE SPECIMENS - GESELSKAPBANK DOMAIN

DST7	Grt1	Grt2	Grt3	Grt4	Grt5	Crd1	Bt1	Bt2
SiO2	37.69	37.33	37.23	37.28	37.17	48.57	35.08	35.31
TiO2	0.04	0.03	0.04	0.03	0.05	0.00	1.29	1.06
Al2O3	21.35	21.53	21.34	21.51	21.51	33.69	21.30	20.99
FeO	34.21	32.85	33.22	33.70	34.38	7.84	19.33	20.18
MnO	1.76	1.60	1.72	0.78	0.96	0.04	0.00	0.00
MgO	2.96	3.97	3.74	4.23	3.29	8.35	9.72	10.12
CaO	1.91	1.89	1.84	1.68	1.63	0.01	0.03	0.02
Na2O	0.00	0.00	0.00	0.00	0.00	0.10	0.09	0.16
K2O	0.00	0.00	0.00	0.00	0.00	0.00	8.93	9.11
TOTAL	99.93	99.20	99.12	99.22	99.00	98.60	95.78	96.95
Si	3.019	2.995	2.997	2.990	3.000	4.970	5.277	5.273
Ti	0.003	0.002	0.002	0.002	0.003	0.000	0.146	0.119
Al	2.018	2.038	2.027	2.036	2.048	4.068	3.780	3.699
Fe2+	2.292	2.204	2.236	2.260	2.320	0.671	2.431	2.521
Mn	0.120	0.109	0.117	0.053	0.065	0.003	0.000	0.000
Mg	0.354	0.475	0.448	0.506	0.396	1.274	2.179	2.253
Ca	0.164	0.162	0.159	0.144	0.141	0.001	0.004	0.003
Na	0.000	0.000	0.000	0.000	0.000	0.021	0.026	0.045
K	0.000	0.000	0.000	0.000	0.000	0.000	1.713	1.736
TOTAL	7.969	7.984	7.987	7.990	7.973	11.007	15.556	15.649

NMG031	Grt1	Grt2	Crd1	Crd2	Bt1	Bt2
SiO2	36.19	35.87	47.50	48.83	35.57	34.44
TiO2	0.10	0.08	0.08	0.06	1.14	1.12
Al2O3	23.11	22.50	33.81	34.32	20.11	20.04
FeO	34.30	33.10	7.16	8.14	19.75	20.13
MnO	0.68	0.68	0.12	0.15	0.09	0.12
MgO	4.11	4.37	9.18	7.85	9.36	9.51
CaO	1.69	1.63	0.08	0.07	0.12	0.10
Na2O	0.08	0.07	0.10	0.18	0.31	0.13
K2O	0.07	0.07	0.07	0.05	9.80	9.67
TOTAL	100.33	98.37	98.10	99.66	96.25	95.25
Si	2.881	2.902	4.887	4.954	5.372	5.279
Ti	0.006	0.005	0.006	0.005	0.130	0.129
Al	2.171	2.148	4.104	4.109	3.583	3.624
Fe2+	2.283	2.239	0.616	0.691	2.494	2.580
Mn	0.046	0.047	0.010	0.013	0.012	0.015
Mg	0.487	0.527	1.408	1.186	2.106	2.172
Ca	0.144	0.141	0.008	0.008	0.020	0.017
Na	0.013	0.011	0.021	0.036	0.090	0.039
K	0.008	0.007	0.009	0.007	1.888	1.890
TOTAL	8.038	8.028	11.070	11.008	15.694	15.745

SK323	Grt1	Grt2	Bt1	Crd1	Crd2
SiO2	36.83	37.28	34.82	48.80	49.06
TiO2	0.04	0.04	2.24	0.00	0.00
Al2O3	21.30	21.57	20.14	33.88	33.90
FeO	32.92	31.74	20.00	7.52	6.66
MnO	3.30	2.96	0.01	0.09	0.04
MgO	2.79	3.67	11.59	8.66	9.19
CaO	1.86	1.85	0.03	0.00	0.00
Na2O	0.00	0.00	0.02	0.03	0.04
K2O	0.00	0.00	8.66	0.00	0.00
TOTAL	99.03	99.11	97.51	98.98	98.89
Si	2.988	2.997	5.168	4.967	4.977
Ti	0.002	0.002	0.250	0.000	0.000
Al	2.040	2.045	3.527	4.068	4.057
Fe2+	2.234	2.133	2.482	0.640	0.565
Mn	0.227	0.202	0.002	0.007	0.003
Mg	0.337	0.440	2.563	1.314	1.389
Ca	0.162	0.159	0.004	0.000	0.000
Na	0.000	0.000	0.005	0.006	0.009
K	0.000	0.000	1.640	0.000	0.000
TOTAL	7.989	7.978	15.641	11.002	10.999

EENRIET MOUNTAINS

SK419	Opx1	Opx2	Opx3	Opx4	Amp1	Amp3	Amp3
SiO2	56.63	54.44	55.35	54.55	49.64	48.58	50.33
TiO2	0.08	0.05	0.04	0.05	0.46	0.47	0.53
Al2O3	3.82	2.95	2.66	2.99	9.87	9.76	9.60
FeO	9.05	10.11	9.76	10.24	5.38	5.46	5.39
MnO	0.33	0.27	0.27	0.27	0.11	0.12	0.13
MgO	28.79	31.79	32.86	32.33	18.94	19.06	19.35
CaO	0.75	0.16	0.00	0.14	12.38	12.20	12.39
Na2O	0.18	0.00	0.01	0.00	0.64	0.65	0.63
K2O	0.00	0.00	0.00	0.00	0.23	0.20	0.22
TOTAL	99.63	99.77	100.96	100.58	97.64	96.50	98.56
Si	1.977	1.917	1.921	1.907	6.950	6.895	6.977
Ti	0.002	0.001	0.001	0.001	0.048	0.050	0.055
Al	0.157	0.123	0.109	0.124	1.630	1.635	1.570
Fe2+	0.264	0.298	0.283	0.300	0.629	0.648	0.625
Mn	0.010	0.008	0.008	0.008	0.013	0.014	0.015
Mg	1.498	1.668	1.700	1.684	3.953	4.032	3.997
Ca	0.028	0.006	0.000	0.005	1.857	1.855	1.841
Na	0.012	0.000	0.001	0.000	0.173	0.179	0.169
K	0.000	0.000	0.000	0.000	0.041	0.037	0.040
TOTAL	3.948	4.020	4.024	4.030	15.294	15.346	15.288

S765	Opx1	Opx2	Hbl	Sp
SiO2	54.33	55.90	48.20	0.00
TiO2	0.08	0.07	0.51	0.07
Al2O3	3.17	4.07	10.41	61.26
FeO	9.96	8.84	5.63	17.86
MnO	0.22	0.31	0.11	0.18
MgO	31.62	28.07	18.98	17.21
CaO	0.12	0.72	1.69	0.02
Na2O	0.00	0.21	0.94	0.00
K2O	0.01	0.00	0.19	0.00
TOTAL	99.52	98.20	86.67	96.61
Si	1.916	1.978	7.316	0.000
Ti	0.002	0.002	0.059	0.001
Al	0.132	0.170	1.865	1.937
Fe2+	0.294	0.261	0.714	0.400
Mn	0.007	0.009	0.015	0.004
Mg	1.662	1.480	4.292	0.687
Ca	0.005	0.027	0.275	0.000
Na	0.000	0.015	0.277	0.000
K	0.000	0.000	0.037	0.000
TOTAL	4.017	3.943	14.850	3.030

SKELMFONTEIN SE POORT

SK203	Opx	Hbl	Ged1	Ged2
SiO2	50.51	42.51	44.29	43.26
TiO2	0.14	0.95	0.49	0.38
Al2O3	6.39	16.08	18.69	18.31
FeO	14.52	9.36	11.87	11.80
MnO	0.65	0.35	0.70	0.70
MgO	27.31	15.18	21.25	20.64
CaO	0.23	11.24	1.13	0.95
Na2O	0.05	1.85	2.17	2.06
K2O	0.00	0.47	0.02	0.01
TOTAL	99.79	97.99	100.59	98.11
Si	1.82	6.12	6.07	6.08
Ti	0.00	0.10	0.05	0.04
Al	0.27	2.73	3.02	3.03
Fe2+	0.44	1.13	1.36	1.39
Mn	0.02	0.04	0.08	0.08
Mg	1.47	3.26	4.34	4.32
Ca	0.01	1.73	0.17	0.14
Na	0.00	0.52	0.58	0.56
K	0.00	0.09	0.00	0.00
TOTAL	4.04	15.71	15.66	15.65

SK204	Opx1	Hbl	Ged
SiO2	50.70	43.28	43.81
TiO2	0.11	0.85	0.41
Al2O3	6.73	15.84	17.74
FeO	15.12	9.53	12.34
MnO	0.64	0.33	0.70
MgO	26.87	15.33	20.75
CaO	0.15	11.59	1.15
Na2O	0.01	1.48	1.70
K2O	0.02	0.46	0.02
TOTAL	100.36	98.69	98.62
Si	1.823	6.179	6.130
Ti	0.003	0.091	0.043
Al	0.286	2.668	2.929
Fe2+	0.454	1.138	1.444
Mn	0.019	0.040	0.084
Mg	1.440	3.262	4.327
Ca	0.006	1.772	0.173
Na	0.000	0.410	0.462
K	0.001	0.083	0.003
TOTAL	4.032	15.643	15.594

MAFIC METAMORPHITES NORTHERN LIMB OF THE RATELPOORT SYNFORM
COPPER DISTRICT

AMPHIBOLITE

S905	Plg	Hbl
SiO2	56.87	43.74
TiO2	0.15	1.16
Al2O3	26.26	11.46
FeO	0.24	14.85
MnO	0.09	0.30
MgO	0.09	11.65
CaO	8.15	11.88
Na2O	6.39	1.72
K2O	0.26	1.62
TOTAL	98.51	98.38
Si	10.343	6.492
Ti	0.020	0.130
Al	5.636	2.007
Fe2+	0.036	1.843
Mn	0.014	0.038
Mg	0.025	2.576
Ca	1.589	1.889
Na	2.254	0.495
K	0.061	0.307
TOTAL	19.977	15.777

TWO-PYROXENE GRANULITE

S965	Opx1	Opx3A	Opx3B	Cpx1	Cpx2	Cpx3A	Cpx3B	Hbl
SiO2	52.27	52.01	51.71	52.07	52.14	51.50	51.51	43.20
TiO2	0.07	0.08	0.08	0.21	0.18	0.21	0.23	1.85
Al2O3	0.99	1.13	1.24	2.21	2.01	2.02	2.31	11.13
FeO	24.68	22.14	22.02	9.81	9.65	8.32	8.73	13.49
MnO	0.88	1.59	1.57	0.35	0.35	0.64	0.68	0.37
MgO	20.79	22.38	22.35	13.48	13.51	14.06	13.99	13.23
CaO	0.61	0.62	0.67	22.40	22.00	22.56	22.32	11.74
Na2O	0.00	0.01	0.01	0.35	0.34	0.48	0.47	1.47
K2O	0.00	0.01	0.01	0.00	0.00	0.00	0.01	1.50
TOTAL	100.30	99.97	99.65	100.87	100.19	99.79	100.24	97.98
Si	1.967	1.950	1.945	1.937	1.949	1.932	1.925	6.404
Ti	0.002	0.002	0.002	0.006	0.005	0.006	0.006	0.206
Al	0.044	0.050	0.055	0.097	0.089	0.089	0.102	1.946
Fe2+	0.777	0.694	0.693	0.305	0.302	0.261	0.273	1.672
Mn	0.028	0.051	0.050	0.011	0.011	0.020	0.021	0.047
Mg	1.166	1.250	1.253	0.747	0.753	0.786	0.779	2.924
Ca	0.025	0.025	0.027	0.893	0.881	0.906	0.894	1.864
Na	0.000	0.001	0.001	0.025	0.025	0.035	0.034	0.422
K	0.000	0.000	0.001	0.000	0.000	0.000	0.000	0.283
TOTAL	4.009	4.023	4.026	4.021	4.014	4.035	4.035	15.768

TWO-PYROXENE GRANULITE

S969	Opx1	Opx2	Cpx1	Cpx2
SiO2	53.5730	53.8210	52.4940	52.8550
TiO2	0.0930	0.0830	0.2690	0.2780
Al2O3	1.3080	1.3040	2.0310	2.1310
Fe2O3	0.0000	0.0000	0.0000	0.0000
FeO	18.0640	17.7390	6.4120	6.6620
MnO	0.5580	0.5540	0.2360	0.2240
MgO	26.3060	26.2810	15.2840	15.3750
CaO	0.4470	0.4540	22.6900	22.5790
Na2O	0.0080	0.0100	0.3580	0.3590
K2O	0.0000	0.0000	0.0000	0.0000
TOTAL	100.3570	100.2460	99.7740	100.4630
Si	1.9497	1.9567	1.9445	1.9443
Ti	0.0025	0.0023	0.0075	0.0077
Al	0.0562	0.0559	0.0888	0.0925
Fe3+	0.0000	0.0000	0.0000	0.0000
Fe2+	0.5497	0.5393	0.1986	0.2049
Mn	0.0172	0.0171	0.0074	0.0070
Mg	1.4267	1.4238	0.8437	0.8428
Ca	0.0174	0.0177	0.9004	0.8898
Na	0.0006	0.0007	0.0257	0.0256
K	0.0000	0.0000	0.0000	0.0000
TOTAL	4.0200	4.0134	4.0165	4.0146

TWO-PYROXENE GRANULITE

SK289	Opx1	Opx2	Opx3	Cpx1	Cpx2	Cpx3
SiO2	52.17	51.76	51.99	52.29	51.27	52.18
TiO2	0.07	0.09	0.09	0.17	0.28	0.31
Al2O3	1.23	1.30	1.35	1.68	2.38	2.55
FeO	24.04	23.02	23.56	8.29	9.23	8.98
MnO	0.03	0.75	0.76	0.33	0.30	0.30
MgO	21.55	22.94	22.02	14.22	13.58	13.56
CaO	0.52	0.52	0.51	22.49	22.05	21.87
Na2O	0.00	0.00	0.03	0.33	0.40	0.43
K2O	0.00	0.00	0.00	0.00	0.01	0.01
TOTAL	99.61	100.37	100.31	99.79	99.51	100.19
Si	1.964	1.934	1.947	1.953	1.930	1.943
Ti	0.002	0.002	0.003	0.005	0.008	0.009
Al	0.055	0.057	0.060	0.074	0.106	0.112
Fe2+	0.756	0.719	0.738	0.259	0.291	0.280
Mn	0.001	0.024	0.024	0.010	0.009	0.009
Mg	1.208	1.277	1.229	0.792	0.762	0.752
Ca	0.021	0.021	0.020	0.900	0.889	0.872
Na	0.000	0.000	0.002	0.024	0.029	0.031
K	0.000	0.000	0.000	0.000	0.000	0.001
TOTAL	4.007	4.035	4.022	4.017	4.024	4.008

TWO-PYROXENE GRANULITE - COPPER DISTRICT

RATELPOORT

SK406	Plg	Opx1	Cpx1	Hbl
SiO2	54.67	51.97	51.77	43.86
TiO2	0.00	0.03	0.08	0.75
Al2O3	27.83	1.38	2.36	11.74
FeO	0.22	23.48	9.37	14.34
MnO	0.00	0.88	0.62	0.20
MgO	0.00	21.36	13.40	12.96
CaO	10.72	0.53	21.90	11.69
Na2O	5.56	0.00	0.48	1.21
K2O	0.43	0.00	0.00	1.56
TOTAL	99.43	99.64	99.96	98.31
Si	9.944	1.959	1.940	6.475
Ti	0.000	0.001	0.002	0.084
Al	5.972	0.061	0.104	2.045
Fe2+	0.033	0.740	0.294	1.770
Mn	0.000	0.028	0.020	0.025
Mg	0.000	1.200	0.748	2.851
Ca	2.089	0.021	0.879	1.849
Na	1.961	0.000	0.035	0.346
K	0.099	0.000	0.000	0.293
TOTAL	20.100	4.010	4.023	15.738

CAROLUSBERG MINE

GLC059	opx	cpx	bt
SiO2	52.13	52.21	39.39
TiO2	0.07	0.24	3.47
Al2O3	1.29	2.45	12.55
FeO	25.75	10.45	10.81
MnO	0.98	0.50	0.08
MgO	17.77	11.36	17.38
CaO	0.67	21.75	0.00
Na2O	0.03	0.40	0.10
K2O	0.01	0.00	10.63
TOTAL	98.70	99.36	94.41
Si	2.002	1.971	5.852
Ti	0.002	0.007	0.388
Al	0.058	0.109	2.200
Fe2+	0.827	0.330	1.343
Mn	0.032	0.016	0.010
Mg	1.017	0.639	3.848
Ca	0.028	0.880	0.000
Na	0.002	0.029	0.029
K	0.000	0.000	2.014
TOTAL	3.968	3.982	15.682

CAROLUSBERG MINE

GLC053	opx	cpx	bt
SiO2	52.35	50.48	37.05
TiO2	0.08	0.23	4.67
Al2O3	1.25	2.33	12.30
FeO	25.35	10.44	12.88
MnO	0.59	0.23	0.05
MgO	18.05	11.36	13.73
CaO	0.69	20.62	0.01
Na2O	0.02	0.39	0.01
K2O	0.01	0.01	10.20
TOTAL	98.39	96.09	90.90
Si	2.008	1.970	5.794
Ti	0.002	0.007	0.549
Al	0.057	0.107	2.269
Fe2+	0.813	0.341	1.684
Mn	0.019	0.008	0.007
Mg	1.032	0.661	3.199
Ca	0.028	0.862	0.002
Na	0.001	0.030	0.003
K	0.000	0.000	2.034
TOTAL	3.962	3.985	15.541

RATELPOORT

SK420	Opx1	Cpx	Hbl
SiO2	52.33	52.23	43.75
TiO2	0.07	0.22	1.94
Al2O3	1.07	2.19	11.13
FeO	21.96	8.92	14.27
MnO	0.13	0.40	0.25
MgO	22.52	13.80	12.65
CaO	0.46	21.64	11.70
Na2O	0.00	0.45	1.38
K2O	0.00	0.00	1.39
TOTAL	98.54	99.86	98.45
Si	1.972	1.951	6.456
Ti	0.002	0.006	0.215
Al	0.048	0.097	1.939
Fe2+	0.692	0.279	1.760
Mn	0.004	0.013	0.031
Mg	1.265	0.768	2.781
Ca	0.019	0.866	1.850
Na	0.000	0.032	0.394
K	0.000	0.000	0.261
TOTAL	4.002	4.011	15.687

RATELPOORT

SK408	Opx	Cpx
SiO2	51.11	50.91
TiO2	0.11	0.23
Al2O3	1.37	2.15
FeO	24.03	9.63
MnO	0.14	0.49
MgO	21.31	13.56
CaO	1.27	22.29
Na2O	0.00	0.49
K2O	0.00	0.00
TOTAL	99.34	99.75
Si	1.939	1.921
Ti	0.003	0.007
Al	0.061	0.096
Fe2+	0.762	0.304
Mn	0.005	0.016
Mg	1.205	0.763
Ca	0.052	0.901
Na	0.000	0.036
K	0.000	0.000
TOTAL	4.027	4.042

EAST OF RATELPOORT

DKON32	Opx1	Opx1	Hbl
SiO2	51.57	52.30	45.38
TiO2	0.19	0.15	0.84
Al2O3	2.98	2.91	10.95
FeO	15.10	14.42	7.86
MnO	0.53	0.45	0.20
MgO	26.30	27.10	15.75
CaO	0.20	0.32	12.12
Na2O	0.41	0.05	0.69
K2O	0.06	0.05	0.40
TOTAL	97.34	97.75	94.20
Si	1.914	1.922	6.711
Ti	0.005	0.004	0.093
Al	0.130	0.126	1.911
Fe2+	0.469	0.443	0.972
Mn	0.017	0.014	0.025
Mg	1.455	1.485	3.471
Ca	0.008	0.013	1.921
Na	0.030	0.003	0.198
K	0.003	0.002	0.076
TOTAL	4.031	4.013	15.377

TWO-PYROXENE GRANULITE GESELSKAPBENK DOMAIN

DGE20	Opx1	Opx2	Opx3	Cpx1	Cpx2A	Cpx2B	Hbl1	Hbl2	Hbl3
SiO2	49.94	52.10	52.69	50.10	50.24	50.63	46.71	48.36	45.70
TiO2	0.20	0.12	0.17	0.24	0.28	0.29	0.92	0.86	0.88
Al2O3	1.16	1.21	1.24	1.88	2.01	2.07	7.99	7.44	8.40
FeO	19.12	19.11	18.42	6.76	6.92	6.82	9.76	9.40	9.61
MnO	0.63	0.58	0.61	0.30	0.10	0.26	0.22	0.17	0.18
MgO	25.56	25.29	23.77	14.68	14.59	14.91	15.74	17.08	15.64
CaO	0.42	0.43	0.40	22.81	22.66	23.11	11.78	12.15	11.76
Na2O	0.09	0.09	0.09	0.43	0.46	0.49	0.91	0.86	0.86
K2O	0.07	0.05	0.05	0.06	0.06	0.06	0.69	0.60	0.79
TOTAL	97.17	98.97	97.44	97.25	97.31	98.65	94.73	96.91	93.81
Si	1.903	1.939	1.979	1.920	1.922	1.913	6.945	7.001	6.870
Ti	0.006	0.003	0.005	0.007	0.008	0.008	0.103	0.093	0.099
Al	0.052	0.053	0.055	0.085	0.091	0.092	1.401	1.271	1.489
Fe2+	0.609	0.594	0.579	0.217	0.221	0.216	1.214	1.138	1.207
Mn	0.020	0.018	0.019	0.010	0.003	0.008	0.027	0.021	0.023
Mg	1.452	1.402	1.331	0.839	0.832	0.839	3.488	3.686	3.503
Ca	0.017	0.017	0.016	0.937	0.929	0.935	1.877	1.884	1.893
Na	0.007	0.007	0.007	0.032	0.034	0.036	0.262	0.241	0.251
K	0.003	0.002	0.002	0.003	0.003	0.003	0.132	0.110	0.152
TOTAL	4.070	4.036	3.993	4.048	4.043	4.052	15.449	15.445	15.488

DGE61	Opx1	Cpx	Hbl
SiO2	52.12	50.70	46.19
TiO2	0.19	0.23	1.12
Al2O3	1.26	1.51	8.16
FeO	21.35	6.69	10.89
MnO	0.56	0.19	0.22
MgO	23.70	14.65	15.44
CaO	0.44	22.91	11.76
Na2O	0.10	0.38	0.95
K2O	0.05	0.05	0.63
TOTAL	99.77	97.31	95.36
Si	1.942	1.938	6.568
Ti	0.005	0.007	0.119
Al	0.055	0.068	1.369
Fe2+	0.665	0.214	1.295
Mn	0.018	0.006	0.026
Mg	1.316	0.834	3.271
Ca	0.018	0.938	1.791
Na	0.007	0.028	0.261
K	0.002	0.002	0.114
TOTAL	4.030	4.036	14.816

DGE18	Plg1	Plg2	Hbl1	Hbl2
SiO2	47.17	46.65	45.77	45.44
TiO2	0.15	0.15	1.33	1.19
Al2O3	32.90	33.07	10.08	10.45
FeO	0.21	0.20	11.47	11.87
MnO	0.14	0.18	0.28	0.36
MgO	0.07	0.09	14.77	14.30
CaO	16.36	17.14	11.47	11.48
Na2O	1.77	0.98	1.35	1.41
K2O	0.09	1.83	0.67	0.64
TOTAL	98.86	100.31	97.19	97.15
Si	8.751	8.629	6.695	6.665
Ti	0.021	0.021	0.146	0.132
Al	7.202	7.218	1.739	1.809
Fe2+	0.033	0.032	1.403	1.457
Mn	0.022	0.029	0.035	0.044
Mg	0.019	0.024	3.220	3.126
Ca	3.251	3.397	1.798	1.804
Na	0.637	0.350	0.383	0.402
K	0.021	0.433	0.125	0.121
TOTAL	19.956	20.132	15.544	15.560

DGE76	Opx1	Opx2	Cpx1	Cpx2	Hbl
SiO2	51.22	51.10	50.51	50.56	45.24
TiO2	0.17	0.17	0.26	0.27	0.68
Al2O3	1.19	1.26	1.84	1.95	8.98
FeO	20.10	22.20	7.30	7.29	11.78
MnO	0.67	0.86	0.37	0.30	0.19
MgO	22.44	22.88	14.01	14.18	13.52
CaO	1.60	0.44	22.62	22.36	11.33
Na2O	0.14	0.11	0.45	0.38	1.02
K2O	0.07	0.06	0.05	0.05	0.65
TOTAL	97.60	99.07	97.41	97.33	93.39
Si	1.951	1.932	1.934	1.935	6.887
Ti	0.005	0.005	0.008	0.008	0.077
Al	0.054	0.056	0.083	0.088	1.613
Fe2+	0.640	0.702	0.234	0.233	1.499
Mn	0.021	0.027	0.012	0.010	0.025
Mg	1.274	1.289	0.799	0.809	3.067
Ca	0.065	0.018	0.928	0.917	1.847
Na	0.010	0.008	0.034	0.028	0.301
K	0.003	0.003	0.002	0.002	0.127
TOTAL	4.024	4.040	4.034	4.029	15.443

METADOLERITE STEINKOPF DOMAIN

SK464	Plg1	Plg2	Plg3	Plg4	Opx1	Opx2	Cpx1	Hbl
SiO2	51.26	52.04	54.90	55.95	50.97	49.39	50.04	40.21
TiO2	0.08	0.08	0.09	0.08	0.12	0.11	0.19	1.47
Al2O3	31.98	31.51	28.56	27.27	0.97	1.04	2.01	12.38
FeO	0.34	0.29	0.16	0.17	26.31	26.77	11.31	14.46
MnO	0.09	0.10	0.08	0.10	0.56	0.49	0.25	0.18
MgO	0.06	0.07	0.07	0.05	20.40	20.98	12.80	11.51
CaO	14.07	12.45	9.93	8.93	0.64	0.43	22.02	11.87
Na2O	3.11	4.06	5.41	5.79	0.10	0.05	0.40	1.40
K2O	0.08	0.12	0.17	0.19	0.03	0.04	0.03	0.86
TOTAL	101.07	100.72	99.35	98.52	100.11	99.29	99.03	94.34
Si	9.224	9.369	9.939	10.180	1.941	1.907	1.917	6.225
Ti	0.011	0.011	0.012	0.011	0.004	0.003	0.005	0.171
Al	6.790	6.694	6.100	5.854	0.044	0.048	0.091	2.261
Fe2+	0.051	0.044	0.024	0.025	0.838	0.864	0.362	1.872
Mn	0.014	0.016	0.012	0.015	0.018	0.016	0.008	0.024
Mg	0.016	0.018	0.018	0.014	1.158	1.207	0.731	2.656
Ca	2.713	2.401	1.925	1.740	0.026	0.018	0.904	1.969
Na	1.085	1.416	1.900	2.043	0.007	0.003	0.029	0.419
K	0.018	0.026	0.038	0.043	0.002	0.002	0.001	0.171
TOTAL	19.922	19.994	19.968	19.926	4.038	4.069	4.048	15.768

SK338	Opx1	Opx2	Cpx	Hbl
SiO2	49.44	50.29	50.04	42.04
TiO2	0.21	0.21	0.43	2.44
Al2O3	1.49	1.52	2.50	11.27
FeO	24.45	24.02	9.43	14.42
MnO	0.86	0.89	0.42	0.29
MgO	21.65	22.34	13.09	12.24
CaO	0.60	0.58	21.88	11.35
Na2O	0.09	0.08	0.35	1.11
K2O	0.05	0.06	0.05	1.52
TOTAL	98.84	100.00	98.19	96.69
Si	1.901	1.904	1.916	6.343
Ti	0.006	0.006	0.012	0.277
Al	0.068	0.068	0.113	2.006
Fe2+	0.786	0.761	0.302	1.819
Mn	0.028	0.028	0.014	0.038
Mg	1.241	1.261	0.747	2.752
Ca	0.025	0.024	0.897	1.834
Na	0.007	0.006	0.026	0.326
K	0.002	0.003	0.003	0.292
TOTAL	4.064	4.060	4.030	15.686

SK468	Plg	Hbe
SiO2	55.32	42.28
TiO2	0.16	1.60
Al2O3	27.33	10.52
FeO	0.21	16.10
MnO	0.16	0.45
MgO	0.08	11.39
CaO	8.63	11.17
Na2O	5.87	2.03
K2O	0.17	0.58
TOTAL	97.93	96.13
Si	10.132	6.452
Ti	0.021	0.184
Al	5.906	1.895
Fe2+	0.032	2.054
Mn	0.025	0.058
Mg	0.021	2.591
Ca	1.694	1.826
Na	2.084	0.599
K	0.039	0.114
TOTAL	19.955	15.773

SK337	Opx1	Opx2	Opx3	Cpx1	Cpx2	Hbl
SiO2	49.67	49.07	48.97	49.82	48.31	41.59
TiO2	0.22	0.20	0.25	0.35	0.38	2.19
Al2O3	1.33	1.28	1.38	2.29	2.26	11.47
FeO	30.40	31.34	26.40	12.66	12.90	18.00
MnO	0.74	0.81	0.36	0.40	0.37	0.19
MgO	17.29	17.13	16.92	11.84	11.63	10.51
CaO	0.68	0.58	1.48	21.46	21.36	11.45
Na2O	0.10	0.10	0.10	0.36	0.49	1.57
K2O	0.06	0.04	0.11	0.07	0.05	1.33
TOTAL	100.49	100.55	95.97	99.25	97.73	98.29
Si	1.927	1.913	1.957	1.914	1.894	6.281
Ti	0.006	0.006	0.007	0.010	0.011	0.249
Al	0.061	0.059	0.065	0.104	0.104	2.043
Fe2+	0.986	1.022	0.882	0.407	0.423	2.273
Mn	0.024	0.027	0.012	0.013	0.012	0.024
Mg	0.999	0.996	1.008	0.678	0.680	2.366
Ca	0.028	0.024	0.063	0.883	0.898	1.853
Na	0.008	0.007	0.008	0.027	0.037	0.461
K	0.003	0.002	0.006	0.003	0.003	0.256
TOTAL	4.042	4.056	4.009	4.039	4.062	15.806

METADOLERITE GESELSKAPBANK DOMAIN

NNB027	Plg1	Plg2	Plg3	Plg4	Opx1	Opx2	Opx3	Cpx1	Cpx2	Hbe	Btel
SiO2	54.61	56.82	53.21	53.17	52.00	51.90	51.66	52.05	51.89	44.62	36.63
TiO2	0.00	0.00	0.00	0.00	0.05	0.02	0.05	0.09	0.07	1.20	5.83
Al2O3	28.59	28.20	29.39	29.62	0.87	0.71	0.74	1.06	1.12	10.36	15.17
FeO	0.12	0.19	0.52	0.10	25.09	25.11	27.00	9.22	4.78	13.72	16.68
MnO	0.00	0.00	0.00	0.00	0.63	0.68	0.72	0.26	0.23	0.06	0.01
MgO	0.00	0.00	0.00	0.00	17.91	17.88	18.14	13.14	13.10	11.72	11.46
CaO	10.88	9.88	11.76	11.77	4.10	3.50	0.49	22.65	22.91	12.01	0.18
Na2O	5.24	5.66	4.43	4.35	0.07	0.10	0.02	0.34	0.35	0.97	0.26
K2O	0.21	0.20	0.20	0.16	0.02	0.01	0.01	0.01	0.00	1.02	9.39
TOTAL	99.65	100.95	99.51	99.17	100.74	99.91	98.83	98.82	94.45	95.68	95.61
Si	9.885	10.106	9.680	9.680	1.971	1.981	1.994	1.974	2.016	6.715	5.507
Ti	0.000	0.000	0.000	0.000	0.001	0.001	0.001	0.003	0.002	0.136	0.659
Al	6.106	5.918	6.309	6.363	0.039	0.032	0.034	0.047	0.051	1.840	2.691
Fe2+	0.018	0.028	0.079	0.015	0.795	0.802	0.871	0.292	0.155	1.727	2.097
Mn	0.000	0.000	0.000	0.000	0.020	0.022	0.024	0.008	0.008	0.008	0.001
Mg	0.000	0.000	0.000	0.000	1.012	1.017	1.043	0.743	0.758	2.628	2.567
Ca	2.110	1.883	2.292	2.296	0.166	0.143	0.020	0.920	0.953	1.936	0.029
Na	1.839	1.952	1.562	1.535	0.005	0.007	0.001	0.025	0.026	0.283	0.076
K	0.048	0.045	0.046	0.037	0.001	0.000	0.000	0.000	0.000	0.196	1.800
TOTAL	20.006	19.933	19.970	19.925	4.011	4.006	3.989	4.013	3.970	15.469	15.427

KLONDIKE CENTRAL LEUCODIORITE (COPPER DISTRICT)

GLK001	bt	opx	cpx
SiO2	36.76	51.78	52.23
TiO2	4.53	0.10	0.22
Al2O3	13.21	0.94	1.70
FeO	18.69	29.60	12.05
MnO	0.01	0.65	0.23
MgO	10.36	14.99	10.90
CaO	0.65	0.82	21.41
Na2O	0.04	0.01	0.29
K2O	9.52	0.00	0.01
TOTAL	93.77	98.89	99.04
Si	5.712	2.019	1.989
Ti	0.529	0.003	0.006
Al	2.422	0.043	0.076
Fe2+	2.428	0.965	0.384
Mn	0.001	0.021	0.007
Mg	2.399	0.871	0.619
Ca	0.108	0.034	0.874
Na	0.012	0.001	0.021
K	1.886	0.000	0.000
TOTAL	15.498	3.957	3.977

METADOLERITE GESELSKAPBANK DOMAIN

NMG001	Plg1	Ol1	Ol2	Cpx1	Cpx2	Cpx3	Hbe
SiO2	48.43	34.17	34.23	49.82	48.59	51.16	40.07
TiO2	0.06	0.05	0.10	0.22	0.29	0.20	1.61
Al2O3	32.63	0.23	0.28	3.68	5.64	2.70	15.26
FeO	0.34	38.99	39.96	14.11	12.34	13.88	12.52
MnO	0.07	0.34	0.56	0.25	0.15	0.35	0.13
MgO	0.22	23.84	23.98	15.72	14.46	16.95	12.34
CaO	15.37	0.09	0.11	15.55	17.82	14.96	11.21
Na2O	2.90	0.09	0.09	0.10	0.20	0.30	2.38
K2O	0.05	0.04	0.11	0.03	0.03	0.03	0.71
TOTAL	100.06	97.82	99.42	99.47	99.53	100.52	96.23
Si	8.872	1.492	1.478	1.884	1.835	1.908	6.012
Ti	0.008	0.002	0.003	0.006	0.008	0.006	0.182
Al	7.054	0.012	0.014	0.164	0.251	0.119	2.701
Fe2+	0.052	1.423	1.442	0.446	0.390	0.433	1.571
Mn	0.011	0.013	0.021	0.008	0.005	0.011	0.017
Mg	0.060	1.551	1.542	0.886	0.813	0.942	2.758
Ca	3.016	0.004	0.005	0.630	0.721	0.598	1.802
Na	1.029	0.007	0.007	0.007	0.015	0.022	0.692
K	0.012	0.002	0.006	0.002	0.002	0.002	0.136
TOTAL	20.113	4.505	4.519	4.032	4.039	4.039	15.870

NMG005	Plg1	Plg2	Plg3	BI	Hbl	Cpx	Opx
SiO2	50.82	47.12	47.85	37.49	45.73	52.02	52.38
TiO2	0.07	0.08	0.08	2.76	0.93	0.17	0.10
Al2O3	32.16	32.35	33.79	15.60	10.17	1.43	1.01
FeO	0.22	0.22	0.21	13.21	10.85	6.91	21.63
MnO	0.10	0.06	0.08	0.14	0.10	0.26	0.43
MgO	0.05	0.05	0.07	16.03	15.24	15.35	25.22
CaO	13.55	15.58	15.20	0.12	11.19	22.56	0.36
Na2O	3.38	2.13	2.55	0.13	1.33	0.12	0.09
K2O	0.07	0.07	0.09	9.33	1.10	0.06	0.07
TOTAL	100.41	97.66	99.92	94.81	96.64	98.87	101.28
Si	9.196	8.832	8.760	5.573	6.711	1.951	1.925
Ti	0.010	0.011	0.011	0.308	0.103	0.005	0.003
Al	6.866	7.154	7.299	2.737	1.762	0.063	0.044
Fe2+	0.033	0.034	0.032	1.642	1.332	0.217	0.665
Mn	0.015	0.010	0.013	0.017	0.012	0.008	0.013
Mg	0.013	0.015	0.019	3.552	3.334	0.858	1.381
Ca	2.628	3.129	2.981	0.019	1.759	0.906	0.014
Na	1.187	0.775	0.905	0.036	0.378	0.008	0.006
K	0.016	0.017	0.021	1.769	0.206	0.003	0.003
TOTAL	19.963	19.975	20.041	15.653	15.597	4.019	4.055

NMG016	Hb1C	Hb1R	Plg11	Plg12	Plg13	Plg14	Ser1	Ser2
SiO2	47.40	47.10	45.59	49.76	45.61	44.52	47.69	46.65
TiO2	0.71	0.72	0.00	0.00	0.00	0.00	0.00	0.00
Al2O3	8.64	9.16	33.41	31.86	34.17	33.91	36.95	35.89
FeO	13.40	13.12	0.18	1.17	0.23	0.21	2.65	2.52
MnO	0.48	0.46	0.00	0.00	0.00	0.00	0.00	0.00
MgO	14.88	14.25	0.00	0.69	0.00	0.00	0.38	0.34
CaO	11.13	10.67	17.08	9.51	17.16	17.24	0.03	0.34
Na2O	0.77	0.80	1.40	1.48	1.20	0.99	0.12	0.03
K2O	0.33	0.40	0.01	3.64	0.02	0.02	10.92	10.28
TOTAL	97.74	96.68	97.67	98.11	98.39	96.89	98.74	96.05
Si	6.908	6.920	8.575	9.265	8.513	8.446	6.147	6.168
Ti	0.078	0.080	0.000	0.000	0.000	0.000	0.000	0.000
Al	1.486	1.588	7.415	7.000	7.525	7.591	5.620	5.599
Fe2+	1.633	1.612	0.028	0.182	0.036	0.033	0.286	0.279
Mn	0.059	0.057	0.000	0.000	0.000	0.000	0.000	0.000
Mg	3.231	3.120	0.000	0.191	0.000	0.000	0.073	0.067
Ca	1.738	1.679	3.442	1.897	3.431	3.504	0.004	0.048
Na	0.218	0.228	0.511	0.534	0.434	0.364	0.030	0.008
K	0.061	0.075	0.002	0.864	0.005	0.005	1.795	1.734
TOTAL	15.411	15.358	19.974	19.934	19.944	19.943	13.955	13.903

NMG002	Plg 1	Scp	Hbl1
SiO2	50.65	48.65	41.14
TiO2	0.07	0.09	0.95
Al2O3	32.10	28.55	14.41
FeO	0.18	0.41	14.06
MnO	0.10	0.10	0.18
MgO	0.06	0.10	12.10
CaO	14.19	15.35	11.61
Na2O	3.30	4.69	2.84
K2O	0.04	0.13	0.34
TOTAL	100.69	98.08	97.63
Si	9.158	9.465	6.122
Ti	0.010	0.013	0.107
Al	6.849	6.554	2.530
Fe2+	0.027	0.066	1.750
Mn	0.015	0.017	0.023
Mg	0.015	0.029	2.683
Ca	2.749	3.200	1.851
Na	1.157	1.770	0.820
K	0.009	0.032	0.064
TOTAL	19.990	21.146	15.949

APPENDIX 6

GREY GNEISS BIOTITE ANALYSES AND BIOTITE : MAGNETITE RATIOS

No.	POS.	BIOTITE	MAGNETITE	Si02	TiO2	Al203	Fe2O3	FeO	MnO	MgO	CaO	Na20	K20
S1376	10	.9815	.1115	37.17	4.17	14.34	0.71	17.89	0.63	12.27	0.30	0.08	9.52
S1479	13	1.6242	.1418	37.06	2.41	15.64	1.09	17.79	0.76	11.61	0.04	0.09	9.54
S1408	16	1.5170	.0048	36.67	3.71	16.37	0.00	15.68	0.71	11.62	1.02	0.07	9.73
S1425	21	1.7632	.3427	38.76	2.58	16.51	0.47	15.97	0.67	13.39	0.02	0.14	9.28
S648	P24	.2669	.1007	36.77	3.23	14.43	1.07	17.53	0.49	12.57	0.08	0.06	9.64
S776B	S19	.7731	.3028	38.09	2.34	15.64	1.32	17.54	0.68	11.75	0.34	0.07	8.90
S595D	L28	.5066	.1654	37.17	2.28	16.30	0.70	18.09	1.13	11.40	0.03	0.08	9.84
S490B	L39	.8453	.3699	35.65	2.14	18.85	1.50	23.77	0.44	8.26	0.04	0.04	9.11
SK185	Y51	.6526	.2037	36.76	2.93	14.81	0.74	16.40	0.50	13.22	0.05	0.07	9.99
S765J	N25	.5569	.0585	35.36	3.24	14.82	0.73	17.26	0.68	12.07	0.02	0.11	10.19
S595E	L28	.5200	.1897	36.54	2.78	17.06	0.00	16.08	0.87	11.18	0.03	0.11	10.04
S010	Y37	1.0438	.3295	35.48	3.02	16.82	0.63	18.46	0.60	10.29	0.50	0.09	9.66
S988	V39	.5939	.2848	35.81	3.61	15.63	0.24	16.65	0.50	11.86	0.11	0.15	10.19
S024A	W32	1.1733	.1039	35.65	3.53	13.96	0.64	15.08	0.67	14.32	0.07	0.10	9.84
S780E	U17	.1835	.0534	36.26	3.56	15.39	0.50	17.65	0.53	10.96	0.01	0.10	9.96
S605C	L28	.8282	.2450	34.18	2.60	15.54	1.62	18.52	0.67	8.71	0.08	0.08	9.01
S605B	L28	.3473	.1298	35.25	2.53	17.47	0.83	19.14	0.61	10.59	0.07	0.11	9.58
S014	W38	.5034	.1532	37.83	4.32	13.98	0.23	15.73	0.36	13.55	0.00	0.06	9.81
SK193	R64	.9457	.7138	36.28	2.79	16.23	1.32	16.78	0.46	14.12	0.15	0.06	8.11
S982	T39	.4322	.2031	37.67	4.60	13.40	0.83	17.47	0.27	12.57	0.02	0.09	9.43
S373C	A42	.4527	.2690	35.03	2.98	17.50	1.26	23.60	0.50	7.73	0.02	0.04	9.68
S452	G35	1.2500	.3429	36.14	1.94	17.40	1.42	20.17	0.41	9.84	0.17	0.05	9.21
S515	L35	.4325	.1514	37.79	2.83	16.45	0.49	16.37	0.71	11.54	0.03	0.09	9.15
S776E	S19	.8115	.2059	38.43	2.64	14.96	0.94	16.75	1.00	12.09	0.06	0.05	9.21
S553	K31	.5856	.1420	36.90	3.02	16.06	0.28	16.08	0.49	11.10	0.20	0.05	9.78
S601	M27	1.6376	.3801	36.91	3.50	15.09	0.28	15.71	0.45	12.26	0.02	0.10	9.96
S552C	H35	.7315	.1529	38.79	3.25	14.54	1.01	15.25	0.56	12.74	0.06	0.03	8.34
S398	L39	.6693	.1718	37.44	3.46	14.55	1.32	17.94	0.44	10.58	0.46	0.09	8.97
S188	X67	.6054	.2591	36.89	4.89	14.37	0.77	19.17	0.40	9.37	0.02	0.10	9.20
S641B	N25	.7525	.0844	37.00	3.94	13.63	0.33	13.67	0.35	14.27	0.08	0.12	9.83
S575B	M34	.4480	.1489	38.25	3.20	13.69	0.40	13.94	0.46	14.83	0.12	0.12	10.28
S399B	L39	.5011	.1624	37.16	2.84	17.05	0.05	18.42	0.85	10.78	0.01	0.08	10.37
S426	J38	.5442	.1856	36.89	2.58	18.76	0.03	16.76	0.56	9.61	0.01	0.11	9.14
SK015	I19	.8471	.0327	36.41	3.21	16.44	0.77	18.13	0.60	10.35	0.06	0.03	8.94
S217	Z11	.6806	.0001	38.20	4.43	13.38	0.85	16.36	0.20	12.04	0.01	0.10	9.17
SK020	AC45	.3326	.1436	36.15	2.97	17.11	0.17	16.40	1.06	10.64	0.04	0.14	9.36
SK180	W60	.4009	.2005	38.62	2.40	15.19	0.63	15.70	0.48	14.01	0.03	0.04	9.91
SK226	Y42	.3491	.0737	37.71	1.92	17.19	0.00	12.39	0.47	15.10	0.03	0.14	9.61
S237C	P41	.4266	.2380	38.13	2.89	15.35	0.31	17.01	0.50	12.99	0.01	0.04	10.47
S209	Z43	.3906	.1448	36.05	2.10	19.35	0.14	17.77	0.41	11.00	0.14	0.12	9.68
S960	N40	.6183	.2073	38.40	3.53	14.27	0.71	16.32	0.44	13.93	0.04	0.05	9.47
S780I	S19	1.6962	.2585	37.89	2.97	14.89	0.48	16.55	0.82	12.80	0.04	0.03	9.99
S469D	G37	.3528	.1470	38.30	3.97	14.46	0.34	16.69	0.52	13.15	0.02	0.05	9.76
S413F	I40	.6493	.4139	37.12	4.01	13.66	0.76	14.77	0.31	14.22	0.07	0.13	9.25
S373D	K42	.4695	.1956	35.98	3.33	16.49	0.95	20.28	0.51	9.45	0.03	0.12	9.53
S640B	N26	.3111	.0569	36.32	3.27	16.24	0.08	18.85	1.28	10.82	0.00	0.07	10.40
S459B	I40	.1812	.1132	36.72	3.18	17.54	0.40	19.23	0.38	9.79	0.01	0.06	9.52
S780B	S19	1.0126	.2021	34.08	1.98	16.64	2.08	17.84	0.46	13.60	0.13	0.04	7.78
S958	P41	.3133	.2159	35.82	3.83	13.37	1.35	20.13	0.39	10.42	0.00	0.05	10.30
S001	U35	1.0105	.3146	35.87	2.05	15.25	1.75	19.08	0.43	11.19	0.12	0.06	9.65
S416	L40	1.0906	.3247	36.87	3.21	13.01	1.67	16.67	0.29	12.52	0.07	0.26	9.75
S451	G35	.1826	.3452	37.93	3.56	14.06	1.24	19.99	0.54	10.28	0.09	0.08	9.89
S415	L40	1.5200	.3789	39.91	3.08	14.47	1.10	18.65	0.38	12.28	0.08	0.10	9.78
S500	M37	.7700	.1854	38.31	4.53	13.03	1.05	17.76	0.35	11.45	1.73	0.07	9.51
S505	L35	1.1320	.3014	38.02	3.55	13.96	0.91	18.73	0.59	11.26	0.06	0.03	10.04
S405	L41	.9315	.2764	38.52	3.30	13.25	1.11	18.11	0.43	12.23	0.03	0.00	10.12

The 'POS.' column refers to positions in a coordinate sytem, the integer part increasing in value toward the south. The BIOTITE and MAGNETITE columns list mass (in grams) of the biotite and magnetite concentrates obtained for each sample. The Fe2O3 values were calculated according to the method of de Bruiyn et al., (1983)

THE GEOLOGY OF OUTCROP GS-I, S.W. OF STEINKOPF.

LOCALITY MAP

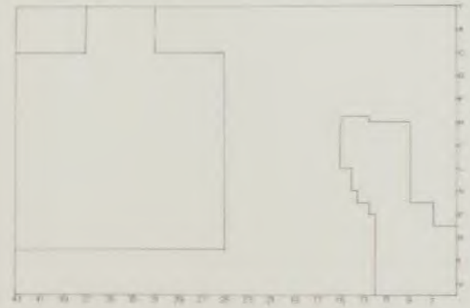

LEGEND

- ALLUVIUM
- LATE PEGMATITE
- LATE GRANITE
- LEUCOGRANITE (ANATEXITE?) WITH MAFIC RESTITE
- SYNTECTONIC PEGMATITE
- GREY META-GRANITOID
- NOENOEMAASBERG GNEISS
- STEINKOPF GNEISS WITH MAFIC COMPONENT
- METAVOLCANIC (?) WITH THIN METAQUARTZITE (METACHERT?)
- LEUCOSOMES
- MINOR SHEARS WITH(——) AND WITHOUT(——) LEUCOSOME VEINS
- SCHLIEREN ⟶ STRIKE LINES IN LEUCOGRANITE
- STRIKE OF PENETRATIVE FOLIATION
- DIP AND STRIKE OF PLANAR STRUCTURE

MAPPED DURING A WEEK IN JULY 1980 BY
J.C. SADDINGHORST, A.L. PEPLER, J.J. PRETORIUS,
D.P. THOMPSON, G. VAN ASWEGEN AND
S.W. VAN DER MERWE.

FINAL PREPARATION BY P. SHAND AND D. DIPPENAAR

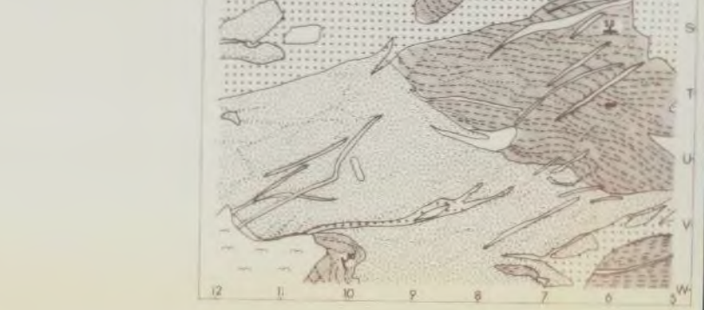

N

THE NAMAQUALAND GEOTRAVERSE

Compiled by H.J. Blignault*, J.A.H. Marais+, S.W. van der Merwe*, G. van Aswegen* and J.A. Muller+ in 1980

CONTRIBUTION BY THE UNIVERSITY OF THE ORANGE FREE STATE AND THE O'OKIEP COPPER COMPANY TO THE SOUTH AFRICAN NATIONAL GEODYNAMICS PROGRAMME

(Annexure to the Spec. Publ. of the Geol. Soc. S. Afr. on the Namaqualand Geotraverse)

*Dept. Geology, University of the Orange Free State, Bloemfontein

+O'okiep Copper Company Ltd., Nababeep

Produced by the Cartographic Division of the Institute for Groundwater Studies, University of the Orange Free State, Bloemfontein, Republic of South Africa

kilometres 10 0 10 20 30 kilometres

1:250 000

GEOLOGICAL DATA SOURCES

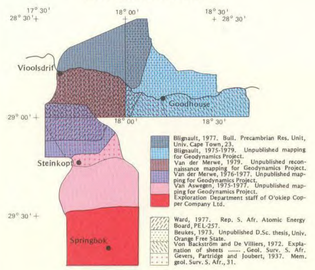

TECTONIC MAP OF SOUTHERN AFRICA SHOWING THE LOCATION OF THE NAMAQUALAND GEOTRAVERSE

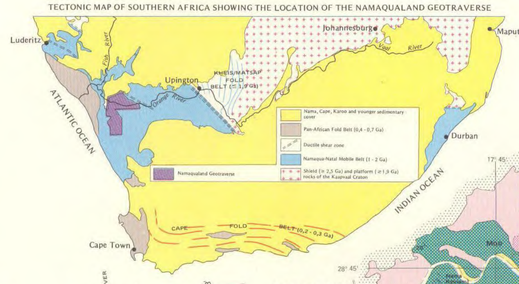

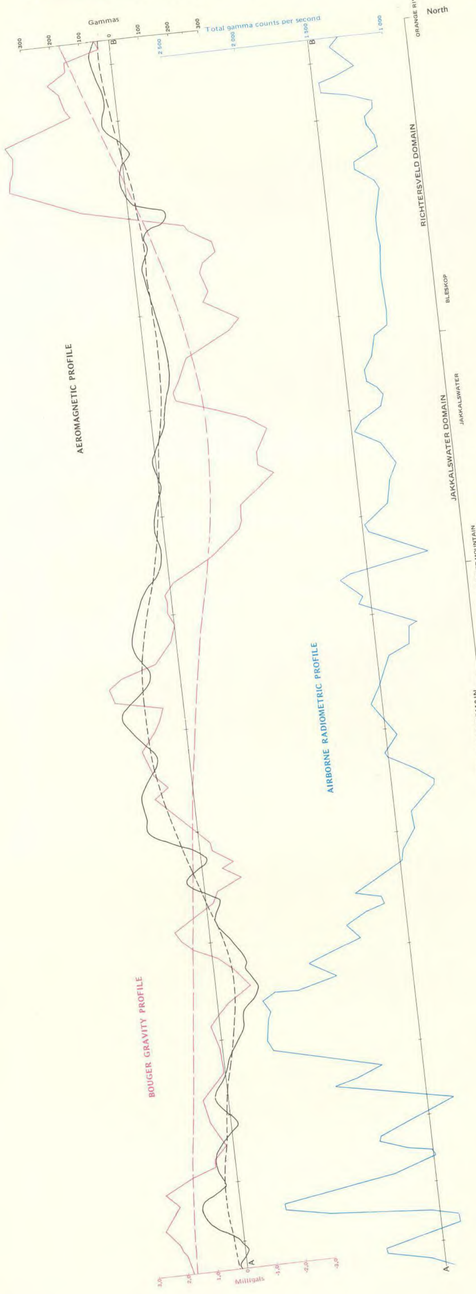

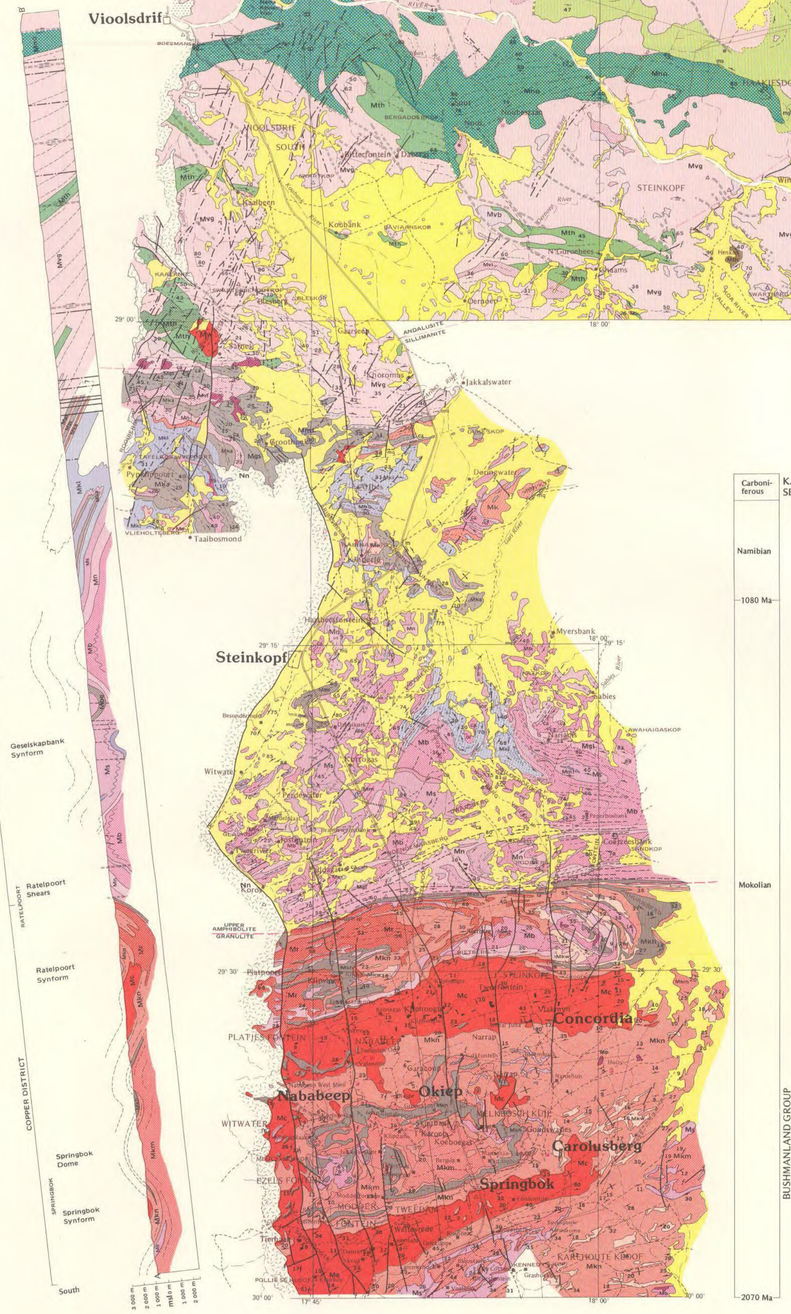

EXPLANATION

METAMORPHIC ZONATION. The area is characterised by low-pressure metamorphism. The andalusite/sillimanite line (———) joins three localities where both minerals coexist; greenschist facies rocks predominate towards the west and amphibolite facies and higher grade rocks towards the east and south. South of Steinkopf upper amphibolite mineral assemblages predominate in common rocks, while granulite facies mineral assemblages characterise the domain south of the upper amphibolite/granulite line (———).

GEOPHYSICAL PROFILES. The gravity, radiometric and magnetic profiles along the national highway N7 are projected onto the reference line AB.

- Bouguer gravity profile. Surveyed by the O'okiep Copper Company Ltd.
- Long wavelength component of the Bouguer gravity field.
- Aeromagnetic profile. Surveyed by the Dept. of Minerals and Energy, Rep. of S. Africa.
- Aeromagnetic profile, upwards continuation of 3 km.
- Airborne radiometric profile. Surveyed by the Dept. of Minerals and Energy, Rep. of S. Africa.

GEOLOGICAL CROSS SECTION. To allow for direct comparison with the geophysical data, the geological data along the national road are projected orthogonally onto the common reference line AB.

LEGEND. Rock units juxtaposed in the double intrusive column suggest possible correlations.

VOLCANO - SEDIMENTARY COLUMN

	FORMATION		LITHOLOGY	
			Sand and calcrete overburden.	
Carboniferous	KAROO SEQUENCE	Dwyka (Cd)	Diamictite and glaciogenic sediments.	Cd
Namibian	NAMA GROUP		Clastic sediments and carbonate rocks.	Nn
1080 Ma				
Mokolian				
2070 Ma				

INTRUSIVE COLUMN

LITHOLOGY

Ng	Dolerite/gabbroid dykes with transitional tholeiitic-alkaline affinities.	GANNAKOURIEP SUITE (Ng)
Nb	Discordant pegmatites constituting a belt along the Orange River.	BLESKOP SUITE (Nb)
Mko	Assemblage of copper-ore-bearing dyke-like bodies ranging from hypersthenite through norite to diorite and anorthosite.	KOPERBERG SUITE (Mko)
Mm	Middelplaat Syenitoid (Mm): Foliated and metamorphosed mesocratic to melanocratic alkaline dykes; normatively a potassium-rich nepheline syenite.	
Me / Mkw	Eyams Granite (Me) / Kweekfontein Granite (Mkw): Compositionally and texturally a variable leucogranite rich in country rock xenoliths in various stages of assimilation. Leucogranite with scattered feldspar megacrysts in places; forms swarms of dykes and sills.	
Mw	Leucogranite, fine to medium grained and equigranular	Wyepoort Granite (Mw)
Mr	Porphyritic (Carlsbad-twinned microcline-microperthite) leucogranite which grades into a biotite-rich syenite in places. Grades into Concordia Granite.	Rietberg Granite (Mr)
Mc	Leucogranite; quartz-microcline with subsidiary oligoclase and variable biotite; garnet plentiful especially near contacts with schist.	Concordia Granite (Mc) — SPEKTAKEL SUITE
Mp	Concordant and subconcordant pegmatites.	
Mkm	A gneissic granite with a variable amount of biotite and prominent augen consisting of granular feldspar.	Modderfontein Gneiss (Mkm)
Mkn	A gneissic biotite-rich granite with prominent augen consisting of granular quartz and feldspar.	Nababeep Gneiss (Mkn) — KLEIN NAMAQUALAND SUITE
Mco	Leucocratic, reddish-brown weathering, gneissic granite with a domainal or megacrystic (feldspar) tendency.	Coboop Gneiss (Mco)
Mvt	Leucocratic granite which becomes a quartzo-feldspathic gneiss towards the south and east.	
Mvg	Undifferentiated granitoids which become gneissic towards the south and east.	
Mvb	Metamorphosed equivalents of tholeiitic gabbroids and ultramafics.	VIOOLSDRIF SUITE
Mam	Foliated, homogeneous amphibolite.	
Mmf	STRUCTURAL POSITION NOT KNOWN: Foliated and metamorphosed mafic dykes and bodies.	
Mho / Mki	NATURE OF PRECURSOR AND STRUCTURAL POSITION NOT KNOWN: Undifferentiated, reddish-brown weathering, leucocratic quartzo-feldspathic gneiss. Leucocratic, reddish-brown weathering quartzo-feldspathic gneiss with sporadic aluminous zones (sillimanite-rich nodules); minor schist ( ) in part an intrusive gneiss.	Hoogoor Gneiss (Mho) / Kinderlé Gneiss (Mki)
Mn	GLADKOP SUITE — Noenoemaasberg Gneiss (Mn): Reddish-brown weathering, leucocratic, gneissic granite; fine grained and finely banded in places.	
Mb	Brandewynsbank Gneiss (Mb): Grey, biotite (± hornblende) granitic gneiss, generally fine grained with a domainal distribution of minerals, locally a megacrystic (K-feldspar) tendency.	
Ms	Steinkopf Gneiss (Ms): Grey, biotite (± hornblende)-granitic to granodioritic gneiss, uniformly fine grained, predominantly of intrusive origin; minor mafic orthogneiss unit ( ).	Mgs**

BUSHMANLAND GROUP

AGGENEYS SUBGROUP (Ma)		Lower metasupracrustite, middle magnetite-quartz-rock - bearing schist and upper (felspathic) metasupracrustite and conglomeratic units.	Ma
HAIB SUBGROUP	Nous (Mno)	Volcaniclastics, andesitic lavas and minor acid flows.	Mno
	Guadom (Mg)	Layered, mafic biotite and hornblende gneiss and schist; minor felsic leucogneiss and sulphide-bearing mica-sillimanite schist ( ).	Mg
	Gaidip (Mga)	Leucocratic quartzo-felspathic gneiss with aluminous nodules and schist layers.	Mga
	Naroep (Mna)	Metaquartzite, laminated felspathic metaquartzite and sulphide-bearing schist.	Mna
	Tsams (Mt)	Volcaniclastics, mafic and felsic lavas; in the east, layered mafic and felsic gneisses and schists.	Mt
	Abbasas (Mab)	Metaquartzite and muscovite schist.	Mab
	Hom (Mh)	Predominantly felsic gneisses with thin layered mafic zones; calc-sediments (——ca) and a muscovite schist/metaquartzite unit ( ).	Mh
	Groothoek (Mg)	A mica-quartz schist unit with muscovite-cordierite-sillimanite layers; minor layers of calc-silicate rock (——si), amphibolite, metaquartzite and cordierite-anthophyllite rock.	Mgs
EENRIET SUBGROUP	Kabina (Mka)	A sequence of metaquartzites, felspathic metaquartzites and biotite-muscovite-sillimanite schists; minor bands of dark metaquartzite, magnetite-quartz rock, amphibolite and cordierite-anthophyllite (± garnet) rock.	Mka
	Besondermeid (Mbe)	Garnet-biotite-sillimanite schist with minor dark metaquartzite (——mq); the schist includes an altered sericite-rich green rock and minor bands of calc-silicate rock, magnetite-quartz rock and amphibolite.	Mbe

STRUCTURAL SEQUENCE

Mkh — Sequence of metaquartzites, felspathic metaquartzites, biotite-sillimanite-garnet schists and minor conglomerate. — KHURISBERG SUBGROUP (Mkh) (Structural position unknown)

* Undifferentiated ** Intimately interbanded

Intrusive relationship

Minor lenses, zones or rafts of ma (metaquartzite), mm (metaquartzite and schist), cn (conglomerate), x (aluminous schist), ca (calc-silicate rock), k (magnetite-quartz rock), sa (sapphirine-bearing rock), cm (cordierite-antophyllite rock) and o (orbicular dykes).

Cu (copper), Ta (tantalite), W (scheelite), Al (corundum), M (muscovite) and D (dolomite) prospects and quarries.

Copper mines

Geological contacts; definite, approximate and concealed.

f——— f Fault or fracture zone.

Strike line of regional foliation/banding; generalised strike line.

Late, open, upright folds; indicated only where structure not obvious.

Strike line of layering. 50

Strike and dip of foliation/banding.

Refoliation, rotated earlier planar fabric and/or shear refoliation.

Strike and dip of bedding; both upright and overturned beds. 12

Ductile shear

National Road

Other Roads

River, Stream

Localities

Farmhouse

Springs

Trigonometrical Beacon

Farm Boundary

PRINTPAK CAPE